NISTIR XXXX Draft

Ongoing Face Recognition Vendor Test (FRVT)

Part 1: Verification

Patrick Grother
Mei Ngan
Kayee Hanaoka
Information Access Division
Information Technology Laboratory

This publication is available free of charge from:
https://www.nist.gov/programs-projects/face-recognition-vendor-test-frvt-ongoing

2020/10/09

National Institute of
Standards and Technology
U.S. Department of Commerce

ACKNOWLEDGMENTS

The authors are grateful to staff in the NIST Biometrics Research Laboratory for infrastructure supporting rapid evaluation of algorithms.

DISCLAIMER

Specific hardware and software products identified in this report were used in order to perform the evaluations described in this document. In no case does identification of any commercial product, trade name, or vendor, imply recommendation or endorsement by the National Institute of Standards and Technology, nor does it imply that the products and equipment identified are necessarily the best available for the purpose.

INSTITUTIONAL REVIEW BOARD

The National Institute of Standards and Technology's Research Protections Office reviewed the protocol for this project and determined it is not human subjects research as defined in Department of Commerce Regulations, 15 CFR 27, also known as the Common Rule for the Protection of Human Subjects (45 CFR 46, Subpart A).

FRVT STATUS

This report is a draft NIST Interagency Report, and is open for comment. It is the twentieth edition of the report since the first was published in June 2017. Prior editions of this report are maintained on the FRVT website, and may contain useful information about older algorithms and datasets no longer used in FRVT.

FRVT remains open: All four tracks of the FRVT are open to new algorithm submissions.

Changes since September 18, 2020:

- This report adds results for first algorithms from five developers: Aigen, Cortica, Kookmin University, Securif AI and Vinai.
- The report also includes results for three developers who have previously submitted algorithms: Fujitsu Laboratories, Hengrui AI, and X-Forward AI.
- In the per-algorithm report-cards linked from tables and the main webpage, we have added a chart to showing reduction in error rates over the course of FRVT i.e. from 2017 onwards for all algorithms supplied by that developer. Similarly we have added a chart showing error rate reductions for our test of protective face mask verification.
- We plan to continue evaluating algorithms on various mask datasets. We hold that algorithms should be capable of detecting masks and verifying identity of all combinations of masked and unmasked faces. We have accordingly increased the amount to time allowed to extract those features from 1.0 to 1.5 seconds.

Changes since August 25, 2020:

- This report adds results for first algorithms from eight new developers. Akurat Satu Indonesia, Cybercore, Decatur Industries, Innef Labs, Satellite Innovation/Eocortex, Expasoft, and Mobai.
- The report includes results for seven developers who have previously submitted algorithms: 3Divi, BioID Technologies, Incode Technologies, Innovatrics, iSAP Solution, Synology, and Tevian.
- We have retired results for five algorithms per our policy to only list results for two algorithms per developer. Results for retired algorithms appear in prior versions of this report in the archive.

Changes since July 27, 2020:

- We have introduced per-algorithm report sheets. These are HTML documents linked from the accuracy tables in this report (i.e. Table 16) and on the FRVT 1:1 homepage. The sheets contain interactive graphics allowing, for example, mouseover exploration of FNMR(T) and FMR(T). Some of their content had previously appeared in this document.
- This report adds results for algorithms from six new developers. ACI Software, Bresee Technology, Fiberhome Telecommunication Technologies, Imageware Systems, Oz Forensics, and Pensees.
- The report includes results for thirteen developers who have previously submitted algorithms: Canon Information Technology (Beijing), Cyberlink, Dahua Technology, Gorilla Technology, ID3 Technology, Intel Research Group, iQIYI Inc, Momentum Digital, Netbridge Technology, Tech5 SA, Shenzhen AiMall Tech, Vigilant Solutions, and VisionLabs.
- We have retired results for nine algorithms per our policy to only list results for two algorithms per developer. Results for retired algorithms appear in prior versions of this report in the archive.

FNMR(T) "False non-match rate"
FMR(T) "False match rate"

Changes since May 18, 2020:

- The report is the first FRVT update since the pandemic closed it from March to June 2020.
- This report includes results for algorithms from nine new developers: GeoVision Inc, Su Zhou NaZhiTianDi Intelligent Technology, YooniK, AYF Technology, PXL Vision AG, Yuan High-Tech Development, Beihang University-ERCACAT, ICM Airport Technics, and Staqu Technologies
- This report includes results for algorithms from 15 returning developers Acer Incorporated, Antheus Technologia, Chosun University, Chunghwa Telecom, Idemia, Moontime Smart Technology, Neurotechnology, Guangzhou Pixel Solutions, Panasonic R+D Center Singapore, Rank One Computing, Scanovate, Shanghai Universiy - Shanghai Film Academy, Synesis, Trueface.ai, and Veridas Digital Authentication Solutions
- We have retired results for ten algorithms per our policy to only list results for two algorithms per developer. Results for retired algorithms appear in prior versions of this report in the archive.
- We separated timing and other resource consumption from the main participation table. The new Table 10 includes template generation durations for four kinds of images, not just mugshots.
- We have published a separate report, NIST Interagency Report 8311 on accuracy of pre-pandemic algorithms on subjects wearing face masks. We plan to track improvements in accuracy on masked images going forward. In particular, we invite submission of algorithms that can detect whether a person is wearing a mask, extract features from the full face or the exposed periocular region, and do appropriate comparison. We do not intend to evaluate algorithms that assume 100% of images will be of masked individuals.

Changes since March 25, 2020:

- The report is a maintenance release - it does not add any new algorithms, and FRVT has been closed to new algorithms since mid March 2020.
- We modified the primary accuracy summary, Table 16, as follows:
  - For visa images, the column for FNMR at FMR = 0.0001 has been removed. The visa images are so highly controlled that the error rates for the most accurate algorithms are dominated by false rejection of very young children and by the presence of a few noisy greyscale images. For now, two visa columns remain: FNMR at FMR= 10^{-6} and, for matched covariates, FNMR at FMR= 10^{-4}.
  - We have inserted a new column labelled "BORDER" giving accuracy for comparison of moderately poor webcam border-crossing photos that exhibit pose variations, poor compression, and low contrast due to strong background illumination. The accuracies are the worst from all cooperative image datasets used in FRVT.
- Accordingly, we updated the failure-to-template rates in Table 21.
- We withdrew a figure showing how false matches are concentrated in certain visa images used in cross-comparison, because it didn't attempt to include demographic information.

Changes since February 27, 2020:

- The report adds results algorithms from two new developers: Beijing Alleyes Technology, and the Chinese Univeristy of Hong Kong. Results for newly submitted algorithms from two other developers will appear in the next report.

FNMR(T) "False non-match rate"
FMR(T) "False match rate"

- The report adds results for algorithms from thirteen returning developers: ASUSTek Computer, Aware, Cyberlink Corp, Gorilla Technology, Innovative Technology, Kakao Enterprise, Lomonosov Moscow State University, Panasonic R+D Center Singapore, Shenzhen AiMall Technology, Shenzhen Intellifusion Technologies, Synology, Tech5 SA, and Via Technologies.
- Per policy to only list results for two algorithms per developer, we have dropped results for algorithms from Aware, Cyberlink, Gorilla Technology, Kakao Enterprise, Lomonosov Moscow State University, Panasonic R+D Center Singapore, and Tech5 SA.

Changes since January 20, 2020:

- The report adds results for five new developers: Ability Enterprise (Andro Video), Chosun University, Fujitsu Research and Development Center, University of Coimbra, and Xforward AI Technology.
- The report adds results for algorithms from six returning developers: AlphaSSTG, Incode Technologies, Kneron. Shanghai Jiao Tong University, Vocord, and X-Laboratory.
- We have corrected template comparison timing numbers for algorithms submitted September 2019 to January 2020. The values reported previously were slower due to a software bug.
- We have dropped results for algorithms from Vocord and Incode per policy to only list results for two algorithms per developer.
- The FRVT 1:1 homepage has been updated with latest accuracy results.
- The FRVT 1:N homepage now includes an update to the September 2019 NIST Interagency Report 8271. The new report adds results for one-to-many search algorithms submitted to NIST from June 2019 to January 2020.

Changes since January 6, 2020:

- Section 2 has been updated to better describe the Visa and Border images. The caption for Table 16 has been updated to better relate the accuracy values to particular image comparisons.
- The report adds results for five new developers: Acer, Advance.AI, Expasoft, Netbridge Technology, and Videmo Intelligente Videoanalyse.
- The report adds results for algorithms from 7 returning developers: China Electronics Import-Export Corp, Intel Research Group, ITMO University, Neurotechnology, N-Tech Lab, Rokid, and VisionLabs.
- We have dropped results from this edition of the report per policy to only list results for two algorithms per developer: N-Tech Lab, Neurotechnology, ITMO, Visionlabs, and CEIEC.
- The FRVT homepage has been updated with latest accuracy results.

Changes since November 11, 2019:

- Table 10 has been updated to include runtime memory usage. This is the first time such a quantity has been reported. The value is the peak size of the resident set size logged during enrollment of single images.
- We have migrated summary results table to a new platform that supports sortable tables: https://pages.nist.gov/frvt/html/frvt11.html
- The report adds results for four new developers: Antheus Technologia, BioID Technologies SA, Canon Information Tech. (Beijing), Samsung S1 (listed in the tables as S1), and Taiwan AI Labs.

- The report adds results for algorithms from 13 returning developers: Anke Investments, Chunghwa Telecom, Deepglint, Institute of Information Technologies, iQIYI, Kneron, Ping An Technology, Paravision, KanKan Ai, Rokid Corporation, Shanghai Universiy - Shanghai Film Academy, Veridas Digital Authentication Solutions, and Videonetics Technology.
- We have dropped results from this edition of the report per policy to only list results for two algorithms per developer: remarkai-000, veridas-001, sensetime-001, iit-000, anke-003, and everai-002. Results for these are available in prior editions of this report linked from the FRVT page.
- We issued NIST Interagency Report 8280: FRVT Part 3: Demographics on 2019-12-19. It includes results for many of the algorithms covered by this report.

Changes since October 16, 2019:

- The report adds results for ten new developers: Ai-Union Technology, ASUSTek Computer, DiDi ChuXing Technology, Innovative Technology, Luxand, MVision, Pyramid Cyber Security + Forensic, Scanovate, Shenzhen AiMall Tech, and TUPU Technology.
- The report adds results for 12 returning developers: CTBC Bank Glory Gorilla Technology Guangzhou Pixel Solutions Imagus Technology Incode Technologies Lomonosov Moscow State University Rank One Computing Samtech InfoNet Shanghai Ulucu Electronics Technology Synesis, and Winsense.
- We have dropped results from this edition of the report per policy to only list results for two algorithms per developer: glory-000, gorilla-002, incode-003, rankone-006, and synesis-004.
- Results for five recently submitted algorithms will appear in the next report.

Changes since September 11, 2019:

- The report adds results for five new participants: Awidit Systems (Awiros), Momemtum Digital (Sertis), Trueface AI, Shanghai Jiao Tong University, and X-Laboratory.
- The reports adds results for five new algorithms from returning developers: Cyberlink, Hengrui AI Technology, Idemia, Panasonic R+D Singapore, and Tevian. This causes three algorithm, to be de-listed from the report per policy to list results for two algorithms per developer.

Changes since July 31 2019:

- The HTML table on the FRVT 1:1 homepage has been updated to include a column for cross-domain Visa-Border verification. Results for this new dataset appeared in the July 29 report under the name "CrossEV" - these are now renamed "Visa-Border".
- The FRVT 1:1 homepage lists algorithms according to lowest mean rank accuracy:
  Rank($\text{FNMR}_{\text{VISA}}$ at FMR = 0.000001) +
  Rank($\text{FNMR}_{\text{VISA-BORDER}}$ at FMR = 0.000001) +
  Rank($\text{FNMR}_{\text{MUGSHOT}}$ at FMR = 0.00001 after 14 years) +
  Rank($\text{FNMR}_{\text{WILD}}$ at FMR = 0.00001)
  This ordering rewards high accuracy across all datasets.
- The main results in Table 16 is now in landscape format to accomodate extra columns for the Visa-Border set, and mugshot comparisons after at least 12 years.
- The report adds results for nine new participants: Alpha SSTG, Intel Research, ULSee, Chungwa Telecon, iSAP Solution, Rokid, Shenzhen EI Networks, CSA Intellicloud, Shenzhen Intellifusion Technologies.

FNMR(T) "False non-match rate"
FMR(T) "False match rate"

- The reports adds results for six new algorithms from returning developers: Innovatrics, Dahua Technology, Tech5 SA, Intellivision, Nodeflux and Imperial College, London. One algorithm, from Imperial has been retired, per policy to list results for two algorithms per developer.
- The cross-country false match rate heatmaps have been replotted to reveal more structure by listing countries by region instead of alphabetically.
- The next version of this report will be posted around October 18, 2019.

Changes since July 3 2019:

- The HTML table on the FRVT 1:1 homepage has been updated to list the 20 most accurate developers rather than algorithms, choosing the most accurate algorithm from each developer based on visa and mugshot results. Also, the algorithms are ordered in terms of lowest mean rank across mugshot, visa and wild datasets, rewarding broad accuracy over a good result on one particular dataset.
- This report includes results for a new dataset - see the column labelled "visa-border" in Table 5. It compares a new set of high quality visa-like portraits with a set webcam border-crossing photos that exhibit moderately poor pose variations and background illumination. The two new sets are described in sections 2.3 and 2.4. The comparisons are "cross-domain" in that the algorithm must compare "visa" and "wild" images. Results for other algorithms will be added in future reports as they become available.
- This report adds results for algorithms from 9 developers submitted in early July 2019. These are from 3DiVi, Camvi, EverAI-Paravision, Facesoft, Farbar (F8), Institute of Information Technologies, Shanghai U. Film Academy, Via Technologies, and Ulucu Electronics Tech. Six of these are new participants.
- Several other algorithms have been submitted and are being evaluated. Results will be released in the next report, scheduled for September 5. That report will include results for new datasets.
- Older algorithms from Everai, Camvi and 3DiVi, have been retired, per the policy to list only two algorithms per developer.

Changes since June 20 2019:

- This report adds results for algorithms from 18 developers submitted in early June 2019. These are from CTBC Bank, Deep Glint, Thales Cogent, Ever AI Paravision, Gorilla Technology, Imagus, Incode, Kneron, N-Tech Lab, Neurotechnology, Notiontag Technologies, Star Hybrid, Videonetics, Vigilant Solutions, Winsense, Anke Investments, CEIEC, and DSK. Nine of these are new participants.
- Several other algorithms have been submitted and are being evaluated. Results will be released in the next report, scheduled for August 1.
- Older algorithms from Everai, Thales Cogent, Gorilla Technology, Incode, Neurotechnology, N-Tech Lab and Vigilant Solutions have been retired, per the policy to list only two algorithms per developer.

Changes since April 2019:

- This report adds results for nine algorithms from nine developers submitted in early June 2019. These are from Tencent Deepsea, Hengrui, Kedacom, Moontime, Guangzhou Pixel, Rank One Computing, Synesis, Sensetime and Vocord.
- Another 23 algorithms have been submitted and are being evaluated. Results will be released in the next report, scheduled for July 3.
- Older algorithms for Rank One, Synesis, and Vocord have been retired, per the policy to list only two algorithms per developer.

Changes since February 2019:

- This report adds results for 49 algorithms from 42 developers submitted in early March 2019.

FNMR(T) "False non-match rate"
FMR(T) "False match rate"

- This report omits results for algorithms that we retired. We retired for three reasons: 1. The developer submitted a new algorithm, and we only list two. 2. The algorithm needs a GPU, and we no longer allow GPU-based algorithms. 3. Inoperable algorithms.
- Previous results for retired algorithms are available in older editions of this report linked here.
- The mugshot database used from February 2017 to January 2019 has been replaced with an extract of the mugshot database documented in NIST Interagency Report 8238, November 2018. The new mugshot set is described in section 2.5 and is adopted because:
  - It has much better identity label integrity, so that false non-match rates are substantially lower than those reported in FRVT 1:1 reports to date - see Figure 52.
  - It includes images collected over a 17 year period such that ageing can be much better characterized - - see Figure 192.
- Using the new mugshot database, Figure 192 shows accuracy for four demographic groups identified in the biographic metadata that accompanies the data: black females, black males, white females and white males.
- The report adds Figure 14 with results for the twenty human-difficult pairs used in the May 2018 paper *Face recognition accuracy of forensic examiners, superrecognizers, and face recognition algorithms* by Phillips et al. [1].
- The report uses an update to the wild image database that corrects some ground truth labels.
- Some results for the child exploitation database are not complete. They are typically updated less frequently than for other image sets.

Contents

ACKNOWLEDGMENTS 1

DISCLAIMER 1

INSTITUTIONAL REVIEW BOARD 1

1 METRICS 32
1.1 CORE ACCURACY . . . 32

2 DATASETS 33
2.1 CHILD EXPLOITATION IMAGES . . . 33
2.2 VISA IMAGES . . . 33
2.3 APPLICATION IMAGES . . . 33
2.4 BORDER CROSSING IMAGES . . . 34
2.5 MUGSHOT IMAGES . . . 34
2.6 WILD IMAGES . . . 34

3 RESULTS 35
3.1 TEST GOALS . . . 35
3.2 TEST DESIGN . . . 35
3.3 FAILURE TO ENROLL . . . 38
3.4 RECOGNITION ACCURACY . . . 43
3.5 GENUINE DISTRIBUTION STABILITY . . . 197
3.5.1 EFFECT OF BIRTH PLACE ON THE GENUINE DISTRIBUTION . . . 197
3.5.2 EFFECT OF AGEING . . . 219
3.5.3 EFFECT OF AGE ON GENUINE SUBJECTS . . . 235
3.6 IMPOSTOR DISTRIBUTION STABILITY . . . 258
3.6.1 EFFECT OF BIRTH PLACE ON THE IMPOSTOR DISTRIBUTION . . . 258
3.6.2 EFFECT OF AGE ON IMPOSTORS . . . 262

List of Tables

1 PARTICIPANT INFORMATION . . . 14
2 PARTICIPANT INFORMATION . . . 15
3 PARTICIPANT INFORMATION . . . 16
4 PARTICIPANT INFORMATION . . . 17
5 ALGORITHM SUMMARY . . . 18
6 ALGORITHM SUMMARY . . . 19
7 ALGORITHM SUMMARY . . . 20
8 ALGORITHM SUMMARY . . . 21
9 ALGORITHM SUMMARY . . . 22
10 ALGORITHM SUMMARY . . . 23
11 FALSE NON-MATCH RATE . . . 24
12 FALSE NON-MATCH RATE . . . 25
13 FALSE NON-MATCH RATE . . . 26
14 FALSE NON-MATCH RATE . . . 27
15 FALSE NON-MATCH RATE . . . 28
16 FALSE NON-MATCH RATE . . . 29
17 FAILURE TO ENROL RATES . . . 38
18 FAILURE TO ENROL RATES . . . 39
19 FAILURE TO ENROL RATES . . . 40
20 FAILURE TO ENROL RATES . . . 41

FNMR(T) "False non-match rate"
FMR(T) "False match rate"

21 FAILURE TO ENROL RATES 42

List of Figures

1 PERFORMANCE SUMMARY: FNMR VS. TEMPLATE SIZE TRADEOFF 30
2 PERFORMANCE SUMMARY: FNMR VS. TEMPLATE TIME TRADEOFF 31
3 EXAMPLE IMAGES 35
(A) VISA 35
(B) MUGSHOT 35
(C) WILD 35
(D) BORDER 35
4 PERFORMANCE ON 20 HUMAN-DIFFICULT PAIRS 44
5 PERFORMANCE ON 20 HUMAN-DIFFICULT PAIRS 45
6 PERFORMANCE ON 20 HUMAN-DIFFICULT PAIRS 46
7 PERFORMANCE ON 20 HUMAN-DIFFICULT PAIRS 47
8 PERFORMANCE ON 20 HUMAN-DIFFICULT PAIRS 48
9 PERFORMANCE ON 20 HUMAN-DIFFICULT PAIRS 49
10 PERFORMANCE ON 20 HUMAN-DIFFICULT PAIRS 50
11 PERFORMANCE ON 20 HUMAN-DIFFICULT PAIRS 51
12 PERFORMANCE ON 20 HUMAN-DIFFICULT PAIRS 52
13 PERFORMANCE ON 20 HUMAN-DIFFICULT PAIRS 53
14 PERFORMANCE ON 20 HUMAN-DIFFICULT PAIRS 54
15 ERROR TRADEOFF CHARACTERISTIC: VISA IMAGES 55
16 ERROR TRADEOFF CHARACTERISTIC: VISA IMAGES 56
17 ERROR TRADEOFF CHARACTERISTIC: VISA IMAGES 57
18 ERROR TRADEOFF CHARACTERISTIC: VISA IMAGES 58
19 ERROR TRADEOFF CHARACTERISTIC: VISA IMAGES 59
20 ERROR TRADEOFF CHARACTERISTIC: VISA IMAGES 60
21 ERROR TRADEOFF CHARACTERISTIC: VISA IMAGES 61
22 ERROR TRADEOFF CHARACTERISTIC: VISA IMAGES 62
23 ERROR TRADEOFF CHARACTERISTIC: VISA IMAGES 63
24 ERROR TRADEOFF CHARACTERISTIC: VISA IMAGES 64
25 ERROR TRADEOFF CHARACTERISTIC: VISA IMAGES 65
26 ERROR TRADEOFF CHARACTERISTIC: VISA IMAGES 66
27 ERROR TRADEOFF CHARACTERISTIC: VISA IMAGES 67
28 ERROR TRADEOFF CHARACTERISTIC: VISA IMAGES 68
29 ERROR TRADEOFF CHARACTERISTIC: VISA IMAGES 69
30 ERROR TRADEOFF CHARACTERISTIC: VISA IMAGES 70
31 ERROR TRADEOFF CHARACTERISTIC: VISA IMAGES 71
32 ERROR TRADEOFF CHARACTERISTIC: VISA IMAGES 72
33 ERROR TRADEOFF CHARACTERISTIC: VISA IMAGES 73
34 ERROR TRADEOFF CHARACTERISTIC: VISA IMAGES 74
35 ERROR TRADEOFF CHARACTERISTIC: VISA IMAGES 75
36 ERROR TRADEOFF CHARACTERISTIC: VISA IMAGES 76
37 ERROR TRADEOFF CHARACTERISTIC: VISA IMAGES 77
38 ERROR TRADEOFF CHARACTERISTIC: VISA IMAGES 78
39 ERROR TRADEOFF CHARACTERISTIC: VISA IMAGES 79
40 ERROR TRADEOFF CHARACTERISTIC: MUGSHOT IMAGES 80
41 ERROR TRADEOFF CHARACTERISTIC: MUGSHOT IMAGES 81
42 ERROR TRADEOFF CHARACTERISTIC: MUGSHOT IMAGES 82
43 ERROR TRADEOFF CHARACTERISTIC: MUGSHOT IMAGES 83
44 ERROR TRADEOFF CHARACTERISTIC: MUGSHOT IMAGES 84
45 ERROR TRADEOFF CHARACTERISTIC: MUGSHOT IMAGES 85
46 ERROR TRADEOFF CHARACTERISTIC: MUGSHOT IMAGES 86
47 ERROR TRADEOFF CHARACTERISTIC: MUGSHOT IMAGES 87

FNMR(T) "False non-match rate"
FMR(T) "False match rate"

48 ERROR TRADEOFF CHARACTERISTIC: MUGSHOT IMAGES . . . 88
49 ERROR TRADEOFF CHARACTERISTIC: MUGSHOT IMAGES . . . 89
50 ERROR TRADEOFF CHARACTERISTIC: MUGSHOT IMAGES . . . 90
51 ERROR TRADEOFF CHARACTERISTIC: MUGSHOT IMAGES . . . 91
52 ERROR TRADEOFF CHARACTERISTIC: MUGSHOT IMAGES . . . 92
53 ERROR TRADEOFF CHARACTERISTIC: WILD IMAGES . . . 93
54 ERROR TRADEOFF CHARACTERISTIC: WILD IMAGES . . . 94
55 ERROR TRADEOFF CHARACTERISTIC: WILD IMAGES . . . 95
56 ERROR TRADEOFF CHARACTERISTIC: WILD IMAGES . . . 96
57 ERROR TRADEOFF CHARACTERISTIC: WILD IMAGES . . . 97
58 ERROR TRADEOFF CHARACTERISTIC: WILD IMAGES . . . 98
59 ERROR TRADEOFF CHARACTERISTIC: WILD IMAGES . . . 99
60 ERROR TRADEOFF CHARACTERISTIC: WILD IMAGES . . . 100
61 ERROR TRADEOFF CHARACTERISTIC: WILD IMAGES . . . 101
62 ERROR TRADEOFF CHARACTERISTIC: WILD IMAGES . . . 102
63 ERROR TRADEOFF CHARACTERISTIC: WILD IMAGES . . . 103
64 ERROR TRADEOFF CHARACTERISTICS: CHILD EXPLOITATION IMAGES . . . 104
65 ERROR TRADEOFF CHARACTERISTICS: CHILD EXPLOITATION IMAGES . . . 105
66 ERROR TRADEOFF CHARACTERISTICS: CHILD EXPLOITATION IMAGES . . . 106
67 ERROR TRADEOFF CHARACTERISTICS: CHILD EXPLOITATION IMAGES . . . 107
68 CMC CHARACTERISTICS: CHILD EXPLOITATION IMAGES . . . 108
69 CMC CHARACTERISTICS: CHILD EXPLOITATION IMAGES . . . 109
70 CMC CHARACTERISTICS: CHILD EXPLOITATION IMAGES . . . 110
71 CMC CHARACTERISTICS: CHILD EXPLOITATION IMAGES . . . 111
72 CMC CHARACTERISTICS: CHILD EXPLOITATION IMAGES . . . 112
73 FALSE MATCH RATES WITHIN AND ACROSS DEMOGRAPHIC GROUPS . . . 113
74 FALSE MATCH RATES WITHIN AND ACROSS DEMOGRAPHIC GROUPS . . . 114
75 FALSE MATCH RATES WITHIN AND ACROSS DEMOGRAPHIC GROUPS . . . 115
76 FALSE MATCH RATES WITHIN AND ACROSS DEMOGRAPHIC GROUPS . . . 116
77 FALSE MATCH RATES WITHIN AND ACROSS DEMOGRAPHIC GROUPS . . . 117
78 FALSE MATCH RATES WITHIN AND ACROSS DEMOGRAPHIC GROUPS . . . 118
79 FALSE MATCH RATES WITHIN AND ACROSS DEMOGRAPHIC GROUPS . . . 119
80 FALSE MATCH RATES WITHIN AND ACROSS DEMOGRAPHIC GROUPS . . . 120
81 FALSE MATCH RATES WITHIN AND ACROSS DEMOGRAPHIC GROUPS . . . 121
82 FALSE MATCH RATES WITHIN AND ACROSS DEMOGRAPHIC GROUPS . . . 122
83 FALSE MATCH RATES WITHIN AND ACROSS DEMOGRAPHIC GROUPS . . . 123
84 FALSE MATCH RATES WITHIN AND ACROSS DEMOGRAPHIC GROUPS . . . 124
85 SEX AND RACE EFFECTS: MUGSHOT IMAGES . . . 125
86 SEX AND RACE EFFECTS: MUGSHOT IMAGES . . . 126
87 SEX AND RACE EFFECTS: MUGSHOT IMAGES . . . 127
88 SEX AND RACE EFFECTS: MUGSHOT IMAGES . . . 128
89 SEX AND RACE EFFECTS: MUGSHOT IMAGES . . . 129
90 SEX AND RACE EFFECTS: MUGSHOT IMAGES . . . 130
91 SEX AND RACE EFFECTS: MUGSHOT IMAGES . . . 131
92 SEX AND RACE EFFECTS: MUGSHOT IMAGES . . . 132
93 SEX AND RACE EFFECTS: MUGSHOT IMAGES . . . 133
94 SEX AND RACE EFFECTS: MUGSHOT IMAGES . . . 134
95 SEX AND RACE EFFECTS: MUGSHOT IMAGES . . . 135
96 SEX AND RACE EFFECTS: MUGSHOT IMAGES . . . 136
97 SEX AND RACE EFFECTS: MUGSHOT IMAGES . . . 137
98 SEX EFFECTS: VISA IMAGES . . . 138
99 SEX EFFECTS: VISA IMAGES . . . 139
100 SEX EFFECTS: VISA IMAGES . . . 140
101 SEX EFFECTS: VISA IMAGES . . . 141
102 SEX EFFECTS: VISA IMAGES . . . 142
103 SEX EFFECTS: VISA IMAGES . . . 143
104 SEX EFFECTS: VISA IMAGES . . . 144

FNMR(T) "False non-match rate"
FMR(T) "False match rate"

105 SEX EFFECTS: VISA IMAGES . . . 145
106 SEX EFFECTS: VISA IMAGES . . . 146
107 SEX EFFECTS: VISA IMAGES . . . 147
108 SEX EFFECTS: VISA IMAGES . . . 148
109 SEX EFFECTS: VISA IMAGES . . . 149
110 SEX EFFECTS: VISA IMAGES . . . 150
111 SEX EFFECTS: VISA IMAGES . . . 151
112 SEX EFFECTS: VISA IMAGES . . . 152
113 SEX EFFECTS: VISA IMAGES . . . 153
114 SEX EFFECTS: VISA IMAGES . . . 154
115 SEX EFFECTS: VISA IMAGES . . . 155
116 SEX EFFECTS: VISA IMAGES . . . 156
117 SEX EFFECTS: VISA IMAGES . . . 157
118 SEX EFFECTS: VISA IMAGES . . . 158
119 FALSE MATCH RATE CALIBRATION: MUGSHOT IMAGES . . . 159
120 FALSE MATCH RATE CALIBRATION: MUGSHOT IMAGES . . . 160
121 FALSE MATCH RATE CALIBRATION: MUGSHOT IMAGES . . . 161
122 FALSE MATCH RATE CALIBRATION: MUGSHOT IMAGES . . . 162
123 FALSE MATCH RATE CALIBRATION: MUGSHOT IMAGES . . . 163
124 FALSE MATCH RATE CALIBRATION: MUGSHOT IMAGES . . . 164
125 FALSE MATCH RATE CALIBRATION: MUGSHOT IMAGES . . . 165
126 FALSE MATCH RATE CALIBRATION: MUGSHOT IMAGES . . . 166
127 FALSE MATCH RATE CALIBRATION: MUGSHOT IMAGES . . . 167
128 FALSE MATCH RATE CALIBRATION: MUGSHOT IMAGES . . . 168
129 FALSE MATCH RATE CALIBRATION: MUGSHOT IMAGES . . . 169
130 FALSE MATCH RATE CALIBRATION: MUGSHOT IMAGES . . . 170
131 FALSE MATCH RATE CALIBRATION: MUGSHOT IMAGES . . . 171
132 FALSE MATCH RATE CALIBRATION: VISA IMAGES . . . 172
133 FALSE MATCH RATE CALIBRATION: VISA IMAGES . . . 173
134 FALSE MATCH RATE CALIBRATION: VISA IMAGES . . . 174
135 FALSE MATCH RATE CALIBRATION: VISA IMAGES . . . 175
136 FALSE MATCH RATE CALIBRATION: VISA IMAGES . . . 176
137 FALSE MATCH RATE CALIBRATION: VISA IMAGES . . . 177
138 FALSE MATCH RATE CALIBRATION: VISA IMAGES . . . 178
139 FALSE MATCH RATE CALIBRATION: VISA IMAGES . . . 179
140 FALSE MATCH RATE CALIBRATION: VISA IMAGES . . . 180
141 FALSE MATCH RATE CALIBRATION: VISA IMAGES . . . 181
142 FALSE MATCH RATE CALIBRATION: VISA IMAGES . . . 182
143 FALSE MATCH RATE CALIBRATION: VISA IMAGES . . . 183
144 FALSE MATCH RATE CALIBRATION: VISA IMAGES . . . 184
145 FALSE MATCH RATE CALIBRATION: VISA IMAGES . . . 185
146 FALSE MATCH RATE CALIBRATION: VISA IMAGES . . . 186
147 FALSE MATCH RATE CALIBRATION: VISA IMAGES . . . 187
148 FALSE MATCH RATE CALIBRATION: VISA IMAGES . . . 188
149 FALSE MATCH RATE CALIBRATION: VISA IMAGES . . . 189
150 FALSE MATCH RATE CALIBRATION: VISA IMAGES . . . 190
151 FALSE MATCH RATE CALIBRATION: VISA IMAGES . . . 191
152 FALSE MATCH RATE CALIBRATION: VISA IMAGES . . . 192
153 FALSE MATCH RATE CALIBRATION: VISA IMAGES . . . 193
154 FALSE MATCH RATE CALIBRATION: VISA IMAGES . . . 194
155 FALSE MATCH RATE CALIBRATION: VISA IMAGES . . . 195
156 FALSE MATCH RATE CALIBRATION: VISA IMAGES . . . 196
157 EFFECT OF COUNTRY OF BIRTH ON FNMR . . . 198
158 EFFECT OF COUNTRY OF BIRTH ON FNMR . . . 199
159 EFFECT OF COUNTRY OF BIRTH ON FNMR . . . 200
160 EFFECT OF COUNTRY OF BIRTH ON FNMR . . . 201

FNMR(T) "False non-match rate"
FMR(T) "False match rate"

161 EFFECT OF COUNTRY OF BIRTH ON FNMR . . . 202
162 EFFECT OF COUNTRY OF BIRTH ON FNMR . . . 203
163 EFFECT OF COUNTRY OF BIRTH ON FNMR . . . 204
164 EFFECT OF COUNTRY OF BIRTH ON FNMR . . . 205
165 EFFECT OF COUNTRY OF BIRTH ON FNMR . . . 206
166 EFFECT OF COUNTRY OF BIRTH ON FNMR . . . 207
167 EFFECT OF COUNTRY OF BIRTH ON FNMR . . . 208
168 EFFECT OF COUNTRY OF BIRTH ON FNMR . . . 209
169 EFFECT OF COUNTRY OF BIRTH ON FNMR . . . 210
170 EFFECT OF COUNTRY OF BIRTH ON FNMR . . . 211
171 EFFECT OF COUNTRY OF BIRTH ON FNMR . . . 212
172 EFFECT OF COUNTRY OF BIRTH ON FNMR . . . 213
173 EFFECT OF COUNTRY OF BIRTH ON FNMR . . . 214
174 EFFECT OF COUNTRY OF BIRTH ON FNMR . . . 215
175 EFFECT OF COUNTRY OF BIRTH ON FNMR . . . 216
176 EFFECT OF COUNTRY OF BIRTH ON FNMR . . . 217
177 EFFECT OF COUNTRY OF BIRTH ON FNMR . . . 218
178 ERROR TRADEOFF CHARACTERISTIC: MUGSHOT IMAGES . . . 220
179 ERROR TRADEOFF CHARACTERISTIC: MUGSHOT IMAGES . . . 221
180 ERROR TRADEOFF CHARACTERISTIC: MUGSHOT IMAGES . . . 222
181 ERROR TRADEOFF CHARACTERISTIC: MUGSHOT IMAGES . . . 223
182 ERROR TRADEOFF CHARACTERISTIC: MUGSHOT IMAGES . . . 224
183 ERROR TRADEOFF CHARACTERISTIC: MUGSHOT IMAGES . . . 225
184 ERROR TRADEOFF CHARACTERISTIC: MUGSHOT IMAGES . . . 226
185 ERROR TRADEOFF CHARACTERISTIC: MUGSHOT IMAGES . . . 227
186 ERROR TRADEOFF CHARACTERISTIC: MUGSHOT IMAGES . . . 228
187 ERROR TRADEOFF CHARACTERISTIC: MUGSHOT IMAGES . . . 229
188 ERROR TRADEOFF CHARACTERISTIC: MUGSHOT IMAGES . . . 230
189 ERROR TRADEOFF CHARACTERISTIC: MUGSHOT IMAGES . . . 231
190 ERROR TRADEOFF CHARACTERISTIC: MUGSHOT IMAGES . . . 232
191 ERROR TRADEOFF CHARACTERISTIC: MUGSHOT IMAGES . . . 233
192 ERROR TRADEOFF CHARACTERISTIC: MUGSHOT IMAGES . . . 234
193 EFFECT OF SUBJECT AGE ON FNMR . . . 236
194 EFFECT OF SUBJECT AGE ON FNMR . . . 237
195 EFFECT OF SUBJECT AGE ON FNMR . . . 238
196 EFFECT OF SUBJECT AGE ON FNMR . . . 239
197 EFFECT OF SUBJECT AGE ON FNMR . . . 240
198 EFFECT OF SUBJECT AGE ON FNMR . . . 241
199 EFFECT OF SUBJECT AGE ON FNMR . . . 242
200 EFFECT OF SUBJECT AGE ON FNMR . . . 243
201 EFFECT OF SUBJECT AGE ON FNMR . . . 244
202 EFFECT OF SUBJECT AGE ON FNMR . . . 245
203 EFFECT OF SUBJECT AGE ON FNMR . . . 246
204 EFFECT OF SUBJECT AGE ON FNMR . . . 247
205 EFFECT OF SUBJECT AGE ON FNMR . . . 248
206 EFFECT OF SUBJECT AGE ON FNMR . . . 249
207 EFFECT OF SUBJECT AGE ON FNMR . . . 250
208 EFFECT OF SUBJECT AGE ON FNMR . . . 251
209 EFFECT OF SUBJECT AGE ON FNMR . . . 252
210 EFFECT OF SUBJECT AGE ON FNMR . . . 253
211 EFFECT OF SUBJECT AGE ON FNMR . . . 254
212 EFFECT OF SUBJECT AGE ON FNMR . . . 255
213 EFFECT OF SUBJECT AGE ON FNMR . . . 256
214 WORST CASE REGIONAL EFFECT FNMR . . . 259

215 IMPOSTOR DISTRIBUTION SHIFTS FOR SELECT COUNTRY PAIRS 261

FNMR(T) "False non-match rate"
FMR(T) "False match rate"

	Developer Name	Short Name	Seq. Num.	Validation Date
1	3Divi	3divi-004	004	2019-07-22
2	3Divi	3divi-005	005	2020-08-28
3	ACI Software	acisw-003	003	2020-08-03
4	ADVANCE.AI	advance-002	002	2019-12-19
5	ASUSTek Computer Inc	asusaics-000	000	2019-10-24
6	ASUSTek Computer Inc	asusaics-001	001	2020-02-25
7	AYF Technology	ayftech-001	001	2020-07-06
8	Acer Incorporated	acer-000	000	2020-01-08
9	Acer Incorporated	acer-001	001	2020-06-30
10	Adera Global PTE	adera-001	001	2019-06-17
11	Ai First	aifirst-001	001	2019-11-21
12	AiUnion Technology	aiunionface-000	000	2019-10-22
13	Aigen	aigen-001	001	2020-10-06
14	Akurat Satu Indonesia	ptakuratsatu-000	000	2020-09-11
15	Alchera Inc	alchera-000	000	2019-03-01
16	Alchera Inc	alchera-001	001	2019-03-01
17	Alivia / Innovation Sys	isystems-001	001	2018-06-12
18	Alivia / Innovation Sys	isystems-002	002	2018-10-18
19	AllGoVision	allgovision-000	000	2019-03-01
20	AlphaSSTG	alphaface-001	001	2019-09-03
21	AlphaSSTG	alphaface-002	002	2020-02-20
22	Amplified Group	amplifiedgroup-001	001	2019-03-01
23	Anke Investments	anke-004	004	2019-06-27
24	Anke Investments	anke-005	005	2019-11-21
25	Antheus Technologia	antheus-000	000	2019-12-05
26	Antheus Technologia	antheus-001	001	2020-06-25
27	AnyVision	anyvision-002	002	2018-01-31
28	AnyVision	anyvision-004	004	2018-06-15
29	Aware	aware-004	004	2019-03-01
30	Aware	aware-005	005	2020-02-27
31	Awidit Systems	awiros-001	001	2019-09-23
32	Ayonix	ayonix-000	000	2017-06-22
33	Beihang University-ERCACAT	ercacat-001	001	2020-07-06
34	Beijing Alleyes Technology	alleyes-000	000	2020-03-09
35	Beijing Vion Technology Inc	vion-000	000	2018-10-19
36	BioID Technologies SA	bioidtechswiss-000	000	2019-11-15
37	BioID Technologies SA	bioidtechswiss-001	001	2020-08-28
38	Bitmain	bm-001	001	2018-10-17
39	Bresee Technology	bresee-000	000	2020-08-07
40	CSA IntelliCloud Technology	intellicloudai-001	001	2019-08-13
41	CTBC Bank	ctbcbank-000	000	2019-06-28
42	CTBC Bank	ctbcbank-001	001	2019-10-28
43	Camvi Technologies	camvi-002	002	2018-10-19
44	Camvi Technologies	camvi-004	004	2019-07-12
45	Canon Information Technology (Beijing)	cib-000	000	2019-12-11
46	Canon Information Technology (Beijing)	cib-001	001	2020-08-05
47	China Electronics Import-Export Corp	ceiec-002	002	2019-06-12
48	China Electronics Import-Export Corp	ceiec-003	003	2020-01-06
49	China University of Petroleum	upc-001	001	2019-06-05
50	Chinese Univeristy of Hong Kong	cuhkee-001	001	2020-03-18
51	Chosun University	chosun-000	000	2020-02-12
52	Chosun University	chosun-001	001	2020-07-01
53	Chunghwa Telecom	chtface-002	002	2019-12-07
54	Chunghwa Telecom	chtface-003	003	2020-06-24
55	Cognitec Systems GmbH	cognitec-000	000	2018-10-19
56	Cognitec Systems GmbH	cognitec-001	001	2019-03-01
57	Cortica	cor-001	001	2020-09-24
58	Cybercore	cybercore-000	000	2020-08-26
59	Cyberextruder	cyberextruder-001	001	2017-08-02
60	Cyberextruder	cyberextruder-002	002	2018-01-30
61	Cyberlink Corp	cyberlink-004	004	2020-02-27
62	Cyberlink Corp	cyberlink-005	005	2020-07-31
63	DSK	dsk-000	000	2019-06-28
64	Dahua Technology	dahua-004	004	2019-12-18
65	Dahua Technology	dahua-005	005	2020-08-13
66	Decatur Industries Inc	decatur-000	000	2020-08-18
67	Deepglint	deepglint-001	001	2019-06-21
68	Deepglint	deepglint-002	002	2019-11-15
69	Dermalog	dermalog-005	005	2018-02-02
70	Dermalog	dermalog-006	006	2018-10-18

Table 1: Summary of participant information included in this report.

FNMR(T) "False non-match rate"
FMR(T) "False match rate"

	Developer Name	Short Name	Seq. Num.	Validation Date
71	DiDi ChuXing Technology	didiglobalface-001	001	2019-10-23
72	Digital Barriers	digitalbarriers-002	002	2019-03-01
73	Expasoft LLC	expasoft-000	000	2020-01-06
74	Expasoft LLC	expasoft-001	001	2020-09-03
75	FaceSoft	facesoft-000	000	2019-07-10
76	FarBar Inc	f8-001	001	2019-07-11
77	Fujitsu Research and Development Center	fujitsulab-000	000	2020-02-04
78	Fujitsu Research and Development Center	fujitsulab-001	001	2020-09-30
79	Gemalto Cogent	cogent-003	003	2019-03-01
80	Gemalto Cogent	cogent-004	004	2019-06-14
81	GeoVision Inc	geo-000	000	2020-06-29
82	Glory	glory-001	001	2018-06-08
83	Glory	glory-002	002	2019-11-12
84	Gorilla Technology	gorilla-005	005	2020-03-11
85	Gorilla Technology	gorilla-006	006	2020-07-31
86	Guangzhou Pixel Solutions	pixelall-003	003	2019-10-15
87	Guangzhou Pixel Solutions	pixelall-004	004	2020-07-02
88	Hengrui AI Technology	hr-002	002	2019-10-08
89	Hengrui AI Technology	hr-003	003	2020-09-25
90	Hikvision Research Institute	hik-001	001	2019-03-01
91	ID3 Technology	id3-004	004	2019-03-01
92	ID3 Technology	id3-005	005	2020-08-04
93	ITMO University	itmo-006	006	2019-03-01
94	ITMO University	itmo-007	007	2020-01-06
95	Idemia	idemia-005	005	2019-10-11
96	Idemia	idemia-006	006	2020-07-06
97	Imageware Systems	iws-000	000	2020-08-12
98	Imagus Technology Pty	imagus-000	000	2019-06-19
99	Imagus Technology Pty	imagus-001	001	2019-10-22
100	Imperial College London	imperial-000	000	2019-03-01
101	Imperial College London	imperial-002	002	2019-08-28
102	Incode Technologies Inc	incode-006	006	2020-02-20
103	Incode Technologies Inc	incode-007	007	2020-08-25
104	Innef Labs	innefulabs-000	000	2020-09-04
105	Innovative Technology	innovativetechnologyltd-001	001	2019-10-22
106	Innovative Technology	innovativetechnologyltd-002	002	2020-02-26
107	Innovatrics	innovatrics-006	006	2019-08-13
108	Innovatrics	innovatrics-007	007	2020-08-19
109	Institute of Information Technologies	iit-001	001	2019-07-05
110	Institute of Information Technologies	iit-002	002	2019-12-04
111	Intel Research Group	intelresearch-001	001	2020-01-14
112	Intel Research Group	intelresearch-002	002	2020-07-24
113	Intellivision	intellivision-001	001	2017-10-10
114	Intellivision	intellivision-002	002	2019-08-23
115	Is It You	isityou-000	000	2017-06-26
116	Kakao Enterprise	kakao-002	002	2019-06-19
117	Kakao Enterprise	kakao-003	003	2020-02-26
118	Kedacom International Pte	kedacom-000	000	2019-06-03
119	Kneron Inc	kneron-003	003	2019-07-01
120	Kneron Inc	kneron-005	005	2020-02-21
121	Kookmin University	kookmin-001	001	2020-09-28
122	Lomonosov Moscow State University	intsysmsu-001	001	2019-10-22
123	Lomonosov Moscow State University	intsysmsu-002	002	2020-03-12
124	Lookman Electroplast Industries	lookman-002	002	2018-06-13
125	Lookman Electroplast Industries	lookman-004	004	2019-06-03
126	Luxand Inc	luxand-000	000	2019-11-07
127	MVision	mvision-001	001	2019-11-12
128	Megvii/Face++	megvii-001	001	2018-06-15
129	Megvii/Face++	megvii-002	002	2018-10-19
130	MicroFocus	microfocus-001	001	2018-06-13
131	MicroFocus	microfocus-002	002	2018-10-17
132	Mobai	mobai-000	000	2020-08-26
133	Momentum Digital	sertis-000	000	2019-10-07
134	Momentum Digital	sertis-001	001	2020-07-30
135	Moontime Smart Technology	mt-000	000	2019-06-03
136	Moontime Smart Technology	mt-002	002	2020-07-02
137	N-Tech Lab	ntechlab-007	007	2019-06-25
138	N-Tech Lab	ntechlab-008	008	2020-01-06
139	Netbridge Technology Incoporation	netbridgetech-001	001	2020-01-08
140	Netbridge Technology Incoporation	netbridgetech-002	002	2020-08-11

Table 2: Summary of participant information included in this report.

FNMR(T) "False non-match rate"
FMR(T) "False match rate"

	Developer Name	Short Name	Seq. Num.	Validation Date
141	Neurotechnology	neurotechnology-008	008	2020-01-08
142	Neurotechnology	neurotechnology-009	009	2020-07-07
143	Nodeflux	nodeflux-002	002	2019-08-13
144	NotionTag Technologies Private Limited	notiontag-000	000	2019-06-12
145	Oz Forensics LLC	oz-001	001	2020-07-29
146	PXL Vision AG	pxl-001	001	2020-06-30
147	Panasonic R+D Center Singapore	psl-003	003	2019-10-01
148	Panasonic R+D Center Singapore	psl-005	005	2020-07-06
149	Paravision (EverAI)	paravision	003	2019-07-01
150	Paravision (EverAI)	paravision-004	004	2019-12-11
151	Pensees Pte	pensees-001	001	2020-08-17
152	Pyramid Cyber Security + Forensic (P)	pyramid-000	000	2019-11-04
153	Rank One Computing	rankone-008	008	2019-11-12
154	Rank One Computing	rankone-009	009	2020-06-26
155	Realnetworks Inc	realnetworks-002	002	2019-02-28
156	Realnetworks Inc	realnetworks-003	003	2019-06-12
157	Remark Holdings	remarkai-001	001	2019-03-01
158	Remark Holdings	remarkai-002	002	2019-11-21
159	Rokid Corporation	rokid-000	000	2019-08-01
160	Rokid Corporation	rokid-001	001	2019-12-13
161	Saffe	saffe-001	001	2018-10-19
162	Saffe	saffe-002	002	2019-03-01
163	Samsung S1 Corp	s1-001	001	2019-12-06
164	Samtech InfoNet Limited	samtech-001	001	2019-10-15
165	Satellite Innovation/Eocortex	eocortex-000	000	2020-08-26
166	Scanovate	scanovate-001	001	2019-11-12
167	Scanovate	scanovate-002	002	2020-06-26
168	Securif AI	securifai-001	001	2020-10-06
169	Sensetime Group	sensetime-002	002	2018-10-19
170	Sensetime Group	sensetime-003	003	2019-06-04
171	Shaman Software	shaman-000	000	2017-12-05
172	Shaman Software	shaman-001	001	2018-01-13
173	Shanghai Jiao Tong University	sjtu-001	001	2019-09-27
174	Shanghai Jiao Tong University	sjtu-002	002	2020-02-12
175	Shanghai Ulucu Electronics Technology	uluface-002	002	2019-07-10
176	Shanghai Ulucu Electronics Technology	uluface-003	003	2019-11-12
177	Shanghai University - Shanghai Film Academy	shu-002	002	2019-12-10
178	Shanghai University - Shanghai Film Academy	shu-003	003	2020-06-24
179	Shanghai Yitu Technology	yitu-003	003	2019-03-01
180	Shenzhen AiMall Tech	aimall-002	002	2020-03-12
181	Shenzhen AiMall Tech	aimall-003	003	2020-08-12
182	Shenzhen EI Networks	einetworks-000	000	2019-08-13
183	Shenzhen Inst Adv Integrated Tech CAS	siat-002	002	2018-06-13
184	Shenzhen Inst Adv Integrated Tech CAS	siat-004	004	2019-03-01
185	Shenzhen Intellifusion Technologies	intellifusion-001	001	2019-08-22
186	Shenzhen Intellifusion Technologies	intellifusion-002	002	2020-03-18
187	Smilart	smilart-002	002	2018-02-06
188	Smilart	smilart-003	003	2018-06-18
189	Staqu Technologies	staqu-000	000	2020-07-15
190	Star Hybrid Limited	starhybrid-001	001	2019-06-19
191	Su Zhou NaZhiTianDi intelligent technology	nazhiai-000	000	2020-06-25
192	Synesis	synesis-006	006	2019-10-10
193	Synesis	synesis-007	007	2020-06-24
194	Synology Inc	synology-000	000	2019-10-23
195	Synology Inc	synology-002	002	2020-08-20
196	TUPU Technology	tuputech-000	000	2019-10-11
197	Taiwan AI Labs	ailabs-001	001	2019-12-18
198	Tech5 SA	tech5-004	004	2020-03-09
199	Tech5 SA	tech5-005	005	2020-07-24
200	Tencent Deepsea Lab	deepsea-001	001	2019-06-03
201	Tevian	tevian-005	005	2019-09-21
202	Tevian	tevian-006	006	2020-09-11
203	TigerIT Americas LLC	tiger-002	002	2018-06-13
204	TigerIT Americas LLC	tiger-003	003	2018-10-16
205	TongYi Transportation Technology	tongyi-005	005	2019-06-12
206	Toshiba	toshiba-002	002	2018-10-19
207	Toshiba	toshiba-003	003	2019-03-01
208	Trueface.ai	trueface-000	000	2019-10-08
209	Trueface.ai	trueface-001	001	2020-07-20
210	ULSee Inc	ulsee-001	001	2019-07-31

Table 3: Summary of participant information included in this report.

FNMR(T) "False non-match rate"
FMR(T) "False match rate"

	Developer Name	Short Name	Seq. Num.	Validation Date
211	Universidade de Coimbra	visteam-000	000	2020-01-14
212	VCognition	vcog-002	002	2017-06-12
213	Veridas Digital Authentication Solutions S.L.	veridas-003	003	2019-11-27
214	Veridas Digital Authentication Solutions S.L.	veridas-004	004	2020-07-21
215	Via Technologies Inc	via-000	000	2019-07-08
216	Via Technologies Inc	via-001	001	2020-01-08
217	Videmo Intelligente Videoanalyse	videmo-000	000	2019-12-19
218	Videonetics Technology Pvt	videonetics-001	001	2019-06-19
219	Videonetics Technology Pvt	videonetics-002	002	2019-11-21
220	Vigilant Solutions	vigilantsolutions-007	007	2019-06-27
221	Vigilant Solutions	vigilantsolutions-008	008	2020-08-03
222	VinAI Research VietNam	vinai-000	000	2020-09-24
223	Visidon	vd-001	001	2019-02-26
224	Vision-Box	visionbox-000	000	2019-02-26
225	Vision-Box	visionbox-001	001	2019-03-01
226	VisionLabs	visionlabs-008	008	2020-01-06
227	VisionLabs	visionlabs-009	009	2020-07-27
228	Vocord	vocord-007	007	2019-06-06
229	Vocord	vocord-008	008	2020-01-031
230	Winsense	winsense-000	000	2019-06-17
231	Winsense	winsense-001	001	2019-10-16
232	Xforward AI Technology	xforwardai-000	000	2020-02-06
233	Xforward AI Technology	xforwardai-001	001	2020-09-25
234	Xiamen Meiya Pico Information	meiya-001	001	2019-03-01
235	YooniK	yoonik-000	000	2020-06-24
236	Yuan High-Tech Development	yuan-000	000	2020-06-30
237	Zhuhai Yisheng Electronics Technology	yisheng-004	004	2018-06-12
238	iQIYI Inc	iqface-000	000	2019-06-04
239	iQIYI Inc	iqface-002	002	2020-07-30
240	iSAP Solution Corporation	isap-001	001	2019-08-07
241	iSAP Solution Corporation	isap-002	002	2020-09-01

Table 4: Summary of participant information included in this report.

FNMR(T) "False non-match rate"
FMR(T) "False match rate"

	ALGORITHM	CONFIG	LIBRARY	TEMPLATE						COMPARISON[4]	
	NAME	DATA	DATA	MEMORY	SIZE	GENERATION TIME (ms)[4]				TIME (ns)[5]	
		(KB)[1]	(KB)[2]	(MB)[3]	(B)	MUGSHOT	ISO	PHOTOJOURN.	WILD	GENUINE	IMPOSTOR
1	3divi-004	263670	50794	[54]430	[116]2048 ± 0	[222]984 ± 131	[158]746 ± 43	[131]682 ± 71	[157]729 ± 35	[42]794 ± 35	[42]801 ± 40
2	3divi-005	264098	53870	[55]431	[162]2048 ± 0	[224]993 ± 83	[167]788 ± 36	[143]719 ± 58	[168]778 ± 37	[41]790 ± 20	[39]791 ± 23
3	acer-000	109735	88323	[71]478	[112]2048 ± 0	[28]222 ± 0	[30]223 ± 1	[31]229 ± 2	[34]241 ± 24	[66]1065 ± 40	[75]1109 ± 35
4	acer-001	36650	66086	[50]417	[30]512 ± 0	[25]199 ± 0	[27]198 ± 0	[28]198 ± 0	[27]198 ± 0	[130]2453 ± 44	[131]2461 ± 62
5	acisw-003	282029	35664	[36]282	[239]18467 ± 8	[30]232 ± 1	[24]187 ± 0	[27]177 ± 7	[24]184 ± 0	[238]847908 ± 16757	[238]851850 ± 17018
6	adera-001	0	79272	[27]190	[204]2560 ± 0	[10]97 ± 0	-	-	-	[100]1604 ± 71	[101]1649 ± 56
7	advance-002	257173	20434	[38]295	[74]2048 ± 0	[182]811 ± 2	-	-	-	[57]987 ± 10	[56]988 ± 45
8	aifirst-001	224157	808777	[72]485	[72]2048 ± 0	[107]587 ± 2	[104]573 ± 2	[94]571 ± 20	[109]590 ± 1	[72]1099 ± 14	[74]1087 ± 45
9	aigen-001	256958	595227	[173]1136	[123]2048 ± 0	[239]1448 ± 9	[213]1370 ± 5	[200]1353 ± 10	[213]1363 ± 2	[165]3772 ± 57	[161]3736 ± 56
10	ailabs-001	1054663	338989	[179]1252	[89]2048 ± 0	[141]664 ± 4	[89]526 ± 1	[70]491 ± 60	[86]513 ± 2	[230]104034 ± 661	[230]103415 ± 7722
11	aimall-002	370156	25210	[203]1576	[122]2048 ± 0	[175]776 ± 4	[166]775 ± 3	[154]775 ± 4	[167]774 ± 3	[228]72811 ± 7399	[228]71216 ± 6286
12	aimall-003	504324	171935	[212]1913	[48]1024 ± 0	[140]662 ± 1	[130]660 ± 1	[119]660 ± 2	[129]661 ± 1	[222]34565 ± 93	[223]34598 ± 118
13	aiunionface-000	241642	840295	[49]402	[118]2048 ± 0	[128]637 ± 13	[111]592 ± 7	[99]585 ± 15	[112]598 ± 8	[67]1072 ± 19	[73]1080 ± 47
14	alchera-000	258450	18848	[101]614	[98]2048 ± 0	[108]587 ± 13	[76]489 ± 8	[65]473 ± 21	[74]483 ± 7	[152]3189 ± 32	[149]3031 ± 142
15	alchera-001	174013	18848	[70]473	[90]2048 ± 0	[122]627 ± 11	[91]527 ± 6	[78]513 ± 21	[91]525 ± 7	[153]3342 ± 81	[154]3243 ± 47
16	alleyes-000	507636	997090	[138]857	[127]2048 ± 0	[178]784 ± 1	[178]826 ± 2	[166]823 ± 40	[189]895 ± 2	[91]1298 ± 34	[92]1303 ± 51
17	allgovision-000	172509	155862	[91]561	[144]2048 ± 0	[58]384 ± 8	[55]374 ± 11	[52]392 ± 26	[58]383 ± 16	[220]29903 ± 406	[221]29735 ± 194
18	alphaface-001	259849	81636	[87]527	[106]2048 ± 0	[117]612 ± 1	[119]612 ± 1	[105]613 ± 1	[117]615 ± 1	[60]1008 ± 10	[60]1002 ± 19
19	alphaface-002	768995	70692	[195]1434	[128]2048 ± 0	[123]628 ± 2	[123]627 ± 1	[42]326 ± 1	[46]327 ± 1	[48]945 ± 25	[50]935 ± 17
20	amplifiedgroup-001	0	47053	[9]81	[41]866 ± 2	[7]93 ± 0	-	-	-	[227]57803 ± 4210	[227]56365 ± 1196
21	anke-004	349388	410776	[108]706	[182]2056 ± 0	[121]625 ± 1	[115]599 ± 9	-	[106]581 ± 2	[23]633 ± 22	[27]632 ± 34
22	anke-005	328553	429160	[172]1134	[184]2056 ± 0	[109]590 ± 2	[102]561 ± 2	[85]535 ± 32	[96]545 ± 1	[28]685 ± 19	[31]687 ± 26
23	antheus-000	119453	41994	[16]116	[32]520 ± 0	[12]109 ± 1	[18]159 ± 1	[26]173 ± 14	[16]140 ± 1	[190]6901 ± 268	[188]6936 ± 103
24	antheus-001	119453	41962	[17]118	[33]520 ± 0	[15]120 ± 1	[28]204 ± 1	[30]221 ± 20	[23]178 ± 1	[186]6218 ± 47	[183]6216 ± 45
25	anyvision-002	662659	520039	[67]468	[47]1024 ± 0	[31]248 ± 0	[26]194 ± 0	-	[26]190 ± 1	[229]74069 ± 188	[229]74019 ± 198
26	anyvision-004	401001	630797	[170]1102	[45]1024 ± 0	[53]355 ± 1	[50]344 ± 1	[58]425 ± 112	[50]342 ± 1	[115]1891 ± 51	[111]1829 ± 85
27	asusaics-000	257418	245320	[99]605	[103]2048 ± 0	[80]484 ± 13	[63]407 ± 10	[53]396 ± 18	[62]404 ± 7	[176]5455 ± 78	[177]5422 ± 112
28	asusaics-001	257418	245330	[94]595	[224]4096 ± 0	[195]842 ± 17	[161]759 ± 7	[149]747 ± 28	[164]759 ± 10	[197]8618 ± 42	[197]8638 ± 136
29	aware-004	427829	28219	[209]1820	[196]2084 ± 0	[207]900 ± 10	[184]872 ± 11	[173]872 ± 30	[186]881 ± 33	[89]1279 ± 50	[91]1287 ± 100
30	aware-005	300017	26320	[182]1265	[64]1572 ± 0	[203]886 ± 23	[182]861 ± 14	[171]858 ± 151	[187]889 ± 45	[96]1475 ± 63	[94]1427 ± 115
31	awiros-001	15499	87480	[12]88	[19]512 ± 0	[9]97 ± 6	[7]87 ± 6	-	[7]86 ± 7	[69]1079 ± 44	[67]1050 ± 45
32	ayftech-001	195423	43580	[114]731	[28]512 ± 0	[66]408 ± 23	[48]339 ± 10	[41]319 ± 18	[47]336 ± 11	[19]615 ± 16	[46]885 ± 44
33	ayonix-000	58505	5252	[5]69	[50]1036 ± 0	[2]18 ± 2	[1]10 ± 1	[4]2 ± 4	[1]10 ± 1	[21]621 ± 23	[26]620 ± 26
34	bioidtechswiss-000	758466	119955	[159]1039	[10]256 ± 0	[125]630 ± 2	[116]608 ± 1	[111]629 ± 2	[123]630 ± 1	[221]34416 ± 137	[222]34403 ± 126
35	bioidtechswiss-001	1178769	120811	[198]1455	[18]512 ± 0	[219]966 ± 4	[198]954 ± 2	[185]954 ± 6	[200]980 ± 4	[138]2610 ± 25	[138]2624 ± 32
36	bm-001	287734	38076	[20]148	[1]64 ± 0	[71]444 ± 88	[43]292 ± 25	[25]173 ± 37	[40]276 ± 71	[114]1887 ± 31	[113]1877 ± 26
37	bresee-000	287880	22872	[40]333	[88]2048 ± 0	[237]1309 ± 1	[210]1212 ± 1	[197]1215 ± 0	[210]1211 ± 1	[225]45317 ± 228	[226]48256 ± 425
38	camvi-002	236278	225285	[115]737	[46]1024 ± 0	[147]677 ± 7	[124]628 ± 4	[109]624 ± 7	[122]627 ± 3	[18]612 ± 26	[20]603 ± 20
39	camvi-004	280733	615819	[147]919	[135]2048 ± 0	[170]759 ± 10	[156]733 ± 3	[147]730 ± 10	[158]731 ± 4	[49]948 ± 40	[52]963 ± 31
40	ceiec-002	269063	90975	[51]426	[91]2048 ± 0	[118]612 ± 17	[100]557 ± 6	[90]554 ± 21	[100]555 ± 7	[122]2188 ± 57	[127]2301 ± 56
41	ceiec-003	260371	88707	[53]430	[92]2048 ± 0	[185]817 ± 4	-	-	-	[125]2256 ± 38	[125]2241 ± 54
42	chosun-000	167093	694	[18]136	[83]2048 ± 0	[70]441 ± 1	[60]402 ± 1	[6]9 ± 13	[61]399 ± 1	[55]983 ± 20	[55]983 ± 29
43	chosun-001	765615	707	[74]491	[148]2048 ± 0	[177]783 ± 2	[114]599 ± 1	[92]562 ± 31	[107]589 ± 1	[58]998 ± 25	[65]1035 ± 11
44	chtface-002	363153	369529	[169]1100	[111]2048 ± 0	[106]584 ± 14	[94]530 ± 9	[80]521 ± 18	[93]528 ± 7	[126]2264 ± 26	[124]2234 ± 103

Notes	
1	The configuration size does not capture static data included in libraries.
2	The library size is the combined total of all files provided in the submission lib folder. These libraries e.g. OpenCV may or may not be installed on any end user's platform natively and would not need to be installed with the algorithm.
4	The memory usage is the peak resident set size reported by the ps system call during template generation.
5	The median template creation times are measured on Intel®Xeon®CPU E5-2630 v4 @ 2.20GHz processors.
6	The comparison durations, in nanoseconds, are estimated using std::chrono::high_resolution_clock which on the machine in (2) counts 1ns clock ticks. Precision is somewhat worse than that however. The ± value is the median absolute deviation times 1.48 for Normal consistency.

Table 5: Summary of algorithms and properties included in this report. The red superscripts give ranking for the quantity in that column.

	ALGORITHM	CONFIG	LIBRARY	TEMPLATE						COMPARISON[4]	
	NAME	DATA	DATA	MEMORY	SIZE	GENERATION TIME (ms)[4]				TIME (ns)[5]	
		(KB)[1]	(KB)[2]	(MB)[3]	(B)	MUGSHOT	ISO	PHOTOJOURN.	WILD	GENUINE	IMPOSTOR
45	chtface-003	363153	369529	174 1178	151 2048 ± 0	111 594 ± 16	92 528 ± 7	82 523 ± 19	92 527 ± 7	118 2110 ± 37	123 2219 ± 65
46	cib-000	340288	69515	90 557	126 2048 ± 0	225 993 ± 40	181 859 ± 21	170 845 ± 41	182 858 ± 22	217 24340 ± 60	217 25972 ± 97
47	cib-001	436253	133766	133 836	115 2048 ± 0	134 651 ± 2	128 654 ± 2	127 674 ± 20	124 632 ± 2	166 3783 ± 38	163 3765 ± 37
48	cogent-003	698290	40430	196 1445	42 973 ± 0	215 952 ± 0	-	-	-	202 12496 ± 75	201 11822 ± 163
49	cogent-004	722919	389164	162 1059	69 1983 ± 0	223 987 ± 50	-	-	-	208 15536 ± 75	208 15964 ± 708
50	cognitec-000	474759	27371	76 495	169 2052 ± 0	29 224 ± 1	-	-	-	167 3835 ± 108	164 3782 ± 83
51	cognitec-001	476809	27487	78 498	175 2052 ± 0	43 293 ± 17	-	-	-	171 4253 ± 59	169 4102 ± 167
52	cor-001	1194948	11240	178 1249	194 2060 ± 0	156 699 ± 3	145 699 ± 3	136 699 ± 7	144 699 ± 5	234 270145 ± 2259	234 282686 ± 11788
53	ctbcbank-000	257208	599238	92 570	100 2048 ± 0	100 568 ± 43	80 498 ± 19	-	81 498 ± 15	158 3551 ± 87	171 4805 ± 209
54	ctbcbank-001	275511	599238	96 603	150 2048 ± 0	135 652 ± 35	113 595 ± 20	-	111 595 ± 17	168 3926 ± 45	167 3924 ± 56
55	cuhkee-001	787853	74917	223 2515	170 2052 ± 0	220 977 ± 31	-	-	-	141 2719 ± 60	141 2783 ± 56
56	cybercore-000	86008	55441	30 200	27 512 ± 0	138 655 ± 3	71 475 ± 3	60 439 ± 26	72 459 ± 3	206 14800 ± 75	207 15757 ± 782
57	cyberextruder-001	121211	13629	24 178	9 256 ± 0	206 893 ± 25	170 791 ± 17	-	165 765 ± 24	70 1083 ± 16	72 1079 ± 19
58	cyberextruder-002	168909	13924	29 194	75 2048 ± 0	89 532 ± 6	83 505 ± 7	81 522 ± 25	88 515 ± 10	111 1803 ± 14	108 1779 ± 22
59	cyberlink-004	340894	104662	160 1046	233 4140 ± 0	160 712 ± 1	148 713 ± 1	140 716 ± 1	148 716 ± 1	163 3693 ± 51	166 3898 ± 71
60	cyberlink-005	341680	111358	158 1037	232 4140 ± 0	161 721 ± 1	153 724 ± 1	145 721 ± 1	153 720 ± 1	161 3680 ± 37	168 4021 ± 97
61	dahua-004	832455	141070	233 4885	107 2048 ± 0	164 735 ± 3	157 738 ± 8	148 734 ± 4	159 734 ± 2	35 730 ± 25	33 707 ± 44
62	dahua-005	1586899	169478	236 7360	223 4096 ± 0	238 1418 ± 34	214 1400 ± 8	201 1403 ± 10	214 1402 ± 10	52 957 ± 23	54 969 ± 19
63	decatur-000	350495	171271	143 907	225 4100 ± 0	227 1024 ± 2	203 1056 ± 2	188 1012 ± 98	204 1106 ± 3	200 11439 ± 80	200 11418 ± 112
64	deepglint-001	569802	206788	146 917	218 4096 ± 0	162 721 ± 4	151 718 ± 1	139 715 ± 1	150 717 ± 1	162 3680 ± 35	159 3517 ± 182
65	deepglint-002	459642	272878	206 1614	215 4096 ± 0	146 677 ± 2	139 675 ± 2	133 683 ± 2	130 661 ± 2	205 13633 ± 87	203 12905 ± 440
66	deepsea-001	147497	336250	45 358	43 1024 ± 0	124 630 ± 7	121 619 ± 3	108 623 ± 8	121 625 ± 2	93 1401 ± 37	95 1467 ± 50
67	dermalog-005	0	317687	44 357	2 128 ± 0	17 130 ± 11	13 121 ± 13	13 107 ± 21	10 122 ± 11	8 499 ± 22	9 500 ± 22
68	dermalog-006	0	452387	153 970	3 128 ± 0	88 532 ± 12	90 526 ± 20	77 513 ± 27	94 529 ± 20	9 506 ± 23	6 459 ± 23
69	didiglobalface-001	259849	70680	86 527	105 2048 ± 0	116 612 ± 1	117 612 ± 1	104 612 ± 1	115 612 ± 1	54 973 ± 20	57 988 ± 20
70	digitalbarriers-002	83002	598577	214 1930	186 2056 ± 0	26 209 ± 11	22 180 ± 12	23 170 ± 15	25 184 ± 15	203 13409 ± 228	204 13267 ± 206
71	dsk-000	11967	782905	32 252	21 512 ± 0	47 304 ± 47	14 131 ± 18	14 110 ± 40	17 143 ± 29	193 7152 ± 115	190 7134 ± 111
72	einetworks-000	372608	219883	141 880	190 2056 ± 0	130 645 ± 3	-	-	-	172 4876 ± 66	172 5156 ± 77
73	eocortex-000	255937	59432	31 224	84 2048 ± 0	48 305 ± 22	35 238 ± 6	-	32 228 ± 6	47 923 ± 11	48 918 ± 11
74	ercacat-001	811623	58012	228 2816	179 2052 ± 0	228 1052 ± 3	200 972 ± 2	187 989 ± 31	194 936 ± 2	134 2551 ± 62	132 2501 ± 81
75	everai-paravision-003	539802	118876	177 1225	217 4096 ± 0	144 674 ± 4	138 673 ± 1	126 673 ± 2	138 672 ± 1	31 699 ± 20	35 713 ± 47
76	expasoft-000	15341	240451	13 100	156 2048 ± 0	4 68 ± 0	5 72 ± 6	8 68 ± 0	4 68 ± 0	108 1779 ± 26	107 1757 ± 97
77	expasoft-001	39057	983064	19 142	137 2048 ± 0	5 70 ± 0	4 69 ± 0	9 69 ± 0	5 69 ± 0	103 1660 ± 35	103 1676 ± 48
78	f8-001	272977	19668	183 1276	87 2048 ± 0	190 822 ± 39	-	-	-	207 15262 ± 139	206 15277 ± 212
79	facesoft-000	370120	10612	124 796	163 2048 ± 0	145 675 ± 18	134 666 ± 2	121 666 ± 3	132 664 ± 2	124 2239 ± 28	126 2277 ± 96
80	fujitsulab-000	0	205894	63 453	23 512 ± 0	67 419 ± 1	62 405 ± 1	54 399 ± 12	68 441 ± 1	160 3613 ± 37	160 3621 ± 29
81	fujitsulab-001	0	548917	180 1252	230 4104 ± 0	236 1300 ± 5	212 1289 ± 4	199 1276 ± 14	212 1319 ± 5	143 2853 ± 16	142 2847 ± 14
82	geo-000	114483	304983	34 279	99 2048 ± 0	196 851 ± 1	188 880 ± 3	128 675 ± 290	193 935 ± 1	231 137544 ± 6225	231 137925 ± 6548
83	glory-001	0	144786	185 1331	66 1726 ± 0	61 393 ± 2	54 372 ± 5	49 367 ± 22	57 381 ± 3	199 9607 ± 128	199 9539 ± 182
84	glory-002	0	385177	154 982	199 2106 ± 0	112 594 ± 3	99 553 ± 2	96 572 ± 7	104 575 ± 3	189 6787 ± 85	185 6551 ± 249
85	gorilla-005	100684	1297614	103 629	202 2192 ± 0	63 407 ± 3	61 402 ± 2	55 407 ± 5	63 415 ± 4	139 2678 ± 42	140 2770 ± 112
86	gorilla-006	172743	1318812	140 874	234 4240 ± 0	73 454 ± 3	69 445 ± 2	64 450 ± 5	71 456 ± 3	164 3755 ± 38	162 3737 ± 44
87	hik-001	667866	9290	235 6597	58 1408 ± 0	133 651 ± 0	125 629 ± 1	112 629 ± 3	120 624 ± 1	7 488 ± 19	7 477 ± 22
88	hr-002	390059	327494	186 1337	192 2057 ± 0	209 908 ± 3	-	-	-	215 22530 ± 416	215 21651 ± 533

Notes	
1	The configuration size does not capture static data included in libraries.
2	The library size is the combined total of all files provided in the submission lib folder. These libraries e.g. OpenCV may or may not be installed on any end user's platform natively and would not need to be installed with the algorithm.
4	The memory usage is the peak resident set size reported by the ps system call during template generation.
5	The median template creation times are measured on Intel®Xeon®CPU E5-2630 v4 @ 2.20GHz processors.
6	The comparison durations, in nanoseconds, are estimated using std::chrono::high_resolution_clock which on the machine in (2) counts 1ns clock ticks. Precision is somewhat worse than that however. The ± value is the median absolute deviation times 1.48 for Normal consistency.

Table 6: Summary of algorithms and properties included in this report. The red superscripts give ranking for the quantity in that column.

	ALGORITHM	CONFIG	LIBRARY	TEMPLATE						COMPARISON[4]	
	NAME	DATA	DATA	MEMORY	SIZE	GENERATION TIME (ms)[4]				TIME (ns)[5]	
		(KB)[1]	(KB)[2]	(MB)[3]	(B)	MUGSHOT	ISO	PHOTOJOURN.	WILD	GENUINE	IMPOSTOR
89	hr-003	383739	144263	[155]984	[191]2057 ± 0	[114]606 ± 0	[109]591 ± 0	[115]641 ± 2	[119]621 ± 0	[191]6982 ± 80	[189]6972 ± 84
90	id3-004	171526	49725	[100]613	[12]264 ± 0	[93]541 ± 11	[84]510 ± 8	[76]510 ± 21	[85]513 ± 11	[77]1135 ± 23	[83]1156 ± 32
91	id3-005	153439	22125	[116]740	[13]264 ± 0	[79]479 ± 1	[70]451 ± 0	[63]446 ± 8	[69]451 ± 1	[185]6072 ± 35	[182]6077 ± 38
92	idemia-005	509824	116761	[102]618	[39]588 ± 0	[84]514 ± 15	[82]505 ± 3	[72]494 ± 31	[82]501 ± 4	[188]6657 ± 54	[186]6616 ± 53
93	idemia-006	570566	115633	[149]932	[40]668 ± 0	[149]679 ± 4	[140]676 ± 2	[124]671 ± 27	[136]670 ± 2	[173]5223 ± 80	[173]5193 ± 72
94	iit-001	269176	52055	[121]788	[121]2048 ± 0	[154]699 ± 4	[144]697 ± 1	[135]697 ± 1	[143]697 ± 1	[65]1060 ± 48	[70]1074 ± 54
95	iit-002	259579	52070	[113]731	[147]2048 ± 0	[85]514 ± 1	[88]523 ± 1	[79]521 ± 2	[90]523 ± 1	[61]1023 ± 7	[61]1011 ± 66
96	imagus-000	183453	599571	[66]466	[153]2048 ± 0	[68]425 ± 24	[64]418 ± 22	[57]421 ± 19	[70]454 ± 15	[79]1145 ± 25	[106]1718 ± 63
97	imagus-001	282680	256875	[130]826	[117]2048 ± 0	[181]807 ± 29	[174]799 ± 20	[168]836 ± 49	[176]805 ± 12	[62]1045 ± 22	[49]934 ± 45
98	imperial-000	370120	10623	[125]796	[114]2048 ± 0	[142]669 ± 1	[135]668 ± 2	[122]668 ± 2	[133]667 ± 1	[120]2130 ± 32	[118]2052 ± 100
99	imperial-002	472327	16134	[210]1826	[77]2048 ± 0	[101]569 ± 1	[103]569 ± 1	[93]569 ± 1	[102]569 ± 1	[127]2278 ± 90	[119]2131 ± 44
100	incode-006	266095	63518	[128]814	[79]2048 ± 0	[78]472 ± 1	[72]478 ± 0	[68]479 ± 13	[79]497 ± 1	[109]1788 ± 41	[110]1798 ± 59
101	incode-007	266103	63524	[129]818	[119]2048 ± 0	[77]470 ± 1	[73]480 ± 1	[67]478 ± 13	[83]504 ± 1	[110]1799 ± 35	[109]1789 ± 59
102	innefulabs-000	370588	162172	[57]439	[155]2048 ± 0	[226]1006 ± 3	[201]1007 ± 2	[189]1041 ± 5	[202]1014 ± 5	[180]5782 ± 41	[181]5741 ± 45
103	innovativetechnologyltd-001	177232	335757	[41]341	[124]2048 ± 0	[69]433 ± 7	[68]439 ± 5	[62]445 ± 10	[66]432 ± 6	[113]1877 ± 42	[114]1924 ± 97
104	innovativetechnologyltd-002	173939	372324	[144]912	[136]2048 ± 0	[139]661 ± 2	[105]573 ± 1	[91]554 ± 21	[101]566 ± 2	[112]1841 ± 50	[112]1857 ± 59
105	innovatrics-006	0	466269	[171]1107	[34]538 ± 0	[187]820 ± 5	[183]868 ± 4	[164]815 ± 80	[155]726 ± 5	[181]5855 ± 204	[175]5266 ± 118
106	innovatrics-007	0	493269	[215]1937	[53]1064 ± 0	[240]1485 ± 7	[215]1651 ± 7	[194]1150 ± 180	[215]1471 ± 8	[183]5978 ± 88	[180]5690 ± 102
107	intellicloudai-001	220831	868246	[105]655	[159]2048 ± 0	[76]468 ± 2	[74]481 ± 2	[69]482 ± 16	[73]473 ± 2	[64]1056 ± 4	[68]1051 ± 72
108	intellifusion-001	271872	289387	[117]762	[81]2048 ± 0	[171]764 ± 38	[143]684 ± 32	[116]646 ± 41	[137]671 ± 22	[73]1112 ± 28	[77]1128 ± 41
109	intellifusion-002	762731	385841	[150]941	[219]4096 ± 0	[213]950 ± 2	[196]942 ± 2	[177]884 ± 3	[188]892 ± 2	[106]1713 ± 57	[102]1665 ± 87
110	intellivision-001	43692	11649	[7]74	[188]2056 ± 0	[3]62 ± 2	[3]49 ± 1	-	[3]47 ± 0	[136]2573 ± 91	[136]2544 ± 38
111	intellivision-002	43692	14505	[10]81	[183]2056 ± 0	[50]322 ± 1	[41]280 ± 1	[17]123 ± 88	[35]244 ± 0	[204]13525 ± 134	[202]12782 ± 278
112	intelresearch-001	353997	272602	[194]1433	[133]2048 ± 0	[150]682 ± 4	[136]671 ± 1	[123]669 ± 10	[139]676 ± 12	[159]3553 ± 57	[157]3462 ± 161
113	intelresearch-002	452850	86454	[191]1420	[104]2048 ± 0	[157]707 ± 2	[147]711 ± 4	[138]709 ± 5	[145]708 ± 4	[170]4204 ± 91	[170]4153 ± 93
114	intsysmsu-001	384409	172480	[123]789	[109]2048 ± 0	[119]614 ± 2	[118]612 ± 2	[106]613 ± 2	[116]613 ± 2	[20]621 ± 8	[22]611 ± 31
115	intsysmsu-002	765921	172298	[120]786	[49]1024 ± 0	[110]593 ± 1	[110]592 ± 2	[101]592 ± 1	[110]593 ± 1	[12]549 ± 25	[14]548 ± 29
116	iqface-000	268819	596337	[107]704	[235]4750 ± 32	[90]538 ± 26	[75]488 ± 1	[71]493 ± 1	[75]487 ± 1	[237]636433 ± 38446	[237]632654 ± 85615
117	iqface-002	268831	596337	[110]717	[236]4763 ± 37	[241]3705 ± 11	[216]3698 ± 7	[202]3699 ± 11	[216]3700 ± 11	[236]573908 ± 3063	[236]575909 ± 7068
118	isap-001	99049	204201	[1]18	[221]4096 ± 0	[1]0 ± 0	-	-	-	[4]459 ± 17	[5]456 ± 11
119	isap-002	256765	49931	[37]288	[101]2048 ± 0	[174]769 ± 3	[163]766 ± 1	[152]763 ± 6	[199]974 ± 1	[149]3045 ± 94	[144]2973 ± 66
120	isityou-000	48010	36621	[14]110	[240]19200 ± 0	[13]113 ± 5	[9]96 ± 18	[19]135 ± 68	[11]123 ± 41	[233]237517 ± 1318	[233]237374 ± 1279
121	isystems-001	274621	639268	[168]1091	[71]2048 ± 0	[42]291 ± 9	[38]261 ± 6	[35]261 ± 15	[38]261 ± 6	[13]557 ± 16	[17]564 ± 22
122	isystems-002	358984	803389	[204]1595	[134]2048 ± 0	[189]822 ± 8	[168]789 ± 6	[157]787 ± 16	[169]788 ± 7	[37]749 ± 31	[28]632 ± 28
123	itmo-006	599187	96762	[200]1489	[201]2121 ± 0	[184]814 ± 1	[176]807 ± 3	[163]804 ± 6	[177]806 ± 3	[219]26154 ± 148	[218]26217 ± 260
124	itmo-007	415979	245376	[219]2199	[141]2048 ± 0	[165]741 ± 2	[165]769 ± 2	[155]775 ± 26	[162]750 ± 2	[133]2551 ± 50	[135]2529 ± 80
125	iws-000	30875	3063	[8]77	[22]512 ± 0	[37]277 ± 5	[32]226 ± 1	-	[31]226 ± 4	[59]999 ± 40	[59]992 ± 22
126	kakao-002	479406	412822	[97]603	[165]2048 ± 0	[166]747 ± 6	[142]681 ± 3	[125]672 ± 17	[140]677 ± 3	[107]1720 ± 62	[105]1715 ± 83
127	kakao-003	414379	113944	[208]1754	[110]2048 ± 0	[202]878 ± 3	[186]879 ± 1	[174]877 ± 2	[184]877 ± 2	[119]2128 ± 34	[121]2134 ± 60
128	kedacom-000	245292	37401	[239]23574	[14]292 ± 0	[82]506 ± 3	[77]492 ± 1	[1]1 ± 1	[78]491 ± 2	[26]684 ± 14	[29]682 ± 16
129	kneron-003	58366	1747	[25]188	[108]2048 ± 0	[39]281 ± 3	[40]276 ± 1	-	[41]277 ± 1	[175]5237 ± 63	[176]5274 ± 99
130	kneron-005	375374	13633	[64]457	[80]2048 ± 0	[87]518 ± 2	[86]514 ± 3	[75]510 ± 5	[87]514 ± 3	[116]1922 ± 11	[115]1926 ± 20
131	kookmin-001	234001	31875	[58]439	[129]2048 ± 0	[14]114 ± 1	[12]116 ± 1	[15]116 ± 5	[13]124 ± 2	[22]629 ± 35	[25]616 ± 11
132	lookman-002	138200	25410	[237]16518	[37]548 ± 0	[20]173 ± 1	[19]160 ± 1	[3]1 ± 1	[18]158 ± 1	[17]610 ± 19	[23]612 ± 22

Notes	
1	The configuration size does not capture static data included in libraries.
2	The library size is the combined total of all files provided in the submission lib folder. These libraries e.g. OpenCV may or may not be installed on any end user's platform natively and would not need to be installed with the algorithm.
4	The memory usage is the peak resident set size reported by the ps system call during template generation.
5	The median template creation times are measured on Intel®Xeon®CPU E5-2630 v4 @ 2.20GHz processors.
6	The comparison durations, in nanoseconds, are estimated using std::chrono::high_resolution_clock which on the machine in (2) counts 1ns clock ticks. Precision is somewhat worse than that however. The ± value is the median absolute deviation times 1.48 for Normal consistency.

Table 7: Summary of algorithms and properties included in this report. The red superscripts give ranking for the quantity in that column.

	ALGORITHM	CONFIG	LIBRARY	TEMPLATE						COMPARISON[4]	
	NAME	DATA	DATA	MEMORY	SIZE	GENERATION TIME (ms)[4]				TIME (ns)[5]	
		(KB)[1]	(KB)[2]	(MB)[3]	(B)	MUGSHOT	ISO	PHOTOJOURN.	WILD	GENUINE	IMPOSTOR
133	lookman-004	244775	37401	238 23548	36 548 ± 0	83 507 ± 5	78 494 ± 4	2 1 ± 1	77 490 ± 2	45 871 ± 29	45 878 ± 29
134	luxand-000	0	57908	189 1366	51 1040 ± 0	65 407 ± 23	59 386 ± 14	51 386 ± 29	51 344 ± 13	44 828 ± 28	44 828 ± 32
135	megvii-001	1361523	16486	192 1426	158 2048 ± 0	94 543 ± 0	-	-	-	174 5228 ± 32	174 5252 ± 60
136	megvii-002	1809564	16491	211 1879	227 4100 ± 0	129 644 ± 0	-	-	-	226 50630 ± 183	225 47591 ± 716
137	meiya-001	280055	264913	80 507	168 2049 ± 0	120 622 ± 12	101 559 ± 7	88 541 ± 24	99 553 ± 8	196 8356 ± 615	196 8134 ± 97
138	microfocus-001	104524	27242	26 190	7 256 ± 0	35 264 ± 18	25 188 ± 7	21 144 ± 40	21 170 ± 8	1 215 ± 8	1 217 ± 10
139	microfocus-002	96288	27362	23 176	5 256 ± 0	33 259 ± 18	23 185 ± 7	20 141 ± 36	20 167 ± 8	2 337 ± 34	2 230 ± 25
140	mobai-000	365451	80573	119 786	237 6144 ± 0	173 766 ± 8	149 716 ± 4	-	154 725 ± 6	209 16458 ± 333	209 16423 ± 1473
141	mt-000	372169	282036	161 1056	167 2049 ± 0	163 724 ± 12	150 717 ± 2	141 717 ± 4	149 717 ± 2	104 1678 ± 47	100 1614 ± 85
142	mt-002	290753	145340	134 844	166 2049 ± 0	102 573 ± 1	108 588 ± 4	95 571 ± 1	103 572 ± 1	194 7205 ± 204	191 7211 ± 244
143	mvision-001	227502	149531	111 723	25 512 ± 0	152 691 ± 21	131 661 ± 12	118 657 ± 20	134 669 ± 14	76 1123 ± 40	81 1154 ± 38
144	nazhiai-000	547484	16141	226 2716	130 2048 ± 0	151 683 ± 3	141 679 ± 1	130 678 ± 1	141 679 ± 1	123 2230 ± 34	120 2133 ± 81
145	netbridgetech-001	133108	205875	81 508	216 4096 ± 0	6 85 ± 1	8 88 ± 0	11 86 ± 3	8 94 ± 1	198 9280 ± 74	198 9446 ± 512
146	netbridgetech-002	257687	49931	39 299	95 2048 ± 0	194 838 ± 6	180 843 ± 1	169 842 ± 7	180 849 ± 2	144 2893 ± 65	150 3050 ± 123
147	neurotechnology-008	119718	53462	106 694	8 256 ± 0	52 339 ± 0	47 337 ± 1	44 337 ± 1	49 337 ± 1	5 467 ± 19	8 486 ± 26
148	neurotechnology-009	137515	53213	122 789	6 256 ± 0	59 388 ± 1	58 385 ± 1	50 385 ± 1	59 385 ± 1	10 513 ± 10	10 512 ± 16
149	nodeflux-002	774668	690213	65 466	160 2048 ± 0	159 708 ± 4	146 710 ± 3	137 705 ± 3	147 711 ± 3	156 3475 ± 62	156 3408 ± 143
150	notiontag-000	92753	406791	85 525	38 584 ± 0	96 548 ± 64	46 330 ± 20	38 269 ± 52	44 302 ± 23	224 44672 ± 269	224 44593 ± 358
151	ntechlab-007	2509686	52474	234 5070	210 3348 ± 0	179 792 ± 3	169 789 ± 1	158 788 ± 2	171 791 ± 2	84 1209 ± 59	89 1267 ± 65
152	ntechlab-008	1138002	52483	225 2707	57 1300 ± 0	99 556 ± 1	98 550 ± 1	89 549 ± 1	98 550 ± 1	71 1095 ± 45	66 1049 ± 51
153	oz-001	303723	238311	156 1021	231 4125 ± 0	232 1147 ± 3	207 1149 ± 3	193 1142 ± 11	207 1135 ± 4	232 228011 ± 5455	232 220746 ± 5572
154	paravision-004	556670	145440	202 1572	214 4096 ± 0	191 829 ± 2	179 829 ± 1	167 825 ± 2	179 829 ± 2	36 737 ± 31	37 718 ± 38
155	pensees-001	1619431	408932	213 1922	238 8200 ± 0	230 1108 ± 3	206 1106 ± 3	191 1107 ± 3	206 1107 ± 3	151 3151 ± 34	152 3143 ± 25
156	pixelall-003	0	707030	139 865	205 2560 ± 0	155 699 ± 8	137 672 ± 6	129 678 ± 30	135 669 ± 4	82 1174 ± 28	78 1139 ± 68
157	pixelall-004	0	550919	88 529	203 2560 ± 0	72 451 ± 11	65 421 ± 7	61 440 ± 28	64 425 ± 12	78 1139 ± 65	85 1186 ± 31
158	psl-003	1159643	1434859	232 3960	200 2120 ± 0	198 865 ± 3	185 879 ± 4	159 789 ± 12	170 790 ± 2	63 1052 ± 14	63 1025 ± 51
159	psl-005	774031	1560153	220 2239	209 3144 ± 0	211 922 ± 37	191 926 ± 13	179 924 ± 21	191 926 ± 7	32 703 ± 32	34 708 ± 26
160	ptakuratsatu-000	0	585434	187 1347	35 538 ± 0	201 875 ± 3	202 1040 ± 2	84 534 ± 168	183 860 ± 5	182 5900 ± 103	179 5687 ± 167
161	pxl-001	110116	78231	21 168	29 512 ± 0	11 101 ± 5	6 79 ± 3	10 75 ± 6	6 78 ± 3	179 5598 ± 45	178 5590 ± 68
162	pyramid-000	372608	219883	127 804	180 2056 ± 0	105 583 ± 2	-	-	-	192 7147 ± 59	194 7586 ± 425
163	rankone-008	2	141234	6 70	4 165 ± 0	36 272 ± 3	36 251 ± 2	34 253 ± 11	37 260 ± 7	38 750 ± 20	24 613 ± 23
164	rankone-009	0	107688	3 41	11 260 ± 0	23 179 ± 4	21 163 ± 3	24 172 ± 19	22 172 ± 8	33 710 ± 32	15 552 ± 25
165	realnetworks-002	95328	107088	46 370	68 1848 ± 0	32 250 ± 2	34 234 ± 4	32 234 ± 8	33 231 ± 3	90 1285 ± 17	87 1247 ± 42
166	realnetworks-003	95334	104498	42 345	67 1848 ± 0	22 177 ± 10	20 162 ± 2	22 163 ± 6	19 161 ± 2	98 1516 ± 29	97 1522 ± 60
167	remarkai-001	241857	868314	112 730	174 2052 ± 0	192 831 ± 6	171 794 ± 8	156 787 ± 15	172 793 ± 8	86 1229 ± 20	43 805 ± 56
168	remarkai-002	224157	808777	59 443	96 2048 ± 0	214 950 ± 6	199 968 ± 5	182 938 ± 24	201 997 ± 3	74 1115 ± 25	69 1068 ± 54
169	rokid-000	258612	396624	176 1218	189 2056 ± 0	95 546 ± 3	85 514 ± 1	102 594 ± 15	84 511 ± 1	155 3457 ± 62	158 3463 ± 77
170	rokid-001	641223	413733	164 1071	193 2060 ± 0	210 911 ± 2	189 902 ± 2	172 858 ± 71	181 851 ± 1	154 3345 ± 50	155 3346 ± 149
171	s1-001	435491	844340	118 772	198 2092 ± 0	113 605 ± 24	93 530 ± 10	83 523 ± 21	95 529 ± 5	94 1428 ± 34	93 1415 ± 85
172	saffe-001	85973	62488	22 168	56 1280 ± 0	38 281 ± 1	16 134 ± 1	12 98 ± 12	12 124 ± 1	88 1274 ± 19	90 1277 ± 26
173	saffe-002	260622	28285	137 855	146 2048 ± 0	186 817 ± 11	172 794 ± 15	160 791 ± 31	175 802 ± 22	34 717 ± 7	36 714 ± 29
174	samtech-001	288082	219883	98 605	185 2056 ± 0	44 294 ± 3	-	-	-	195 7694 ± 59	195 7678 ± 91
175	scanovate-001	257083	328532	95 601	85 2048 ± 0	103 577 ± 24	-	-	-	201 12054 ± 699	205 13795 ± 705
176	scanovate-002	256986	457227	136 850	161 2048 ± 0	153 696 ± 32	154 726 ± 25	134 697 ± 31	146 710 ± 16	148 3021 ± 38	151 3120 ± 163

Notes	
1	The configuration size does not capture static data included in libraries.
2	The library size is the combined total of all files provided in the submission lib folder. These libraries e.g. OpenCV may or may not be installed on any end user's platform natively and would not need to be installed with the algorithm.
4	The memory usage is the peak resident set size reported by the ps system call during template generation.
5	The median template creation times are measured on Intel®Xeon®CPU E5-2630 v4 @ 2.20GHz processors.
6	The comparison durations, in nanoseconds, are estimated using std::chrono::high_resolution_clock which on the machine in (2) counts 1ns clock ticks. Precision is somewhat worse than that however. The ± value is the median absolute deviation times 1.48 for Normal consistency.

Table 8: Summary of algorithms and properties included in this report. The red superscripts give ranking for the quantity in that column.

	ALGORITHM	CONFIG	LIBRARY	TEMPLATE						COMPARISON[4]	
	NAME	DATA	DATA	MEMORY	SIZE	GENERATION TIME (ms)[4]				TIME (ns)[5]	
		(KB)[1]	(KB)[2]	(MB)[3]	(B)	MUGSHOT	ISO	PHOTOJOURN.	WILD	GENUINE	IMPOSTOR
177	securifai-001	120291	12456	197 1445	229 4104 ± 0	27 211 ± 1	29 211 ± 1	29 211 ± 1	28 211 ± 1	105 1681 ± 29	104 1701 ± 25
178	sensetime-002	531783	7203	216 2094	177 2052 ± 0	180 797 ± 3	152 718 ± 2	144 720 ± 7	151 717 ± 2	140 2713 ± 90	128 2301 ± 25
179	sensetime-003	787853	74950	224 2519	176 2052 ± 0	208 908 ± 4	-	-	-	132 2527 ± 65	147 3004 ± 174
180	sertis-000	265572	68770	52 427	78 2048 ± 0	168 754 ± 0	160 755 ± 0	151 755 ± 2	163 752 ± 0	97 1497 ± 29	99 1582 ± 38
181	sertis-001	292591	68831	47 374	142 2048 ± 0	127 634 ± 1	126 633 ± 0	113 633 ± 1	125 634 ± 1	129 2449 ± 23	139 2685 ± 41
182	shaman-000	0	120033	79 507	220 4096 ± 0	136 653 ± 16	162 761 ± 76	114 639 ± 17	142 683 ± 37	3 380 ± 25	3 379 ± 31
183	shaman-001	0	174446	83 511	213 4096 ± 0	45 294 ± 2	45 305 ± 9	5 8 ± 11	43 298 ± 6	24 635 ± 19	4 441 ± 25
184	shu-002	731250	148309	142 890	212 4096 ± 0	167 751 ± 2	120 618 ± 1	142 718 ± 8	152 719 ± 1	241 2930763 ± 47355	241 2929759 ± 39149
185	shu-003	428774	146940	82 511	125 2048 ± 0	188 820 ± 6	173 798 ± 3	162 798 ± 7	174 799 ± 2	131 2506 ± 26	133 2512 ± 38
186	siat-002	486842	7738	221 2434	178 2052 ± 0	104 579 ± 0	106 579 ± 8	98 577 ± 3	105 575 ± 1	39 769 ± 13	38 750 ± 13
187	siat-004	940063	6984	231 3860	226 4100 ± 0	143 670 ± 0	132 662 ± 2	120 663 ± 9	131 662 ± 3	169 4013 ± 45	165 3782 ± 173
188	sjtu-001	347115	148322	56 438	76 2048 ± 0	132 650 ± 2	122 620 ± 1	107 615 ± 6	118 617 ± 1	240 2243804 ± 12751	240 2249915 ± 19380
189	sjtu-002	446215	148306	89 538	149 2048 ± 0	193 835 ± 2	175 802 ± 3	161 794 ± 9	173 796 ± 1	239 2211198 ± 26052	239 2210428 ± 21877
190	smilart-002	111826	87805	33 263	44 1024 ± 0	21 176 ± 16	10 112 ± 11	37 266 ± 158	52 349 ± 39	211 18784 ± 136	212 18795 ± 151
191	smilart-003	67339	91670	28 192	20 512 ± 0	24 180 ± 12	17 139 ± 8	16 119 ± 22	15 136 ± 8	92 1395 ± 74	64 1027 ± 66
192	staqu-000	879661	624676	163 1064	222 4096 ± 0	183 813 ± 25	-	-	-	145 2979 ± 31	148 3007 ± 75
193	starhybrid-001	100509	289356	135 845	102 2048 ± 0	55 358 ± 82	44 293 ± 22	39 298 ± 27	42 284 ± 19	68 1075 ± 51	71 1078 ± 53
194	synesis-006	731941	21817	199 1472	228 4104 ± 0	97 549 ± 1	97 549 ± 0	100 588 ± 1	108 589 ± 1	30 697 ± 32	32 688 ± 31
195	synesis-007	1442961	24145	222 2443	208 3080 ± 0	234 1215 ± 5	209 1196 ± 7	196 1204 ± 5	209 1202 ± 4	27 684 ± 32	30 686 ± 25
196	synology-000	221021	25809	62 453	86 2048 ± 0	64 407 ± 14	51 344 ± 7	43 333 ± 17	53 349 ± 9	214 19720 ± 203	213 19767 ± 379
197	synology-002	256713	25943	73 488	82 2048 ± 0	204 886 ± 4	187 879 ± 3	175 877 ± 4	185 878 ± 3	95 1466 ± 32	96 1496 ± 45
198	tech5-004	2410272	118858	227 2733	15 321 ± 0	199 872 ± 2	190 926 ± 10	178 908 ± 4	197 944 ± 2	16 597 ± 13	19 592 ± 16
199	tech5-005	1178769	120517	193 1426	24 512 ± 0	235 1272 ± 109	211 1239 ± 120	198 1252 ± 113	211 1289 ± 135	135 2573 ± 37	137 2545 ± 32
200	tevian-005	921043	16556	166 1083	143 2048 ± 0	126 633 ± 21	112 592 ± 15	103 600 ± 45	127 646 ± 1	14 568 ± 22	21 607 ± 35
201	tevian-006	692492	19339	151 954	97 2048 ± 0	115 611 ± 1	107 584 ± 1	97 576 ± 39	113 603 ± 1	15 591 ± 19	18 573 ± 28
202	tiger-002	341638	178194	84 522	187 2056 ± 0	62 393 ± 20	57 378 ± 21	48 364 ± 42	60 387 ± 22	121 2135 ± 29	122 2137 ± 38
203	tiger-003	426164	560292	109 708	181 2056 ± 0	74 458 ± 21	67 436 ± 21	56 421 ± 41	67 438 ± 22	117 2031 ± 35	117 2029 ± 38
204	tongyi-005	1140701	138919	217 2121	197 2089 ± 0	19 165 ± 1	-	-	-	212 18924 ± 65	214 20158 ± 103
205	toshiba-002	813606	114260	-	62 1560 ± 0	92 541 ± 0	-	-	-	157 3521 ± 369	130 2449 ± 124
206	toshiba-003	984125	114264	175 1197	63 1560 ± 0	91 540 ± 0	95 538 ± 2	176 882 ± 5	161 749 ± 4	128 2390 ± 41	129 2407 ± 81
207	trueface-000	255123	796861	75 493	152 2048 ± 0	56 367 ± 8	52 356 ± 6	47 354 ± 11	54 355 ± 7	6 482 ± 13	13 528 ± 20
208	trueface-001	255123	186754	104 638	16 500 ± 0	60 390 ± 1	53 358 ± 1	46 353 ± 6	55 355 ± 1	25 676 ± 26	16 558 ± 50
209	tuputech-000	11476	17185	2 33	94 2048 ± 0	16 122 ± 4	11 114 ± 2	-	9 114 ± 3	216 23893 ± 406	216 25279 ± 406
210	ulsee-001	370519	57261	-	145 2048 ± 0	137 654 ± 2	-	-	-	184 6065 ± 94	184 6228 ± 77
211	uluface-002	0	480761	167 1088	120 2048 ± 0	200 873 ± 42	177 825 ± 7	165 818 ± 13	178 825 ± 7	213 19207 ± 1114	211 18501 ± 274
212	uluface-003	97357	529422	181 1264	207 3072 ± 0	218 965 ± 11	194 937 ± 7	181 934 ± 16	195 938 ± 6	218 26057 ± 195	220 26865 ± 566
213	upc-001	0	89914	165 1077	52 1052 ± 0	98 551 ± 15	96 541 ± 5	87 539 ± 10	97 546 ± 6	150 3114 ± 44	153 3165 ± 97
214	vcog-002	3229434	118946	229 3666	241 61504 ± 5	54 357 ± 25	42 289 ± 22	40 313 ± 43	45 307 ± 28	235 296154 ± 3077	235 296436 ± 4183
215	vd-001	170262	44058	35 281	171 2052 ± 0	49 316 ± 6	-	-	-	87 1258 ± 38	80 1148 ± 109
216	veridas-003	293109	141587	68 469	113 2048 ± 0	205 890 ± 33	129 659 ± 16	110 628 ± 46	128 654 ± 16	177 5484 ± 42	192 7306 ± 410
217	veridas-004	196585	160684	69 472	164 2048 ± 0	148 678 ± 22	87 522 ± 9	73 499 ± 29	89 520 ± 12	178 5516 ± 42	193 7425 ± 130
218	via-000	124422	11151	152 964	138 2048 ± 0	158 707 ± 8	133 662 ± 1	132 682 ± 36	114 603 ± 2	53 966 ± 28	62 1021 ± 44
219	via-001	370255	11151	207 1697	93 2048 ± 0	217 964 ± 3	193 934 ± 5	186 965 ± 36	190 918 ± 3	56 983 ± 31	58 989 ± 40
220	videmo-000	139643	39470	48 390	157 2048 ± 0	18 142 ± 5	15 133 ± 3	18 132 ± 6	14 136 ± 4	11 513 ± 16	11 523 ± 38

Notes	
1	The configuration size does not capture static data included in libraries.
2	The library size is the combined total of all files provided in the submission lib folder. These libraries e.g. OpenCV may or may not be installed on any end user's platform natively and would not need to be installed with the algorithm.
4	The memory usage is the peak resident set size reported by the ps system call during template generation.
5	The median template creation times are measured on Intel®Xeon®CPU E5-2630 v4 @ 2.20GHz processors.
6	The comparison durations, in nanoseconds, are estimated using std::chrono::high_resolution_clock which on the machine in (2) counts 1ns clock ticks. Precision is somewhat worse than that however. The ± value is the median absolute deviation times 1.48 for Normal consistency.

Table 9: Summary of algorithms and properties included in this report. The red superscripts give ranking for the quantity in that column.

	ALGORITHM	CONFIG	LIBRARY	TEMPLATE						COMPARISON[4]	
	NAME	DATA	DATA	MEMORY	SIZE	GENERATION TIME (ms)[4]				TIME (ns)[5]	
		(KB)[1]	(KB)[2]	(MB)[3]	(B)	MUGSHOT	ISO	PHOTOJOURN.	WILD	GENUINE	IMPOSTOR
221	videonetics-001	30875	5963	[4]61	[17]512 ± 0	[34]262 ± 3	[31]226 ± 4	-	[29]223 ± 4	[80]1153 ± 38	[79]1142 ± 65
222	videonetics-002	121981	6289	[15]115	[173]2052 ± 0	[40]282 ± 5	[33]231 ± 3	[86]536 ± 444	[30]226 ± 0	[85]1219 ± 57	[88]1262 ± 56
223	vigilantsolutions-007	255600	125715	[145]912	[61]1548 ± 0	[81]493 ± 6	[79]494 ± 3	[74]499 ± 27	[76]489 ± 3	[43]803 ± 35	[41]800 ± 40
224	vigilantsolutions-008	441835	47824	[126]802	[60]1548 ± 0	[131]647 ± 2	[127]648 ± 1	[117]652 ± 27	[126]643 ± 2	[46]889 ± 23	[47]903 ± 44
225	vinai-000	402391	866522	[157]1032	[73]2048 ± 0	[229]1099 ± 1	[204]1093 ± 2	[192]1108 ± 1	[203]1104 ± 1	[146]2996 ± 20	[146]2993 ± 26
226	vion-000	228219	7533	[77]498	[172]2052 ± 0	[51]333 ± 1	[49]341 ± 1	-	[48]337 ± 2	[223]39839 ± 3561	[219]26830 ± 2241
227	visionbox-000	176501	190645	[43]355	[154]2048 ± 0	[46]304 ± 7	[37]252 ± 5	[33]243 ± 12	[36]250 ± 5	[102]1648 ± 57	[86]1192 ± 42
228	visionbox-001	256869	190645	[93]579	[139]2048 ± 0	[221]983 ± 7	[192]933 ± 9	[180]928 ± 20	[192]932 ± 7	[81]1161 ± 22	[82]1154 ± 20
229	visionlabs-008	706099	19705	[61]446	[26]512 ± 0	[75]467 ± 1	[66]434 ± 1	[59]431 ± 10	[65]431 ± 1	[50]955 ± 23	[51]962 ± 25
230	visionlabs-009	706099	19862	[60]444	[31]513 ± 0	[86]515 ± 41	[81]498 ± 51	[66]475 ± 40	[80]497 ± 54	[51]957 ± 28	[53]965 ± 32
231	visteam-000	32729	17740	[11]83	[59]1536 ± 0	[8]96 ± 7	[2]38 ± 4	[7]27 ± 10	[2]36 ± 4	[187]6361 ± 87	[187]6668 ± 277
232	vocord-007	587489	344995	[188]1352	[65]1664 ± 0	[176]780 ± 2	[164]768 ± 2	[153]765 ± 3	[166]767 ± 2	[137]2593 ± 83	[134]2526 ± 59
233	vocord-008	603867	345047	[201]1559	[206]2688 ± 0	[216]962 ± 2	[197]952 ± 2	[184]949 ± 4	[198]953 ± 2	[147]3015 ± 50	[145]2988 ± 62
234	winsense-000	270819	32034	[131]833	[54]1280 ± 0	[41]283 ± 1	[39]262 ± 1	[36]262 ± 4	[39]265 ± 1	[99]1551 ± 31	[98]1532 ± 42
235	winsense-001	264428	32035	[148]922	[55]1280 ± 0	[172]766 ± 7	[155]729 ± 4	[146]726 ± 9	[156]727 ± 4	[101]1631 ± 28	[116]1964 ± 171
236	xforwardai-000	242457	175556	[190]1392	[70]2048 ± 0	[169]757 ± 6	[159]753 ± 6	[150]752 ± 1	[160]747 ± 1	[83]1185 ± 44	[84]1157 ± 44
237	xforwardai-001	340100	51163	[218]2173	[132]2048 ± 0	[233]1180 ± 2	[208]1189 ± 2	[195]1187 ± 2	[208]1179 ± 2	[40]779 ± 17	[40]797 ± 13
238	yisheng-004	486351	38653	[184]1279	[211]3704 ± 0	[57]378 ± 12	[56]375 ± 14	[45]352 ± 16	[56]367 ± 13	[29]693 ± 137	[12]526 ± 34
239	yitu-003	1525719	138919	[230]3737	[195]2082 ± 0	[197]860 ± 0	-	-	-	[210]18305 ± 71	[210]18286 ± 62
240	yoonik-000	290414	206059	[132]836	[131]2048 ± 0	[212]941 ± 3	[195]937 ± 4	[183]939 ± 3	[196]938 ± 2	[75]1116 ± 34	[76]1113 ± 54
241	yuan-000	370472	331437	[205]1605	[140]2048 ± 0	[231]1112 ± 6	[205]1105 ± 3	[190]1106 ± 3	[205]1106 ± 2	[142]2777 ± 44	[143]2937 ± 87

Notes	
1	The configuration size does not capture static data included in libraries.
2	The library size is the combined total of all files provided in the submission lib folder. These libraries e.g. OpenCV may or may not be installed on any end user's platform natively and would not need to be installed with the algorithm.
4	The memory usage is the peak resident set size reported by the ps system call during template generation.
5	The median template creation times are measured on Intel®Xeon®CPU E5-2630 v4 @ 2.20GHz processors.
6	The comparison durations, in nanoseconds, are estimated using std::chrono::high_resolution_clock which on the machine in (2) counts 1ns clock ticks. Precision is somewhat worse than that however. The ± value is the median absolute deviation times 1.48 for Normal consistency.

Table 10: Summary of algorithms and properties included in this report. The red superscripts give ranking for the quantity in that column.

		FALSE NON-MATCH RATE (FNMR)																	
	Algorithm	CONSTRAINED, COOPERATIVE														LESS CONSTRAINED, NON-COOP.			
	Name	VISAMC		VISA		MUGSHOT		MUGSHOT12+YRS		VISABORDER		BORDER		BORDER		WILD		CHILDEXP	
	FMR	0.0001		1E-06		1E-05		1E-05		1E-06		1E-06		1E-05		0.0001		0.01	
1	3divi-004	0.0095	86	0.0153	88	0.0097	99	0.0145	96	0.0175	98	0.0330	86	0.0242	113	0.0665	167	0.5025	23
2	3divi-005	0.0094	85	0.0151	86	0.0078	73	0.0121	70	0.0135	71	0.0231	61	0.0156	74	0.0351	118	-	
3	acer-000	0.1393	208	0.9075	238	0.9981	238	-		1.0000	232	1.0000	224	0.9998	228	0.9841	233	-	
4	acer-001	0.0294	175	0.0504	175	0.0240	171	0.0463	172	0.0436	167	0.0622	123	0.0360	141	0.0307	84	-	
5	acisw-003	0.9682	244	0.9971	244	0.7892	233	0.8738	231	0.8752	225	0.8275	203	0.6698	216	0.4470	222	-	
6	adera-001	0.1021	205	0.1757	202	0.1823	211	0.2967	209	0.1714	198	0.6357	184	0.1127	178	0.1965	199	0.7202	55
7	advance-002	0.0089	78	0.0137	78	0.0073	63	0.0115	65	0.0400	160	0.0722	129	0.0593	161	0.0498	151	-	
8	aifirst-001	0.0119	109	0.0170	100	0.0084	82	0.0127	78	0.0131	68	0.0212	54	0.0138	61	0.0432	138	0.4301	16
9	aigen-001	0.0124	115	0.0219	125	0.0143	142	0.0217	132	0.0236	128	0.8960	206	0.3255	202	0.0681	168	-	
10	ailabs-001	0.0158	144	0.0276	151	0.0192	160	0.0317	156	0.0352	153	0.0608	119	0.0434	149	0.0338	112	-	
11	aimall-002	0.0119	108	0.0167	96	0.0224	166	0.0411	167	0.0233	124	0.0373	99	0.0235	110	0.0327	103	-	
12	aimall-003	0.0033	12	0.0041	8	0.0033	12	0.0035	5	0.0056	13	0.0109	17	0.0087	21	0.0312	92	-	
13	aiunionface-000	0.0104	93	0.0154	91	0.0082	80	0.0122	71	0.0141	74	0.0243	63	0.0169	80	0.0306	82	-	
14	alchera-000	0.0165	147	0.0243	139	0.0125	130	0.0186	122	0.0204	113	0.0349	93	0.0243	115	0.0370	125	-	
15	alchera-001	0.0183	153	0.0299	152	0.0142	139	0.0234	138	0.0239	130	0.0388	101	0.0267	124	0.0372	126	-	
16	alleyes-000	0.0058	41	0.0090	48	0.0055	36	0.0087	46	0.0068	20	0.0105	15	0.0076	12	0.0282	31	-	
17	allgovision-000	0.0346	181	0.0527	177	0.0232	168	0.0339	158	0.0372	158	0.0620	122	0.0443	151	0.0607	162	-	
18	alphaface-001	0.0065	53	0.0097	54	0.0039	19	0.0063	24	0.0083	34	-		-		0.0280	20	-	
19	alphaface-002	0.0052	32	0.0075	32	0.0030	4	0.0044	9	1.0000	235	0.0115	20	0.0084	19	0.0279	17	-	
20	amplifiedgroup-001	0.5034	231	0.5848	228	0.6973	228	0.8316	226	0.7807	219	0.7724	195	0.6354	213	0.4250	219	-	
21	anke-004	0.0080	70	0.0154	90	0.0073	62	0.0112	63	0.0102	55	0.0178	46	0.0118	53	0.0288	52	0.3577	8
22	anke-005	0.0070	60	0.0109	64	0.0059	48	0.0094	49	0.0105	56	0.0142	31	0.0102	38	0.0289	55	0.3337	6
23	antheus-000	0.2564	217	0.3776	217	0.7240	229	0.8699	229	0.8899	226	0.9872	212	0.9483	221	0.7668	226	0.9233	76
24	antheus-001	0.1311	206	0.2306	209	0.5113	220	0.6797	219	0.8748	224	0.9908	213	0.9649	224	0.7586	225	-	
25	anyvision-002	0.0660	197	0.0898	192	0.0928	202	0.1512	198	0.0899	187	0.1191	145	0.0801	172	0.2227	203	0.6960	49
26	anyvision-004	0.0267	172	0.0385	167	0.0258	174	0.0487	175	0.0234	126	0.0301	76	0.0191	95	0.0470	145	0.4633	19
27	asusaics-000	0.0125	118	0.0209	118	0.0085	83	0.0134	86	0.0143	76	0.7189	190	0.0285	129	0.0295	67	-	
28	asusaics-001	0.0125	119	0.0210	119	0.0085	85	0.0134	87	0.0143	77	0.7437	193	0.0289	130	0.0295	66	-	
29	aware-004	0.0690	198	0.0949	196	0.0837	199	0.1436	197	0.1171	193	0.8137	200	0.1056	177	0.0516	153	-	
30	aware-005	0.0457	186	0.0643	183	0.0603	192	0.1094	189	0.0613	176	0.1075	144	0.0491	156	0.0314	95	-	
31	awiros-001	0.4044	223	0.4622	221	0.5530	221	0.6518	218	0.2008	200	0.1994	154	0.1386	182	0.5584	223	-	
32	ayftech-001	0.0946	203	0.1941	206	0.2438	213	0.3625	210	0.1558	196	0.1589	150	0.0936	175	0.0785	173	-	
33	ayonix-000	0.4351	226	0.4872	222	0.6150	225	0.7510	223	0.6557	214	0.6361	185	0.4981	209	0.3635	216	0.8434	67
34	bioidtechswiss-000	0.0066	55	0.0082	42	0.0113	118	0.0225	135	0.0078	28	0.0139	29	0.0092	25	0.0278	14	-	
35	bioidtechswiss-001	0.0054	35	0.0072	29	0.0069	58	0.0124	74	0.0060	15	0.0094	10	0.0065	5	0.0313	93	-	
36	bm-001	0.7431	237	0.9494	241	0.9586	234	0.9843	232	0.9049	227	0.9021	209	0.8395	219	0.9935	234	0.8845	73
37	bresee-000	0.8467	239	0.9472	239	0.9819	235	0.9903	233	0.9940	228	0.9919	214	0.9760	225	0.8992	230	-	
38	camvi-002	0.0125	120	0.0221	127	0.0089	90	0.0145	98	0.0142	75	0.2650	162	0.0166	79	0.0288	50	0.5760	35
39	camvi-004	0.0171	150	0.0316	155	0.0042	22	0.0049	16	0.0097	52	0.6636	187	0.0141	64	0.0284	39	0.5788	37
40	ceiec-002	0.0161	146	0.0193	112	0.0122	127	0.0164	111	0.0270	137	0.0555	112	0.0472	154	0.0465	144	0.5156	27
41	ceiec-003	0.0071	63	0.0107	62	0.0061	50	0.0079	38	0.0160	88	0.0316	78	0.0260	122	0.0308	88	-	
42	chosun-000	0.8481	240	1.0000	245	1.0000	245	-		1.0000	244	1.0000	243	1.0000	243	1.0000	244	-	
43	chosun-001	0.0525	189	0.0936	194	0.0742	197	0.1263	194	0.0978	192	1.0000	231	0.9354	220	0.4446	221	-	
44	chtface-002	0.0150	136	0.0268	147	0.0096	98	0.0140	92	0.0186	103	0.0320	80	0.0194	97	0.0306	83	-	

Table 11: FNMR is the proportion of mated comparisons below a threshold set to achieve the FMR given in the header on the fourth row. FMR is the proportion of impostor comparisons at or above that threshold. The light grey values give rank over all algorithms in that column. The pink columns use only same-sex impostors; others are selected regardless of demographics. The exception, in the green column, uses "matched-covariates" i.e. impostors of the same sex, age group, and country of birth. The second pink column includes effects of extended ageing. Missing entries for border, visa, mugshot and wild images generally mean the algorithm did not run to completion. For child exploitation, missing entries arise because NIST executes those runs only infrequently. The VISA *columns compare images described in section 2.2. The* MUGSHOT *columns compare images described in section 2.5. The* VISA-BORDER *column compare images described in section 2.3 with those of section 2.4. The* BORDER *column compares images described in section 2.4. The* WILD *columns compare images described in section 2.6. The* CHILD-EXPLOITATION *columns compare images described in section 2.1.*

		FALSE NON-MATCH RATE (FNMR)																	
	Algorithm	CONSTRAINED, COOPERATIVE														LESS CONSTRAINED, NON-COOP.			
	Name	VISAMC		VISA		MUGSHOT		MUGSHOT12+YRS		VISABORDER		BORDER		BORDER		WILD		CHILDEXP	
	FMR	0.0001		1E-06		1E-05		1E-05		1E-06		1E-06		1E-05		0.0001		0.01	
45	chtface-003	0.0091	80	0.0146	83	0.0083	81	0.0128	80	0.0132	69	0.0220	58	0.0149	70	0.0301	77	-	
46	cib-000	0.0084	74	0.0156	93	0.0049	28	0.0051	18	0.0275	140	0.1371	148	0.0138	62	0.0294	65	-	
47	cib-001	0.0041	21	0.0061	22	0.0030	7	0.0041	8	0.0048	9	0.0578	114	0.0069	7	0.0279	16	-	
48	cogent-003	0.0091	79	0.0188	111	0.0098	101	0.0132	83	0.0187	104	0.0319	79	0.0224	108	0.0406	132	-	
49	cogent-004	0.0064	51	0.0116	69	0.0096	97	0.0134	88	0.0157	84	0.0325	84	0.0204	101	0.0379	128	0.7177	54
50	cognitec-000	0.0116	105	0.0177	101	0.0118	123	0.0167	113	0.0285	143	0.9924	215	0.0435	150	0.0953	180	0.8365	66
51	cognitec-001	0.0126	121	0.0185	108	0.0120	125	0.0168	114	0.0270	136	0.0554	111	0.0357	138	0.0598	161	-	
52	cor-001	0.0075	69	0.0113	68	0.0055	39	0.0084	39	0.0091	43	0.0148	36	0.0092	26	0.0277	12	-	
53	ctbcbank-000	0.0168	148	0.0250	143	0.0146	144	0.0224	134	0.0211	116	0.8964	208	0.3779	205	1.0000	243	0.8803	71
54	ctbcbank-001	0.0155	139	0.0235	137	0.0148	149	0.0243	141	0.0207	114	0.9279	210	0.3469	203	1.0000	246	-	
55	cuhkee-001	0.0036	14	0.0045	12	0.0031	8	0.0046	11	0.0051	12	0.0095	12	0.0079	14	0.1492	192	-	
56	cybercore-000	0.0728	200	0.1110	199	0.1521	209	0.2375	208	0.1874	199	0.1907	153	0.1178	181	0.1191	187	-	
57	cyberextruder-001	0.1972	211	0.2547	210	0.4686	219	0.6387	217	0.3807	211	0.3806	171	0.2582	194	0.1747	195	0.7804	64
58	cyberextruder-002	0.0811	201	0.1336	201	0.1465	208	0.2266	207	0.2086	202	1.0000	242	1.0000	242	0.1000	182	0.6105	39
59	cyberlink-004	0.0074	68	0.0105	60	0.0068	56	0.0089	48	0.0094	48	0.0176	44	0.0117	52	0.0283	33	-	
60	cyberlink-005	0.0060	49	0.0092	50	0.0058	47	0.0067	28	0.0074	25	0.0146	35	0.0105	46	0.0283	36	-	
61	dahua-004	0.0045	26	0.0058	18	0.0036	16	0.0048	13	0.0051	10	0.0086	6	0.0070	8	0.0281	23	-	
62	dahua-005	0.0031	11	0.0046	14	0.0035	14	0.0049	17	0.0046	6	0.0076	2	0.0062	2	0.0277	11	-	
63	decatur-000	0.0714	199	0.1115	200	0.0608	193	0.1106	190	0.0866	185	1.0000	228	0.0714	168	0.0658	166	-	
64	deepglint-001	0.0040	18	0.0062	26	0.0047	27	0.0067	27	0.0069	21	1.0000	229	1.0000	231	0.0278	13	0.4006	11
65	deepglint-002	0.0016	2	0.0027	4	0.0032	10	0.0033	4	0.0043	3	0.0084	5	0.0077	13	0.0280	19	0.3422	7
66	deepsea-001	0.0136	128	0.0215	122	0.0142	140	0.0214	130	0.0163	92	0.0250	65	0.0192	96	0.0347	113	0.5606	32
67	dermalog-005	0.1526	210	0.1823	205	0.2580	214	0.4018	212	-		0.2651	163	0.1585	184	0.0855	175	0.6842	45
68	dermalog-006	0.0253	170	0.0369	164	0.0171	155	0.0283	150	0.0217	119	0.0358	96	0.0230	109	0.0623	164	0.5852	38
69	didiglobalface-001	0.0055	37	0.0092	49	0.0030	5	0.0045	10	0.0088	39	0.0119	21	0.0085	20	0.0282	29	0.4270	14
70	digitalbarriers-002	0.3360	220	0.3690	215	0.0877	201	0.1557	199	0.0971	191	0.0951	136	0.0497	157	0.0436	140	-	
71	dsk-000	0.1526	209	0.2169	207	0.3787	216	0.5426	215	0.3115	206	0.3089	167	0.1994	190	0.2201	201	0.7313	57
72	einetworks-000	0.0099	88	0.0180	104	0.0088	89	0.0140	94	0.0130	66	0.0225	60	0.0147	69	0.0293	62	-	
73	eocortex-000	0.3485	221	0.6943	233	0.1122	206	0.1574	200	0.2155	203	0.2257	159	0.1606	186	0.2546	208	-	
74	ercacat-001	0.0036	15	0.0044	11	0.0033	11	0.0047	12	0.0106	57	0.0202	53	0.0184	89	0.0258	1	-	
75	paravision-003	0.0034	13	0.0050	15	0.0036	18	0.0052	20	0.0092	45	0.0193	51	0.0156	73	0.0278	15	0.2669	2
76	expasoft-000	0.0427	184	0.0655	185	0.0239	170	0.0393	164	0.0673	181	0.8963	207	0.3832	206	0.0565	159	-	
77	expasoft-001	0.0328	180	0.0488	174	0.0211	165	0.0342	159	0.0629	178	0.6483	186	0.2816	198	0.0552	158	-	
78	f8-001	0.0249	169	0.0336	157	0.0178	157	0.0232	137	0.0303	148	0.0615	121	0.0408	146	0.0475	147	0.5272	28
79	facesoft-000	0.0085	75	0.0112	67	0.0064	53	0.0107	59	0.0091	42	0.0171	42	0.0107	47	0.0275	7	0.4992	22
80	fiberhome-nanjing-002	0.0217	161	0.0381	166	0.0874	200	0.1770	204	0.0271	138	0.0351	94	0.0188	91	0.0361	123	-	
81	fujitsulab-000	0.0123	113	0.0212	120	0.0091	91	0.0133	84	0.0251	133	0.4200	174	0.0360	140	0.0445	142	-	
82	fujitsulab-001	0.0059	46	0.0082	40	0.0132	134	0.0258	143	0.0140	73	0.0246	64	0.0142	65	0.0271	2	-	
83	geo-000	0.0543	191	0.0814	189	0.1042	203	0.1592	201	0.1637	197	0.8533	205	0.1800	187	0.1211	188	-	
84	glory-001	0.0902	202	0.1082	198	0.1642	210	0.2065	206	0.2186	204	0.2669	164	0.2089	191	0.4261	220	0.8831	72
85	glory-002	0.0241	163	0.0311	154	0.0116	120	0.0151	103	0.0157	86	0.0264	68	0.0188	93	0.1265	189	-	
86	gorilla-005	-		-		0.0142	141	0.0267	148	0.0228	123	0.0358	95	0.0195	98	0.0307	85	-	
87	gorilla-006	0.0105	99	0.0152	87	0.0106	106	0.0203	126	0.0155	81	0.0218	57	0.0136	60	0.0289	53	-	
88	hik-001	0.0096	87	0.0125	74	0.0093	94	0.0164	110	0.0108	60	0.0937	133	0.0127	57	0.0271	3	-	

Table 12: FNMR is the proportion of mated comparisons below a threshold set to achieve the FMR given in the header on the fourth row. FMR is the proportion of impostor comparisons at or above that threshold. The light grey values give rank over all algorithms in that column. The pink columns use only same-sex impostors; others are selected regardless of demographics. The exception, in the green column, uses "matched-covariates" i.e. impostors of the same sex, age group, and country of birth. The second pink column includes effects of extended ageing. Missing entries for border, visa, mugshot and wild images generally mean the algorithm did not run to completion. For child exploitation, missing entries arise because NIST executes those runs only infrequently. The VISA *columns compare images described in section 2.2. The* MUGSHOT *columns compare images described in section 2.5. The* VISA-BORDER *column compare images described in section 2.3 with those of section 2.4. The* BORDER *column compares images described in section 2.4. The* WILD *columns compare images described in section 2.6. The* CHILD-EXPLOITATION *columns compare images described in section 2.1.*

FNMR(T) "False non-match rate"
FMR(T) "False match rate"

	Algorithm	FALSE NON-MATCH RATE (FNMR)																	
		CONSTRAINED, COOPERATIVE														LESS CONSTRAINED, NON-COOP.			
	Name	VISAMC		VISA		MUGSHOT		MUGSHOT12+YRS		VISABORDER		BORDER		BORDER		WILD		CHILDEXP	
	FMR	0.0001		1E-06		1E-05		1E-05		1E-06		1E-06		1E-05		0.0001		0.01	
89	hr-002	0.0043	23	0.0059	19	0.0054	32	0.0076	34	0.0076	27	0.5932	182	0.0093	27	0.0338	111	-	
90	hr-003	0.0026	7	0.0041	9	0.0040	21	0.0058	22	0.0060	17	0.9992	220	0.0094	28	0.7206	224	-	
91	id3-004	0.0198	157	0.0344	159	0.0238	169	0.0423	169	0.0289	144	0.0416	105	0.0257	120	-		-	
92	id3-005	0.0104	97	0.0169	98	0.0080	77	0.0133	85	0.0194	110	0.0334	90	0.0262	123	0.0713	170	-	
93	idemia-005	0.0132	124	0.0216	124	0.0121	126	0.0218	133	0.0215	117	0.0323	83	0.0188	92	0.0294	64	0.4343	17
94	idemia-006	0.0046	27	0.0062	27	0.0047	26	0.0066	25	0.0073	24	0.2882	166	0.0094	30	0.0281	22	-	
95	iit-001	0.0104	94	0.0179	103	0.0099	102	0.0142	95	0.1222	194	0.2677	165	0.2171	192	0.3092	214	0.4836	20
96	iit-002	0.0111	102	0.0177	102	0.0085	84	0.0140	93	0.0193	109	0.0332	89	0.0260	121	0.1373	190	-	
97	imagus-000	0.0642	195	0.0882	190	0.0497	186	0.0905	184	0.0848	184	0.1026	141	0.0618	162	0.1158	185	0.6936	48
98	imagus-001	0.0245	166	0.0407	168	0.0257	173	0.0497	177	0.0514	170	0.0656	126	0.0400	145	0.0971	181	-	
99	imperial-000	0.0067	57	0.0108	63	0.0080	76	0.0134	89	0.0087	38	0.0581	116	0.0102	39	0.0281	25	-	
100	imperial-002	0.0058	40	0.0081	38	0.0055	38	0.0085	41	0.0083	35	0.0157	38	0.0103	40	0.0273	4	0.5151	24
101	incode-006	0.0156	140	0.0273	149	0.0117	121	0.0238	139	0.0202	112	0.0339	92	0.0164	77	0.0325	101	-	
102	incode-007	0.0109	101	0.0155	92	0.0056	41	0.0099	55	0.0107	59	0.0168	41	0.0102	37	0.0291	60	-	
103	innefulabs-000	0.0122	111	0.0199	114	0.0112	116	0.0197	125	0.0222	121	0.0372	98	0.0271	125	0.0348	114	-	
104	innovativetechnologyltd-001	0.0578	193	0.0938	195	0.0501	187	0.0981	185	0.0592	175	0.0779	131	0.0422	147	0.0449	143	-	
105	innovativetechnologyltd-002	0.0451	185	0.0716	186	0.0541	189	0.1009	187	0.0506	169	0.0682	127	0.0371	143	0.0804	174	-	
106	innovatrics-006	0.0058	43	0.0089	46	0.0061	51	0.0096	53	0.0096	50	0.0165	40	0.0103	41	0.0281	21	0.3056	4
107	innovatrics-007	0.0040	20	0.0054	17	0.0057	43	0.0078	35	0.0079	29	0.0123	22	0.0088	22	0.0282	32	-	
108	intellicloudai-001	0.0142	131	0.0234	135	0.0092	93	0.0145	97	0.0162	90	0.0371	97	0.0171	83	0.0409	133	-	
109	intellifusion-001	0.0072	64	0.0094	52	0.0056	42	0.0085	42	0.0111	62	0.0212	55	0.0143	66	0.0289	54	0.5454	30
110	intellifusion-002	0.0059	44	0.0077	34	0.0040	20	0.0074	31	0.0085	37	0.5352	179	0.0104	44	0.0305	80	-	
111	intellivision-001	0.1335	207	0.2205	208	0.1090	205	0.1670	202	0.1385	195	0.1676	151	0.1170	180	0.2445	204	0.7766	63
112	intellivision-002	0.1000	204	0.1775	203	0.0610	194	0.1009	186	0.0805	183	0.1074	143	0.0682	165	0.0768	171	-	
113	intelresearch-001	0.0242	164	0.0595	181	0.0129	133	0.0292	153	0.0351	152	0.9993	221	0.1854	189	0.0919	179	-	
114	intelresearch-002	0.0058	42	0.0082	41	0.0050	31	0.0086	44	0.0136	72	0.0434	106	0.0216	106	0.0285	45	-	
115	intsysmsu-001	0.9543	243	0.9888	243	0.9923	236	-		0.9977	229	0.9955	216	0.9892	226	0.7871	227	-	
116	intsysmsu-002	0.0130	122	0.0254	144	0.0137	136	0.0267	149	0.0160	87	0.0267	70	0.0145	68	0.0289	56	-	
117	iqface-000	0.0091	82	0.0143	80	0.0075	68	0.0110	62	0.0171	97	0.2234	157	0.0359	139	0.0381	129	0.6490	42
118	iqface-002	0.0057	39	0.0083	43	0.0049	29	0.0058	23	0.0093	46	1.0000	227	0.9999	229	0.0359	122	-	
119	isap-001	0.5092	232	0.6588	231	0.6899	227	0.7978	224	0.7200	216	0.7253	191	0.5373	211	0.1931	197	-	
120	isap-002	0.0114	104	0.0186	110	0.0087	88	0.0151	102	0.0156	83	0.5134	177	0.0333	136	0.0354	121	-	
121	isityou-000	0.5682	234	0.7033	234	1.0000	240	-		1.0000	236	1.0000	232	1.0000	233	1.0000	237	1.0000	83
122	isystems-001	0.0149	135	0.0245	141	0.0138	138	0.0210	128	0.0209	115	0.0332	88	0.0223	107	0.0524	156	0.5152	26
123	isystems-002	0.0118	106	0.0182	105	0.0111	113	0.0162	108	0.0166	94	0.0284	73	0.0195	99	0.0516	154	0.4876	21
124	itmo-006	0.0125	117	0.0220	126	0.0149	150	0.0266	147	0.0233	125	0.0383	100	0.0285	128	0.0329	105	-	
125	itmo-007	0.0080	71	0.0125	75	0.0107	107	0.0185	120	0.0167	95	0.0222	59	0.0144	67	0.0300	74	-	
126	iws-000	0.4824	230	0.5801	227	0.6859	226	0.8155	225	0.8251	221	0.7756	196	0.6400	214	0.3251	215	-	
127	kakao-002	0.0625	194	0.1779	204	0.0791	198	0.1381	196	0.0636	179	1.0000	233	1.0000	234	1.0000	239	1.0000	94
128	kakao-003	0.0130	123	0.0185	109	0.0261	176	0.0464	173	0.0252	134	0.2380	161	0.0284	127	0.0274	5	-	
129	kedacom-000	0.0055	36	0.0081	39	0.0111	115	0.0120	69	0.0415	162	0.0966	139	0.0686	166	0.2511	206	0.7650	61
130	kneron-003	0.0542	190	0.0902	193	0.0346	180	0.0562	179	0.0919	188	0.1251	147	0.0973	176	0.3053	213	0.6962	50
131	kneron-005	0.0157	142	0.0259	146	0.0126	132	0.0212	129	0.0406	161	0.0693	128	0.0542	160	0.0471	146	-	
132	kookmin-001	0.0462	187	0.0750	187	0.0489	185	0.0842	183	0.0659	180	0.8380	204	0.3212	201	0.0491	150	-	

Table 13: FNMR is the proportion of mated comparisons below a threshold set to achieve the FMR given in the header on the fourth row. FMR is the proportion of impostor comparisons at or above that threshold. The light grey values give rank over all algorithms in that column. The pink columns use only same-sex impostors; others are selected regardless of demographics. The exception, in the green column, uses "matched-covariates" i.e. impostors of the same sex, age group, and country of birth. The second pink column includes effects of extended ageing. Missing entries for border, visa, mugshot and wild images generally mean the algorithm did not run to completion. For child exploitation, missing entries arise because NIST executes those runs only infrequently. The VISA *columns compare images described in section 2.2. The* MUGSHOT *columns compare images described in section 2.5. The* VISA-BORDER *column compare images described in section 2.3 with those of section 2.4. The* BORDER *column compares images described in section 2.4. The* WILD *columns compare images described in section 2.6. The* CHILD-EXPLOITATION *columns compare images described in section 2.1.*

	Algorithm	FALSE NON-MATCH RATE (FNMR)																	
		CONSTRAINED, COOPERATIVE														LESS CONSTRAINED, NON-COOP.			
	Name	VISAMC		VISA		MUGSHOT		MUGSHOT12+YRS		VISABORDER		BORDER		BORDER		WILD		CHILDEXP	
	FMR	0.0001		1E-06		1E-05		1E-05		1E-06		1E-06		1E-05		0.0001		0.01	
133	lookman-002	0.0297	176	0.0547	179	0.0339	179	0.0562	178	0.0614	177	0.0960	138	0.0790	170	0.2640	210	-	
134	lookman-004	0.0074	66	0.0099	56	0.0124	129	0.0149	101	0.0430	166	0.0866	132	0.0694	167	0.2516	207	0.7664	62
135	luxand-000	0.2056	213	0.2814	211	0.4053	217	0.5365	214	0.3497	208	0.3743	169	0.2605	195	0.2222	202	-	
136	megvii-001	0.0157	143	0.0244	140	0.0392	183	0.0671	181	0.0168	96	0.0455	107	0.0164	76	0.0916	178	0.4418	18
137	megvii-002	0.0104	95	0.0145	82	0.0225	167	0.0345	160	0.0099	53	0.0286	74	0.0240	112	0.0692	169	0.3013	3
138	meiya-001	0.0171	149	0.0275	150	0.0159	153	0.0261	146	0.0311	149	0.2250	158	0.0245	117	0.0363	124	-	
139	microfocus-001	0.4482	227	0.5524	226	0.7256	230	0.8416	227	0.7301	217	0.6926	189	0.5180	210	0.2567	209	0.6890	47
140	microfocus-002	0.3605	222	0.5057	223	0.5783	222	0.7223	220	0.5909	213	0.5963	183	0.4160	207	0.1582	194	0.6517	43
141	mobai-000	0.0360	182	0.0439	171	0.0372	182	0.0700	182	0.0367	156	0.0939	134	0.0795	171	0.2640	211	-	
142	mt-000	0.0100	89	0.0170	99	0.0074	67	0.0118	67	0.0127	65	0.0197	52	0.0129	58	0.0326	102	0.3773	10
143	mt-002	0.0064	52	0.0085	44	0.0054	34	0.0098	54	0.0070	23	0.0108	16	0.0076	11	0.0283	37	-	
144	mvision-001	0.0191	155	0.0233	132	0.0204	162	0.0356	161	0.0198	111	0.0337	91	0.0242	114	0.0431	137	-	
145	nazhiai-000	0.0040	17	0.0059	20	0.0036	15	0.0048	15	0.0057	14	0.0125	23	0.0083	18	0.0275	8	-	
146	netbridgetech-001	0.4749	229	0.6599	232	0.4438	218	0.5676	216	0.4491	212	1.0000	223	0.9541	222	0.1098	184	-	
147	netbridgetech-002	0.0101	91	0.0166	95	0.0077	72	0.0127	77	0.0133	70	0.8215	201	0.0523	159	0.0351	119	-	
148	neurotechnology-008	0.0091	81	0.0184	107	0.0076	70	0.0116	66	0.0157	85	0.9973	218	0.1803	188	0.0301	76	-	
149	neurotechnology-009	0.0049	28	0.0087	45	0.0057	46	0.0094	50	0.0079	31	1.0000	225	0.0101	35	0.0300	73	-	
150	nodeflux-002	0.0186	154	0.0340	158	0.0261	175	0.0451	171	0.0548	172	1.0000	230	1.0000	232	0.0299	71	-	
151	notiontag-000	0.6669	235	0.7885	235	0.3715	215	0.4978	213	0.8571	222	0.8102	199	0.6460	215	0.1807	196	0.6479	41
152	ntechlab-007	0.0056	38	0.0076	33	0.0073	65	0.0128	81	0.0079	30	0.0144	33	0.0102	36	0.0276	10	0.3316	5
153	ntechlab-008	0.0041	22	0.0061	21	0.0056	40	0.0108	60	0.0042	2	0.0080	4	0.0063	3	0.0289	58	-	
154	oz-001	0.0133	125	0.0215	123	0.0109	111	0.0160	106	0.0235	127	1.0000	236	1.0000	237	0.0417	134	-	
155	paravision-004	0.0030	10	0.0046	13	0.0030	6	0.0036	6	0.0091	44	0.0188	49	0.0173	84	0.0288	51	0.2467	1
156	pensees-001	0.0087	77	0.0133	77	0.0071	61	0.0122	73	0.0145	78	0.0252	66	0.0195	100	0.0283	35	-	
157	pixelall-003	0.0074	67	0.0118	70	0.0057	44	0.0079	37	0.0121	64	0.0390	102	0.0170	82	0.0285	46	-	
158	pixelall-004	0.0040	19	0.0061	24	0.0055	37	0.0069	29	0.0100	54	0.5663	181	0.0371	142	0.0285	43	-	
159	psl-003	0.0065	54	0.0099	57	0.0055	35	0.0075	32	1.0000	234	0.0188	50	0.0129	59	0.0296	69	-	
160	psl-005	0.0060	47	0.0094	51	0.0034	13	0.0048	14	0.0081	32	0.0140	30	0.0103	42	0.0281	24	-	
161	ptakuratsatu-000	0.0060	48	0.0089	47	0.0070	59	0.0104	57	0.0096	51	0.0152	37	0.0100	33	0.0284	40	-	
162	pxl-001	0.0488	188	0.0752	188	0.0586	191	0.1087	188	0.0946	189	0.1065	142	0.0625	163	0.1088	183	-	
163	pyramid-000	0.0136	127	0.0233	134	0.0117	122	0.0192	124	0.0185	102	0.0322	82	0.0206	103	0.0304	79	-	
164	rankone-008	0.0124	114	0.0232	131	0.0082	79	0.0107	58	0.0188	106	0.0320	81	0.0244	116	0.0420	135	-	
165	rankone-009	0.0087	76	0.0119	71	0.0065	54	0.0086	45	0.0088	40	0.0161	39	0.0121	55	0.0323	98	-	
166	realnetworks-002	0.0248	167	0.0358	161	0.0513	188	0.1127	191	0.0371	157	0.0614	120	0.0316	134	0.0334	108	-	
167	realnetworks-003	0.0259	171	0.0372	165	0.0541	190	0.1208	193	0.0378	159	0.0578	115	0.0306	133	0.0335	109	0.5152	25
168	remarkai-001	0.0144	132	0.0256	145	0.0102	104	0.0159	105	0.0162	91	0.0582	117	0.0185	90	0.0308	87	-	
169	remarkai-002	0.0151	138	0.0197	113	0.0075	69	0.0108	61	0.0119	63	0.0187	48	0.0127	56	0.0426	136	-	
170	rokid-000	0.0093	84	0.0145	81	0.0073	64	0.0102	56	0.0164	93	0.0280	72	0.0214	105	0.0857	176	-	
171	rokid-001	0.0105	98	0.0162	94	0.0094	95	0.0163	109	0.0181	100	0.0276	71	0.0165	78	0.0325	99	-	
172	s1-001	0.0314	179	0.0651	184	0.0252	172	0.0357	162	0.0444	168	0.0653	125	0.0429	148	0.8493	228	-	
173	saffe-001	0.4339	225	0.5261	224	0.7539	232	0.8736	230	0.7977	220	0.9810	211	0.7435	218	0.3887	217	0.8973	74
174	saffe-002	0.0119	110	0.0206	115	0.0107	110	0.0177	116	0.0244	131	0.9998	222	0.2785	197	0.0308	86	-	
175	samtech-001	0.0197	156	0.0365	162	0.0146	147	0.0241	140	0.0238	129	0.0394	103	0.0251	119	0.0337	110	-	
176	scanovate-001	0.0175	151	0.0331	156	0.0163	154	0.0248	142	0.2476	205	0.3801	170	0.3740	204	0.4060	218	-	

Table 14: FNMR is the proportion of mated comparisons below a threshold set to achieve the FMR given in the header on the fourth row. FMR is the proportion of impostor comparisons at or above that threshold. The light grey values give rank over all algorithms in that column. The pink columns use only same-sex impostors; others are selected regardless of demographics. The exception, in the green column, uses "matched-covariates" i.e. impostors of the same sex, age group, and country of birth. The second pink column includes effects of extended ageing. Missing entries for border, visa, mugshot and wild images generally mean the algorithm did not run to completion. For child exploitation, missing entries arise because NIST executes those runs only infrequently. The VISA *columns compare images described in section 2.2. The* MUGSHOT *columns compare images described in section 2.5. The* VISA-BORDER *column compare images described in section 2.3 with those of section 2.4. The* BORDER *column compares images described in section 2.4. The* WILD *columns compare images described in section 2.6. The* CHILD-EXPLOITATION *columns compare images described in section 2.1.*

	Algorithm	FALSE NON-MATCH RATE (FNMR)															
		CONSTRAINED, COOPERATIVE												LESS CONSTRAINED, NON-COOP.			
	Name	VISAMC		VISA		MUGSHOT		MUGSHOT12+YRS		VISABORDER		BORDER		BORDER		WILD		CHILDEXP	
	FMR	0.0001		1E-06		1E-05		1E-05		1E-06		1E-06		1E-05		0.0001		0.01	
177	scanovate-002	0.0175	152	0.0355	160	0.0146	145	0.0286	151	0.0269	135	0.0301	75	0.0178	86	0.0301	78	-	
178	securifai-001	0.4538	228	0.6142	229	0.5844	223	0.7428	221	0.7051	215	0.9961	217	0.9558	223	0.1963	198	-	
179	sensetime-002	0.0068	58	0.0098	55	0.0143	143	-		0.0278	142	0.0502	109	0.0502	158	0.9999	235	0.5309	29
180	sensetime-003	0.0021	5	0.0027	3	0.0027	2	0.0027	1	0.0051	11	0.0100	13	0.0089	24	0.0329	104	0.3683	9
181	sertis-000	0.0118	107	0.0208	116	0.0080	75	0.0127	75	0.0110	61	0.0176	45	0.0114	50	0.0285	44	-	
182	sertis-001	0.0113	103	0.0182	106	0.0204	163	0.0403	166	0.0216	118	0.0763	130	0.0282	126	0.0310	90	-	
183	shaman-000	0.9297	242	0.9774	242	0.9990	239	-		0.9999	231	1.0000	226	0.9999	230	0.9575	232	0.9618	78
184	shaman-001	0.3346	219	0.4616	220	0.2368	212	0.3723	211	0.3574	209	0.3527	168	0.2304	193	0.1498	193	0.8990	75
185	shu-002	-		0.0079	36	0.0146	146	0.0308	155	1.0000	233	0.0183	47	0.0115	51	0.0284	41	-	
186	shu-003	0.0028	8	0.0041	10	0.0050	30	0.0088	47	0.0081	33	0.0133	25	0.0094	29	0.0283	38	-	
187	siat-002	0.0091	83	0.0126	76	0.0109	112	0.0190	123	0.0276	141	0.0516	110	0.0464	153	0.0520	155	0.4277	15
188	siat-004	0.0067	56	0.0099	58	0.0152	151	-		0.0275	139	0.4823	176	0.4823	208	1.0000	236	-	
189	sjtu-001	0.0051	31	0.0080	37	0.0211	164	0.0446	170	0.0131	67	0.0175	43	0.0110	48	0.0289	57	-	
190	sjtu-002	0.0053	33	0.0078	35	0.0138	137	0.0296	154	0.0084	36	0.0136	27	0.0095	31	0.0284	42	-	
191	smilart-002	0.2440	215	0.3532	214	-		-		0.3785	210	0.4145	173	0.2611	196	-		0.6999	51
192	smilart-003	0.6944	236	0.8836	236	0.0695	195	0.1193	192	0.0894	186	0.1221	146	0.0737	169	0.1190	186	-	
193	staqu-000	0.0139	129	0.0208	117	0.0104	105	0.0145	99	0.0156	82	0.8063	197	0.1408	183	0.0332	107	-	
194	starhybrid-001	0.0108	100	0.0138	79	0.0081	78	0.0113	64	0.0152	79	0.0265	69	0.0189	94	0.0350	117	0.5584	31
195	synesis-006	0.0070	61	0.0096	53	0.0107	108	0.0166	112	-		0.0128	24	0.0089	23	0.0292	61	-	
196	synesis-007	0.0050	29	0.0073	31	0.0062	52	0.0076	33	-		0.0105	14	0.0080	16	0.0288	49	-	
197	synology-000	0.0149	134	0.0238	138	0.0148	148	0.0261	145	0.0221	120	0.0331	87	0.0209	104	0.0330	106	-	
198	synology-002	0.0104	96	0.0153	89	0.0107	109	0.0184	119	0.0189	107	0.2032	156	0.0180	87	0.0312	91	-	
199	tech5-004	0.0123	112	0.0234	136	0.0086	87	0.0162	107	0.0065	19	0.0112	18	0.0082	17	0.0281	27	-	
200	tech5-005	0.0054	34	0.0072	28	0.0069	57	0.0122	72	0.0060	16	0.0094	11	0.0066	6	0.0349	116	-	
201	tevian-005	0.0043	24	0.0062	25	0.0057	45	0.0085	43	0.0070	22	0.0135	26	0.0119	54	0.0300	75	0.5625	34
202	tevian-006	0.0045	25	0.0061	23	0.0045	25	0.0066	26	0.0046	8	0.0091	9	0.0075	10	0.0308	89	-	
203	tiger-002	0.0658	196	0.0889	191	0.1083	204	0.1766	203	0.0952	190	0.1568	149	0.0661	164	0.0512	152	0.7862	65
204	tiger-003	0.0313	178	0.0602	182	0.0188	159	0.0359	163	0.0344	150	-		-		0.0482	149	0.5610	33
205	tongyi-005	0.0073	65	0.0146	84	0.0187	158	0.0421	168	0.0161	89	0.0215	56	0.0149	71	0.0399	131	0.6195	40
206	toshiba-002	0.0134	126	0.0222	128	0.0097	100	0.0154	104	-		0.0327	85	0.0158	75	0.0434	139	0.7103	52
207	toshiba-003	0.0125	116	0.0214	121	0.0085	86	0.0131	82	-		0.0241	62	0.0151	72	0.0282	28	-	
208	trueface-000	0.0249	168	0.4321	219	0.0119	124	0.0180	118	0.0297	147	0.7467	194	0.1602	185	0.0614	163	-	
209	trueface-001	0.0204	159	0.0438	170	0.0095	96	0.0138	91	0.0154	80	0.0253	67	0.0169	81	0.0772	172	-	
210	tuputech-000	0.3218	218	0.3696	216	-		-		0.3237	207	0.4304	175	0.2973	200	0.9415	231	-	
211	ulsee-001	0.0151	137	0.0246	142	0.0113	117	0.0185	121	0.0187	105	0.6766	188	0.0181	88	0.0316	96	-	
212	ultinous-000	0.2343	214	0.3484	213	-		-		-		-		-		-		0.9447	77
213	ultinous-001	0.2485	216	0.4003	218	-		-		-		-		-		-		0.6847	46
214	uluface-002	0.0081	72	0.0123	72	0.0071	60	0.0095	52	0.0107	58	1.0000	241	0.0140	63	0.0444	141	0.6729	44
215	uluface-003	0.0100	90	0.0150	85	0.0079	74	0.0128	79	-		-		-		0.0635	165	-	
216	upc-001	0.0234	162	0.0519	176	0.0291	178	0.0490	176	0.0294	145	0.2316	160	0.0389	144	0.0314	94	0.4224	13
217	vcog-002	0.7522	238	0.9033	237	-		-		-		-		-		-		0.7523	59
218	vd-001	0.0243	165	0.0452	172	0.0271	177	0.0402	165	0.0424	165	-		-		0.1389	191	-	
219	veridas-003	0.0557	192	0.0983	197	0.0734	196	0.1267	195	0.0694	182	0.0951	137	0.0480	155	0.0299	70	0.5785	36
220	veridas-004	0.0281	173	0.0467	173	0.0353	181	0.0643	180	0.0424	164	0.0644	124	0.0342	137	0.0291	59	-	

Table 15: FNMR is the proportion of mated comparisons below a threshold set to achieve the FMR given in the header on the fourth row. FMR is the proportion of impostor comparisons at or above that threshold. The light grey values give rank over all algorithms in that column. The pink columns use only same-sex impostors; others are selected regardless of demographics. The exception, in the green column, uses "matched-covariates" i.e. impostors of the same sex, age group, and country of birth. The second pink column includes effects of extended ageing. Missing entries for border, visa, mugshot and wild images generally mean the algorithm did not run to completion. For child exploitation, missing entries arise because NIST executes those runs only infrequently. The VISA *columns compare images described in section 2.2. The* MUGSHOT *columns compare images described in section 2.5. The* VISA-BORDER *column compare images described in section 2.3 with those of section 2.4. The* BORDER *column compares images described in section 2.4. The* WILD *columns compare images described in section 2.6. The* CHILD-EXPLOITATION *columns compare images described in section 2.1.*

FNMR(T) "False non-match rate"
FMR(T) "False match rate"

		FALSE NON-MATCH RATE (FNMR)																	
	Algorithm	CONSTRAINED, COOPERATIVE														LESS CONSTRAINED, NON-COOP.			
	Name	VISAMC		VISA		MUGSHOT		MUGSHOT12+YRS		VISABORDER		BORDER		BORDER		WILD		CHILDEXP	
	FMR	0.0001		1E-06		1E-05		1E-05		1E-06		1E-06		1E-05		0.0001		0.01	
221	via-000	0.0216	160	0.0365	163	0.0177	156	0.0287	152	0.0296	146	0.0572	113	0.0290	131	0.0349	115	0.7638	60
222	via-001	0.0149	133	0.0229	130	0.0114	119	0.0177	117	0.0183	101	0.4056	172	0.0176	85	0.0373	127	-	
223	videmo-000	0.0298	177	0.0423	169	0.0155	152	0.0260	144	0.0246	132	0.0397	104	0.0239	111	0.0541	157	-	
224	videonetics-001	0.5483	233	0.6446	230	0.7517	231	0.8607	228	0.8664	223	0.8255	202	0.6956	217	0.2986	212	0.7297	56
225	videonetics-002	0.4274	224	0.5329	225	0.6081	224	0.7438	222	0.7775	218	0.7297	192	0.5756	212	0.1976	200	0.7435	58
226	vigilantsolutions-007	0.0202	158	0.0307	153	0.0136	135	0.0227	136	0.0356	155	1.0000	246	1.0000	246	0.0306	81	1.0000	221
227	vigilantsolutions-008	0.0156	141	0.0233	133	0.0101	103	0.0147	100	0.0355	154	0.0492	108	0.0293	132	0.0285	47	-	
228	vinai-000	0.0081	73	0.0124	73	0.0045	24	0.0072	30	0.0089	41	0.1814	152	0.0112	49	0.0274	6	-	
229	vion-000	0.0419	183	0.0590	180	0.0422	184	0.0478	174	0.0581	174	0.0968	140	0.0847	173	0.2479	205	0.8765	70
230	visionbox-000	0.0293	174	0.0541	178	0.0197	161	0.0339	157	0.0349	151	0.0593	118	0.0329	135	0.0476	148	-	
231	visionbox-001	0.0159	145	0.0270	148	0.0111	114	0.0173	115	0.0190	108	0.0315	77	0.0205	102	0.0389	130	-	
232	visionlabs-008	0.0026	6	0.0036	6	0.0031	9	0.0040	7	0.0045	4	0.0079	3	0.0064	4	0.0282	30	-	
233	visionlabs-009	0.0018	3	0.0025	1	0.0026	1	0.0029	3	0.0035	1	0.0064	1	0.0054	1	0.0283	34	-	
234	visteam-000	0.9200	241	0.9489	240	0.9959	237	-		0.9994	230	0.9978	219	0.9914	227	0.8783	229	-	
235	vocord-007	0.0039	16	0.0053	16	0.0061	49	0.0094	51	0.0520	171	0.0939	135	0.0910	174	0.0280	18	0.8468	68
236	vocord-008	0.0029	9	0.0038	7	0.0042	23	0.0055	21	0.0045	5	0.0086	7	0.0073	9	0.0286	48	-	
237	winsense-000	0.0140	130	0.0228	129	0.0125	131	0.0215	131	0.0226	122	0.8091	198	0.0461	152	0.0352	120	0.8600	69
238	winsense-001	0.0062	50	0.0099	59	0.0092	92	0.0210	127	0.0093	47	0.0144	34	0.0098	32	0.0320	97	0.4155	12
239	x-laboratory-000	0.0071	62	0.0106	61	0.0123	128	0.0138	90	0.0419	163	0.5629	180	0.2852	199	0.0295	68	0.9686	79
240	x-laboratory-001	0.0059	45	0.0110	65	0.0054	33	0.0078	36	0.0094	49	0.0142	32	0.0100	34	0.0294	63	-	
241	xforwardai-000	0.0050	30	0.0072	30	0.0036	17	0.0051	19	0.0074	26	0.0136	28	0.0105	45	0.0276	9	-	
242	xforwardai-001	0.0021	4	0.0034	5	0.0027	3	0.0028	2	0.0046	7	0.0088	8	0.0079	15	0.0281	26	-	
243	yisheng-004	0.1988	212	0.3329	212	0.1147	207	0.1849	205	0.2044	201	-		-		0.0908	177	0.7152	53
244	yitu-003	0.0015	1	0.0026	2	0.0066	55	0.0085	40	0.0064	18	0.0114	19	0.0103	43	0.0325	100	-	
245	yoonik-000	0.0070	59	0.0112	66	0.0074	66	0.0118	68	0.0564	173	0.2013	155	0.1160	179	0.0590	160	-	
246	yuan-000	0.0101	92	0.0168	97	0.0077	71	0.0127	76	0.0178	99	0.5189	178	0.0245	118	0.0299	72	-	

Table 16: FNMR is the proportion of mated comparisons below a threshold set to achieve the FMR given in the header on the fourth row. FMR is the proportion of impostor comparisons at or above that threshold. The light grey values give rank over all algorithms in that column. The pink columns use only same-sex impostors; others are selected regardless of demographics. The exception, in the green column, uses "matched-covariates" i.e. impostors of the same sex, age group, and country of birth. The second pink column includes effects of extended ageing. Missing entries for border, visa, mugshot and wild images generally mean the algorithm did not run to completion. For child exploitation, missing entries arise because NIST executes those runs only infrequently. The VISA *columns compare images described in section 2.2. The* MUGSHOT *columns compare images described in section 2.5. The* VISA-BORDER *column compare images described in section 2.3 with those of section 2.4. The* BORDER *column compares images described in section 2.4. The* WILD *columns compare images described in section 2.6. The* CHILD-EXPLOITATION *columns compare images described in section 2.1.*

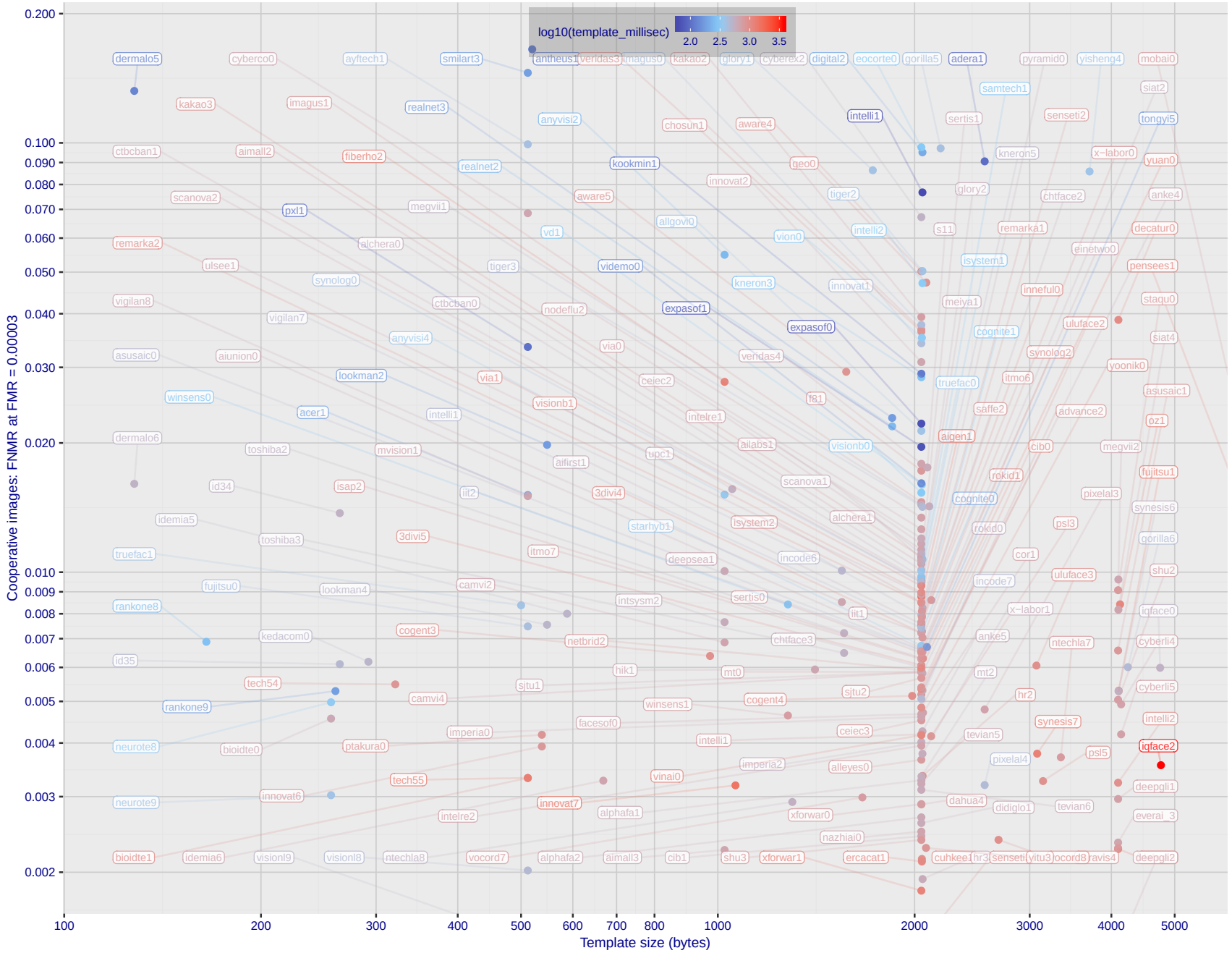

Figure 1: The points show false non-match rates (FNMR) versus the size of the encoded template. FNMR is the geometric mean of FNMR values for visa and mugshot images (from Figs. 39 and 52) at a false match rate (FMR) of 0.0001. The color of the points encodes template generation time - which spans at least one order of magnitude. Durations are measured on a single core of a c. 2016 Intel Xeon CPU E5-2630 v4 running at 2.20GHz. Algorithms with poor FNMR are omitted.

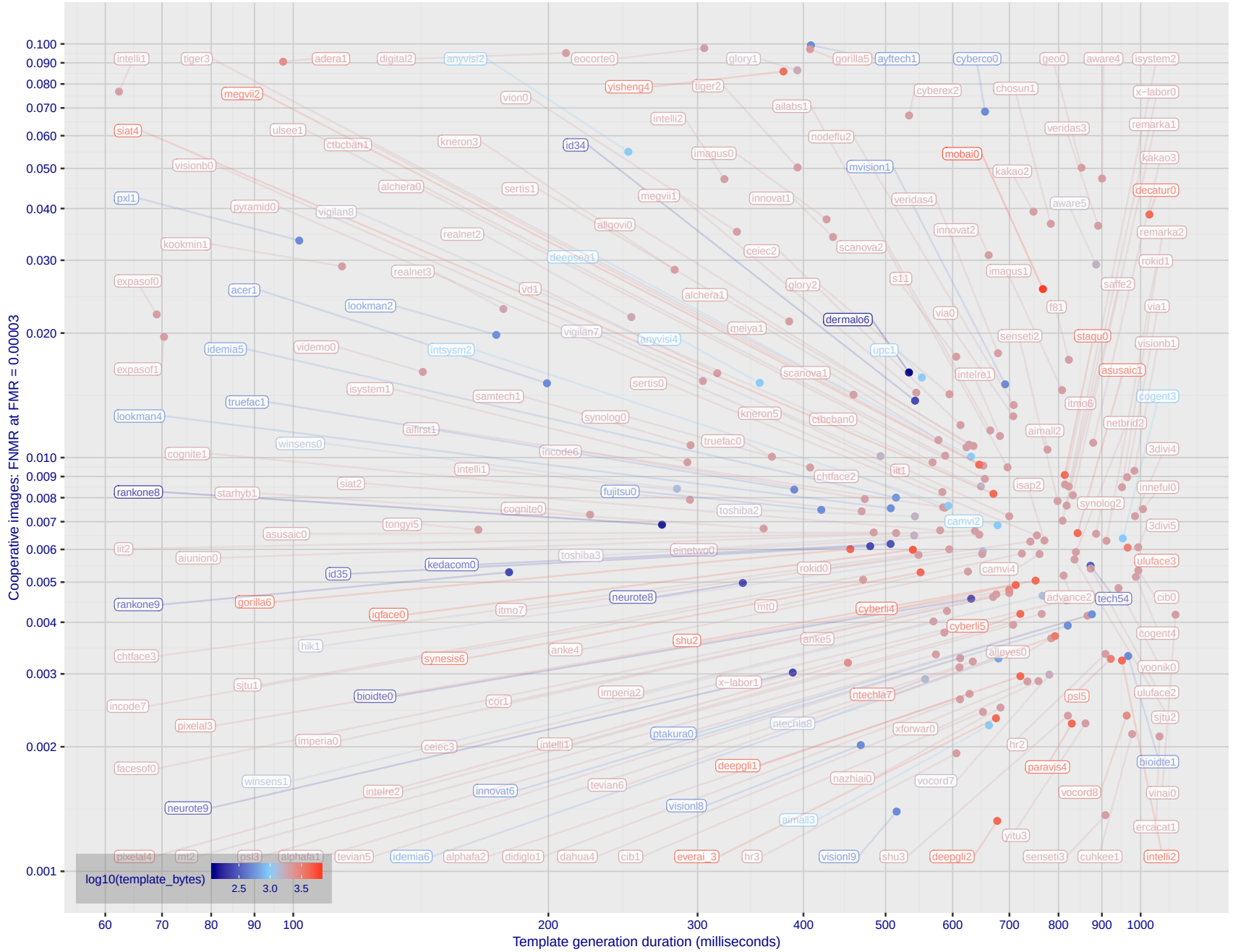

Figure 2: The points show false non-match rates (FNMR) versus the duration of the template generation operation. FNMR is the geometric mean of FNMR values for visa and mugshot images (from Figs. 39 and 52) at a false match rate (FMR) of 0.0001. Template generation time is a median estimated over 640 x 480 pixel portraits. It is measured on a single core of a c. 2016 Intel Xeon CPU E5-2630 v4 running at 2.20GHz. The color of the points encodes template size - which span two orders of magnitude. Algorithms with poor FNMR are omitted.

1 Metrics

1.1 Core accuracy

Given a vector of N genuine scores, u, the false non-match rate (FNMR) is computed as the proportion below some threshold, T:

$$\text{FNMR}(T) = 1 - \frac{1}{N}\sum_{i=1}^{N} H(u_i - T) \tag{1}$$

where $H(x)$ is the unit step function, and $H(0)$ taken to be 1.

Similarly, given a vector of N impostor scores, v, the false match rate (FMR) is computed as the proportion above T:

$$\text{FMR}(T) = \frac{1}{N}\sum_{i=1}^{N} H(v_i - T) \tag{2}$$

The threshold, T, can take on any value. We typically generate a set of thresholds from quantiles of the observed impostor scores, v, as follows. Given some interesting false match rate range, $[\text{FMR}_L, \text{FMR}_U]$, we form a vector of K thresholds corresponding to FMR measurements evenly spaced on a logarithmic scale

$$T_k = Q_v(1 - \text{FMR}_k) \tag{3}$$

where Q is the quantile function, and FMR_k comes from

$$\log_{10}\text{FMR}_k = \log_{10}\text{FMR}_L + \frac{k}{K}\ [\log_{10}\text{FMR}_U - \log_{10}\text{FMR}_L] \tag{4}$$

Error tradeoff characteristics are plots of FNMR(T) vs. FMR(T). These are plotted with $\text{FMR}_U \to 1$ and FMR_L as low as is sustained by the number of impostor comparisons, N. This is somewhat higher than the "rule of three" limit $3/N$ because samples are not independent, due to re-use of images.

2 Datasets

2.1 Child exploitation images

- ▷ The number of images is on the order of 10^4.
- ▷ The number of subjects is on the order of 10^3.
- ▷ The number of subjects with two images on the order of 10^3.
- ▷ The images are operational. They are taken from ongoing investigations of child exploitation crimes. The images are arbitrarily unconstrained. Pose varies considerably around all three axes, including subject lying down. Resolution varies very widely. Faces can be occluded by other objects, including hair and hands. Lighting varies, although the images are intended for human viewing. Mis-focus is rare. Images are given to the algorithm without any cropping; faces may occupy widely varying areas.
- ▷ The images are usually large from contemporary cameras. The mean interocular distance (IOD) is 70 pixels.
- ▷ The images are of subjects from several countries, due to the global production of this imagery.
- ▷ The images are of children, from infancy to late adolescence.
- ▷ All of the images are live capture, none are scanned. Many have been cropped.
- ▷ When these images are input to the algorithm, they are labelled as being of type "EXPLOITATION" - see Table 4 of the FRVT API.

2.2 Visa images

- ▷ The number of images is on the order of 10^5.
- ▷ The number of subjects is on the order of 10^5.
- ▷ The number of subjects with two images is on the order of 10^4.
- ▷ The images have geometry in reasonable conformance with the ISO/IEC 19794-5 Full Frontal image type. Pose is generally excellent.
- ▷ The images are of size 252x300 pixels. The mean interocular distance (IOD) is 69 pixels.
- ▷ The images are of subjects from greater than 100 countries, with significant imbalance due to visa issuance patterns.
- ▷ The images are of subjects of all ages, including children, again with imbalance due to visa issuance demand.
- ▷ Many of the images are live capture. A substantial number of the images are photographs of paper photographs.
- ▷ When these images are input to the algorithm, they are labelled as being of type "ISO" - see Table 4 of the FRVT API.

2.3 Application images

- ▷ The number of images is on the order of 10^6.
- ▷ The number of subjects is on the order of 10^6.
- ▷ The number of subjects with two images is on the order of 10^6.
- ▷ The images have geometry in good conformance with the ISO/IEC 19794-5 Full Frontal image type. Pose is generally excellent.
- ▷ The images are of size 300x300 pixels. The mean interocular distance (IOD) is 61 pixels.
- ▷ The images are of subjects from greater than 100 countries, with significant imbalance due to population and immigration patterns.

- ▷ The images are of subjects of adults with imbalance due due to population and immigration patterns and demand.
- ▷ All of the images are live capture.
- ▷ When these images are input to the algorithm, they are labelled as being of type ”ISO” - see Table 4 of the FRVT API.

2.4 Border crossing images

- ▷ The number of images is on the order of 10^6.
- ▷ The number of subjects is on the order of 10^6.
- ▷ The number of subjects with two images is on the order of 10^6.
- ▷ The images are taken with at camera oriented by an attendant toward a cooperating subject. This is done under time constraints so there are role, pitch and yaw angle variations. Also background illumination is sometimes strong, so the face is under-exposed. There is some perspective distortion due to close range images. Some faces are partially cropped.
- ▷ The images are of subjects from greater than 100 countries, with significant imbalance due to population and immigration patterns.
- ▷ The images are of subjects of adults with imbalance due due to population and immigration patterns and demand.
- ▷ The images have mean IOD of 38 pixels.
- ▷ The images are all live capture.
- ▷ When these images are input to the algorithm, they are labelled as being of type ”WILD” - see Table 4 of the FRVT API.

2.5 Mugshot images

- ▷ The number of images is on the order of 10^6.
- ▷ The number of subjects is on the order of 10^6.
- ▷ The number of subjects with two images is on the order of 10^6.
- ▷ The images have geometry in reasonable conformance with the ISO/IEC 19794-5 Full Frontal image type.
- ▷ The images are of variable sizes. The median IOD is 105 pixels. The mean IOD is 113 pixels. The 1-st, 5-th, 10-th, 25-th, 75-th, 90-th and 99-th percentiles are 34, 58, 70, 87, 121, 161 and 297 pixels.
- ▷ The images are of subjects from the United States.
- ▷ The images are of adults.
- ▷ The images are all live capture.
- ▷ When these images are input to the algorithm, they are labelled as being of type ”mugshot” - see Table 4 of the FRVT API.

2.6 Wild images

- ▷ The number of images is on the order of 10^5.
- ▷ The number of subjects is on the order of 10^3.
- ▷ The number of subjects with two images on the order of 10^3.
- ▷ The images include many photojournalism-style images. Images are given to the algorithm using a variable but generally tight crop of the head. Resolution varies very widely. The images are very unconstrained, with wide yaw and pitch pose variation. Faces can be occluded, including hair and hands.

FNMR(T) “False non-match rate”
FMR(T) “False match rate”

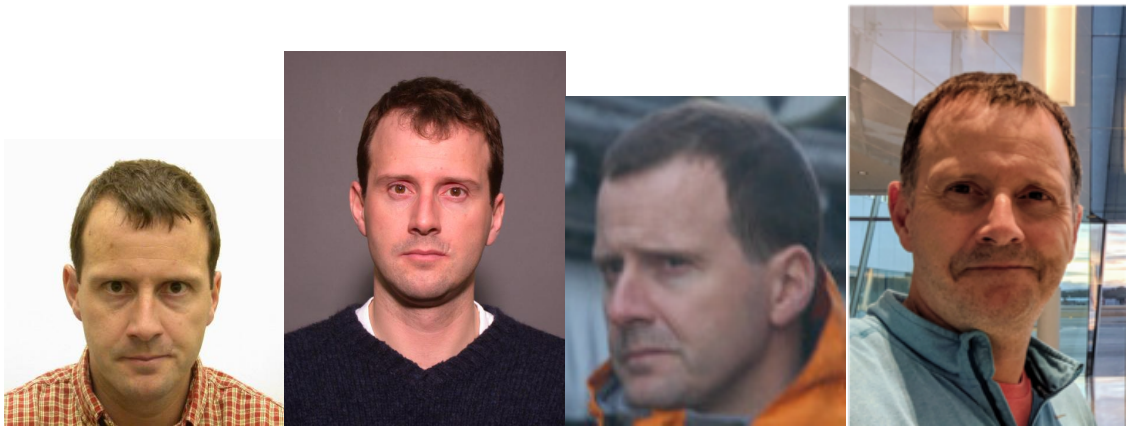

(a) Visa (b) Mugshot (c) Wild (d) Border

Figure 3: The figure gives simulated samples of image types used in this report.

- The images are of adults.
- All of the images are live capture, none are scanned.
- When these images are input to the algorithm, they are labelled as being of type "WILD" - see Table 4 of the FRVT API.

3 Results

3.1 Test goals

- To state absolute accuracy for different kinds of images, including those with and without subject cooperation.
- To state comparative accuracy, across algorithms.

3.2 Test design

Method: For visa images:

- The comparisons are of visa photos against visa photos.
- The number of genuine comparisons is on the order of 10^4.
- The number of impostor comparisons is on the order of 10^{10}.
- The comparisons are fully zero-effort, meaning impostors are paired without attention to sex, age or other covariates. However, later analysis is conducted on subsets.
- The number of persons is on the order of 10^5.
- The number of images used to make 1 template is 1.
- The number of templates used to make each comparison score is two corresponding to simple one-to-one verification.

Method: For mugshot images:

- The comparisons are of mugshot photos against mugshot photos.

- ▷ The number of genuine comparisons is on the order of 10^6.
- ▷ The number of impostor comparisons is on the order of 10^8.
- ▷ The impostors are paired by sex, but not by age or other covariates.
- ▷ The number of persons is on the order of 10^6.
- ▷ The number of images used to make 1 template is 1.
- ▷ The number of templates used to make each comparison score is two corresponding to simple one-to-one verification.

Method: For visa-border comparisons:

- ▷ The comparisons are of visa-like frontals against border crossing webcam photos.
- ▷ The number of genuine comparisons is on the order of 10^6.
- ▷ The number of impostor comparisons is on the order of 10^8.
- ▷ The impostors are paired by sex, but not by age or other covariates.
- ▷ The number of persons is on the order of 10^6.
- ▷ The number of images used to make 1 template is 1.
- ▷ The number of templates used to make each comparison score is two corresponding to simple one-to-one verification.

Method: For border-border comparisons:

- ▷ The comparisons are of border crossing webcam photos.
- ▷ The number of genuine comparisons is on the order of 10^6.
- ▷ The number of impostor comparisons is on the order of 10^8.
- ▷ The impostors are paired by sex, but not by age or other covariates.
- ▷ The number of persons is on the order of 10^6.
- ▷ The number of images used to make 1 template is 1.
- ▷ The number of templates used to make each comparison score is two corresponding to simple one-to-one verification.

Method: For wild images:

- ▷ The comparisons are of wild photos against wild photos.
- ▷ The number of genuine comparisons is on the order of 10^6.
- ▷ The number of impostor comparisons is on the order of 10^7.
- ▷ The comparisons are fully zero-effort, meaning impostors are paired without attention to sex, age or other covariates.
- ▷ The number of persons is on the order of 10^4.
- ▷ The number of images used to make 1 template is 1.
- ▷ The number of templates used to make each comparison score is two corresponding to simple one-to-one verification.

Method: For child exploitation images:

- ▷ The comparisons are of unconstrained child exploitation photos against others of the same type.

FNMR(T) "False non-match rate"
FMR(T) "False match rate"

- The number of genuine comparisons is on the order of 10^4.
- The number of impostor comparisons is on the order of 10^7.
- The comparisons are fully zero-effort, meaning impostors are paired without attention to sex, age or other covariates.
- The number of persons is on the order of 10^3.
- The number of images used to make 1 template is 1.
- The number of templates used to make each comparison score is two corresponding to simple one-to-one verification.
- We produce two performance statements. First, is a DET as used for visa and mugshot images. The second is a cumulative match characteristic (CMC) summarizing a simulated one-to-many search process. This is done as follows.
  - We regard M enrollment templates as items in a gallery.
  - These M templates come from $M > N$ individuals, because multiple images of a subject are present in the gallery under separate identifiers.
  - We regard the verification templates as search templates.
  - For each search we compute the rank of the highest scoring mate.
  - This process should properly be conducted with a 1:N algorithm, such as those tested in NIST IR 8009. We use the 1:1 algorithms in a simulated 1:N mode here to a) better reflect what a child exploitation analyst does, and b) to show algorithm efficacy is better than that revealed in the verification DETs.

FNMR(T) "False non-match rate"
FMR(T) "False match rate"

3.3 Failure to enroll

	Algorithm	Failure to Enrol Rate[1]											
	Name	APPLICATION		BORDER		CHILD-EXPLOIT		MUGSHOT		VISA		WILD	
	Name	SEC. 2.3		SEC. 2.4		SEC. 2.1		SEC. 2.5		SEC. 2.2		SEC. 2.6	
1	3divi-004	0.0001	205	0.0059	208	0.2302	63	0.0008	198	0.0006	191	0.0222	201
2	3divi-005	0.0000	159	0.0008	109	-	247	0.0000	80	0.0002	76	0.0003	77
3	acer-000	0.0000	177	0.0024	165	-	160	0.0002	139	0.0004	159	0.0008	137
4	acer-001	0.0000	141	0.0011	129	-	245	0.0001	99	0.0004	140	0.0004	102
5	acisw-003	0.0000	58	0.0000	44	-	182	0.0000	43	0.0000	46	0.0001	69
6	adera-001	0.0000	176	0.0034	182	0.1928	59	0.0003	157	0.0005	183	0.0505	220
7	advance-002	0.0000	98	0.0013	144	-	96	0.0000	88	0.0004	138	0.0009	144
8	aifirst-001	0.0000	3	0.0000	3	0.0000	2	0.0000	3	0.0000	3	0.0000	59
9	aigen-001	0.0000	52	0.0000	40	-	174	0.0000	39	0.0000	42	0.0000	34
10	ailabs-001	0.0000	108	0.0090	216	-	126	0.0007	197	0.0005	169	0.0016	159
11	aimall-002	0.0000	179	0.0043	192	-	173	0.0012	212	0.0005	182	0.0005	121
12	aimall-003	0.0000	165	0.0012	141	-	197	0.0004	168	0.0005	167	0.0004	105
13	aiunionface-000	0.0000	47	0.0000	35	-	167	0.0000	34	0.0000	37	0.0000	62
14	alchera-000	0.0000	199	0.0041	191	-	141	0.0004	172	0.0014	222	0.0038	170
15	alchera-001	0.0000	198	0.0041	190	-	127	0.0004	171	0.0014	221	0.0038	169
16	alleyes-000	0.0000	120	0.0010	119	-	185	0.0002	131	0.0004	147	0.0004	111
17	allgovision-000	0.0007	228	0.0062	209	-	213	0.0026	226	0.0052	239	0.0131	191
18	alphaface-001	0.0000	114	0.0012	135	-	149	0.0000	90	0.0004	146	0.0004	95
19	alphaface-002	0.0000	121	0.0012	136	-	186	0.0000	91	0.0004	148	0.0004	97
20	amplifiedgroup-001	0.0114	238	0.1023	240	-	156	0.0189	241	0.0279	245	0.1390	236
21	anke-004	0.0000	105	0.0011	128	0.0944	48	0.0001	115	0.0004	149	0.0006	127
22	anke-005	0.0000	110	0.0012	137	0.1228	52	0.0001	125	0.0004	158	0.0007	130
23	antheus-000	0.0000	77	0.0000	58	0.0000	26	0.0000	57	0.0000	63	0.0242	203
24	antheus-001	0.0000	90	0.0000	66	-	243	0.0000	64	0.0000	70	0.0242	204
25	anyvision-002	0.0060	235	0.0230	223	0.4866	77	0.0070	237	0.0090	243	0.1146	230
26	anyvision-004	0.0000	170	0.0017	151	0.1660	55	0.0001	124	0.0004	134	0.0080	177
27	asusaics-000	0.0000	33	0.0000	27	-	146	0.0000	27	0.0000	28	0.0000	23
28	asusaics-001	0.0000	91	0.0000	67	-	246	0.0000	65	0.0000	71	0.0000	56
29	aware-004	0.0000	149	0.0023	163	-	142	0.0002	134	0.0005	166	0.0014	156
30	aware-005	0.0000	154	0.0020	159	-	169	0.0001	130	0.0004	152	0.0011	150
31	awiros-001	0.0039	231	0.0369	232	-	90	0.0386	242	0.0872	246	0.3415	241
32	ayftech-001	0.0002	217	0.0046	198	-	216	0.0043	231	0.0011	209	0.0091	182
33	ayonix-000	0.0053	234	0.0341	231	0.0000	19	0.0113	239	0.0137	244	0.1194	231
34	bioidtechswiss-000	0.0000	131	0.0008	105	-	211	0.0003	154	0.0004	162	0.0006	122
35	bioidtechswiss-001	0.0000	94	0.0007	97	-	86	0.0000	75	0.0004	142	0.0025	165
36	bm-001	0.0000	34	0.0000	28	0.0000	12	0.0000	67	0.0000	29	0.0000	24
37	bresee-000	0.0000	107	0.0010	123	-	124	0.0002	137	0.0003	90	0.0003	74
38	camvi-002	0.0000	54	0.0000	42	0.0000	20	0.0000	41	0.0000	44	0.0000	36
39	camvi-004	0.0000	65	0.0000	71	0.0000	22	0.0000	48	0.0000	53	0.0000	43
40	ceiec-002	0.0002	216	0.0056	205	0.2482	66	0.0036	230	0.0031	235	0.0081	178
41	ceiec-003	0.0000	23	0.0013	145	-	128	0.0001	102	0.0004	143	0.0004	91
42	chosun-000	0.0000	18	0.0000	16	-	117	0.0000	15	0.0000	16	0.0000	14
43	chosun-001	0.0000	80	0.0000	60	-	220	0.0000	59	0.0000	65	0.0000	52
44	chtface-002	0.0000	182	0.0021	161	-	155	0.0002	151	0.0007	194	0.0014	155
45	chtface-003	0.0000	175	0.0018	153	-	229	0.0001	108	0.0006	189	0.0010	148
46	cib-000	0.0000	60	0.0000	46	-	184	0.0001	127	0.0000	48	0.0000	38
47	cib-001	0.0000	46	0.0000	34	-	164	0.0000	33	0.0000	36	0.0000	30
48	cogent-003	0.0000	174	0.0018	154	-	201	0.0001	107	0.0004	130	0.0009	147
49	cogent-004	0.0000	8	0.0000	9	0.0000	3	0.0000	8	0.0000	9	0.0000	7
50	cognitec-000	0.0005	225	0.0112	219	0.6342	81	0.0007	194	0.0007	198	0.0388	216
51	cognitec-001	0.0003	221	0.0110	218	-	172	0.0008	202	0.0010	201	0.0185	197
52	cor-001	0.0000	115	0.0006	88	-	152	0.0002	149	0.0004	135	0.0004	114
53	ctbcbank-000	0.0001	204	0.0051	201	0.3285	70	0.0011	209	0.0019	226	0.0868	228
54	ctbcbank-001	0.0000	183	0.0036	186	-	225	0.0005	186	0.0010	202	0.0844	227
55	cuhkee-001	0.0000	109	0.0011	132	-	131	0.0000	71	0.0004	126	0.1278	233
56	cybercore-000	0.0000	132	0.0073	211	-	212	0.0001	111	0.0005	170	0.0383	215
57	cyberextruder-001	0.0029	230	0.0293	225	0.5338	79	0.0024	223	0.0029	233	0.0597	224
58	cyberextruder-002	0.0013	229	0.0840	239	0.2672	69	0.0027	227	0.0028	232	0.0335	212

Table 17: FTE is the proportion of failed template generation attempts. Failures can occur because the software throws an exception, or because the software electively refuses to process the input image. This would typically occur if a face is not detected. FTE is measured as the number of function calls that give EITHER a non-zero error code OR that give a "small" template. This is defined as one whose size is less than 0.3 times the median template size for that algorithm. This second rule is needed because some algorithms incorrectly fail to return a non-zero error code when template generation fails.

[1] *The effects of FTE are included in the accuracy results of this report by regarding any template comparison involving a failed template to produce a low similarity score. Thus higher FTE results in higher FNMR and lower FMR.*

FNMR(T) "False non-match rate"
FMR(T) "False match rate"

	Algorithm	Failure to Enrol Rate[1]											
	Name	APPLICATION		BORDER		CHILD-EXPLOIT		MUGSHOT		VISA		WILD	
	Name	SEC. 2.3		SEC. 2.4		SEC. 2.1		SEC. 2.5		SEC. 2.2		SEC. 2.6	
59	cyberlink-004	0.0000	137	0.0010	127	-	234	0.0004	169	0.0003	99	0.0003	84
60	cyberlink-005	0.0000	93	0.0009	114	-	85	0.0003	164	0.0003	98	0.0003	80
61	dahua-004	0.0000	37	0.0009	117	-	150	0.0001	123	0.0003	79	0.0002	70
62	dahua-005	0.0000	79	0.0000	69	-	218	0.0000	81	0.0003	91	0.0000	51
63	decatur-000	0.0000	145	0.0020	158	-	102	0.0004	175	0.0005	165	0.0236	202
64	deepglint-001	0.0000	36	0.0000	29	0.0000	13	0.0000	28	0.0000	30	0.0000	25
65	deepglint-002	0.0000	96	0.0004	80	0.0669	42	0.0002	145	0.0004	116	0.0003	81
66	deepsea-001	0.0000	13	0.0000	13	0.0000	6	0.0000	12	0.0000	13	0.0000	11
67	dermalog-005	-	246	0.0031	174	0.1796	56	0.0013	216	0.0041	236	0.0163	195
68	dermalog-006	0.0005	226	0.0031	175	0.1797	57	0.0013	215	0.0041	237	0.0163	196
69	didiglobalface-001	0.0000	113	0.0012	134	0.2175	61	0.0000	89	0.0004	145	0.0004	94
70	digitalbarriers-002	0.0001	208	0.0045	195	-	176	0.0028	228	0.0027	231	0.0071	176
71	dsk-000	0.0000	24	0.0000	20	0.0000	9	0.0000	19	0.0000	20	0.0000	18
72	einetworks-000	0.0000	184	0.0017	150	-	228	0.0002	142	0.0005	181	0.0008	140
73	eocortex-000	0.0095	237	0.0602	236	-	118	0.0094	238	0.0059	240	0.1405	237
74	ercacat-001	0.0000	83	0.0005	86	-	231	0.0000	84	0.0003	92	0.0002	71
75	everai-paravision-003	0.0000	150	0.0008	112	0.0705	44	0.0002	133	0.0004	115	0.0004	109
76	expasoft-000	0.0000	85	0.0000	63	-	237	0.0000	61	0.0000	67	0.0000	55
77	expasoft-001	0.0000	69	0.0000	53	-	203	0.0000	51	0.0000	56	0.0000	46
78	f8-001	0.0003	220	0.0059	207	0.2026	60	0.0035	229	0.0030	234	0.0087	181
79	facesoft-000	0.0000	92	0.0000	68	0.0000	28	0.0000	66	0.0000	72	0.0000	57
80	fiberhome-nanjing-002	0.0000	144	0.0006	92	-	97	0.0001	109	0.0004	114	0.0016	158
81	fujitsulab-000	0.0000	193	0.0033	178	-	151	0.0005	181	0.0002	75	0.0099	184
82	fujitsulab-001	0.0000	84	0.0014	146	-	236	0.0002	146	0.0003	97	0.0003	76
83	geo-000	0.0000	30	0.0000	24	-	143	0.0000	24	0.0000	25	0.0000	20
84	glory-001	0.0160	239	0.0314	229	0.0000	25	0.0051	234	0.0010	204	0.1651	238
85	glory-002	0.0003	218	0.0045	194	-	113	0.0015	218	0.0011	214	0.0557	222
86	gorilla-005	0.0000	44	0.0008	110	-	162	0.0000	78	0.0003	86	0.0004	100
87	gorilla-006	0.0000	41	0.0006	93	-	158	0.0000	74	0.0003	85	0.0003	75
88	hik-001	0.0000	70	0.0000	72	-	204	0.0000	52	0.0000	57	0.0000	47
89	hr-002	0.0000	111	0.0007	100	-	139	0.0002	141	0.0004	150	0.0004	93
90	hr-003	0.0000	106	0.0008	111	-	119	0.0001	106	0.0004	111	0.0113	187
91	id3-004	0.0000	201	0.0052	202	-	166	0.0015	220	0.0011	213	-	247
92	id3-005	0.0000	124	0.0074	213	-	193	0.0002	136	0.0005	168	0.0256	207
93	idemia-005	0.0000	11	0.0004	81	0.0239	32	0.0000	72	0.0003	93	0.0003	78
94	idemia-006	0.0000	57	0.0004	82	-	181	0.0000	73	0.0003	95	0.0003	79
95	iit-001	0.0000	162	0.0806	238	0.0843	47	0.0001	129	0.0004	139	0.0104	185
96	iit-002	0.0000	185	0.0021	160	-	217	0.0009	205	0.0005	186	0.0443	219
97	imagus-000	0.0002	214	0.0028	170	0.1107	51	0.0010	208	0.0012	217	0.0347	213
98	imagus-001	0.0000	152	0.0030	172	-	165	0.0001	116	0.0004	141	0.0396	217
99	imperial-000	0.0000	45	0.0000	33	-	163	0.0000	32	0.0000	35	0.0000	29
100	imperial-002	0.0000	12	0.0000	12	0.0000	5	0.0000	11	0.0000	12	0.0000	10
101	incode-006	0.0000	103	0.0005	85	-	110	0.0001	126	0.0004	101	0.0004	99
102	incode-007	0.0000	153	0.0009	115	-	168	0.0002	138	0.0004	118	0.0007	136
103	innefulabs-000	0.0000	138	0.0024	164	-	235	0.0003	159	0.0005	178	0.0004	103
104	innovativetechnologyltd-001	0.0001	212	0.0050	200	-	179	0.0024	225	0.0025	230	0.0055	175
105	innovativetechnologyltd-002	0.0000	166	0.0046	197	-	199	0.0057	236	0.0005	179	0.0247	206
106	innovatrics-006	0.0000	127	0.0009	116	0.0350	35	0.0000	82	0.0004	108	0.0003	90
107	innovatrics-007	0.0000	97	0.0007	101	-	93	0.0001	94	0.0003	84	0.0003	82
108	intellicloudai-001	0.0000	88	0.0000	64	-	239	0.0000	62	0.0000	68	0.0001	68
109	intellifusion-001	0.0000	104	0.0005	87	0.0949	49	0.0001	105	0.0003	96	0.0005	120
110	intellifusion-002	0.0000	42	0.0000	70	-	161	0.0000	68	0.0000	33	0.0001	67
111	intellivision-001	0.0042	232	0.0296	226	0.5495	80	0.0048	233	0.0042	238	0.1358	234
112	intellivision-002	0.0000	200	0.0046	196	-	125	0.0012	211	0.0005	187	0.0146	192
113	intelresearch-001	0.0000	191	0.0082	215	-	192	0.0005	185	0.0010	203	0.0407	218
114	intelresearch-002	0.0000	112	0.0022	162	-	147	0.0000	85	0.0004	103	0.0003	88
115	intsysmsu-001	0.0000	38	0.0010	121	-	153	0.0001	113	0.0004	136	0.0004	106
116	intsysmsu-002	0.0000	66	0.0010	122	-	198	0.0001	114	0.0004	137	0.0004	108

Table 18: FTE is the proportion of failed template generation attempts. Failures can occur because the software throws an exception, or because the software electively refuses to process the input image. This would typically occur if a face is not detected. FTE is measured as the number of function calls that give EITHER a non-zero error code OR that give a "small" template. This is defined as one whose size is less than 0.3 times the median template size for that algorithm. This second rule is needed because some algorithms incorrectly fail to return a non-zero error code when template generation fails.

[1] *The effects of FTE are included in the accuracy results of this report by regarding any template comparison involving a failed template to produce a low similarity score. Thus higher FTE results in higher FNMR and lower FMR.*

	Algorithm	Failure to Enrol Rate[1]											
	Name	APPLICATION		BORDER		CHILD-EXPLOIT		MUGSHOT		VISA		WILD	
	Name	SEC. 2.3		SEC. 2.4		SEC. 2.1		SEC. 2.5		SEC. 2.2		SEC. 2.6	
117	iqface-000	0.0000	68	0.0000	52	0.0000	23	0.0000	50	0.0000	55	0.0000	45
118	iqface-002	0.0000	6	0.0000	7	-	100	0.0000	6	0.0000	7	0.0000	5
119	isap-001	0.0000	64	0.0000	50	-	195	0.0000	47	0.0000	52	0.0000	42
120	isap-002	0.0000	31	0.0000	25	-	144	0.0000	25	0.0000	26	0.0000	21
121	isityou-000	0.0068	236	0.0316	230	0.4714	75	0.0023	221	0.0010	206	0.0663	226
122	isystems-001	0.0000	187	0.0035	183	0.1421	53	0.0010	206	0.0007	195	0.0128	189
123	isystems-002	0.0000	188	0.0035	184	0.1421	54	0.0010	207	0.0007	196	0.0128	190
124	itmo-006	0.0000	15	0.0015	148	-	111	0.0004	176	0.0004	133	0.0006	126
125	itmo-007	0.0000	73	0.0009	113	-	208	0.0003	165	0.0000	60	0.0004	101
126	iws-000	0.0005	227	0.0650	237	-	134	0.0024	224	0.0012	215	0.0936	229
127	kakao-002	0.0000	167	0.0057	206	0.2494	67	0.0002	147	0.0005	173	0.0310	209
128	kakao-003	0.0000	39	0.0000	30	-	154	0.0000	29	0.0000	31	0.0000	26
129	kedacom-000	0.0000	32	0.0000	26	0.0000	11	0.0000	26	0.0000	27	0.0000	22
130	kneron-003	0.0239	241	0.0306	227	0.4883	78	0.0044	232	0.0016	225	0.1823	239
131	kneron-005	0.0000	190	0.0226	222	-	112	0.0006	190	0.0005	174	0.0097	183
132	kookmin-001	0.0000	61	0.0000	47	-	187	0.0000	44	0.0000	49	0.0000	39
133	lookman-002	0.0000	63	0.0000	49	-	194	0.0000	46	0.0000	51	0.0000	41
134	lookman-004	0.0000	51	0.0000	39	0.0000	18	0.0000	38	0.0000	41	0.0000	33
135	luxand-000	0.0000	17	0.0000	15	-	116	0.0000	14	0.0000	15	0.0000	13
136	megvii-001	0.0000	87	0.0006	90	0.0274	34	0.0007	195	0.0004	113	0.0152	193
137	megvii-002	0.0000	86	0.0006	89	0.0274	33	0.0054	235	0.0004	112	0.0126	188
138	meiya-001	0.0000	186	0.0028	171	-	233	0.0004	177	0.0010	207	0.0025	164
139	microfocus-001	0.0001	210	0.0053	204	0.0791	46	0.0008	201	0.0016	224	0.0220	200
140	microfocus-002	0.0001	209	0.0053	203	0.0791	45	0.0008	200	0.0016	223	0.0220	199
141	mobai-000	0.0000	172	0.0114	220	-	136	0.0003	161	0.0012	216	0.1242	232
142	mt-000	0.0000	116	0.0008	108	0.1043	50	0.0002	143	0.0004	151	0.0004	96
143	mt-002	0.0000	100	0.0003	75	-	106	0.0001	96	0.0004	105	0.0004	104
144	mvision-001	0.0000	53	0.0000	41	-	177	0.0000	40	0.0000	43	0.0000	35
145	nazhiai-000	0.0000	62	0.0000	48	-	188	0.0000	45	0.0000	50	0.0000	40
146	netbridgetech-001	0.0000	10	0.0000	11	-	104	0.0000	10	0.0000	11	0.0000	9
147	netbridgetech-002	0.0000	27	0.0000	22	-	137	0.0000	22	0.0000	23	0.0000	19
148	neurotechnology-008	0.0000	163	0.0006	91	-	178	0.0004	170	0.0004	119	0.0018	162
149	neurotechnology-009	0.0000	143	0.0008	107	-	87	0.0002	135	0.0004	110	0.0018	161
150	nodeflux-002	0.0000	140	0.0261	224	-	242	0.0008	199	0.0005	180	0.0008	142
151	notiontag-000	0.0000	48	0.0000	36	0.0000	16	0.0000	35	0.0000	38	0.0000	31
152	ntechlab-007	0.0000	157	0.0019	155	0.0682	43	0.0001	100	0.0004	109	0.0005	119
153	ntechlab-008	0.0000	151	0.0005	84	-	145	0.0001	103	0.0004	106	0.0005	115
154	null-000	-	245	-	245	-	98	-	246	-	248	-	245
155	null-082	-	244	-	244	-	89	-	245	-	247	-	244
156	oz-001	0.0000	169	0.0011	133	-	129	0.0006	193	0.0004	122	0.0014	154
157	paravision-004	0.0000	168	0.0007	103	0.0570	38	0.0002	140	0.0004	125	0.0008	138
158	pensees-001	0.0000	95	0.0000	4	-	91	0.0000	4	0.0000	4	0.0000	2
159	pixelall-003	0.0000	75	0.0000	56	-	210	0.0000	55	0.0000	61	0.0000	49
160	pixelall-004	0.0000	7	0.0000	8	-	101	0.0000	7	0.0000	8	0.0000	6
161	psl-003	0.0000	129	0.0007	95	-	205	0.0000	86	0.0004	131	0.0003	87
162	psl-005	0.0000	99	0.0007	94	-	103	0.0000	76	0.0004	120	0.0003	85
163	ptakuratsatu-000	0.0000	133	0.0007	102	-	219	0.0001	95	0.0003	87	0.0003	83
164	pxl-001	0.0000	203	0.0044	193	-	221	0.0005	183	0.0022	228	0.0323	211
165	pyramid-000	0.0001	207	0.0041	189	-	94	0.0005	182	0.0007	197	0.0015	157
166	rankone-008	0.0000	197	0.0049	199	-	88	0.0003	152	0.0004	100	0.0040	171
167	rankone-009	0.0000	89	0.0000	65	-	240	0.0000	63	0.0000	69	0.0000	60
168	realnetworks-002	0.0000	164	0.0003	78	-	190	0.0004	167	0.0003	82	0.0004	107
169	realnetworks-003	0.0000	161	0.0003	77	0.0076	31	0.0004	166	0.0003	81	0.0004	110
170	remarkai-001	0.0000	50	0.0000	38	-	170	0.0000	37	0.0000	40	0.0000	63
171	remarkai-002	0.0000	28	0.0000	23	-	138	0.0000	23	0.0000	24	0.0000	61
172	rokid-000	0.0000	81	0.0072	210	-	224	0.0001	112	0.0005	175	0.0354	214
173	rokid-001	0.0000	26	0.0013	143	-	132	0.0000	21	0.0000	22	0.0007	135
174	s1-001	0.0000	202	0.0073	212	-	105	0.0013	213	0.0007	193	0.0600	225

Table 19: FTE is the proportion of failed template generation attempts. Failures can occur because the software throws an exception, or because the software electively refuses to process the input image. This would typically occur if a face is not detected. FTE is measured as the number of function calls that give EITHER a non-zero error code OR that give a "small" template. This is defined as one whose size is less than 0.3 times the median template size for that algorithm. This second rule is needed because some algorithms incorrectly fail to return a non-zero error code when template generation fails.

[1] *The effects of FTE are included in the accuracy results of this report by regarding any template comparison involving a failed template to produce a low similarity score. Thus higher FTE results in higher FNMR and lower FMR.*

FNMR(T) "False non-match rate"
FMR(T) "False match rate"

	Algorithm	Failure to Enrol Rate[1]											
	Name	APPLICATION		BORDER		CHILD-EXPLOIT		MUGSHOT		VISA		WILD	
	Name	SEC. 2.3		SEC. 2.4		SEC. 2.1		SEC. 2.5		SEC. 2.2		SEC. 2.6	
175	saffe-001	0.0000	43	0.0000	32	0.0000	15	0.0000	31	0.0000	34	0.0000	28
176	saffe-002	0.0000	78	0.0000	59	-	215	0.0000	58	0.0000	64	0.0000	50
177	samtech-001	0.0001	206	0.0032	177	-	157	0.0004	174	0.0008	199	0.0013	153
178	scanovate-001	0.0208	240	0.2388	241	-	122	0.0024	222	0.0014	220	0.2751	240
179	scanovate-002	0.0000	158	0.0018	152	-	244	0.0000	92	0.0004	163	0.0008	139
180	securifai-001	0.0000	59	0.0000	45	-	183	0.0000	69	0.0000	47	0.0017	160
181	sensetime-002	0.0004	224	0.0082	214	0.3345	71	0.0011	210	0.0005	185	0.0218	198
182	sensetime-003	0.0000	130	0.0011	131	0.0554	37	0.0000	70	0.0004	127	0.0004	112
183	sertis-000	0.0000	14	0.0007	98	-	109	0.0000	93	0.0004	117	0.0004	98
184	sertis-001	0.0000	74	0.0004	83	-	209	0.0002	144	0.0005	188	0.0003	89
185	shaman-000	0.0000	55	0.0000	43	0.0000	21	0.0000	42	0.0000	45	0.0000	37
186	shaman-001	0.0000	2	0.0000	2	0.0000	1	0.0000	2	0.0000	2	0.0000	58
187	shu-002	0.0000	142	0.0010	124	-	83	0.0005	178	0.0004	154	0.0007	131
188	shu-003	0.0000	56	0.0007	96	-	180	0.0001	98	0.0003	83	0.0004	113
189	siat-002	0.0000	135	0.0012	140	0.0616	39	0.0000	83	0.0004	128	0.0048	173
190	siat-004	0.0000	118	0.0011	130	-	171	0.0000	79	0.0004	124	0.0003	86
191	sjtu-001	0.0000	146	0.0010	126	-	107	0.0005	180	0.0004	161	0.0008	141
192	sjtu-002	0.0000	155	0.0010	125	-	222	0.0005	179	0.0004	157	0.0007	134
193	smilart-002	0.0000	192	0.0036	185	0.2422	65	0.0003	163	0.0011	210	0.0575	223
194	smilart-003	0.0003	219	0.0100	217	-	114	0.0014	217	0.0013	219	0.0555	221
195	staqu-000	0.0000	67	0.0000	51	-	200	0.0000	49	0.0000	54	0.0000	44
196	starhybrid-001	0.0001	211	0.0033	181	0.2340	64	0.0009	204	0.0023	229	0.0044	172
197	synesis-006	0.0000	35	0.0003	79	-	148	0.0000	87	0.0003	80	0.0002	73
198	synesis-007	0.0000	139	0.0013	142	-	241	0.0002	148	0.0004	129	0.0005	116
199	synology-000	0.0000	21	0.0000	18	-	123	0.0000	17	0.0000	18	0.0000	16
200	synology-002	0.0000	16	0.0000	14	-	115	0.0000	13	0.0000	14	0.0000	12
201	tech5-004	0.0000	134	0.0008	106	-	223	0.0003	155	0.0004	160	0.0006	123
202	tech5-005	0.0000	117	0.0007	104	-	159	0.0000	77	0.0004	144	0.0049	174
203	tevian-005	0.0001	213	0.0041	188	0.3606	72	0.0006	191	0.0006	192	0.0012	151
204	tevian-006	0.0000	29	0.0012	138	-	140	0.0003	158	0.0005	177	0.0007	132
205	tiger-002	0.0000	125	0.0010	120	0.0619	41	0.0001	119	0.0004	123	0.0082	180
206	tiger-003	0.0000	101	-	246	0.0619	40	0.0001	117	0.0004	121	0.0082	179
207	tongyi-005	0.0000	9	0.0000	10	0.0000	4	0.0000	9	0.0000	10	0.0000	8
208	toshiba-002	0.0000	22	0.0000	19	0.0000	8	0.0000	18	0.0000	19	0.0000	17
209	toshiba-003	0.0000	82	0.0001	73	-	227	0.0001	120	0.0001	74	0.0002	72
210	trueface-000	0.0000	136	0.0000	61	-	230	0.0000	60	0.0000	66	0.0000	53
211	trueface-001	0.0000	147	0.0038	187	-	120	0.0007	196	0.0005	176	0.0277	208
212	tuputech-000	0.0003	222	0.0116	221	-	135	0.0632	243	0.0081	242	0.6383	242
213	ulsee-001	0.0000	76	0.0000	57	-	214	0.0000	56	0.0000	62	0.0001	64
214	ultinous-000	-	243	-	243	0.0007	29	-	244	0.0003	88	-	243
215	ultinous-001	-	248	-	248	0.0007	30	-	248	0.0003	89	-	248
216	uluface-002	0.0000	49	0.0000	37	0.0000	17	0.0000	36	0.0000	39	0.0000	32
217	uluface-003	0.0000	20	0.0001	74	-	121	0.0002	132	0.0002	77	0.0244	205
218	upc-001	0.0000	181	0.0003	76	0.0450	36	0.0003	153	0.0003	94	0.0011	149
219	vcog-002	-	247	0.3719	242	0.2209	62	-	247	0.0019	227	-	246
220	vd-001	0.0000	189	0.0030	173	-	133	0.0004	173	0.0009	200	0.0024	163
221	veridas-003	0.0000	178	0.0026	166	0.1893	58	0.0001	118	0.0005	171	0.0006	124
222	veridas-004	0.0000	180	0.0026	167	-	248	0.0001	121	0.0005	172	0.0006	125
223	via-000	0.0000	71	0.0000	54	0.0000	24	0.0000	53	0.0000	58	0.0001	66
224	via-001	0.0000	25	0.0000	21	-	130	0.0000	20	0.0000	21	0.0001	65
225	videmo-000	0.0000	156	0.0019	156	-	238	0.0003	160	0.0012	218	0.0158	194
226	videonetics-001	0.0004	223	0.0309	228	0.4799	76	0.0015	219	0.0010	205	0.0112	186
227	videonetics-002	0.0000	160	0.0459	234	0.4598	74	0.0006	192	0.0005	184	0.0013	152
228	vigilantsolutions-007	0.0000	173	0.0028	169	0.2538	68	0.0001	104	0.0004	107	0.0005	118
229	vigilantsolutions-008	0.0000	171	0.0028	168	-	95	0.0001	101	0.0004	104	0.0005	117
230	vinai-000	0.0000	4	0.0000	5	-	92	0.0000	5	0.0000	5	0.0000	3
231	vion-000	0.0050	233	0.0392	233	0.6388	82	0.0130	240	0.0078	241	0.1389	235
232	visionbox-000	0.0000	196	0.0033	180	-	232	0.0005	189	0.0011	212	0.0028	168

Table 20: FTE is the proportion of failed template generation attempts. Failures can occur because the software throws an exception, or because the software electively refuses to process the input image. This would typically occur if a face is not detected. FTE is measured as the number of function calls that give EITHER a non-zero error code OR that give a "small" template. This is defined as one whose size is less than 0.3 times the median template size for that algorithm. This second rule is needed because some algorithms incorrectly fail to return a non-zero error code when template generation fails.

[1] *The effects of FTE are included in the accuracy results of this report by regarding any template comparison involving a failed template to produce a low similarity score. Thus higher FTE results in higher FNMR and lower FMR.*

FNMR(T) "False non-match rate"
FMR(T) "False match rate"

	Algorithm	Failure to Enrol Rate[1]											
	Name	APPLICATION		BORDER		CHILD-EXPLOIT		MUGSHOT		VISA		WILD	
	Name	SEC. 2.3		SEC. 2.4		SEC. 2.1		SEC. 2.5		SEC. 2.2		SEC. 2.6	
233	visionbox-001	0.0000	195	0.0033	179	-	206	0.0005	188	0.0011	211	0.0028	167
234	visionlabs-008	0.0000	126	0.0015	147	-	196	0.0002	150	0.0004	164	0.0009	143
235	visionlabs-009	0.0000	102	0.0010	118	-	108	0.0001	97	0.0004	132	0.0006	128
236	visteam-000	0.0000	194	0.0031	176	-	226	0.0005	184	0.0011	208	0.0026	166
237	vocord-007	0.0000	148	0.0535	235	0.0000	10	0.0001	128	0.0004	102	0.0009	145
238	vocord-008	0.0000	119	0.0015	149	-	175	0.0003	162	0.0001	73	0.0007	133
239	winsense-000	0.0000	19	0.0000	17	0.0000	7	0.0000	16	0.0000	17	0.0000	15
240	winsense-001	0.0000	40	0.0000	31	0.0000	14	0.0000	30	0.0000	32	0.0000	27
241	x-laboratory-000	0.0247	242	0.0000	62	0.0000	27	0.0005	187	0.0002	78	0.0000	54
242	x-laboratory-001	0.0000	128	0.0012	139	-	202	0.0001	122	0.0004	156	0.0007	129
243	xforwardai-000	0.0000	1	0.0000	1	-	84	0.0000	1	0.0000	1	0.0000	1
244	xforwardai-001	0.0000	123	0.0007	99	-	191	0.0003	156	0.0004	153	0.0004	92
245	yisheng-004	0.0002	215	-	247	0.4279	73	0.0013	214	0.0006	190	0.0321	210
246	yitu-003	0.0000	5	0.0000	6	-	99	0.0009	203	0.0000	6	0.0000	4
247	yoonik-000	0.0000	122	0.0019	157	-	189	0.0001	110	0.0004	155	0.0009	146
248	yuan-000	0.0000	72	0.0000	55	-	207	0.0000	54	0.0000	59	0.0000	48

Table 21: FTE is the proportion of failed template generation attempts. Failures can occur because the software throws an exception, or because the software electively refuses to process the input image. This would typically occur if a face is not detected. FTE is measured as the number of function calls that give EITHER a non-zero error code OR that give a "small" template. This is defined as one whose size is less than 0.3 times the median template size for that algorithm. This second rule is needed because some algorithms incorrectly fail to return a non-zero error code when template generation fails.

[1] *The effects of FTE are included in the accuracy results of this report by regarding any template comparison involving a failed template to produce a low similarity score. Thus higher FTE results in higher FNMR and lower FMR.*

FNMR(T) "False non-match rate"
FMR(T) "False match rate"

3.4 Recognition accuracy

Core algorithm accuracy is stated via:

- **Cooperative subjects**
  - The summary table of Figure 16;
  - The visa image DETs of Figure 39;
  - The mugshot DETs of Figure 52;
  - The mugshot ageing profiles of Figure 192;
  - The human-difficult pairs of Figure 14
- **Non-cooperative subjects**
  - The photojournalism DET of Figure 63
  - The child-exploitation DET of Figure 67;
  - The child-exploitation CMC of Figure 71.

Figure 156 shows dependence of false match rate on algorithm score threshold. This allows a deployer to set a threshold to target a particular false match rate appropriate to the security objectives of the application.

Figure 131 likewise shows FMR(T) but for mugshots, and specially four subsets of the population.

Note that in both the mugshot and visa sets false match rates vary with the ethnicity, age, and sex, of the enrollee and impostor. For example figure 84 summarizes FMR for impostors paired from four groups black females, black males, white females, white males.

FNMR(T) "False non-match rate"
FMR(T) "False match rate"

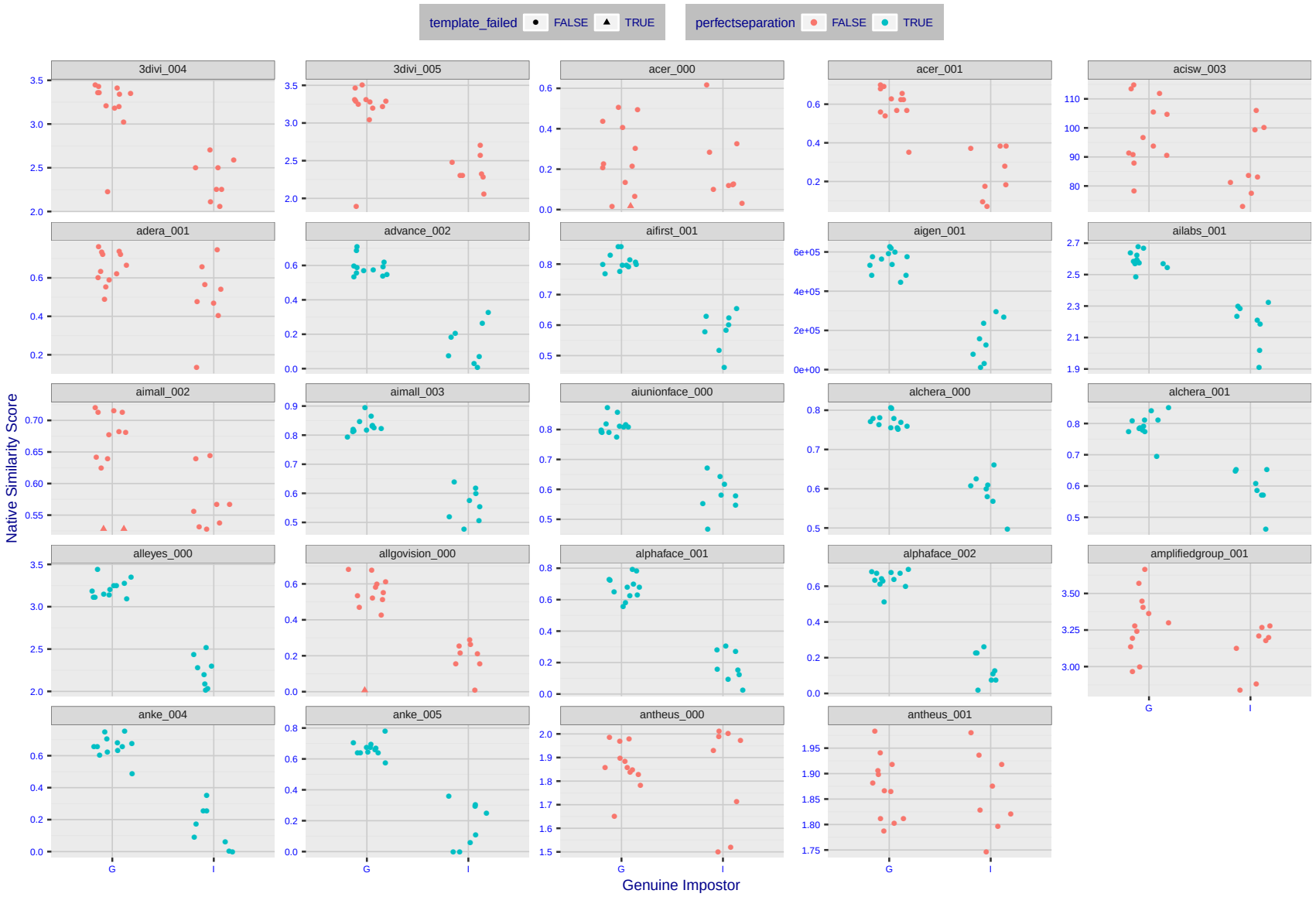

Figure 4: The Figure shows, in blue, algorithms that correctly separate the 12 genuine and 8 impostor pairs used in the May 2018 paper Face recognition accuracy of forensic examiners, superrecognizers, and face recognition algorithms *(Phillips et al. [1]). In red are algorithms that are imperfect. Some algorithms fail only because they failed to make a template e.g. due to face detection failure (shown as a triangle). Others fail because the pairs were selected for that study because they had been difficult for three leading algorithms used in FRVT 2006. Caution: Given the small sample size (n=20) the figure may change substantially if larger or different sets were used. The images can be downloaded from the* Supplemental Information *page provided with that publication.*

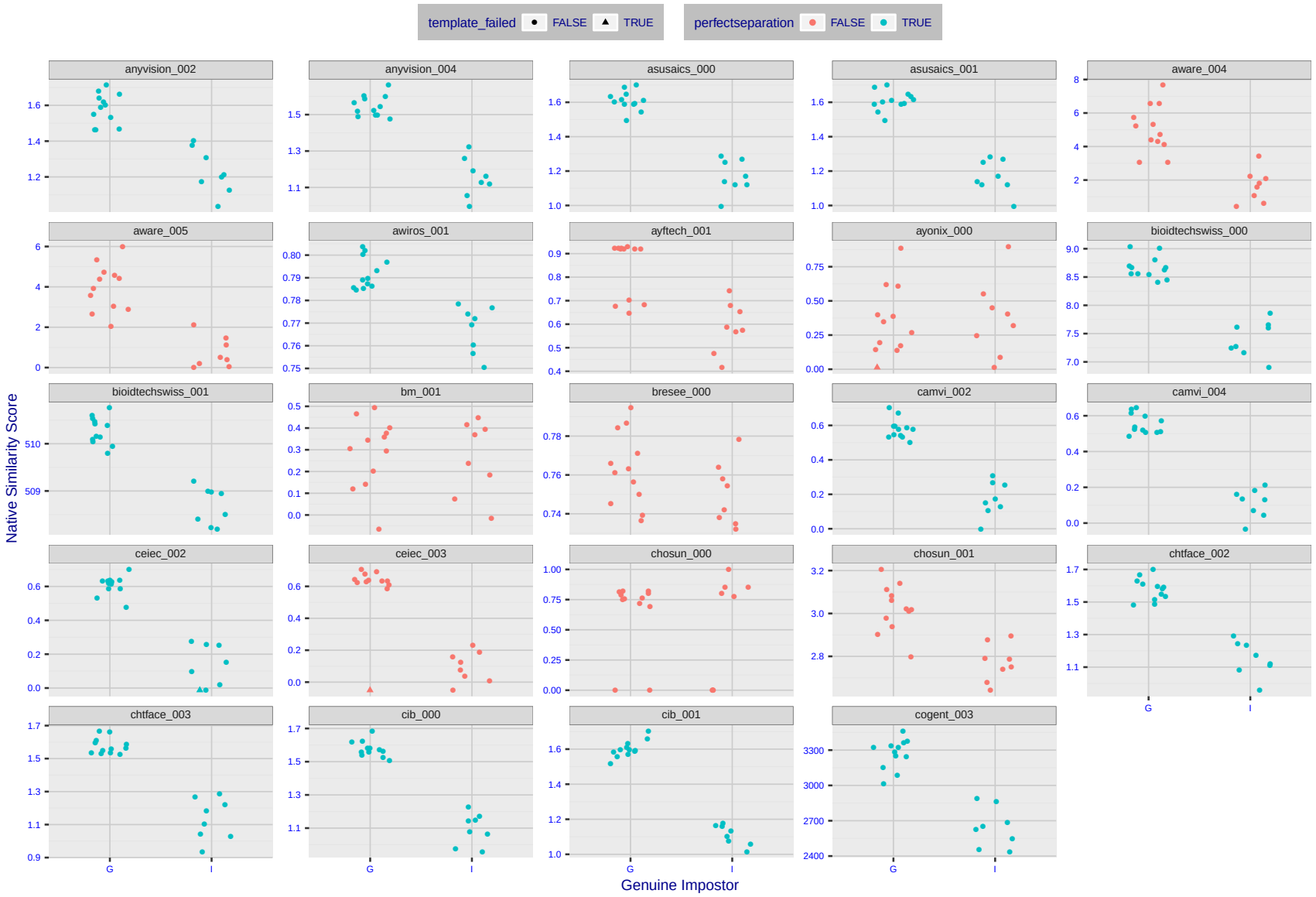

Figure 5: The Figure shows, in blue, algorithms that correctly separate the 12 genuine and 8 impostor pairs used in the May 2018 paper Face recognition accuracy of forensic examiners, superrecognizers, and face recognition algorithms *(Phillips et al. [1]). In red are algorithms that are imperfect. Some algorithms fail only because they failed to make a template e.g. due to face detection failure (shown as a triangle). Others fail because the pairs were selected for that study because they had been difficult for three leading algorithms used in FRVT 2006. Caution: Given the small sample size (n=20) the figure may change substantially if larger or different sets were used. The images can be downloaded from the* Supplemental Information *page provided with that publication.*

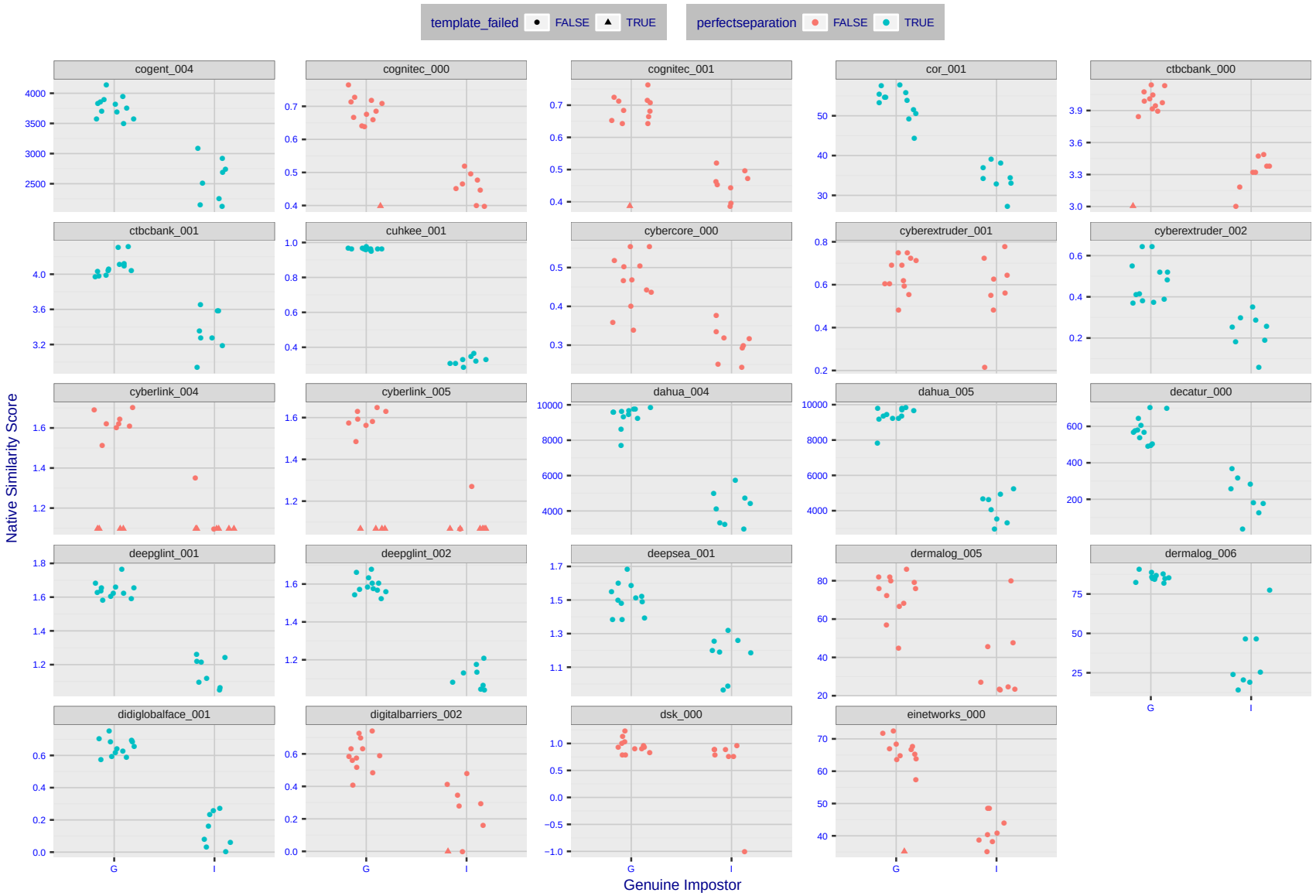

Figure 6: The Figure shows, in blue, algorithms that correctly separate the 12 genuine and 8 impostor pairs used in the May 2018 paper Face recognition accuracy of forensic examiners, superrecognizers, and face recognition algorithms *(Phillips et al. [1]). In red are algorithms that are imperfect. Some algorithms fail only because they failed to make a template e.g. due to face detection failure (shown as a triangle). Others fail because the pairs were selected for that study because they had been difficult for three leading algorithms used in FRVT 2006. Caution: Given the small sample size (n=20) the figure may change substantially if larger or different sets were used. The images can be downloaded from the* Supplemental Information *page provided with that publication.*

Figure 7: The Figure shows, in blue, algorithms that correctly separate the 12 genuine and 8 impostor pairs used in the May 2018 paper Face recognition accuracy of forensic examiners, superrecognizers, and face recognition algorithms *(Phillips et al. [1]). In red are algorithms that are imperfect. Some algorithms fail only because they failed to make a template e.g. due to face detection failure (shown as a triangle). Others fail because the pairs were selected for that study because they had been difficult for three leading algorithms used in FRVT 2006. Caution: Given the small sample size (n=20) the figure may change substantially if larger or different sets were used. The images can be downloaded from the* Supplemental Information *page provided with that publication.*

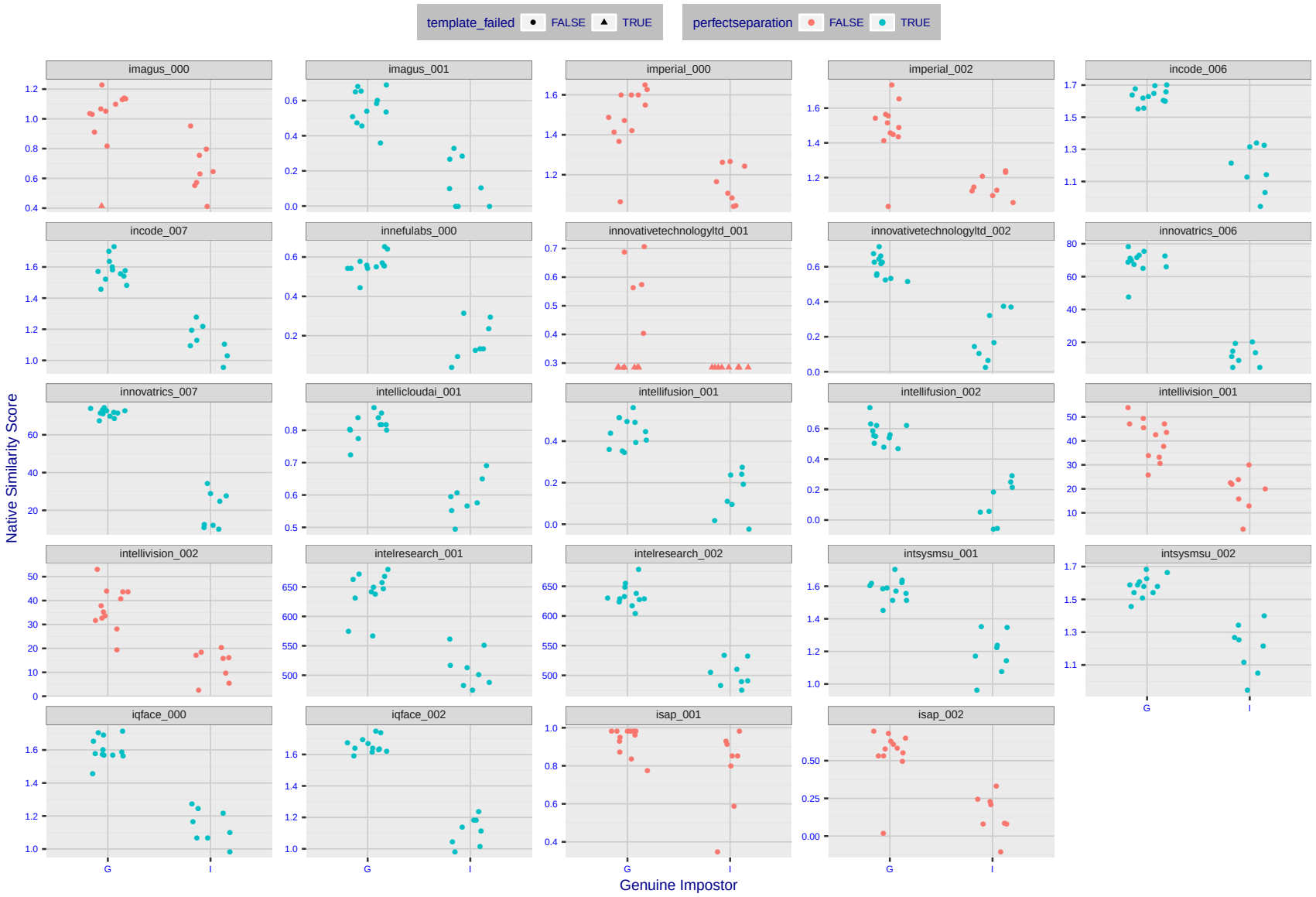

Figure 8: The Figure shows, in blue, algorithms that correctly separate the 12 genuine and 8 impostor pairs used in the May 2018 paper Face recognition accuracy of forensic examiners, superrecognizers, and face recognition algorithms *(Phillips et al. [1]). In red are algorithms that are imperfect. Some algorithms fail only because they failed to make a template e.g. due to face detection failure (shown as a triangle). Others fail because the pairs were selected for that study because they had been difficult for three leading algorithms used in FRVT 2006. Caution: Given the small sample size (n=20) the figure may change substantially if larger or different sets were used. The images can be downloaded from the* Supplemental Information *page provided with that publication.*

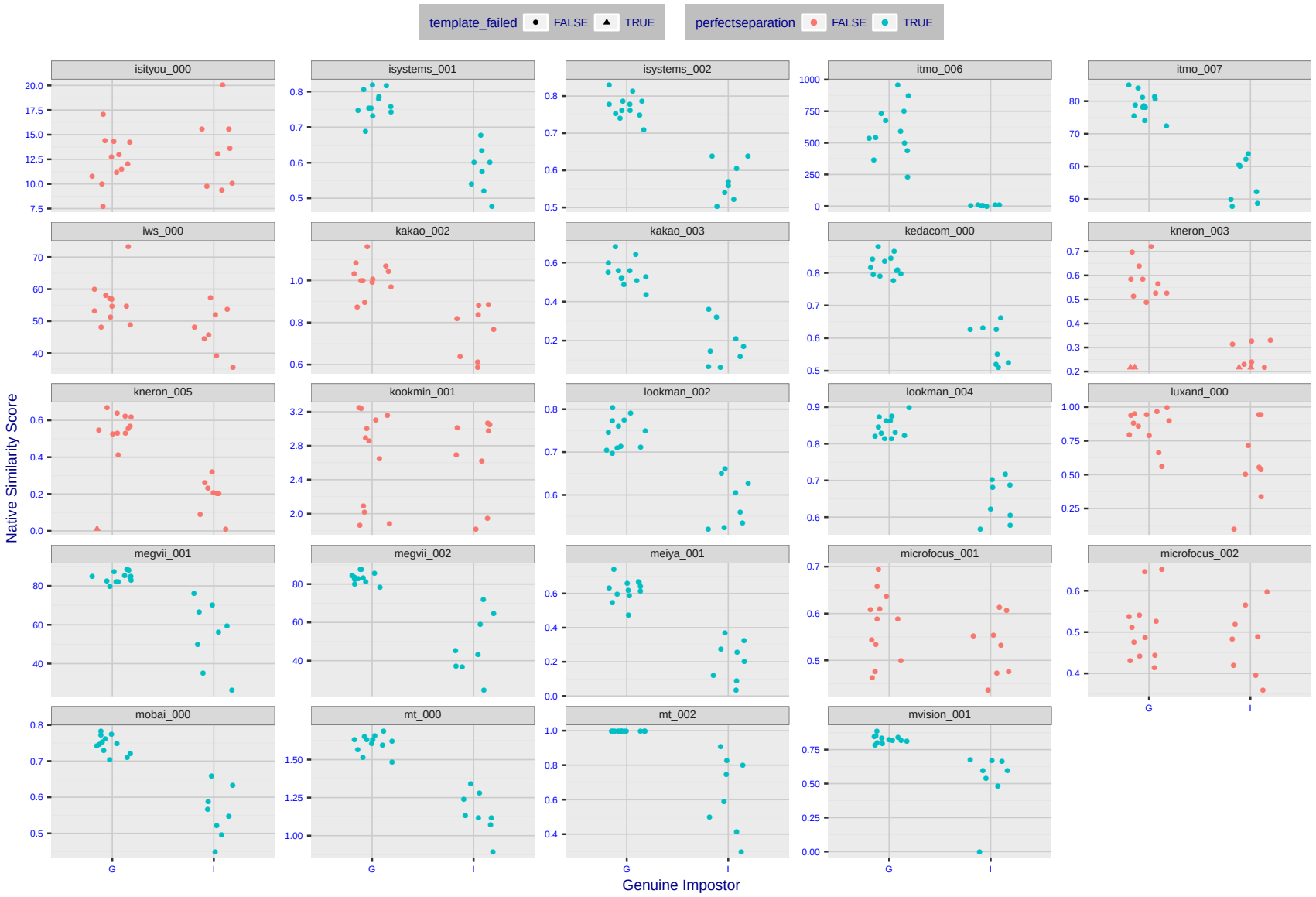

Figure 9: The Figure shows, in blue, algorithms that correctly separate the 12 genuine and 8 impostor pairs used in the May 2018 paper Face recognition accuracy of forensic examiners, superrecognizers, and face recognition algorithms *(Phillips et al. [1]). In red are algorithms that are imperfect. Some algorithms fail only because they failed to make a template e.g. due to face detection failure (shown as a triangle). Others fail because the pairs were selected for that study because they had been difficult for three leading algorithms used in FRVT 2006. Caution: Given the small sample size (n=20) the figure may change substantially if larger or different sets were used. The images can be downloaded from the* Supplemental Information *page provided with that publication.*

Figure 10: The Figure shows, in blue, algorithms that correctly separate the 12 genuine and 8 impostor pairs used in the May 2018 paper Face recognition accuracy of forensic examiners, superrecognizers, and face recognition algorithms *(Phillips et al. [1]). In red are algorithms that are imperfect. Some algorithms fail only because they failed to make a template e.g. due to face detection failure (shown as a triangle). Others fail because the pairs were selected for that study because they had been difficult for three leading algorithms used in FRVT 2006. Caution: Given the small sample size (n=20) the figure may change substantially if larger or different sets were used. The images can be downloaded from the* Supplemental Information *page provided with that publication.*

Figure 11: The Figure shows, in blue, algorithms that correctly separate the 12 genuine and 8 impostor pairs used in the May 2018 paper Face recognition accuracy of forensic examiners, superrecognizers, and face recognition algorithms *(Phillips et al. [1]). In red are algorithms that are imperfect. Some algorithms fail only because they failed to make a template e.g. due to face detection failure (shown as a triangle). Others fail because the pairs were selected for that study because they had been difficult for three leading algorithms used in FRVT 2006. Caution: Given the small sample size (n=20) the figure may change substantially if larger or different sets were used. The images can be downloaded from the* Supplemental Information *page provided with that publication.*

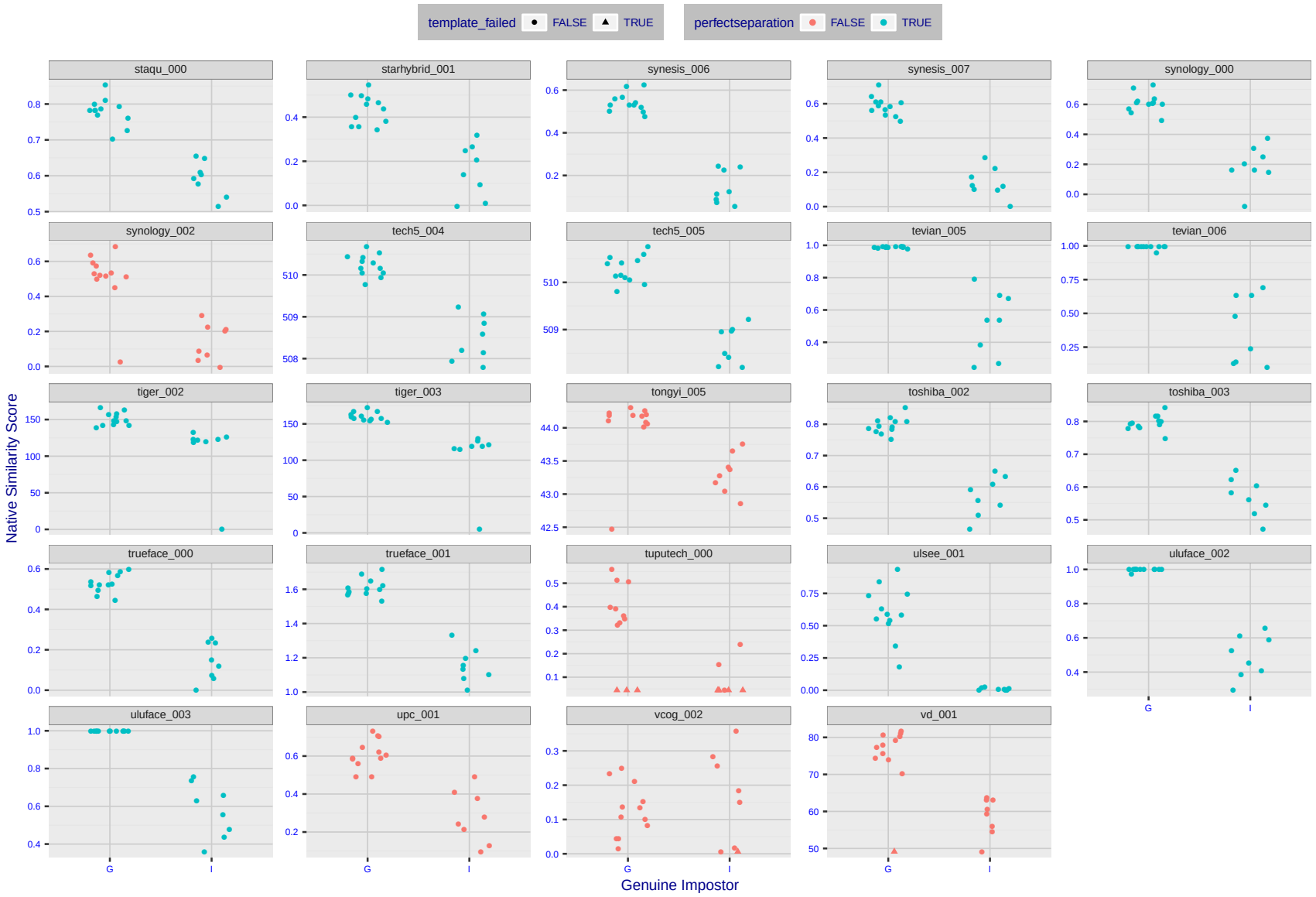

Figure 12: The Figure shows, in blue, algorithms that correctly separate the 12 genuine and 8 impostor pairs used in the May 2018 paper Face recognition accuracy of forensic examiners, superrecognizers, and face recognition algorithms *(Phillips et al. [1]). In red are algorithms that are imperfect. Some algorithms fail only because they failed to make a template e.g. due to face detection failure (shown as a triangle). Others fail because the pairs were selected for that study because they had been difficult for three leading algorithms used in FRVT 2006. Caution: Given the small sample size (n=20) the figure may change substantially if larger or different sets were used. The images can be downloaded from the* Supplemental Information *page provided with that publication.*

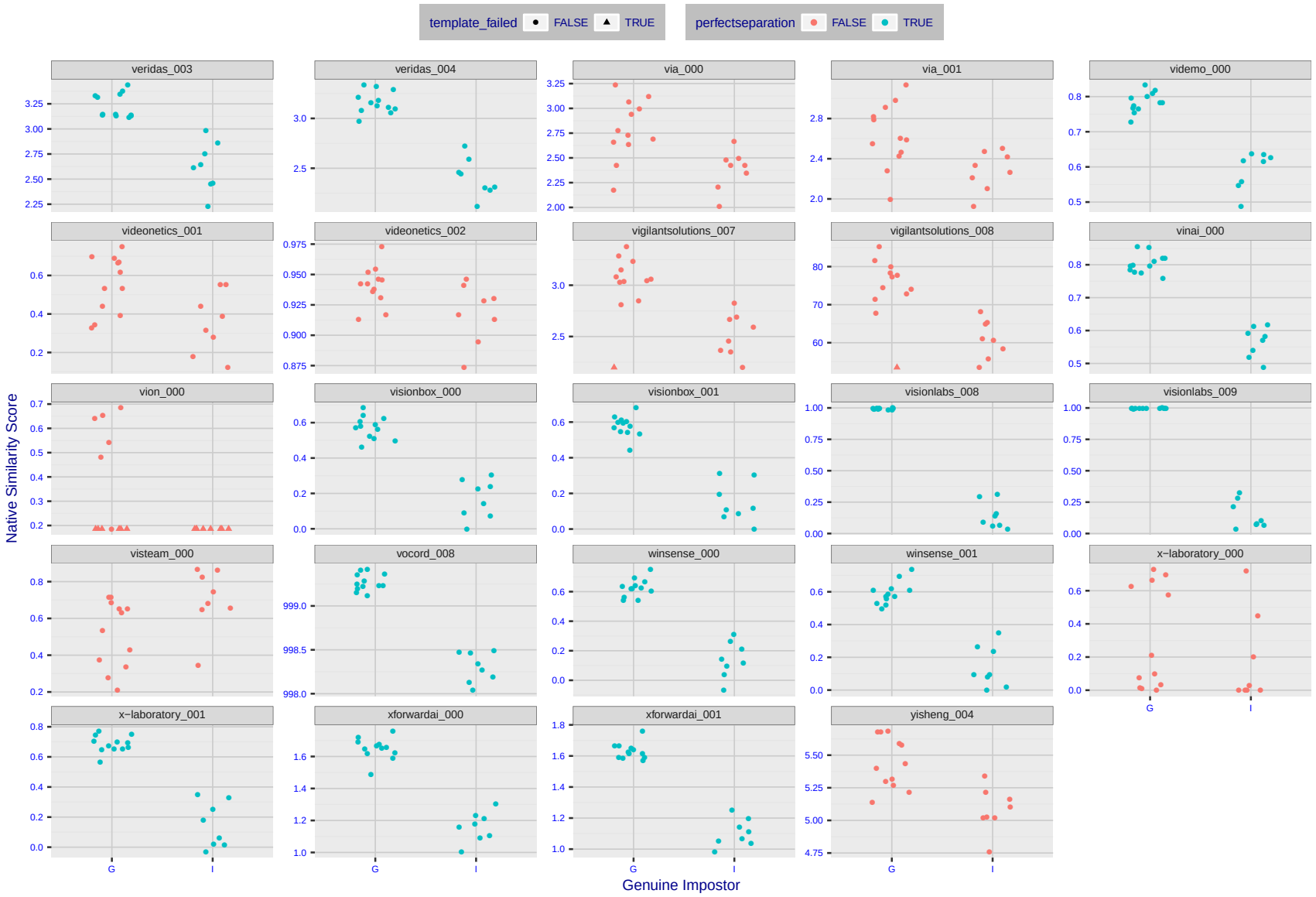

Figure 13: The Figure shows, in blue, algorithms that correctly separate the 12 genuine and 8 impostor pairs used in the May 2018 paper Face recognition accuracy of forensic examiners, superrecognizers, and face recognition algorithms *(Phillips et al. [1]). In red are algorithms that are imperfect. Some algorithms fail only because they failed to make a template e.g. due to face detection failure (shown as a triangle). Others fail because the pairs were selected for that study because they had been difficult for three leading algorithms used in FRVT 2006. Caution: Given the small sample size (n=20) the figure may change substantially if larger or different sets were used. The images can be downloaded from the* Supplemental Information *page provided with that publication.*

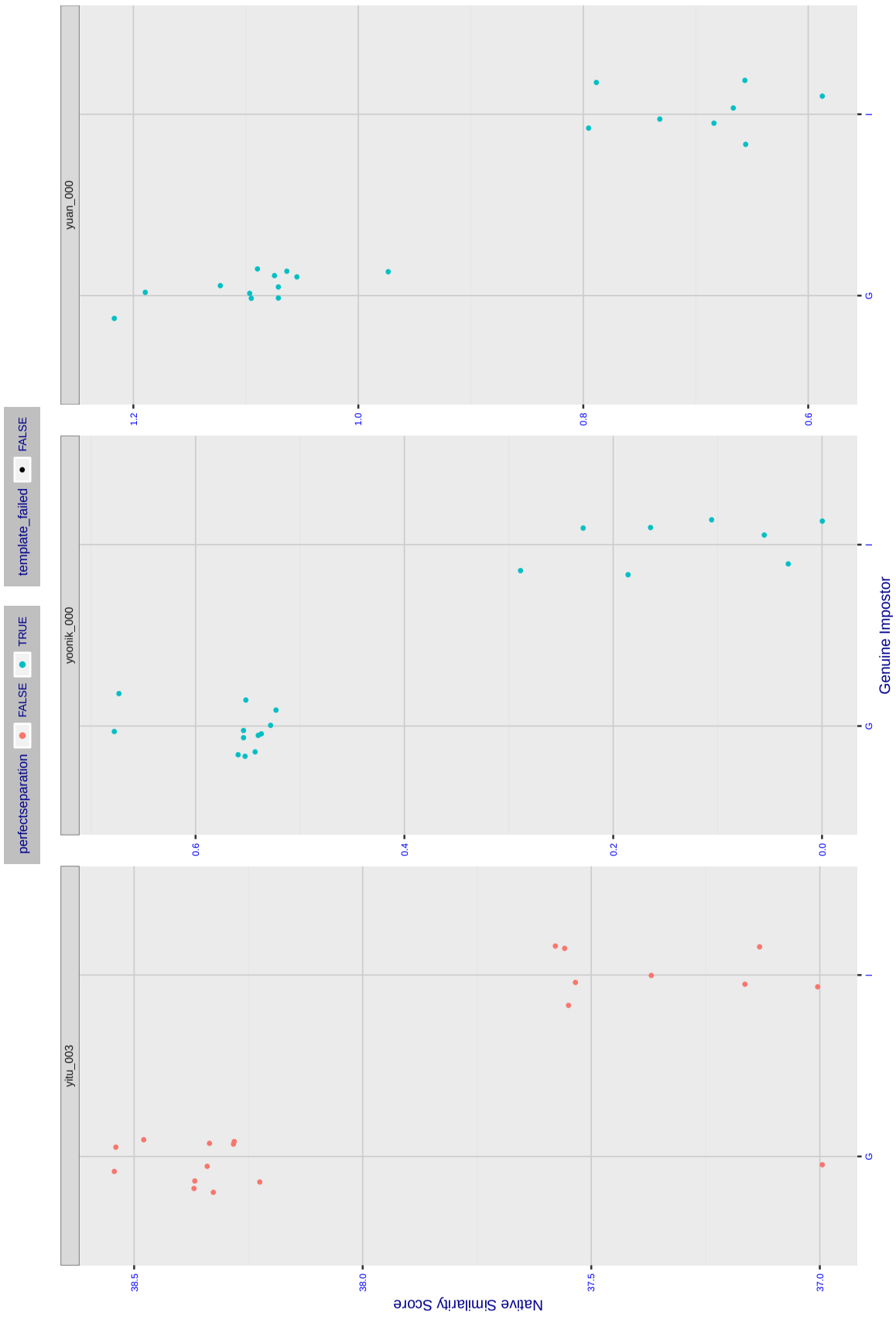

Figure 14: The Figure shows, in blue, algorithms that correctly separate the 12 genuine and 8 impostor pairs used in the May 2018 paper Face recognition accuracy of forensic examiners, superrecognizers, and face recognition algorithms (Phillips et al. [1]). In red are algorithms that are imperfect. Some algorithms fail only because they failed to make a template e.g. due to face detection failure (shown as a triangle). Others fail because the pairs were selected for that study because they had been difficult for three leading algorithms used in FRVT 2006. Caution: Given the small sample size (n=20) the figure may change substantially if larger or different sets were used. The images can be downloaded from the Supplemental Information page provided with that publication.

FNMR(T) "False non-match rate"
FMR(T) "False match rate"

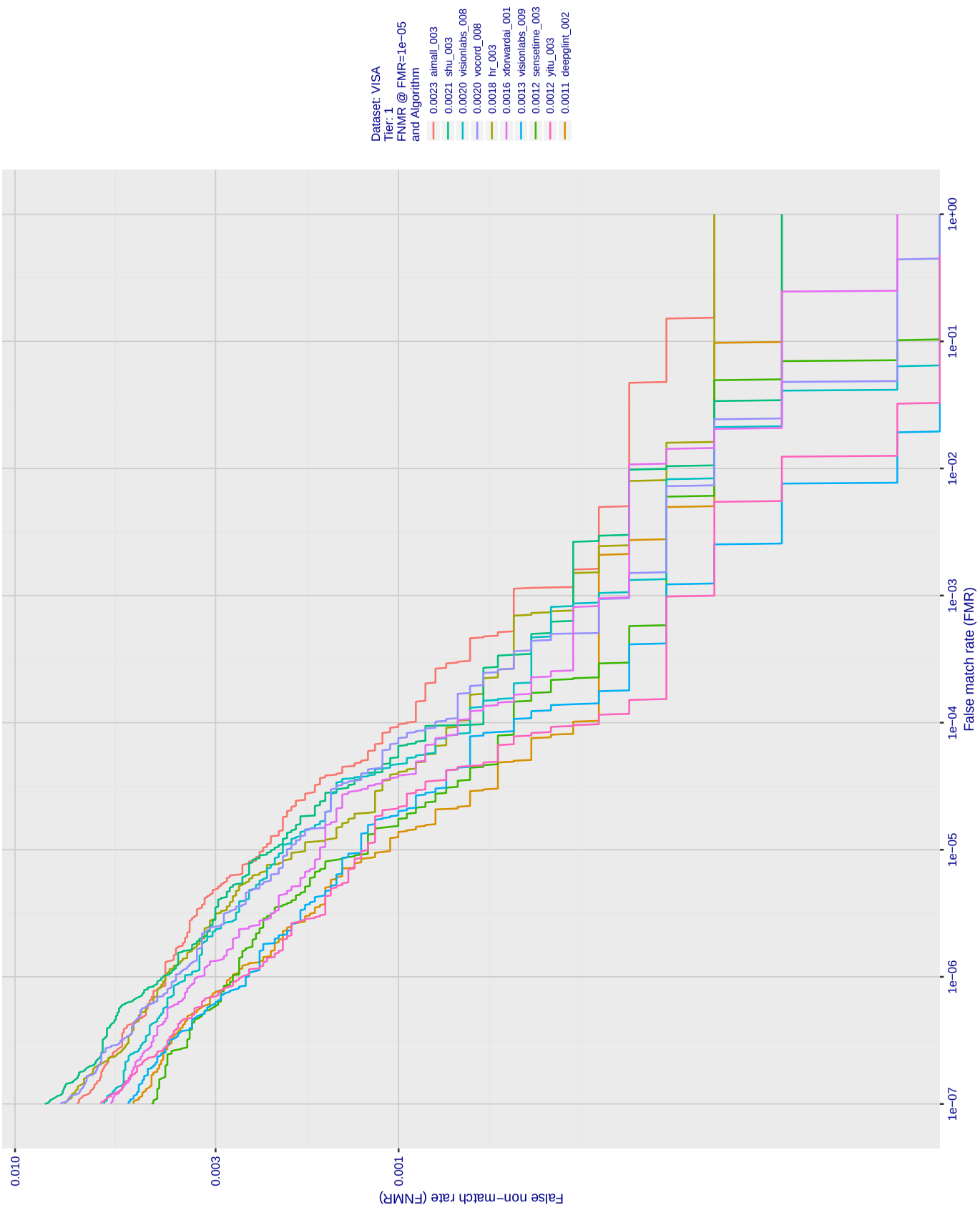

Figure 15: For the visa images, detection error tradeoff (DET) *characteristics showing false non-match rate vs. false match rate plotted parametrically on threshold, T. The scales are logarithmic in order to show many decades of* FMR.

FNMR(T) "False non-match rate"
FMR(T) "False match rate"

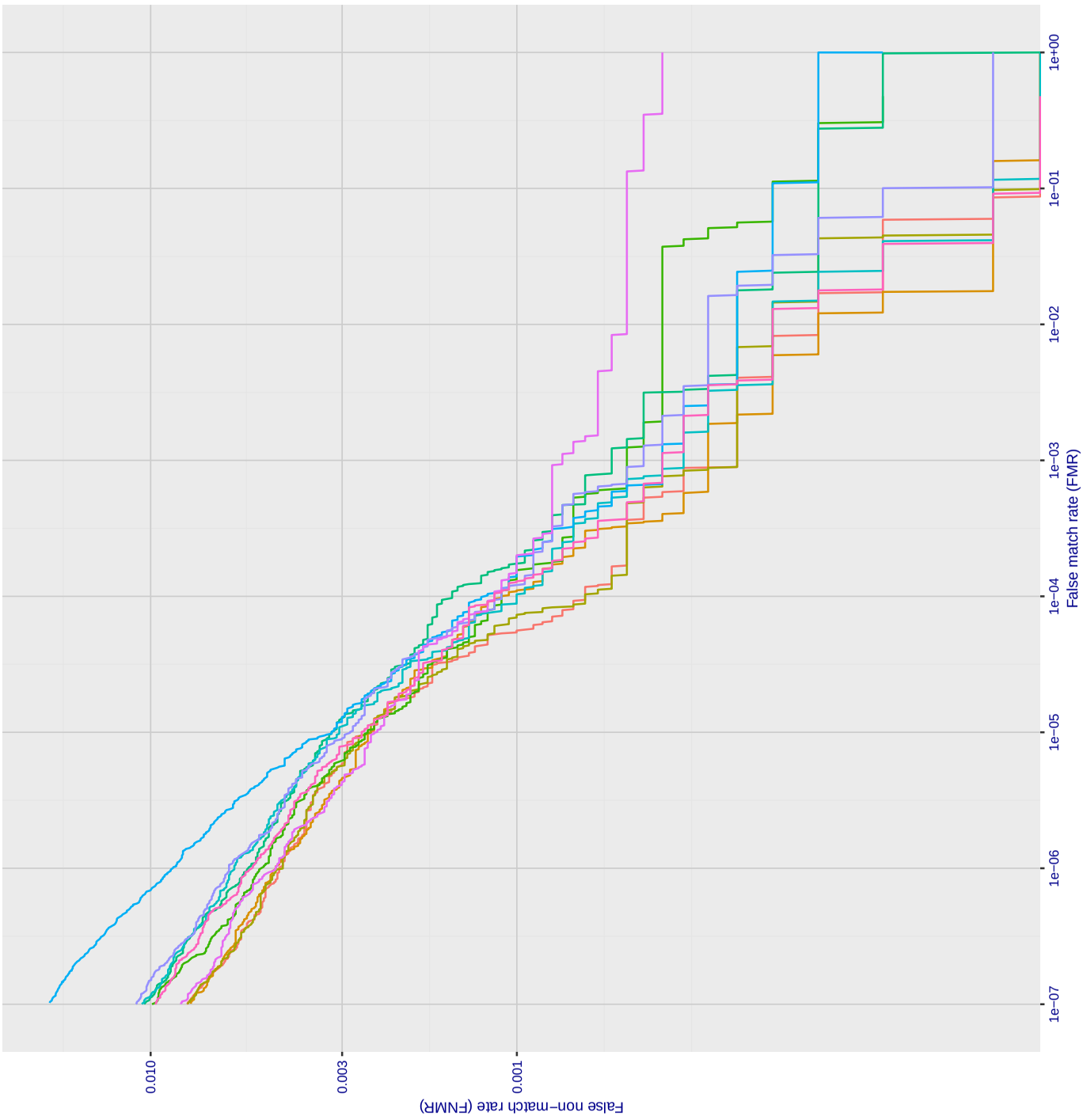

Figure 16: For the visa images, detection error tradeoff (DET) characteristics showing false non-match rate vs. false match rate plotted parametrically on threshold, T. The scales are logarithmic in order to show many decades of FMR.

FNMR(T) "False non-match rate"
FMR(T) "False match rate"

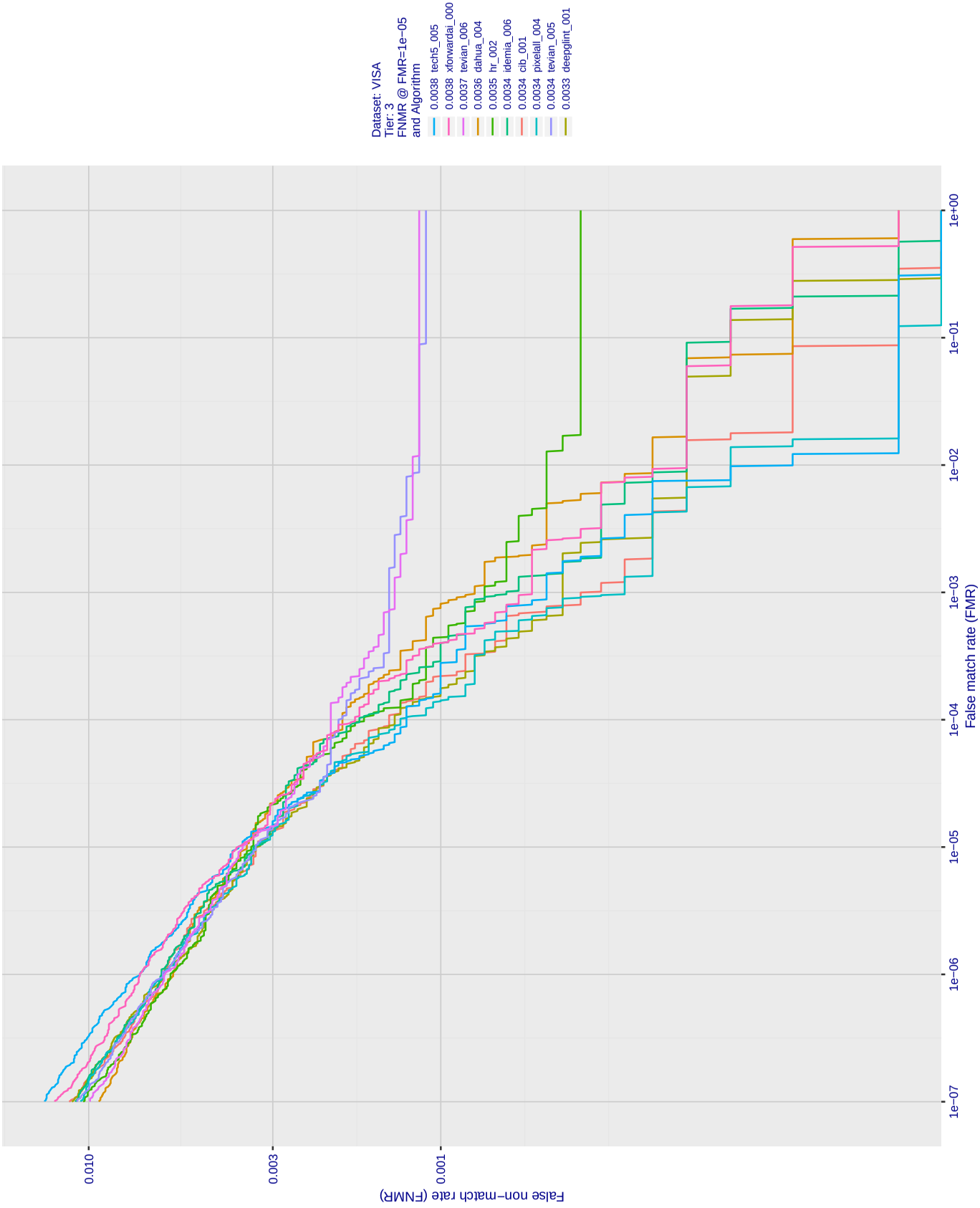

Figure 17: For the visa images, detection error tradeoff (DET) characteristics showing false non-match rate vs. false match rate plotted parametrically on threshold, T. The scales are logarithmic in order to show many decades of FMR.

FNMR(T) "False non-match rate"
FMR(T) "False match rate"

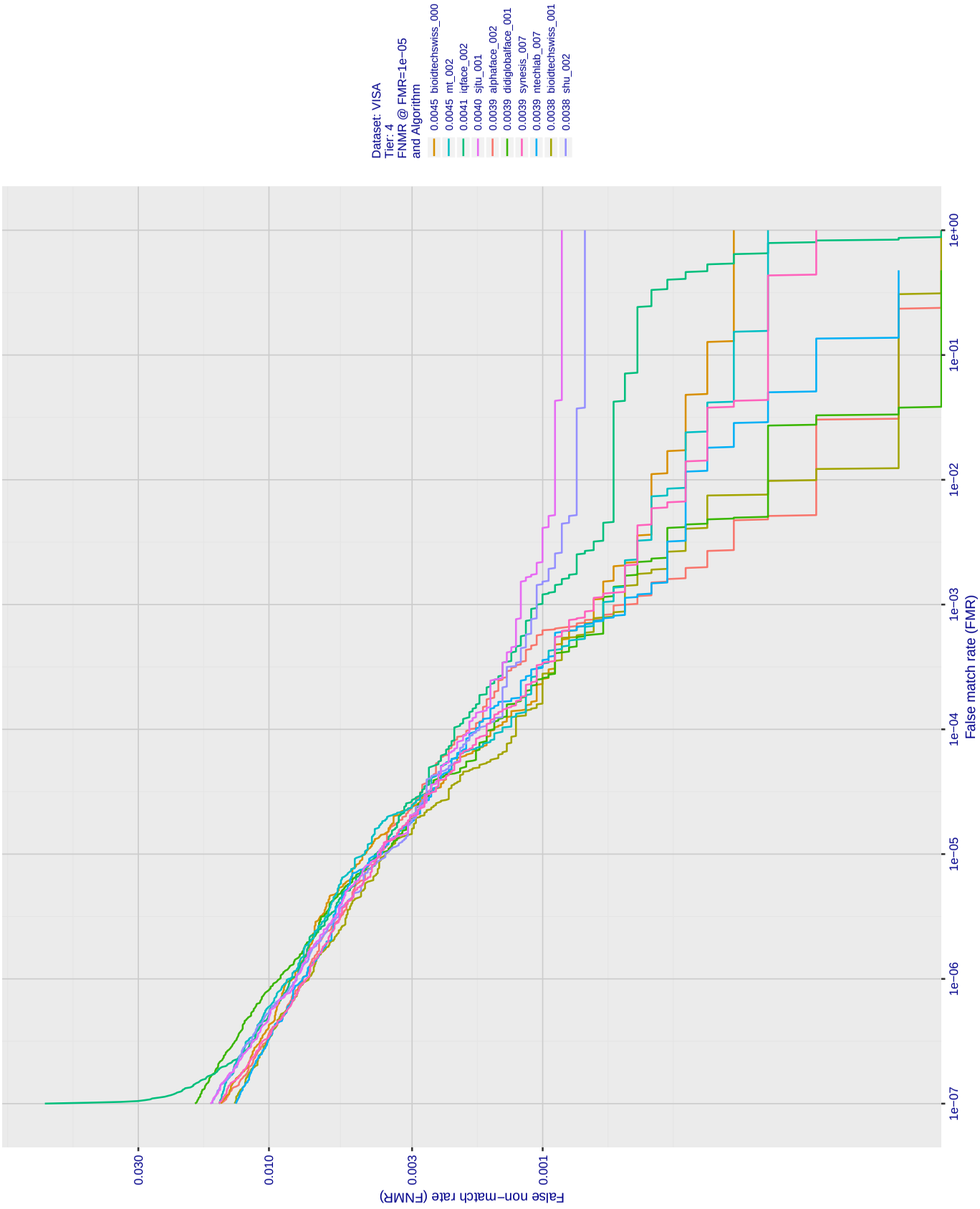

Figure 18: For the visa images, detection error tradeoff (DET) *characteristics showing false non-match rate vs. false match rate plotted parametrically on threshold, T. The scales are logarithmic in order to show many decades of* FMR.

FNMR(T) "False non-match rate"
FMR(T) "False match rate"

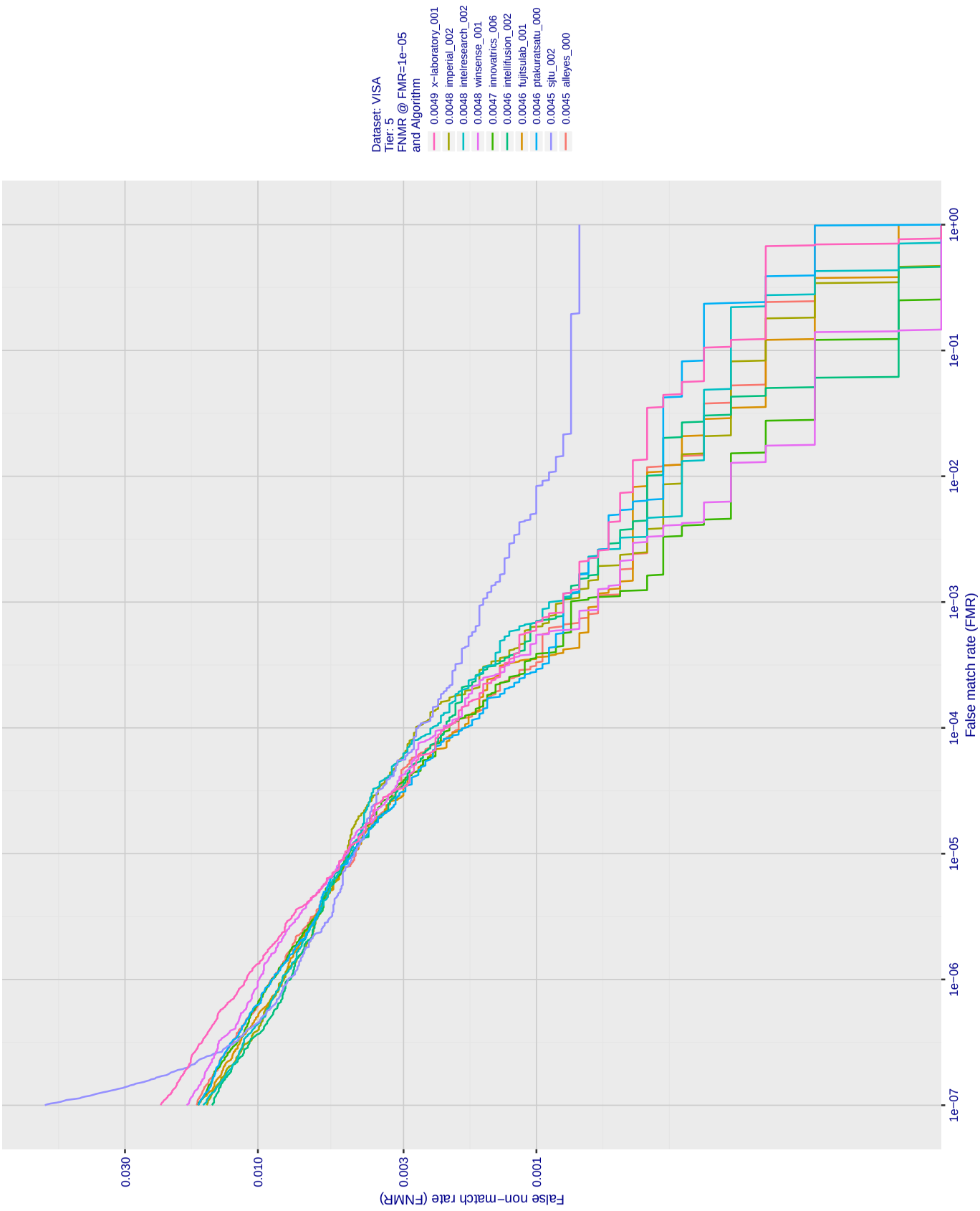

Figure 19: For the visa images, detection error tradeoff (DET) *characteristics showing false non-match rate vs. false match rate plotted parametrically on threshold, T. The scales are logarithmic in order to show many decades of* FMR.

FNMR(T) "False non-match rate"
FMR(T) "False match rate"

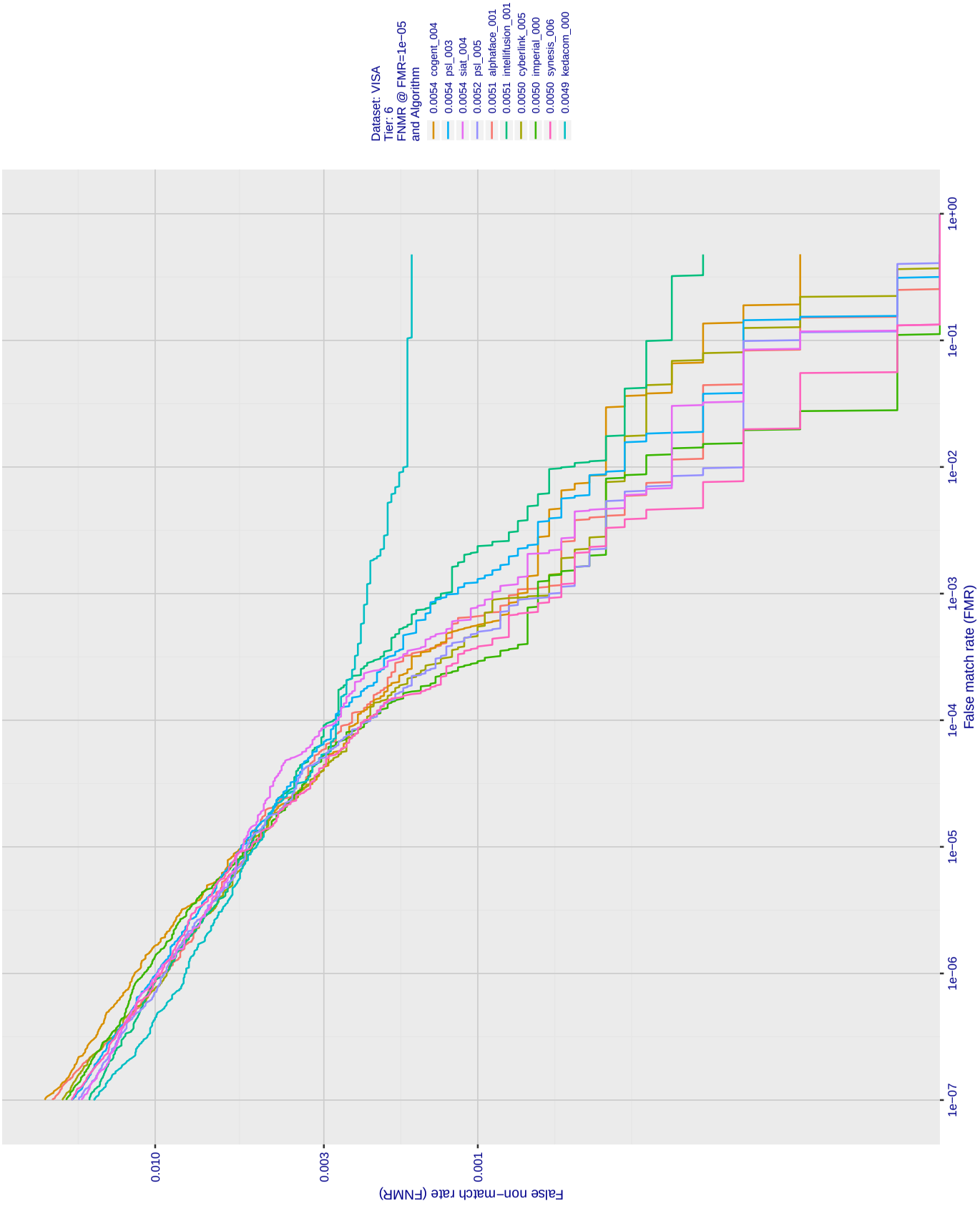

Figure 20: For the visa images, detection error tradeoff (DET) *characteristics showing false non-match rate vs. false match rate plotted parametrically on threshold, T. The scales are logarithmic in order to show many decades of* FMR.

FNMR(T) "False non-match rate"
FMR(T) "False match rate"

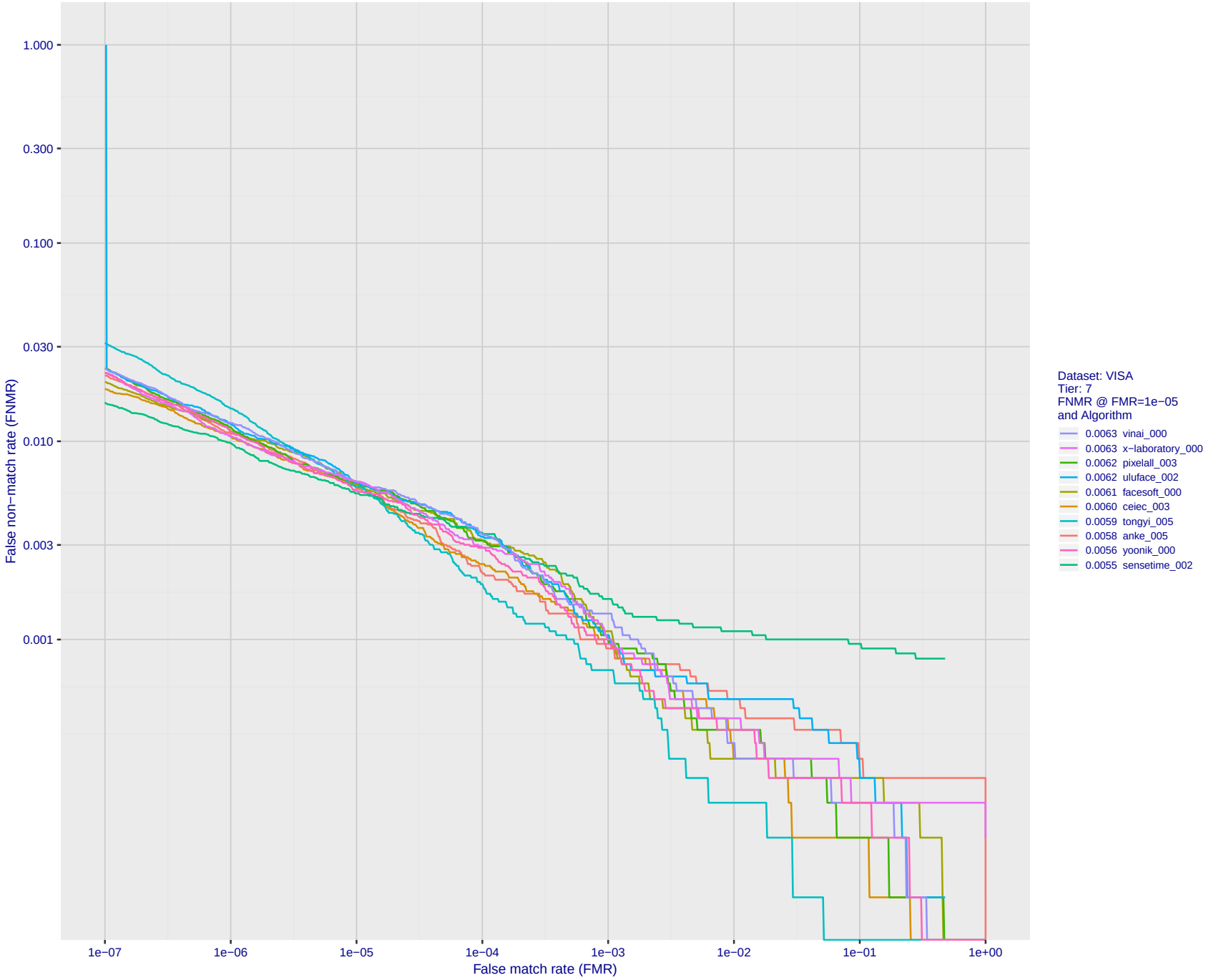

Figure 21: For the visa images, detection error tradeoff (DET) characteristics showing false non-match rate vs. false match rate plotted parametrically on threshold, T. The scales are logarithmic in order to show many decades of FMR.

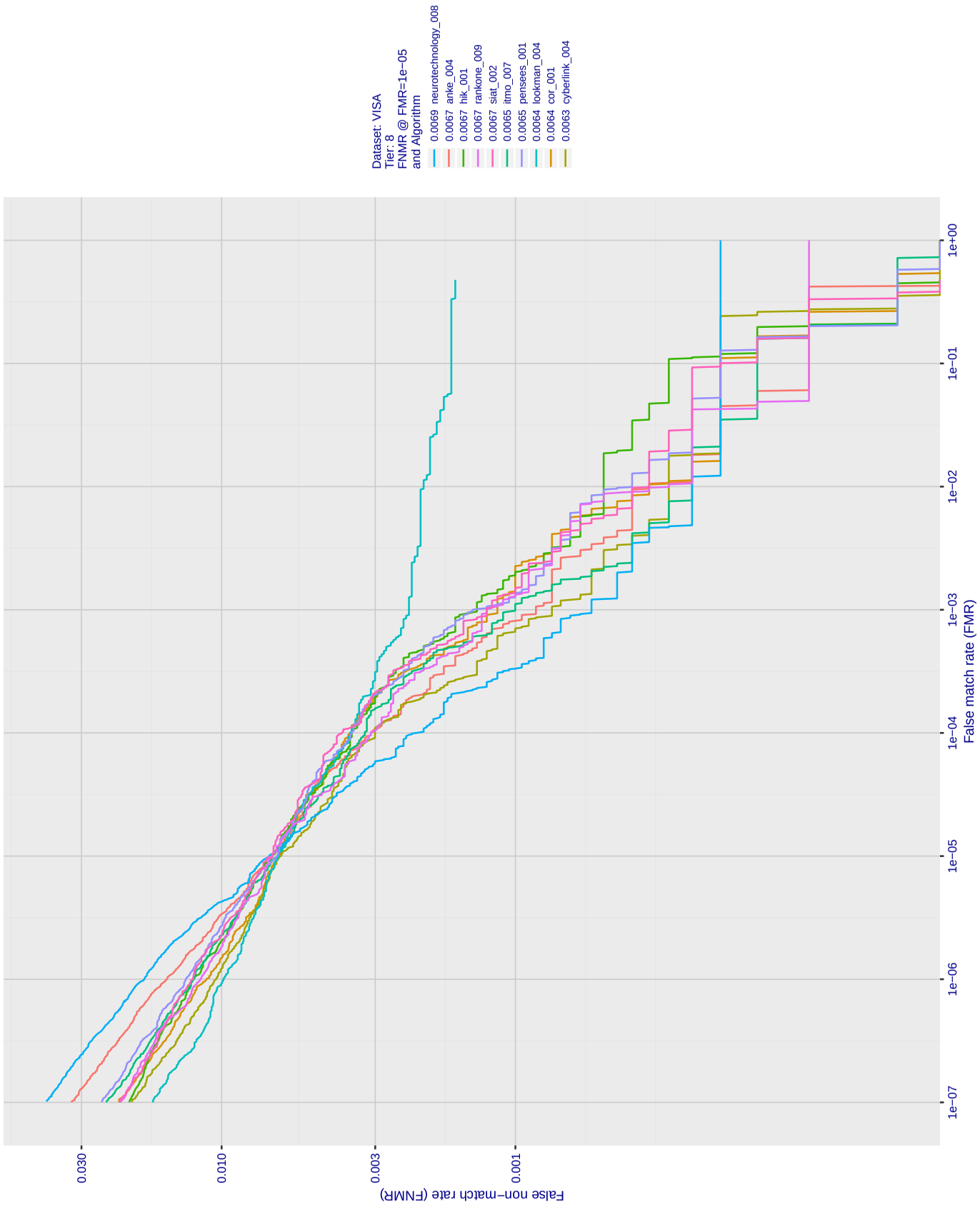

Figure 22: For the visa images, detection error tradeoff (DET) characteristics showing false non-match rate vs. false match rate plotted parametrically on threshold, T. The scales are logarithmic in order to show many decades of FMR.

FNMR(T) "False non-match rate"
FMR(T) "False match rate"

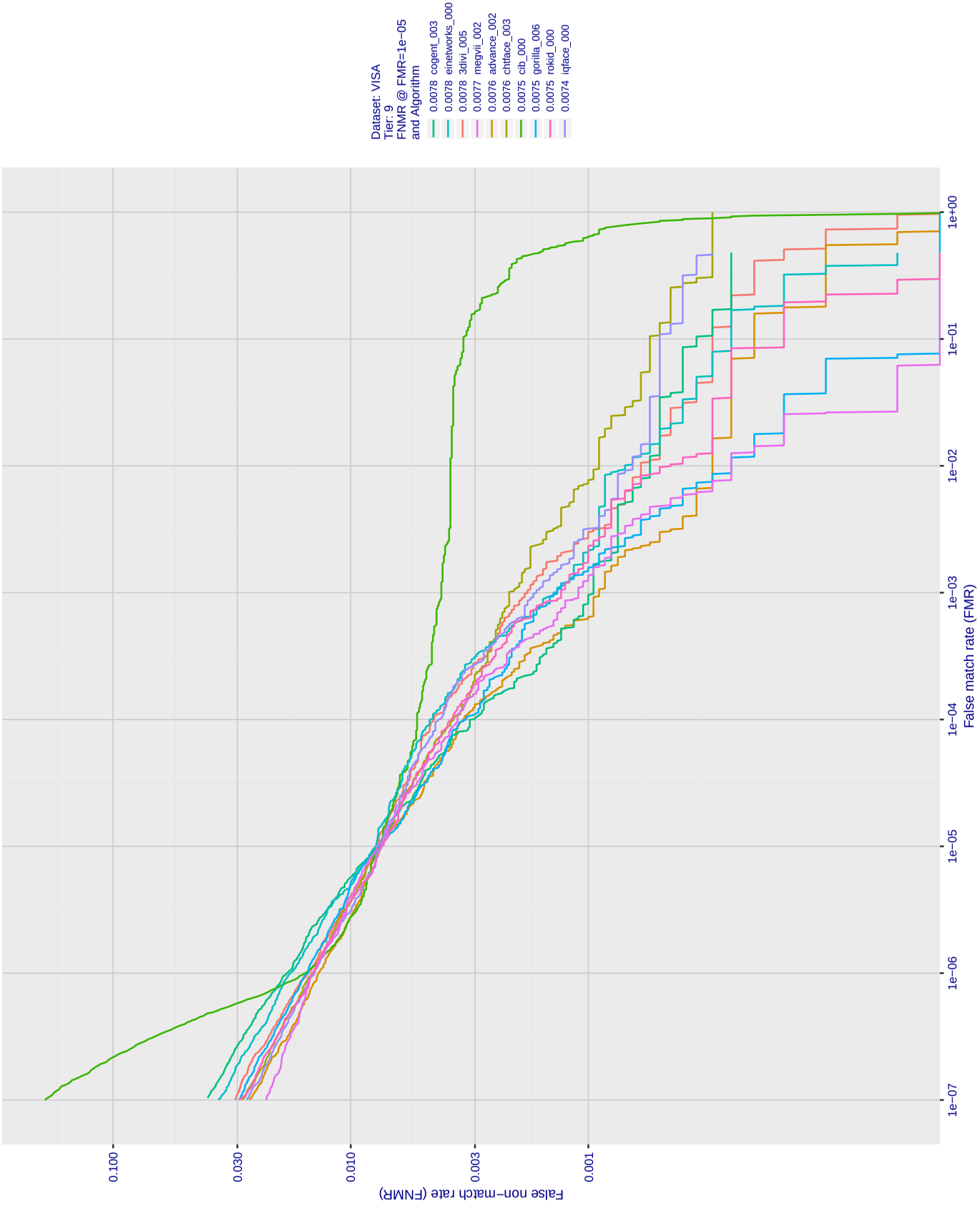

Figure 23: For the visa images, detection error tradeoff (DET) *characteristics showing false non-match rate vs. false match rate plotted parametrically on threshold, T. The scales are logarithmic in order to show many decades of* FMR.

FNMR(T) "False non-match rate"
FMR(T) "False match rate"

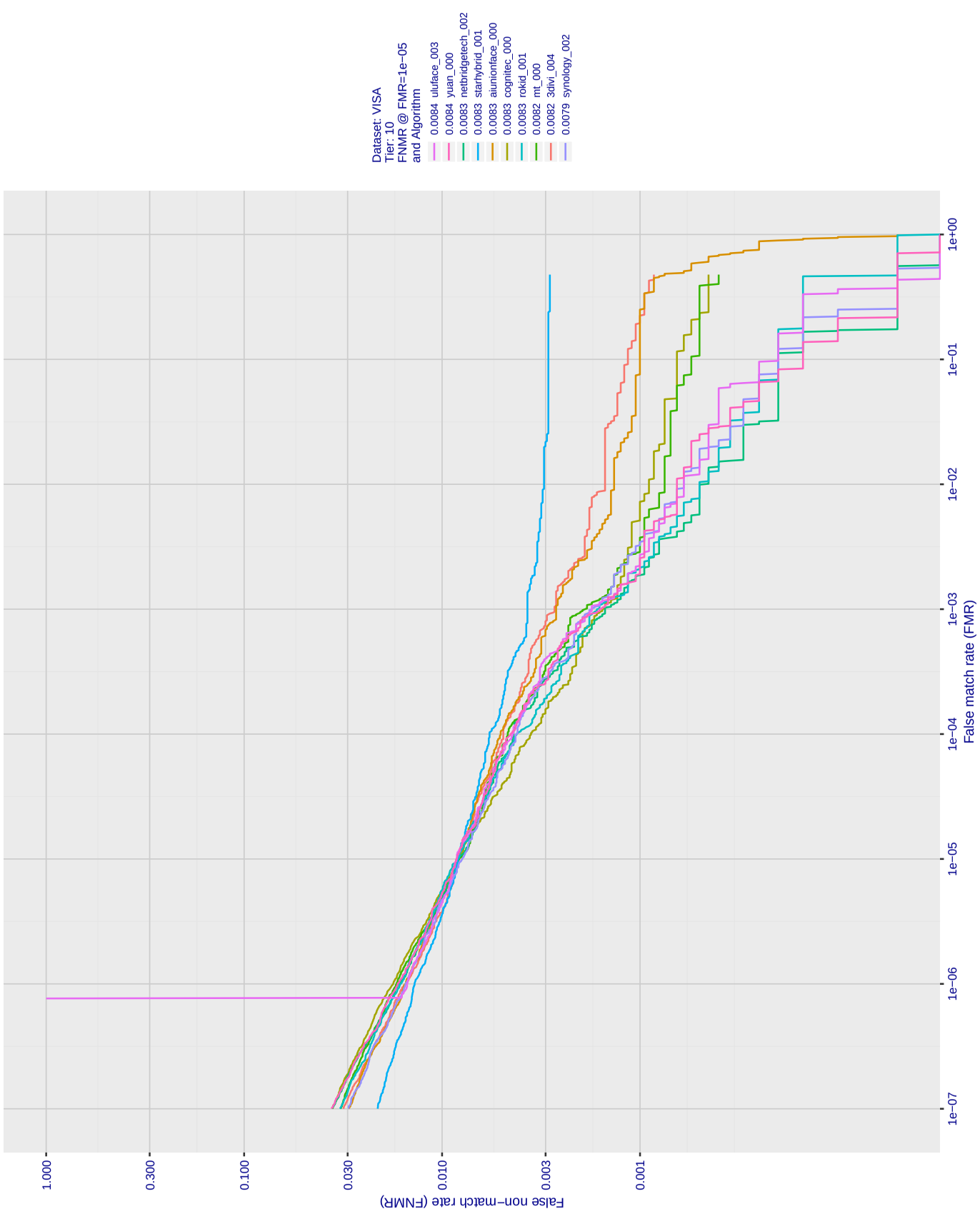

Figure 24: For the visa images, detection error tradeoff (DET) characteristics showing false non-match rate vs. false match rate plotted parametrically on threshold, T. The scales are logarithmic in order to show many decades of FMR.

FNMR(T) "False non-match rate"
FMR(T) "False match rate"

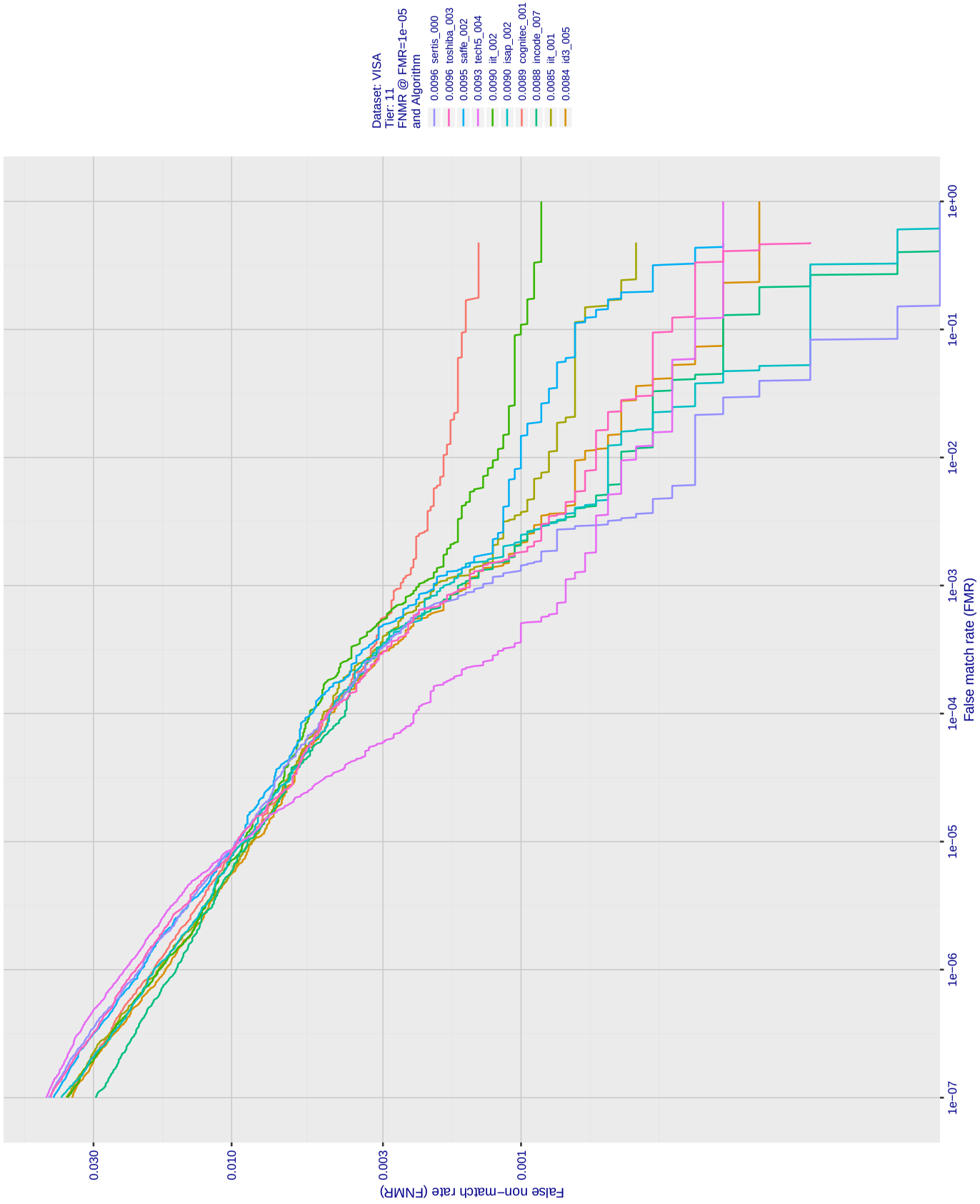

Figure 25: For the visa images, detection error tradeoff (DET) characteristics showing false non-match rate vs. false match rate plotted parametrically on threshold, T. The scales are logarithmic in order to show many decades of FMR.

FNMR(T) "False non-match rate"
FMR(T) "False match rate"

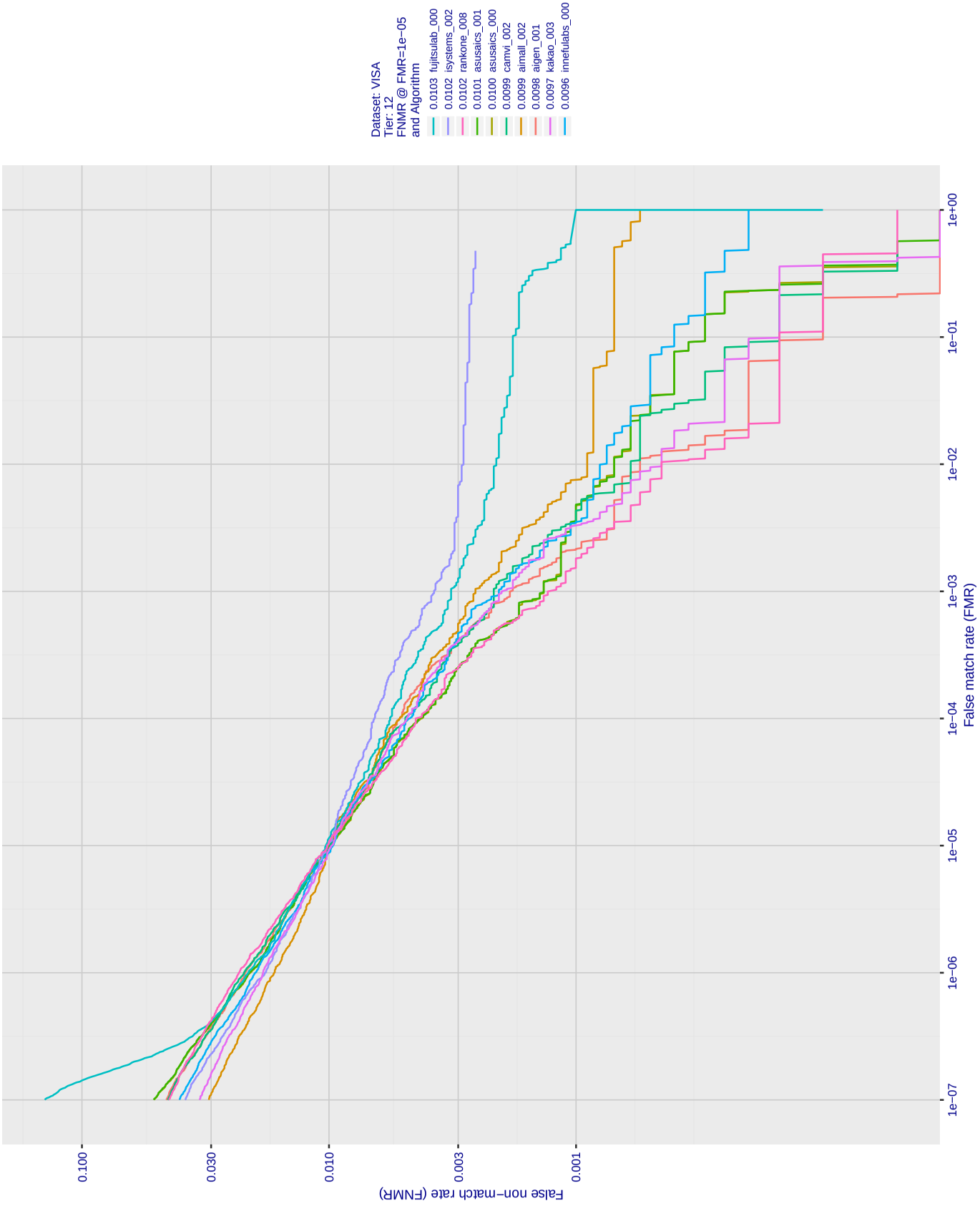

Figure 26: For the visa images, detection error tradeoff (DET) characteristics showing false non-match rate vs. false match rate plotted parametrically on threshold, T. The scales are logarithmic in order to show many decades of FMR.

FNMR(T) "False non-match rate"
FMR(T) "False match rate"

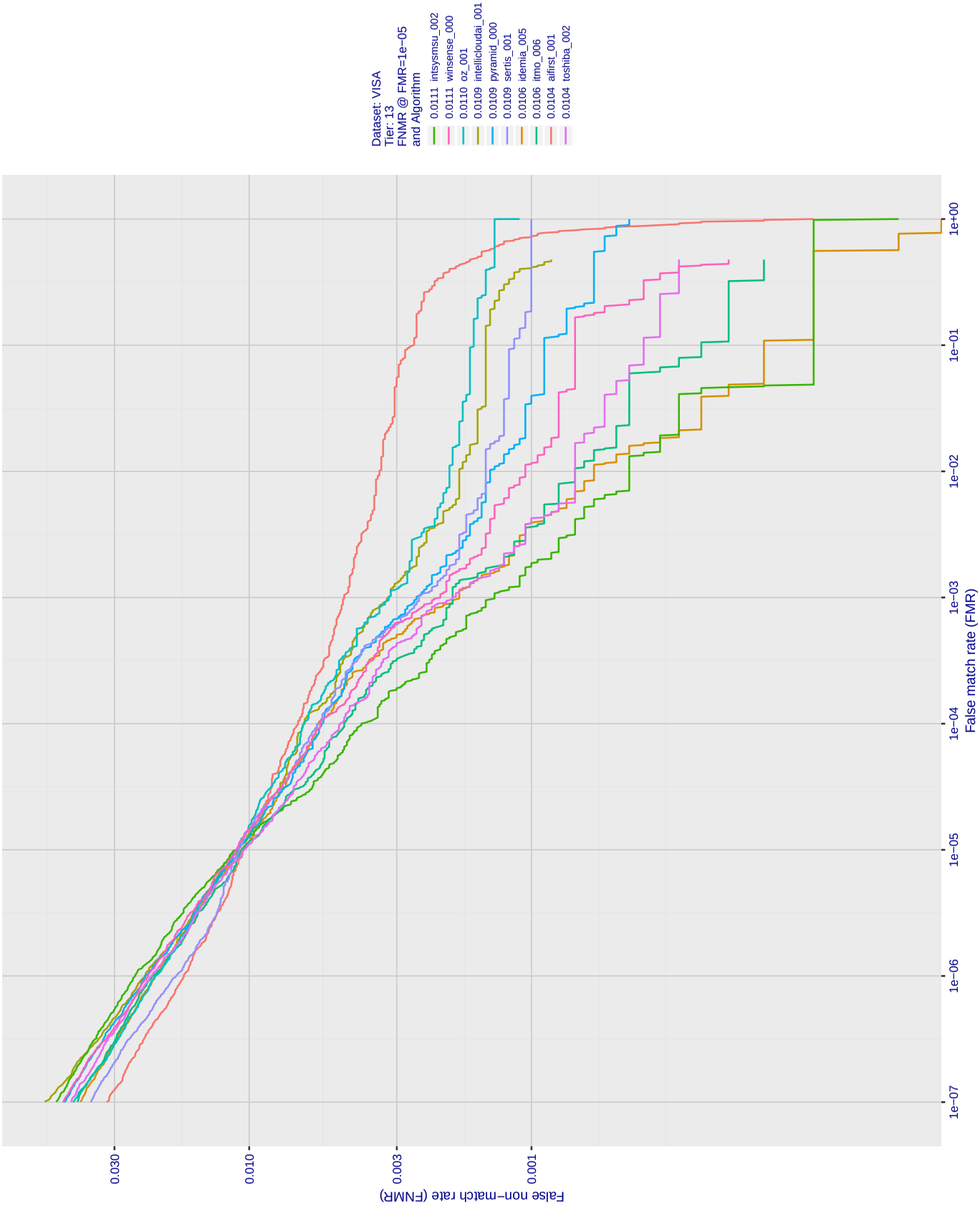

Figure 27: For the visa images, detection error tradeoff (DET) *characteristics showing false non-match rate vs. false match rate plotted parametrically on threshold, T. The scales are logarithmic in order to show many decades of* FMR.

FNMR(T) "False non-match rate"
FMR(T) "False match rate"

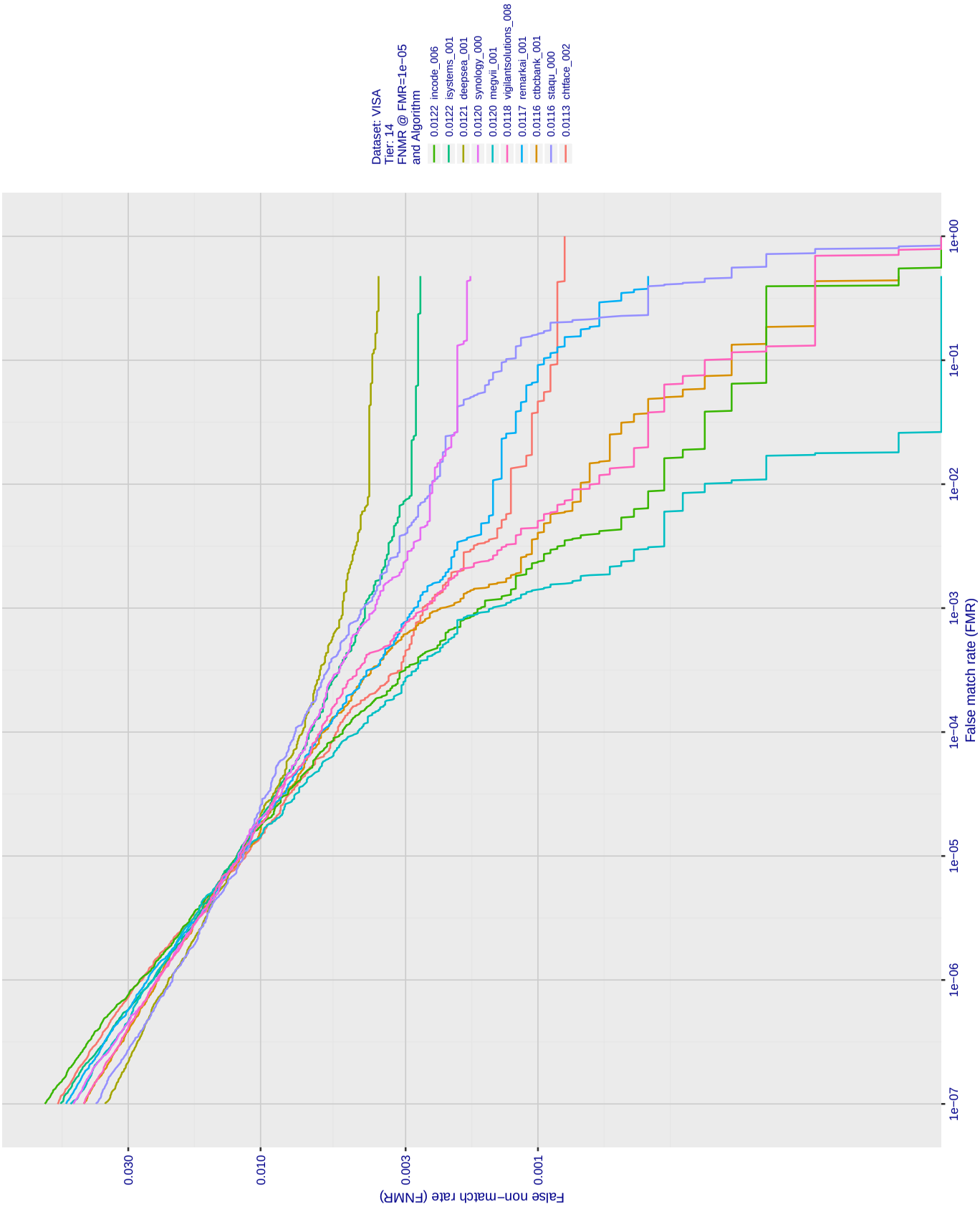

Figure 28: For the visa images, detection error tradeoff (DET) characteristics showing false non-match rate vs. false match rate plotted parametrically on threshold, T. The scales are logarithmic in order to show many decades of FMR.

FNMR(T) "False non-match rate"
FMR(T) "False match rate"

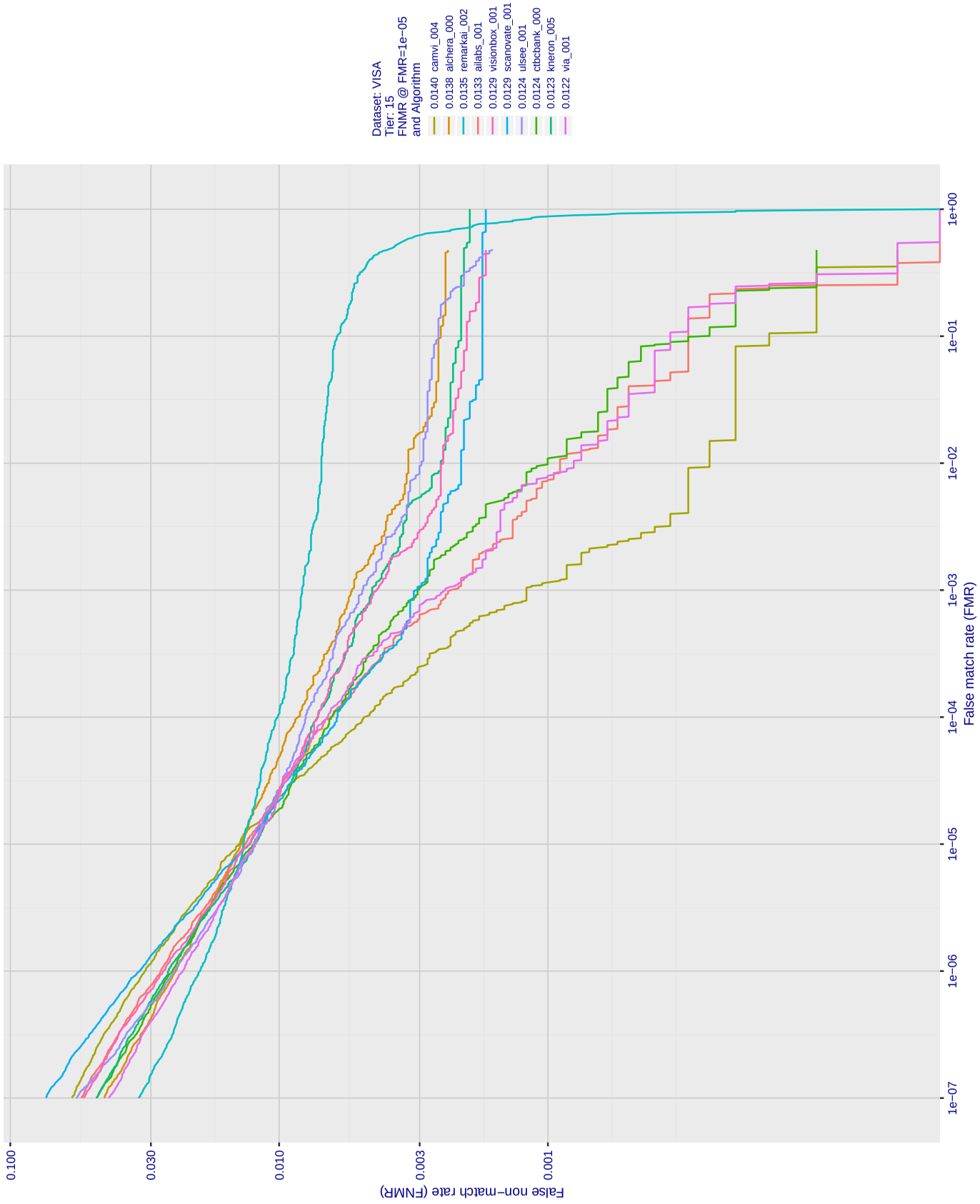

Figure 29: For the visa images, detection error tradeoff (DET) *characteristics showing false non-match rate vs. false match rate plotted parametrically on threshold, T. The scales are logarithmic in order to show many decades of* FMR.

FNMR(T) "False non-match rate"
FMR(T) "False match rate"

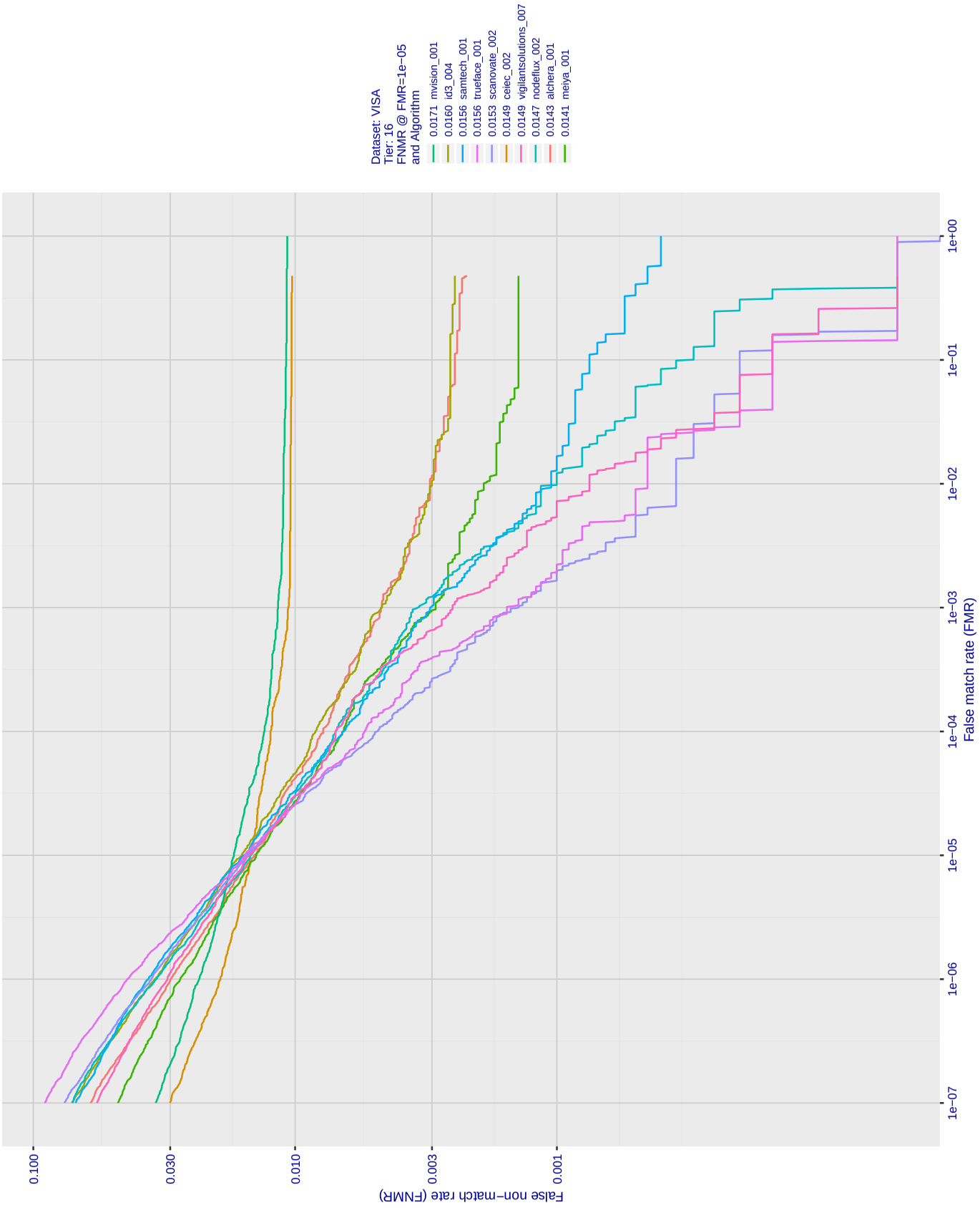

Figure 30: For the visa images, detection error tradeoff (DET) characteristics showing false non-match rate vs. false match rate plotted parametrically on threshold, T. The scales are logarithmic in order to show many decades of FMR.

FNMR(T) "False non-match rate"
FMR(T) "False match rate"

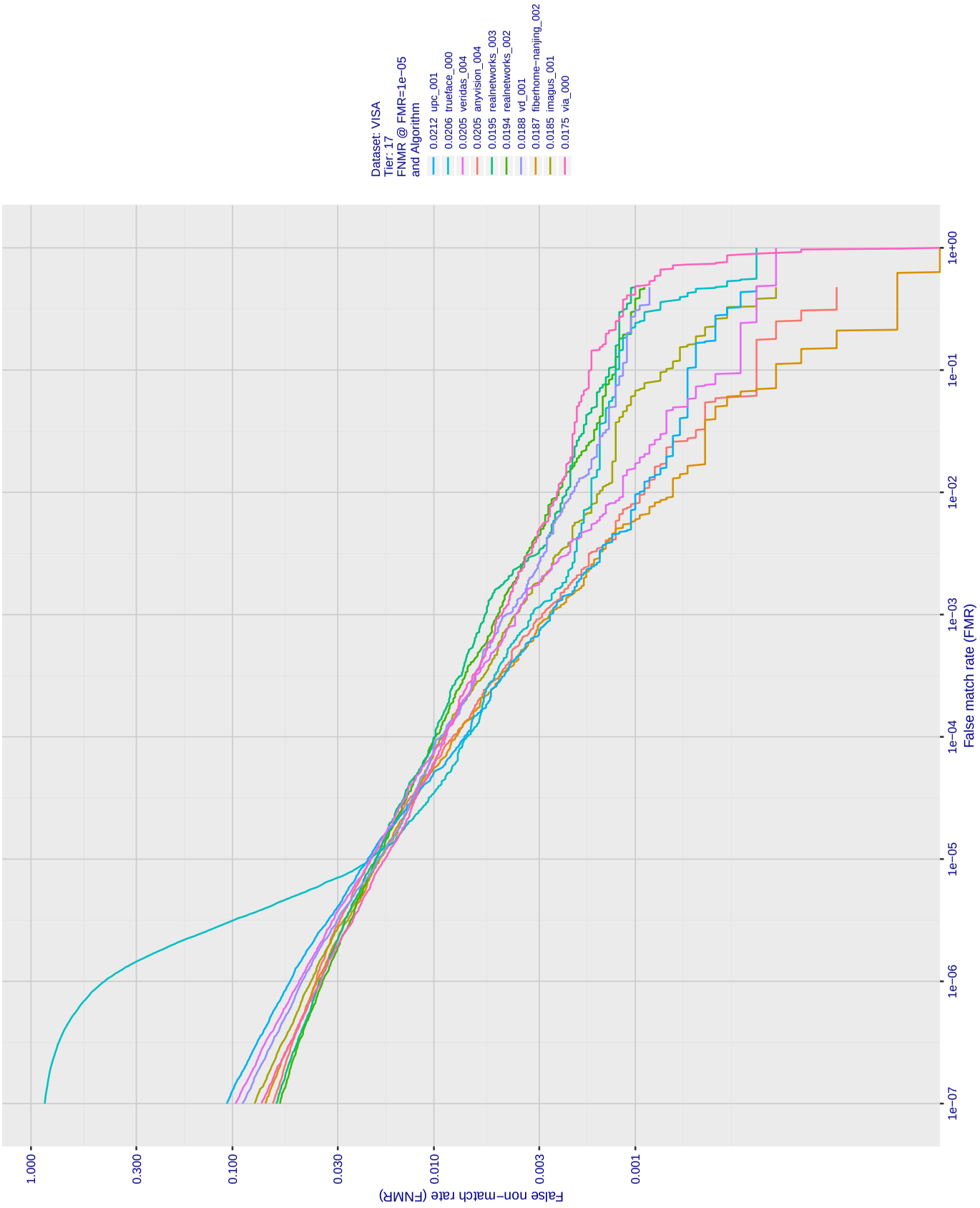

Figure 31: For the visa images, detection error tradeoff (DET) *characteristics showing false non-match rate vs. false match rate plotted parametrically on threshold, T. The scales are logarithmic in order to show many decades of* FMR.

FNMR(T) "False non-match rate"
FMR(T) "False match rate"

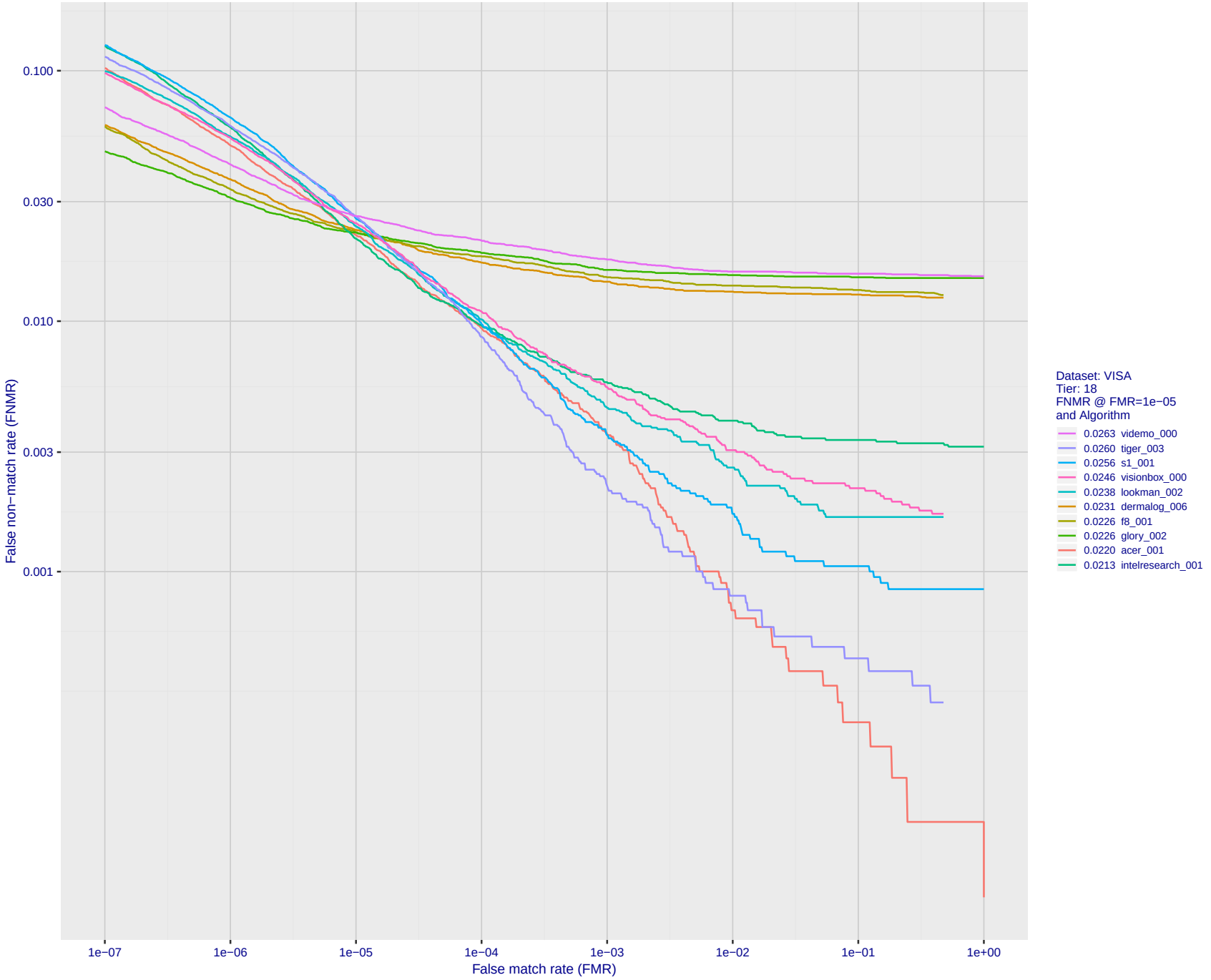

*Figure 32: For the visa images, detection error tradeoff (*DET*) characteristics showing false non-match rate vs. false match rate plotted parametrically on threshold, T. The scales are logarithmic in order to show many decades of* FMR*.*

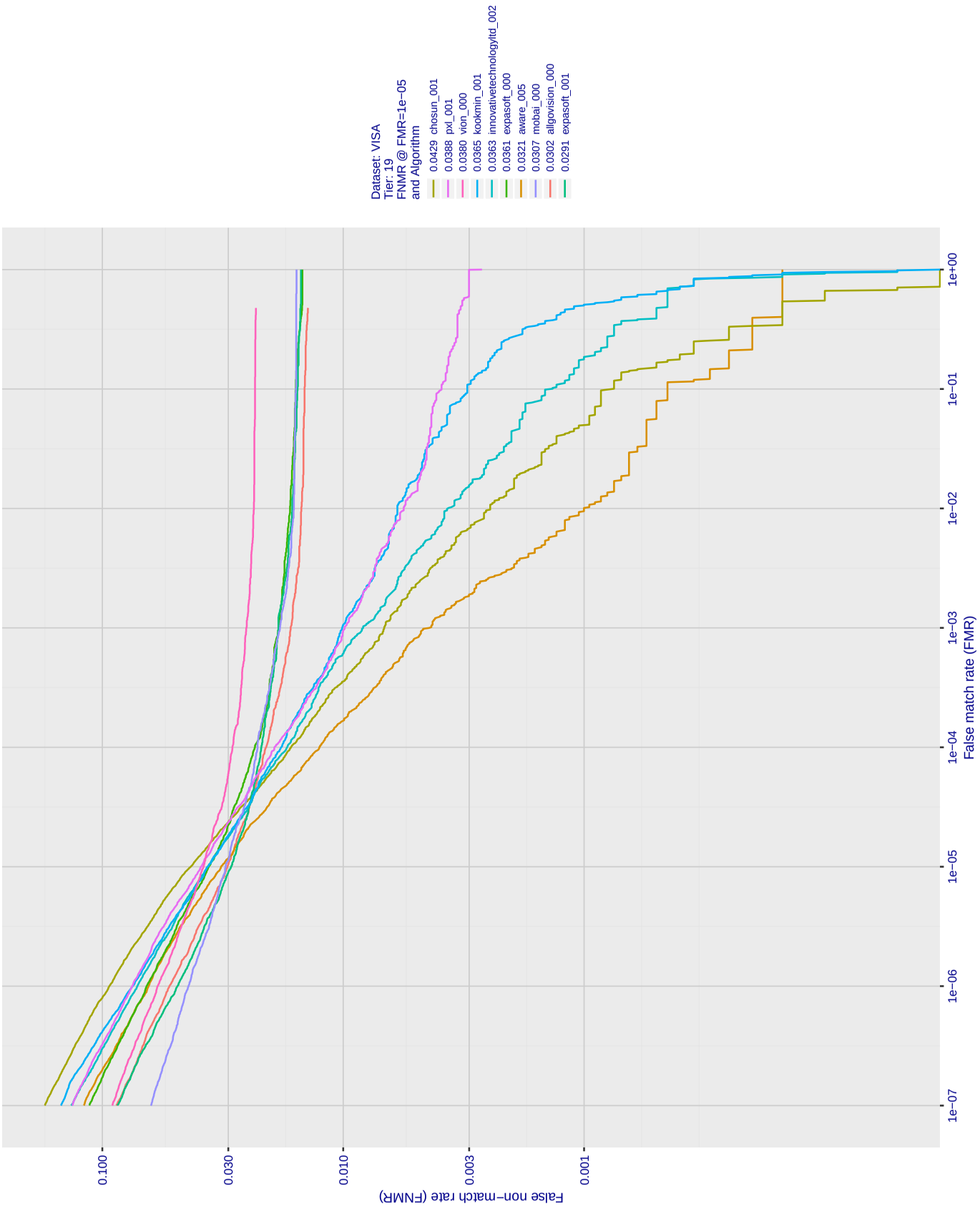

Figure 33: For the visa images, detection error tradeoff (DET) *characteristics showing false non-match rate vs. false match rate plotted parametrically on threshold, T. The scales are logarithmic in order to show many decades of* FMR.

FNMR(T) "False non-match rate"
FMR(T) "False match rate"

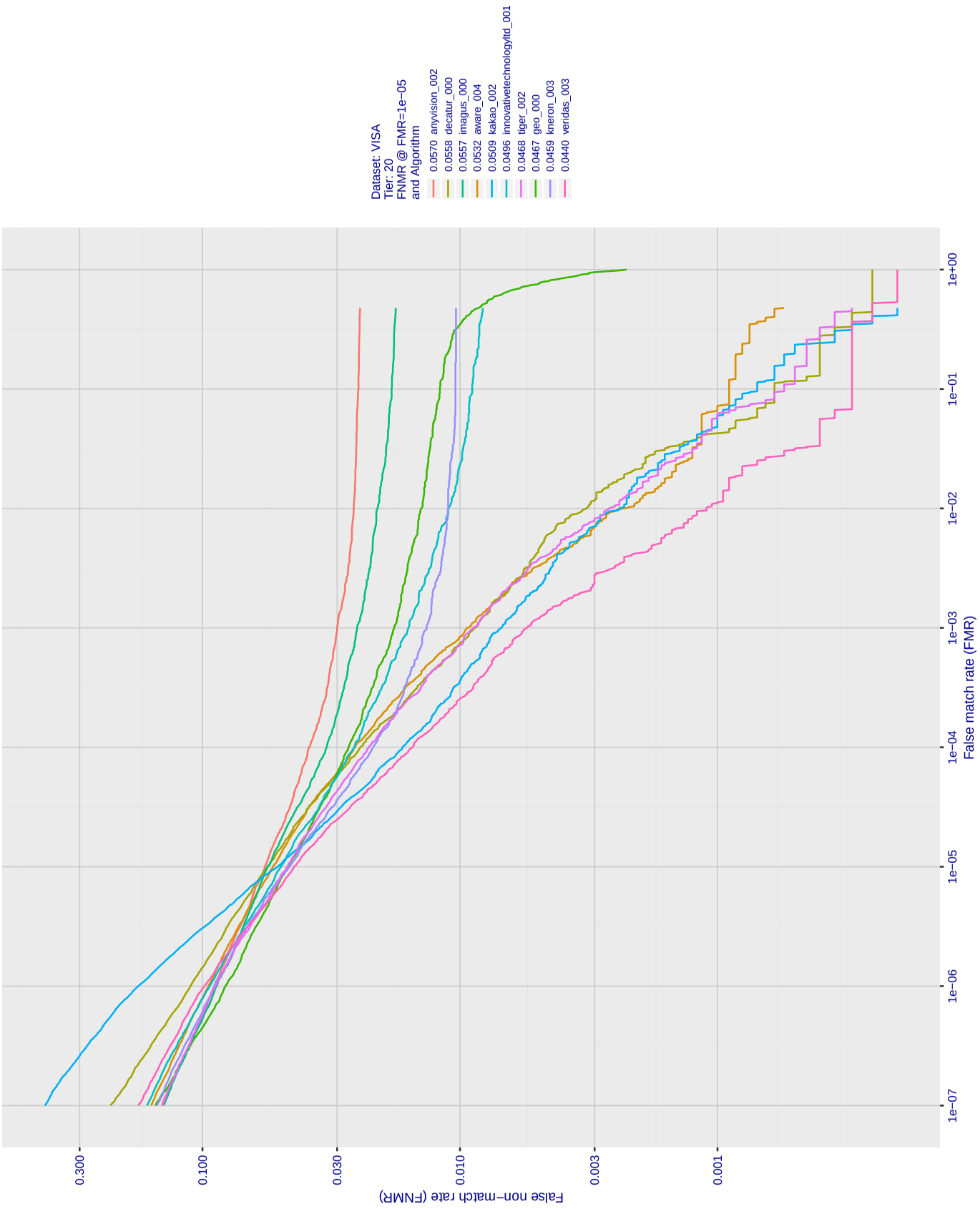

Figure 34: For the visa images, detection error tradeoff (DET) *characteristics showing false non-match rate vs. false match rate plotted parametrically on threshold, T. The scales are logarithmic in order to show many decades of* FMR.

FNMR(T) "False non-match rate"
FMR(T) "False match rate"

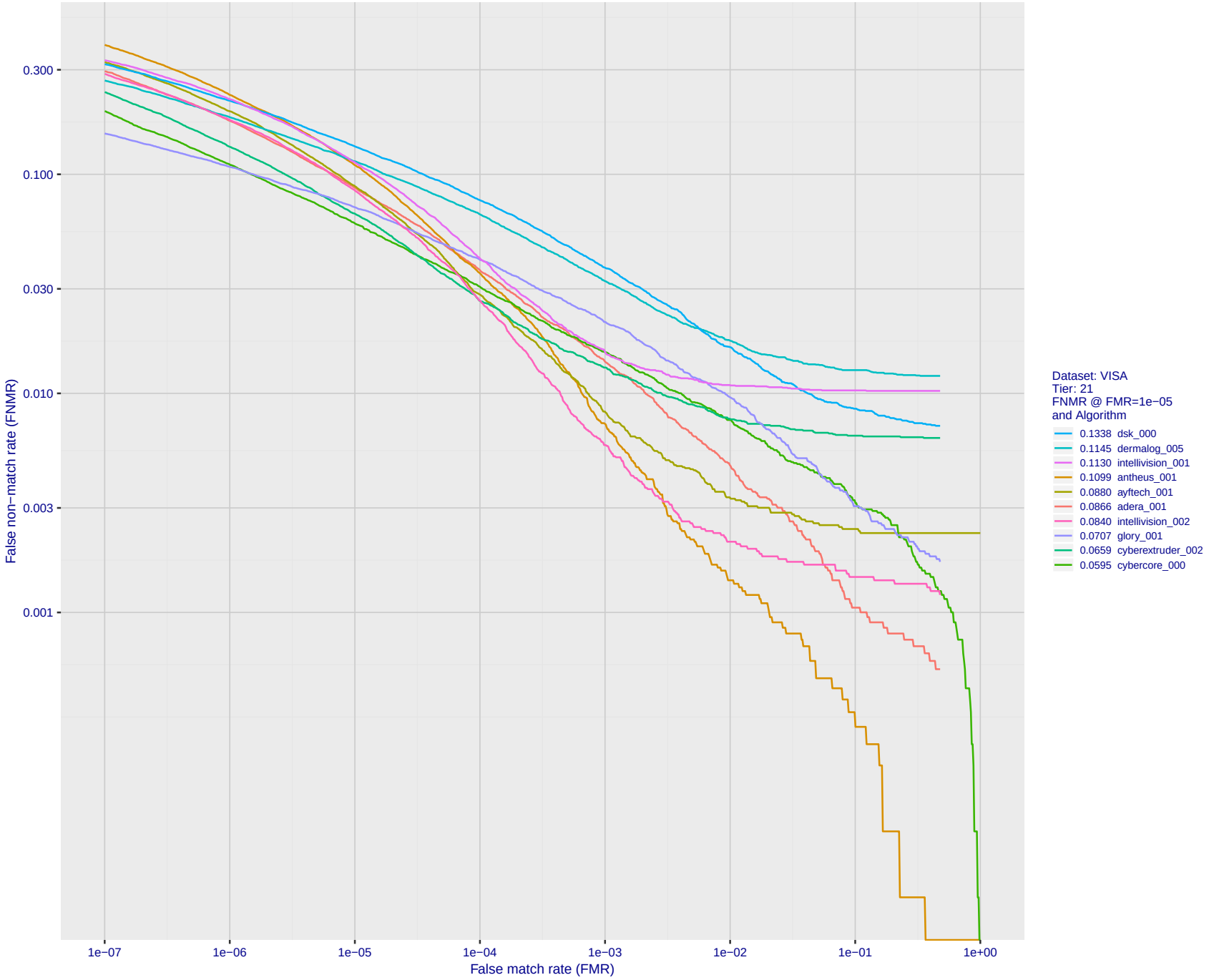

*Figure 35: For the visa images, detection error tradeoff (*DET*) characteristics showing false non-match rate vs. false match rate plotted parametrically on threshold, T. The scales are logarithmic in order to show many decades of* FMR*.*

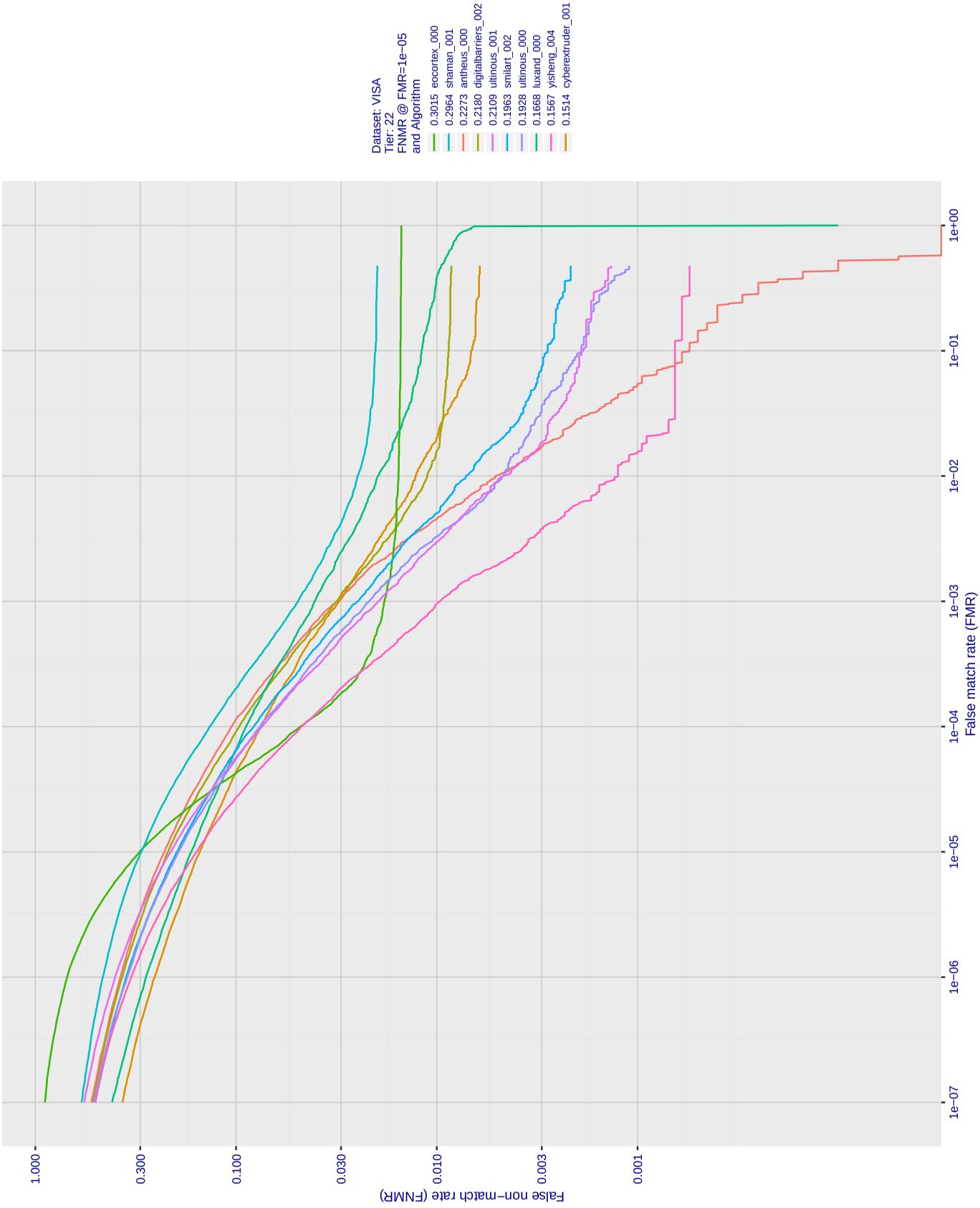

Figure 36: For the visa images, detection error tradeoff (DET) characteristics showing false non-match rate vs. false match rate plotted parametrically on threshold, T. The scales are logarithmic in order to show many decades of FMR.

FNMR(T) "False non-match rate"
FMR(T) "False match rate"

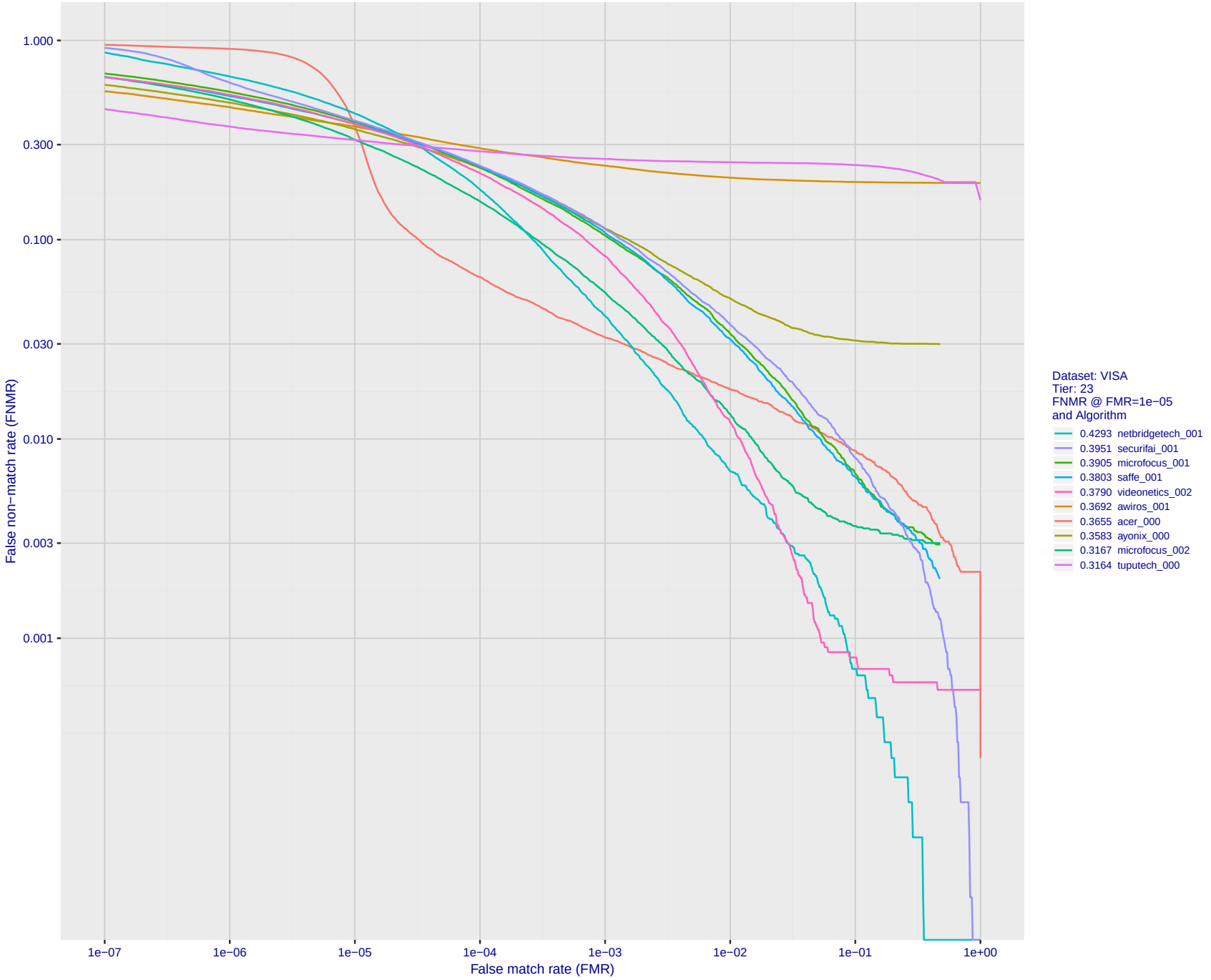

Figure 37: For the visa images, detection error tradeoff (DET) characteristics showing false non-match rate vs. false match rate plotted parametrically on threshold, T. The scales are logarithmic in order to show many decades of FMR.

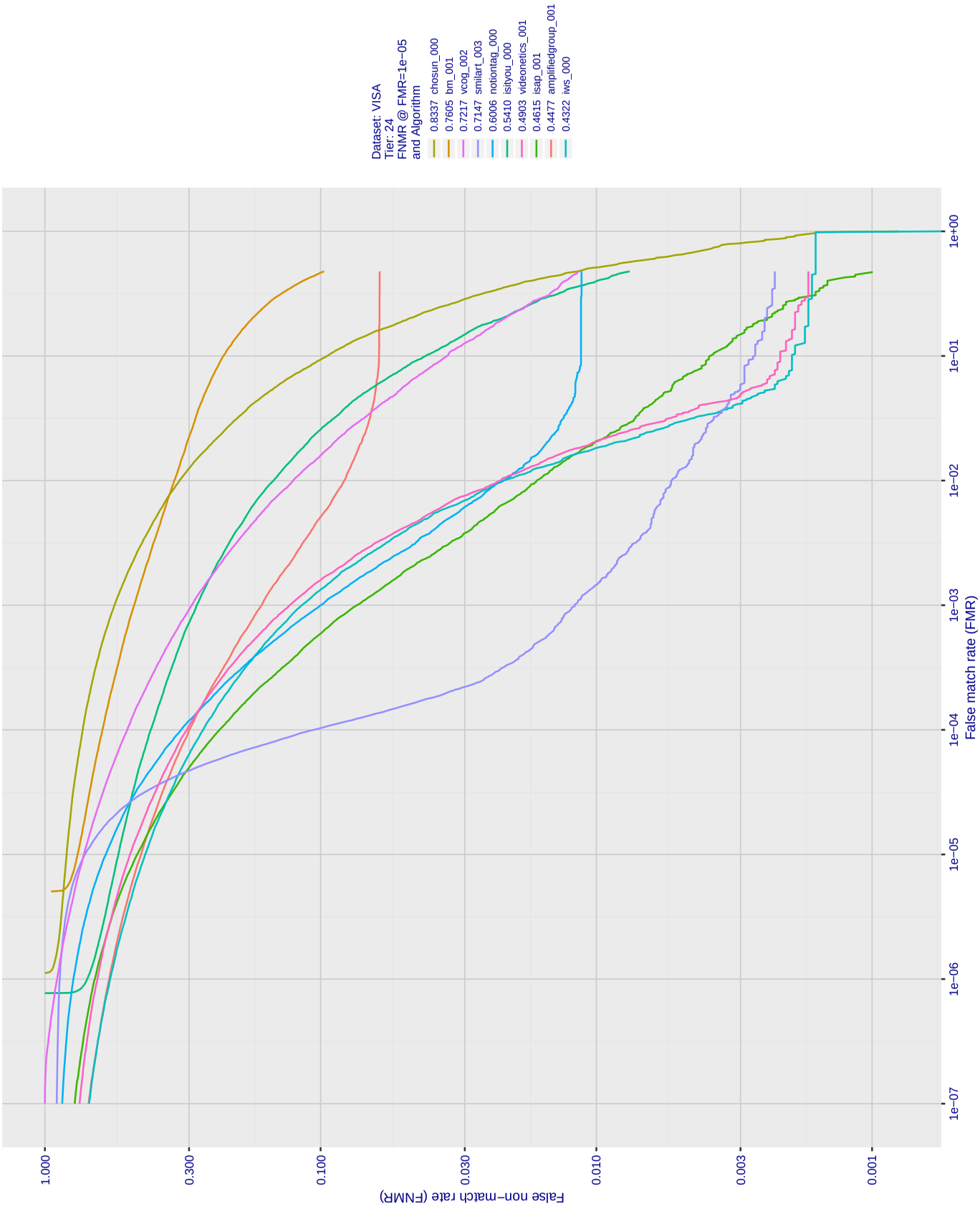

Figure 38: For the visa images, detection error tradeoff (DET) characteristics showing false non-match rate vs. false match rate plotted parametrically on threshold, T. The scales are logarithmic in order to show many decades of FMR.

FNMR(T) "False non-match rate"
FMR(T) "False match rate"

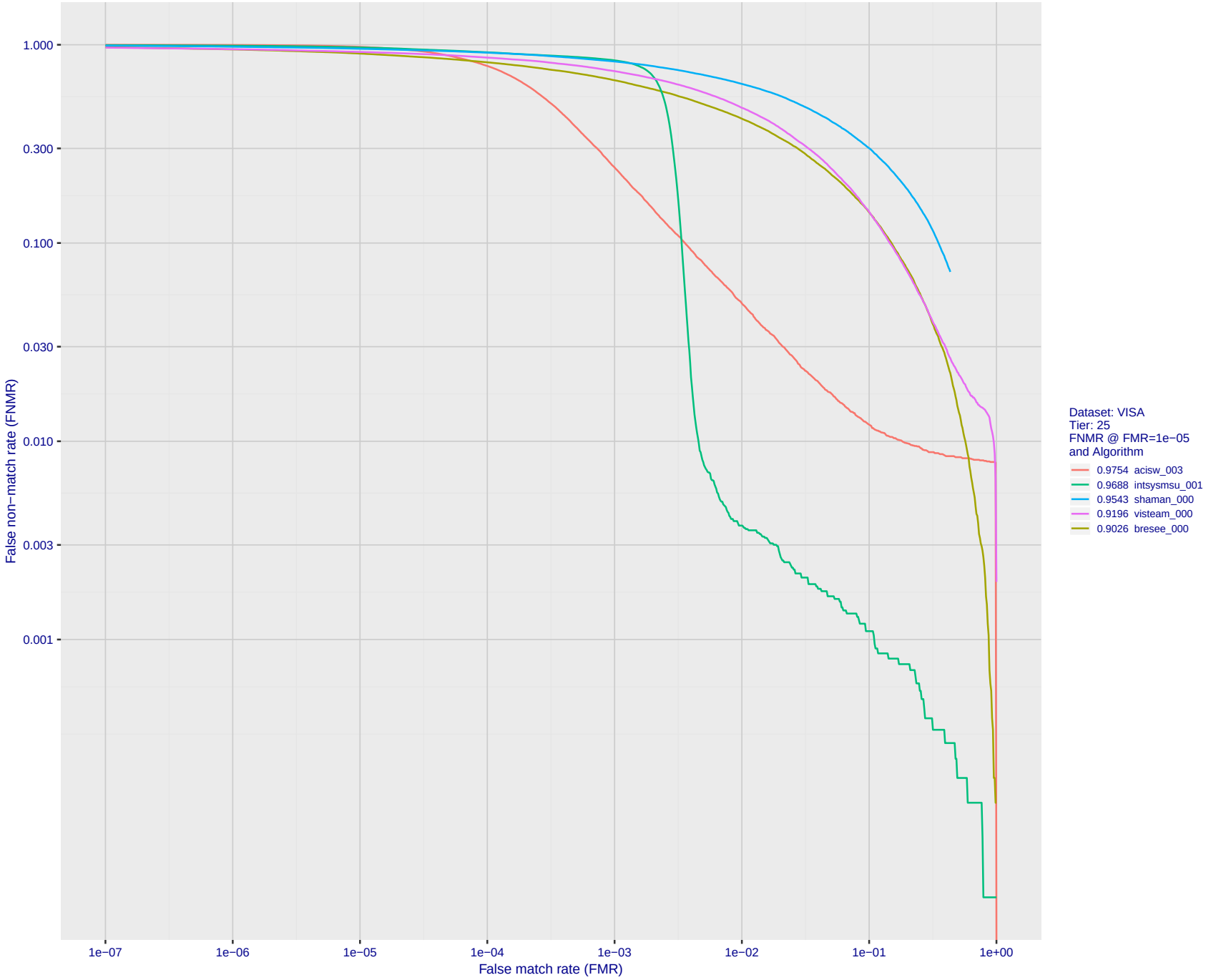

*Figure 39: For the visa images, detection error tradeoff (*DET*) characteristics showing false non-match rate vs. false match rate plotted parametrically on threshold, T. The scales are logarithmic in order to show many decades of* FMR*.*

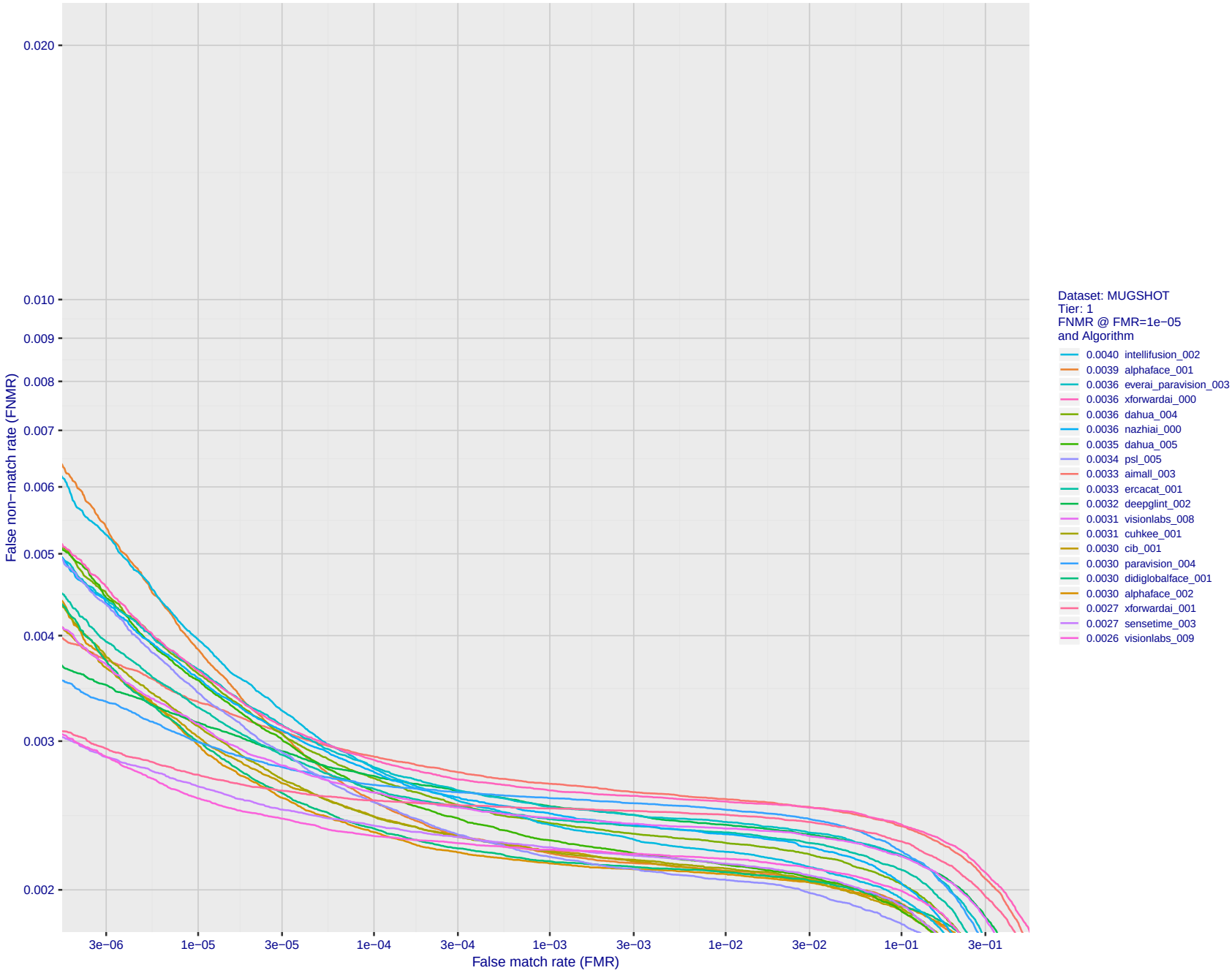

*Figure 40: For the mugshot images, detection error tradeoff (*DET*) characteristics showing false non-match rate vs. false match rate plotted parametrically on threshold, T. The scales are logarithmic in order to show decades of* FMR.

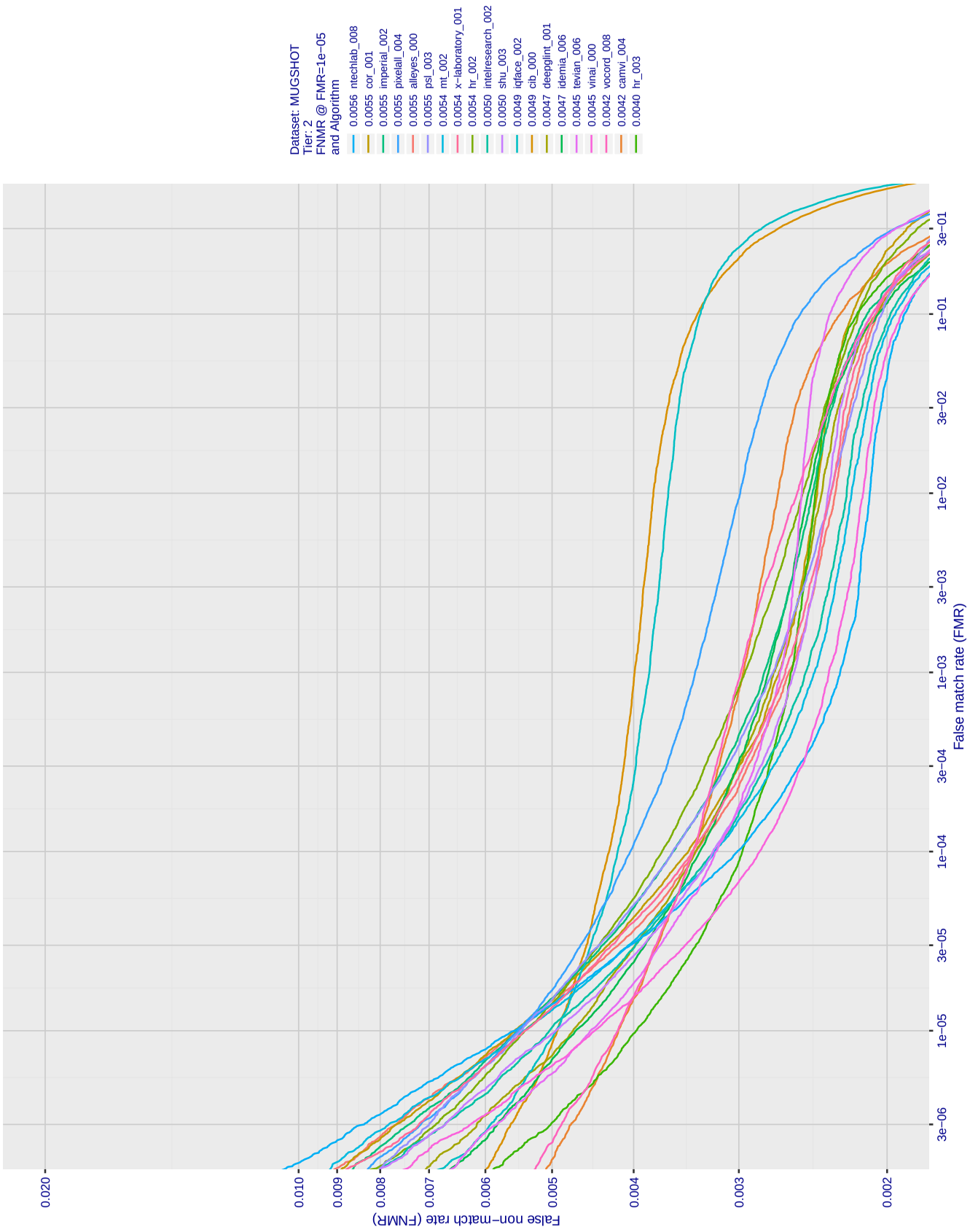

Figure 41: For the mugshot images, detection error tradeoff (DET) *characteristics showing false non-match rate vs. false match rate plotted parametrically on threshold, T. The scales are logarithmic in order to show decades of* FMR.

FNMR(T) "False non-match rate"
FMR(T) "False match rate"

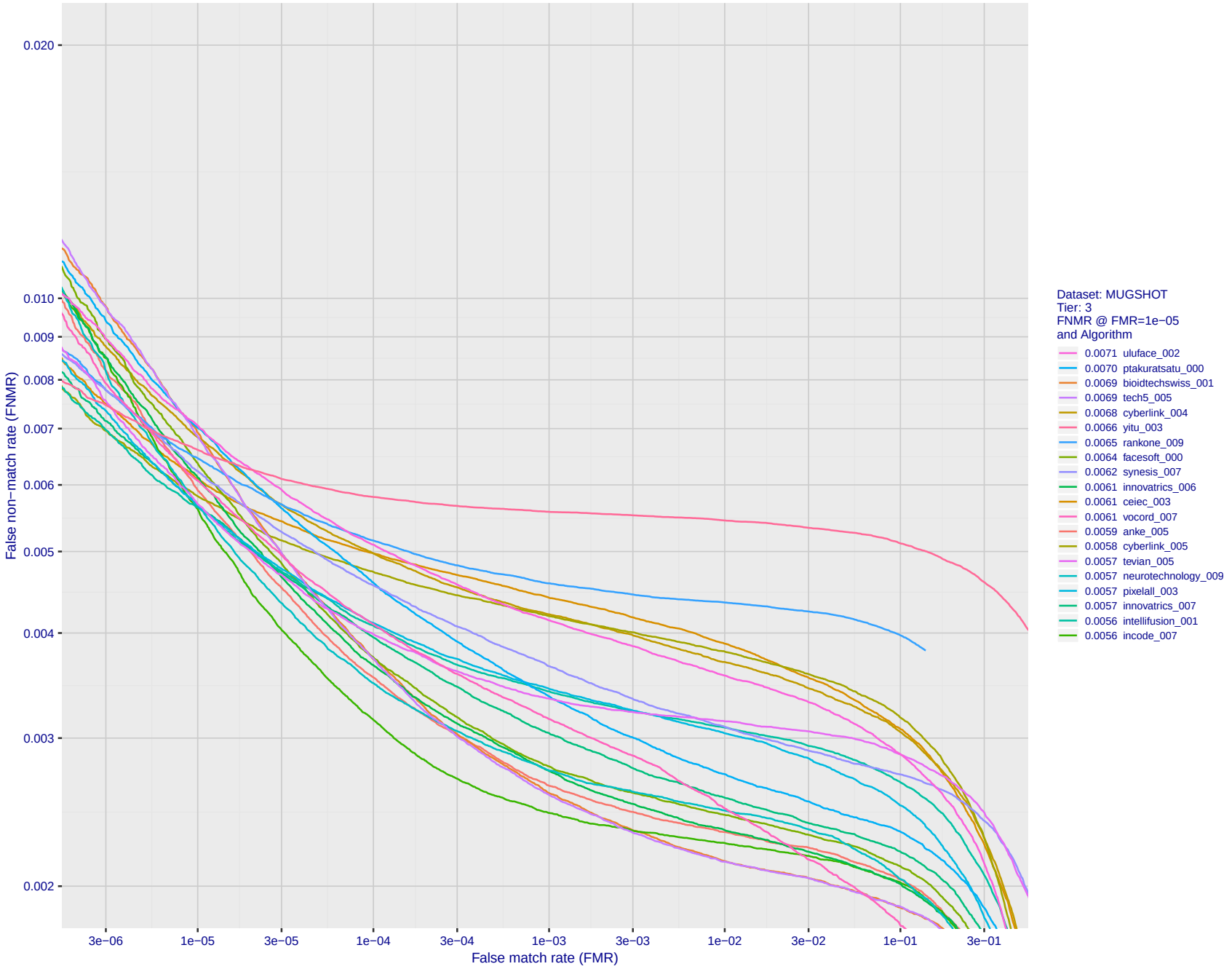

*Figure 42: For the mugshot images, detection error tradeoff (*DET*) characteristics showing false non-match rate vs. false match rate plotted parametrically on threshold, T. The scales are logarithmic in order to show decades of* FMR*.*

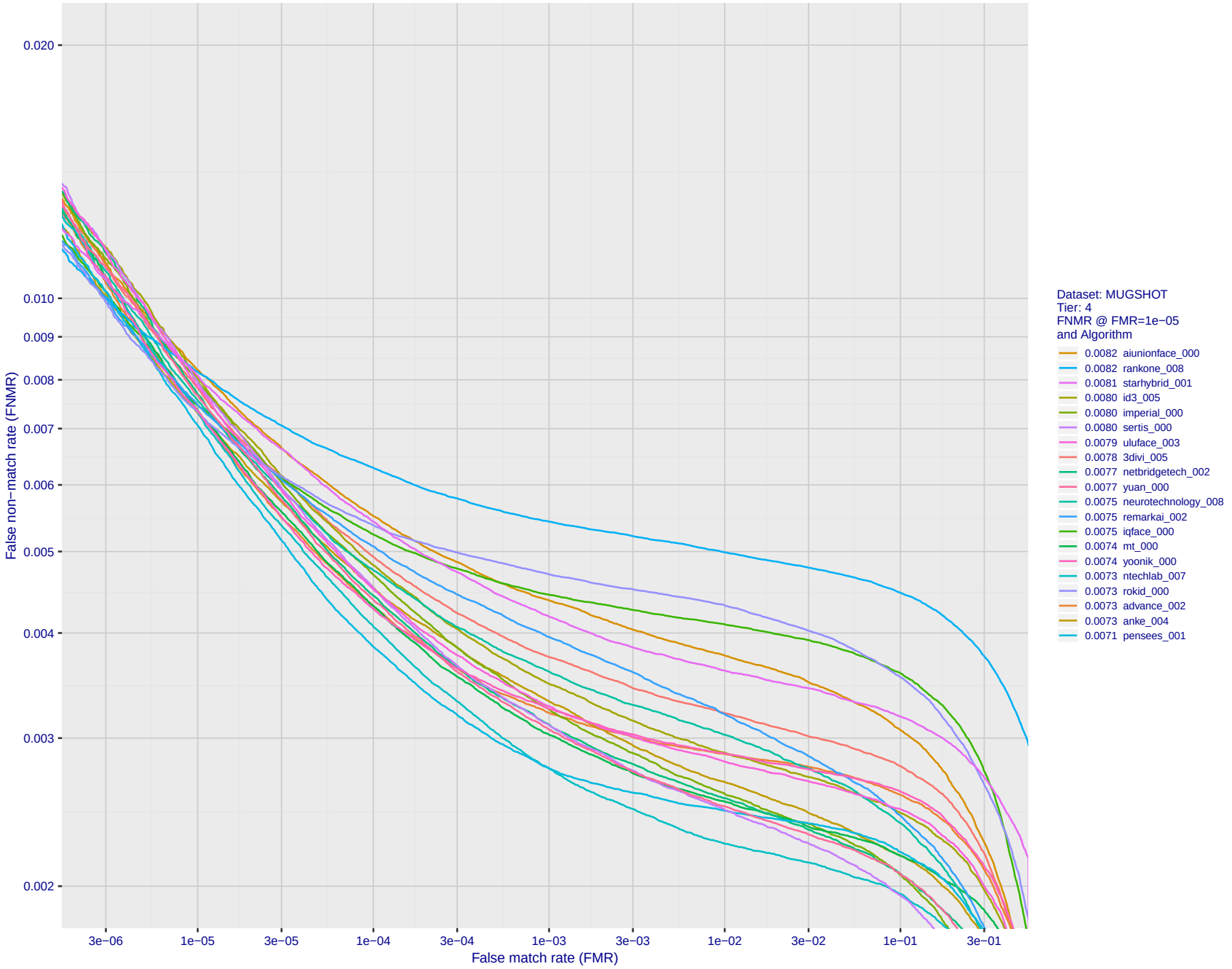

*Figure 43: For the mugshot images, detection error tradeoff (*DET*) characteristics showing false non-match rate vs. false match rate plotted parametrically on threshold, T. The scales are logarithmic in order to show decades of* FMR.

FNMR(T) "False non-match rate"
FMR(T) "False match rate"

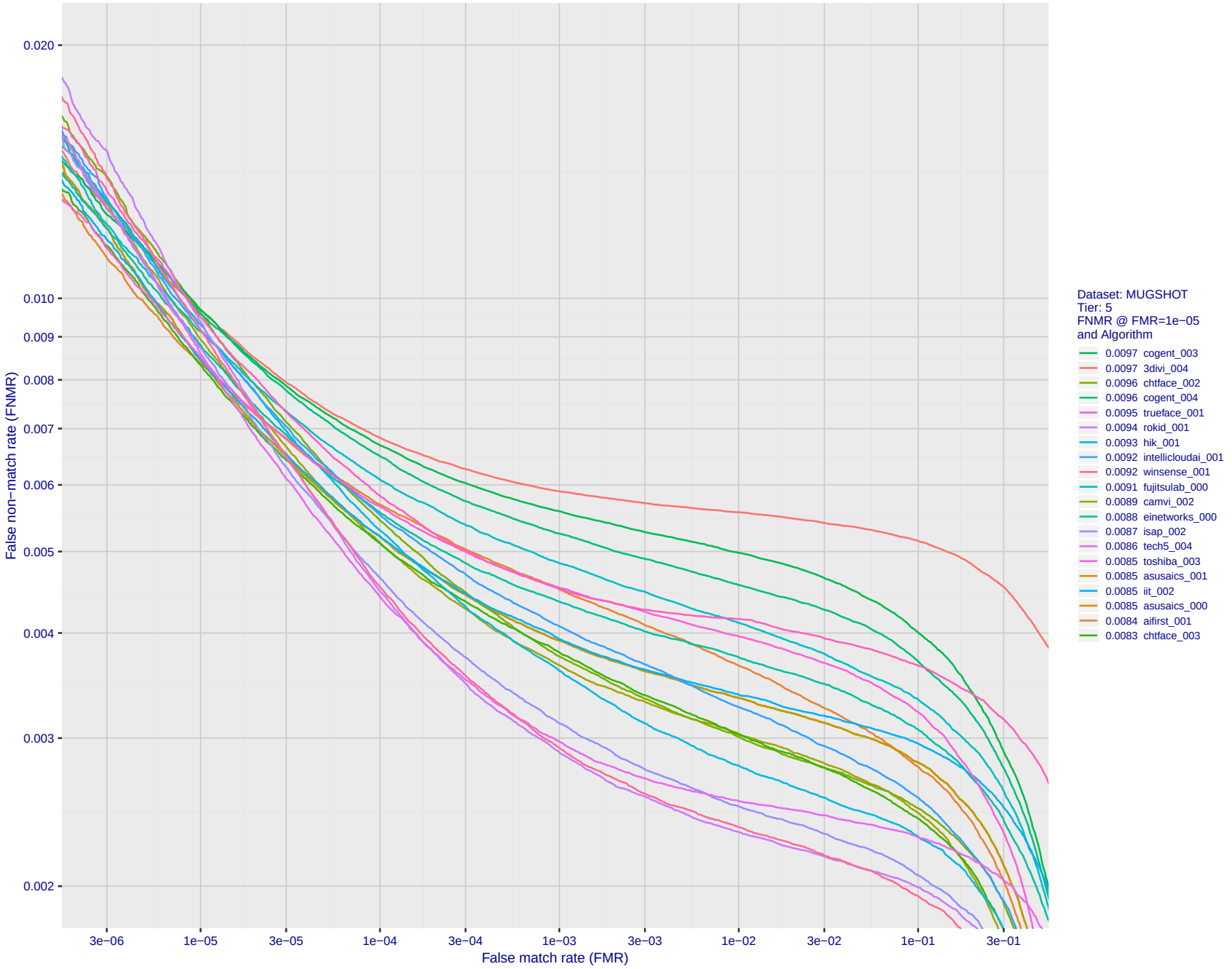

*Figure 44: For the mugshot images, detection error tradeoff (*DET*) characteristics showing false non-match rate vs. false match rate plotted parametrically on threshold, T. The scales are logarithmic in order to show decades of* FMR*.*

FNMR(T) "False non-match rate"
FMR(T) "False match rate"

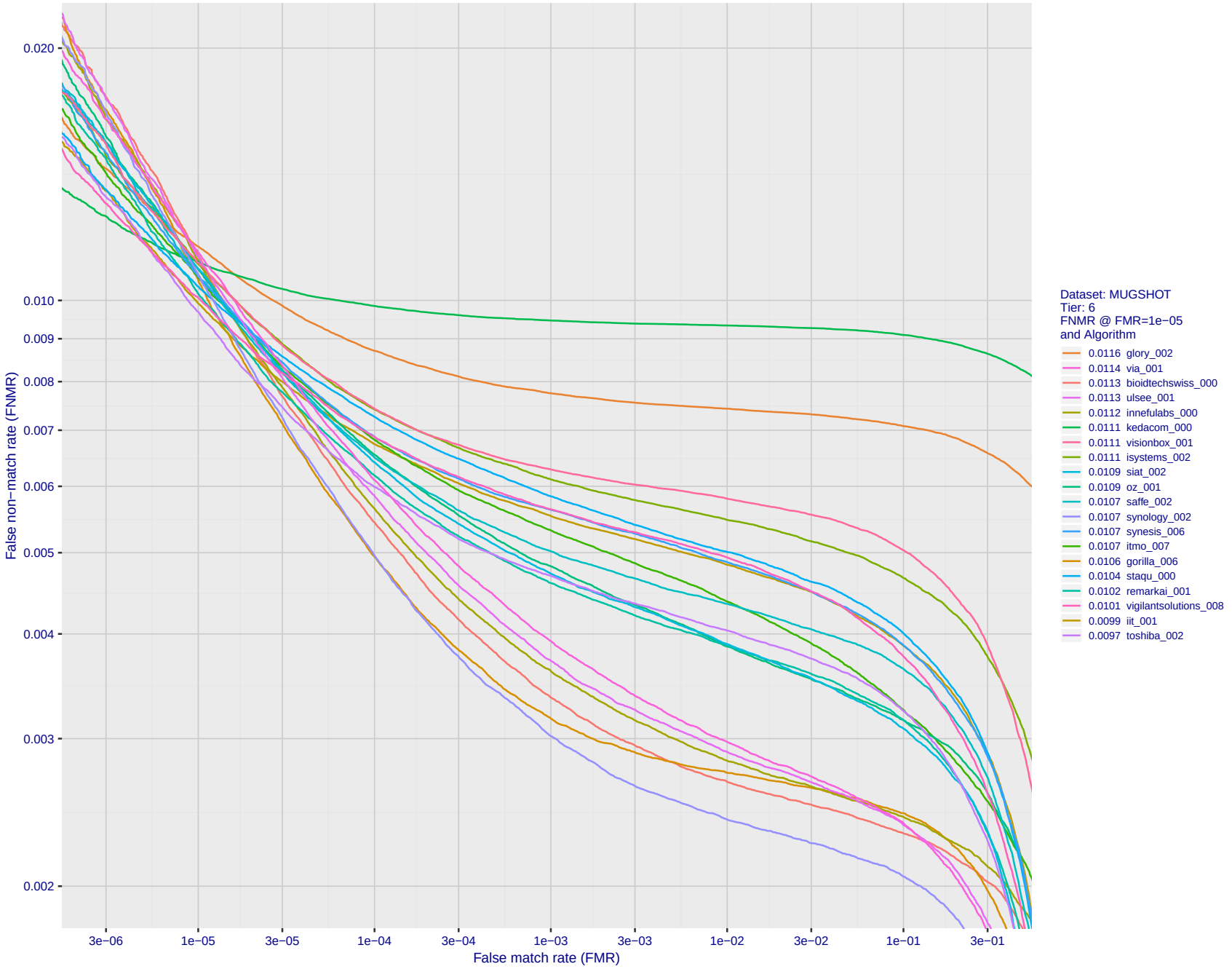

*Figure 45: For the mugshot images, detection error tradeoff (*DET*) characteristics showing false non-match rate vs. false match rate plotted parametrically on threshold, T. The scales are logarithmic in order to show decades of* FMR*.*

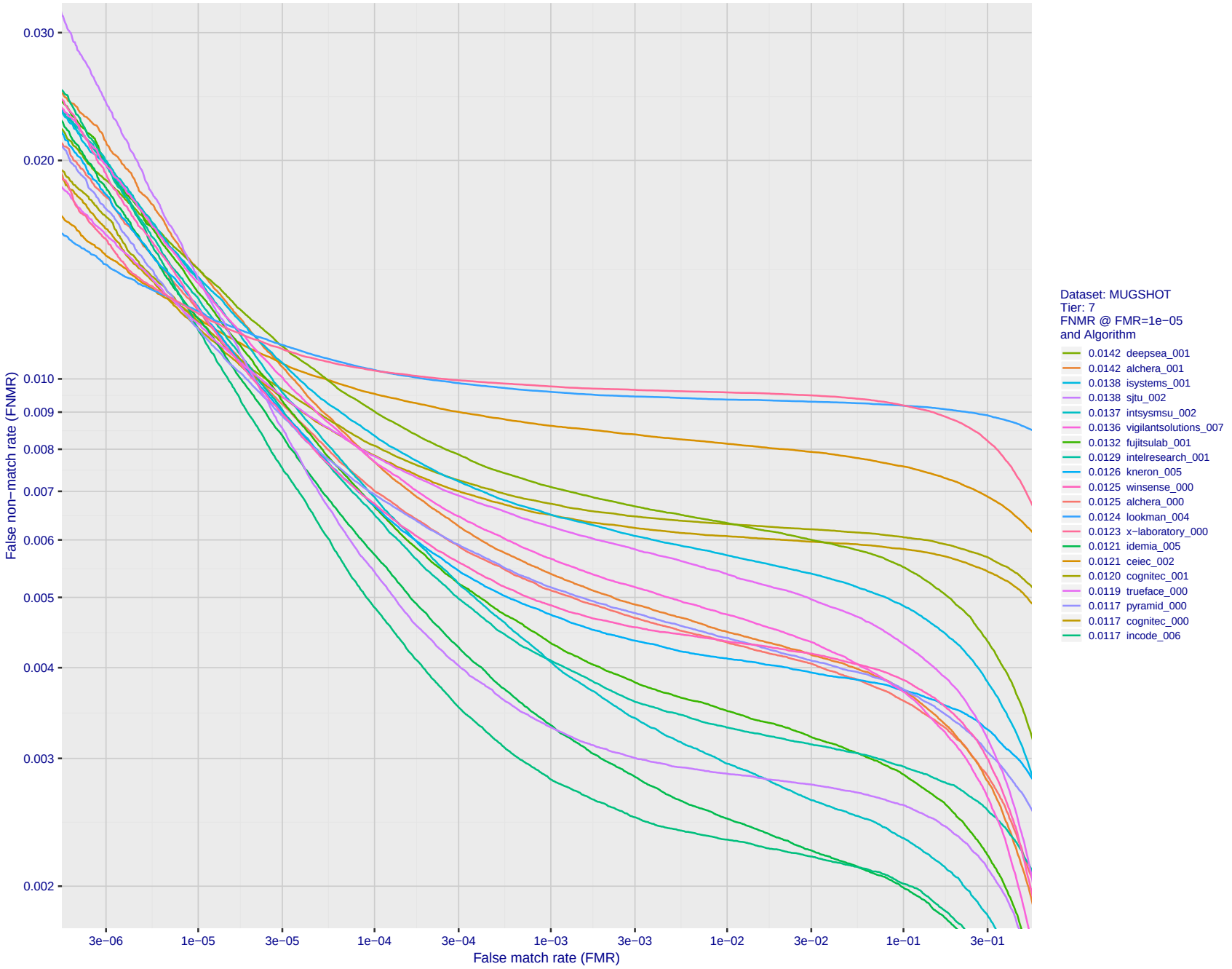

*Figure 46: For the mugshot images, detection error tradeoff (*DET*) characteristics showing false non-match rate vs. false match rate plotted parametrically on threshold, T. The scales are logarithmic in order to show decades of* FMR*.*

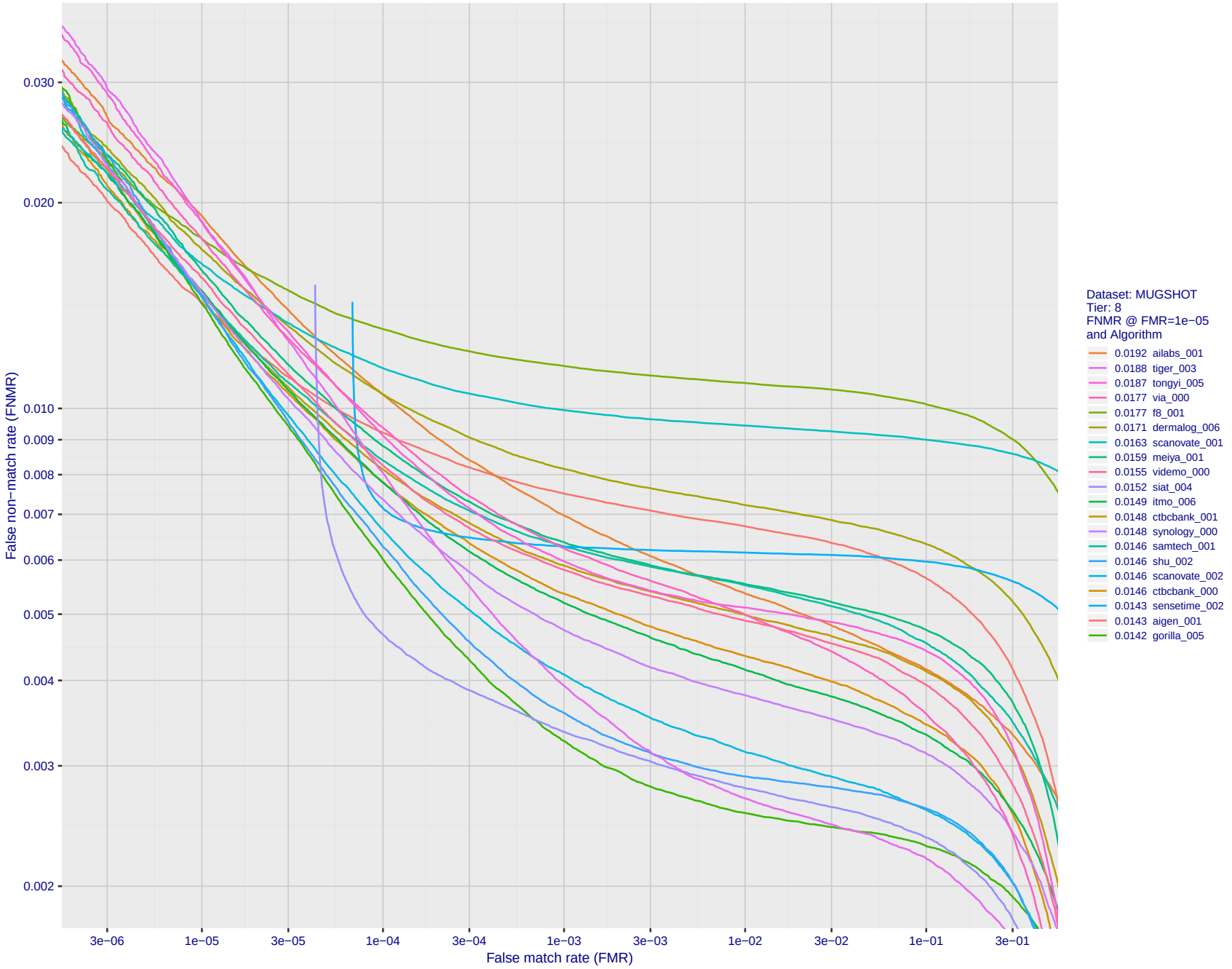

*Figure 47: For the mugshot images, detection error tradeoff (*DET*) characteristics showing false non-match rate vs. false match rate plotted parametrically on threshold, T. The scales are logarithmic in order to show decades of* FMR.

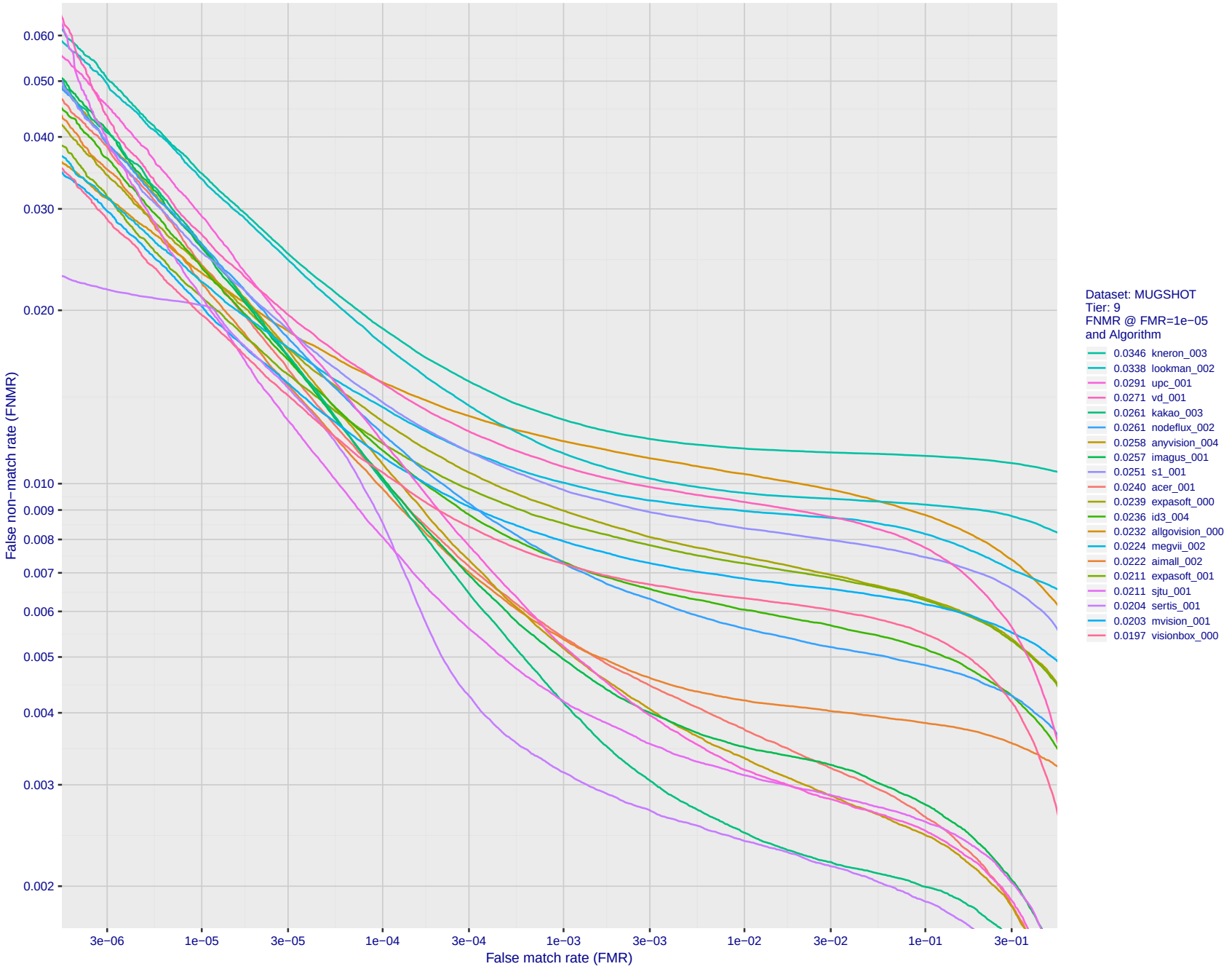

*Figure 48: For the mugshot images, detection error tradeoff (*DET*) characteristics showing false non-match rate vs. false match rate plotted parametrically on threshold, T. The scales are logarithmic in order to show decades of* FMR*.*

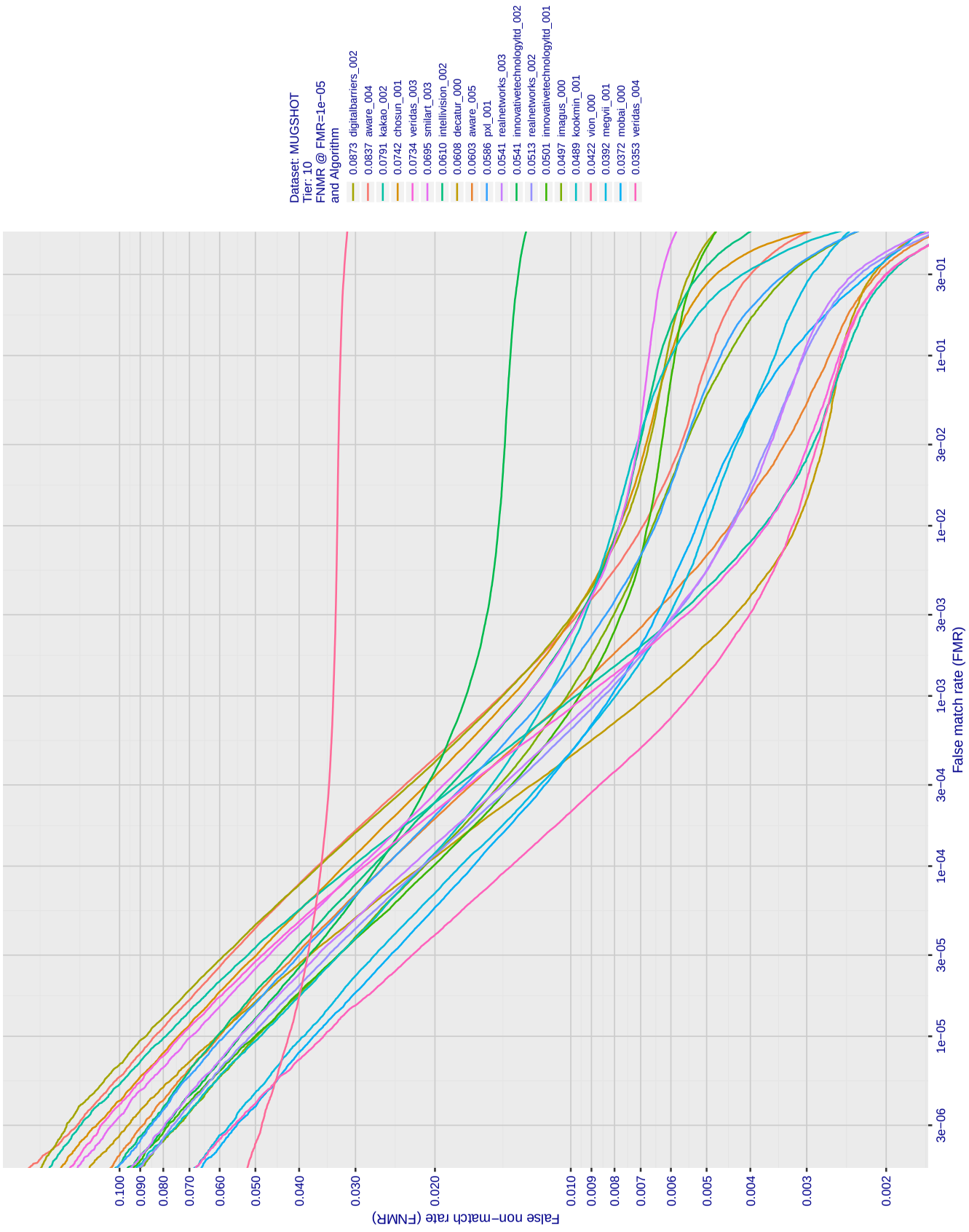

Figure 49: For the mugshot images, detection error tradeoff (DET) characteristics showing false non-match rate vs. false match rate plotted parametrically on threshold, T. The scales are logarithmic in order to show decades of FMR.

FNMR(T) "False non-match rate"
FMR(T) "False match rate"

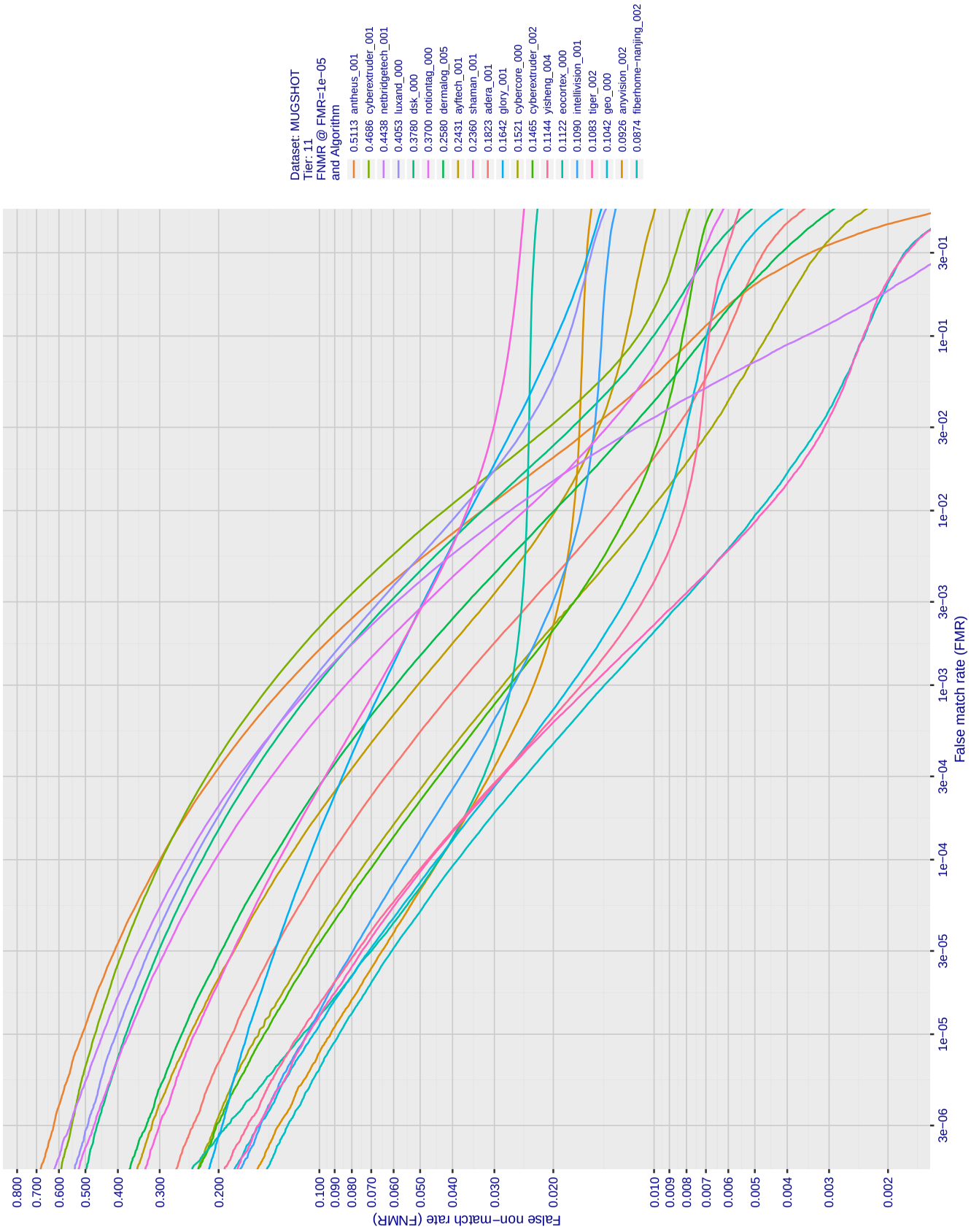

Figure 50: For the mugshot images, detection error tradeoff (DET) *characteristics showing false non-match rate vs. false match rate plotted parametrically on threshold, T. The scales are logarithmic in order to show decades of* FMR.

FNMR(T) "False non-match rate"
FMR(T) "False match rate"

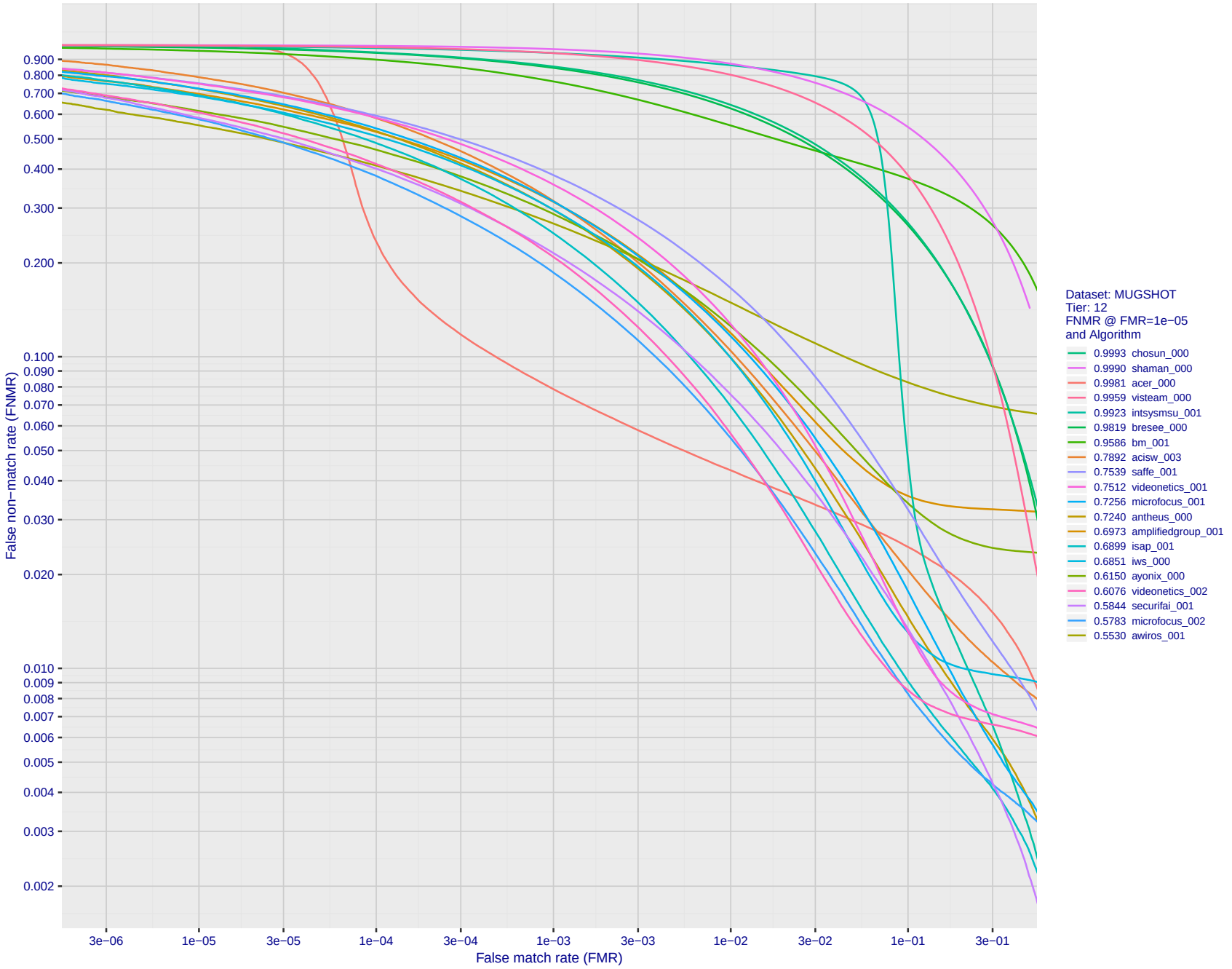

Figure 51: For the mugshot images, detection error tradeoff (DET) characteristics showing false non-match rate vs. false match rate plotted parametrically on threshold, T. The scales are logarithmic in order to show decades of FMR.

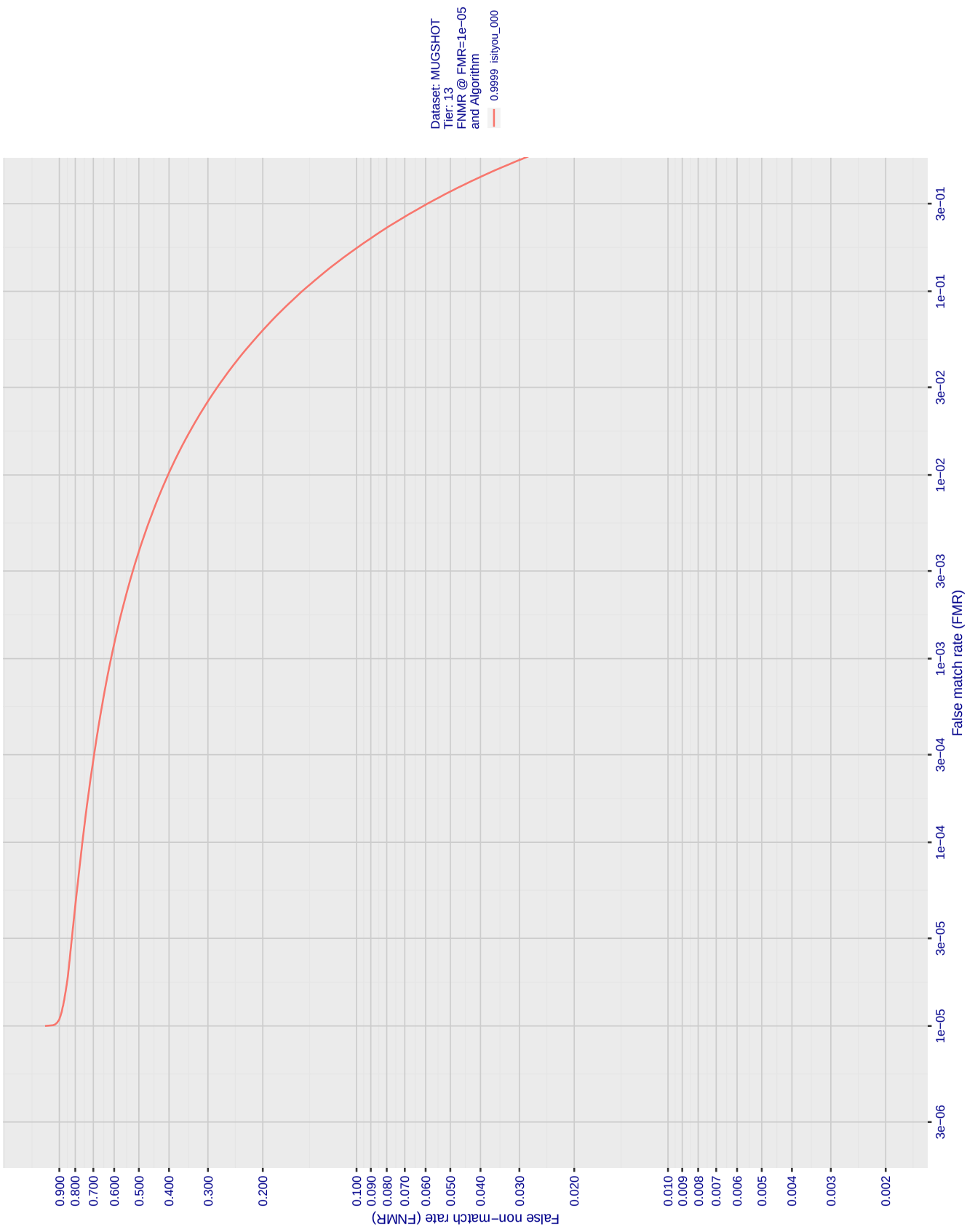

Figure 52: For the mugshot images, detection error tradeoff (DET) *characteristics showing false non-match rate vs. false match rate plotted parametrically on threshold, T. The scales are logarithmic in order to show decades of* FMR.

FNMR(T) "False non-match rate"
FMR(T) "False match rate"

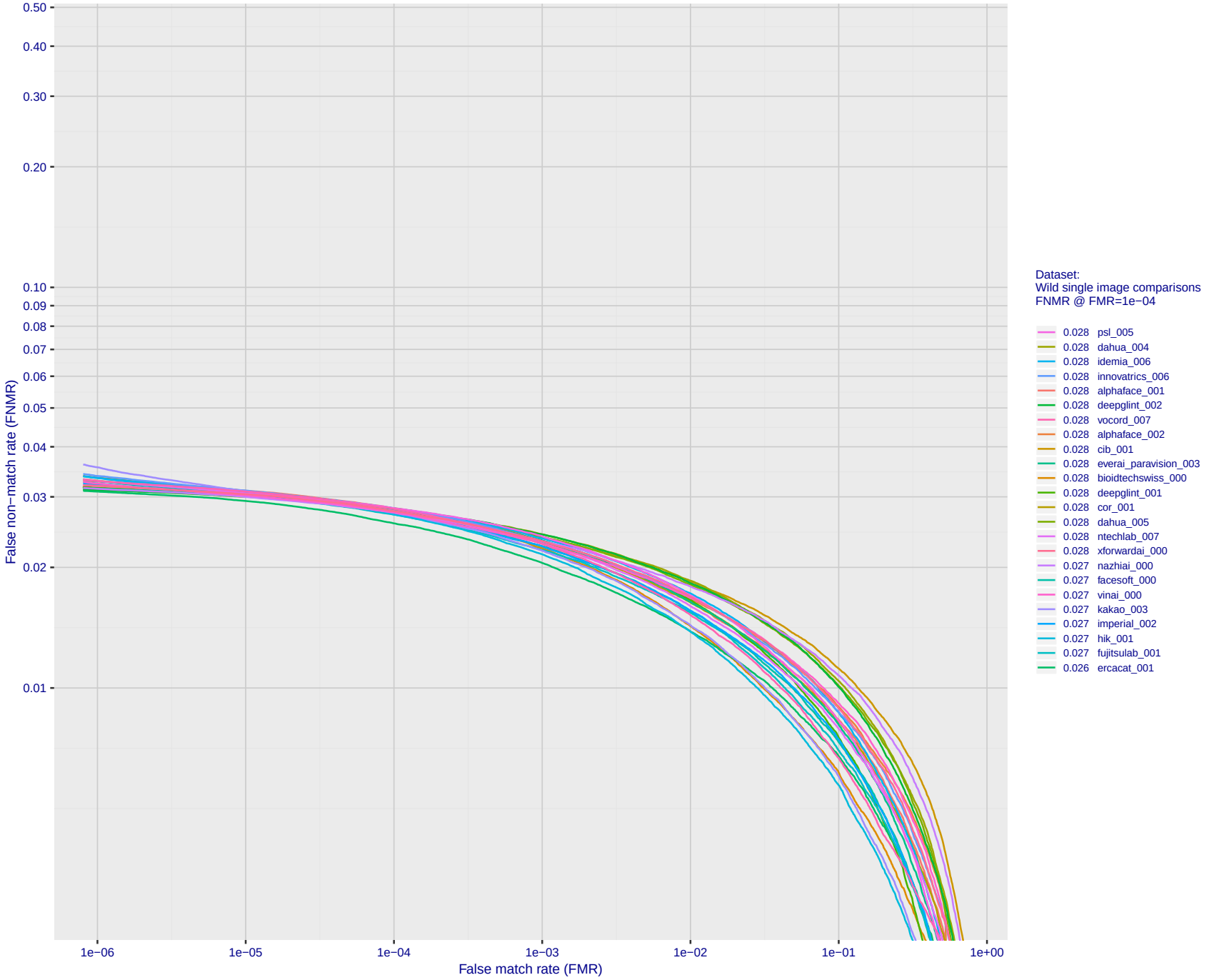

*Figure 53: For the 2018 wild image comparisons, detection error tradeoff (*DET*) characteristics showing false non-match rate vs. false match rate plotted parametrically on threshold, T. The scales are logarithmic in order to show several decades of* FMR*.*

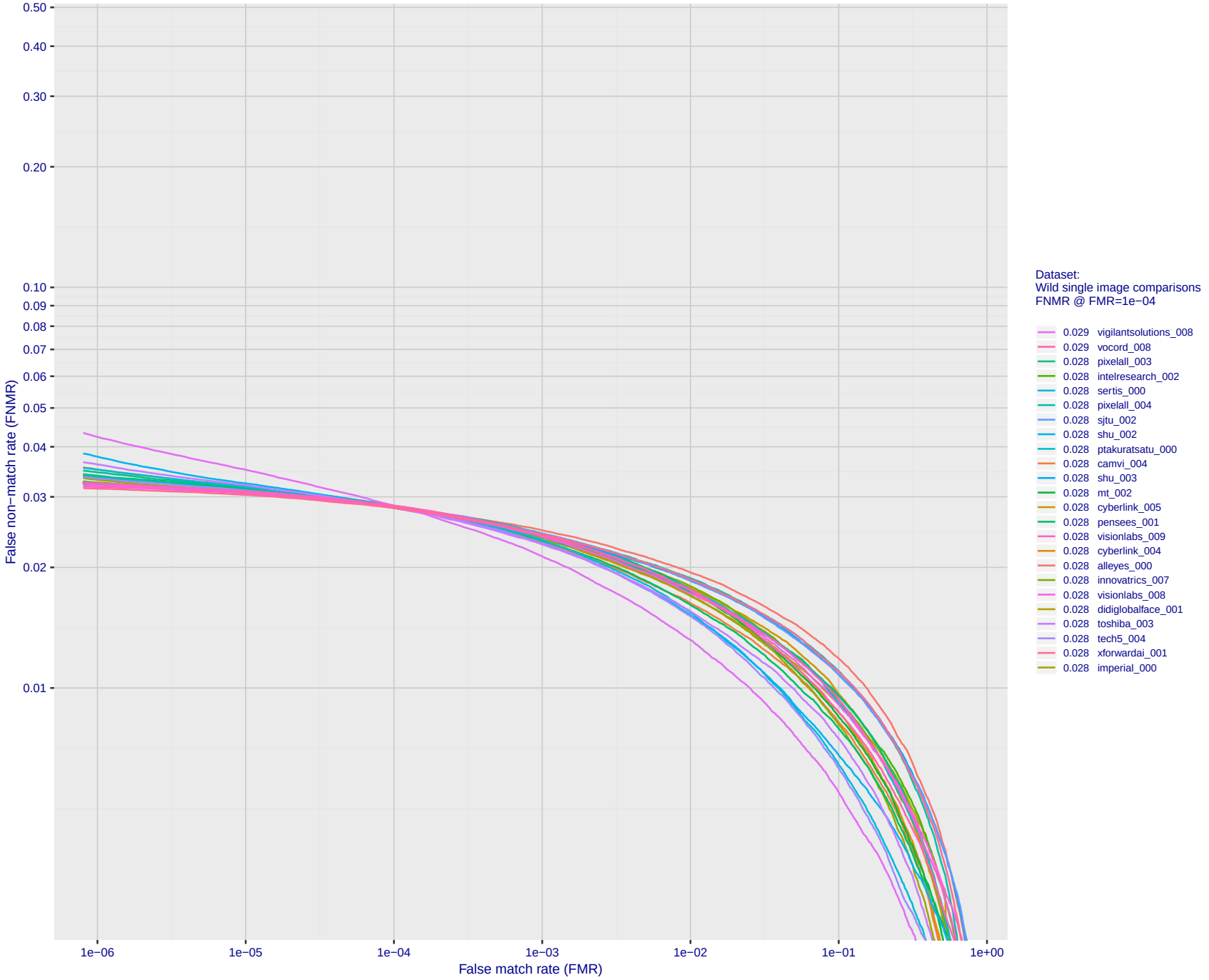

*Figure 54: For the 2018 wild image comparisons, detection error tradeoff (*DET*) characteristics showing false non-match rate vs. false match rate plotted parametrically on threshold, T. The scales are logarithmic in order to show several decades of* FMR.

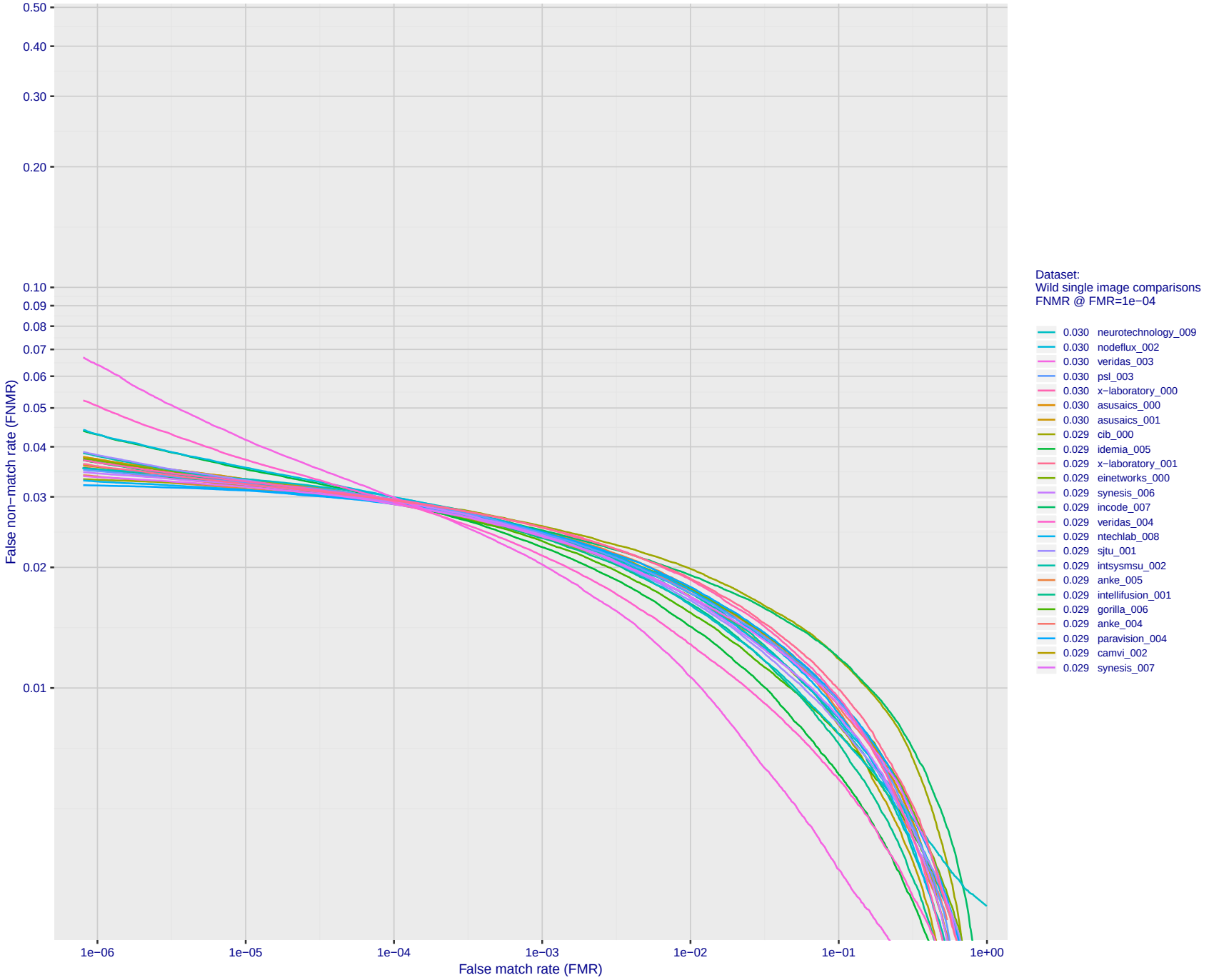

*Figure 55: For the 2018 wild image comparisons, detection error tradeoff (*DET*) characteristics showing false non-match rate vs. false match rate plotted parametrically on threshold, T. The scales are logarithmic in order to show several decades of* FMR.

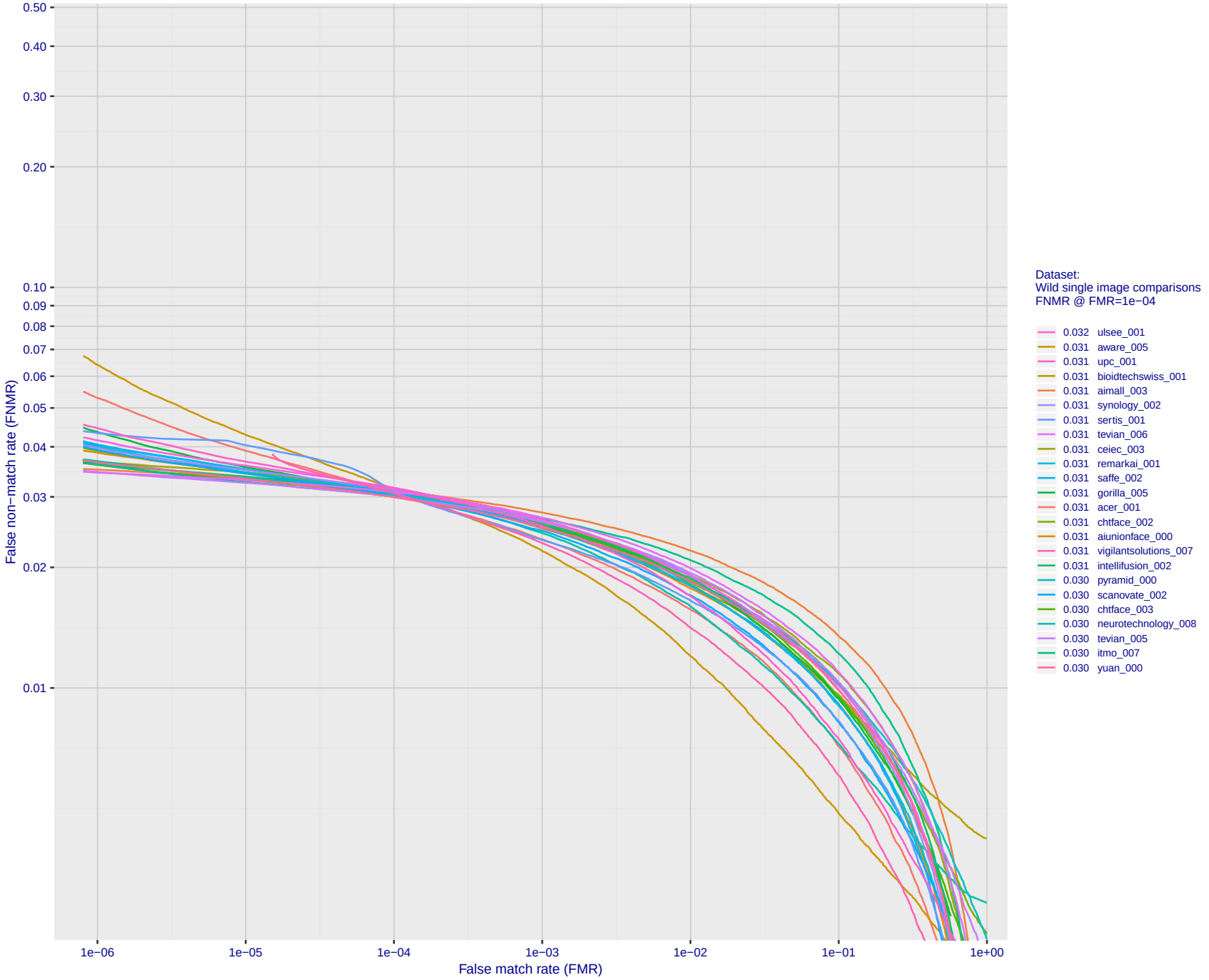

*Figure 56: For the 2018 wild image comparisons, detection error tradeoff (*DET*) characteristics showing false non-match rate vs. false match rate plotted parametrically on threshold, T. The scales are logarithmic in order to show several decades of* FMR*.*

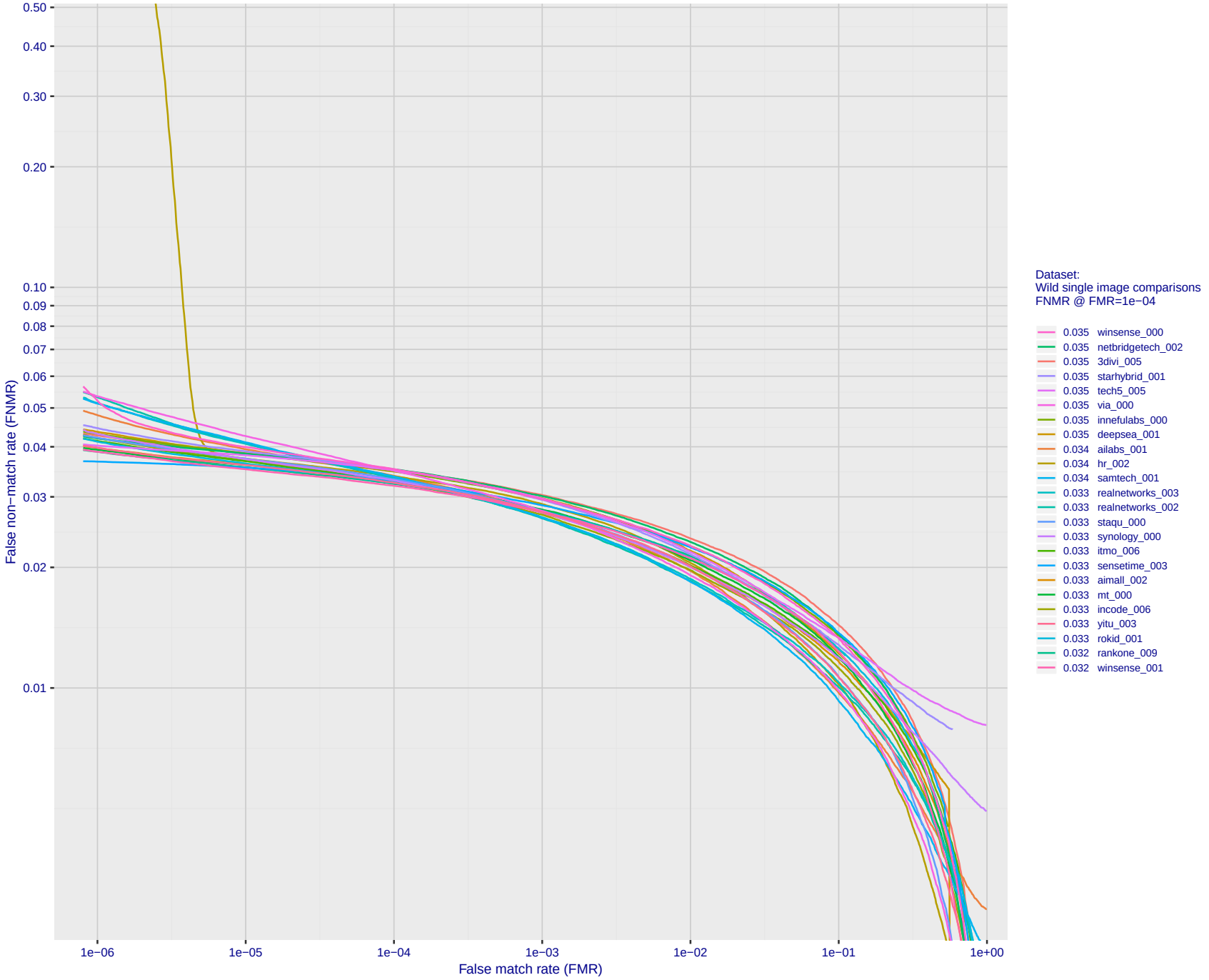

*Figure 57: For the 2018 wild image comparisons, detection error tradeoff (*DET*) characteristics showing false non-match rate vs. false match rate plotted parametrically on threshold, T. The scales are logarithmic in order to show several decades of* FMR.

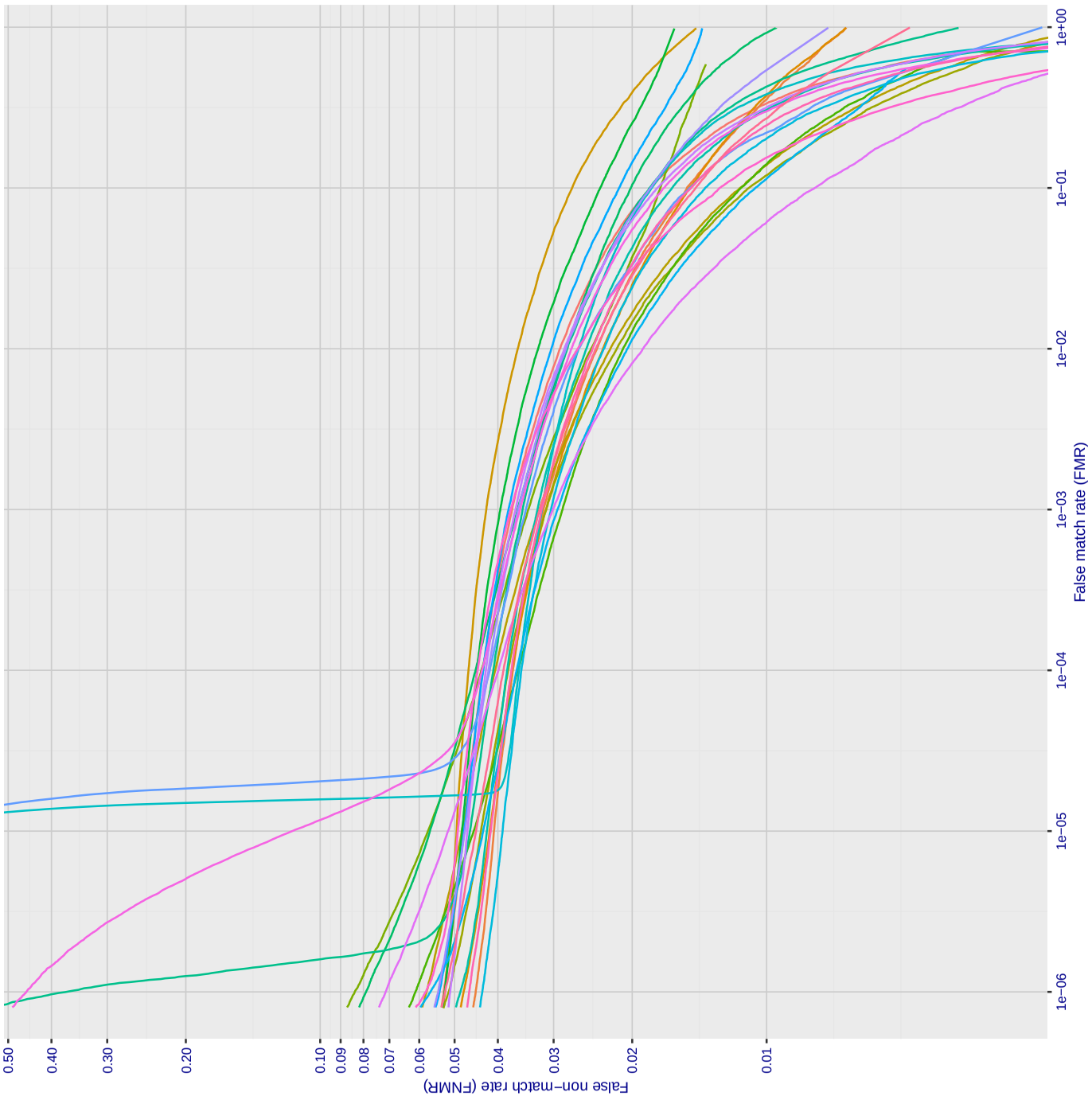

Figure 58: For the 2018 wild image comparisons, detection error tradeoff (DET) characteristics showing false non-match rate vs. false match rate plotted parametrically on threshold, T. The scales are logarithmic in order to show several decades of FMR.

FNMR(T) "False non-match rate"
FMR(T) "False match rate"

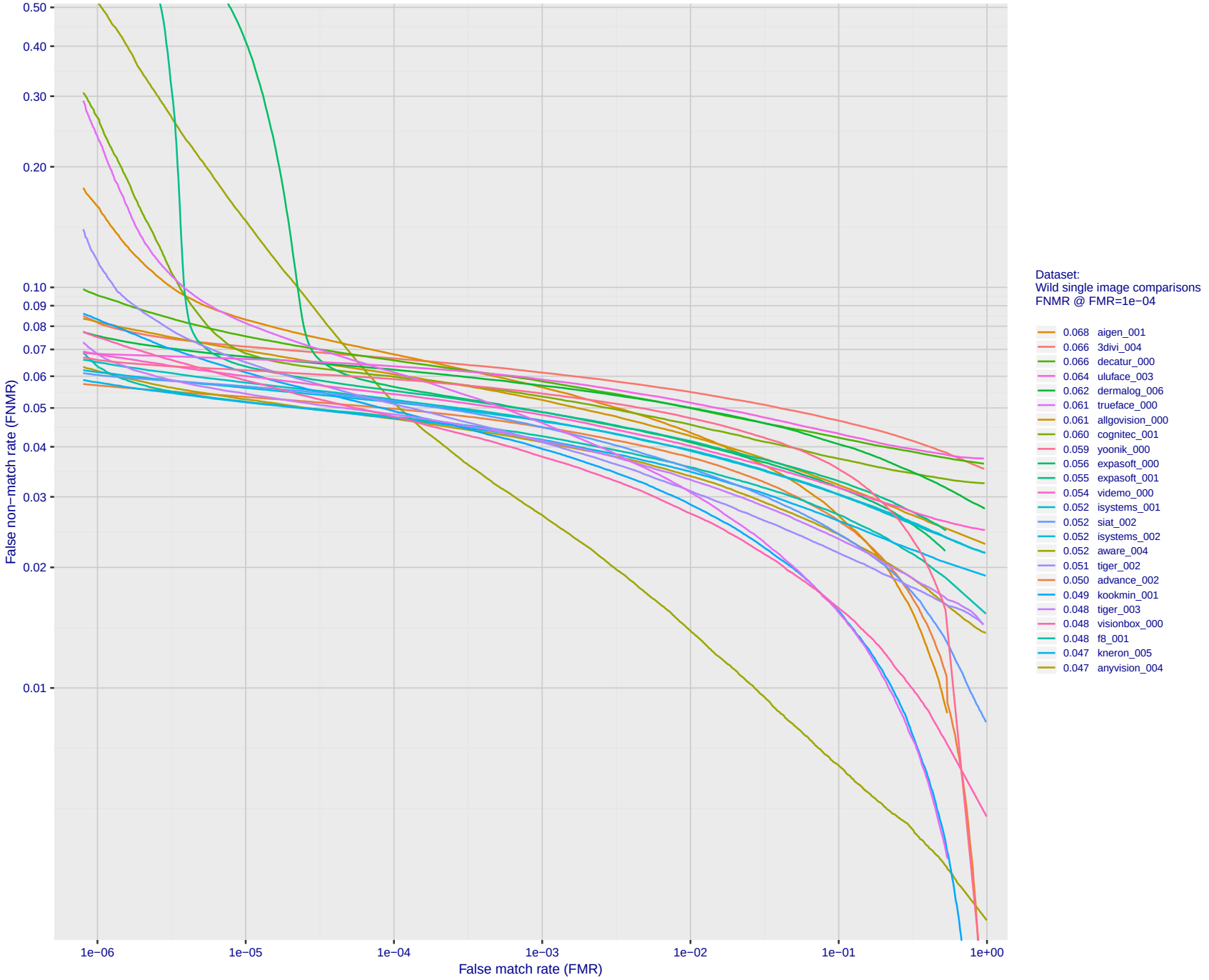

*Figure 59: For the 2018 wild image comparisons, detection error tradeoff (*DET*) characteristics showing false non-match rate vs. false match rate plotted parametrically on threshold, T. The scales are logarithmic in order to show several decades of* FMR*.*

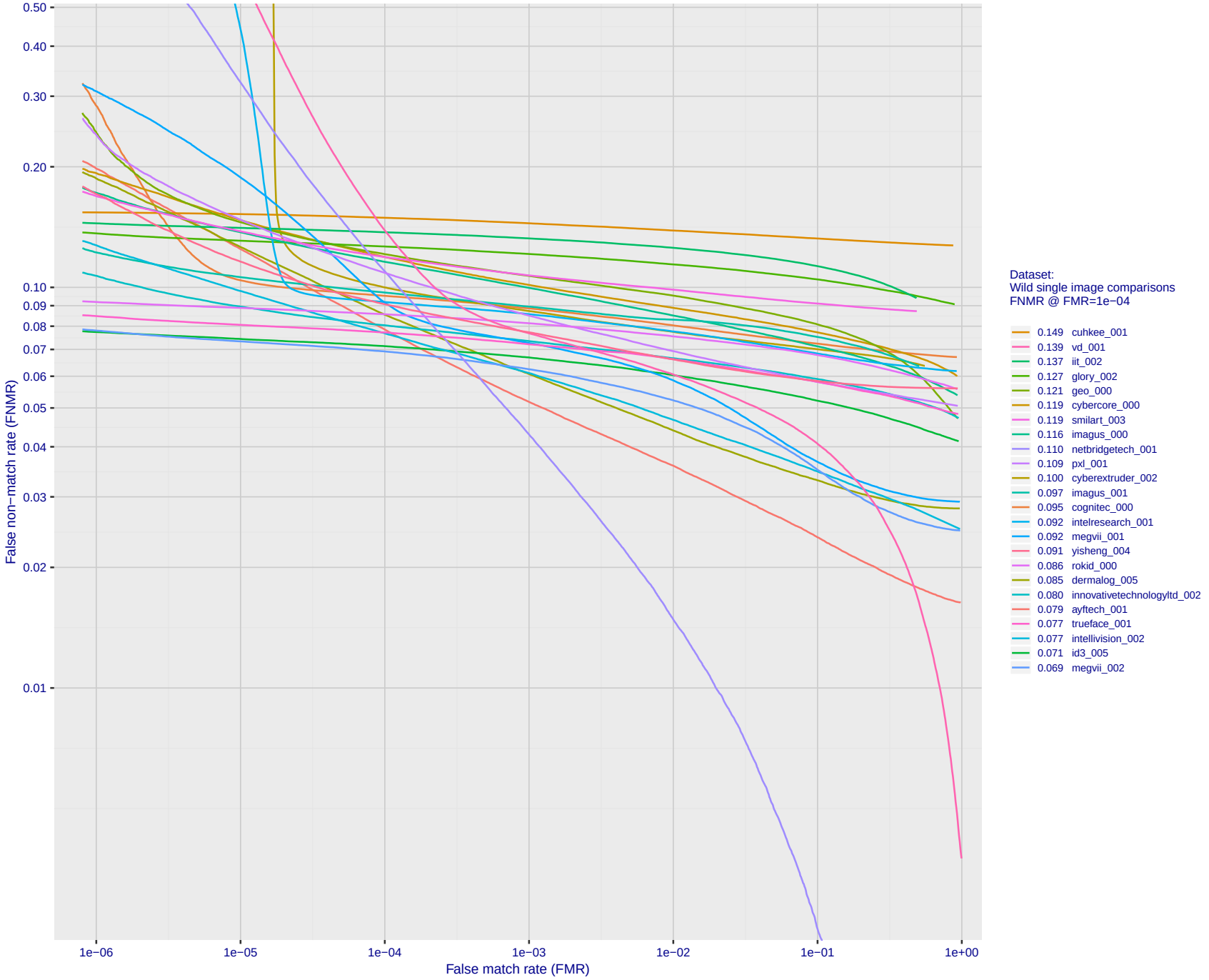

*Figure 60: For the 2018 wild image comparisons, detection error tradeoff (*DET*) characteristics showing false non-match rate vs. false match rate plotted parametrically on threshold, T. The scales are logarithmic in order to show several decades of* FMR.

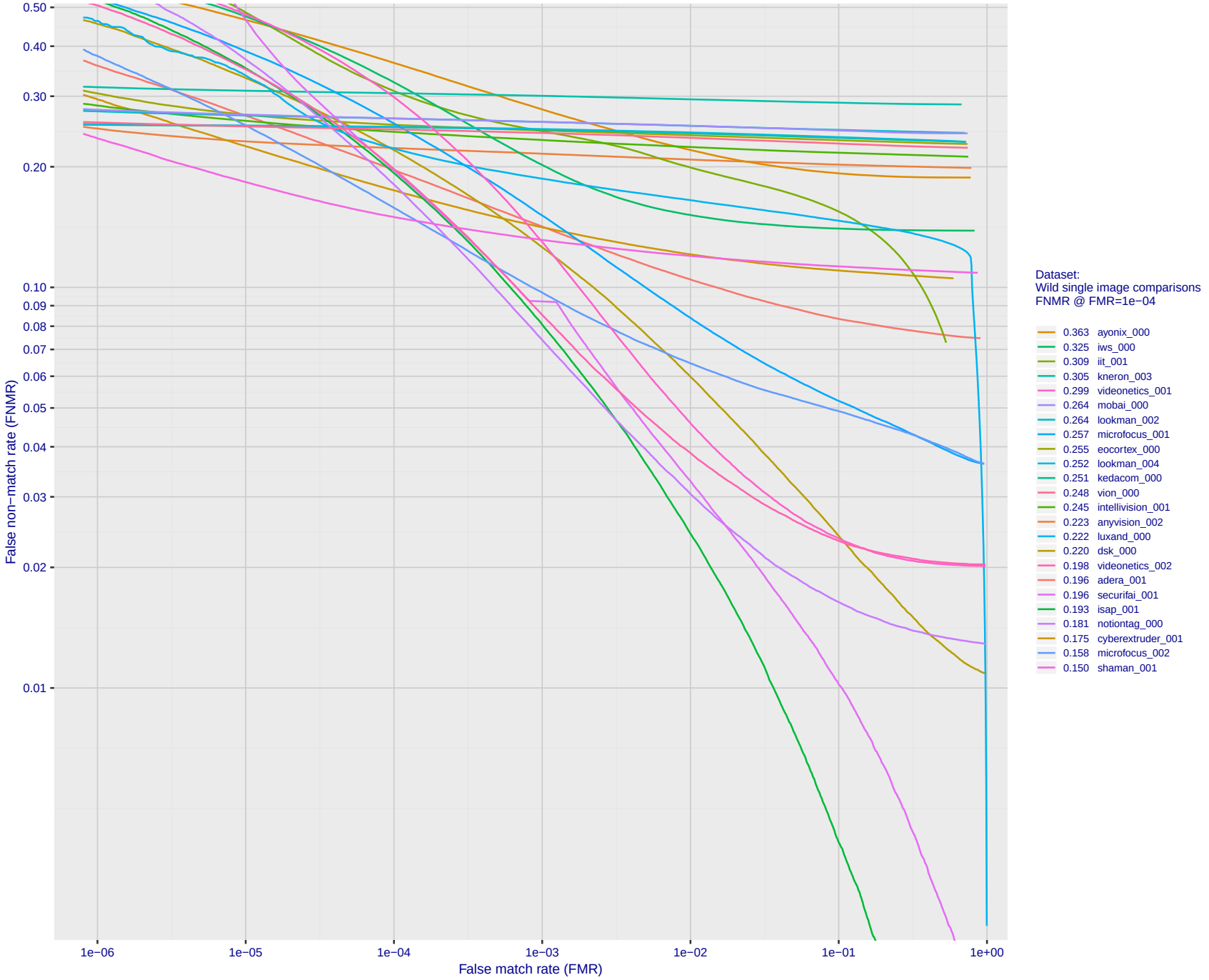

*Figure 61: For the 2018 wild image comparisons, detection error tradeoff (*DET*) characteristics showing false non-match rate vs. false match rate plotted parametrically on threshold, T. The scales are logarithmic in order to show several decades of* FMR*.*

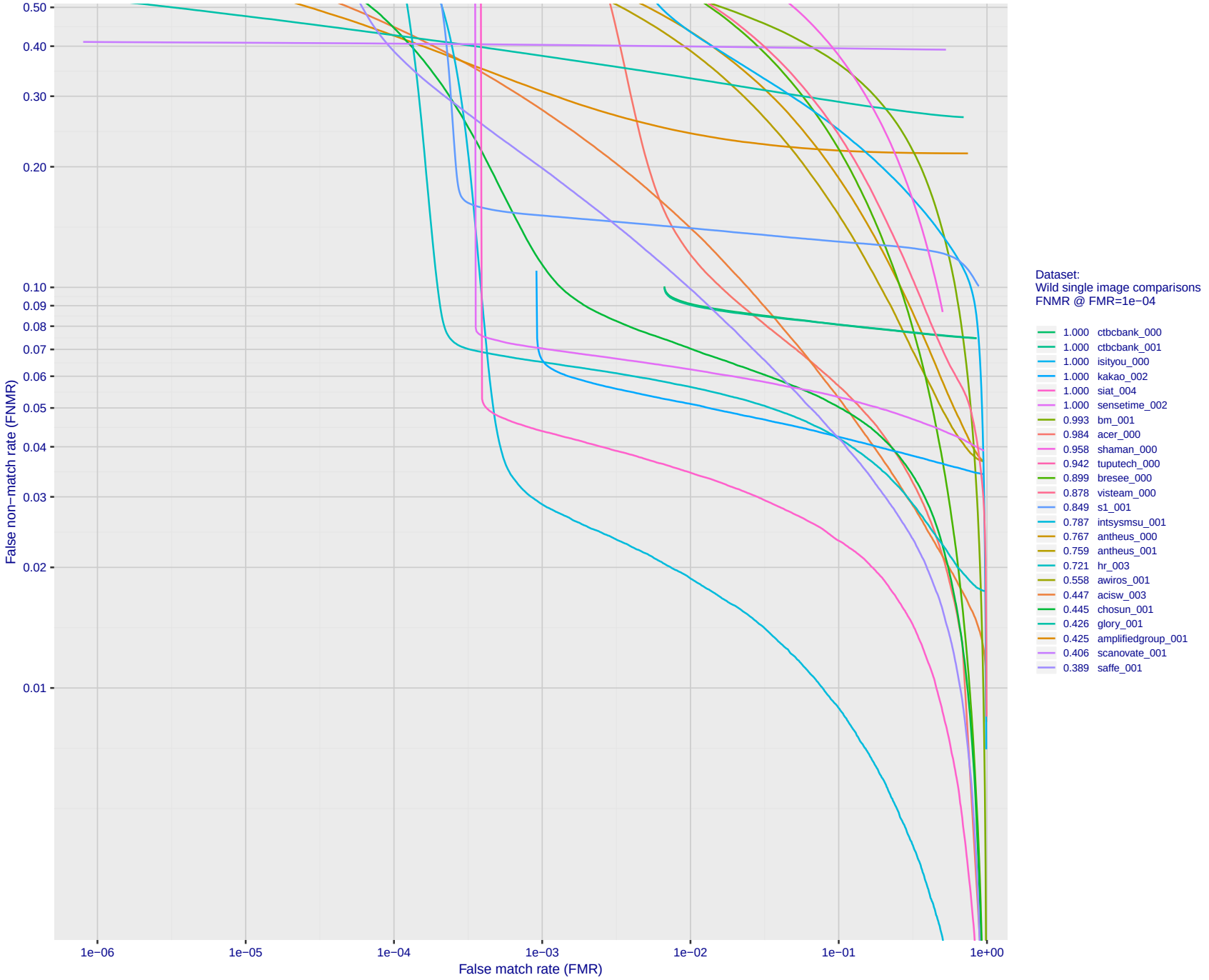

*Figure 62: For the 2018 wild image comparisons, detection error tradeoff (*DET*) characteristics showing false non-match rate vs. false match rate plotted parametrically on threshold, T. The scales are logarithmic in order to show several decades of* FMR.

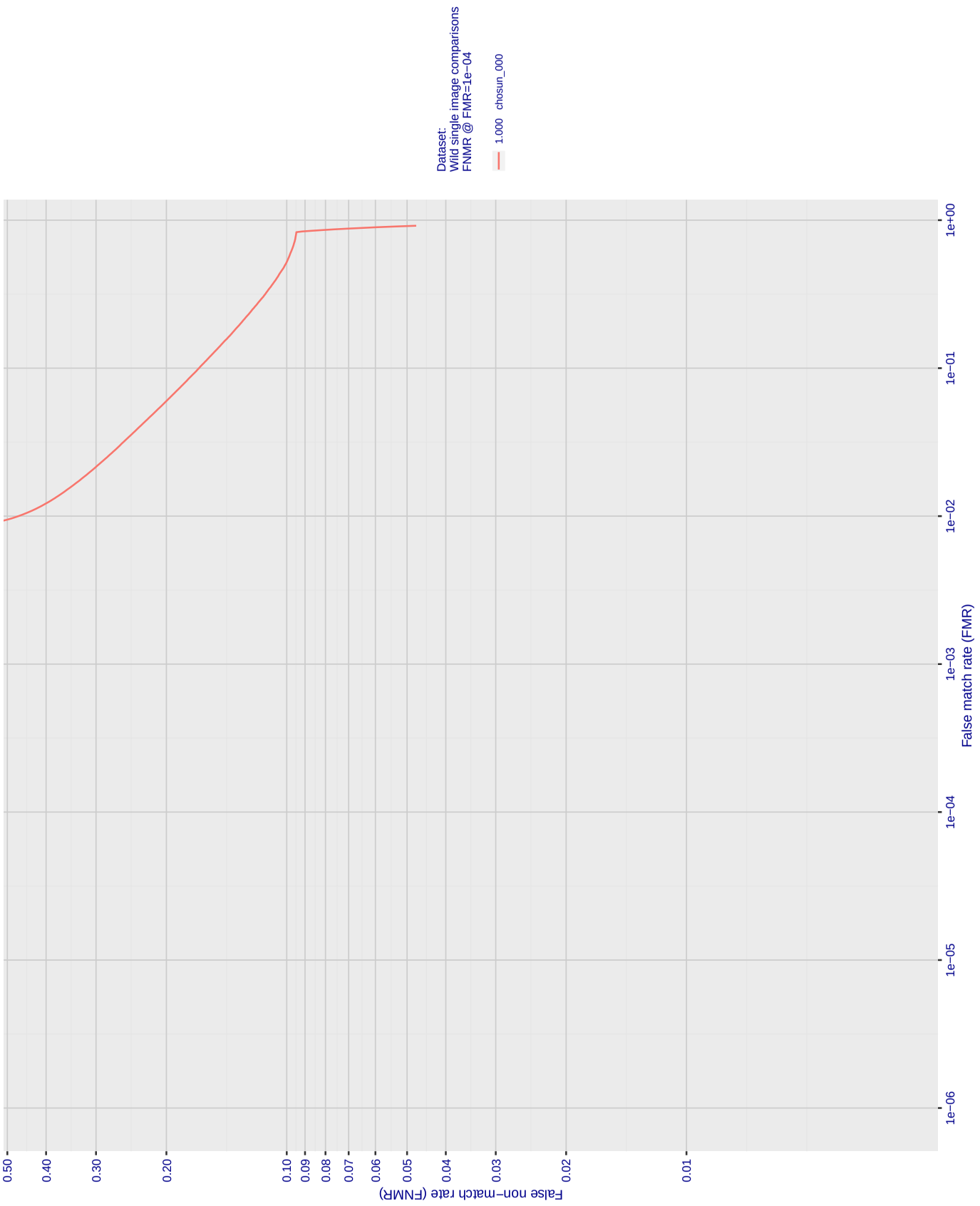

Figure 63: For the 2018 wild image comparisons, detection error tradeoff (DET) characteristics showing false non-match rate vs. false match rate plotted parametrically on threshold, T. The scales are logarithmic in order to show several decades of FMR.

FNMR(T) "False non-match rate"
FMR(T) "False match rate"

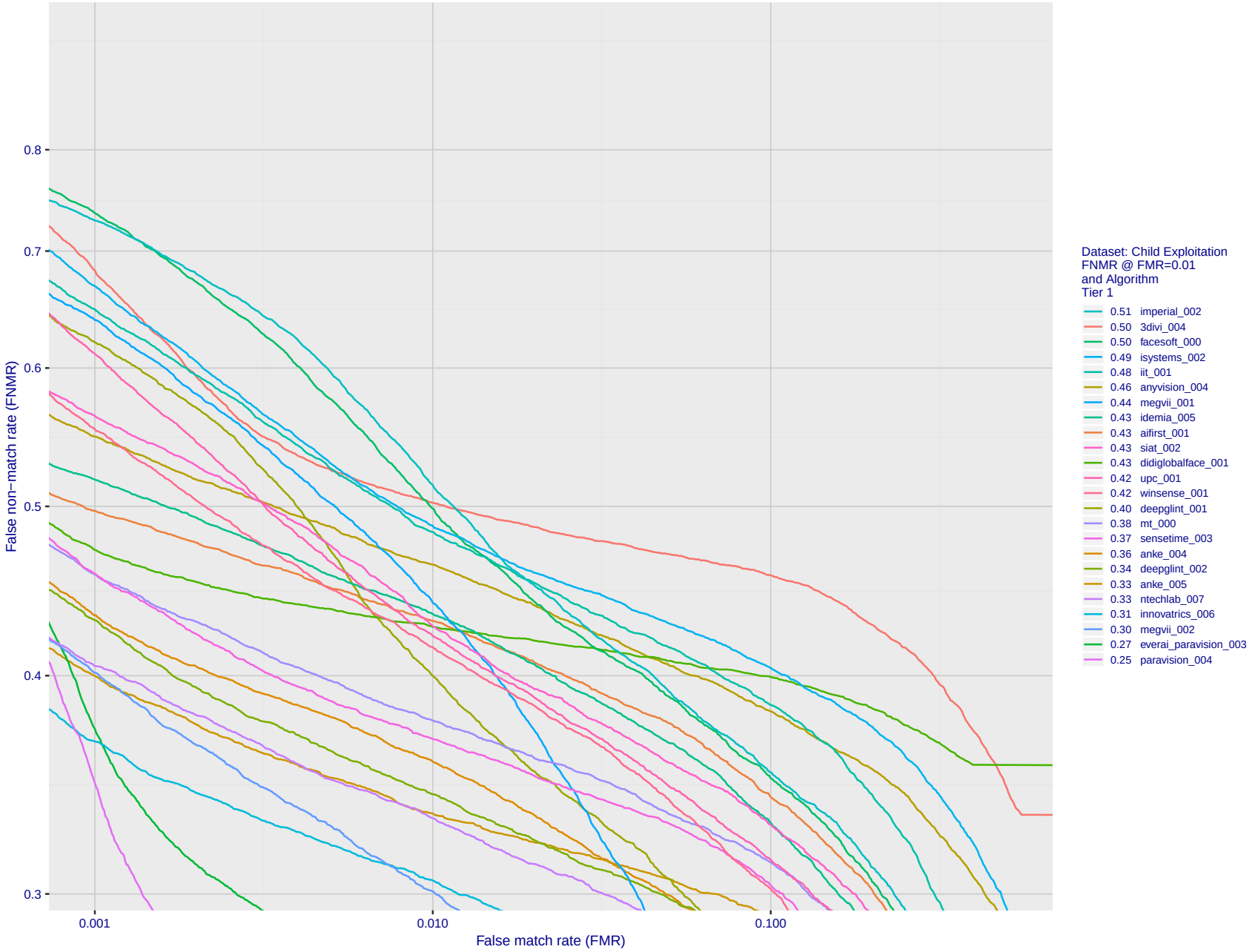

*Figure 64: For child exploitation images, detection error tradeoff (*DET*) characteristics showing false non-match rate vs. false match rate plotted parametrically on threshold, T. The scales are logarithmic in order to show many decades of* FMR*. Accuracy is poor because many images have adverse quality characteristics, and because detection and enrollment fails.*

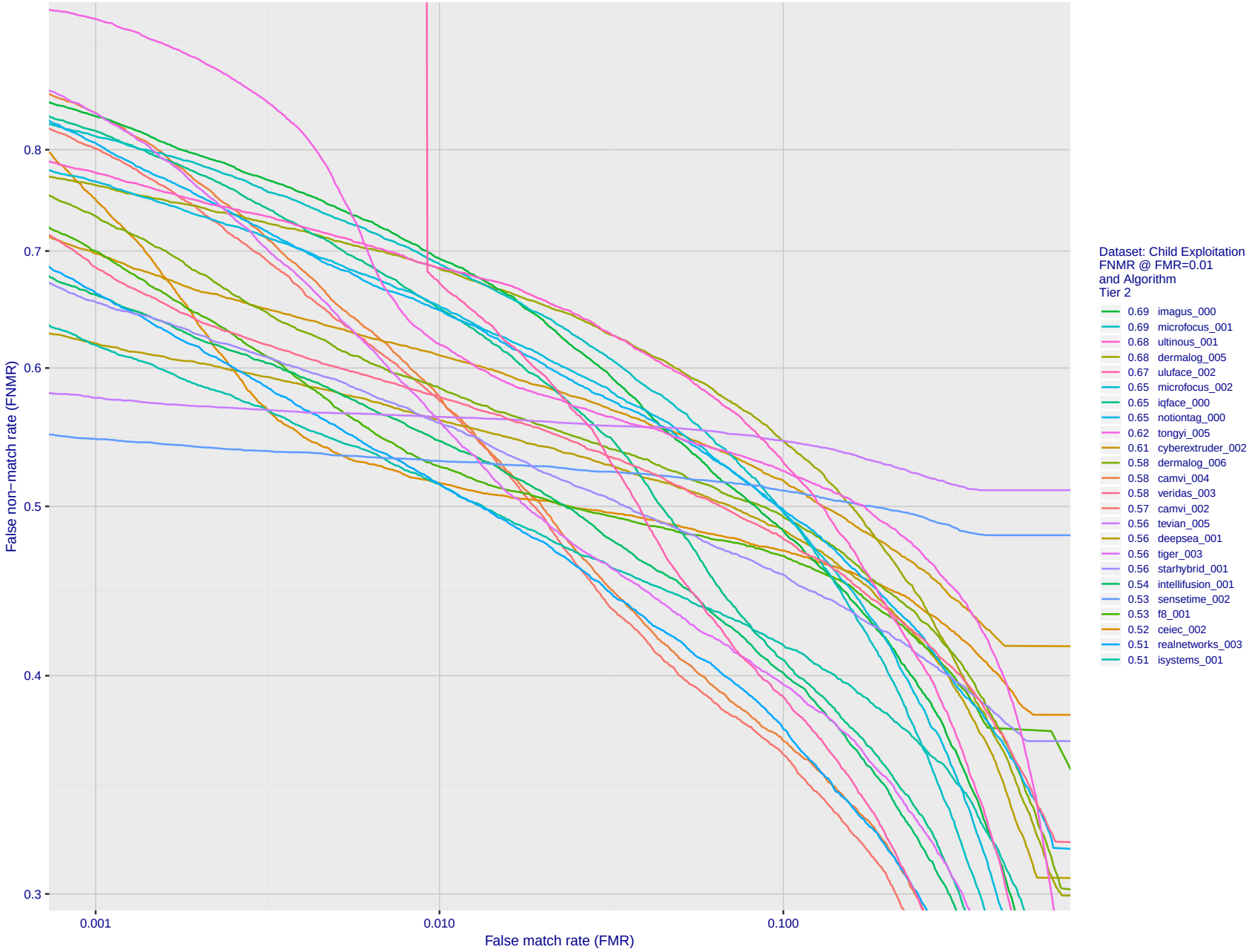

Figure 65: For child exploitation images, detection error tradeoff (DET) characteristics showing false non-match rate vs. false match rate plotted parametrically on threshold, T. The scales are logarithmic in order to show many decades of FMR. Accuracy is poor because many images have adverse quality characteristics, and because detection and enrollment fails.

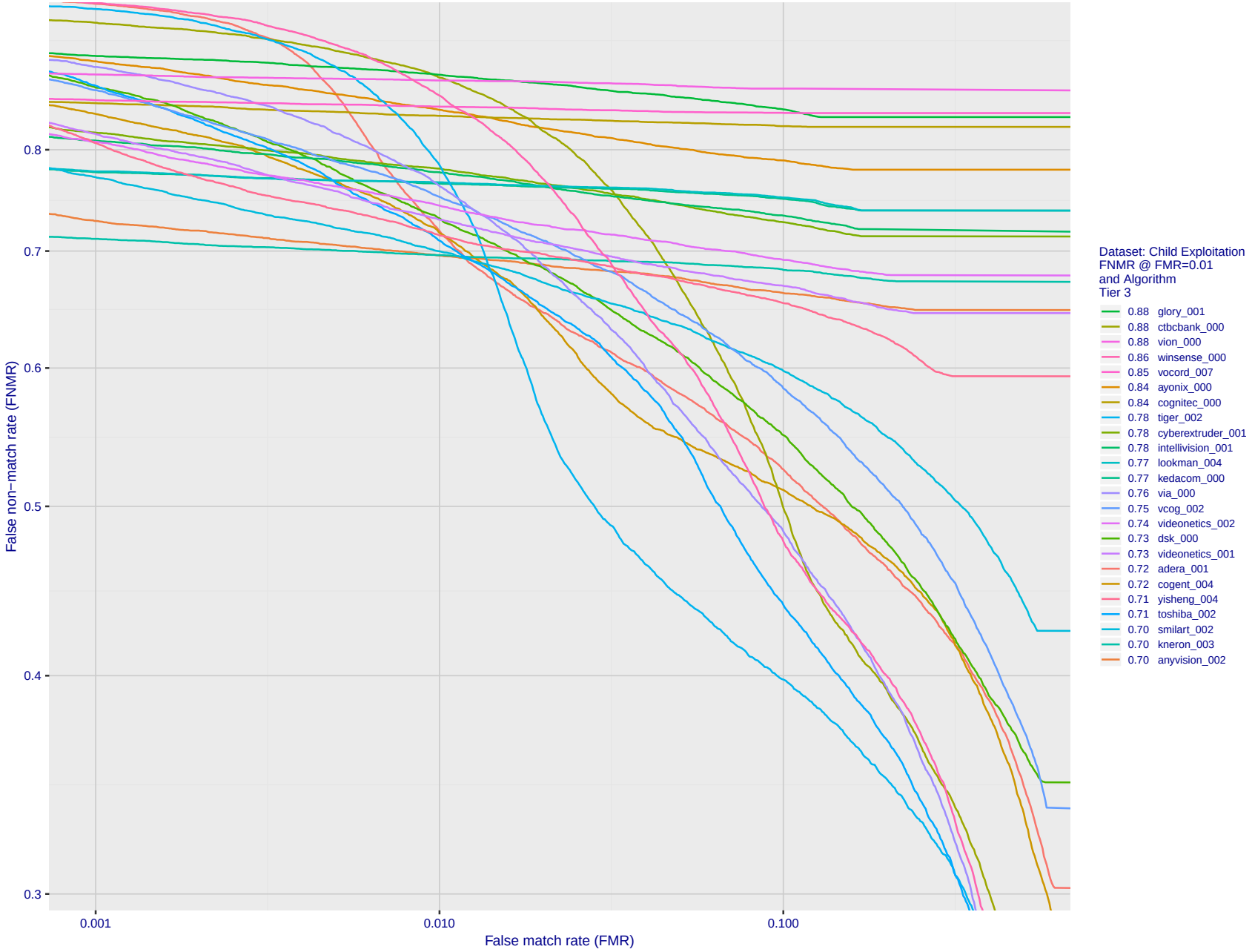

*Figure 66: For child exploitation images, detection error tradeoff (*DET*) characteristics showing false non-match rate vs. false match rate plotted parametrically on threshold, T. The scales are logarithmic in order to show many decades of* FMR*. Accuracy is poor because many images have adverse quality characteristics, and because detection and enrollment fails.*

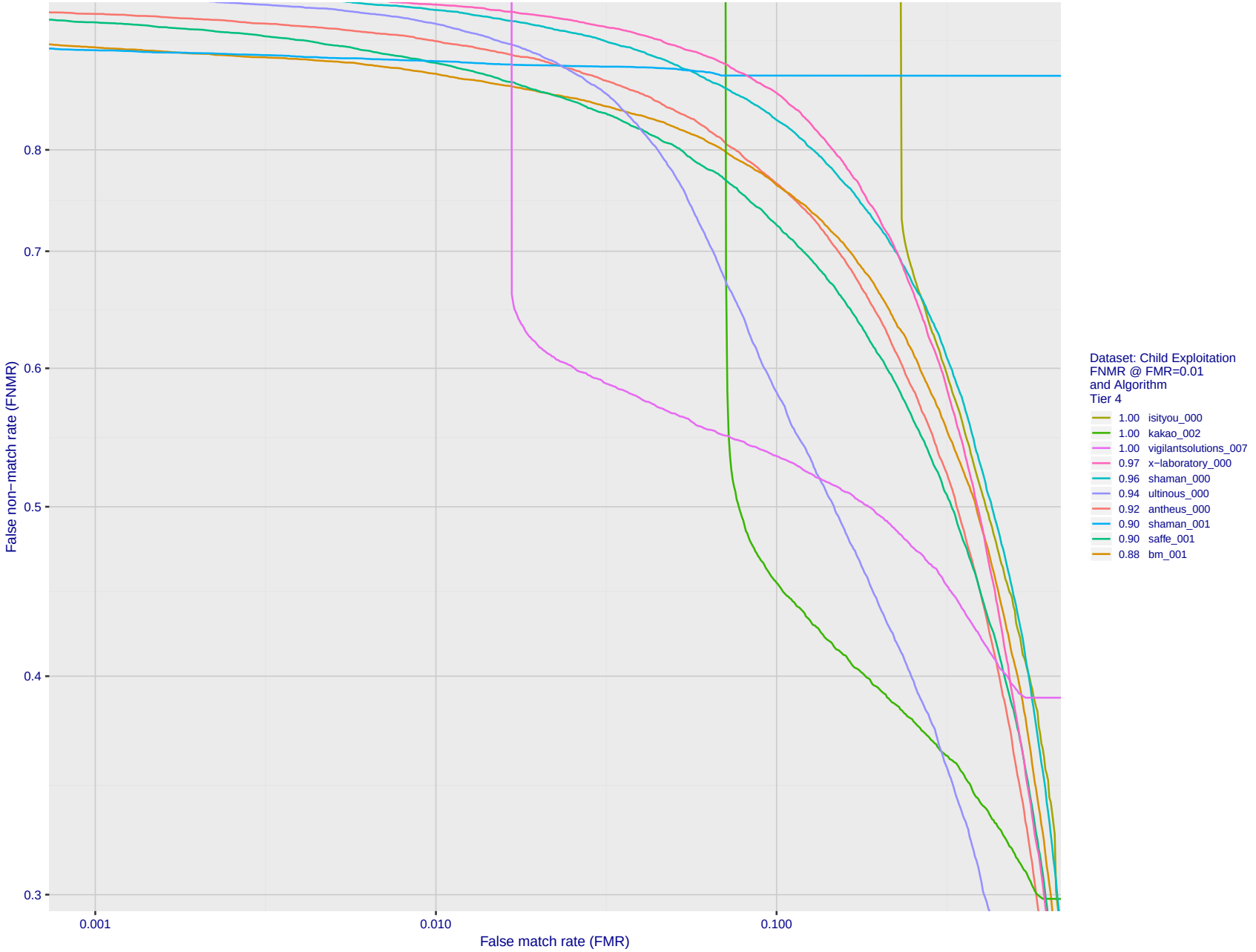

*Figure 67: For child exploitation images, detection error tradeoff (*DET*) characteristics showing false non-match rate vs. false match rate plotted parametrically on threshold, T. The scales are logarithmic in order to show many decades of* FMR*. Accuracy is poor because many images have adverse quality characteristics, and because detection and enrollment fails.*

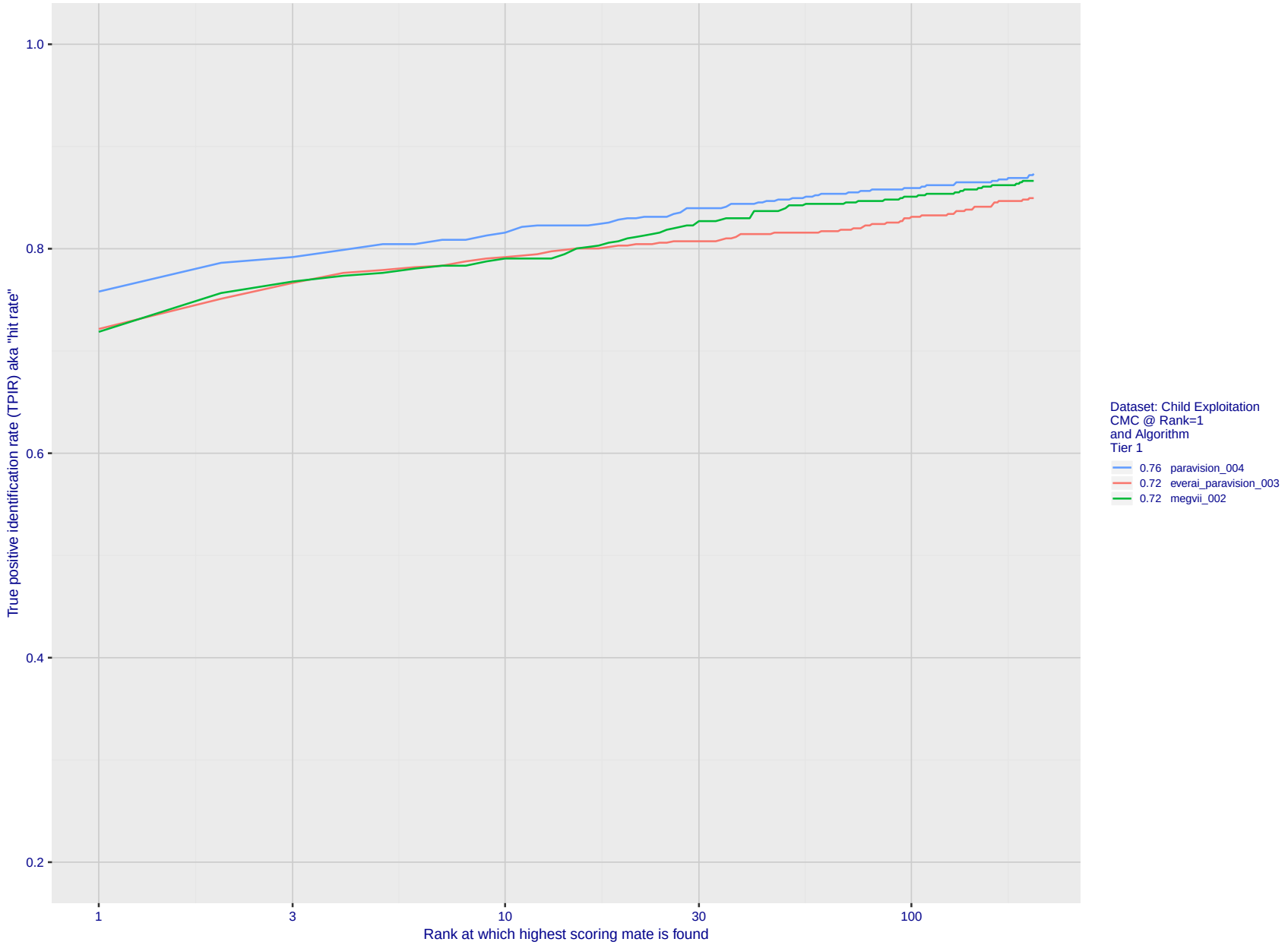

Figure 68: For child exploitation images, cumulative match characteristics (CMC) showing true positive identification rate vs. rank. This is simulation of a one-to-many search experiment - see discussion in section 3.2. The scales are logarithmic in order to show the effect of long candidate lists. Accuracy is poor but much improved relative to the 1:1 DETs of Fig. 67 because a search can succeed if any of a subject's several enrolled images matches the search image with a high score.

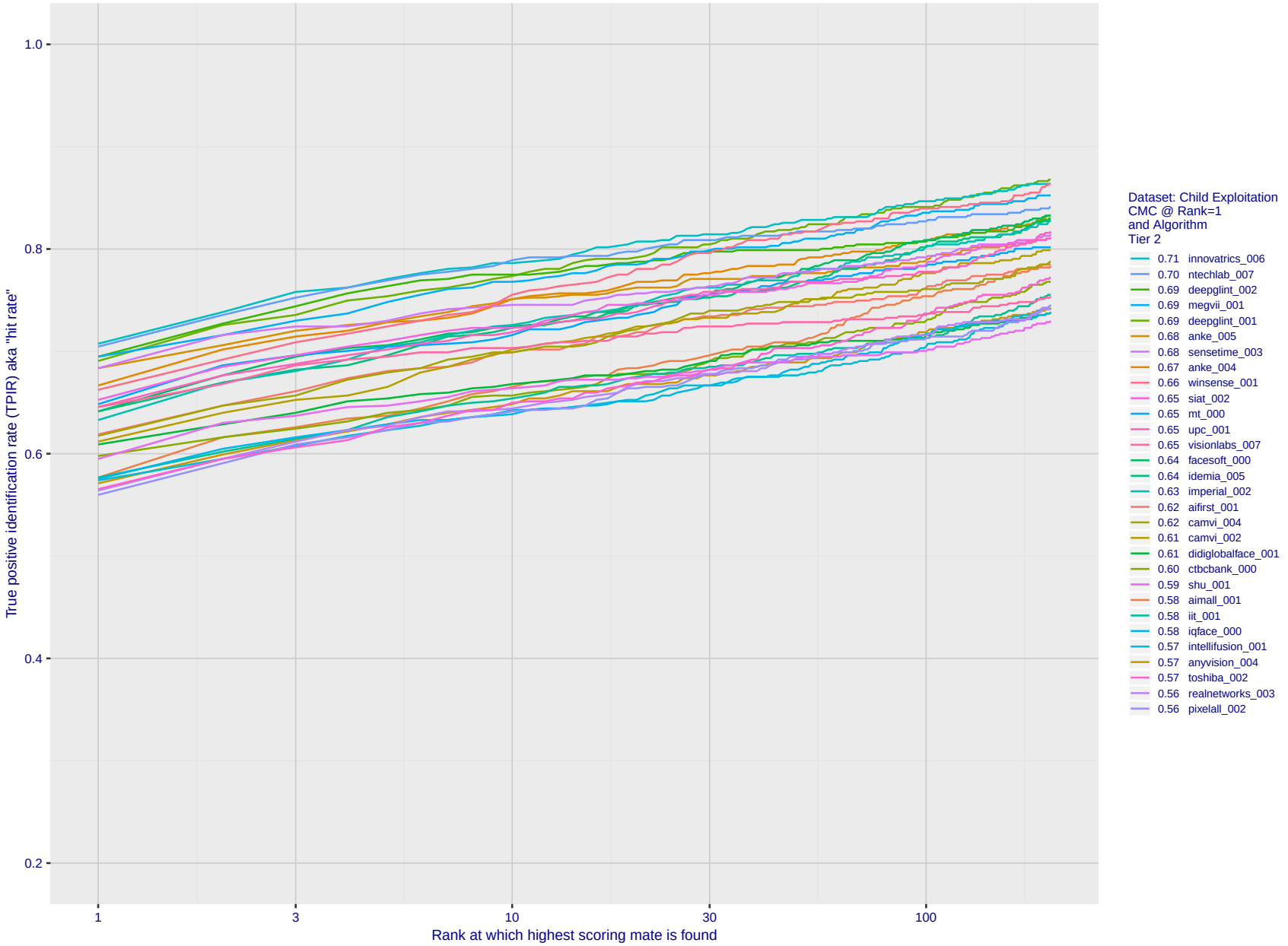

Figure 69: For child exploitation images, cumulative match characteristics (CMC) showing true positive identification rate vs. rank. This is simulation of a one-to-many search experiment - see discussion in section 3.2. The scales are logarithmic in order to show the effect of long candidate lists. Accuracy is poor but much improved relative to the 1:1 DETs of Fig. 67 because a search can succeed if any of a subject's several enrolled images matches the search image with a high score.

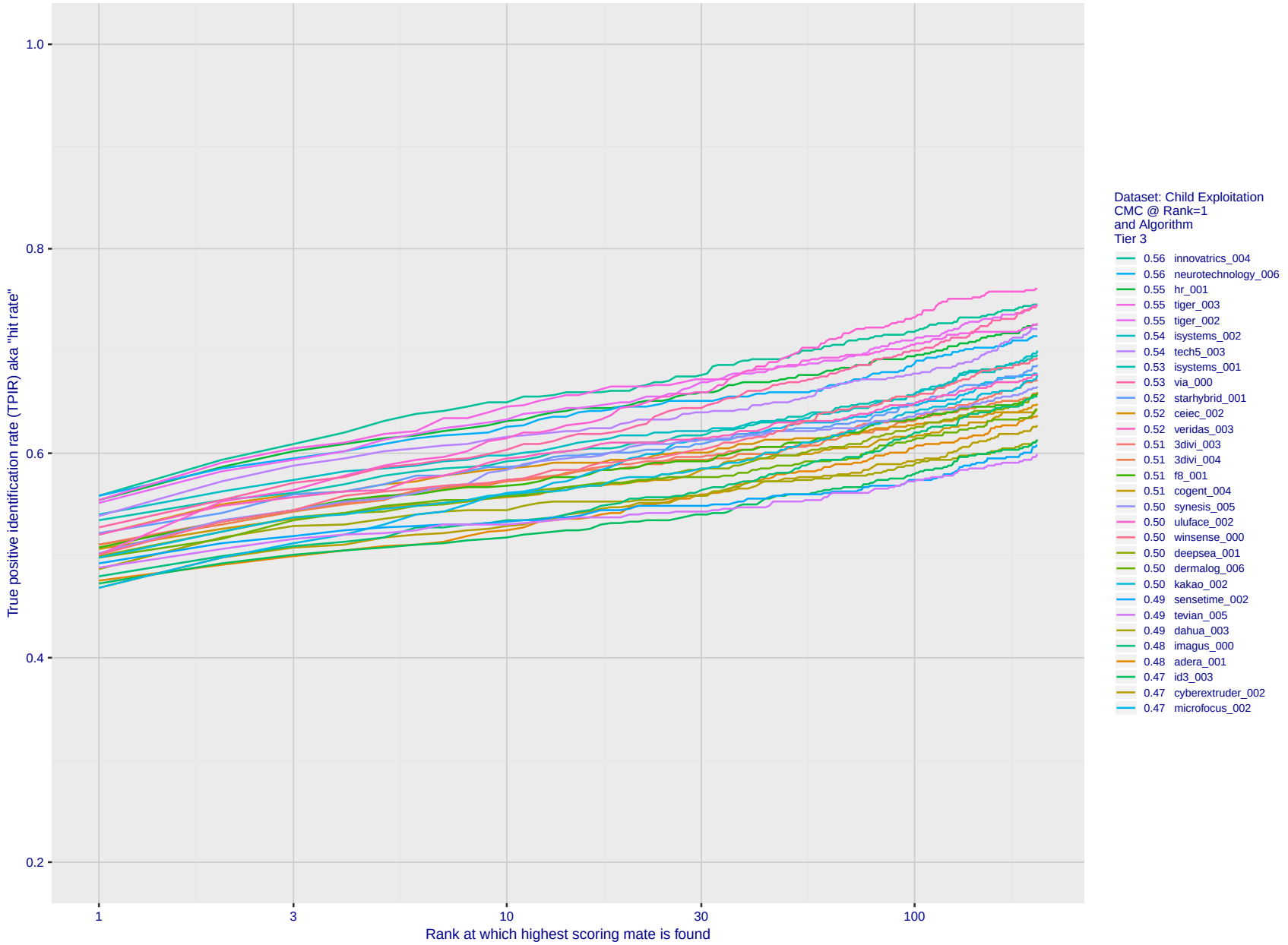

Figure 70: For child exploitation images, cumulative match characteristics (CMC) showing true positive identification rate vs. rank. This is simulation of a one-to-many search experiment - see discussion in section 3.2. The scales are logarithmic in order to show the effect of long candidate lists. Accuracy is poor but much improved relative to the 1:1 DETs of Fig. 67 because a search can succeed if any of a subject's several enrolled images matches the search image with a high score.

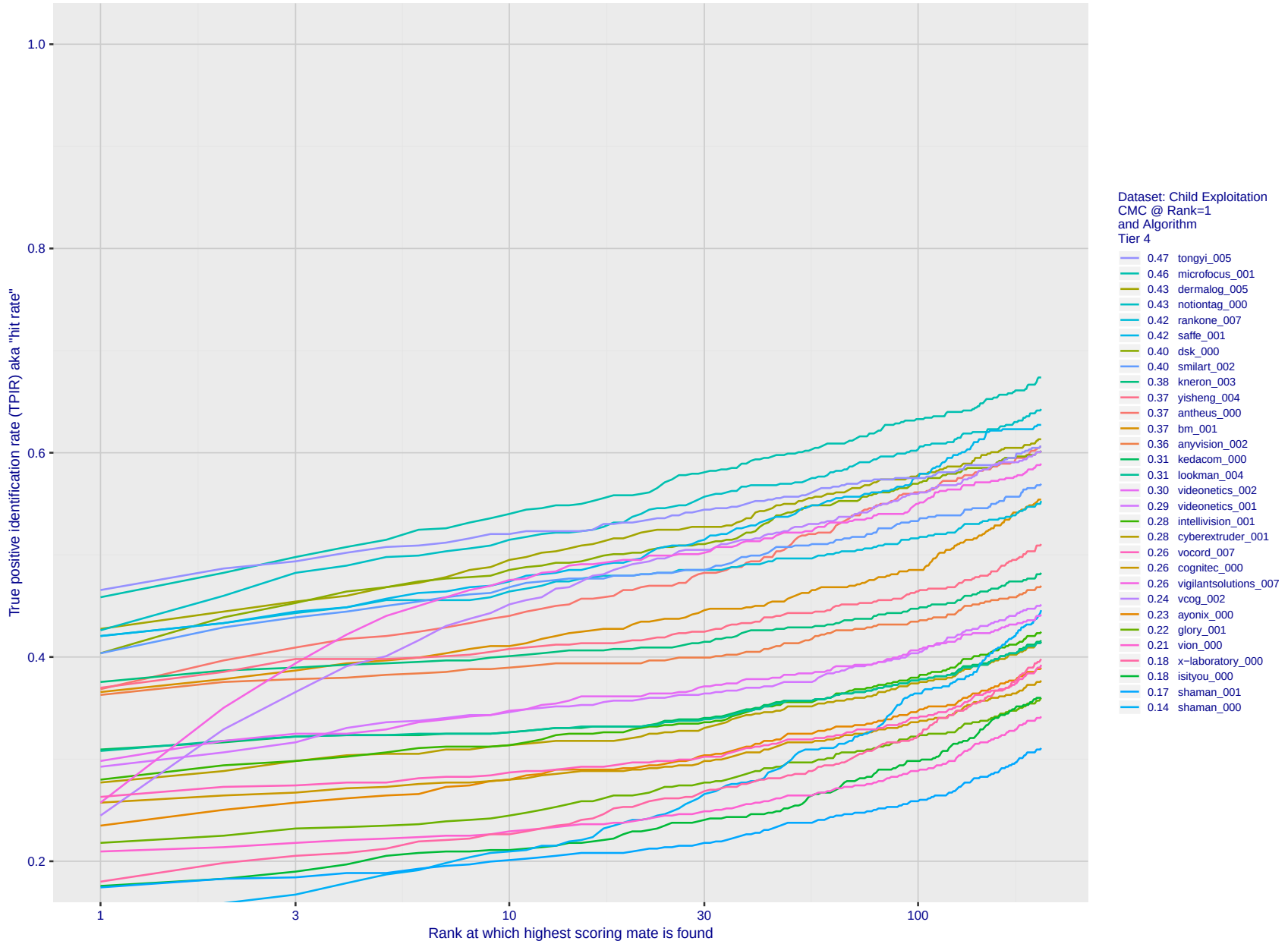

Figure 71: For child exploitation images, cumulative match characteristics (CMC) showing true positive identification rate vs. rank. This is simulation of a one-to-many search experiment - see discussion in section 3.2. The scales are logarithmic in order to show the effect of long candidate lists. Accuracy is poor but much improved relative to the 1:1 DETs of Fig. 67 because a search can succeed if any of a subject's several enrolled images matches the search image with a high score.

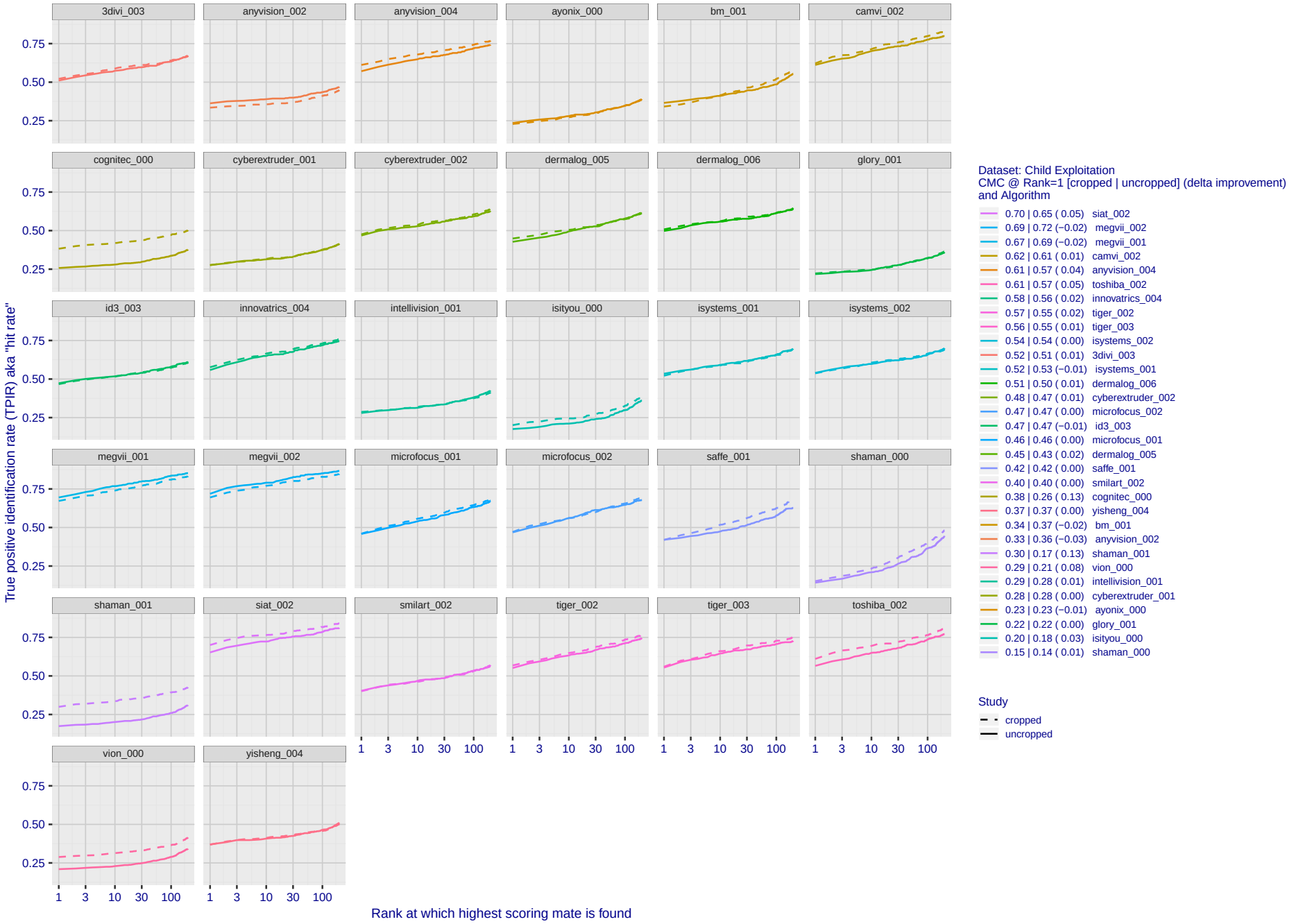

Figure 72: For child exploitation images, cumulative match characteristics (CMC) showing true positive identification rate vs. rank for two cases: 1. Whole image provided to the algorithm; 2. Human annotated rectangular region, cropped and provided to the algorithm. The difference between the traces is associated with detection of difficult faces, and fine localization.

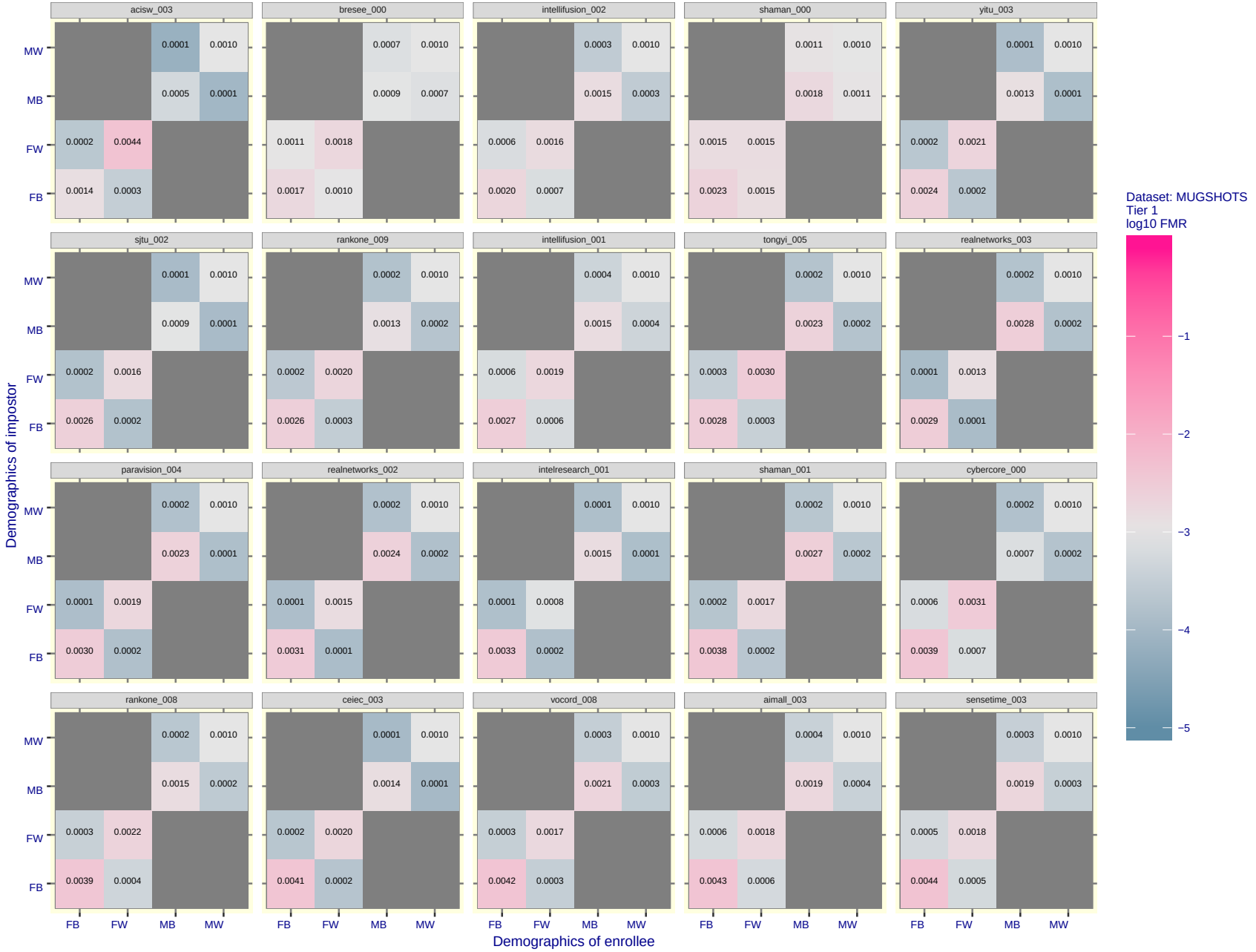

Figure 73: For the mugshot images, FMR *for same-sex impostor pairs of images annotated with codes for black female, black male, white female, white male. The threshold is set for each algorithm to give* FMR *= 0.001 for white males which is the demographc that usually gives the lowest* FMR*. This means the top right box is the same color in all panels. The panels are sorted over multiple pages in order of* FMR *on black females, which is the demographc that usually gives the highest* FMR*.*

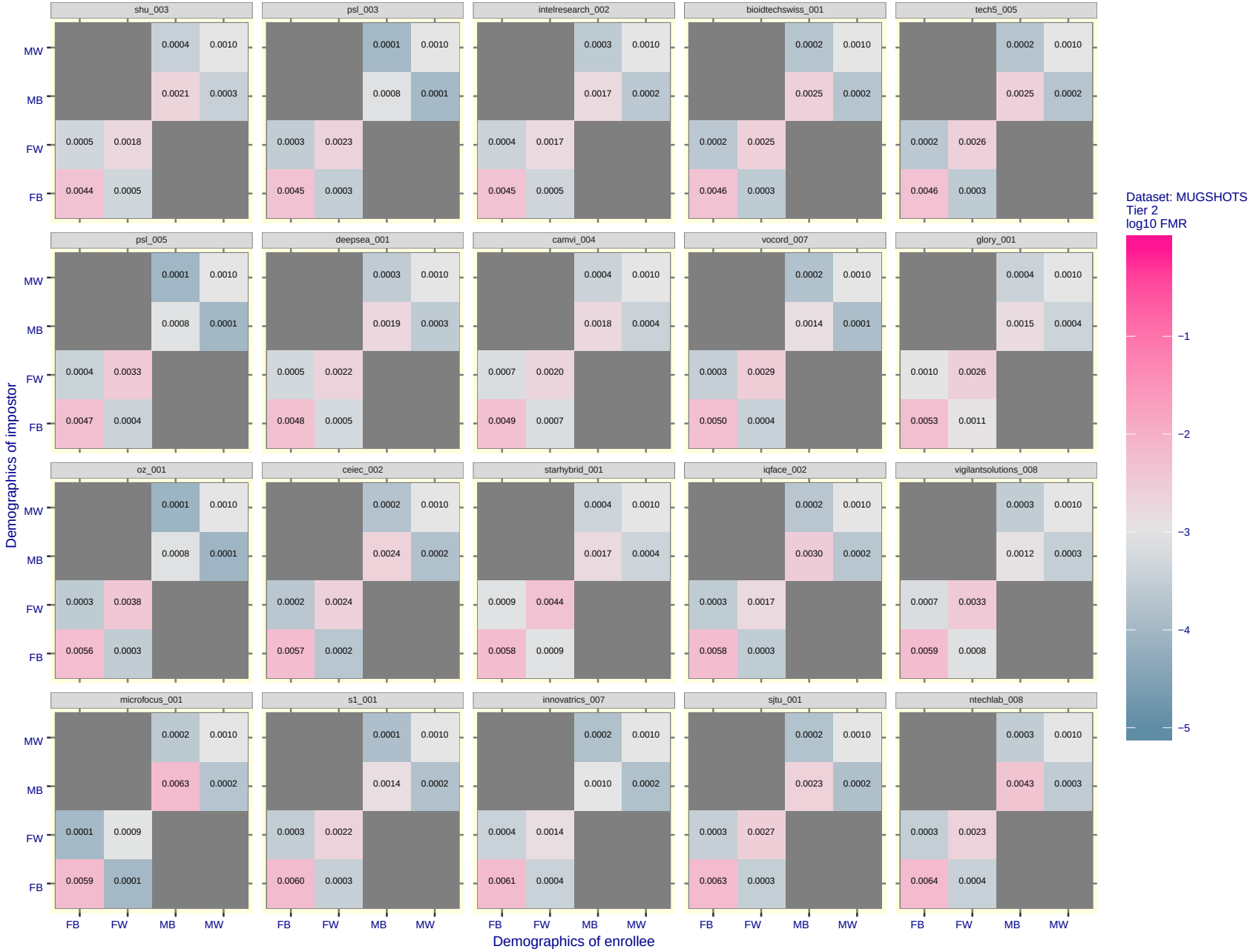

Figure 74: For the mugshot images, FMR *for same-sex impostor pairs of images annotated with codes for black female, black male, white female, white male. The threshold is set for each algorithm to give* FMR *= 0.001 for white males which is the demographc that usually gives the lowest* FMR*. This means the top right box is the same color in all panels. The panels are sorted over multiple pages in order of* FMR *on black females, which is the demographc that usually gives the highest* FMR*.*

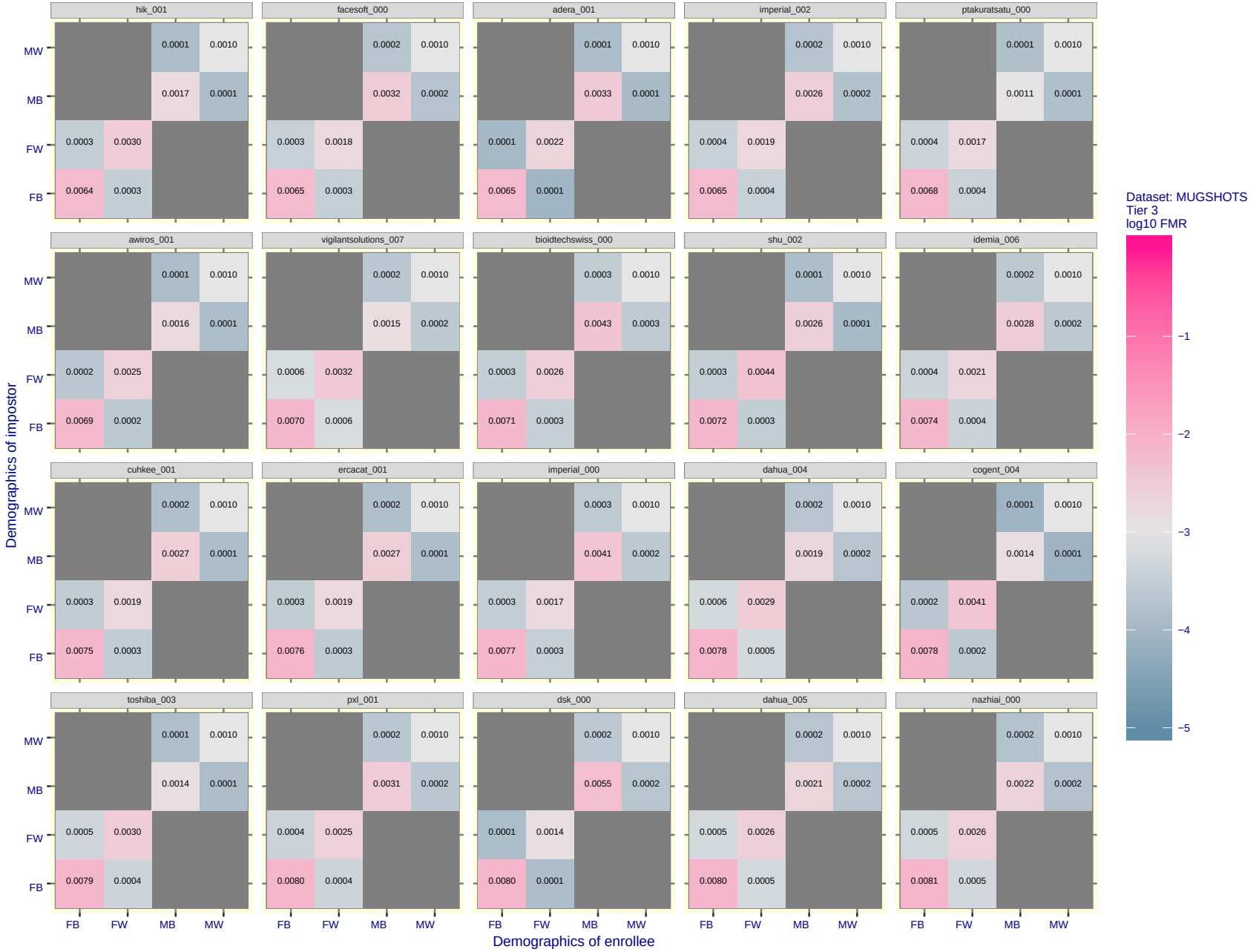

Figure 75: For the mugshot images, FMR *for same-sex impostor pairs of images annotated with codes for black female, black male, white female, white male. The threshold is set for each algorithm to give* FMR *= 0.001 for white males which is the demographc that usually gives the lowest* FMR*. This means the top right box is the same color in all panels. The panels are sorted over multiple pages in order of* FMR *on black females, which is the demographc that usually gives the highest* FMR*.*

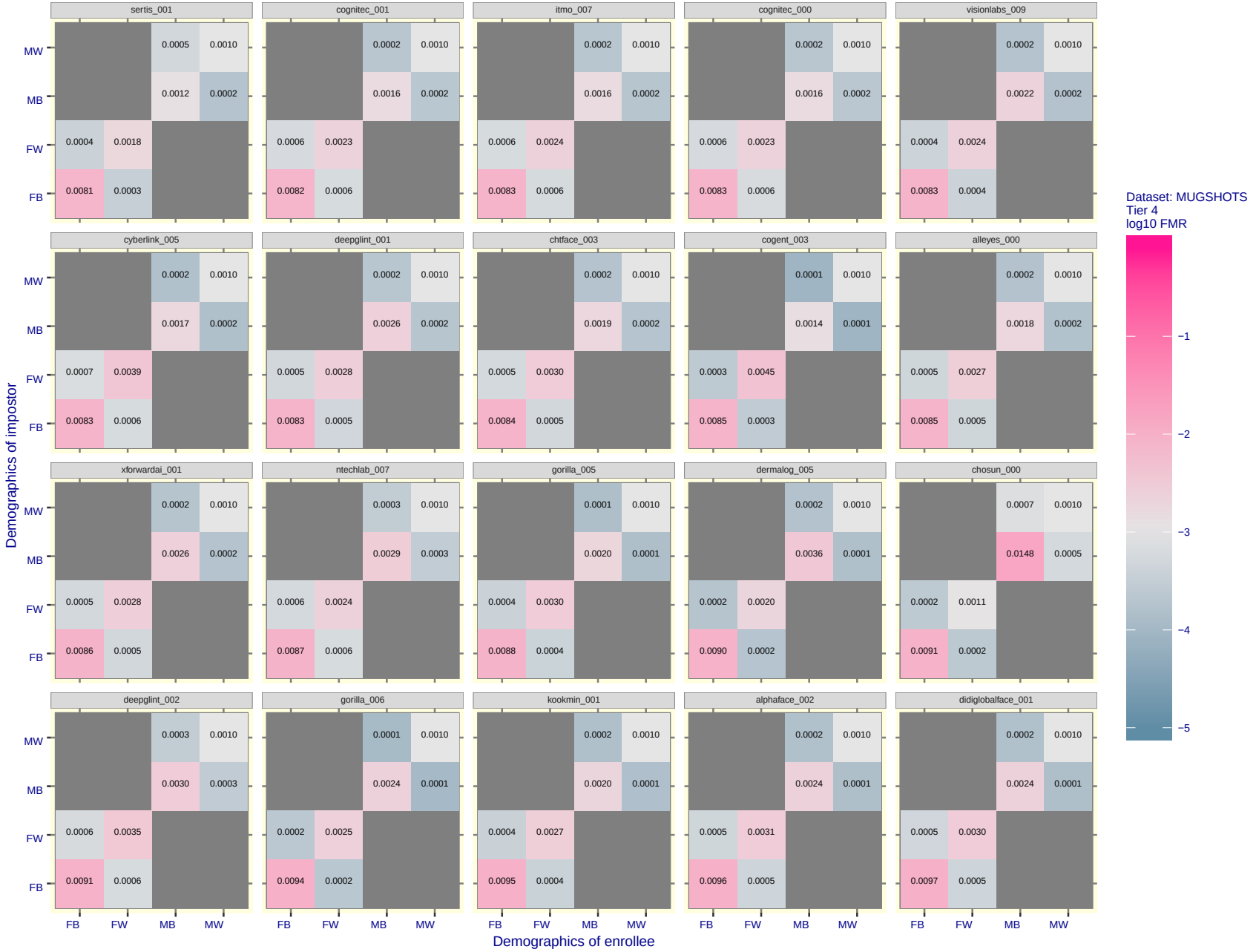

Figure 76: For the mugshot images, FMR *for same-sex impostor pairs of images annotated with codes for black female, black male, white female, white male. The threshold is set for each algorithm to give* FMR *= 0.001 for white males which is the demographc that usually gives the lowest* FMR*. This means the top right box is the same color in all panels. The panels are sorted over multiple pages in order of* FMR *on black females, which is the demographc that usually gives the highest* FMR*.*

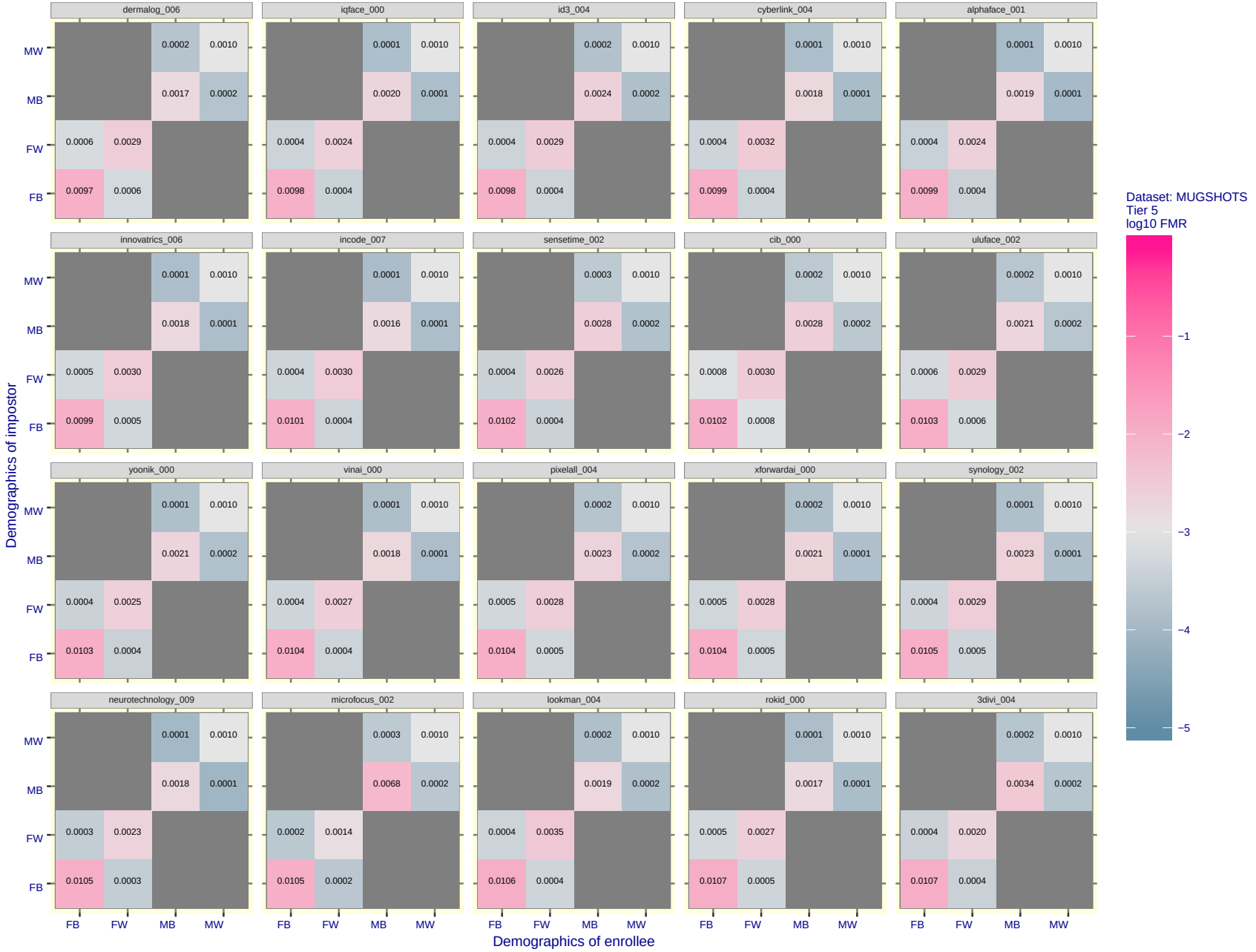

Figure 77: For the mugshot images, FMR *for same-sex impostor pairs of images annotated with codes for black female, black male, white female, white male. The threshold is set for each algorithm to give* FMR *= 0.001 for white males which is the demographc that usually gives the lowest* FMR*. This means the top right box is the same color in all panels. The panels are sorted over multiple pages in order of* FMR *on black females, which is the demographc that usually gives the highest* FMR*.*

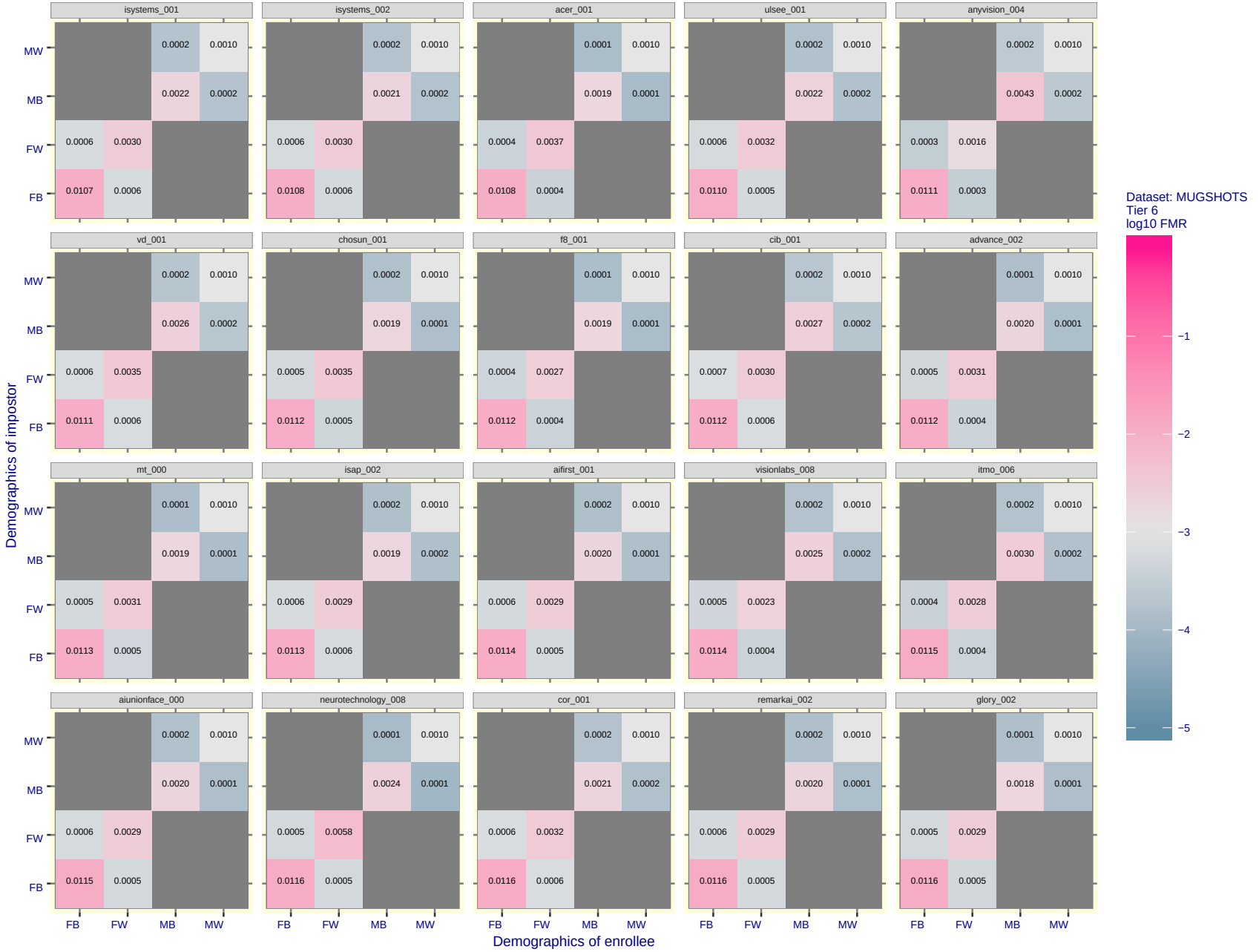

Figure 78: For the mugshot images, FMR *for same-sex impostor pairs of images annotated with codes for black female, black male, white female, white male. The threshold is set for each algorithm to give* FMR *= 0.001 for white males which is the demographc that usually gives the lowest* FMR*. This means the top right box is the same color in all panels. The panels are sorted over multiple pages in order of* FMR *on black females, which is the demographc that usually gives the highest* FMR*.*

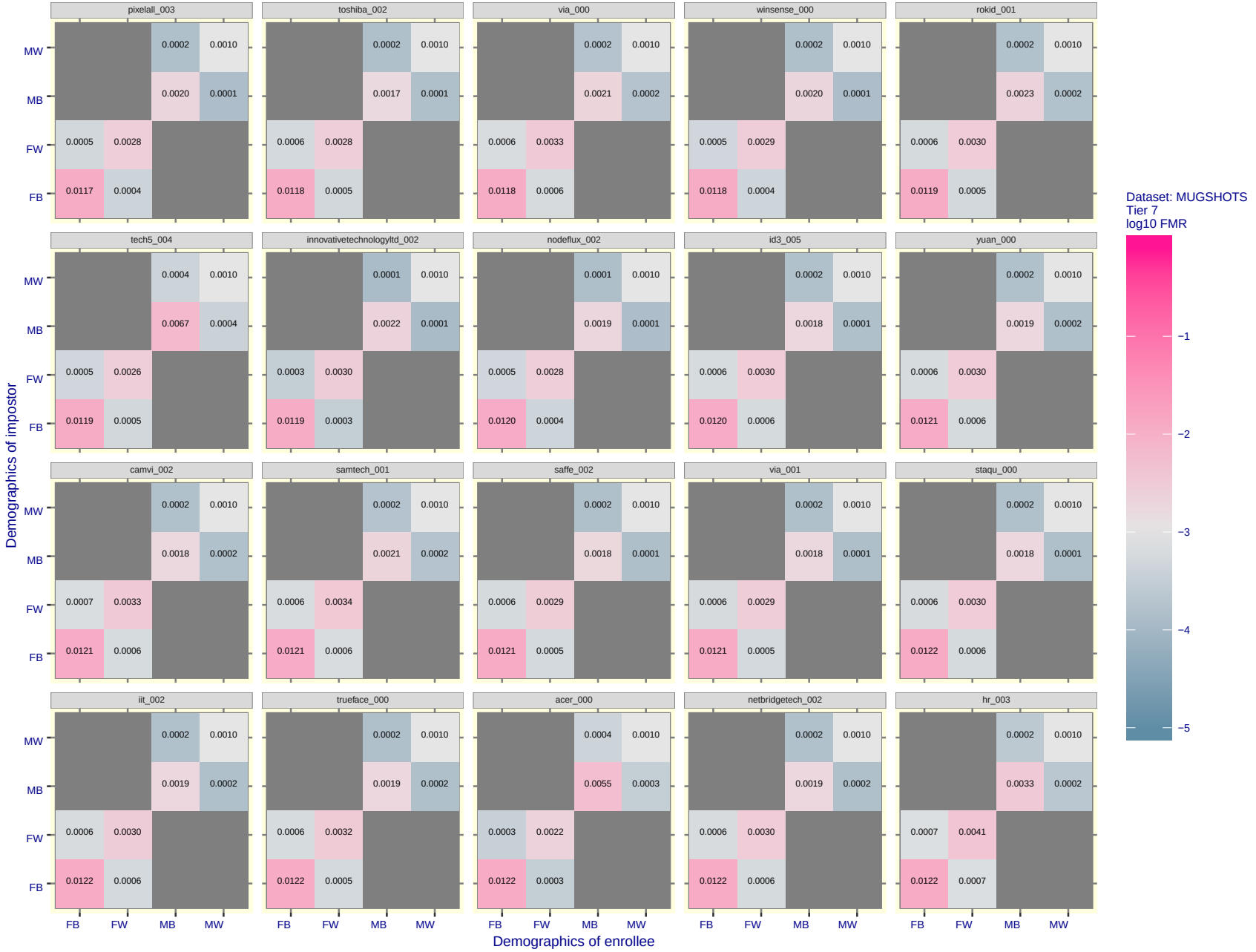

Figure 79: For the mugshot images, FMR *for same-sex impostor pairs of images annotated with codes for black female, black male, white female, white male. The threshold is set for each algorithm to give* FMR *= 0.001 for white males which is the demographc that usually gives the lowest* FMR*. This means the top right box is the same color in all panels. The panels are sorted over multiple pages in order of* FMR *on black females, which is the demographc that usually gives the highest* FMR*.*

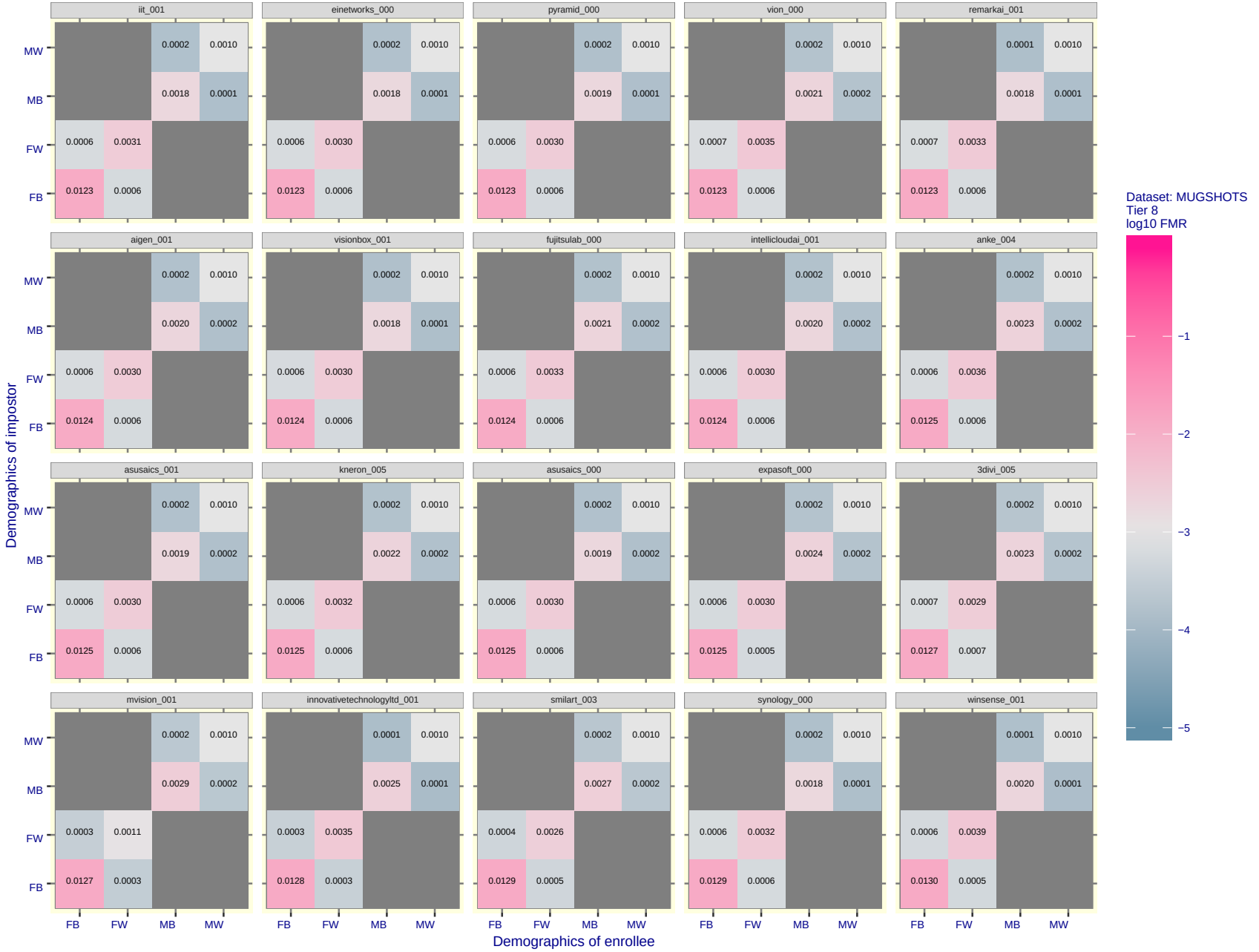

Figure 80: For the mugshot images, FMR *for same-sex impostor pairs of images annotated with codes for black female, black male, white female, white male. The threshold is set for each algorithm to give* FMR *= 0.001 for white males which is the demographc that usually gives the lowest* FMR*. This means the top right box is the same color in all panels. The panels are sorted over multiple pages in order of* FMR *on black females, which is the demographc that usually gives the highest* FMR*.*

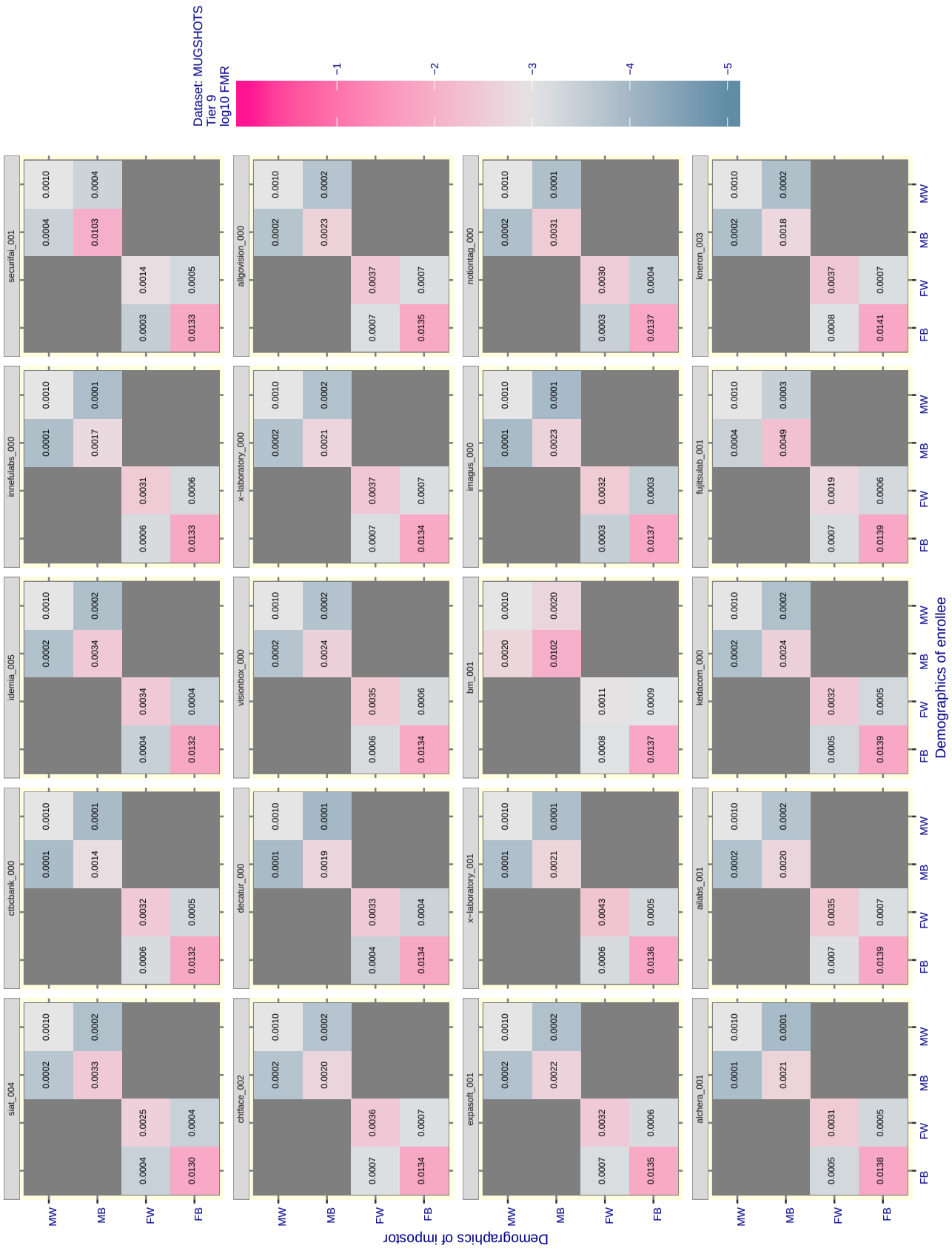

Figure 81: For the mugshot images, FMR for same-sex impostor pairs of images annotated with codes for black female, black male, white female, white male. The threshold is set for each algorithm to give FMR = 0.001 for white males which is the demographic that usually gives the lowest FMR. This means the top right box is the same color in all panels. The panels are sorted over multiple pages in order of FMR on black females, which is the demographic that usually gives the highest FMR.

FNMR(T) "False non-match rate"
FMR(T) "False match rate"

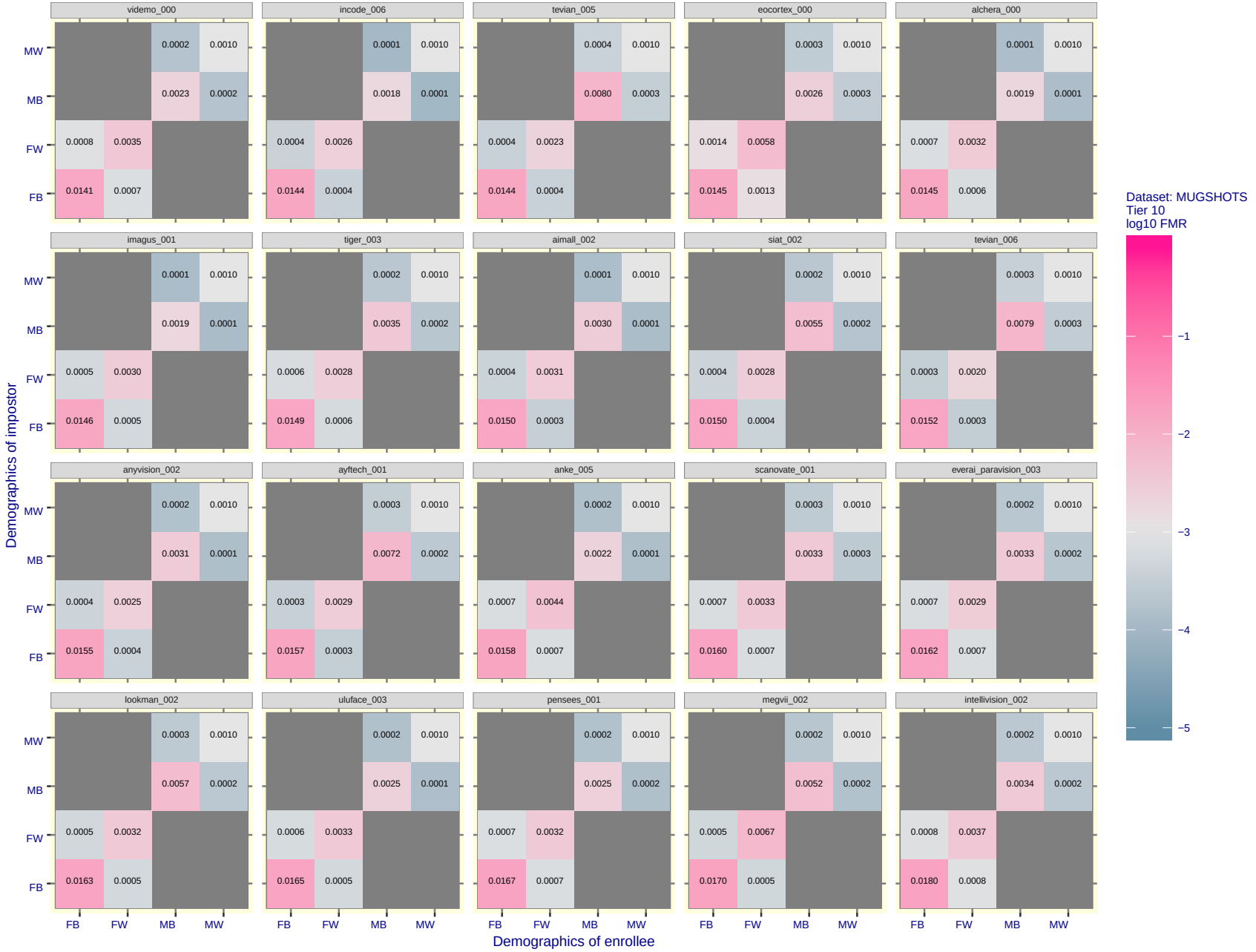

Figure 82: For the mugshot images, FMR *for same-sex impostor pairs of images annotated with codes for black female, black male, white female, white male. The threshold is set for each algorithm to give* FMR *= 0.001 for white males which is the demographc that usually gives the lowest* FMR*. This means the top right box is the same color in all panels. The panels are sorted over multiple pages in order of* FMR *on black females, which is the demographc that usually gives the highest* FMR*.*

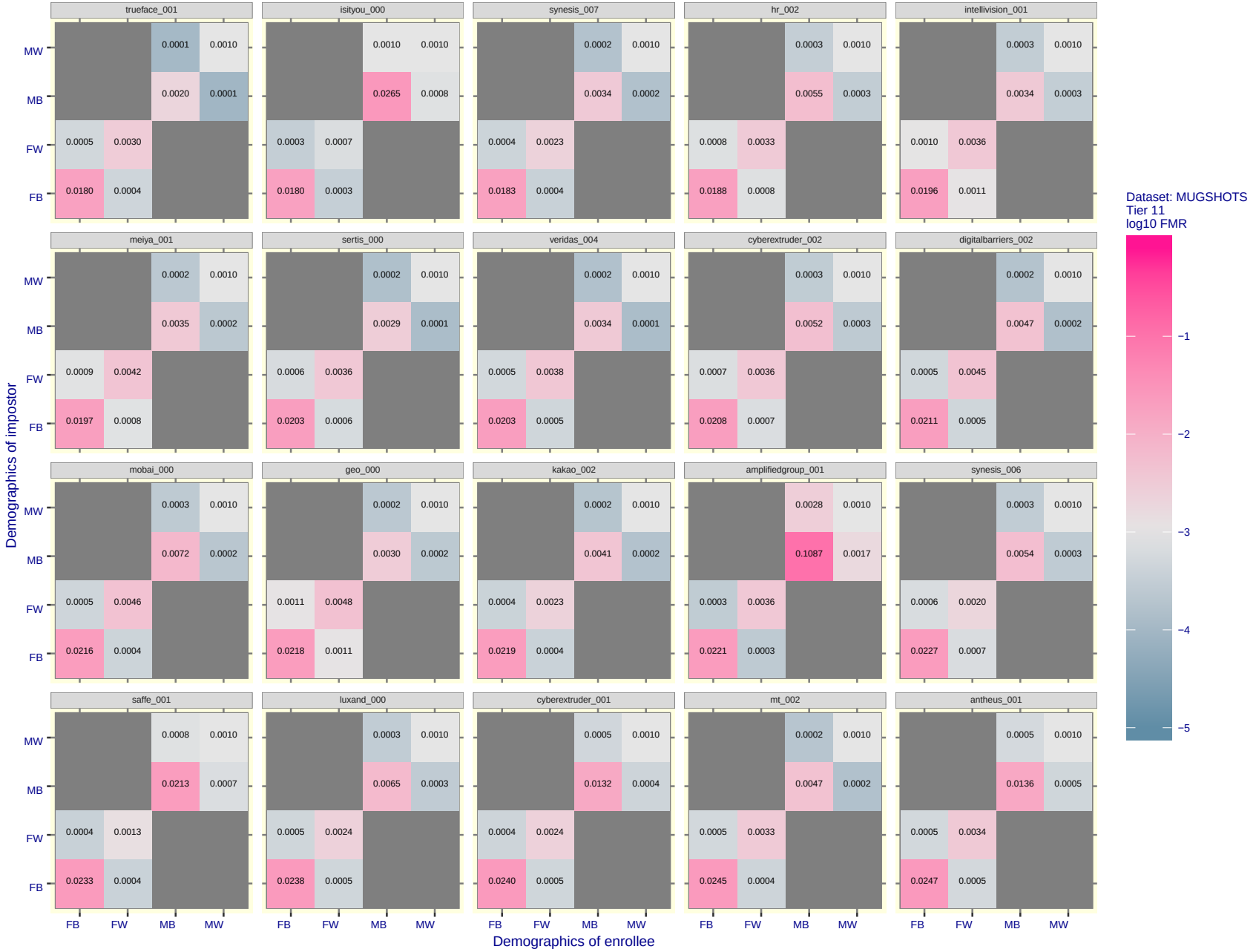

Figure 83: For the mugshot images, FMR *for same-sex impostor pairs of images annotated with codes for black female, black male, white female, white male. The threshold is set for each algorithm to give* FMR *= 0.001 for white males which is the demographc that usually gives the lowest* FMR*. This means the top right box is the same color in all panels. The panels are sorted over multiple pages in order of* FMR *on black females, which is the demographc that usually gives the highest* FMR*.*

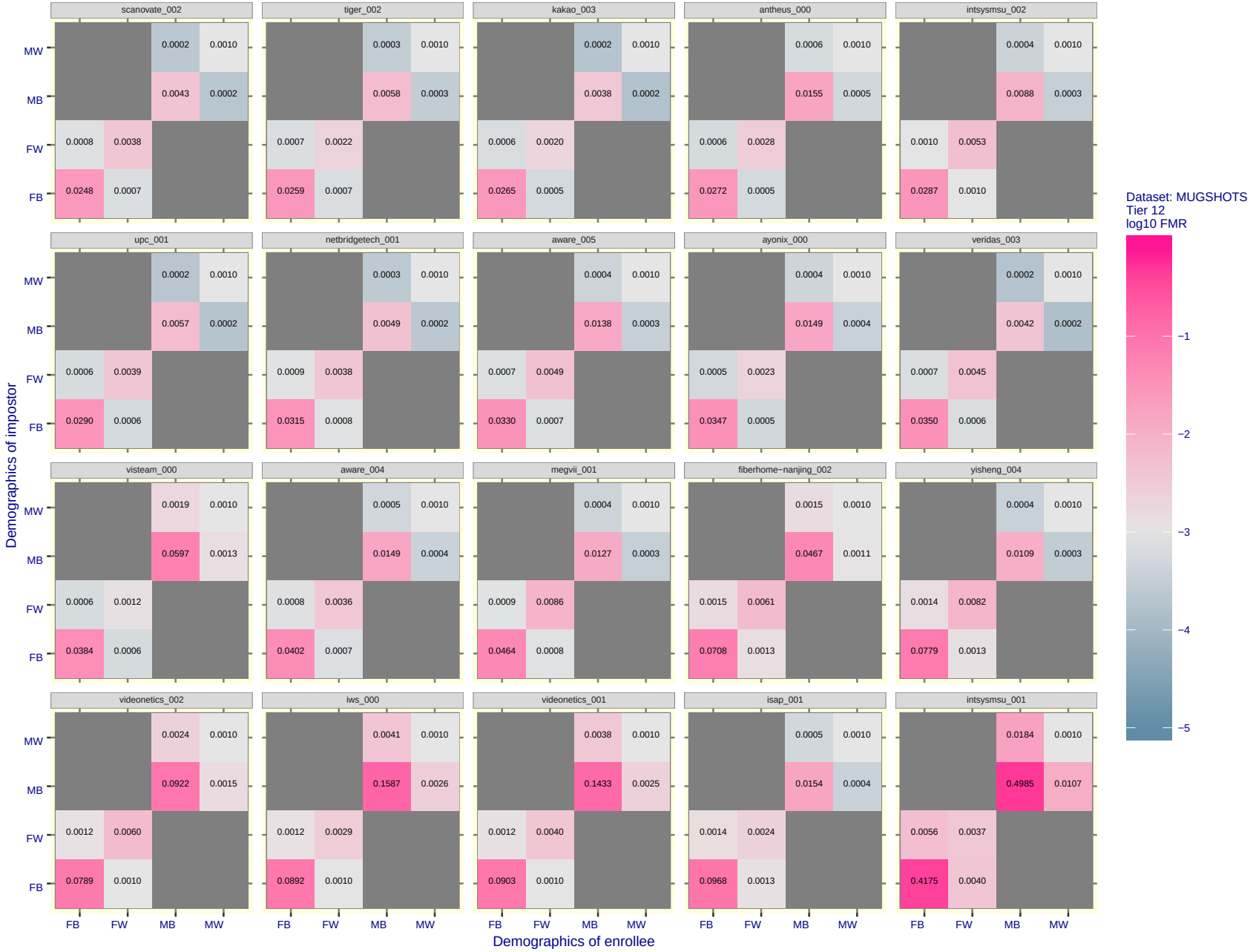

Figure 84: For the mugshot images, FMR *for same-sex impostor pairs of images annotated with codes for black female, black male, white female, white male. The threshold is set for each algorithm to give* FMR *= 0.001 for white males which is the demographc that usually gives the lowest* FMR*. This means the top right box is the same color in all panels. The panels are sorted over multiple pages in order of* FMR *on black females, which is the demographc that usually gives the highest* FMR*.*

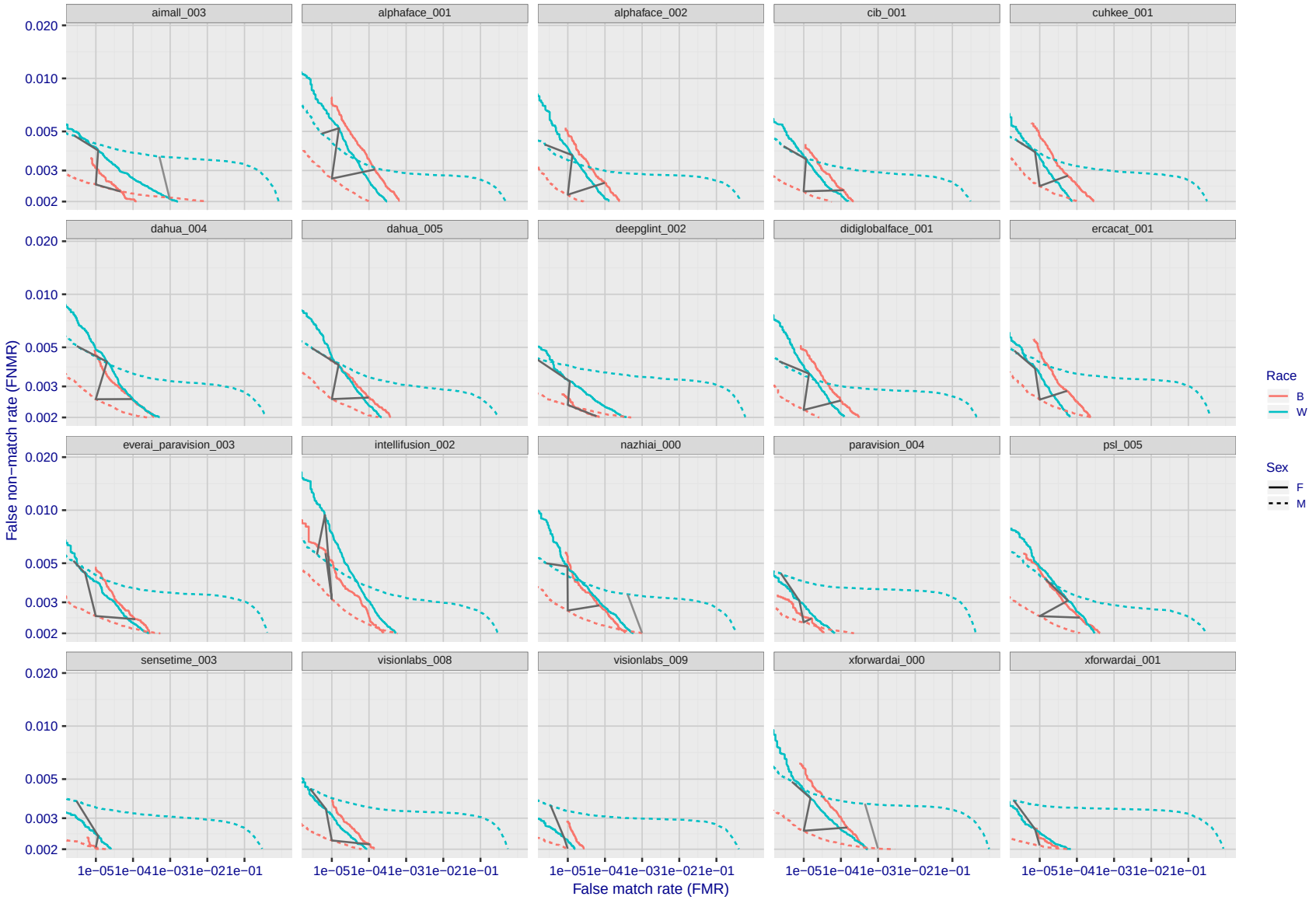

Figure 85: For the mugshot images, error tradeoff characteristics for white females, black females, black males and white males. The Z-shaped grey lines correspond to fixed thresholds, showing both *FNMR and FMR vary at one T value. Note: Many of the plots will naively be read as saying women gives worse error rates than men because the solid traces lie above the dotted ones. However, this is misleading and incomplete: The grey lines show the traces reveal horizontal shifts. Thus for the cogent-003 algorithm FNMR for men is* higher *than for women* at a fixed threshold *but, at the same time, FMR is higher for women - see Figure 131. As access control systems almost always operate at a fixed threshold, the naive interpretation is incorrect.*

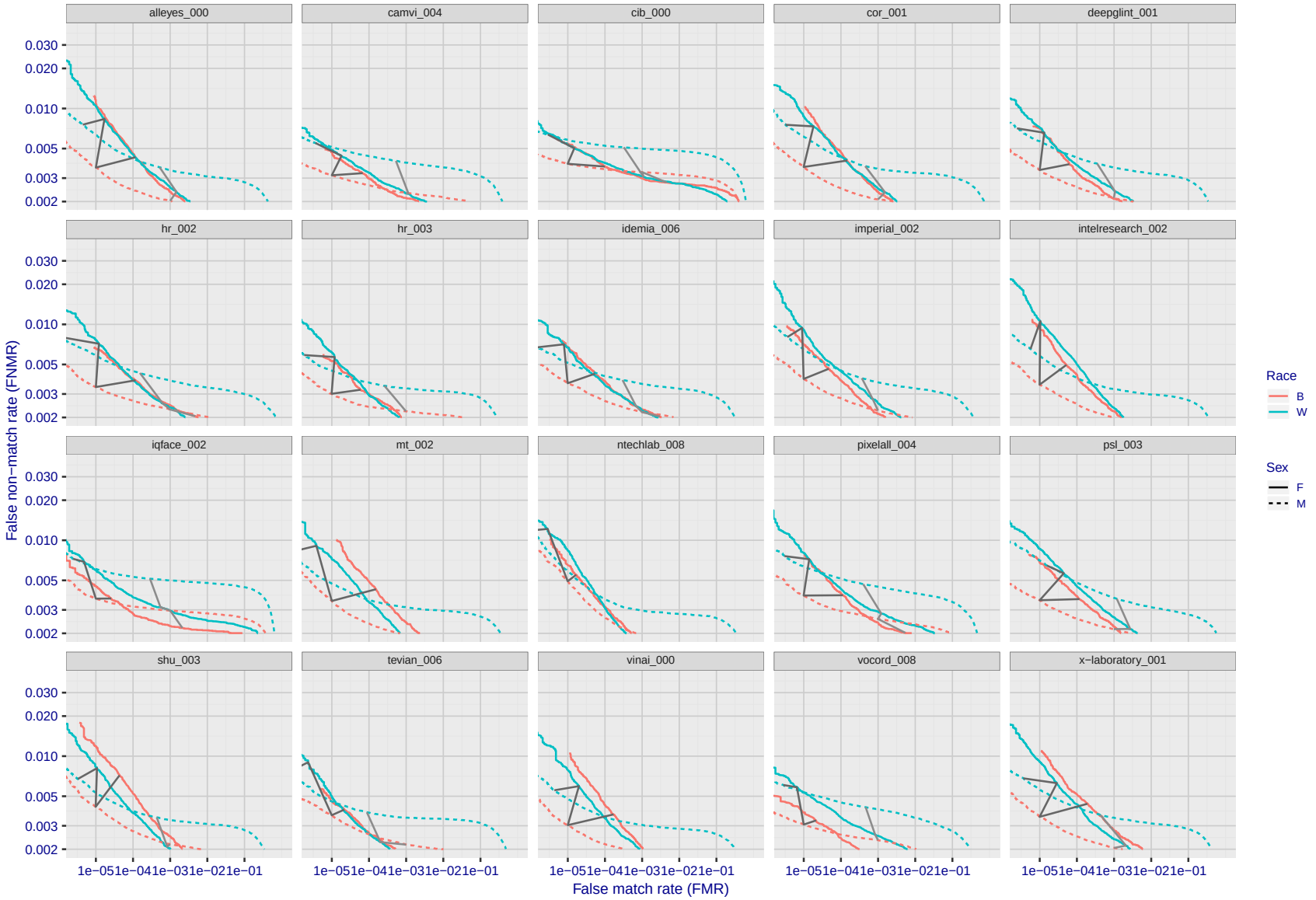

Figure 86: For the mugshot images, error tradeoff characteristics for white females, black females, black males and white males. The Z-shaped grey lines correspond to fixed thresholds, showing both *FNMR and FMR vary at one T value. Note: Many of the plots will naively be read as saying women gives worse error rates than men because the solid traces lie above the dotted ones. However, this is misleading and incomplete: The grey lines show the traces reveal horizontal shifts. Thus for the cogent-003 algorithm FNMR for men is* higher *than for women* at a fixed threshold *but, at the same time, FMR is higher for women - see Figure 131. As access control systems almost always operate at a fixed threshold, the naive interpretation is incorrect.*

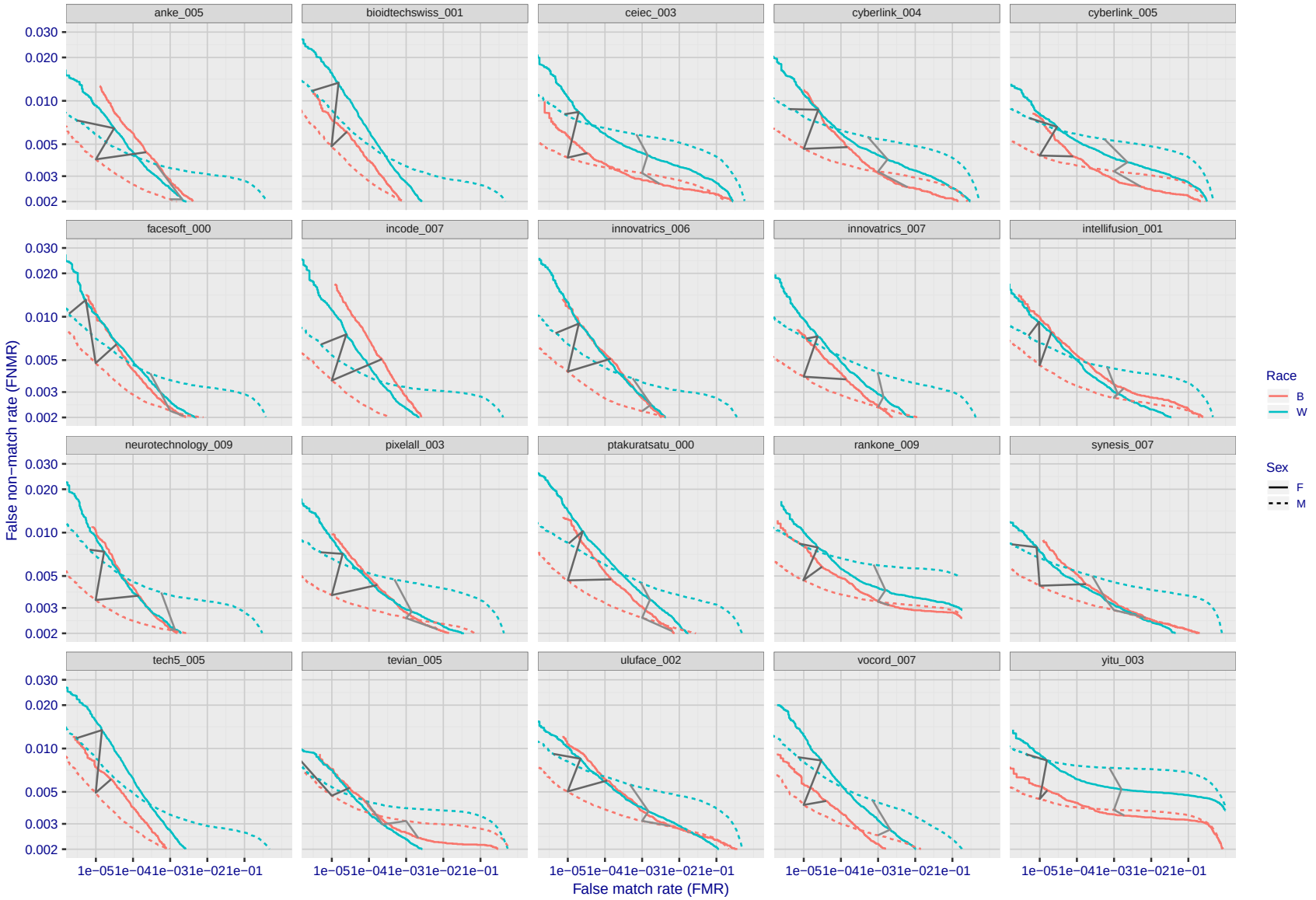

Figure 87: For the mugshot images, error tradeoff characteristics for white females, black females, black males and white males. The Z-shaped grey lines correspond to fixed thresholds, showing both *FNMR and FMR vary at one T value. Note: Many of the plots will naively be read as saying women gives worse error rates than men because the solid traces lie above the dotted ones. However, this is misleading and incomplete: The grey lines show the traces reveal horizontal shifts. Thus for the cogent-003 algorithm FNMR for men is* higher *than for women* at a fixed threshold *but, at the same time, FMR is higher for women - see Figure 131. As access control systems almost always operate at a fixed threshold, the naive interpretation is incorrect.*

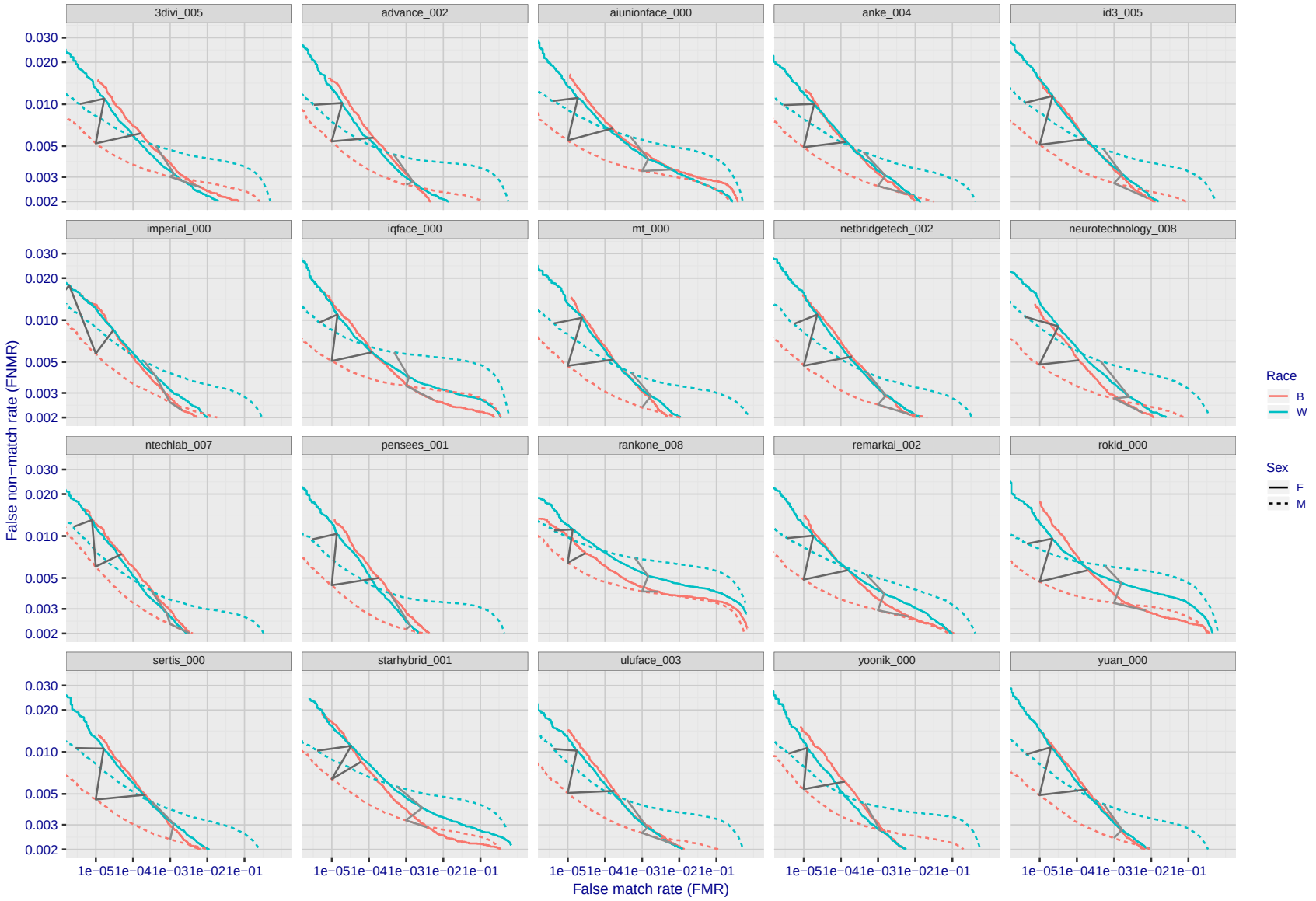

Figure 88: For the mugshot images, error tradeoff characteristics for white females, black females, black males and white males. The Z-shaped grey lines correspond to fixed thresholds, showing both *FNMR and FMR vary at one T value. Note: Many of the plots will naively be read as saying women gives worse error rates than men because the solid traces lie above the dotted ones. However, this is misleading and incomplete: The grey lines show the traces reveal horizontal shifts. Thus for the cogent-003 algorithm FNMR for men is* higher *than for women* at a fixed threshold *but, at the same time, FMR is higher for women - see Figure 131. As access control systems almost always operate at a fixed threshold, the naive interpretation is incorrect.*

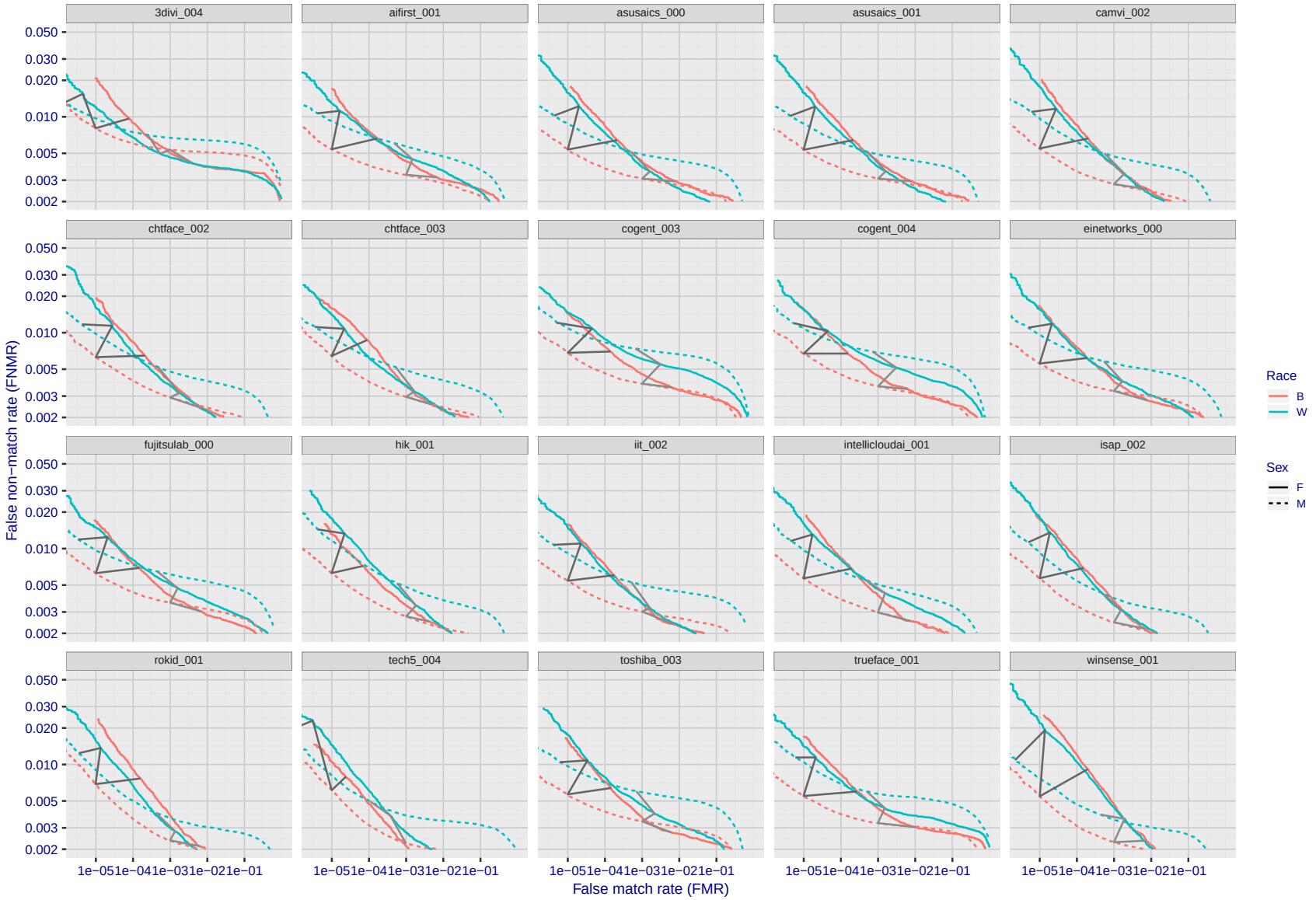

Figure 89: For the mugshot images, error tradeoff characteristics for white females, black females, black males and white males. The Z-shaped grey lines correspond to fixed thresholds, showing both *FNMR and FMR vary at one T value. Note: Many of the plots will naively be read as saying women gives worse error rates than men because the solid traces lie above the dotted ones. However, this is misleading and incomplete: The grey lines show the traces reveal horizontal shifts. Thus for the cogent-003 algorithm FNMR for men is* higher *than for women* at a fixed threshold *but, at the same time, FMR is higher for women - see Figure 131. As access control systems almost always operate at a fixed threshold, the naive interpretation is incorrect.*

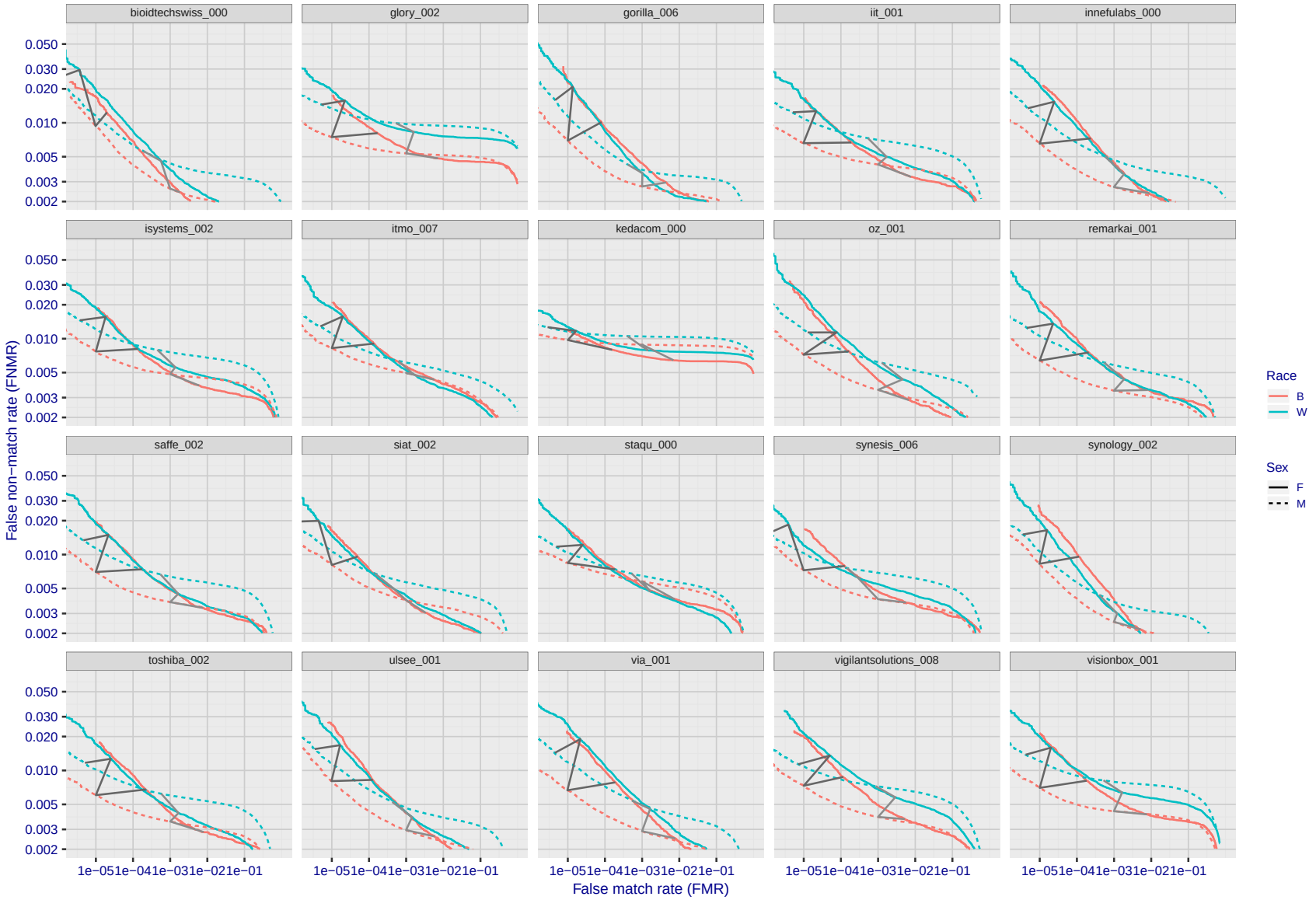

Figure 90: For the mugshot images, error tradeoff characteristics for white females, black females, black males and white males. The Z-shaped grey lines correspond to fixed thresholds, showing both *FNMR and FMR vary at one T value. Note: Many of the plots will naively be read as saying women gives worse error rates than men because the solid traces lie above the dotted ones. However, this is misleading and incomplete: The grey lines show the traces reveal horizontal shifts. Thus for the cogent-003 algorithm FNMR for men is* higher *than for women* at a fixed threshold *but, at the same time, FMR is higher for women - see Figure 131. As access control systems almost always operate at a fixed threshold, the naive interpretation is incorrect.*

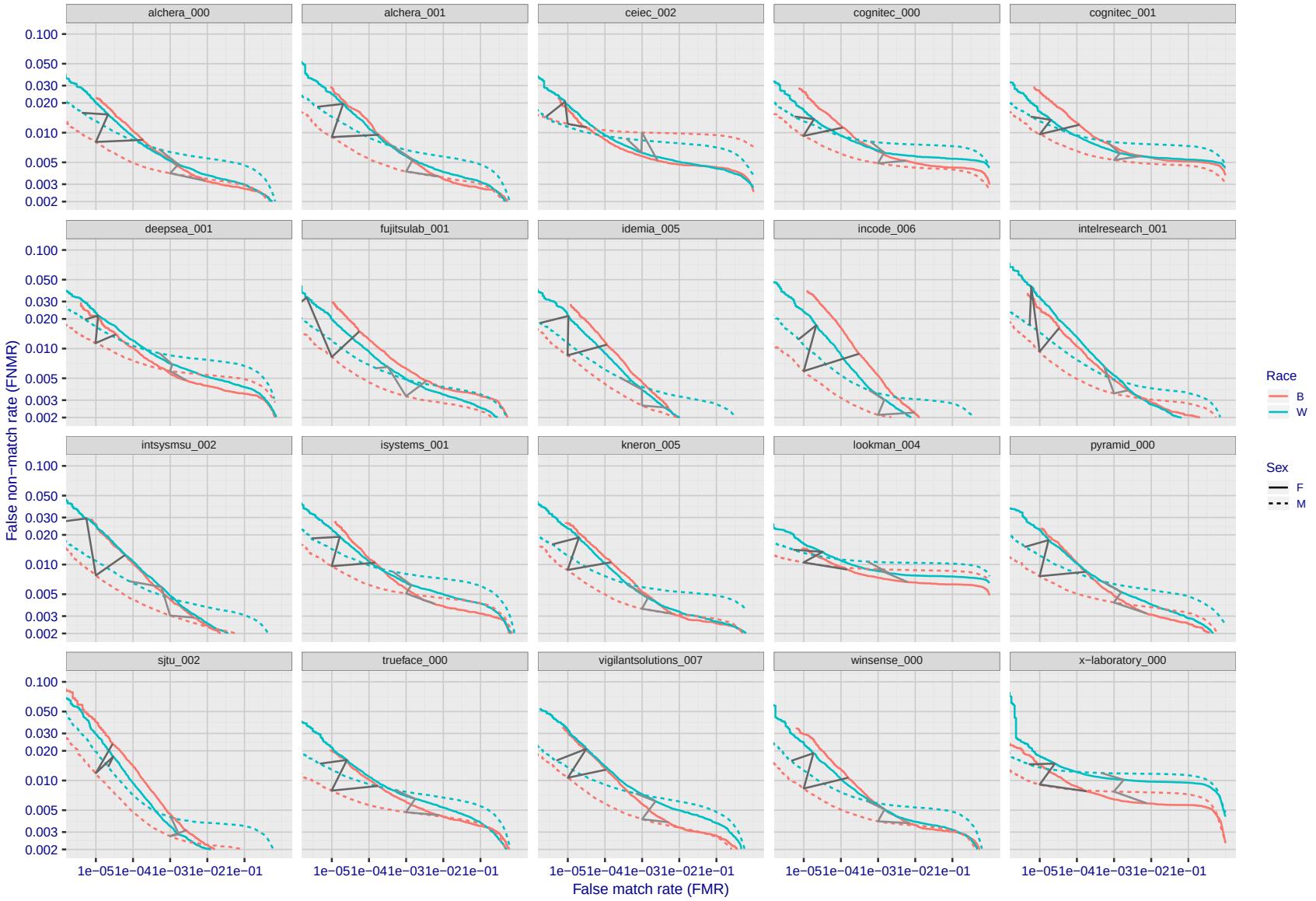

Figure 91: For the mugshot images, error tradeoff characteristics for white females, black females, black males and white males. The Z-shaped grey lines correspond to fixed thresholds, showing both *FNMR and FMR vary at one T value. Note: Many of the plots will naively be read as saying women gives worse error rates than men because the solid traces lie above the dotted ones. However, this is misleading and incomplete: The grey lines show the traces reveal horizontal shifts. Thus for the cogent-003 algorithm FNMR for men is* higher *than for women* at a fixed threshold *but, at the same time, FMR is higher for women - see Figure 131. As access control systems almost always operate at a fixed threshold, the naive interpretation is incorrect.*

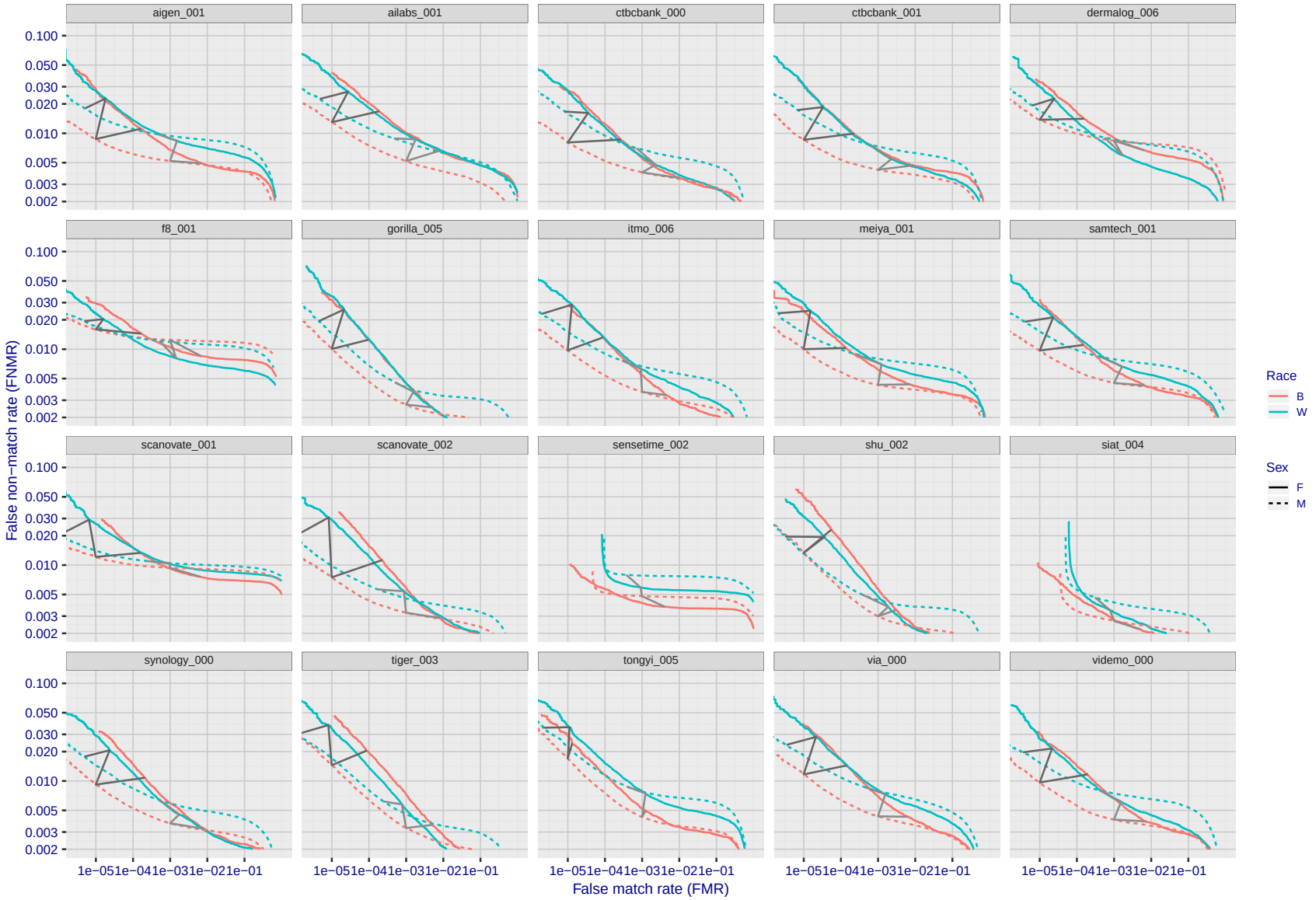

Figure 92: For the mugshot images, error tradeoff characteristics for white females, black females, black males and white males. The Z-shaped grey lines correspond to fixed thresholds, showing both *FNMR and FMR vary at one T value. Note: Many of the plots will naively be read as saying women gives worse error rates than men because the solid traces lie above the dotted ones. However, this is misleading and incomplete: The grey lines show the traces reveal horizontal shifts. Thus for the cogent-003 algorithm FNMR for men is* higher *than for women* at a fixed threshold *but, at the same time, FMR is higher for women - see Figure 131. As access control systems almost always operate at a fixed threshold, the naive interpretation is incorrect.*

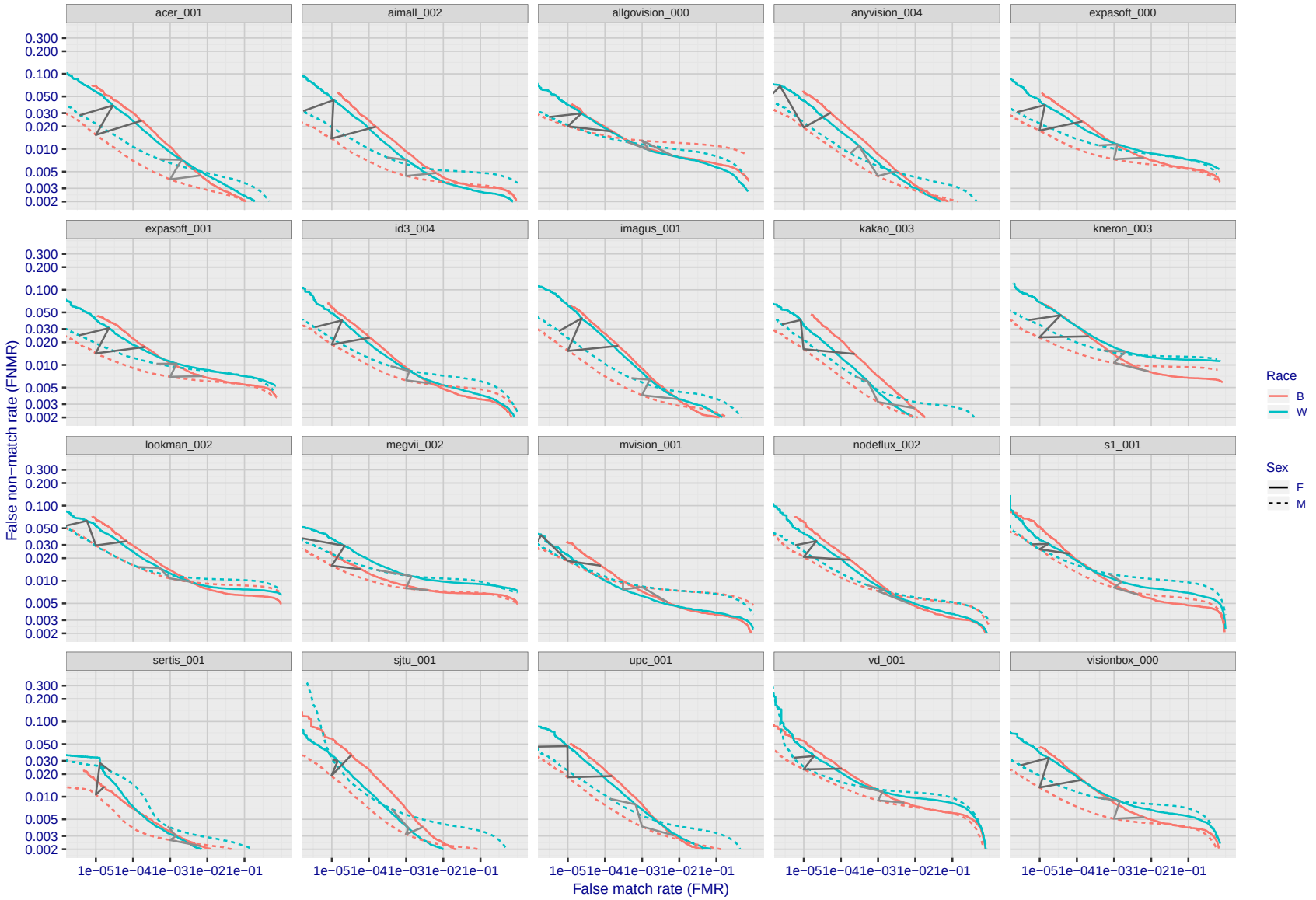

Figure 93: For the mugshot images, error tradeoff characteristics for white females, black females, black males and white males. The Z-shaped grey lines correspond to fixed thresholds, showing both *FNMR and FMR vary at one T value. Note: Many of the plots will naively be read as saying women gives worse error rates than men because the solid traces lie above the dotted ones. However, this is misleading and incomplete: The grey lines show the traces reveal horizontal shifts. Thus for the cogent-003 algorithm FNMR for men is* higher *than for women* at a fixed threshold *but, at the same time, FMR is higher for women - see Figure 131. As access control systems almost always operate at a fixed threshold, the naive interpretation is incorrect.*

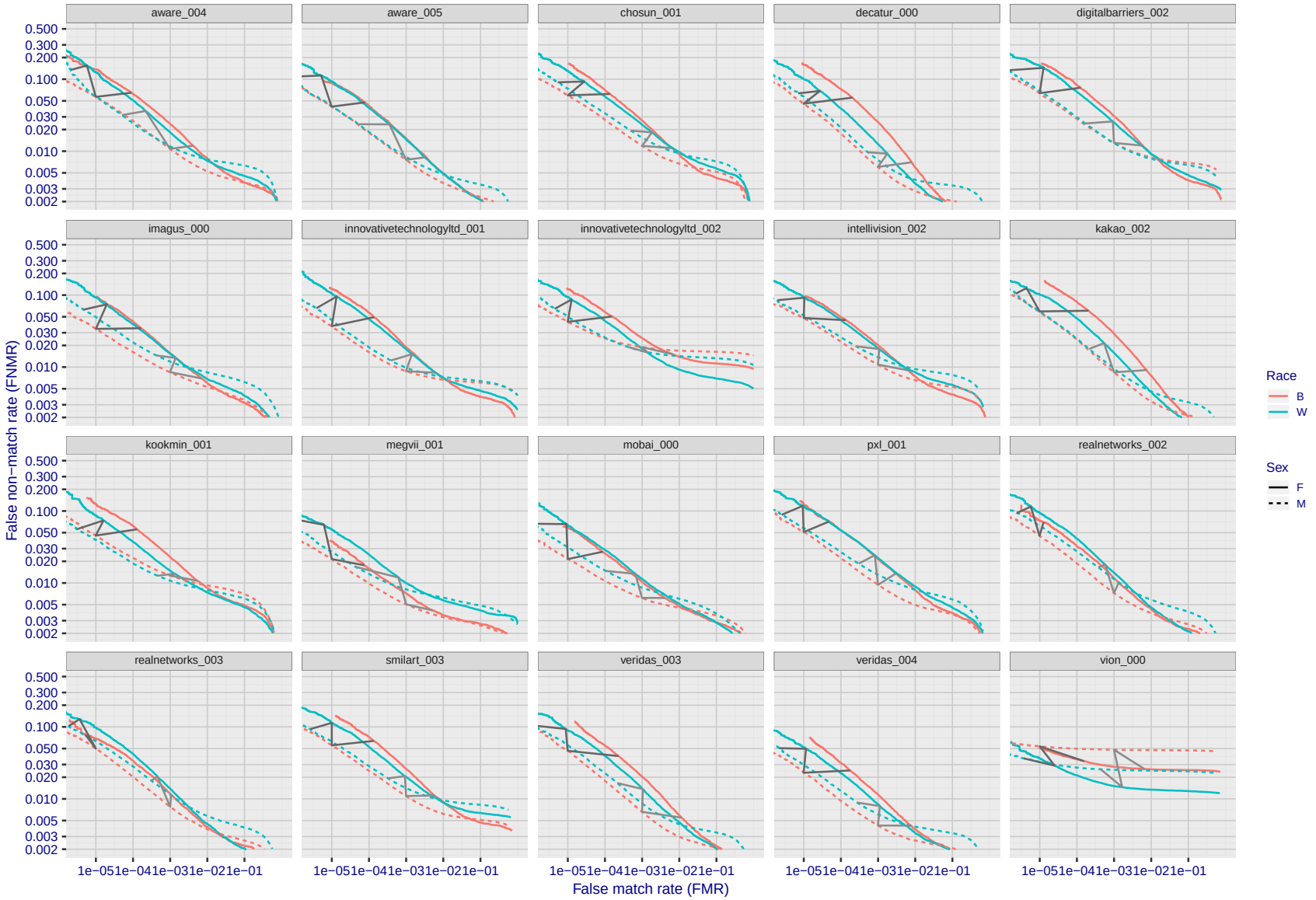

Figure 94: For the mugshot images, error tradeoff characteristics for white females, black females, black males and white males. The Z-shaped grey lines correspond to fixed thresholds, showing both *FNMR and FMR vary at one T value. Note: Many of the plots will naively be read as saying women gives worse error rates than men because the solid traces lie above the dotted ones. However, this is misleading and incomplete: The grey lines show the traces reveal horizontal shifts. Thus for the cogent-003 algorithm FNMR for men is* higher *than for women* at a fixed threshold *but, at the same time, FMR is higher for women - see Figure 131. As access control systems almost always operate at a fixed threshold, the naive interpretation is incorrect.*

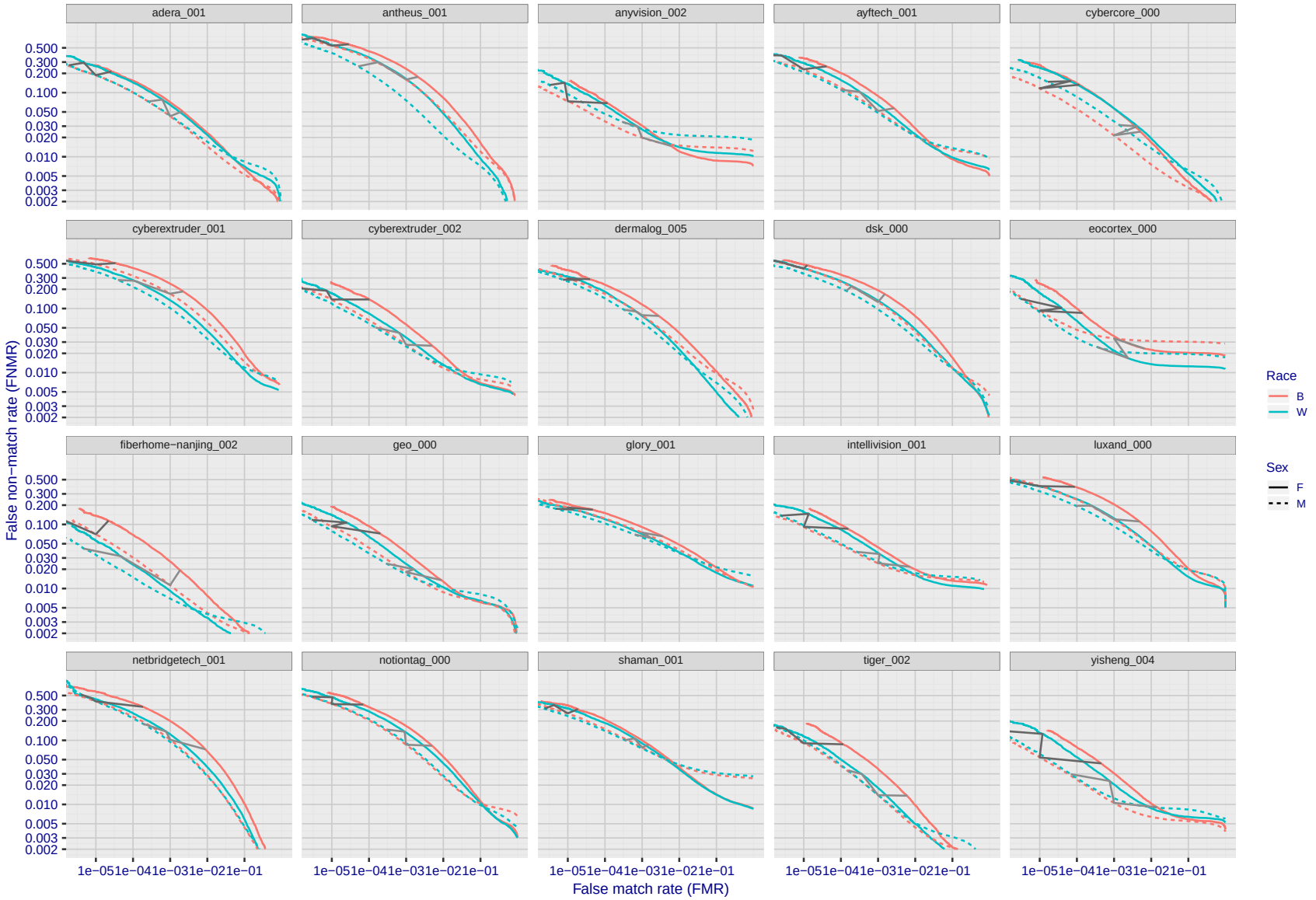

Figure 95: For the mugshot images, error tradeoff characteristics for white females, black females, black males and white males. The Z-shaped grey lines correspond to fixed thresholds, showing both *FNMR and FMR vary at one T value. Note: Many of the plots will naively be read as saying women gives worse error rates than men because the solid traces lie above the dotted ones. However, this is misleading and incomplete: The grey lines show the traces reveal horizontal shifts. Thus for the cogent-003 algorithm FNMR for men is* higher *than for women* at a fixed threshold *but, at the same time, FMR is higher for women - see Figure 131. As access control systems almost always operate at a fixed threshold, the naive interpretation is incorrect.*

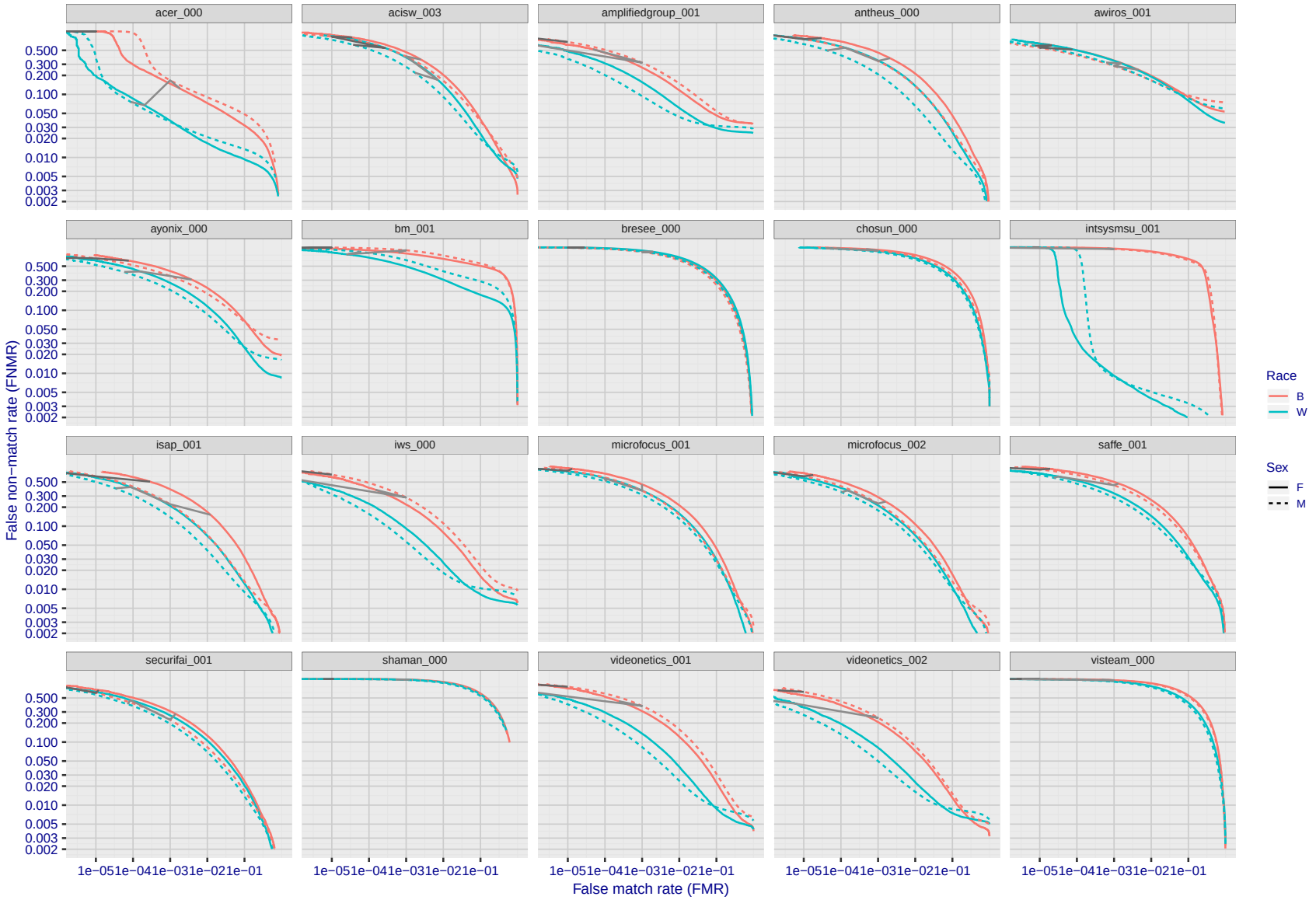

Figure 96: For the mugshot images, error tradeoff characteristics for white females, black females, black males and white males. The Z-shaped grey lines correspond to fixed thresholds, showing both *FNMR and FMR vary at one T value. Note: Many of the plots will naively be read as saying women gives worse error rates than men because the solid traces lie above the dotted ones. However, this is misleading and incomplete: The grey lines show the traces reveal horizontal shifts. Thus for the cogent-003 algorithm FNMR for men is* higher *than for women* at a fixed threshold *but, at the same time, FMR is higher for women - see Figure 131. As access control systems almost always operate at a fixed threshold, the naive interpretation is incorrect.*

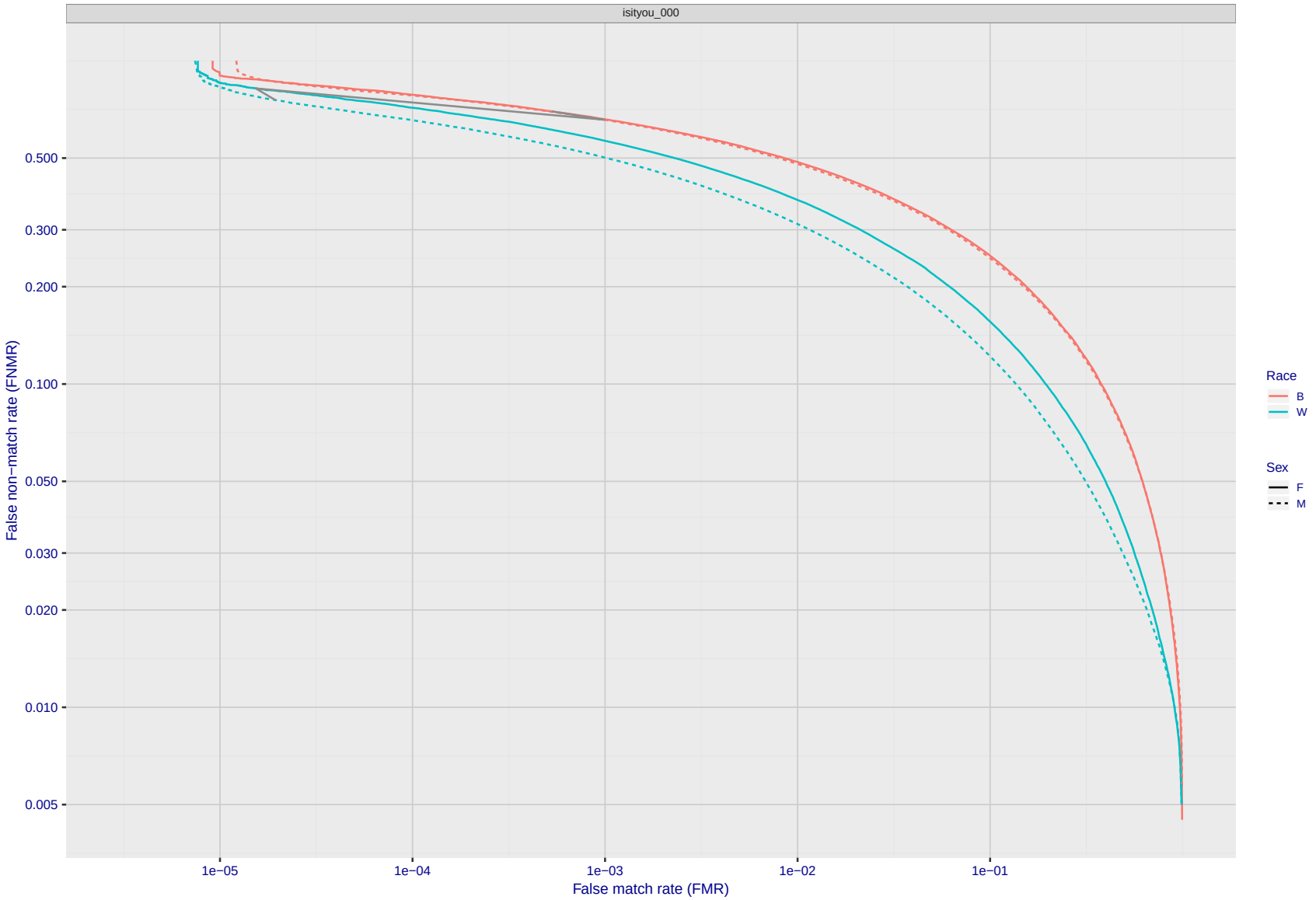

Figure 97: For the mugshot images, error tradeoff characteristics for white females, black females, black males and white males. The Z-shaped grey lines correspond to fixed thresholds, showing both *FNMR and FMR vary at one T value. Note: Many of the plots will naively be read as saying women gives worse error rates than men because the solid traces lie above the dotted ones. However, this is misleading and incomplete: The grey lines show the traces reveal horizontal shifts. Thus for the cogent-003 algorithm FNMR for men is* higher *than for women* at a fixed threshold *but, at the same time, FMR is higher for women - see Figure 131. As access control systems almost always operate at a fixed threshold, the naive interpretation is incorrect.*

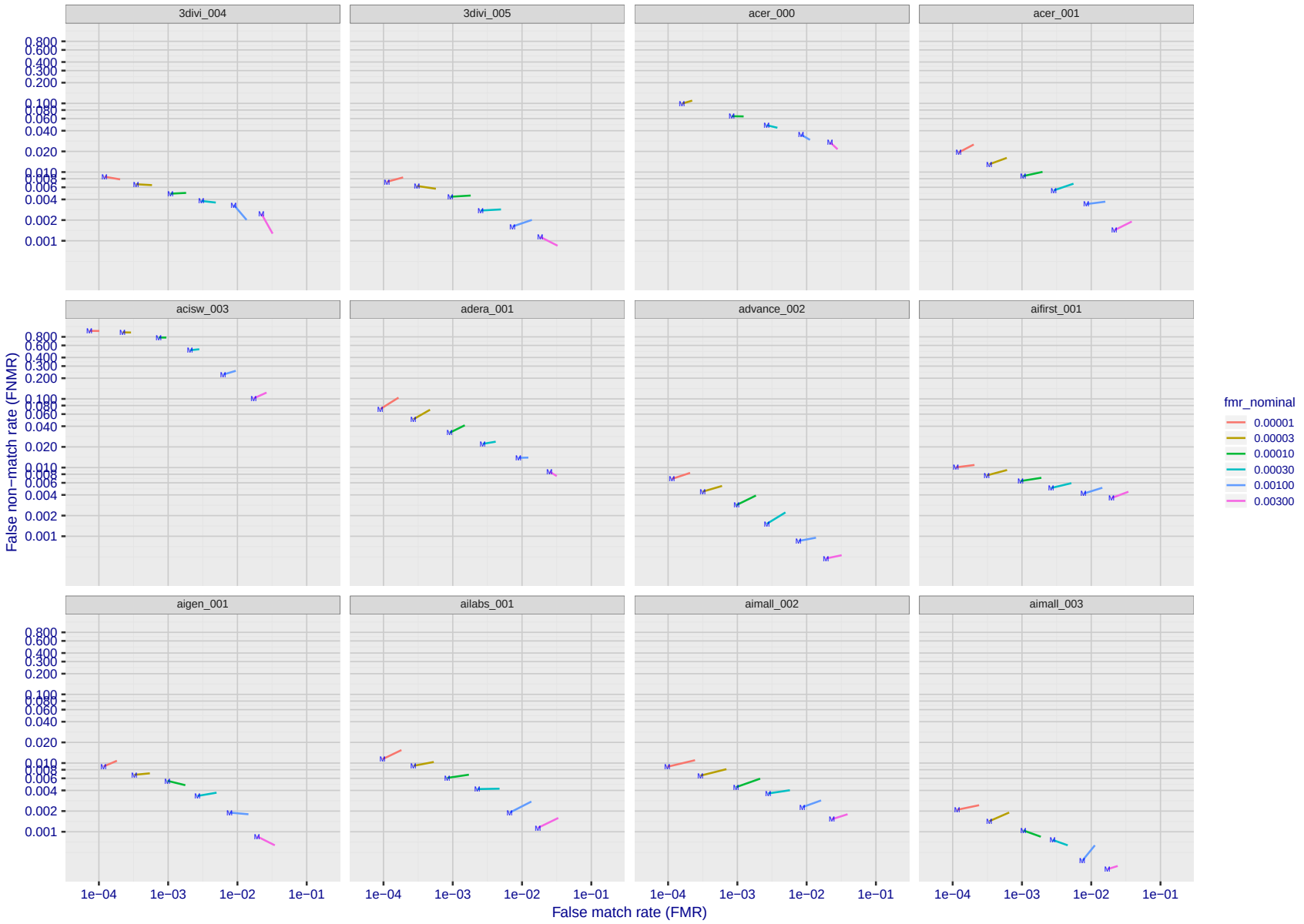

Figure 98: For the visa images, FNMR and FMR at six operating points along the DET characteristic. At each point a line is drawn between (FMR,FNMR)$_{\text{MALE}}$ and (FMR,FNMR)$_{\text{FEMALE}}$ showing how which sex has lower FMR and/or FNMR. The "M" label denotes male, the other end of the line corresponds to female. The six operating thresholds are selected to give the nominal false match rates given in the legend, and are computed over all impostor pairs regardless of age, sex, and place of birth. The plotted FMR values are broadly an order of magnitude larger than the nominal rates because FMR is computed over demographically-matched impostor pairs i.e individuals of the same sex, from the same geographic region (see section 3.6.1), and the same age group (see section 3.6.2).

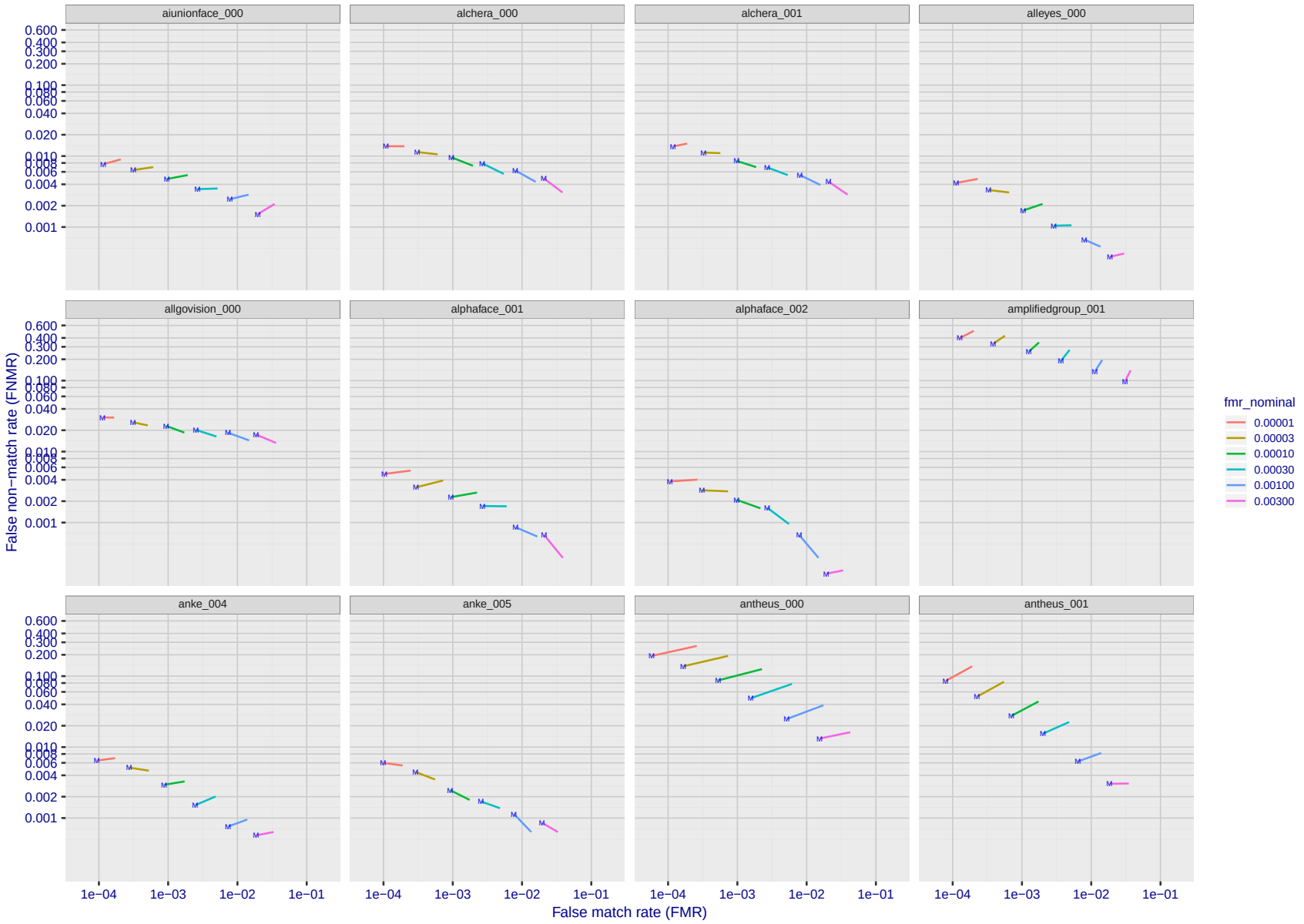

Figure 99: For the visa images, FNMR and FMR at six operating points along the DET characteristic. At each point a line is drawn between (FMR,FNMR)$_{\text{MALE}}$ and (FMR,FNMR)$_{\text{FEMALE}}$ showing how which sex has lower FMR and/or FNMR. The "M" label denotes male, the other end of the line corresponds to female. The six operating thresholds are selected to give the nominal false match rates given in the legend, and are computed over all impostor pairs regardless of age, sex, and place of birth. The plotted FMR values are broadly an order of magnitude larger than the nominal rates because FMR is computed over demographically-matched impostor pairs i.e individuals of the same sex, from the same geographic region (see section 3.6.1), and the same age group (see section 3.6.2).

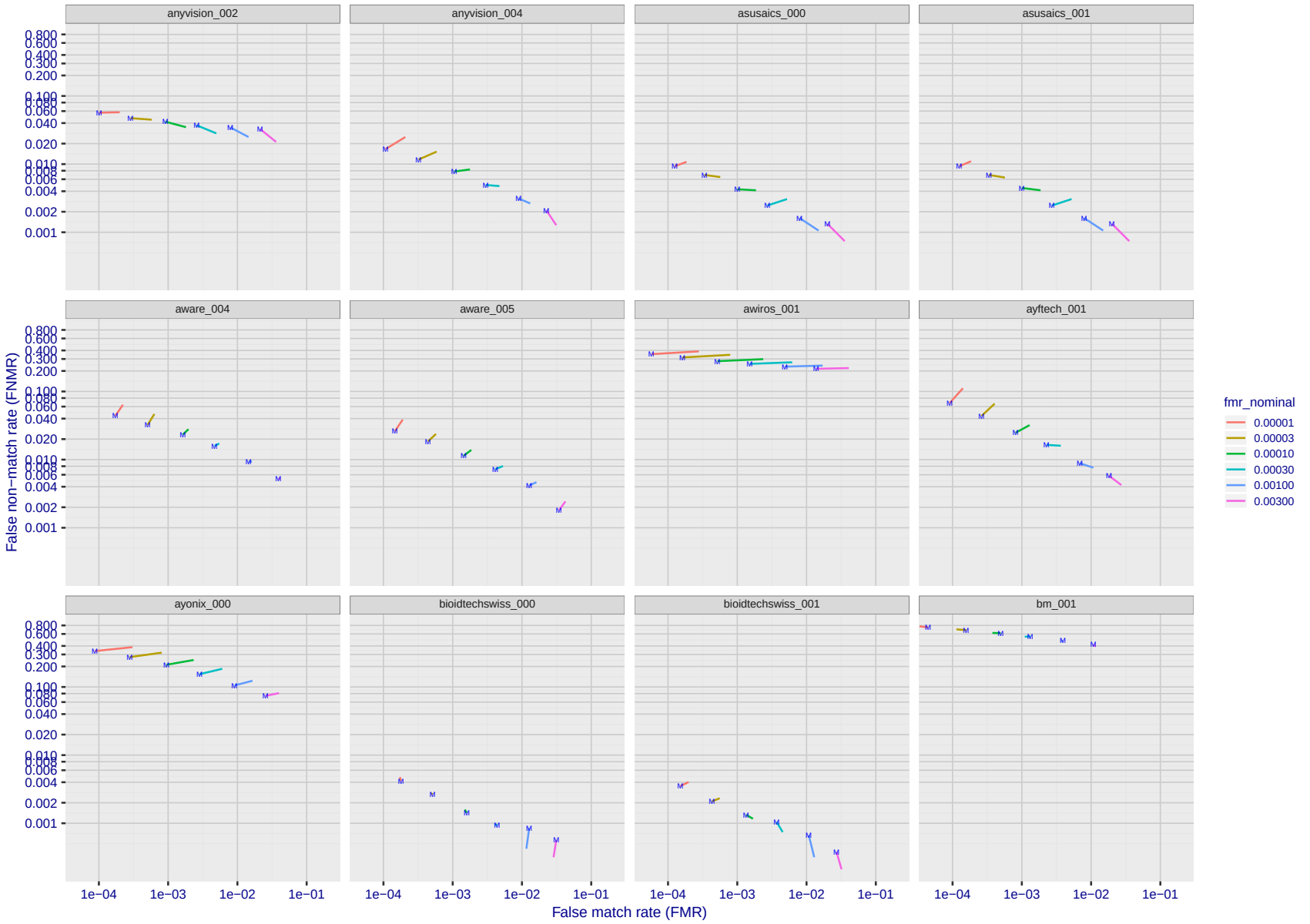

Figure 100: For the visa images, FNMR and FMR at six operating points along the DET characteristic. At each point a line is drawn between (FMR,FNMR)$_{\text{MALE}}$ and (FMR,FNMR)$_{\text{FEMALE}}$ showing how which sex has lower FMR and/or FNMR. The "M" label denotes male, the other end of the line corresponds to female. The six operating thresholds are selected to give the nominal false match rates given in the legend, and are computed over all impostor pairs regardless of age, sex, and place of birth. The plotted FMR values are broadly an order of magnitude larger than the nominal rates because FMR is computed over demographically-matched impostor pairs i.e individuals of the same sex, from the same geographic region (see section 3.6.1), and the same age group (see section 3.6.2).

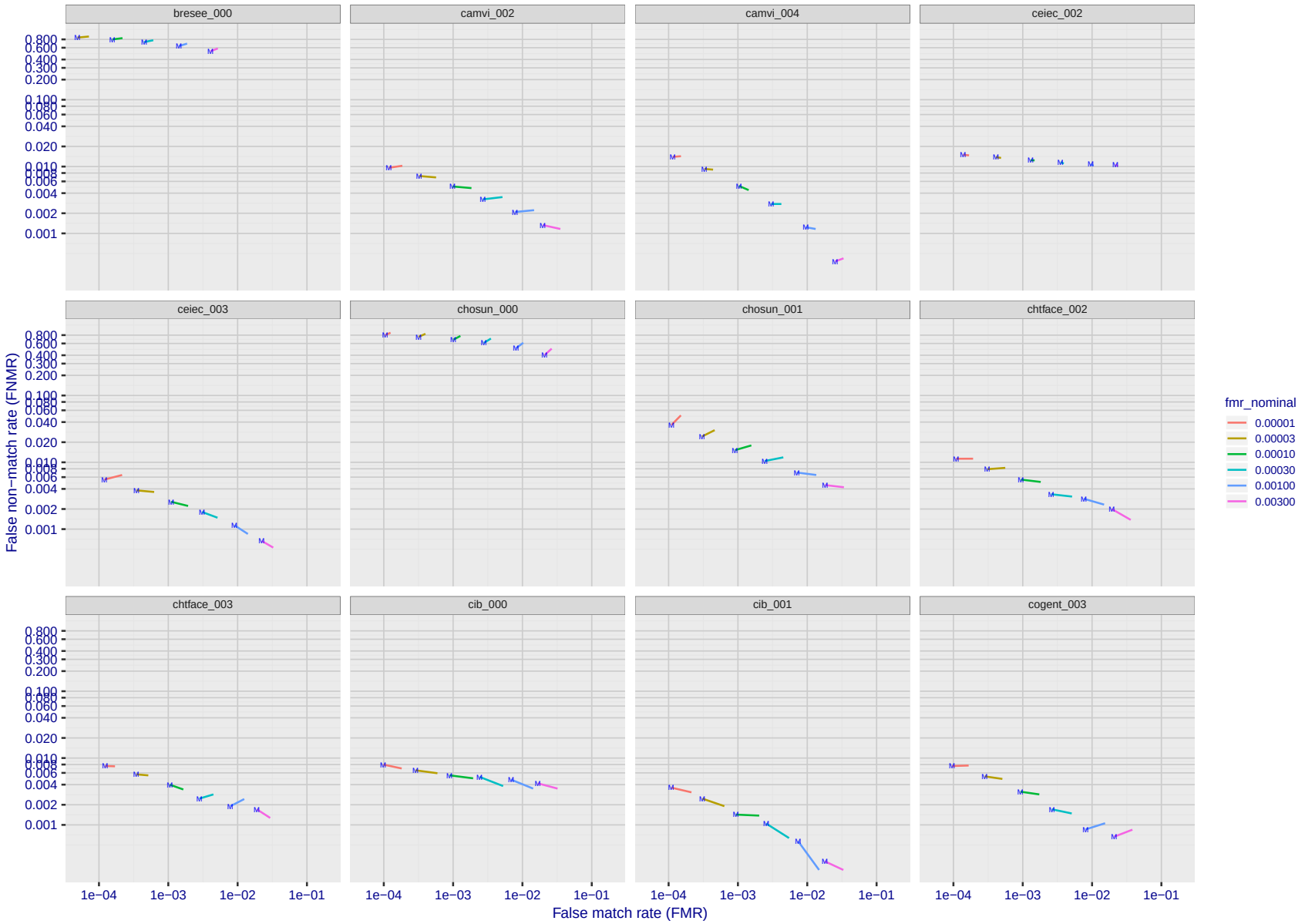

Figure 101: For the visa images, FNMR and FMR at six operating points along the DET characteristic. At each point a line is drawn between (FMR,FNMR)$_{\text{MALE}}$ and (FMR,FNMR)$_{\text{FEMALE}}$ showing how which sex has lower FMR and/or FNMR. The "M" label denotes male, the other end of the line corresponds to female. The six operating thresholds are selected to give the nominal false match rates given in the legend, and are computed over all impostor pairs regardless of age, sex, and place of birth. The plotted FMR values are broadly an order of magnitude larger than the nominal rates because FMR is computed over demographically-matched impostor pairs i.e individuals of the same sex, from the same geographic region (see section 3.6.1), and the same age group (see section 3.6.2).

2020/10/09 13:32:41
FNMR(T) "False non-match rate"
FMR(T) "False match rate"

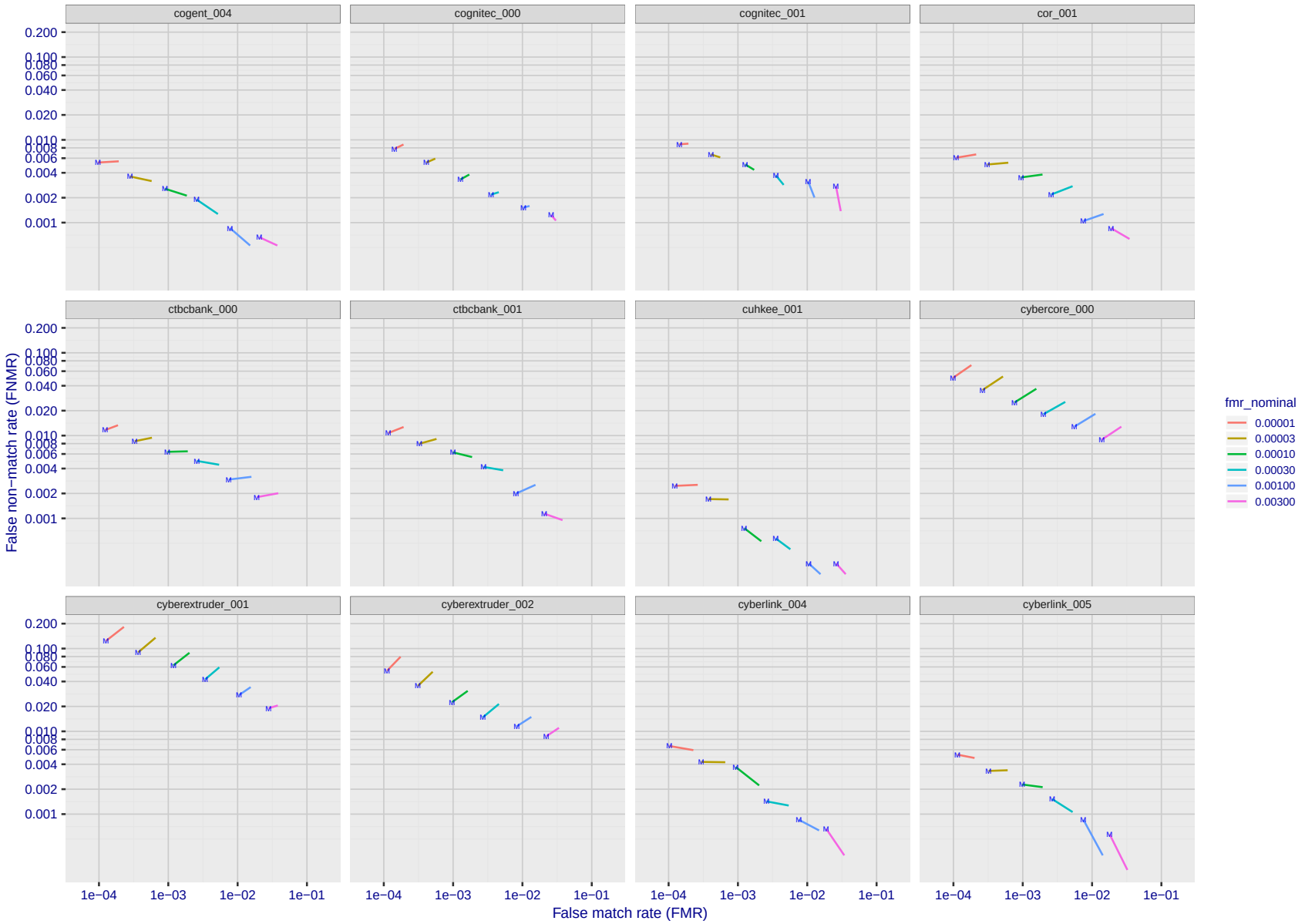

Figure 102: For the visa images, FNMR and FMR at six operating points along the DET characteristic. At each point a line is drawn between (FMR,FNMR)$_{\text{MALE}}$ and (FMR,FNMR)$_{\text{FEMALE}}$ showing how which sex has lower FMR and/or FNMR. The "M" label denotes male, the other end of the line corresponds to female. The six operating thresholds are selected to give the nominal false match rates given in the legend, and are computed over all impostor pairs regardless of age, sex, and place of birth. The plotted FMR values are broadly an order of magnitude larger than the nominal rates because FMR is computed over demographically-matched impostor pairs i.e individuals of the same sex, from the same geographic region (see section 3.6.1), and the same age group (see section 3.6.2).

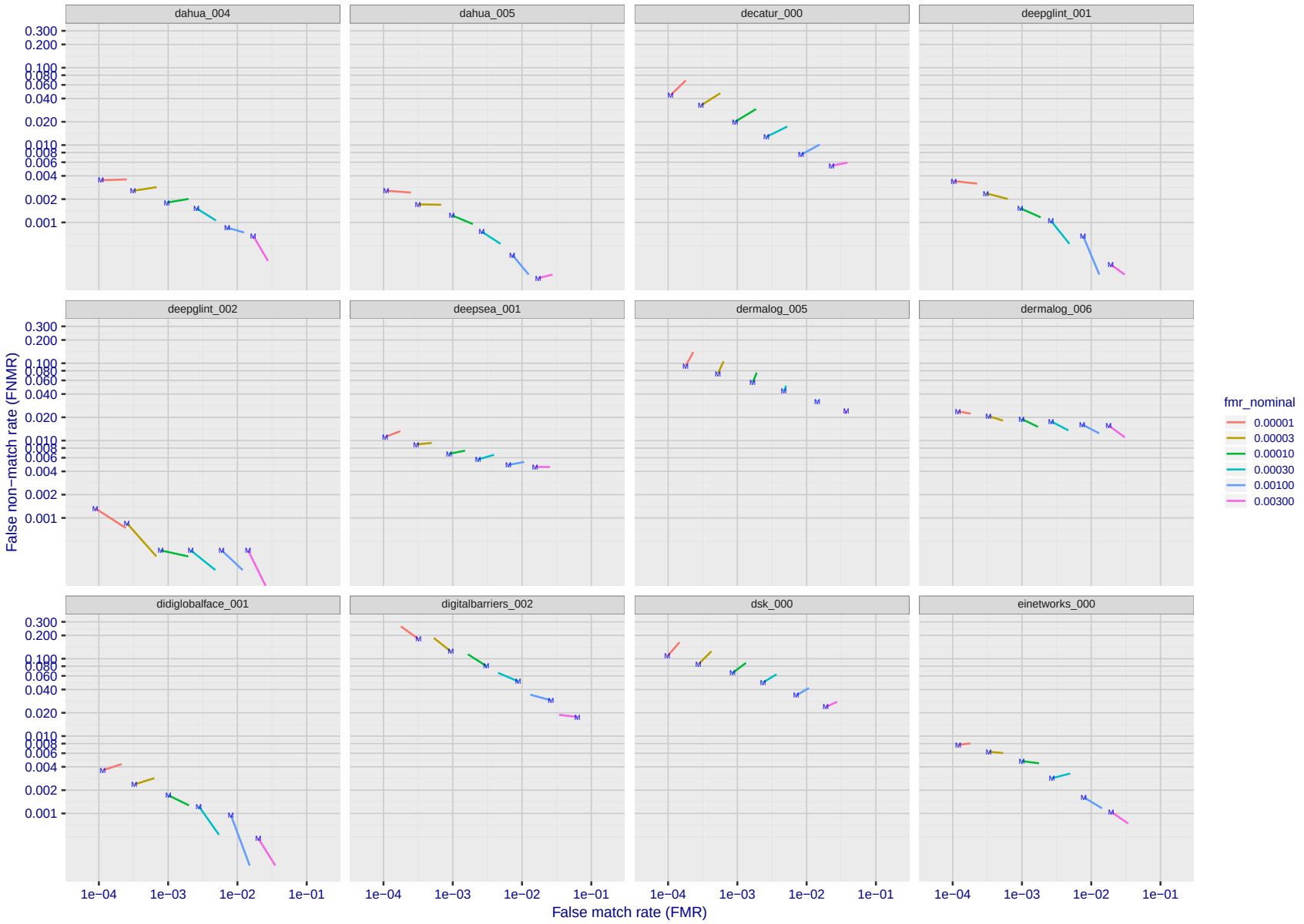

Figure 103: For the visa images, FNMR and FMR at six operating points along the DET characteristic. At each point a line is drawn between (FMR,FNMR)$_{\text{MALE}}$ and (FMR,FNMR)$_{\text{FEMALE}}$ showing how which sex has lower FMR and/or FNMR. The "M" label denotes male, the other end of the line corresponds to female. The six operating thresholds are selected to give the nominal false match rates given in the legend, and are computed over all impostor pairs regardless of age, sex, and place of birth. The plotted FMR values are broadly an order of magnitude larger than the nominal rates because FMR is computed over demographically-matched impostor pairs i.e individuals of the same sex, from the same geographic region (see section 3.6.1), and the same age group (see section 3.6.2).

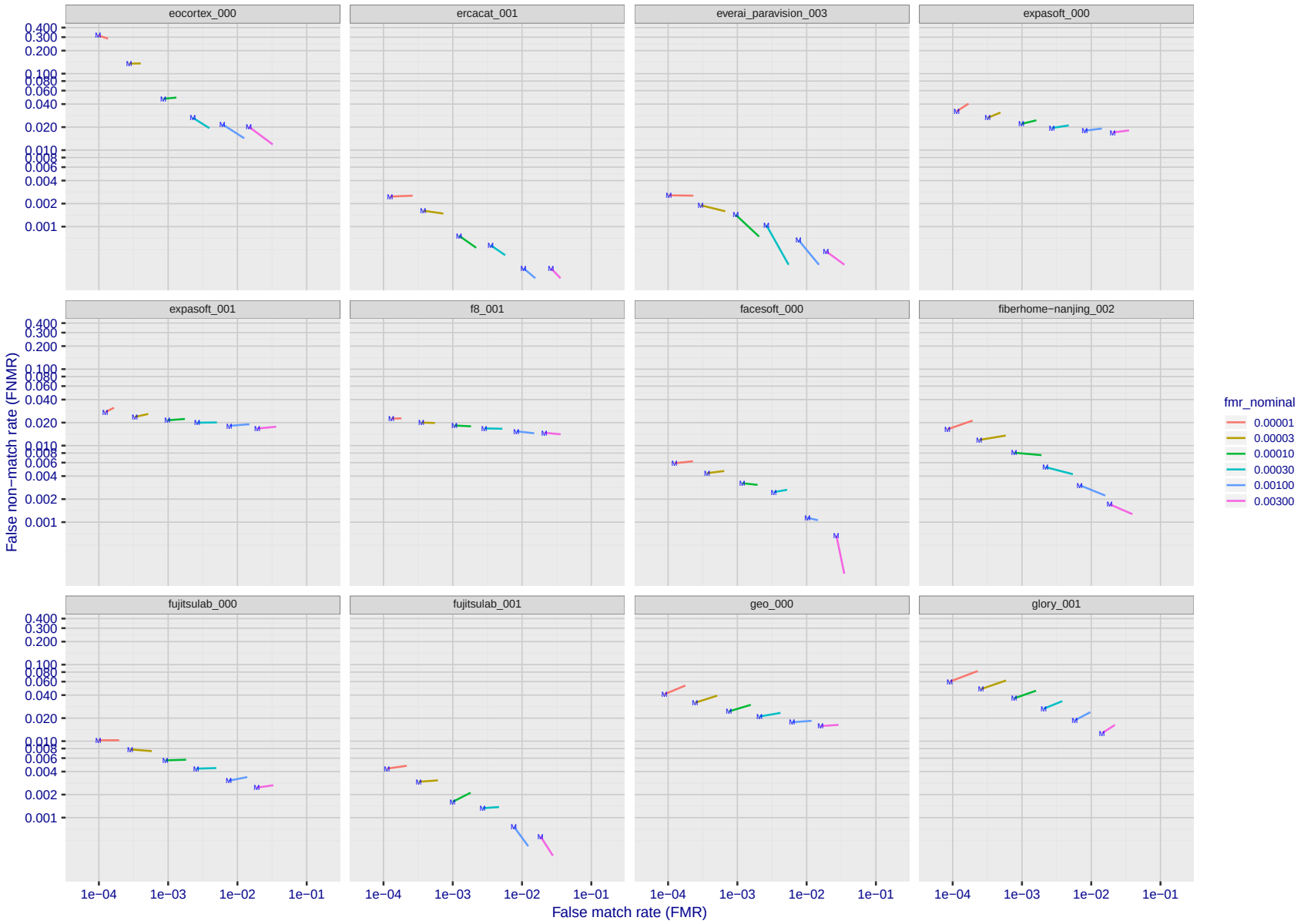

Figure 104: For the visa images, FNMR and FMR at six operating points along the DET characteristic. At each point a line is drawn between (FMR,FNMR)$_{\text{MALE}}$ and (FMR,FNMR)$_{\text{FEMALE}}$ showing how which sex has lower FMR and/or FNMR. The "M" label denotes male, the other end of the line corresponds to female. The six operating thresholds are selected to give the nominal false match rates given in the legend, and are computed over all impostor pairs regardless of age, sex, and place of birth. The plotted FMR values are broadly an order of magnitude larger than the nominal rates because FMR is computed over demographically-matched impostor pairs i.e individuals of the same sex, from the same geographic region (see section 3.6.1), and the same age group (see section 3.6.2).

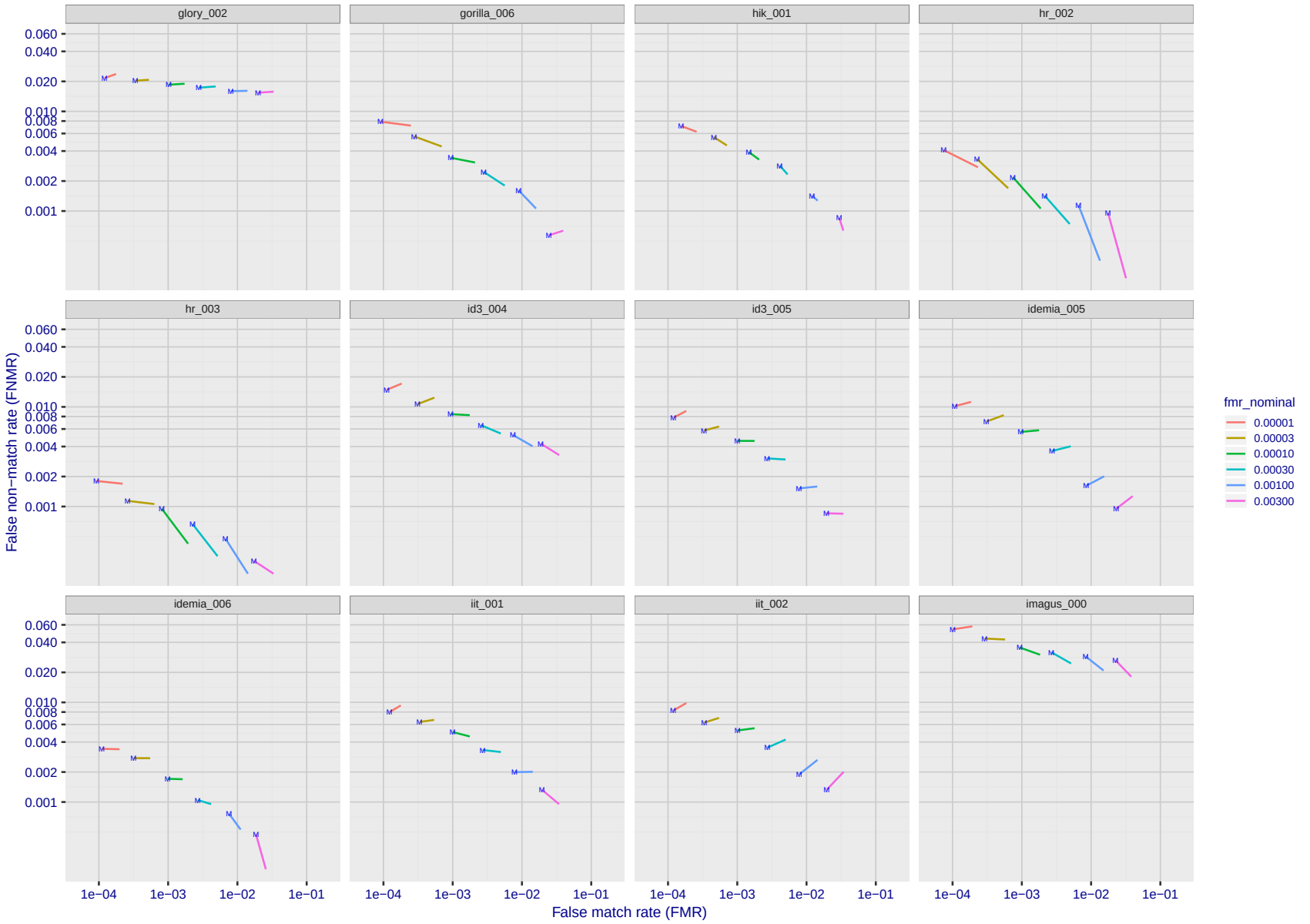

Figure 105: For the visa images, FNMR and FMR at six operating points along the DET characteristic. At each point a line is drawn between (FMR,FNMR)$_{\text{MALE}}$ and (FMR,FNMR)$_{\text{FEMALE}}$ showing how which sex has lower FMR and/or FNMR. The "M" label denotes male, the other end of the line corresponds to female. The six operating thresholds are selected to give the nominal false match rates given in the legend, and are computed over all impostor pairs regardless of age, sex, and place of birth. The plotted FMR values are broadly an order of magnitude larger than the nominal rates because FMR is computed over demographically-matched impostor pairs i.e individuals of the same sex, from the same geographic region (see section 3.6.1), and the same age group (see section 3.6.2).

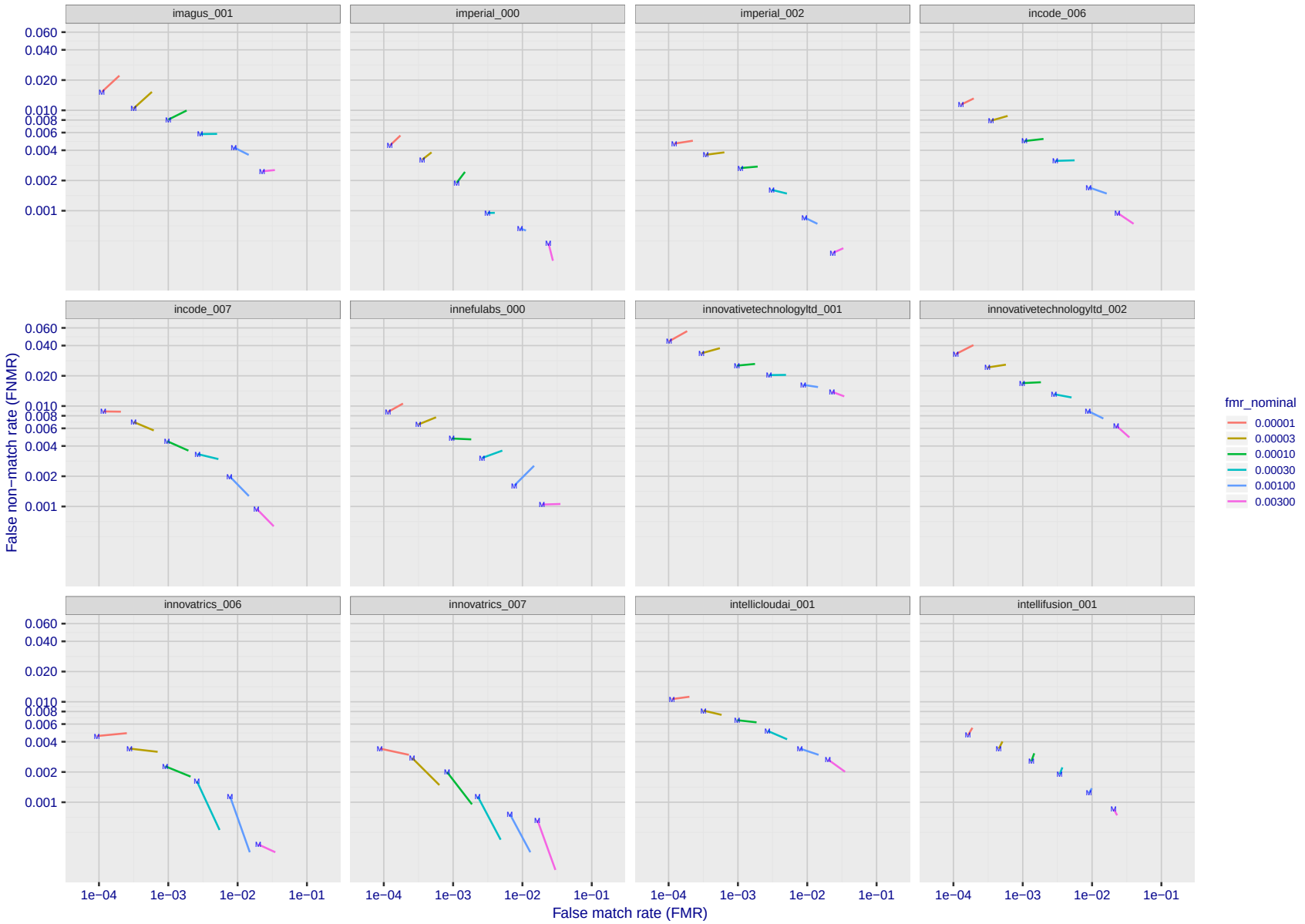

Figure 106: For the visa images, FNMR and FMR at six operating points along the DET characteristic. At each point a line is drawn between (FMR,FNMR)$_{\text{MALE}}$ and (FMR,FNMR)$_{\text{FEMALE}}$ showing how which sex has lower FMR and/or FNMR. The "M" label denotes male, the other end of the line corresponds to female. The six operating thresholds are selected to give the nominal false match rates given in the legend, and are computed over all impostor pairs regardless of age, sex, and place of birth. The plotted FMR values are broadly an order of magnitude larger than the nominal rates because FMR is computed over demographically-matched impostor pairs i.e individuals of the same sex, from the same geographic region (see section 3.6.1), and the same age group (see section 3.6.2).

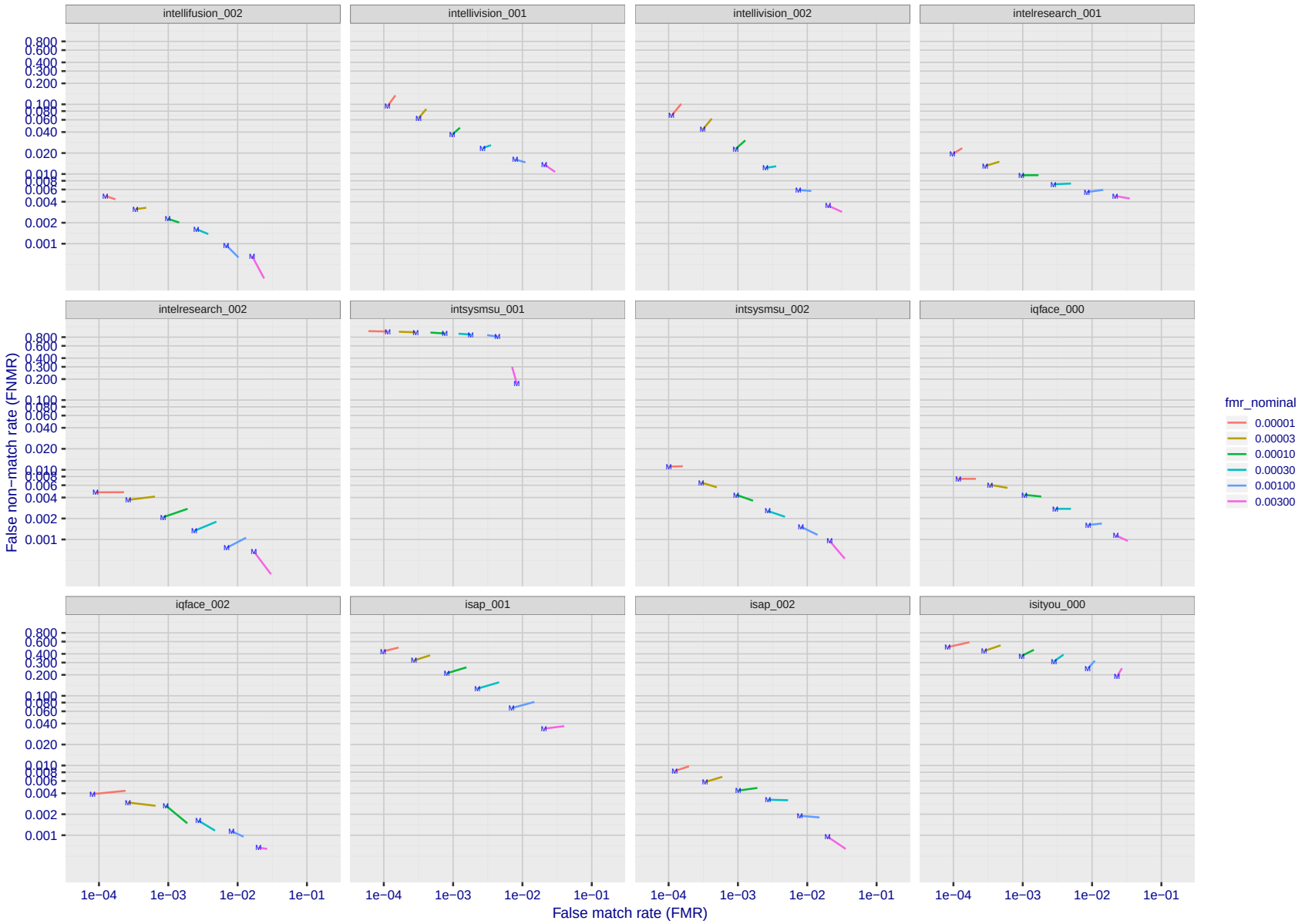

Figure 107: For the visa images, FNMR and FMR at six operating points along the DET characteristic. At each point a line is drawn between (FMR,FNMR)$_{\text{MALE}}$ and (FMR,FNMR)$_{\text{FEMALE}}$ showing how which sex has lower FMR and/or FNMR. The "M" label denotes male, the other end of the line corresponds to female. The six operating thresholds are selected to give the nominal false match rates given in the legend, and are computed over all impostor pairs regardless of age, sex, and place of birth. The plotted FMR values are broadly an order of magnitude larger than the nominal rates because FMR is computed over demographically-matched impostor pairs i.e individuals of the same sex, from the same geographic region (see section 3.6.1), and the same age group (see section 3.6.2).

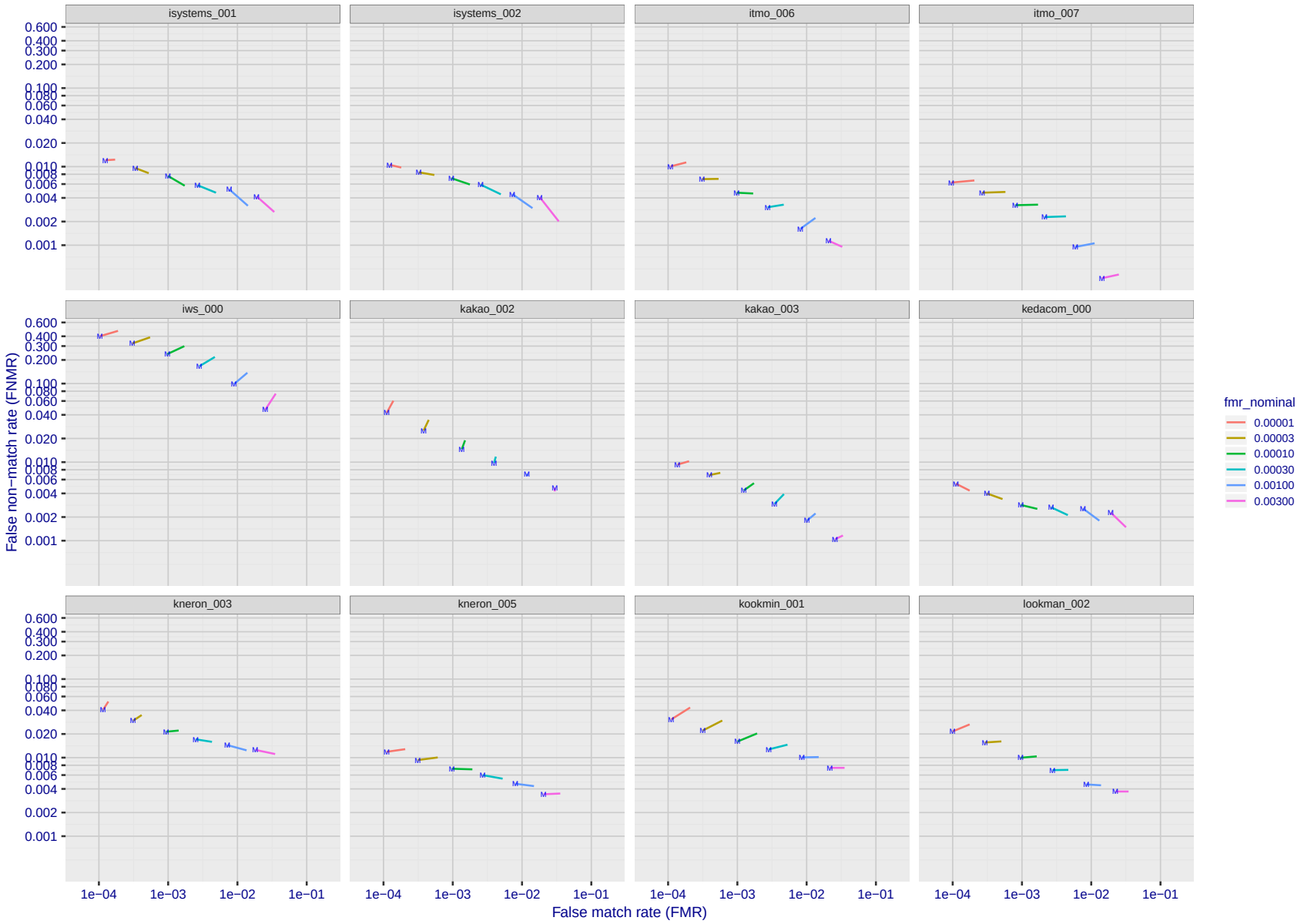

Figure 108: For the visa images, FNMR and FMR at six operating points along the DET characteristic. At each point a line is drawn between (FMR,FNMR)$_{\text{MALE}}$ and (FMR,FNMR)$_{\text{FEMALE}}$ showing how which sex has lower FMR and/or FNMR. The "M" label denotes male, the other end of the line corresponds to female. The six operating thresholds are selected to give the nominal false match rates given in the legend, and are computed over all impostor pairs regardless of age, sex, and place of birth. The plotted FMR values are broadly an order of magnitude larger than the nominal rates because FMR is computed over demographically-matched impostor pairs i.e individuals of the same sex, from the same geographic region (see section 3.6.1), and the same age group (see section 3.6.2).

2020/10/09 13:32:41

FNMR(T) "False non-match rate"
FMR(T) "False match rate"

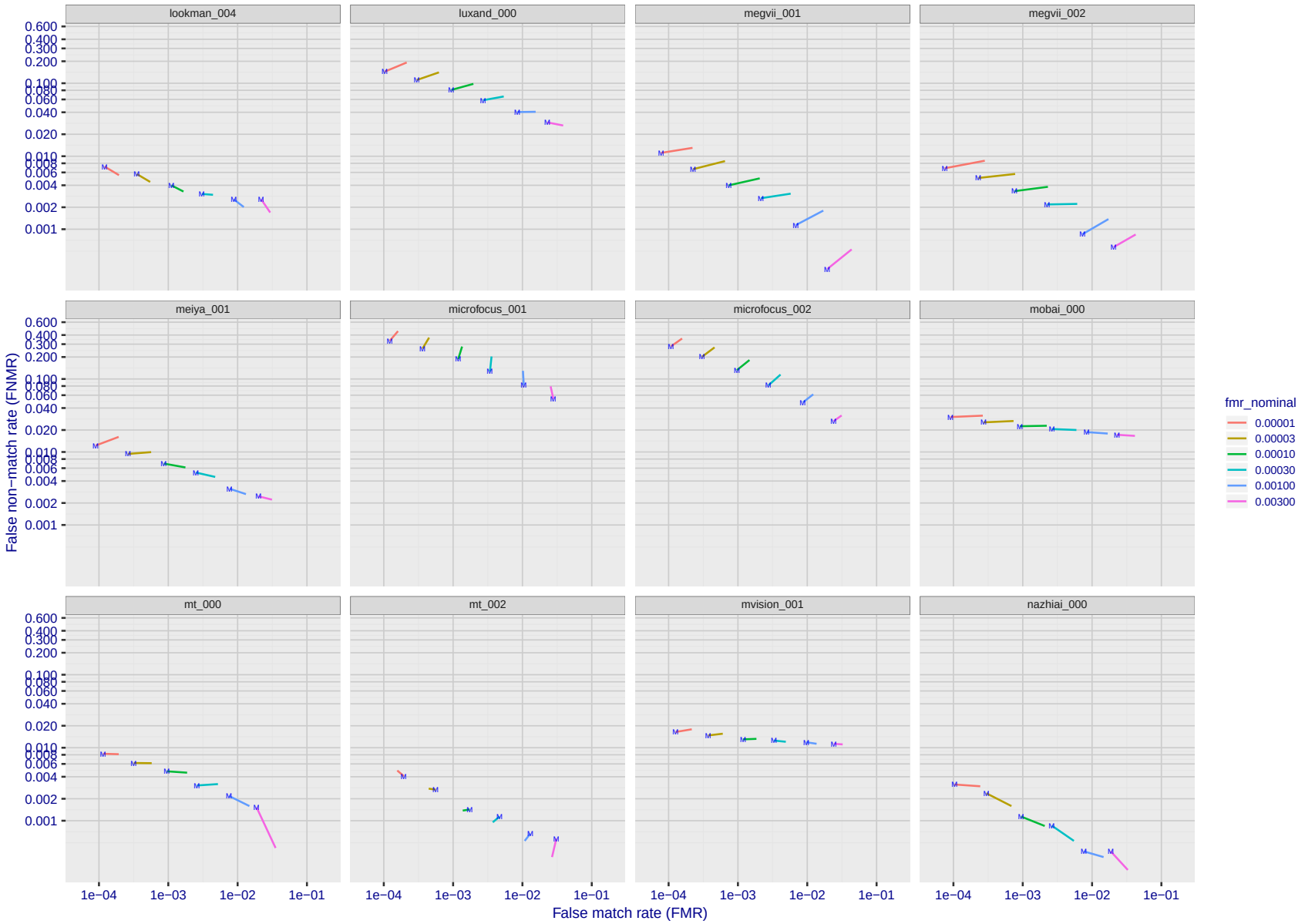

Figure 109: For the visa images, FNMR and FMR at six operating points along the DET characteristic. At each point a line is drawn between (FMR,FNMR)$_{\text{MALE}}$ and (FMR,FNMR)$_{\text{FEMALE}}$ showing how which sex has lower FMR and/or FNMR. The "M" label denotes male, the other end of the line corresponds to female. The six operating thresholds are selected to give the nominal false match rates given in the legend, and are computed over all impostor pairs regardless of age, sex, and place of birth. The plotted FMR values are broadly an order of magnitude larger than the nominal rates because FMR is computed over demographically-matched impostor pairs i.e individuals of the same sex, from the same geographic region (see section 3.6.1), and the same age group (see section 3.6.2).

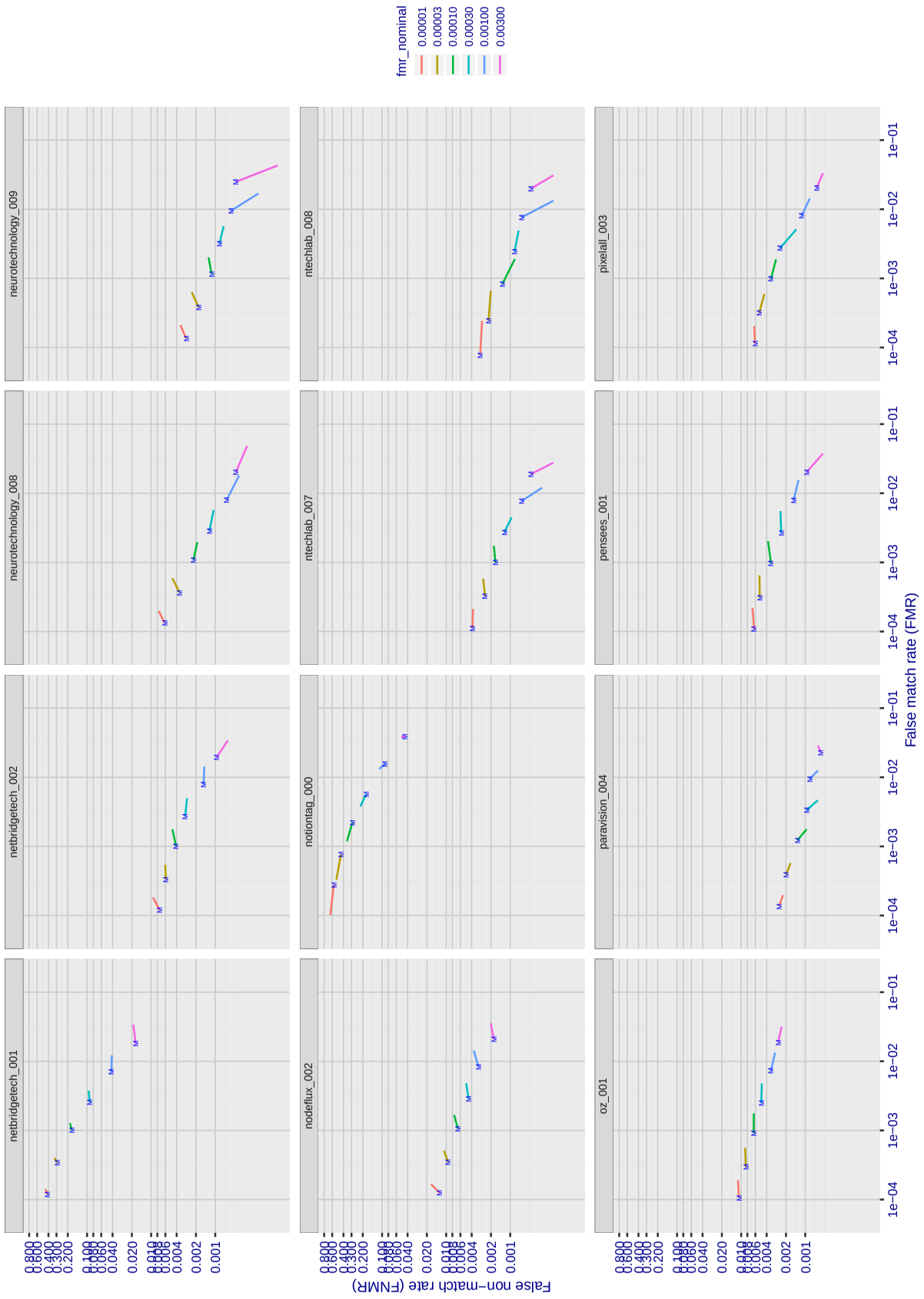

Figure 110: For the visa images, FNMR and FMR at six operating points along the DET characteristic. At each point a line is drawn between (FMR,FNMR)$_{\text{MALE}}$ and (FMR,FNMR)$_{\text{FEMALE}}$ showing how which sex has lower FMR and/or FNMR. The "M" label denotes male, the other end of the line corresponds to female. The six operating thresholds are selected to give the nominal false match rates given in the legend, and are computed over all impostor pairs regardless of age, sex, and place of birth. The plotted FMR values are broadly an order of magnitude larger than the nominal rates because FMR is computed over demographically-matched impostor pairs i.e individuals of the same sex, from the same geographic region (see section 3.6.1), and the same age group (see section 3.6.2).

FNMR(T) "False non-match rate"
FMR(T) "False match rate"

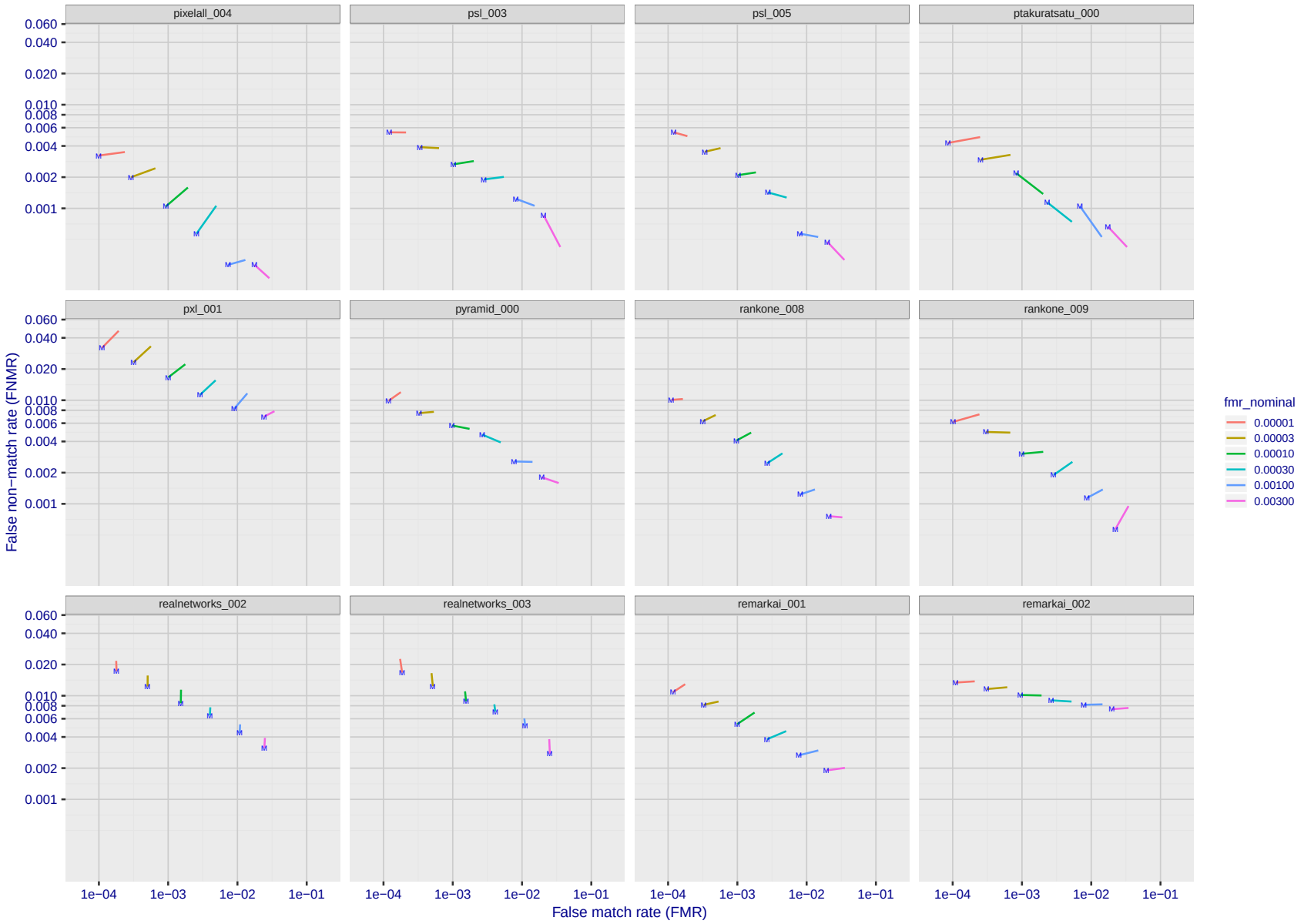

Figure 111: For the visa images, FNMR and FMR at six operating points along the DET characteristic. At each point a line is drawn between (FMR,FNMR)$_{\text{MALE}}$ and (FMR,FNMR)$_{\text{FEMALE}}$ showing how which sex has lower FMR and/or FNMR. The "M" label denotes male, the other end of the line corresponds to female. The six operating thresholds are selected to give the nominal false match rates given in the legend, and are computed over all impostor pairs regardless of age, sex, and place of birth. The plotted FMR values are broadly an order of magnitude larger than the nominal rates because FMR is computed over demographically-matched impostor pairs i.e individuals of the same sex, from the same geographic region (see section 3.6.1), and the same age group (see section 3.6.2).

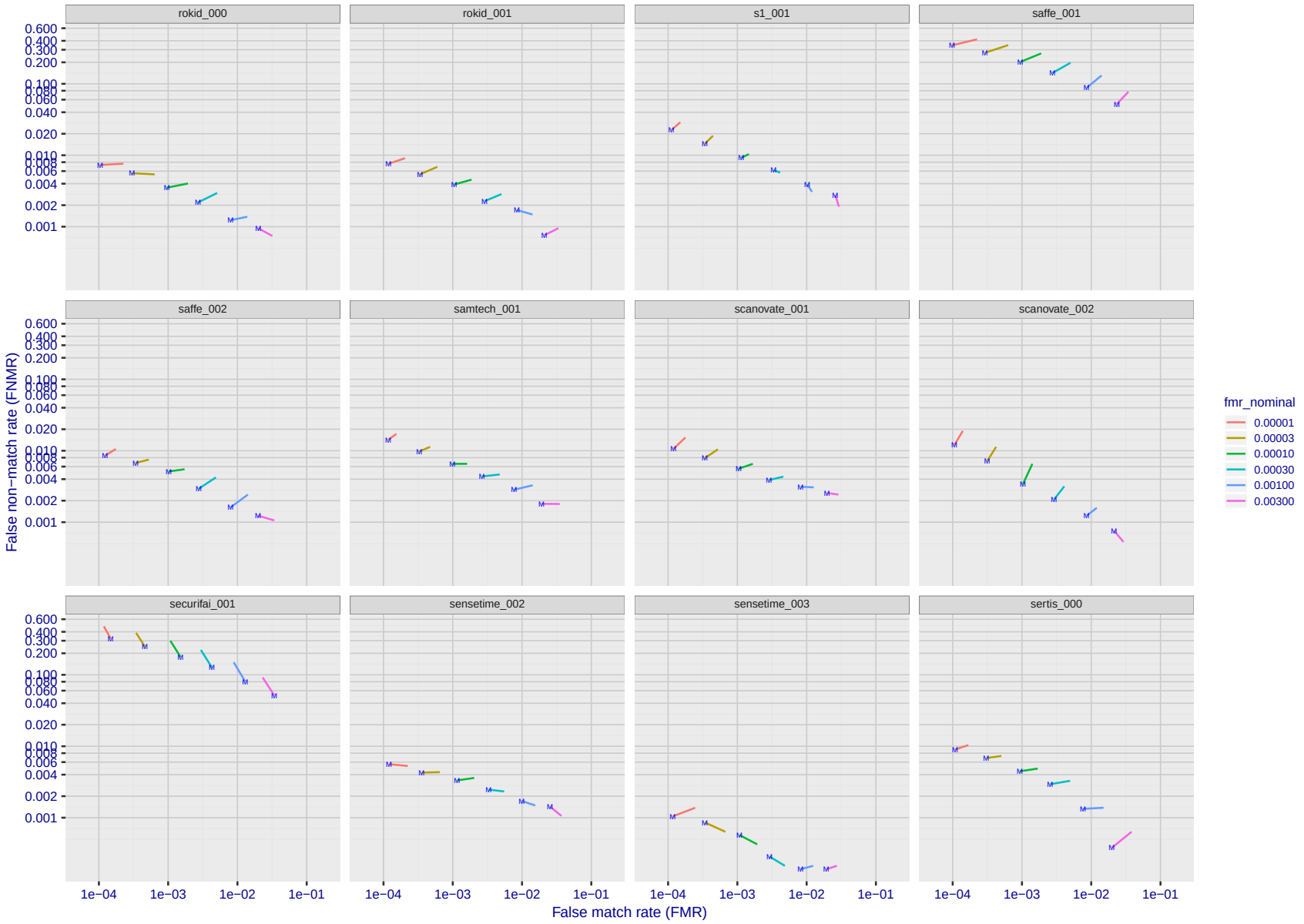

Figure 112: For the visa images, FNMR and FMR at six operating points along the DET characteristic. At each point a line is drawn between (FMR,FNMR)$_{\text{MALE}}$ and (FMR,FNMR)$_{\text{FEMALE}}$ showing how which sex has lower FMR and/or FNMR. The "M" label denotes male, the other end of the line corresponds to female. The six operating thresholds are selected to give the nominal false match rates given in the legend, and are computed over all impostor pairs regardless of age, sex, and place of birth. The plotted FMR values are broadly an order of magnitude larger than the nominal rates because FMR is computed over demographically-matched impostor pairs i.e individuals of the same sex, from the same geographic region (see section 3.6.1), and the same age group (see section 3.6.2).

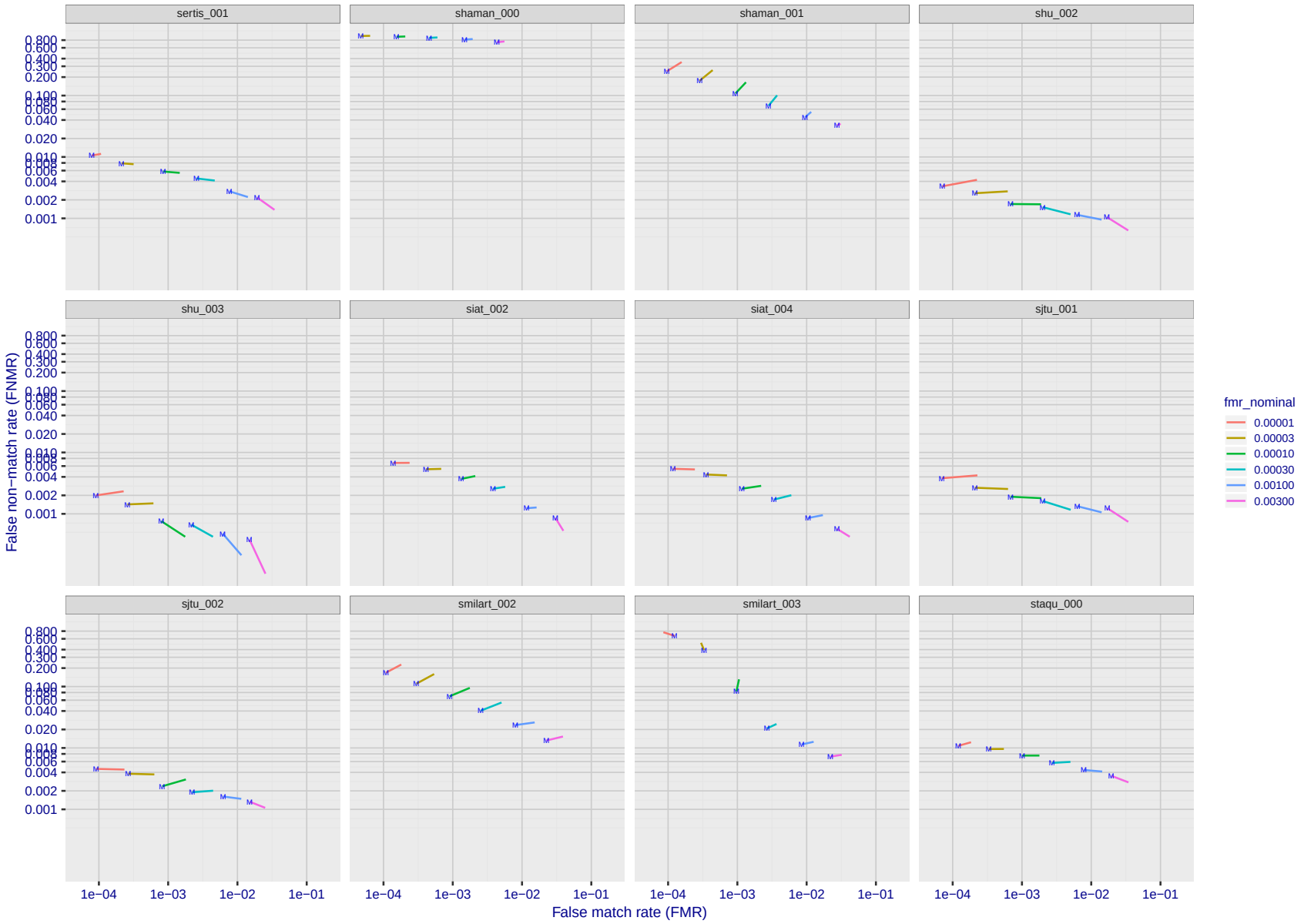

Figure 113: For the visa images, FNMR and FMR at six operating points along the DET characteristic. At each point a line is drawn between (FMR,FNMR)$_{\text{MALE}}$ and (FMR,FNMR)$_{\text{FEMALE}}$ showing how which sex has lower FMR and/or FNMR. The "M" label denotes male, the other end of the line corresponds to female. The six operating thresholds are selected to give the nominal false match rates given in the legend, and are computed over all impostor pairs regardless of age, sex, and place of birth. The plotted FMR values are broadly an order of magnitude larger than the nominal rates because FMR is computed over demographically-matched impostor pairs i.e individuals of the same sex, from the same geographic region (see section 3.6.1), and the same age group (see section 3.6.2).

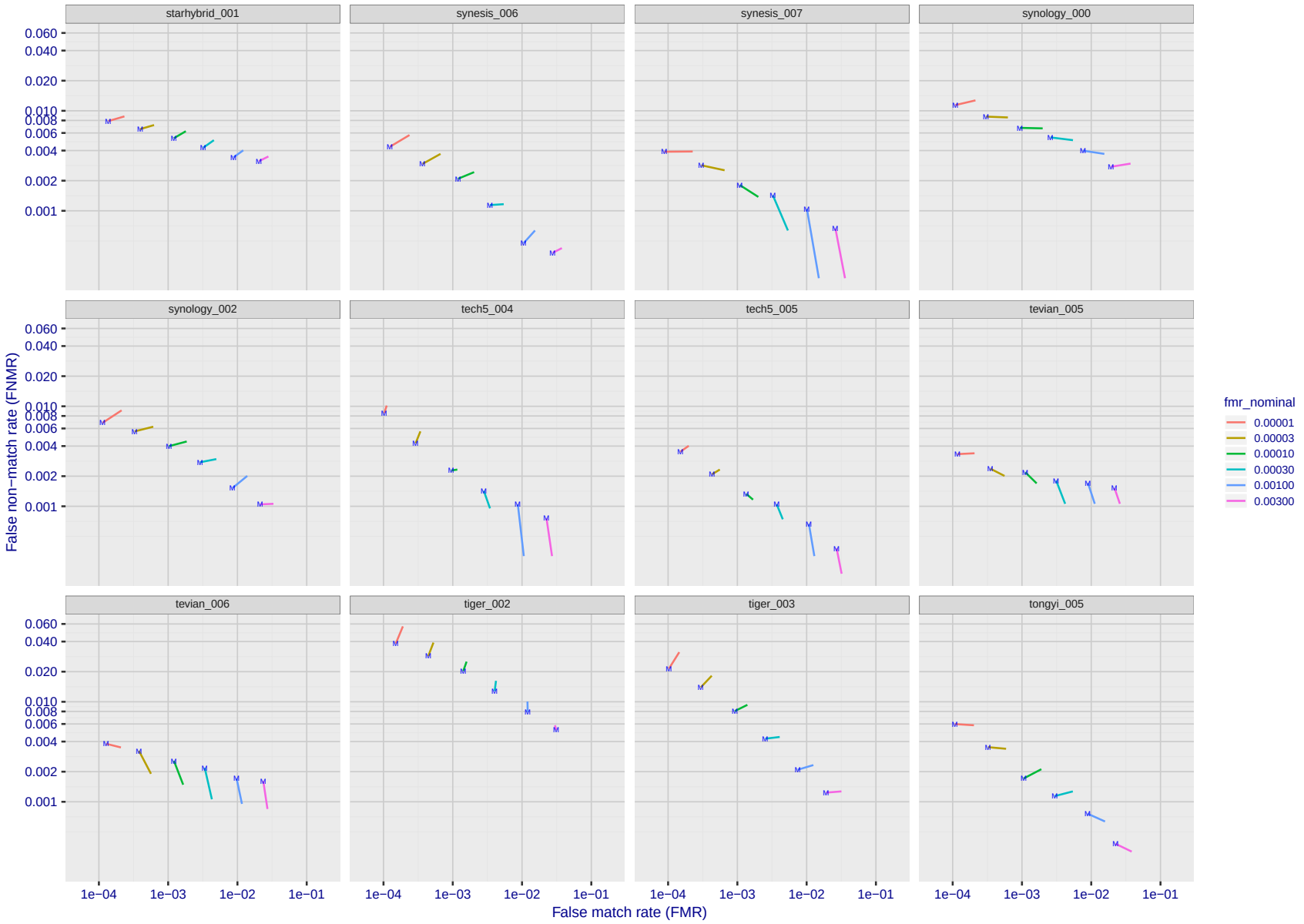

Figure 114: For the visa images, FNMR and FMR at six operating points along the DET characteristic. At each point a line is drawn between (FMR,FNMR)$_{\text{MALE}}$ and (FMR,FNMR)$_{\text{FEMALE}}$ showing how which sex has lower FMR and/or FNMR. The "M" label denotes male, the other end of the line corresponds to female. The six operating thresholds are selected to give the nominal false match rates given in the legend, and are computed over all impostor pairs regardless of age, sex, and place of birth. The plotted FMR values are broadly an order of magnitude larger than the nominal rates because FMR is computed over demographically-matched impostor pairs i.e individuals of the same sex, from the same geographic region (see section 3.6.1), and the same age group (see section 3.6.2).

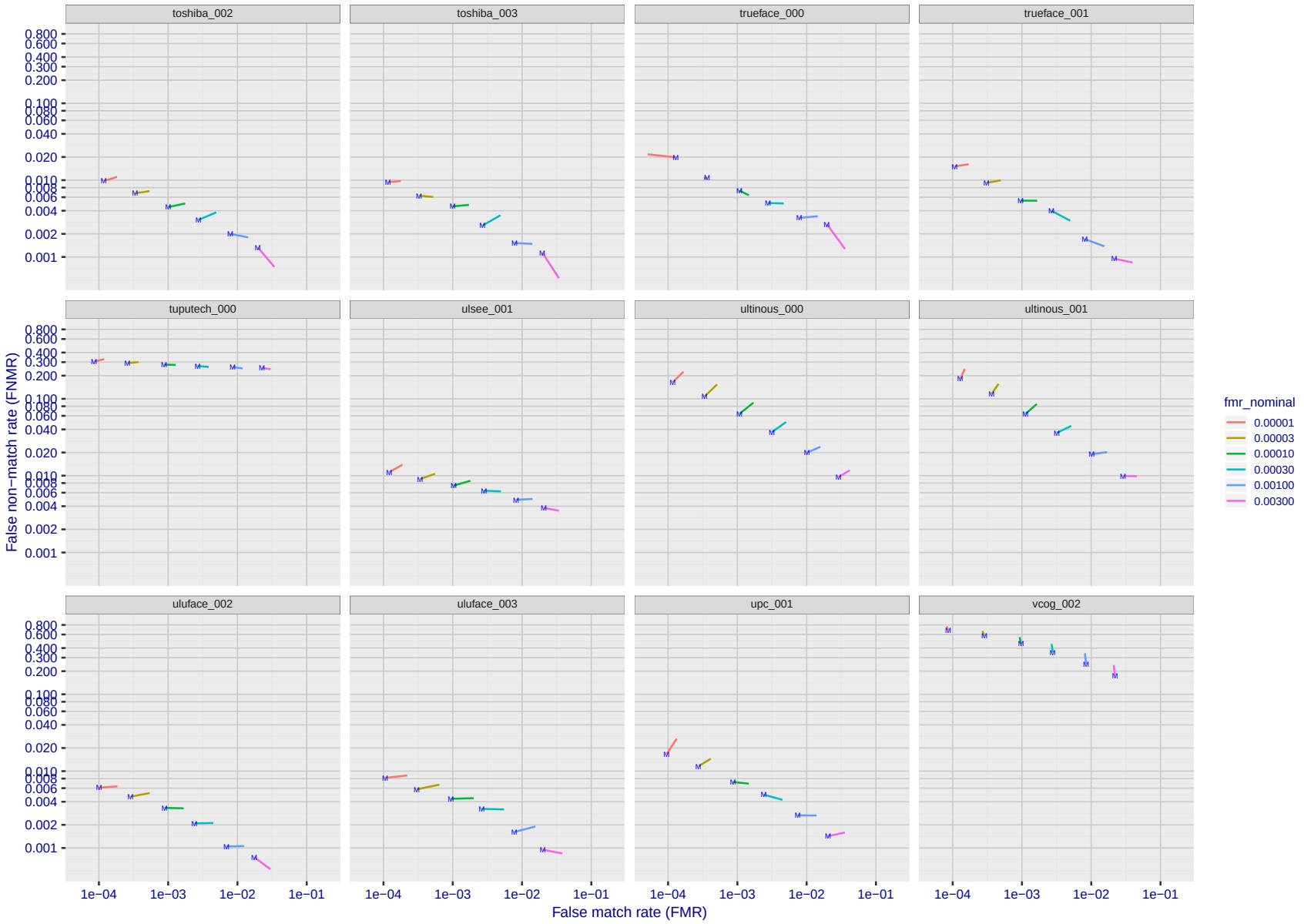

Figure 115: For the visa images, FNMR and FMR at six operating points along the DET characteristic. At each point a line is drawn between (FMR,FNMR)$_{\text{MALE}}$ and (FMR,FNMR)$_{\text{FEMALE}}$ showing how which sex has lower FMR and/or FNMR. The "M" label denotes male, the other end of the line corresponds to female. The six operating thresholds are selected to give the nominal false match rates given in the legend, and are computed over all impostor pairs regardless of age, sex, and place of birth. The plotted FMR values are broadly an order of magnitude larger than the nominal rates because FMR is computed over demographically-matched impostor pairs i.e individuals of the same sex, from the same geographic region (see section 3.6.1), and the same age group (see section 3.6.2).

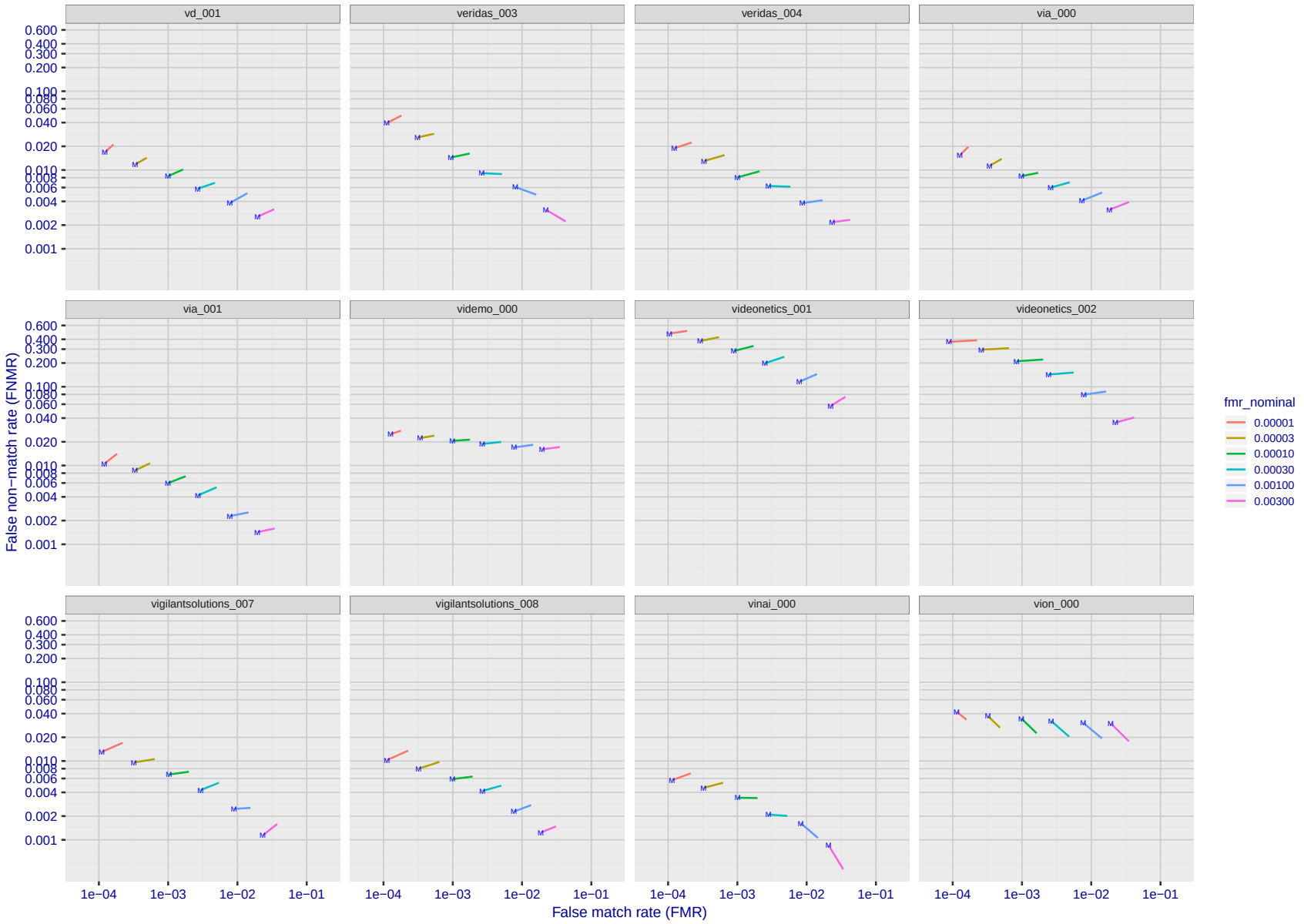

Figure 116: For the visa images, FNMR and FMR at six operating points along the DET characteristic. At each point a line is drawn between (FMR,FNMR)$_{\text{MALE}}$ and (FMR,FNMR)$_{\text{FEMALE}}$ showing how which sex has lower FMR and/or FNMR. The "M" label denotes male, the other end of the line corresponds to female. The six operating thresholds are selected to give the nominal false match rates given in the legend, and are computed over all impostor pairs regardless of age, sex, and place of birth. The plotted FMR values are broadly an order of magnitude larger than the nominal rates because FMR is computed over demographically-matched impostor pairs i.e individuals of the same sex, from the same geographic region (see section 3.6.1), and the same age group (see section 3.6.2).

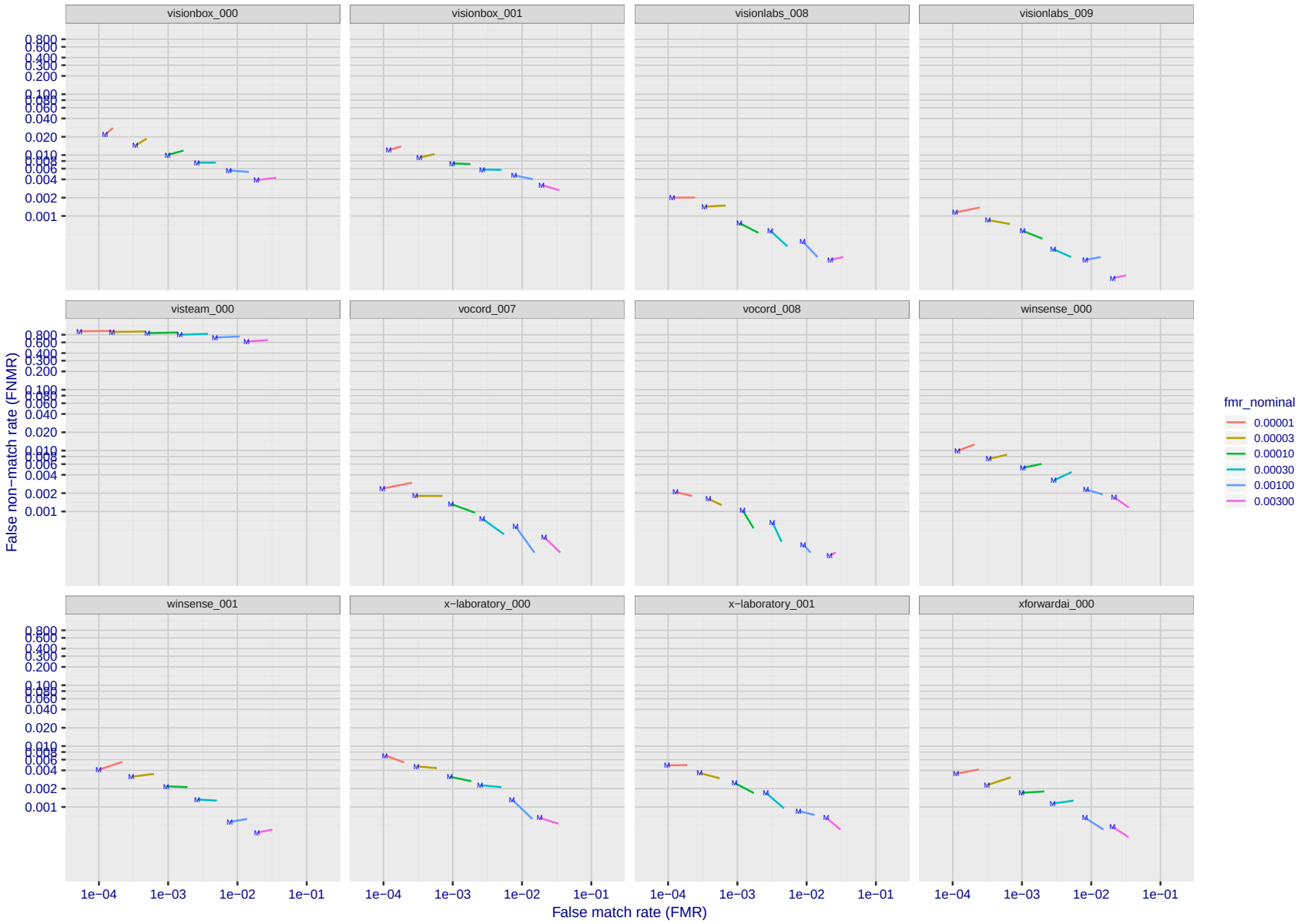

Figure 117: For the visa images, FNMR and FMR at six operating points along the DET characteristic. At each point a line is drawn between (FMR,FNMR)$_{\text{MALE}}$ and (FMR,FNMR)$_{\text{FEMALE}}$ showing how which sex has lower FMR and/or FNMR. The "M" label denotes male, the other end of the line corresponds to female. The six operating thresholds are selected to give the nominal false match rates given in the legend, and are computed over all impostor pairs regardless of age, sex, and place of birth. The plotted FMR values are broadly an order of magnitude larger than the nominal rates because FMR is computed over demographically-matched impostor pairs i.e individuals of the same sex, from the same geographic region (see section 3.6.1), and the same age group (see section 3.6.2).

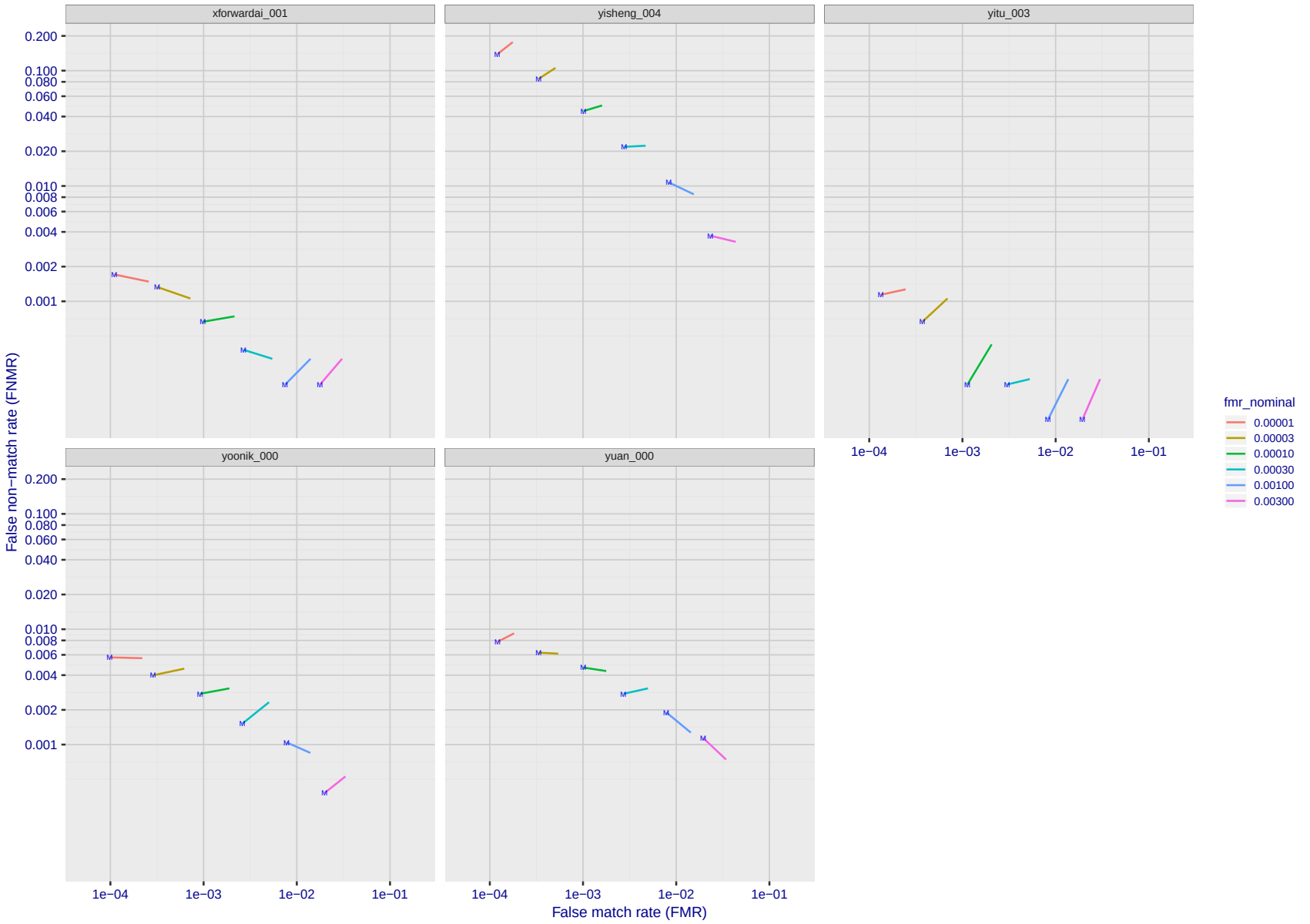

Figure 118: For the visa images, FNMR and FMR at six operating points along the DET characteristic. At each point a line is drawn between (FMR,FNMR)$_{\text{MALE}}$ and (FMR,FNMR)$_{\text{FEMALE}}$ showing how which sex has lower FMR and/or FNMR. The "M" label denotes male, the other end of the line corresponds to female. The six operating thresholds are selected to give the nominal false match rates given in the legend, and are computed over all impostor pairs regardless of age, sex, and place of birth. The plotted FMR values are broadly an order of magnitude larger than the nominal rates because FMR is computed over demographically-matched impostor pairs i.e individuals of the same sex, from the same geographic region (see section 3.6.1), and the same age group (see section 3.6.2).

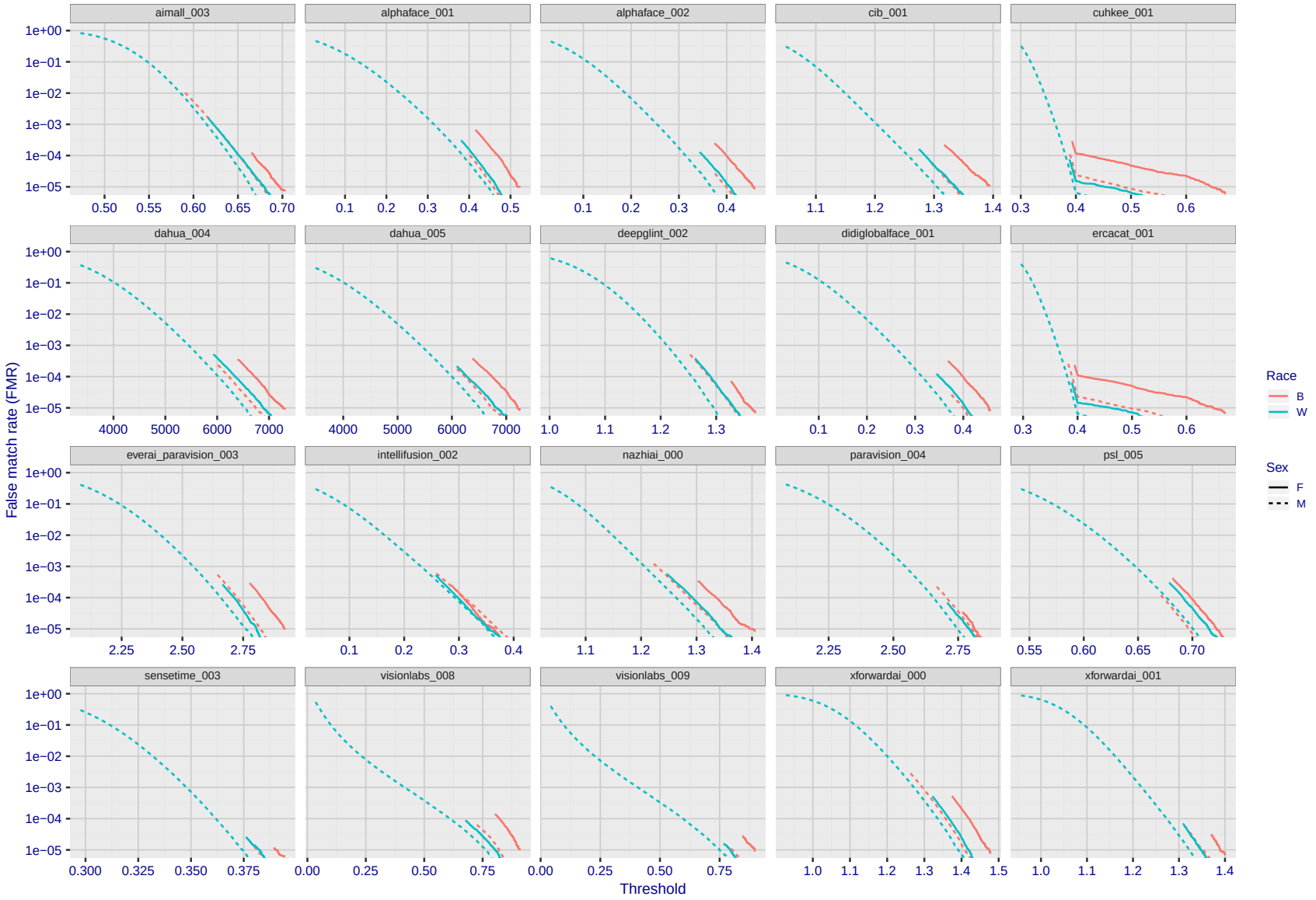

Figure 119: For the mugshot images, the false match calibration curves show false match rate vs. threshold. Separate curves appear for white females, black females, black males and white males.

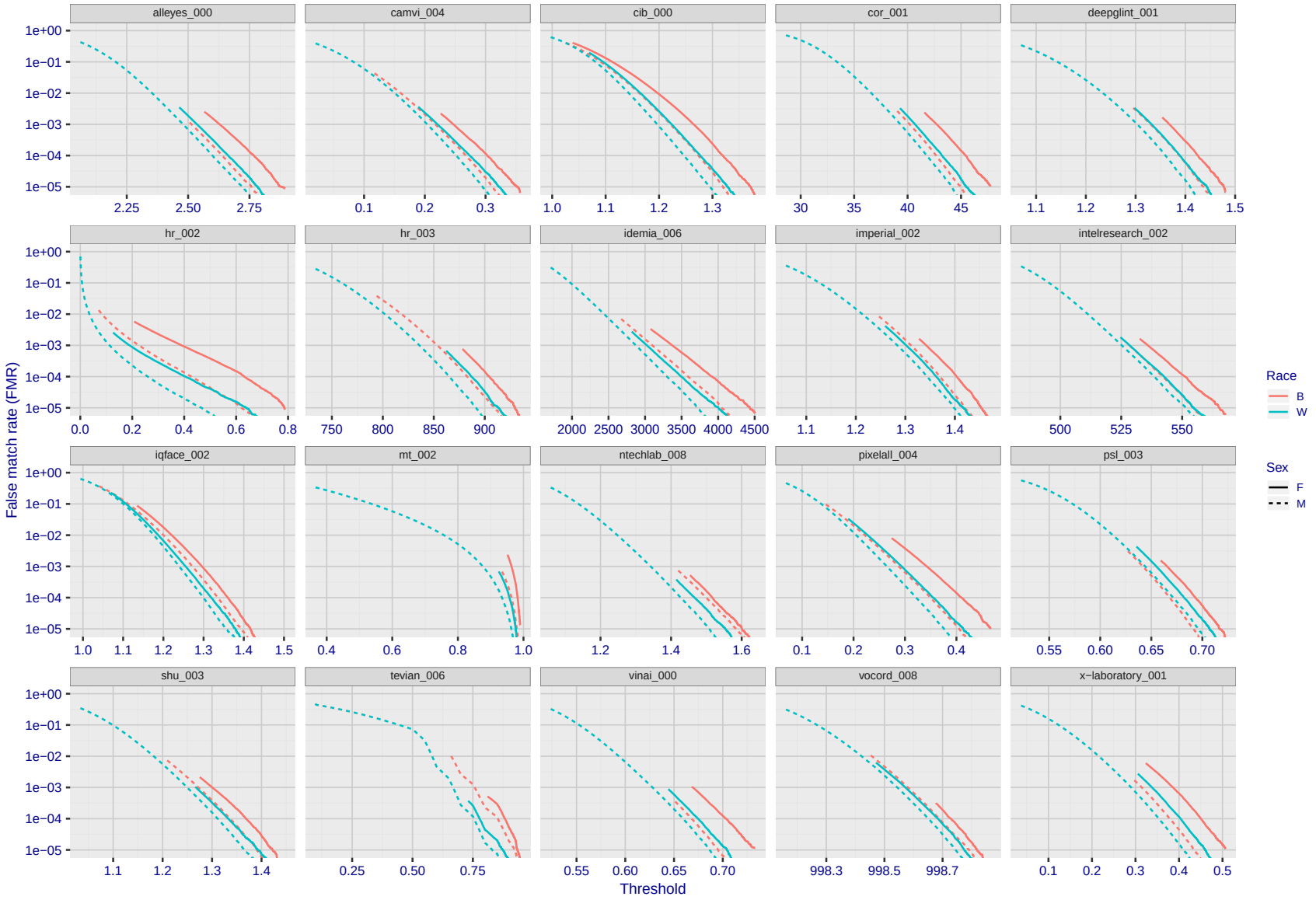

Figure 120: For the mugshot images, the false match calibration curves show false match rate vs. threshold. Separate curves appear for white females, black females, black males and white males.

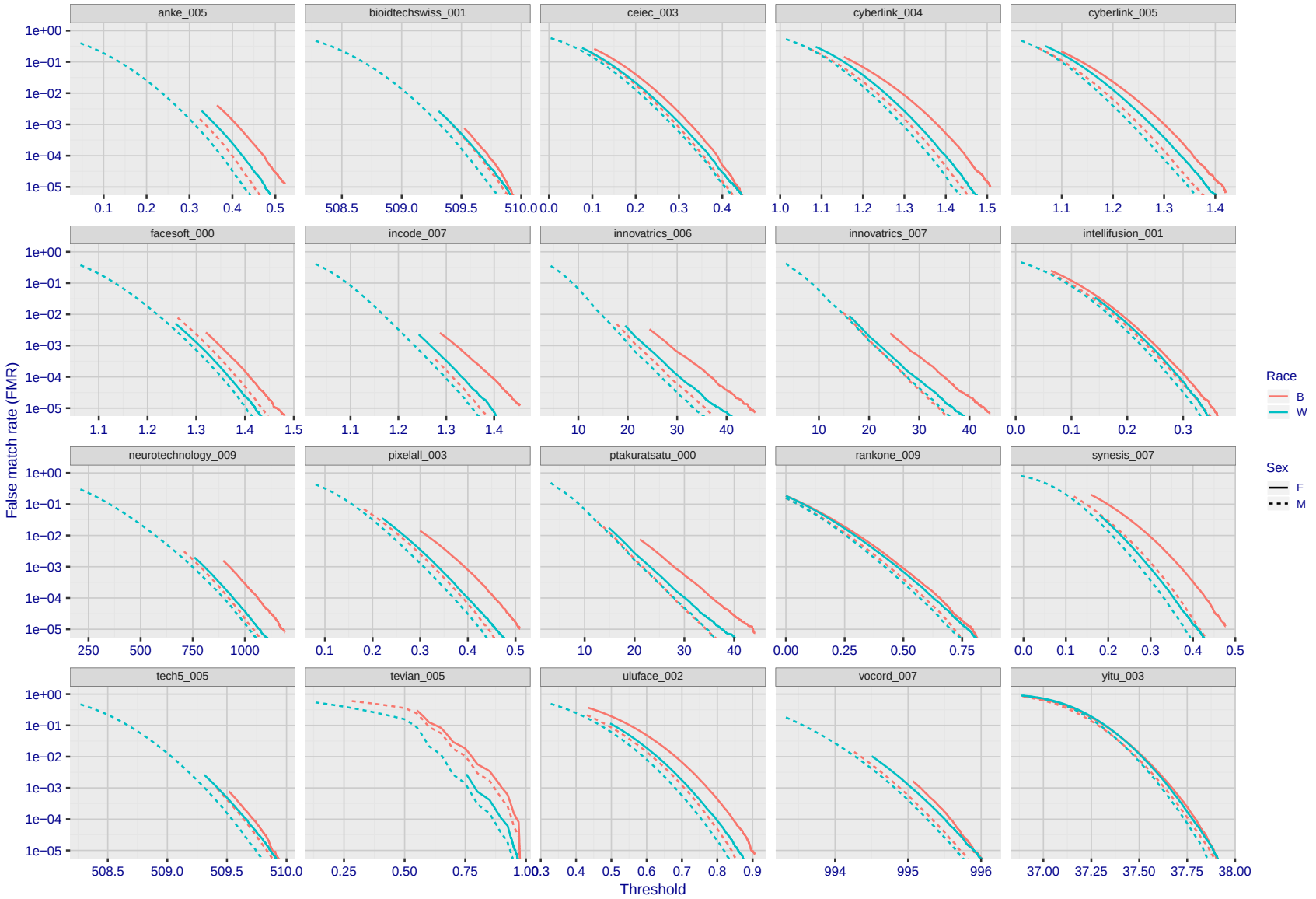

Figure 121: For the mugshot images, the false match calibration curves show false match rate vs. threshold. Separate curves appear for white females, black females, black males and white males.

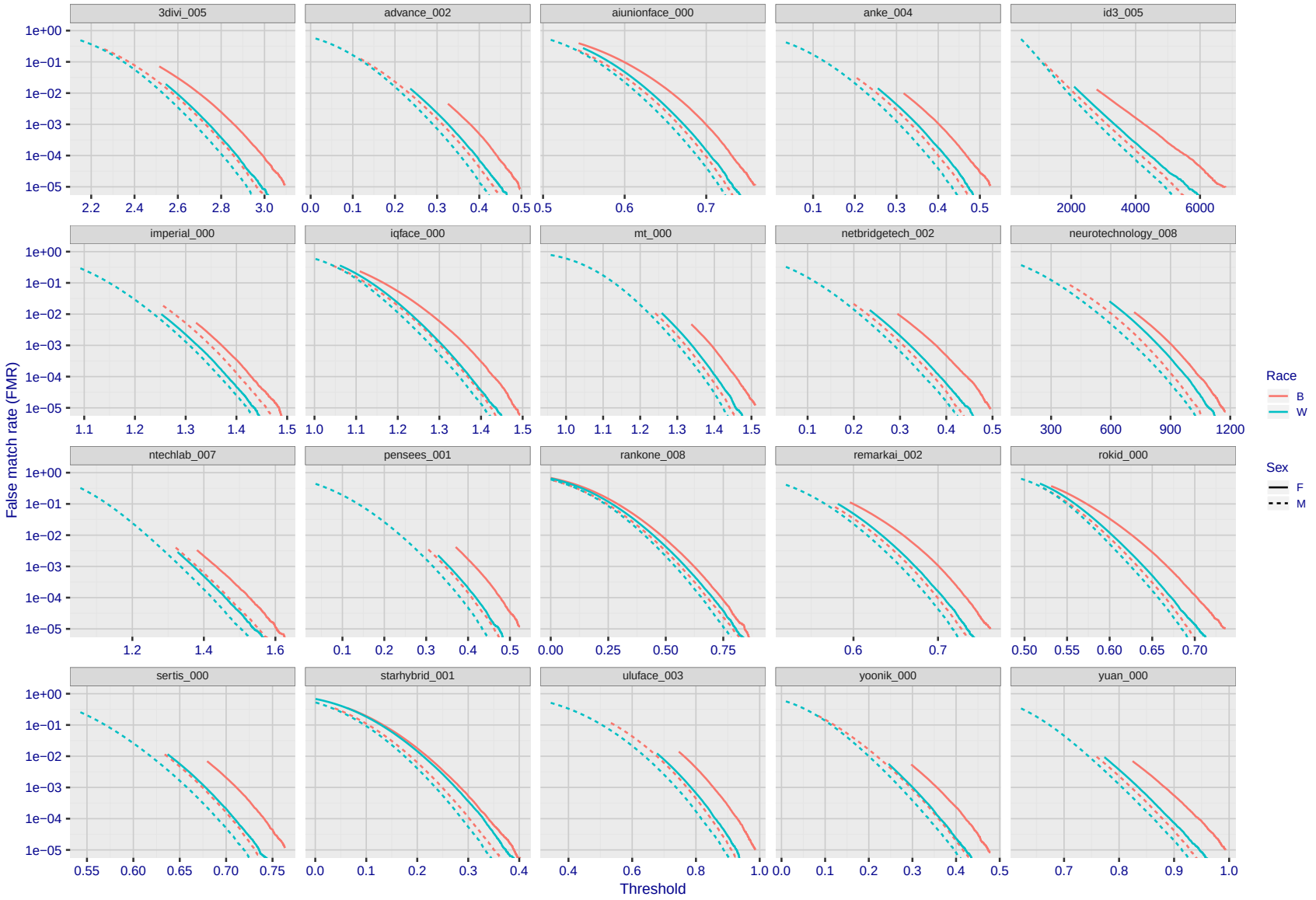

Figure 122: For the mugshot images, the false match calibration curves show false match rate vs. threshold. Separate curves appear for white females, black females, black males and white males.

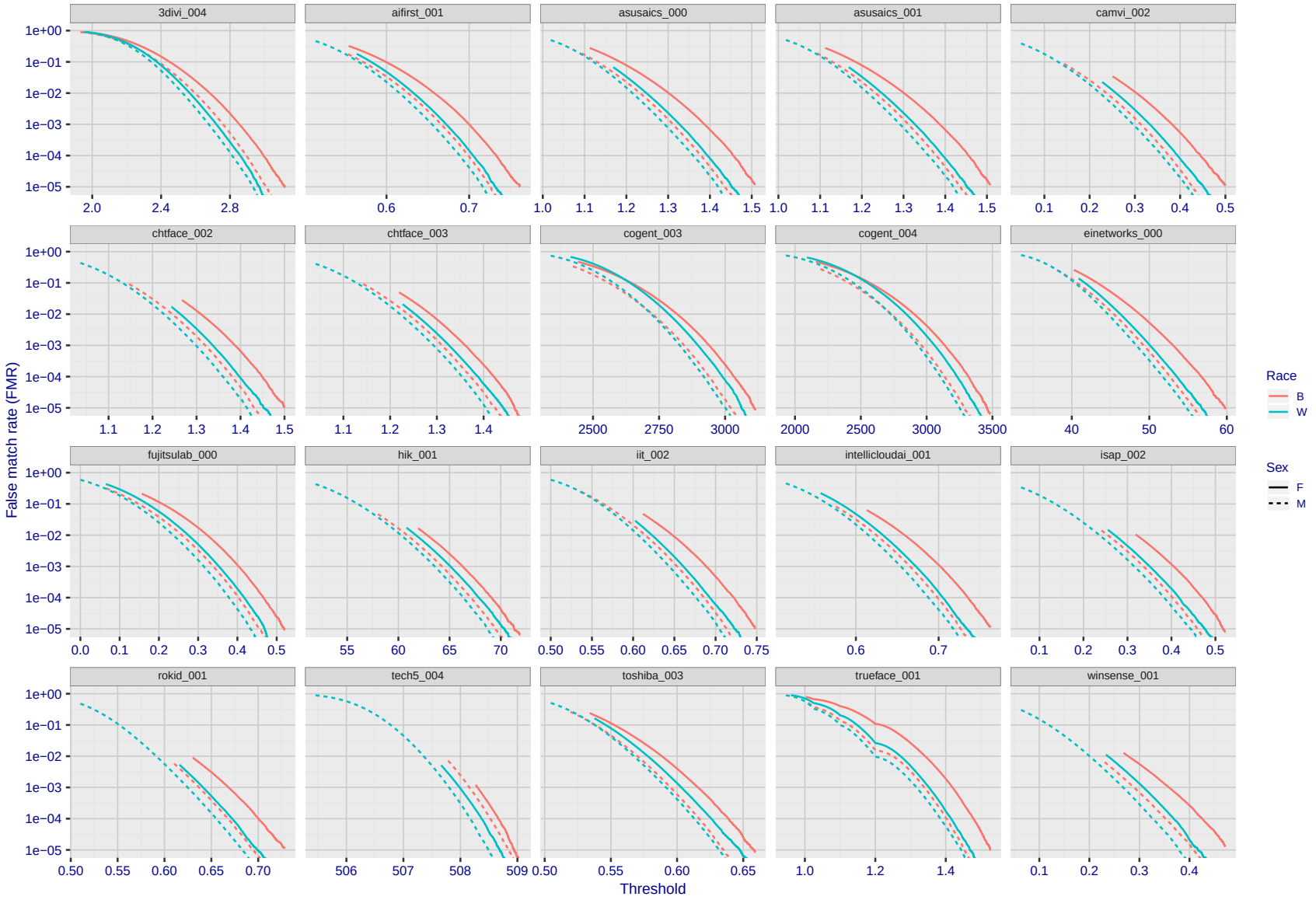

Figure 123: For the mugshot images, the false match calibration curves show false match rate vs. threshold. Separate curves appear for white females, black females, black males and white males.

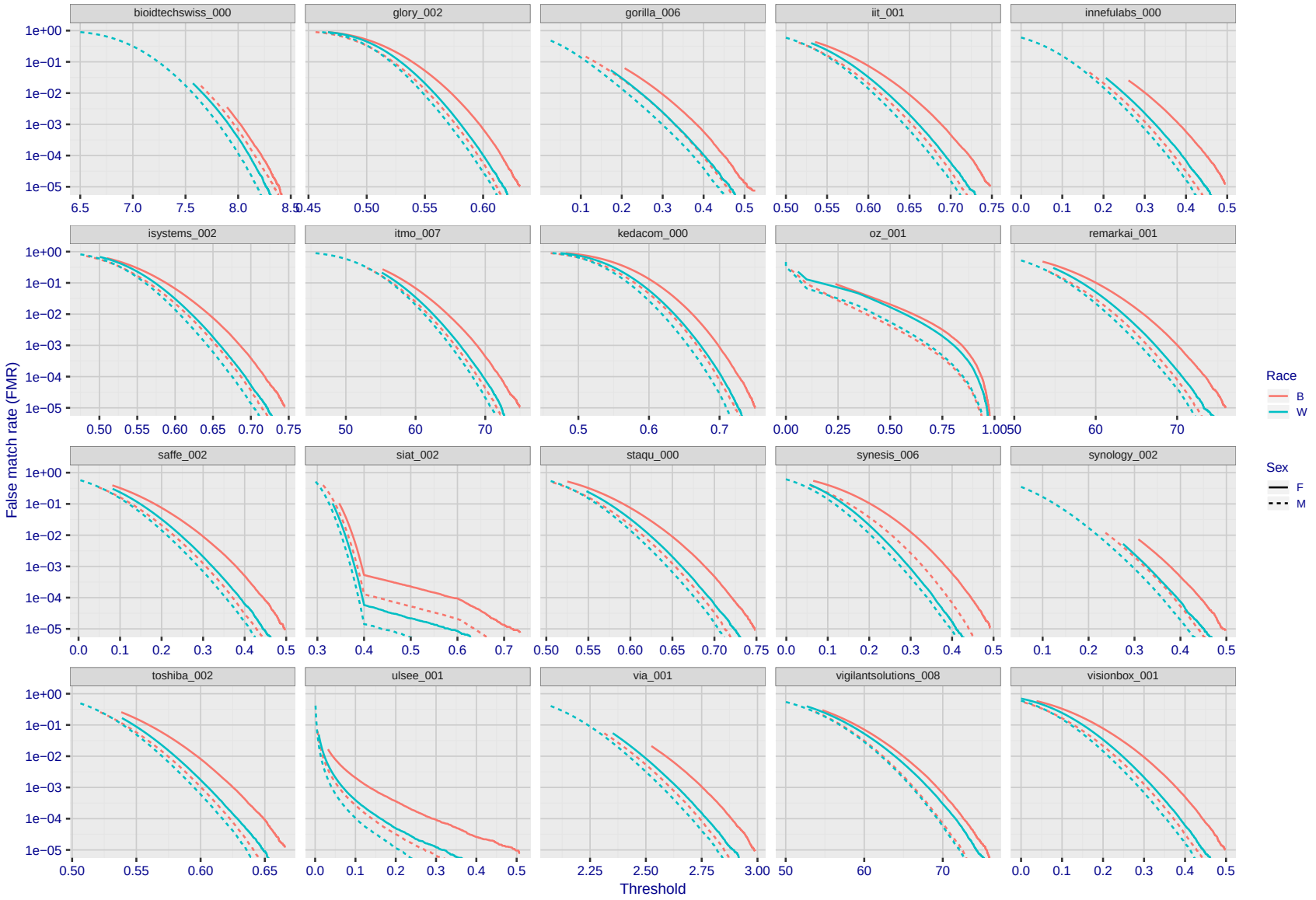

Figure 124: For the mugshot images, the false match calibration curves show false match rate vs. threshold. Separate curves appear for white females, black females, black males and white males.

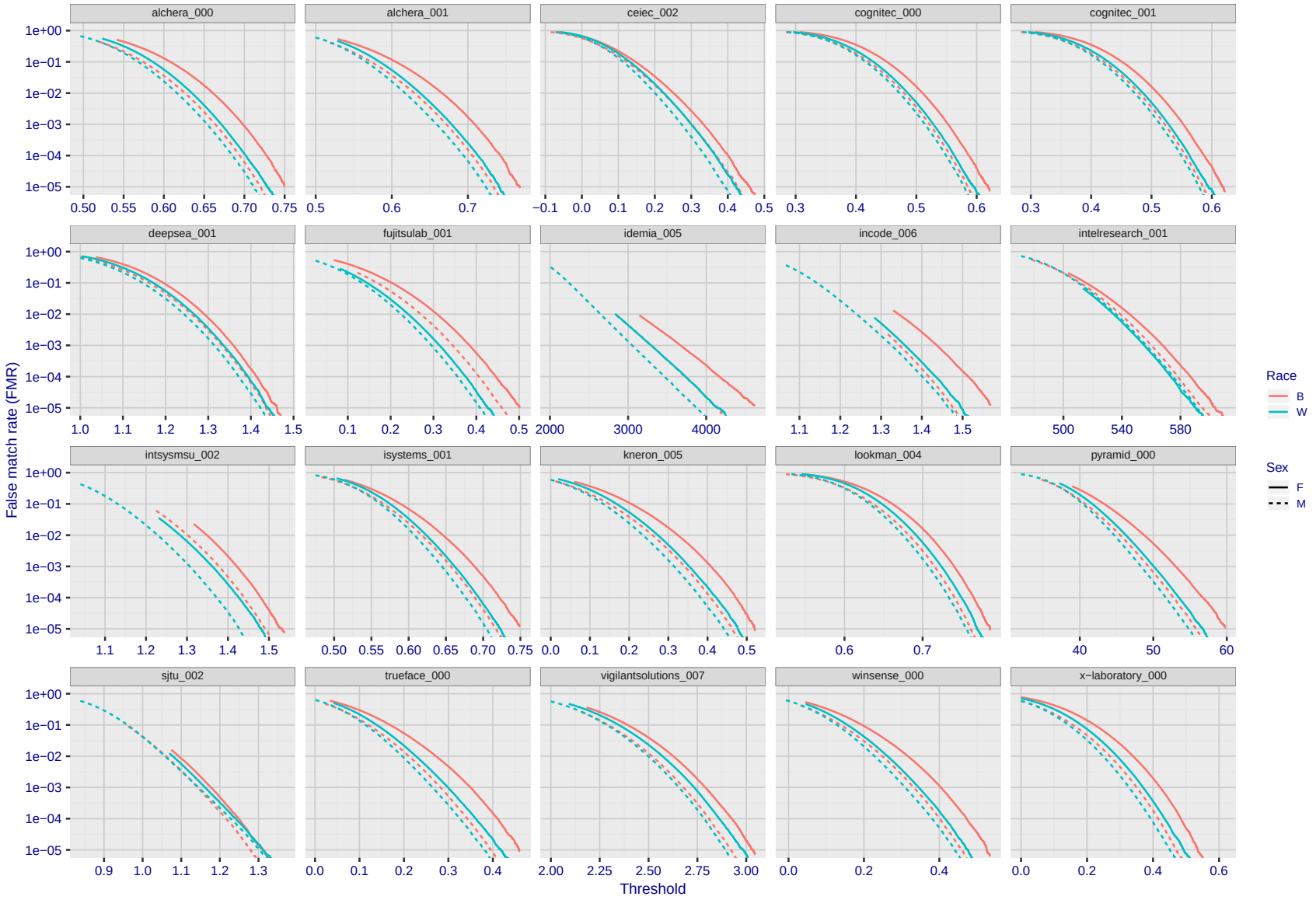

Figure 125: For the mugshot images, the false match calibration curves show false match rate vs. threshold. Separate curves appear for white females, black females, black males and white males.

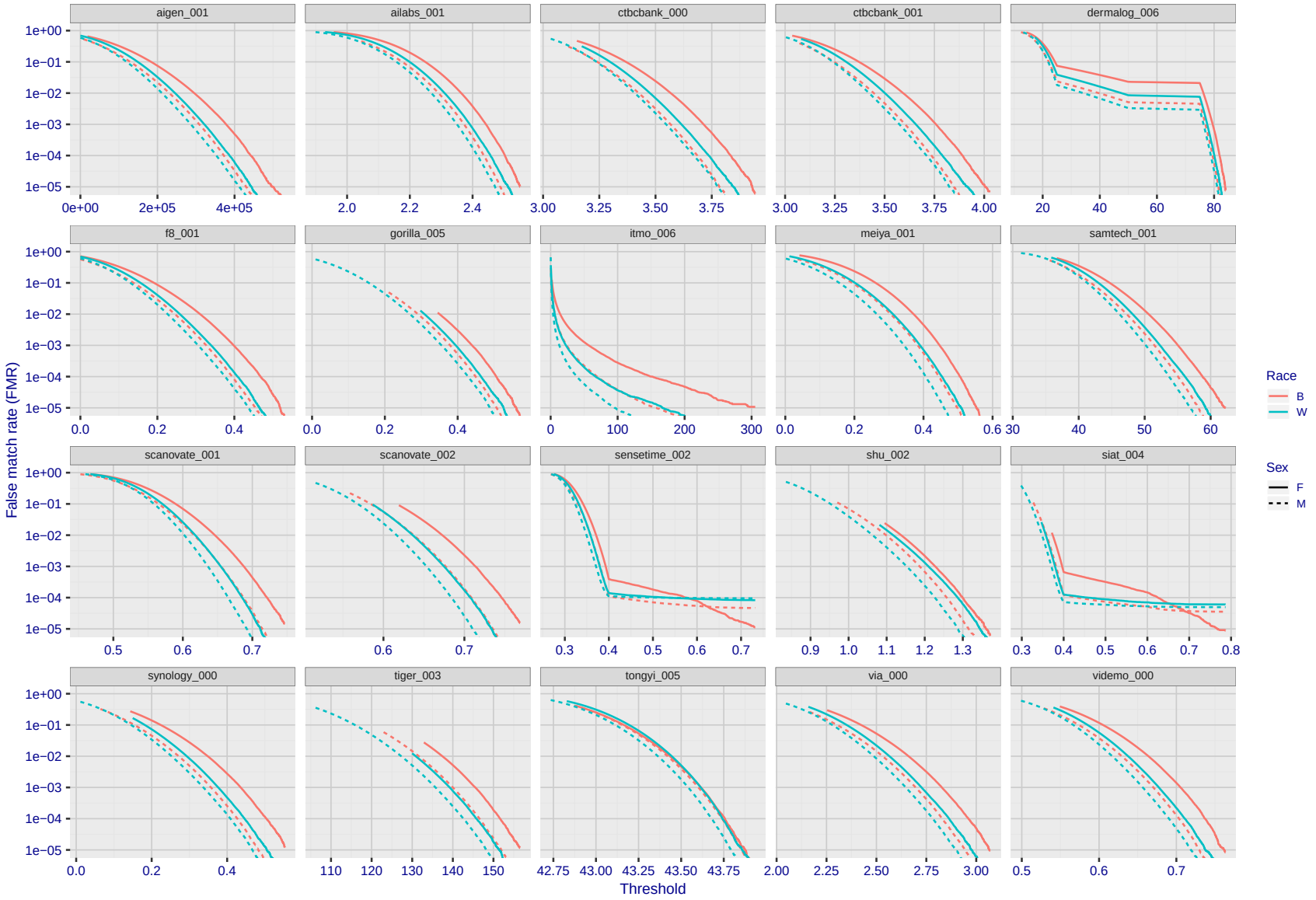

Figure 126: For the mugshot images, the false match calibration curves show false match rate vs. threshold. Separate curves appear for white females, black females, black males and white males.

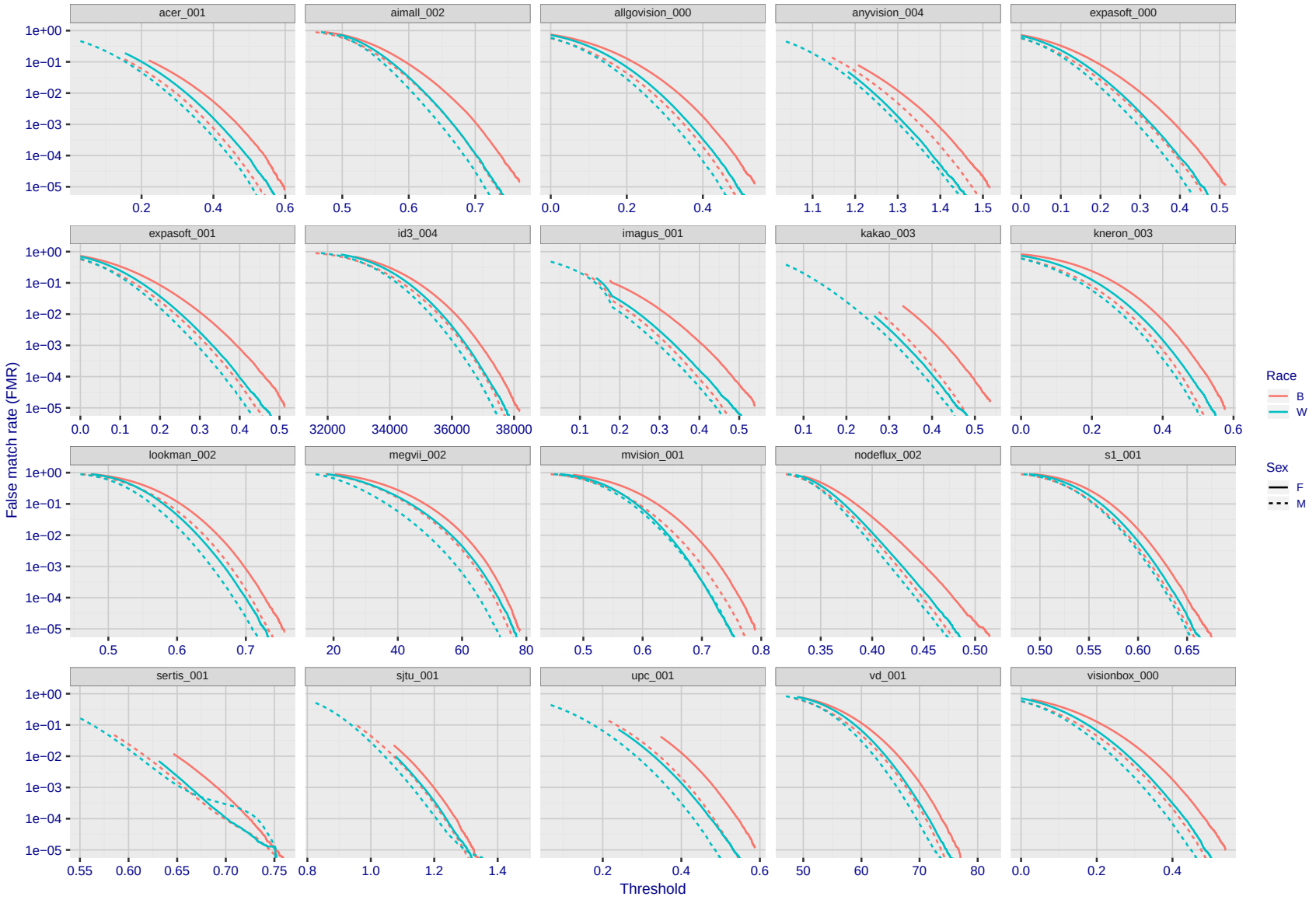

Figure 127: For the mugshot images, the false match calibration curves show false match rate vs. threshold. Separate curves appear for white females, black females, black males and white males.

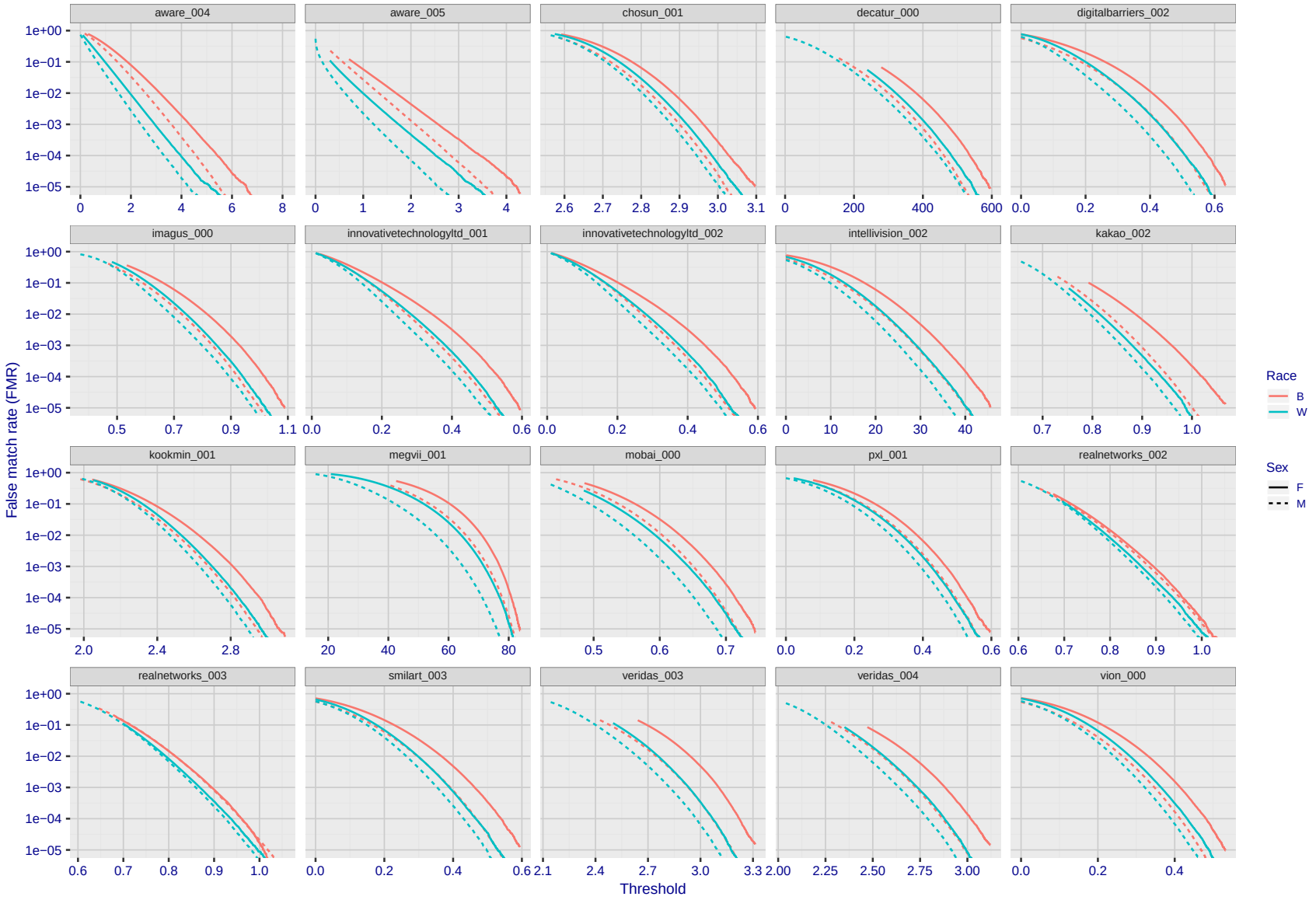

Figure 128: For the mugshot images, the false match calibration curves show false match rate vs. threshold. Separate curves appear for white females, black females, black males and white males.

2020/10/09 13:32:41
FNMR(T) "False non-match rate"
FMR(T) "False match rate"

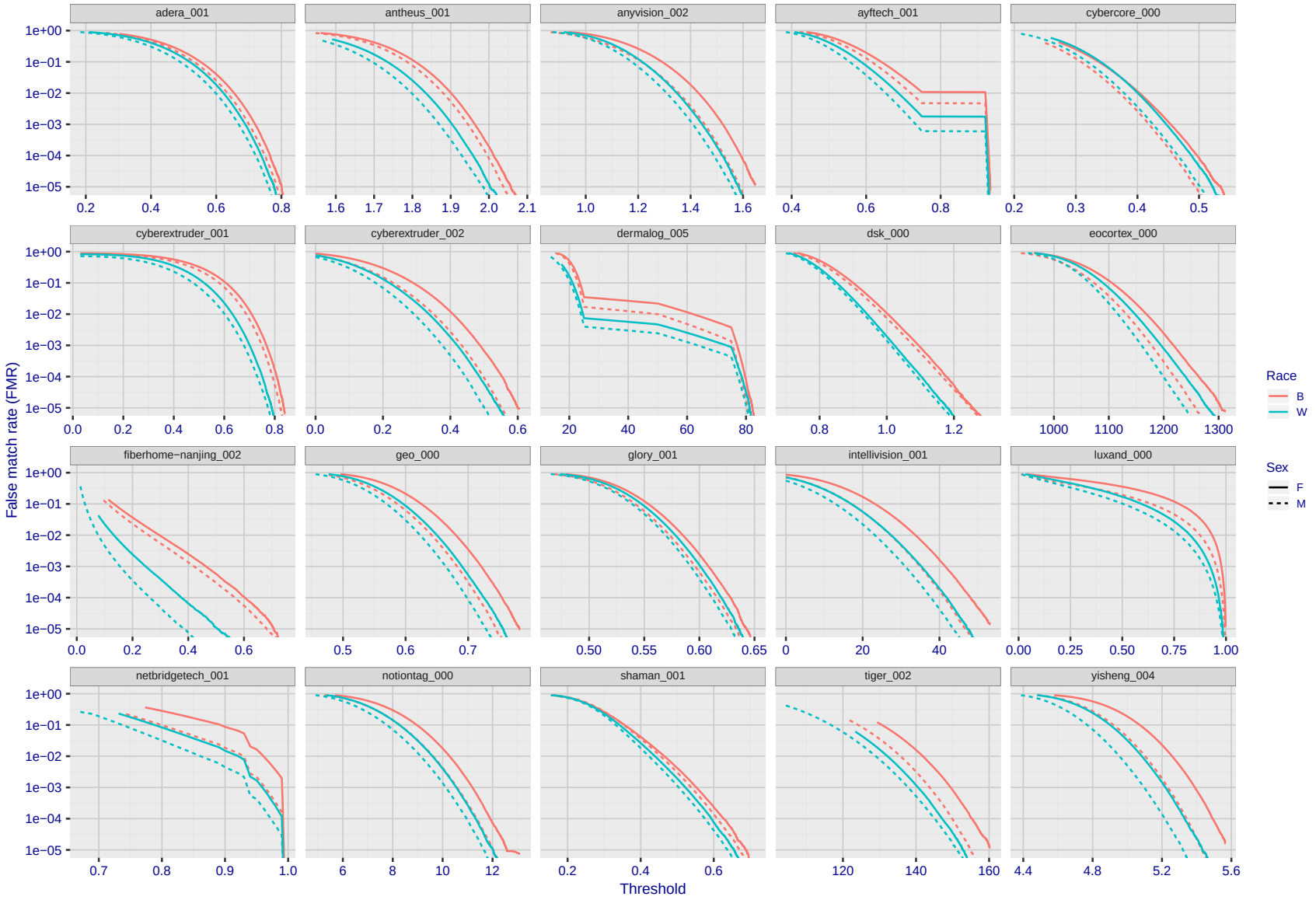

Figure 129: For the mugshot images, the false match calibration curves show false match rate vs. threshold. Separate curves appear for white females, black females, black males and white males.

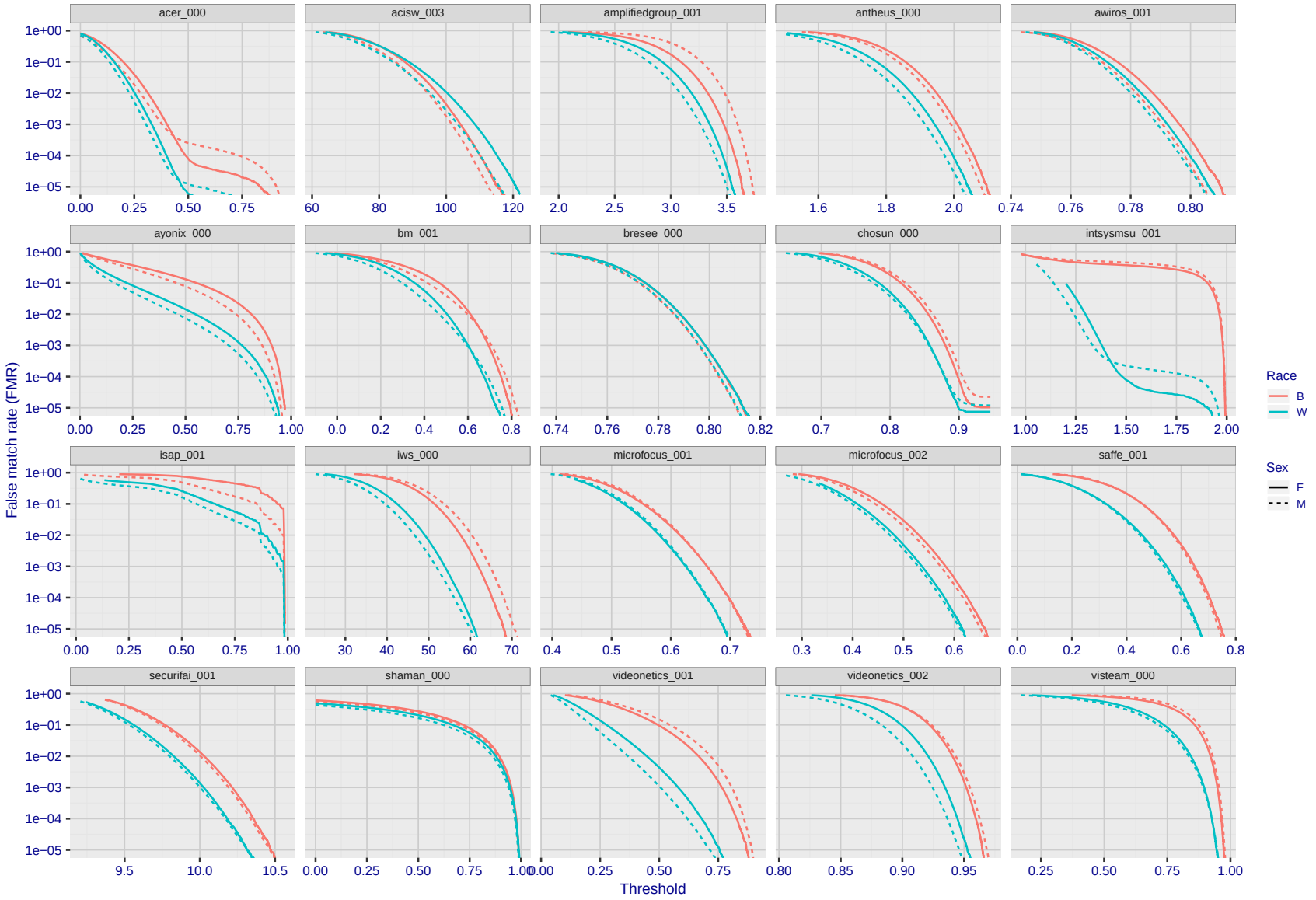

Figure 130: For the mugshot images, the false match calibration curves show false match rate vs. threshold. Separate curves appear for white females, black females, black males and white males.

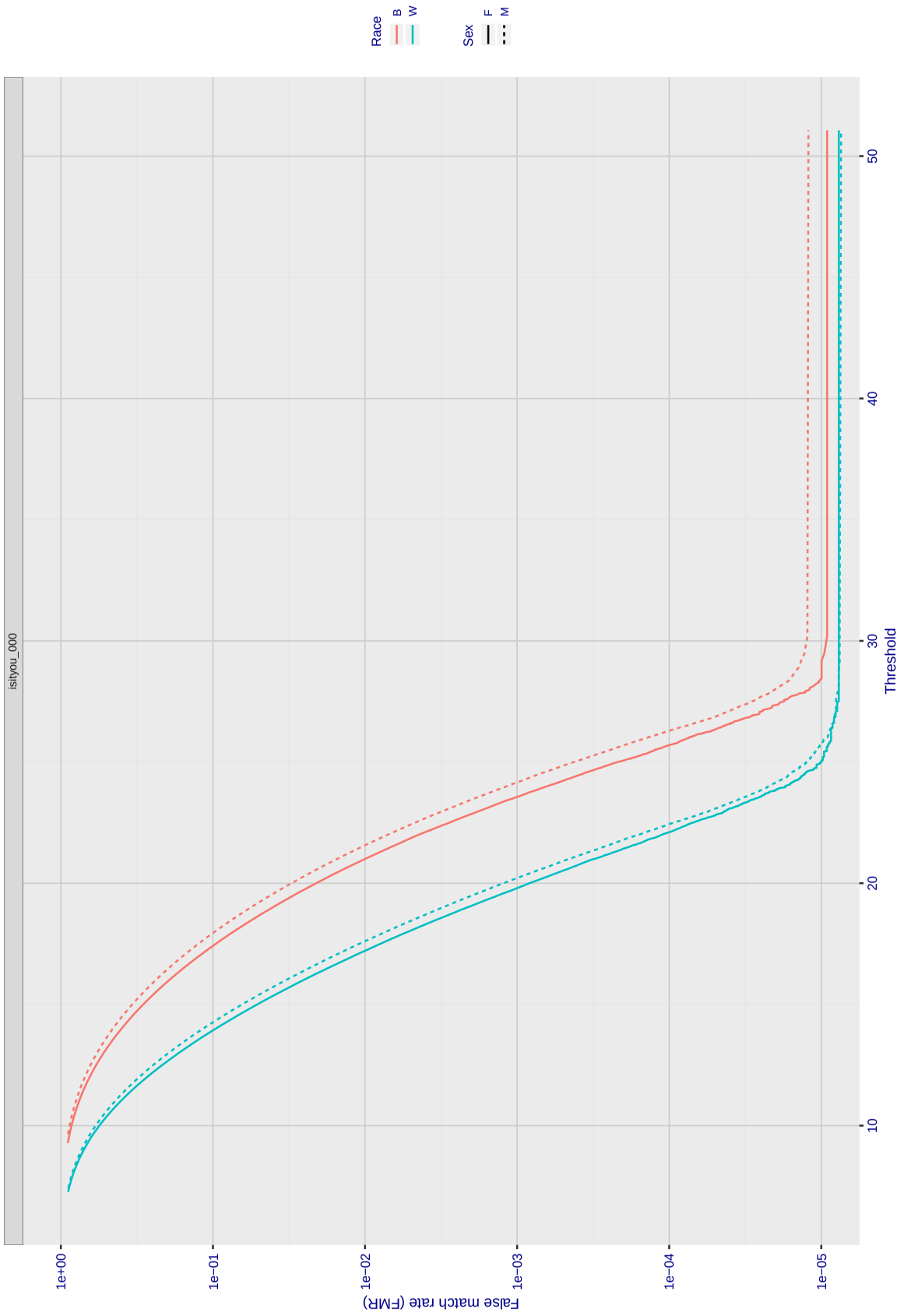

Figure 131: For the mugshot images, the false match calibration curves show false match rate vs. threshold. Separate curves appear for white females, black females, black males and white males.

FNMR(T) "False non-match rate"
FMR(T) "False match rate"

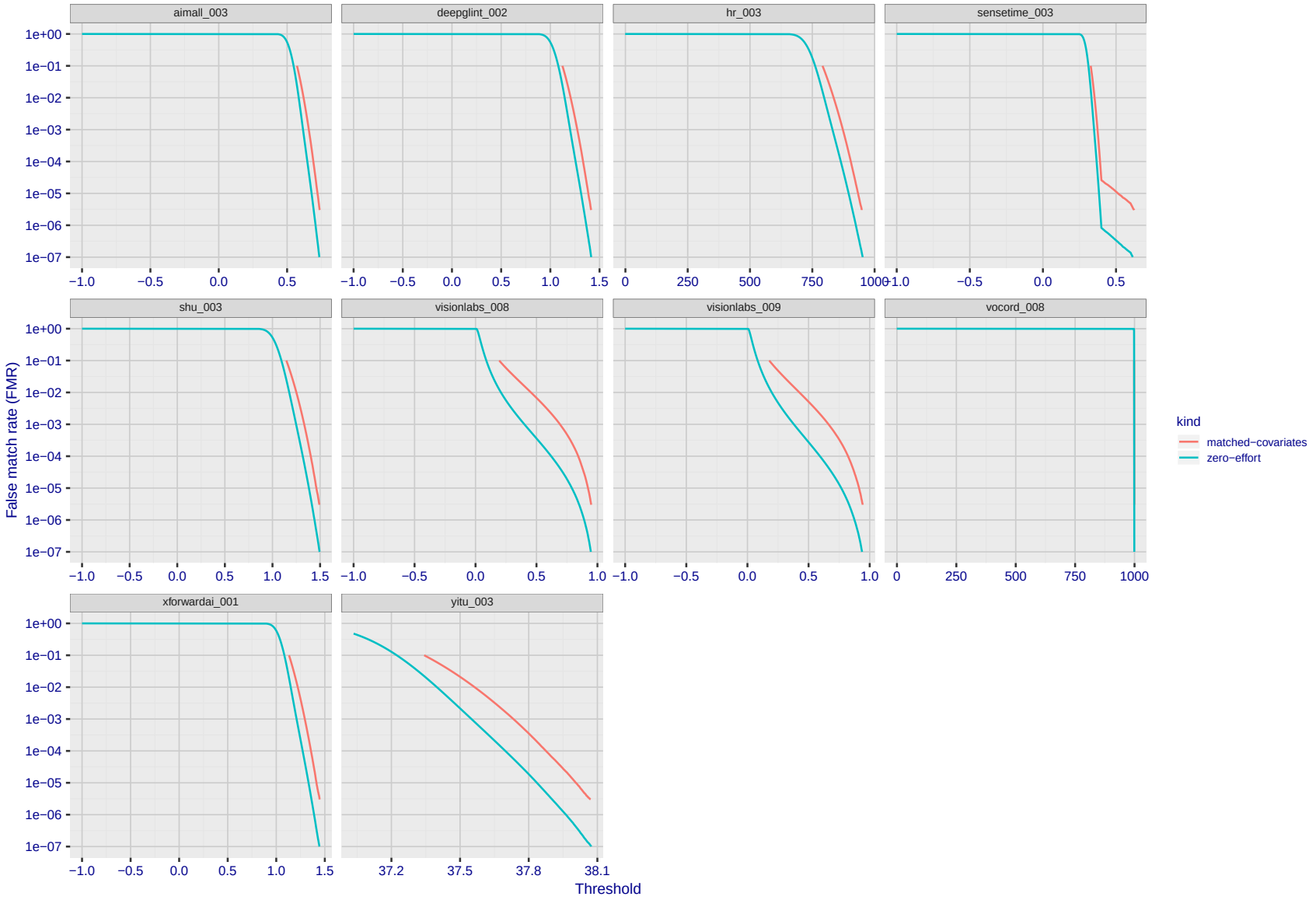

Figure 132: For the visa images, the false match calibration curves show FMR vs. threshold, T. The blue (lower) curves are for zero-effort impostors (i.e. comparing all images against all). The red (upper) curves are for persons of the same-sex, same-age, and same national-origin. This shows that FMR is underestimated (by a factor of 10 or more) by using a zero-effort impostor calculation to calibrate T. As shown later (sec. 3.6), FMR is higher for demographic-matched impostors.

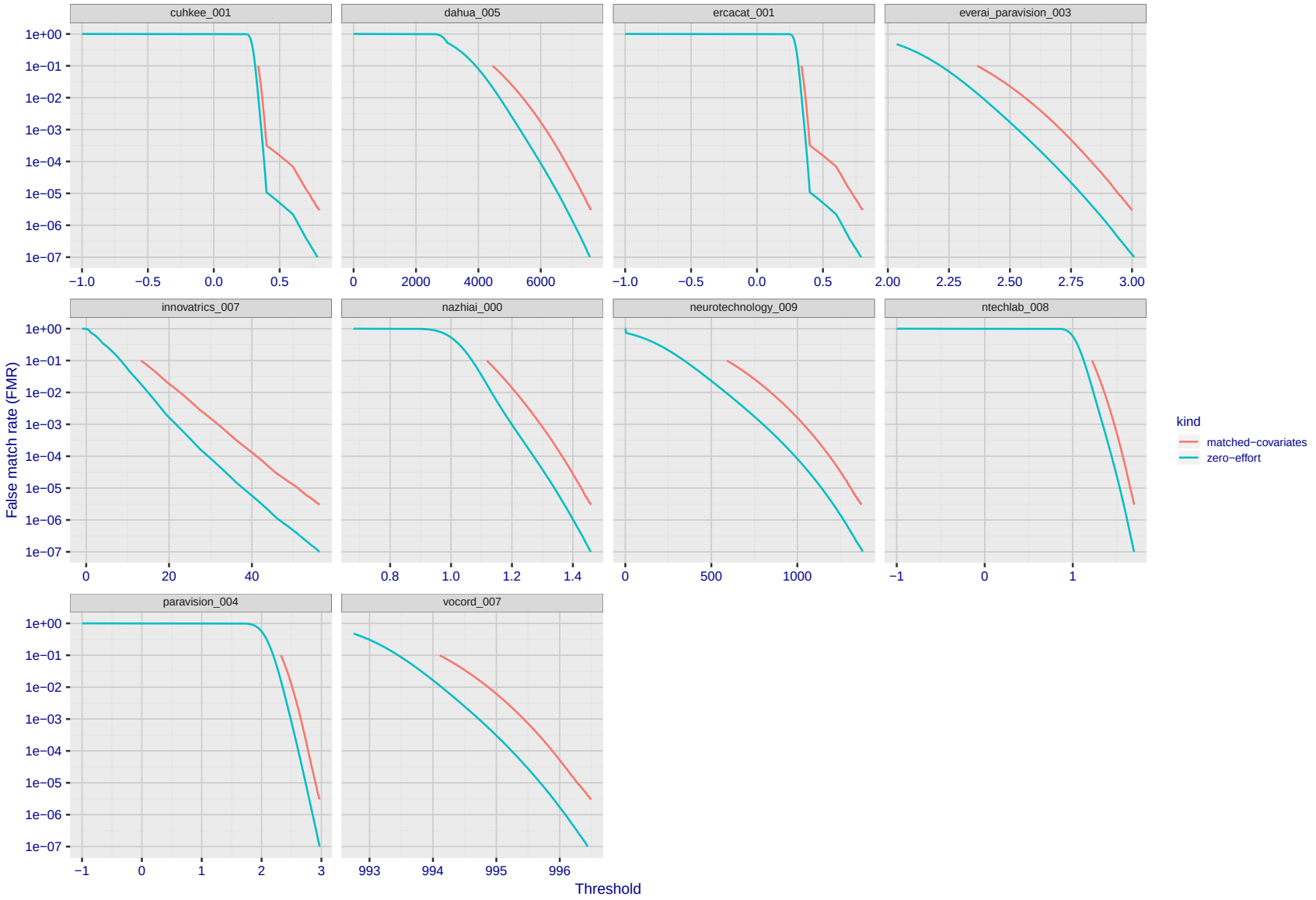

Figure 133: For the visa images, the false match calibration curves show FMR vs. threshold, T. The blue (lower) curves are for zero-effort impostors (i.e. comparing all images against all). The red (upper) curves are for persons of the same-sex, same-age, and same national-origin. This shows that FMR is underestimated (by a factor of 10 or more) by using a zero-effort impostor calculation to calibrate T. As shown later (sec. 3.6), FMR is higher for demographic-matched impostors.

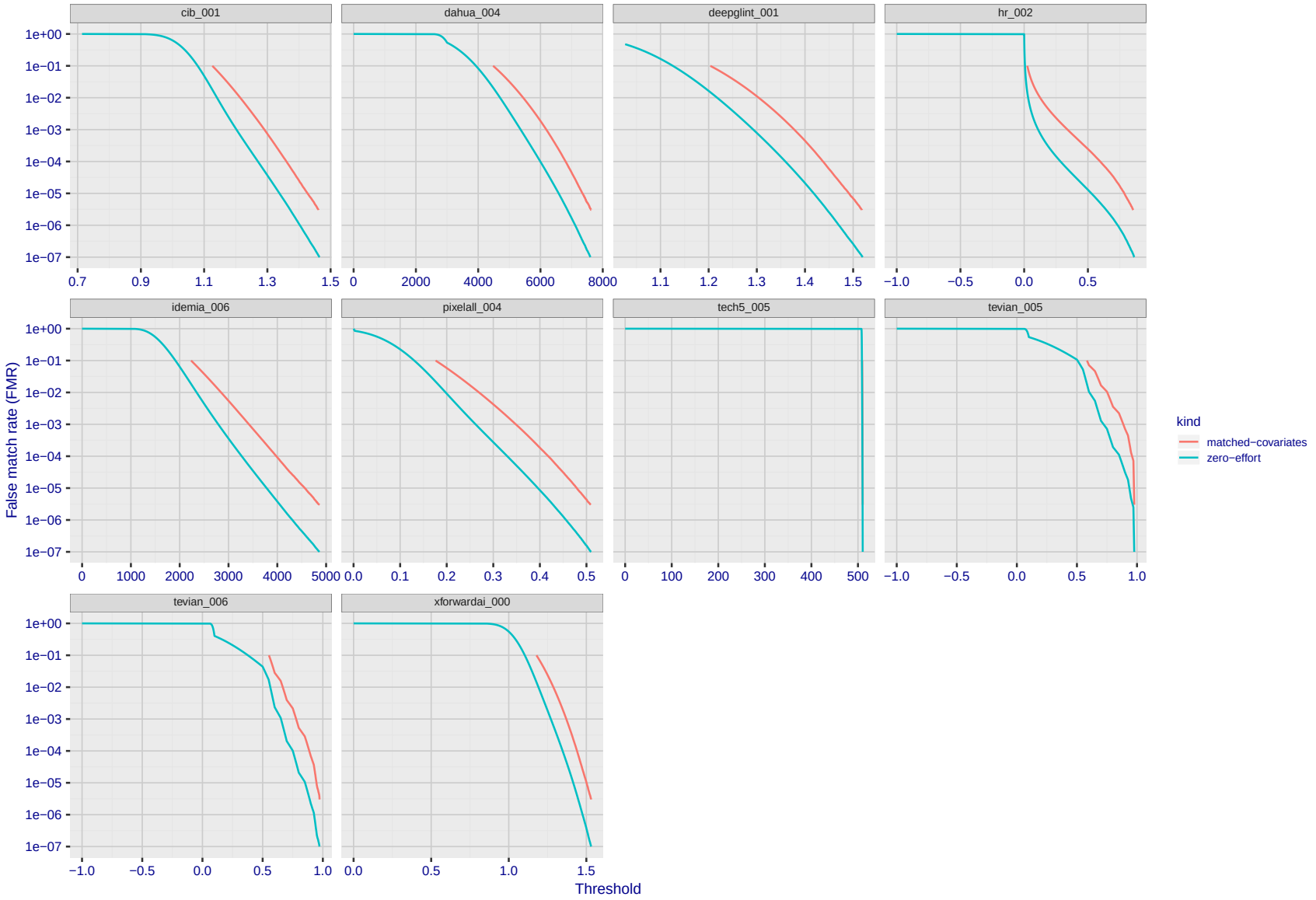

Figure 134: For the visa images, the false match calibration curves show FMR vs. threshold, T. The blue (lower) curves are for zero-effort impostors (i.e. comparing all images against all). The red (upper) curves are for persons of the same-sex, same-age, and same national-origin. This shows that FMR is underestimated (by a factor of 10 or more) by using a zero-effort impostor calculation to calibrate T. As shown later (sec. 3.6), FMR is higher for demographic-matched impostors.

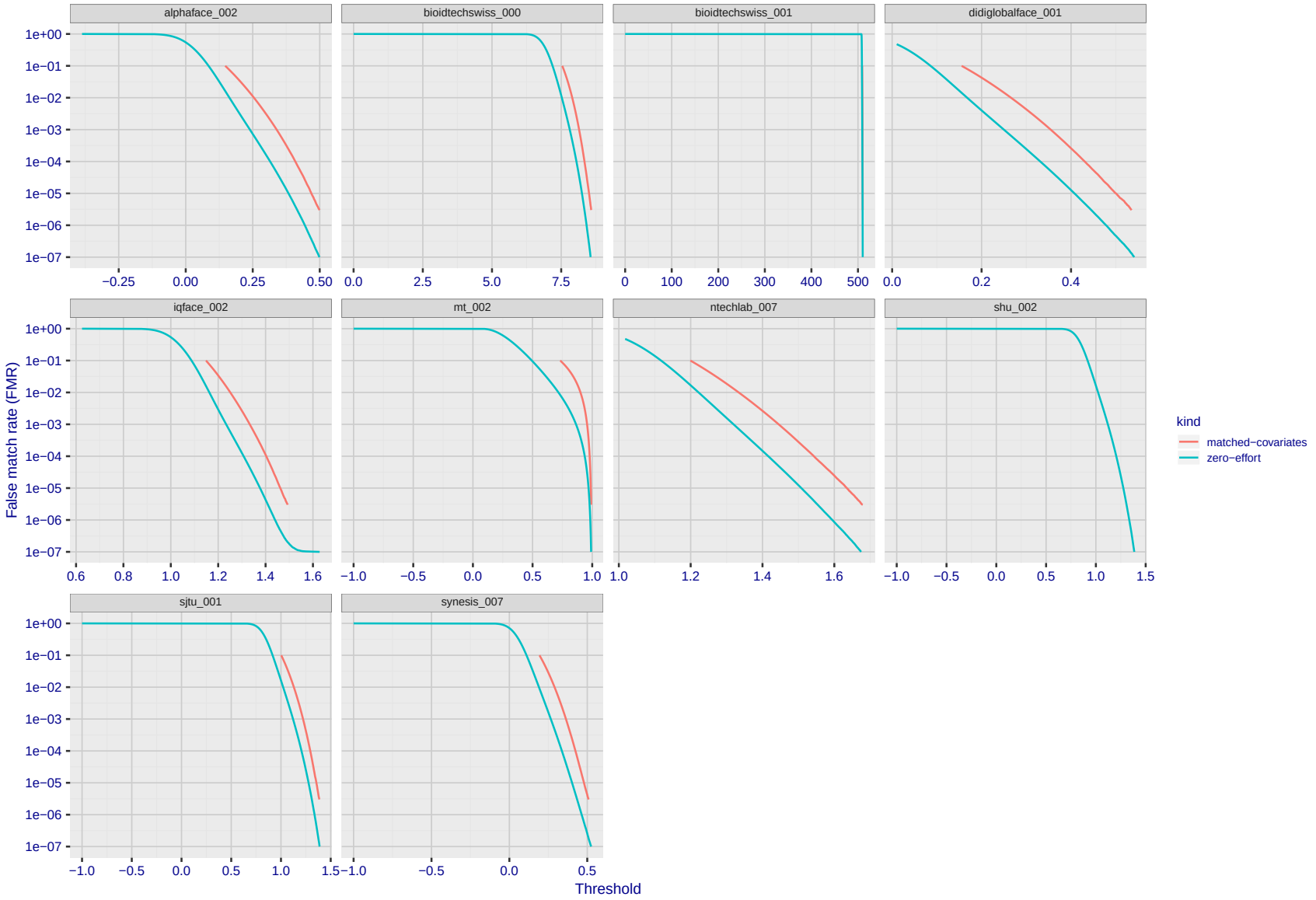

Figure 135: For the visa images, the false match calibration curves show FMR vs. threshold, T. The blue (lower) curves are for zero-effort impostors (i.e. comparing all images against all). The red (upper) curves are for persons of the same-sex, same-age, and same national-origin. This shows that FMR is underestimated (by a factor of 10 or more) by using a zero-effort impostor calculation to calibrate T. As shown later (sec. 3.6), FMR is higher for demographic-matched impostors.

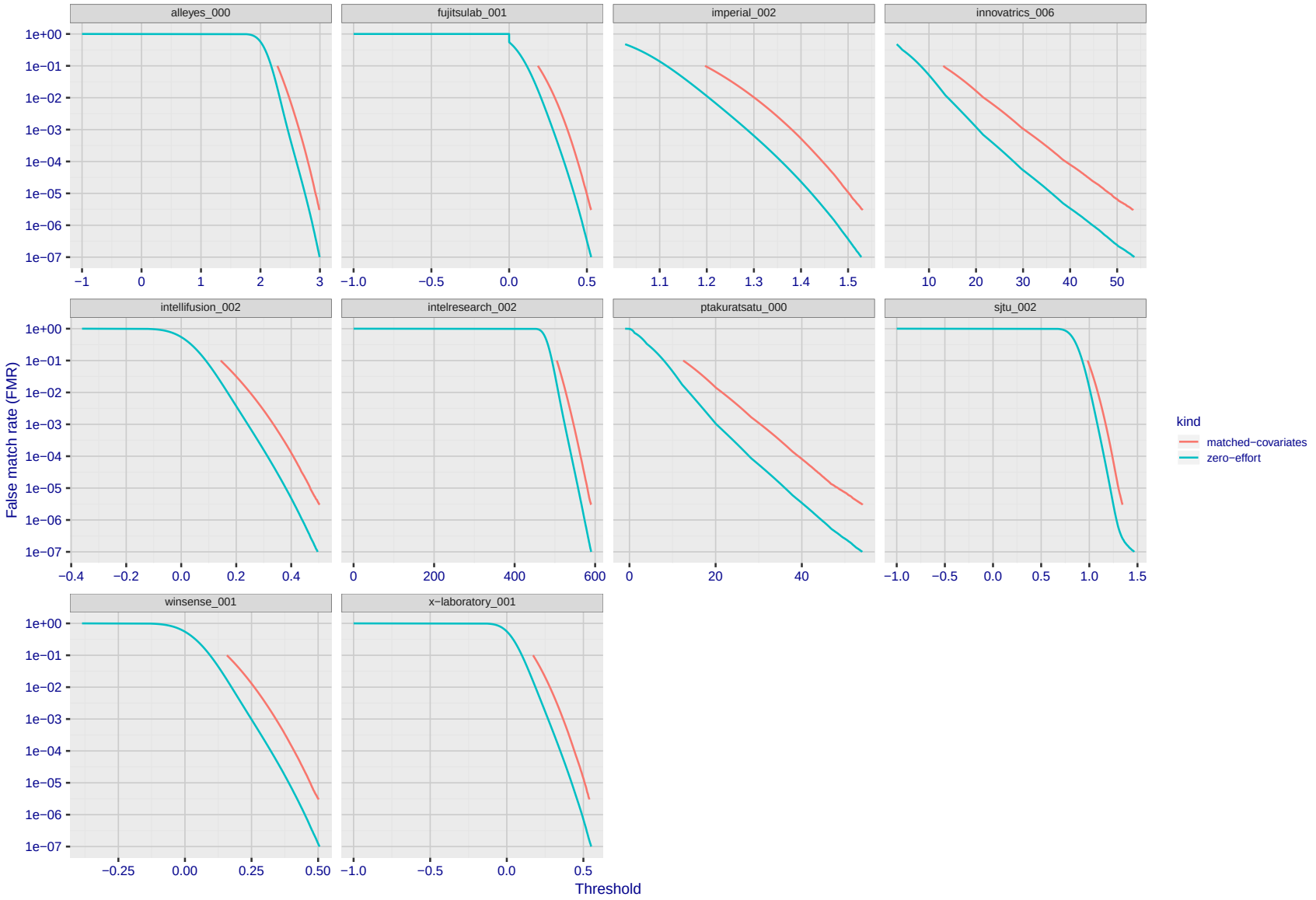

Figure 136: For the visa images, the false match calibration curves show FMR vs. threshold, T. The blue (lower) curves are for zero-effort impostors (i.e. comparing all images against all). The red (upper) curves are for persons of the same-sex, same-age, and same national-origin. This shows that FMR is underestimated (by a factor of 10 or more) by using a zero-effort impostor calculation to calibrate T. As shown later (sec. 3.6), FMR is higher for demographic-matched impostors.

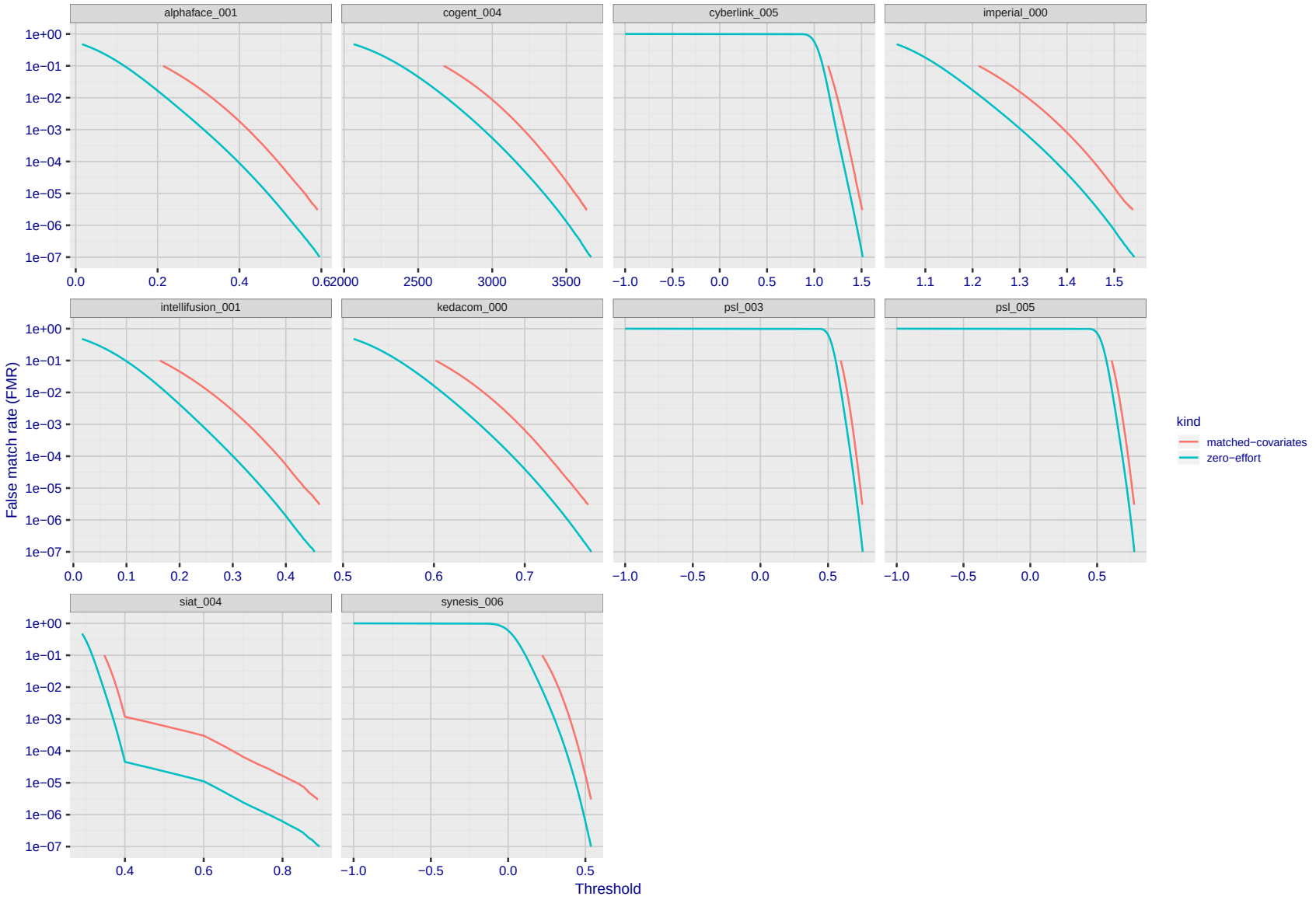

Figure 137: For the visa images, the false match calibration curves show FMR vs. threshold, T. The blue (lower) curves are for zero-effort impostors (i.e. comparing all images against all). The red (upper) curves are for persons of the same-sex, same-age, and same national-origin. This shows that FMR is underestimated (by a factor of 10 or more) by using a zero-effort impostor calculation to calibrate T. As shown later (sec. 3.6), FMR is higher for demographic-matched impostors.

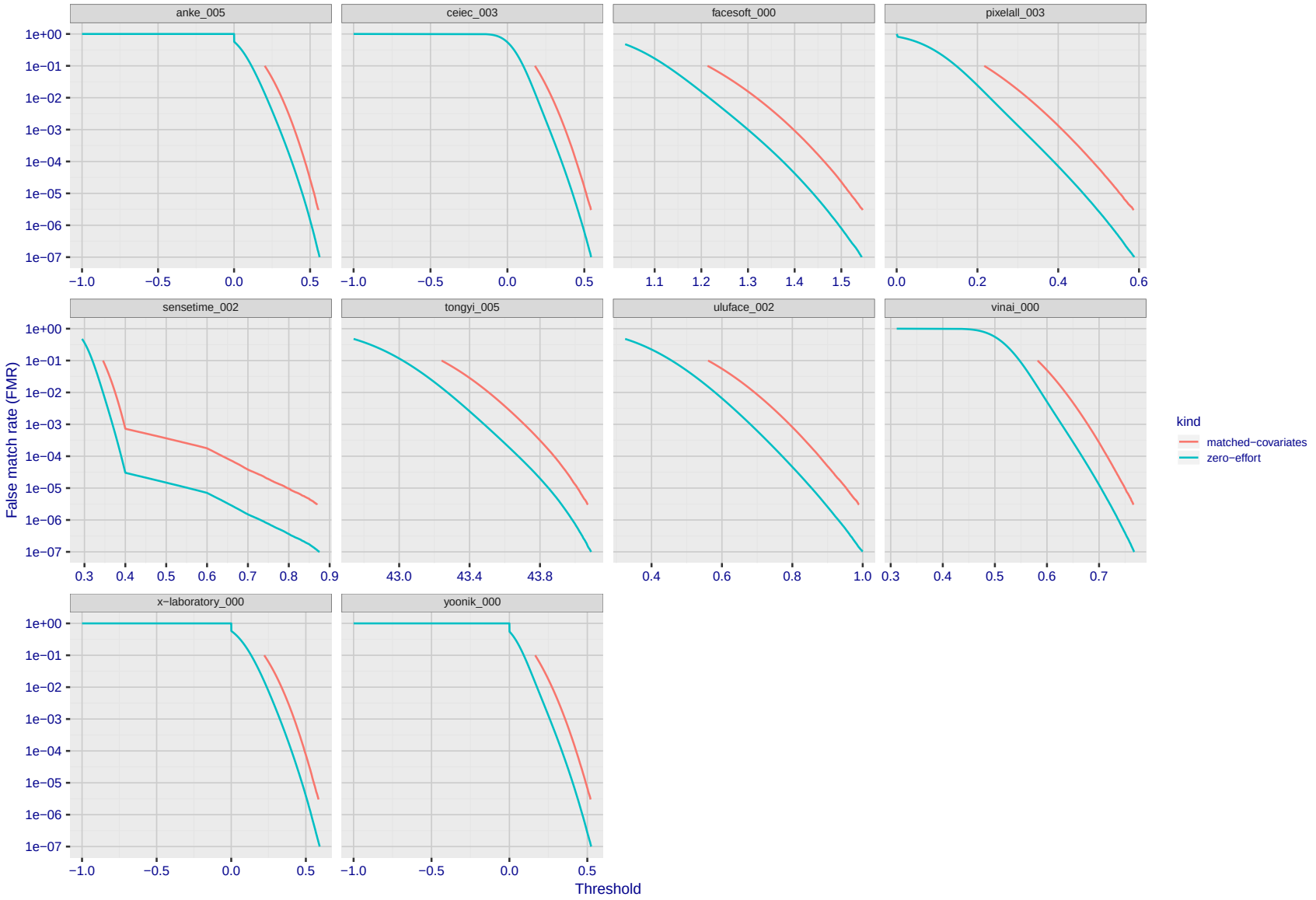

Figure 138: For the visa images, the false match calibration curves show FMR vs. threshold, T. The blue (lower) curves are for zero-effort impostors (i.e. comparing all images against all). The red (upper) curves are for persons of the same-sex, same-age, and same national-origin. This shows that FMR is underestimated (by a factor of 10 or more) by using a zero-effort impostor calculation to calibrate T. As shown later (sec. 3.6), FMR is higher for demographic-matched impostors.

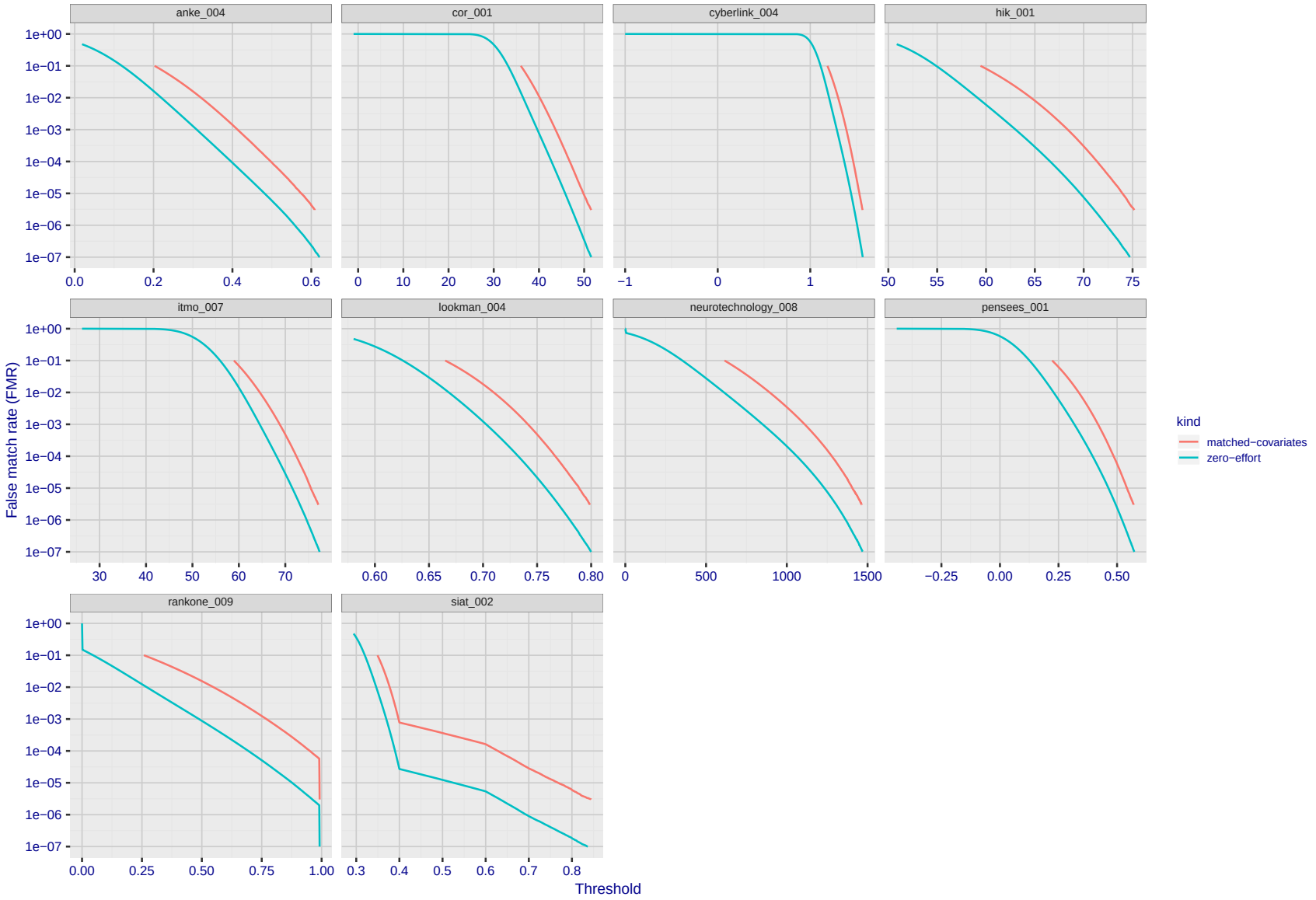

Figure 139: For the visa images, the false match calibration curves show FMR vs. threshold, T. The blue (lower) curves are for zero-effort impostors (i.e. comparing all images against all). The red (upper) curves are for persons of the same-sex, same-age, and same national-origin. This shows that FMR is underestimated (by a factor of 10 or more) by using a zero-effort impostor calculation to calibrate T. As shown later (sec. 3.6), FMR is higher for demographic-matched impostors.

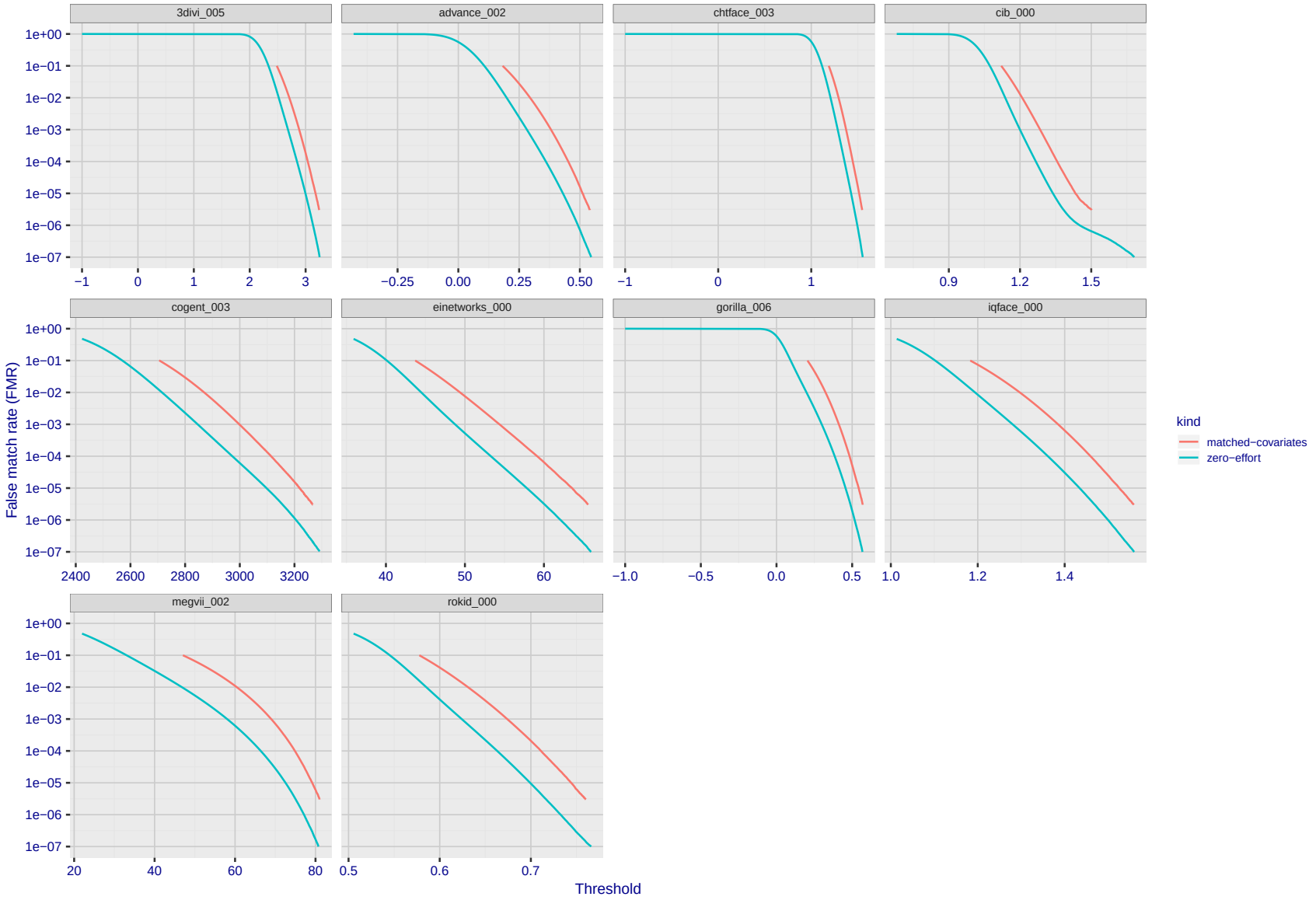

Figure 140: For the visa images, the false match calibration curves show FMR vs. threshold, T. The blue (lower) curves are for zero-effort impostors (i.e. comparing all images against all). The red (upper) curves are for persons of the same-sex, same-age, and same national-origin. This shows that FMR is underestimated (by a factor of 10 or more) by using a zero-effort impostor calculation to calibrate T. As shown later (sec. 3.6), FMR is higher for demographic-matched impostors.

2020/10/09 13:32:41

FNMR(T) "False non-match rate"
FMR(T) "False match rate"

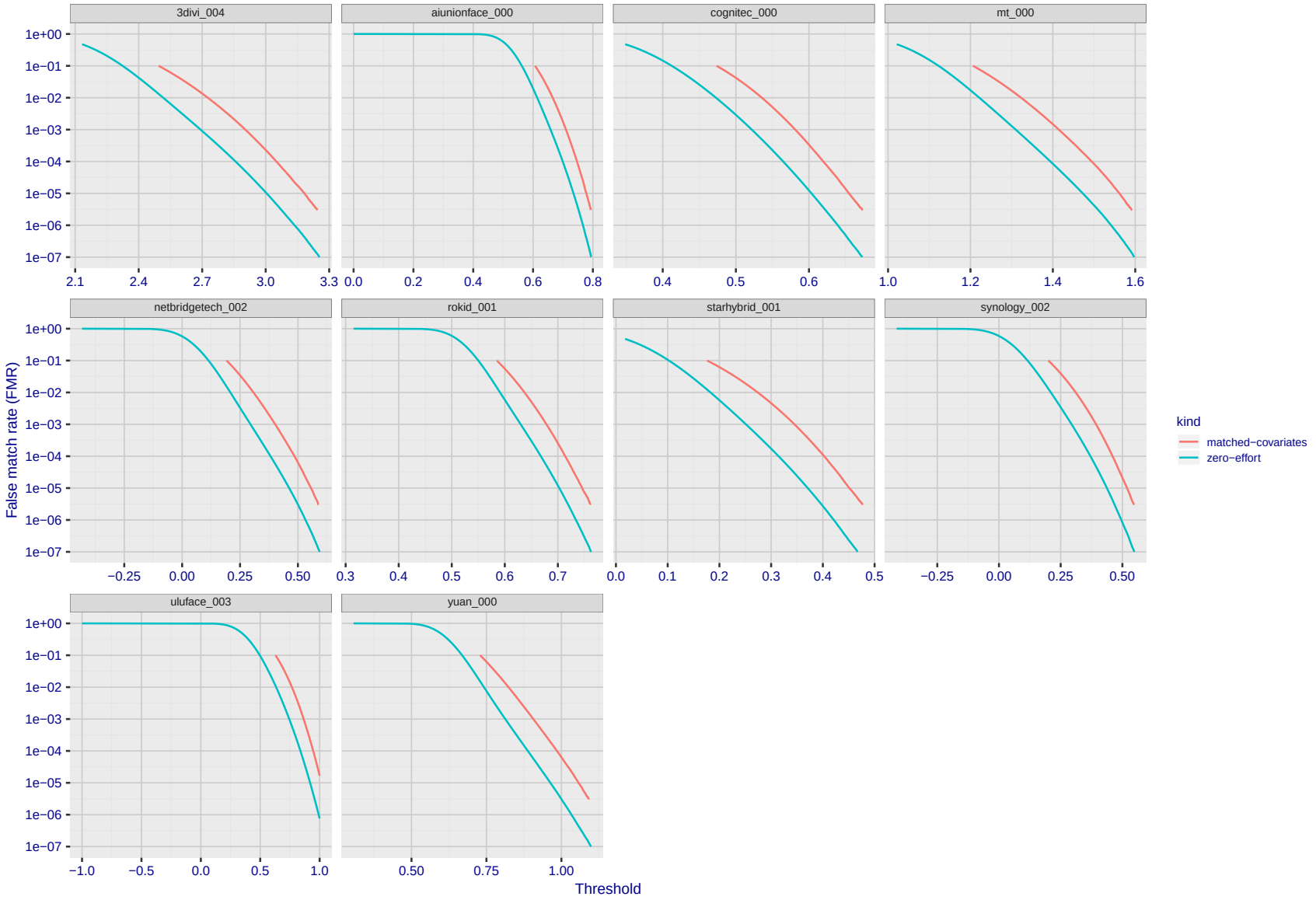

Figure 141: For the visa images, the false match calibration curves show FMR vs. threshold, T. The blue (lower) curves are for zero-effort impostors (i.e. comparing all images against all). The red (upper) curves are for persons of the same-sex, same-age, and same national-origin. This shows that FMR is underestimated (by a factor of 10 or more) by using a zero-effort impostor calculation to calibrate T. As shown later (sec. 3.6), FMR is higher for demographic-matched impostors.

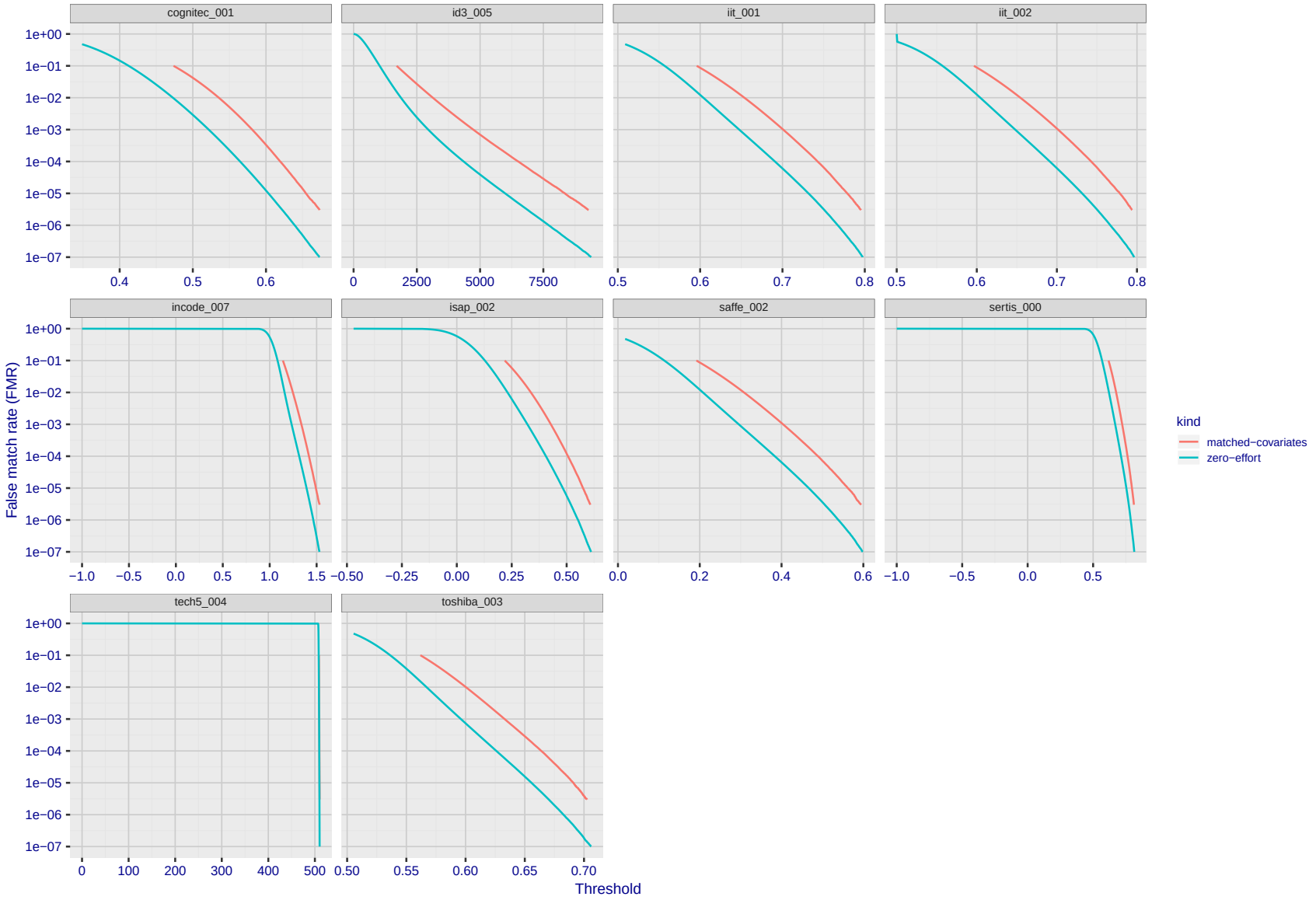

Figure 142: For the visa images, the false match calibration curves show FMR vs. threshold, T. The blue (lower) curves are for zero-effort impostors (i.e. comparing all images against all). The red (upper) curves are for persons of the same-sex, same-age, and same national-origin. This shows that FMR is underestimated (by a factor of 10 or more) by using a zero-effort impostor calculation to calibrate T. As shown later (sec. 3.6), FMR is higher for demographic-matched impostors.

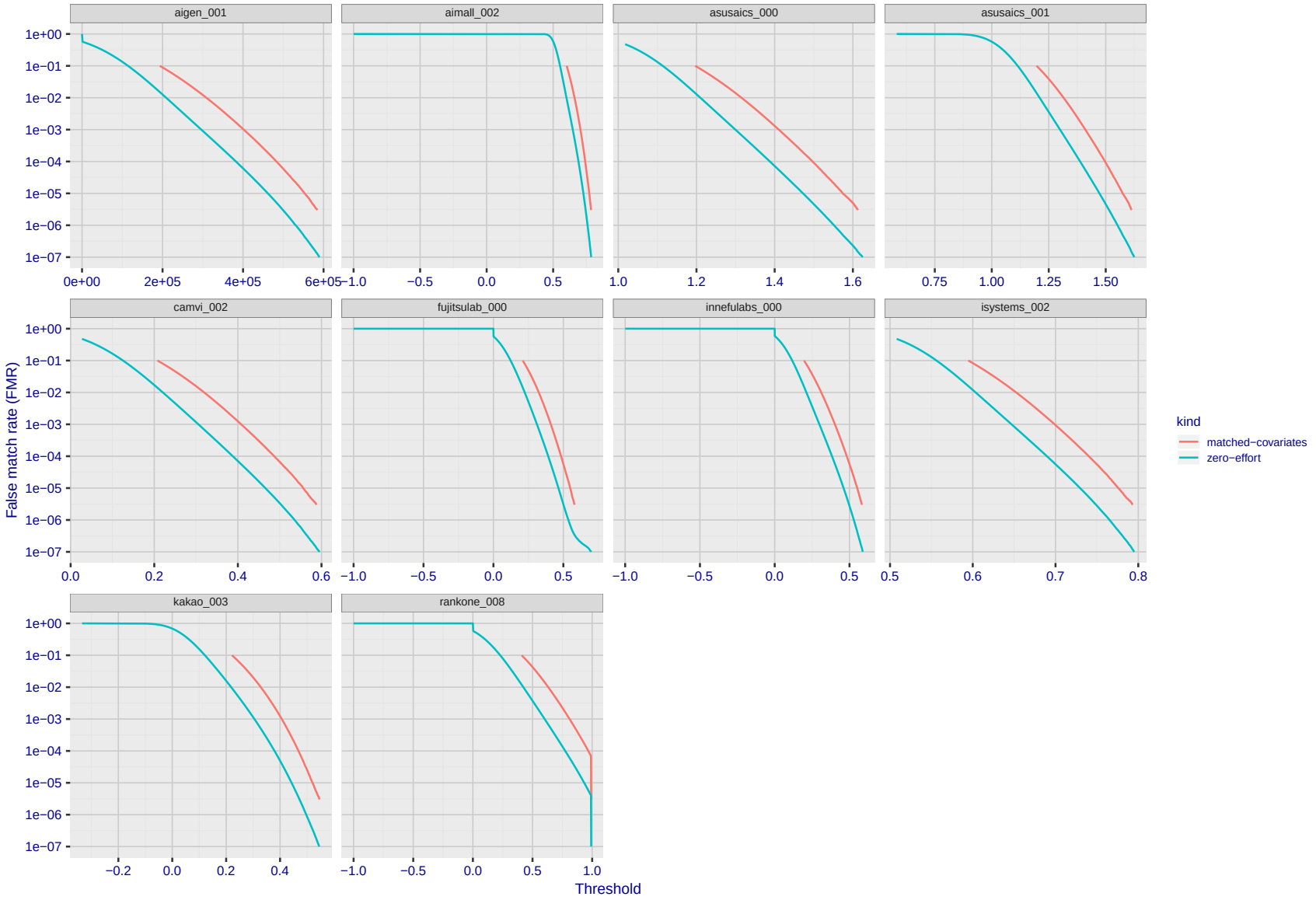

Figure 143: For the visa images, the false match calibration curves show FMR vs. threshold, T. The blue (lower) curves are for zero-effort impostors (i.e. comparing all images against all). The red (upper) curves are for persons of the same-sex, same-age, and same national-origin. This shows that FMR is underestimated (by a factor of 10 or more) by using a zero-effort impostor calculation to calibrate T. As shown later (sec. 3.6), FMR is higher for demographic-matched impostors.

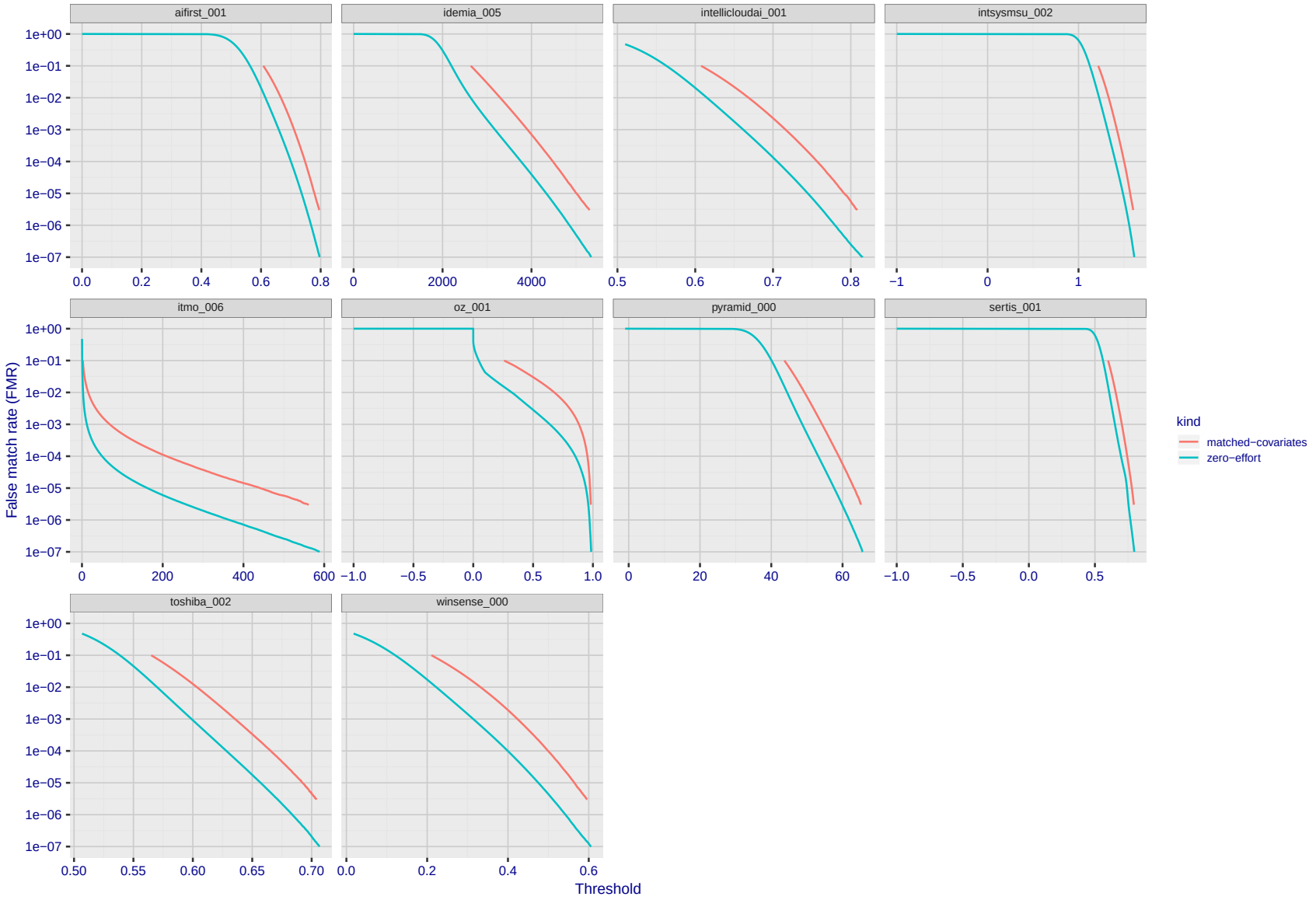

Figure 144: For the visa images, the false match calibration curves show FMR vs. threshold, T. The blue (lower) curves are for zero-effort impostors (i.e. comparing all images against all). The red (upper) curves are for persons of the same-sex, same-age, and same national-origin. This shows that FMR is underestimated (by a factor of 10 or more) by using a zero-effort impostor calculation to calibrate T. As shown later (sec. 3.6), FMR is higher for demographic-matched impostors.

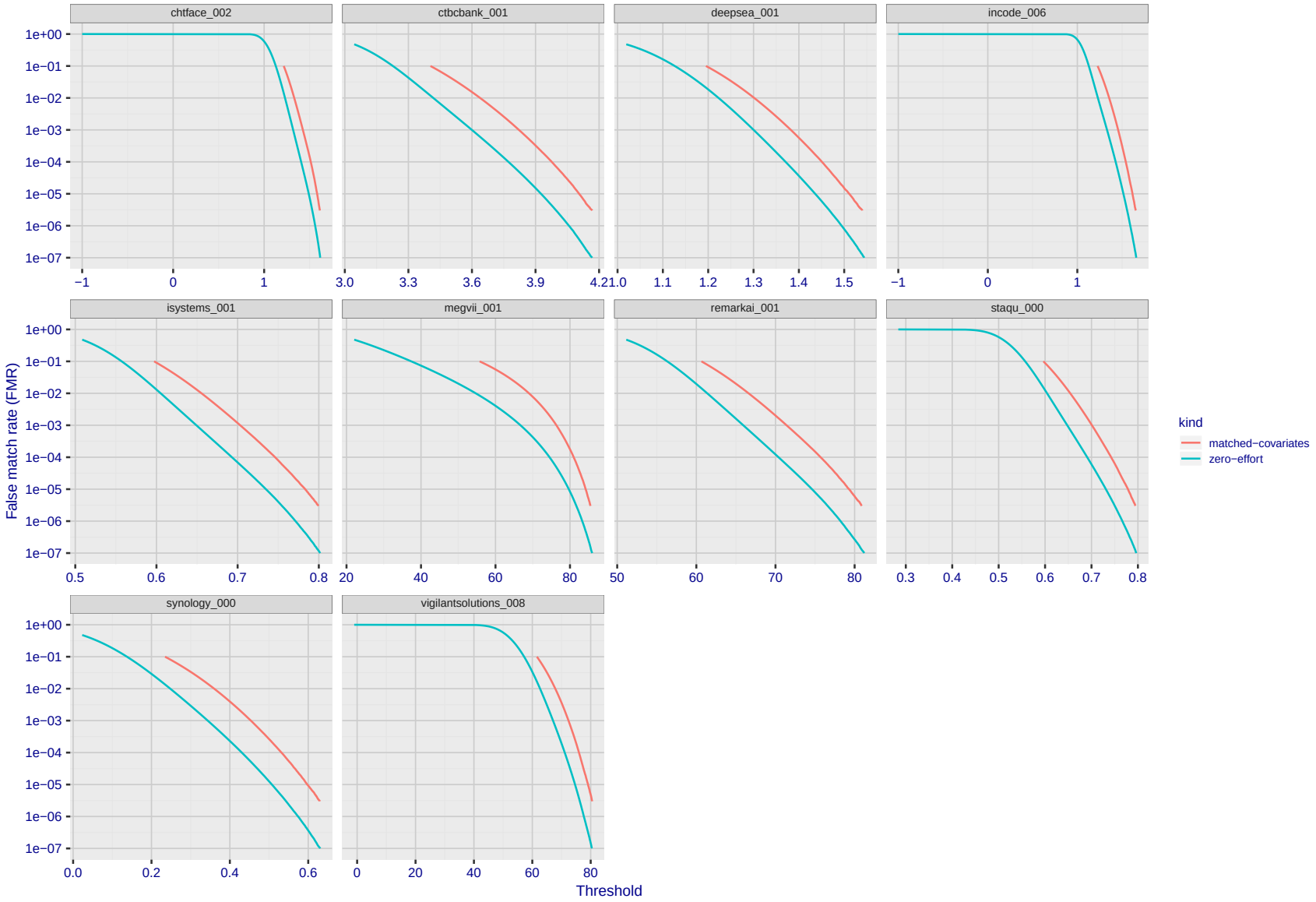

Figure 145: For the visa images, the false match calibration curves show FMR vs. threshold, T. The blue (lower) curves are for zero-effort impostors (i.e. comparing all images against all). The red (upper) curves are for persons of the same-sex, same-age, and same national-origin. This shows that FMR is underestimated (by a factor of 10 or more) by using a zero-effort impostor calculation to calibrate T. As shown later (sec. 3.6), FMR is higher for demographic-matched impostors.

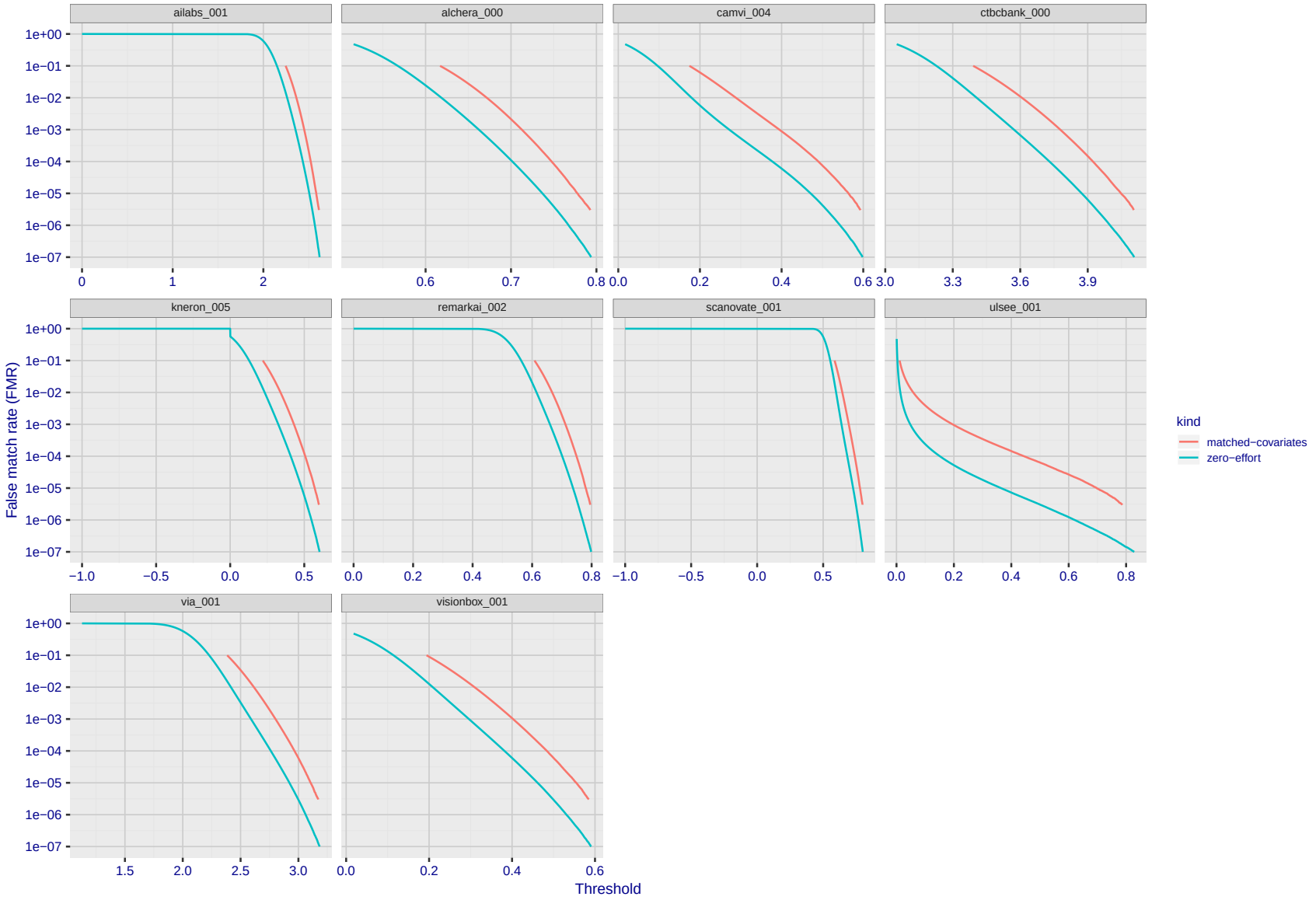

Figure 146: For the visa images, the false match calibration curves show FMR vs. threshold, T. The blue (lower) curves are for zero-effort impostors (i.e. comparing all images against all). The red (upper) curves are for persons of the same-sex, same-age, and same national-origin. This shows that FMR is underestimated (by a factor of 10 or more) by using a zero-effort impostor calculation to calibrate T. As shown later (sec. 3.6), FMR is higher for demographic-matched impostors.

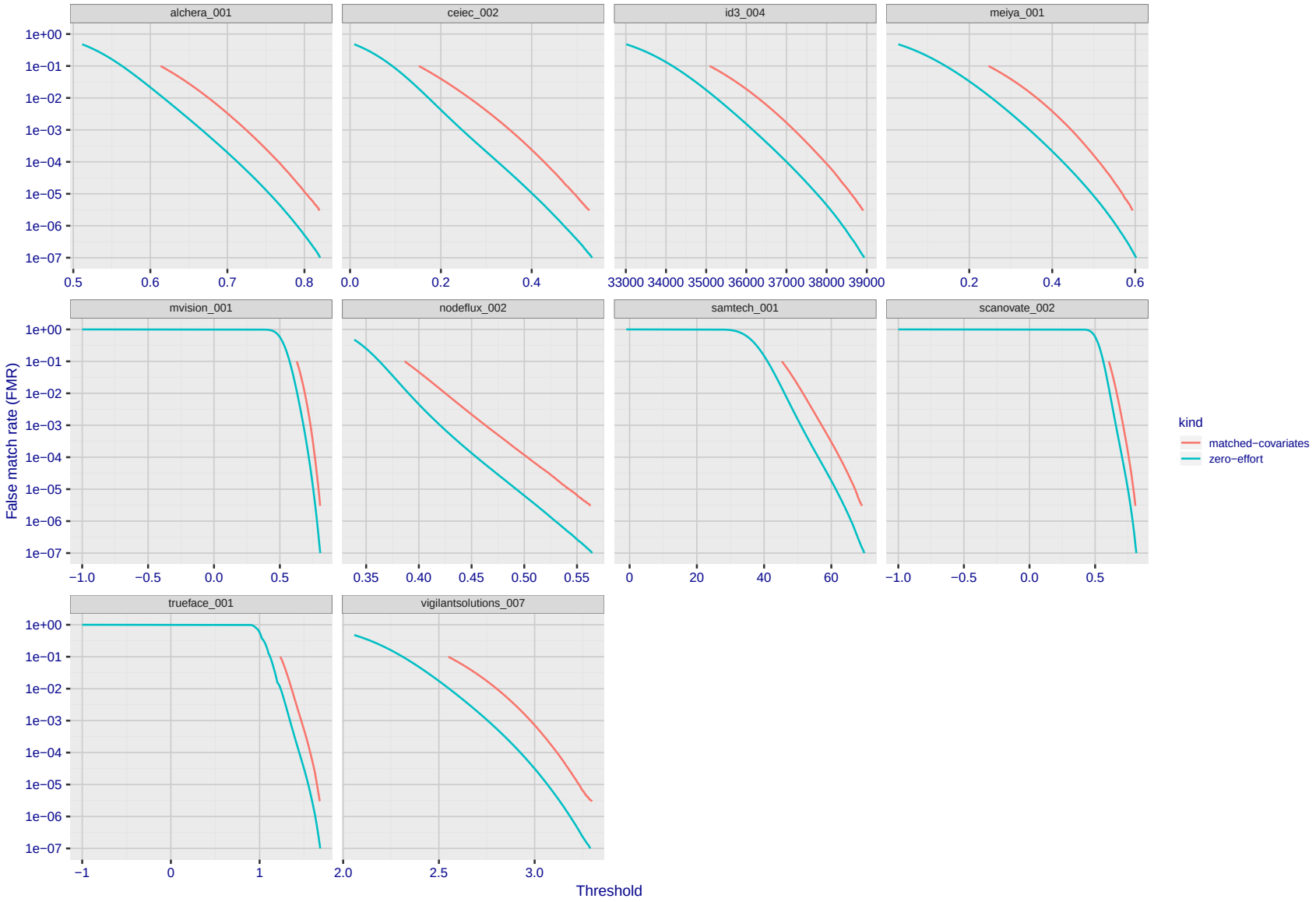

Figure 147: For the visa images, the false match calibration curves show FMR vs. threshold, T. The blue (lower) curves are for zero-effort impostors (i.e. comparing all images against all). The red (upper) curves are for persons of the same-sex, same-age, and same national-origin. This shows that FMR is underestimated (by a factor of 10 or more) by using a zero-effort impostor calculation to calibrate T. As shown later (sec. 3.6), FMR is higher for demographic-matched impostors.

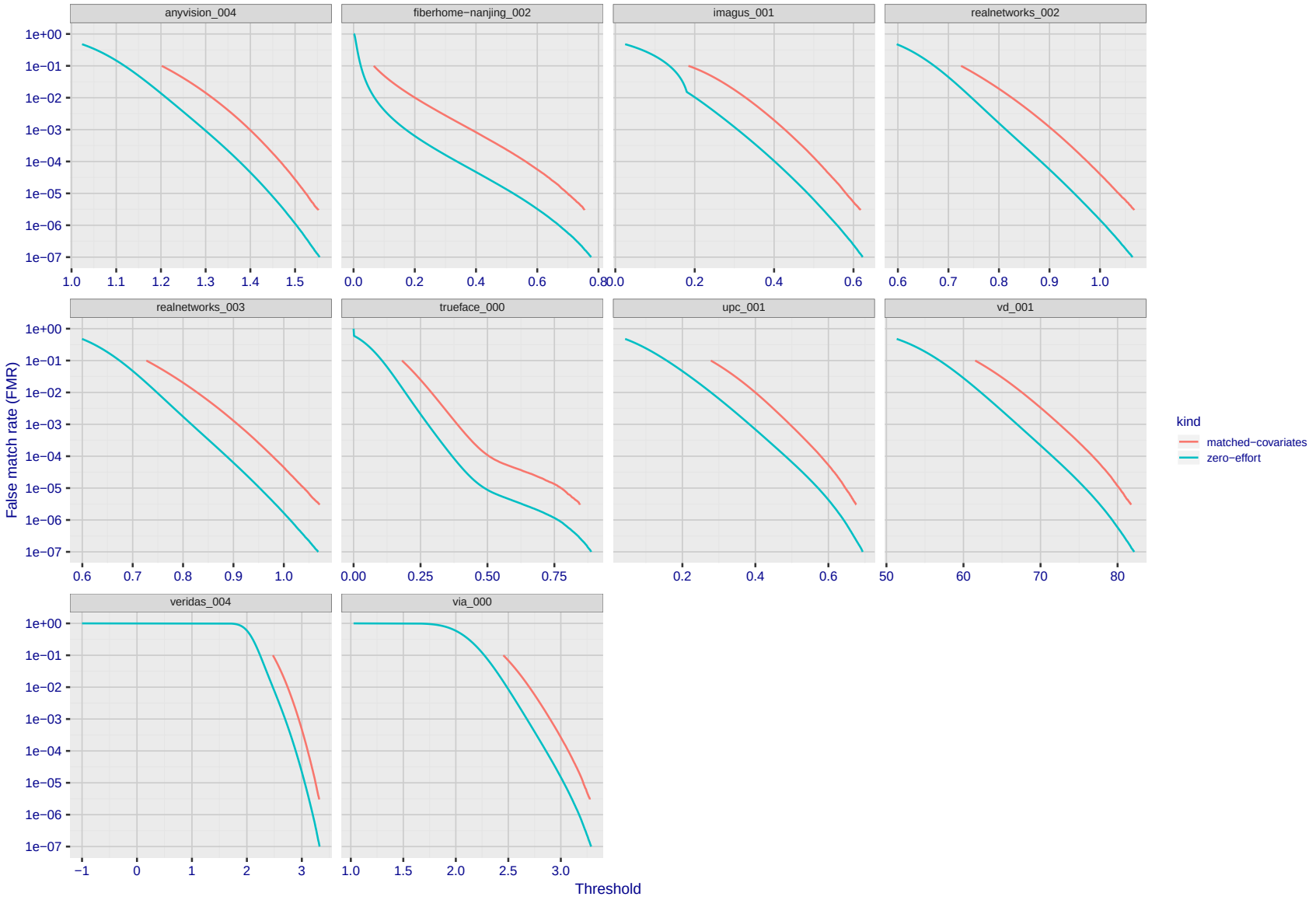

Figure 148: For the visa images, the false match calibration curves show FMR vs. threshold, T. The blue (lower) curves are for zero-effort impostors (i.e. comparing all images against all). The red (upper) curves are for persons of the same-sex, same-age, and same national-origin. This shows that FMR is underestimated (by a factor of 10 or more) by using a zero-effort impostor calculation to calibrate T. As shown later (sec. 3.6), FMR is higher for demographic-matched impostors.

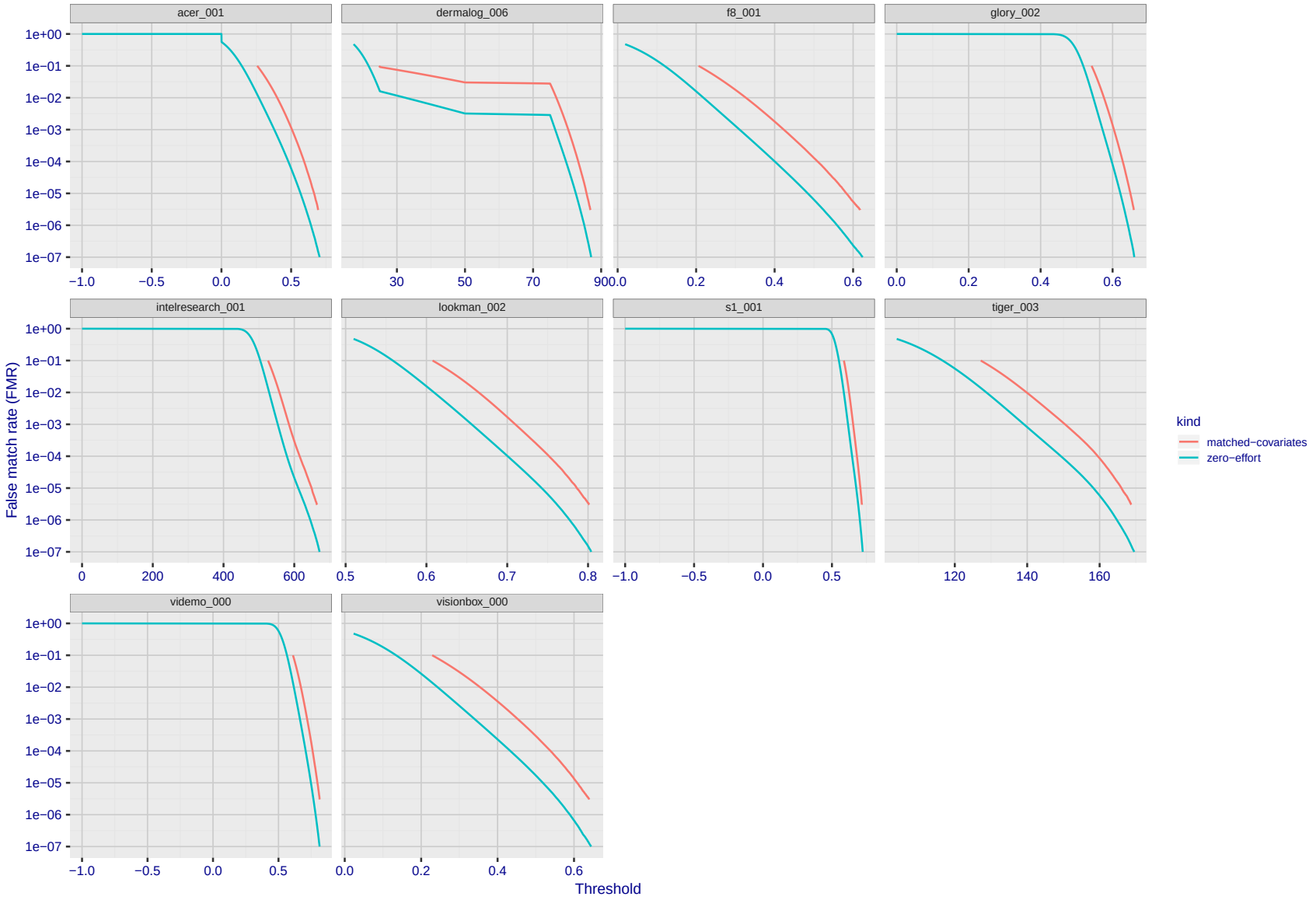

Figure 149: For the visa images, the false match calibration curves show FMR vs. threshold, T. The blue (lower) curves are for zero-effort impostors (i.e. comparing all images against all). The red (upper) curves are for persons of the same-sex, same-age, and same national-origin. This shows that FMR is underestimated (by a factor of 10 or more) by using a zero-effort impostor calculation to calibrate T. As shown later (sec. 3.6), FMR is higher for demographic-matched impostors.

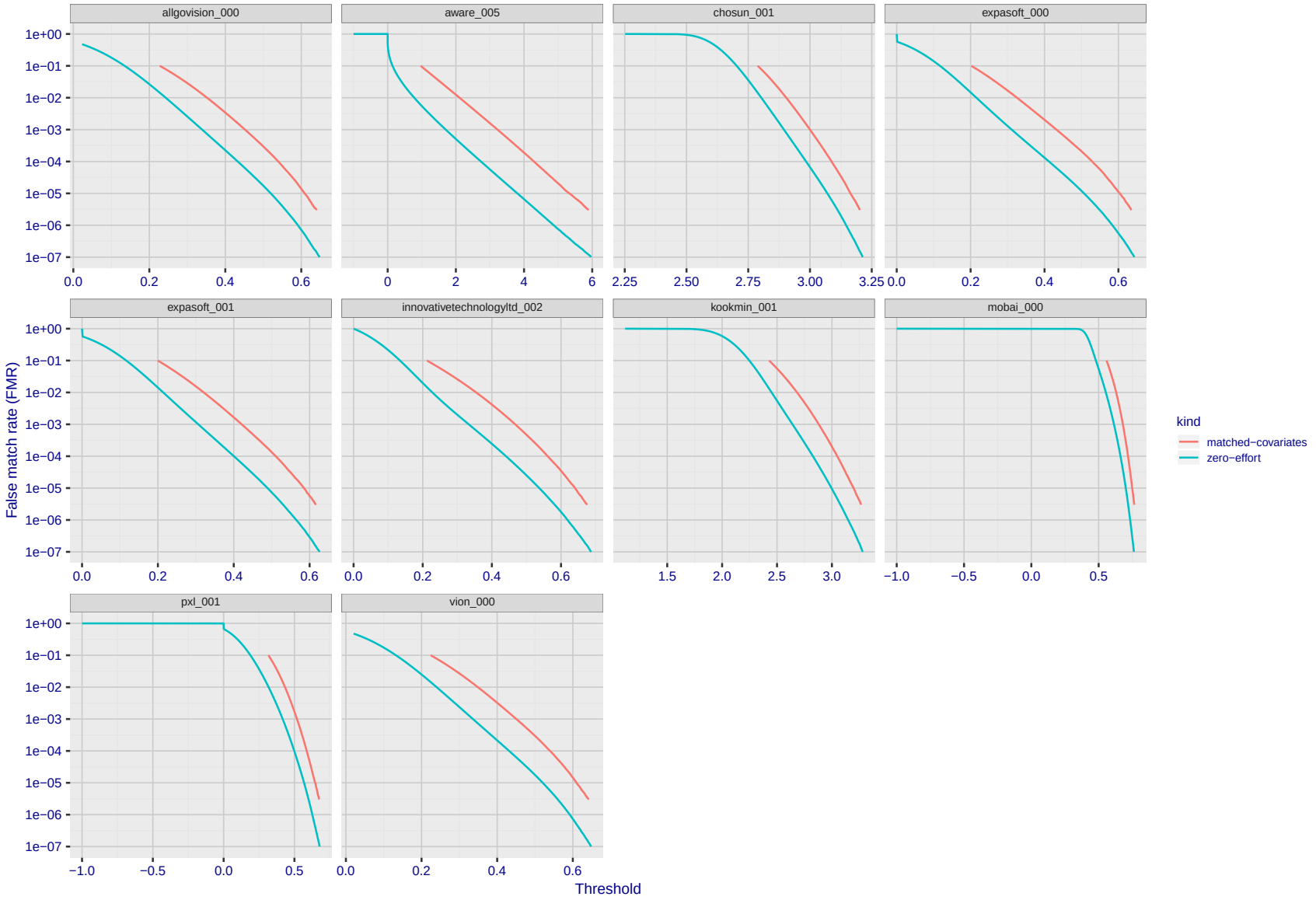

Figure 150: For the visa images, the false match calibration curves show FMR vs. threshold, T. The blue (lower) curves are for zero-effort impostors (i.e. comparing all images against all). The red (upper) curves are for persons of the same-sex, same-age, and same national-origin. This shows that FMR is underestimated (by a factor of 10 or more) by using a zero-effort impostor calculation to calibrate T. As shown later (sec. 3.6), FMR is higher for demographic-matched impostors.

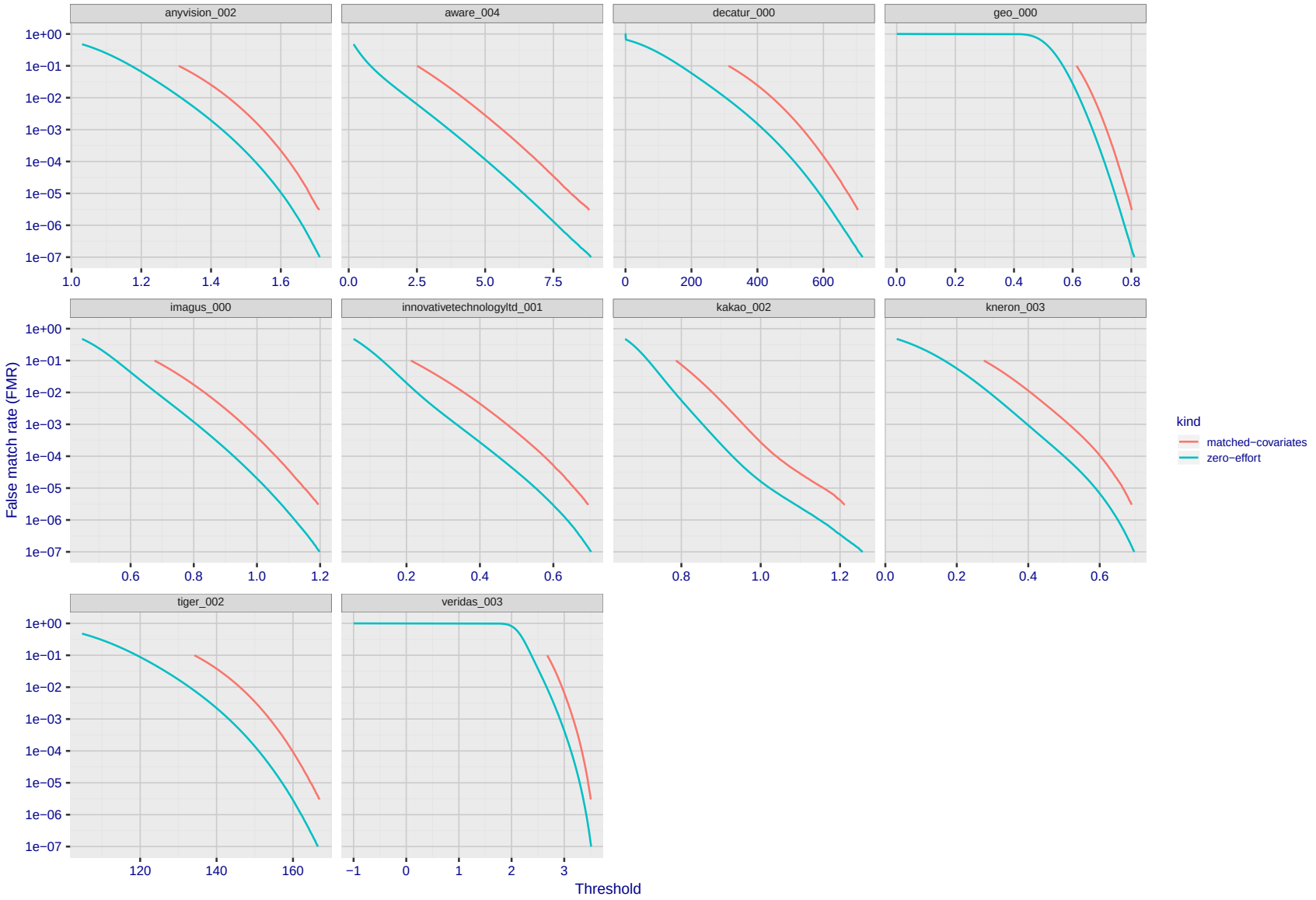

Figure 151: For the visa images, the false match calibration curves show FMR vs. threshold, T. The blue (lower) curves are for zero-effort impostors (i.e. comparing all images against all). The red (upper) curves are for persons of the same-sex, same-age, and same national-origin. This shows that FMR is underestimated (by a factor of 10 or more) by using a zero-effort impostor calculation to calibrate T. As shown later (sec. 3.6), FMR is higher for demographic-matched impostors.

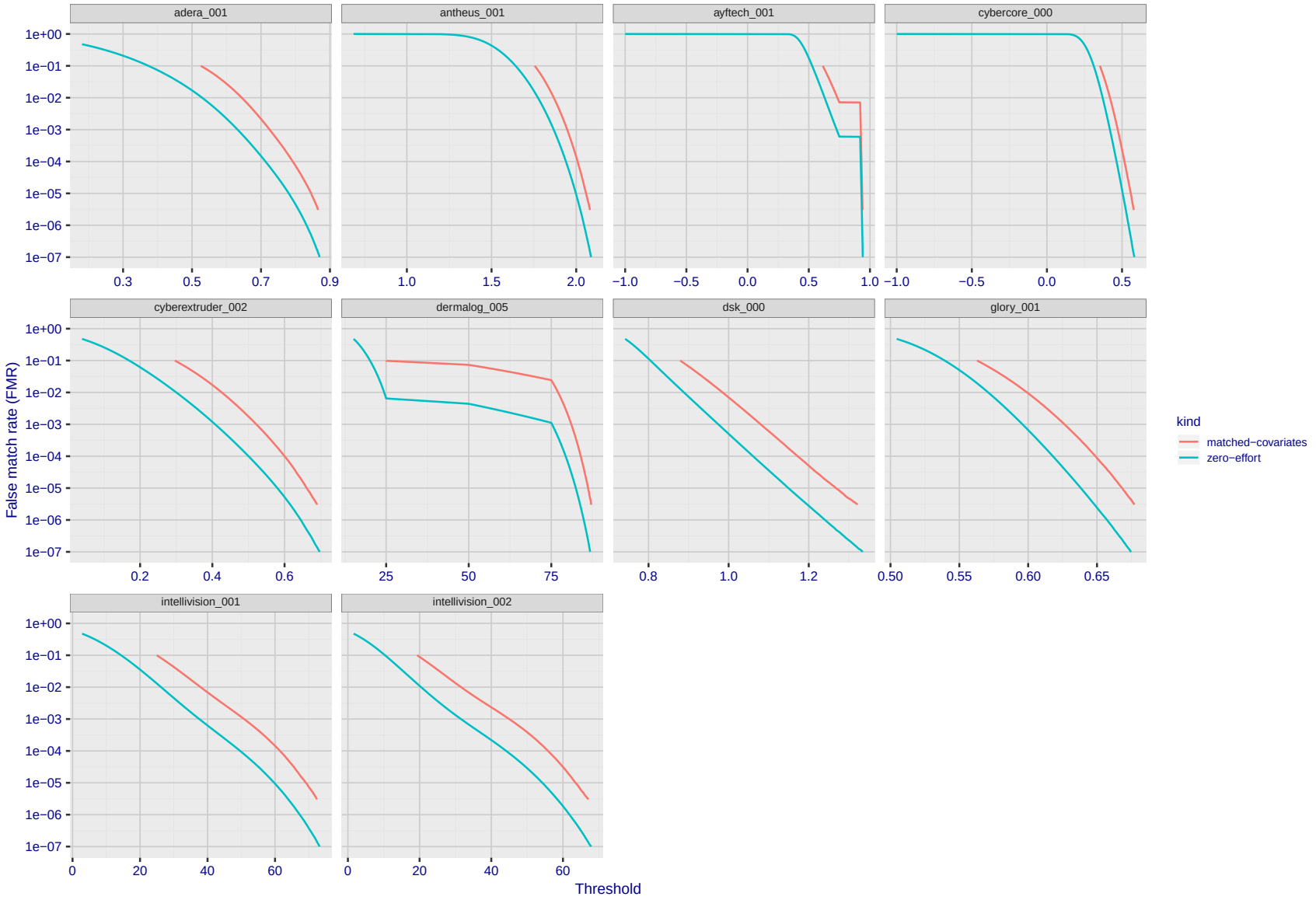

Figure 152: For the visa images, the false match calibration curves show FMR vs. threshold, T. The blue (lower) curves are for zero-effort impostors (i.e. comparing all images against all). The red (upper) curves are for persons of the same-sex, same-age, and same national-origin. This shows that FMR is underestimated (by a factor of 10 or more) by using a zero-effort impostor calculation to calibrate T. As shown later (sec. 3.6), FMR is higher for demographic-matched impostors.

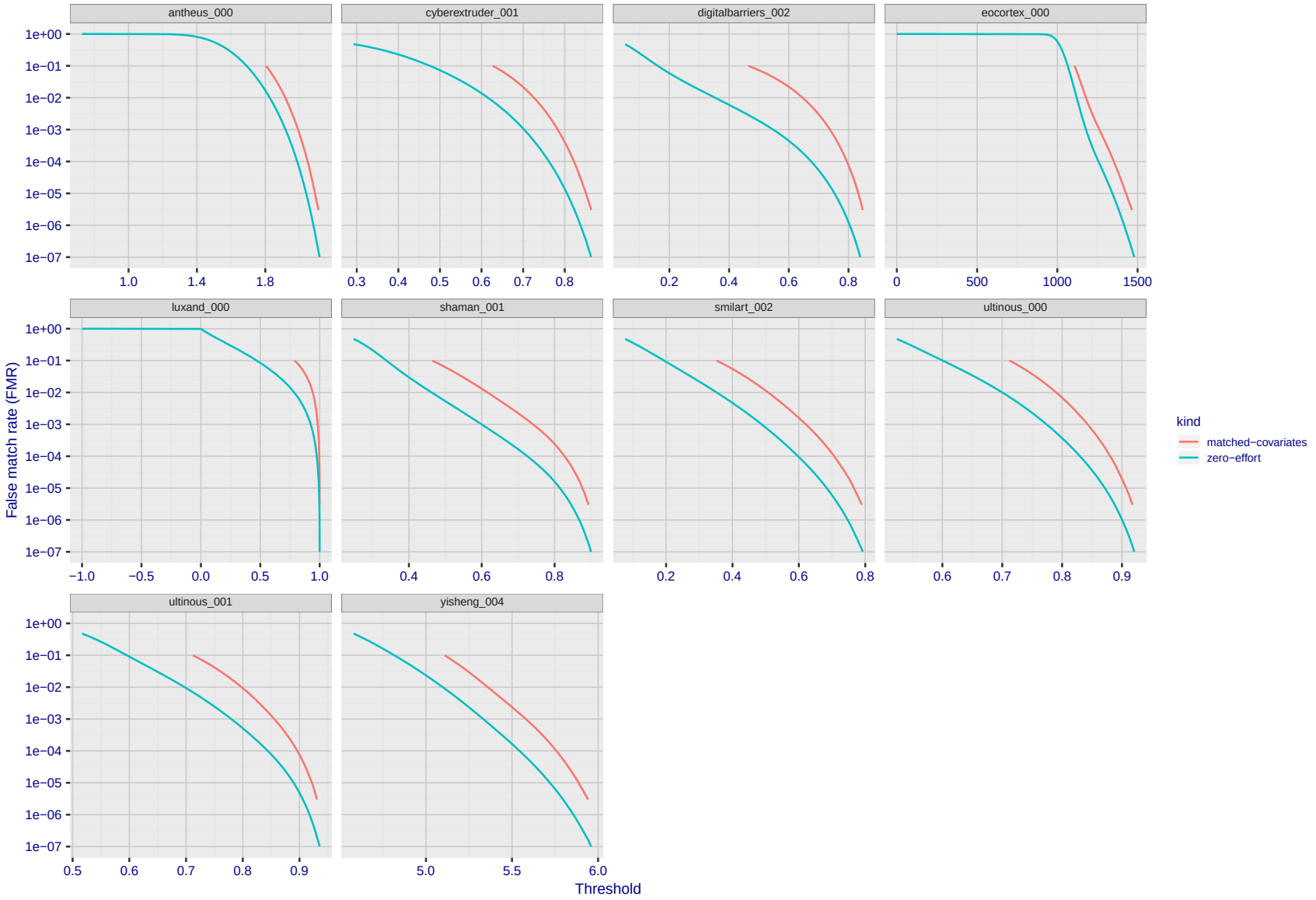

Figure 153: For the visa images, the false match calibration curves show FMR vs. threshold, T. The blue (lower) curves are for zero-effort impostors (i.e. comparing all images against all). The red (upper) curves are for persons of the same-sex, same-age, and same national-origin. This shows that FMR is underestimated (by a factor of 10 or more) by using a zero-effort impostor calculation to calibrate T. As shown later (sec. 3.6), FMR is higher for demographic-matched impostors.

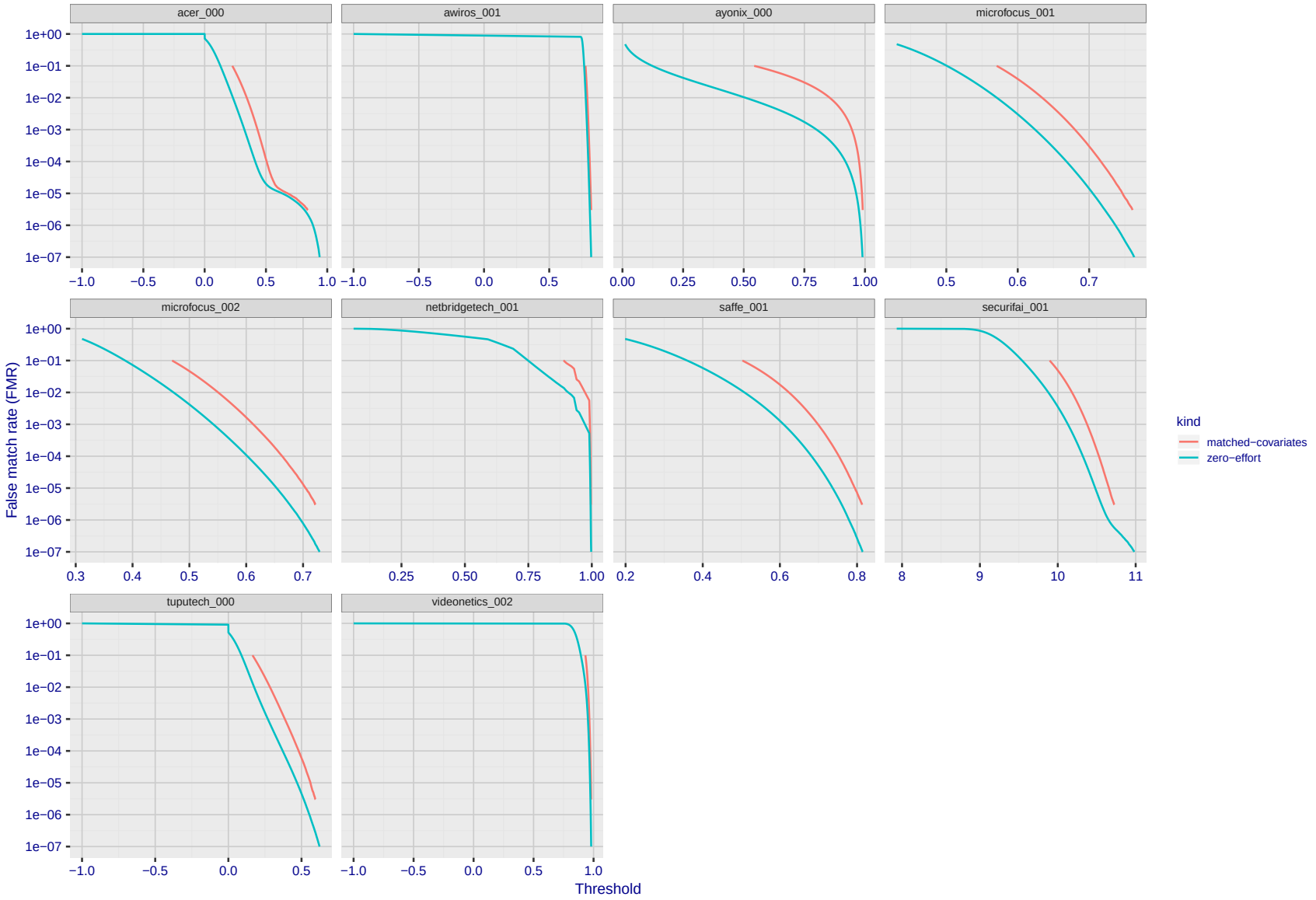

Figure 154: For the visa images, the false match calibration curves show FMR vs. threshold, T. The blue (lower) curves are for zero-effort impostors (i.e. comparing all images against all). The red (upper) curves are for persons of the same-sex, same-age, and same national-origin. This shows that FMR is underestimated (by a factor of 10 or more) by using a zero-effort impostor calculation to calibrate T. As shown later (sec. 3.6), FMR is higher for demographic-matched impostors.

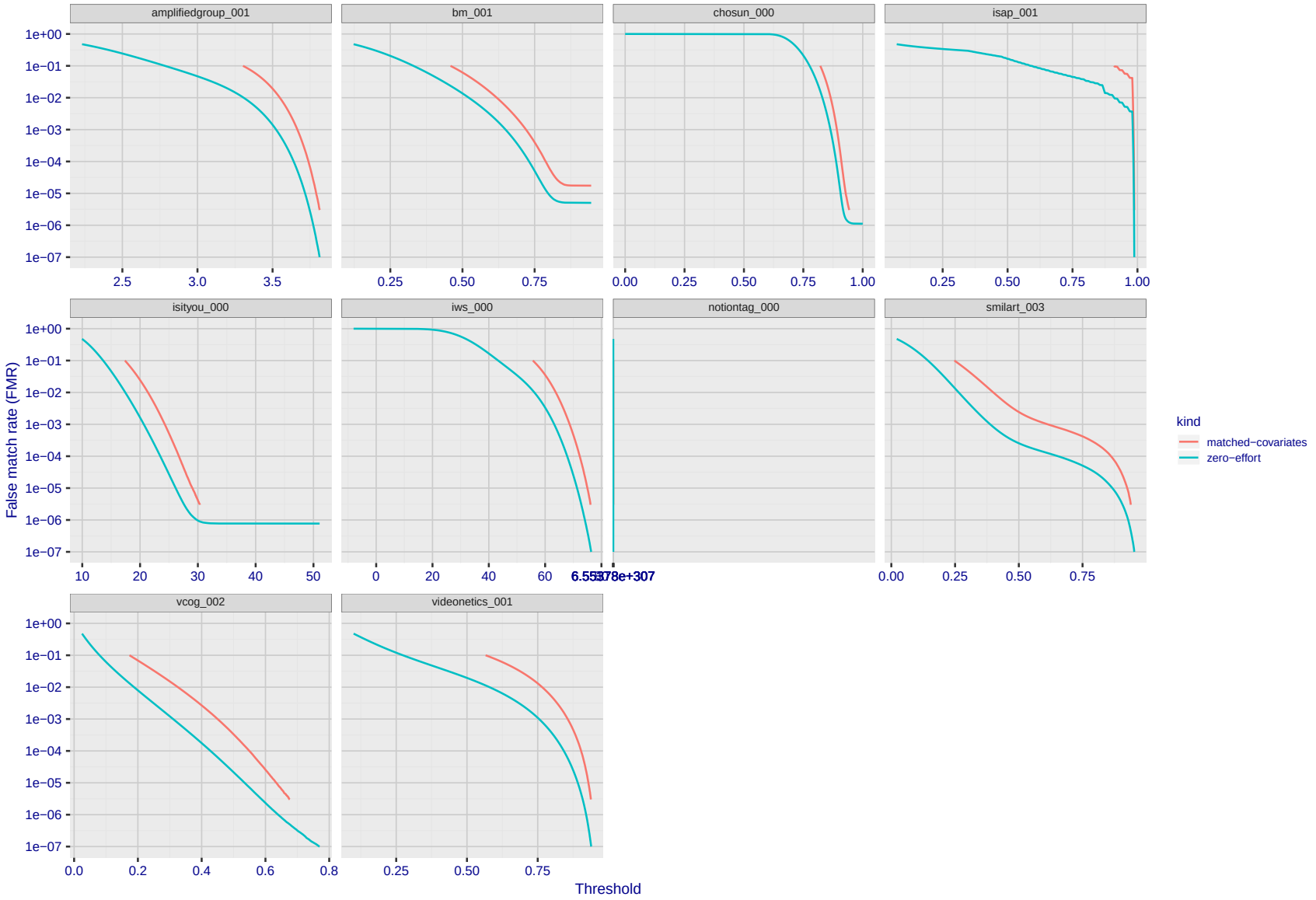

Figure 155: For the visa images, the false match calibration curves show FMR vs. threshold, T. The blue (lower) curves are for zero-effort impostors (i.e. comparing all images against all). The red (upper) curves are for persons of the same-sex, same-age, and same national-origin. This shows that FMR is underestimated (by a factor of 10 or more) by using a zero-effort impostor calculation to calibrate T. As shown later (sec. 3.6), FMR is higher for demographic-matched impostors.

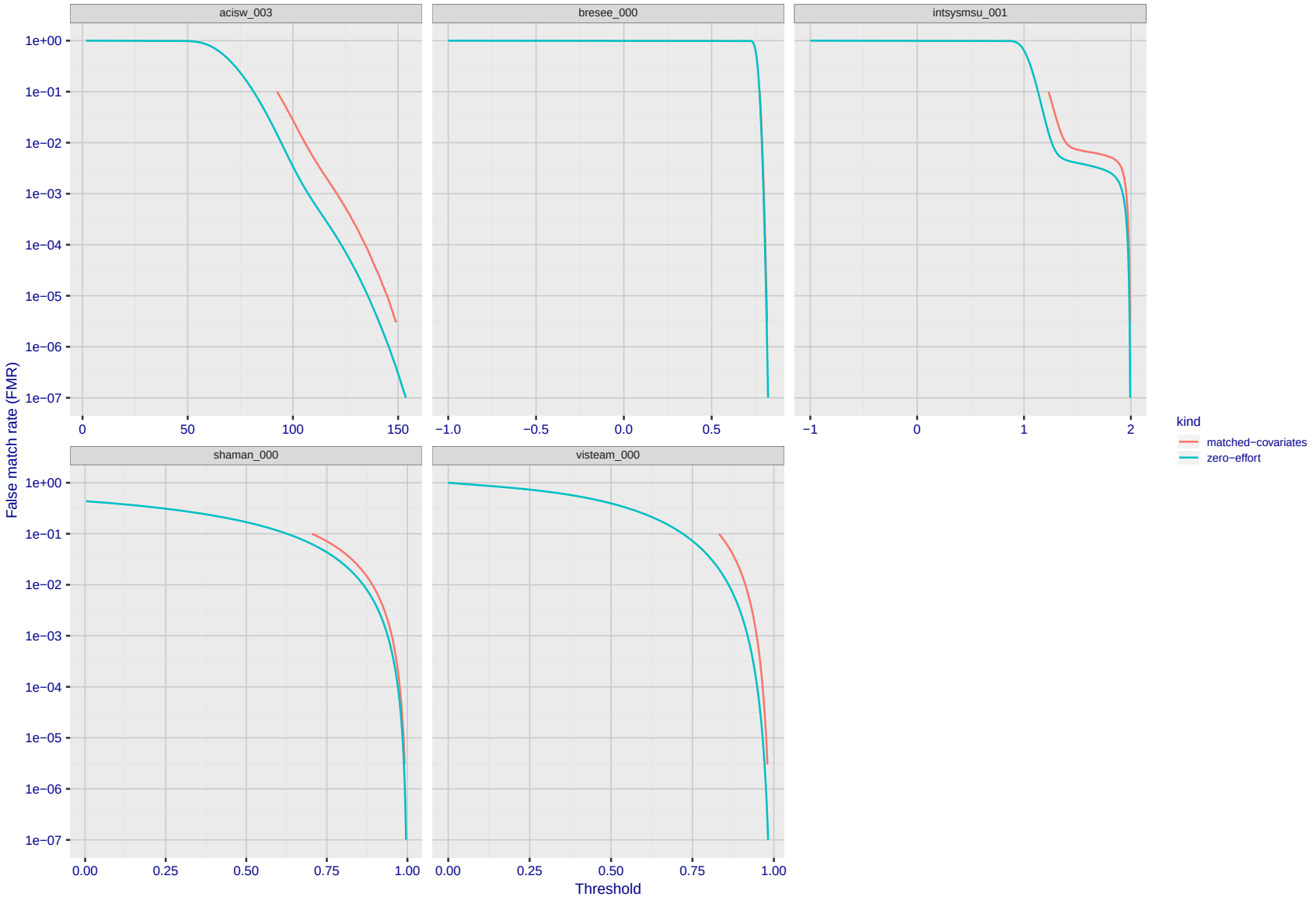

Figure 156: For the visa images, the false match calibration curves show FMR vs. threshold, T. The blue (lower) curves are for zero-effort impostors (i.e. comparing all images against all). The red (upper) curves are for persons of the same-sex, same-age, and same national-origin. This shows that FMR is underestimated (by a factor of 10 or more) by using a zero-effort impostor calculation to calibrate T. As shown later (sec. 3.6), FMR is higher for demographic-matched impostors.

3.5 Genuine distribution stability

3.5.1 Effect of birth place on the genuine distribution

Background: Both skin tone and bone structure vary geographically. Prior studies have reported variations in FNMR and FMR.

Goal: To measure false non-match rate (FNMR) variation with country of birth.

Methods: Thresholds are determined that give FMR = $\{0.001, 0.0001\}$ over the entire impostor set. Then FNMR is measured over 1000 bootstrap replications of the genuine scores. Only those countries with at least 140 individuals are included in the analysis.

Results: Figure 177 shows FNMR by country of birth for the two thresholds.

FNMR(T) "False non-match rate"
FMR(T) "False match rate"

Figure 157: For the visa images, the dots show FNMR by country of birth for two globally set operating thresholds corresponding to FMR = $\{0.001, 0.0001\}$ computed over all on the order of 10^{10} impostor scores. The FMR in each bin will vary also - see subsequent impostor heatmaps in sec. 3.6.1. The figures shows an order of magnitude variation in FNMR across country of birth; these effects are likely due quality variations, then demographics like age and race. The error rates in some cases are zero, and in others the DET is flat so the error rates at the two thresholds are identical. The lines span 1% and 99% of boostrap replicated FNMR estimates.

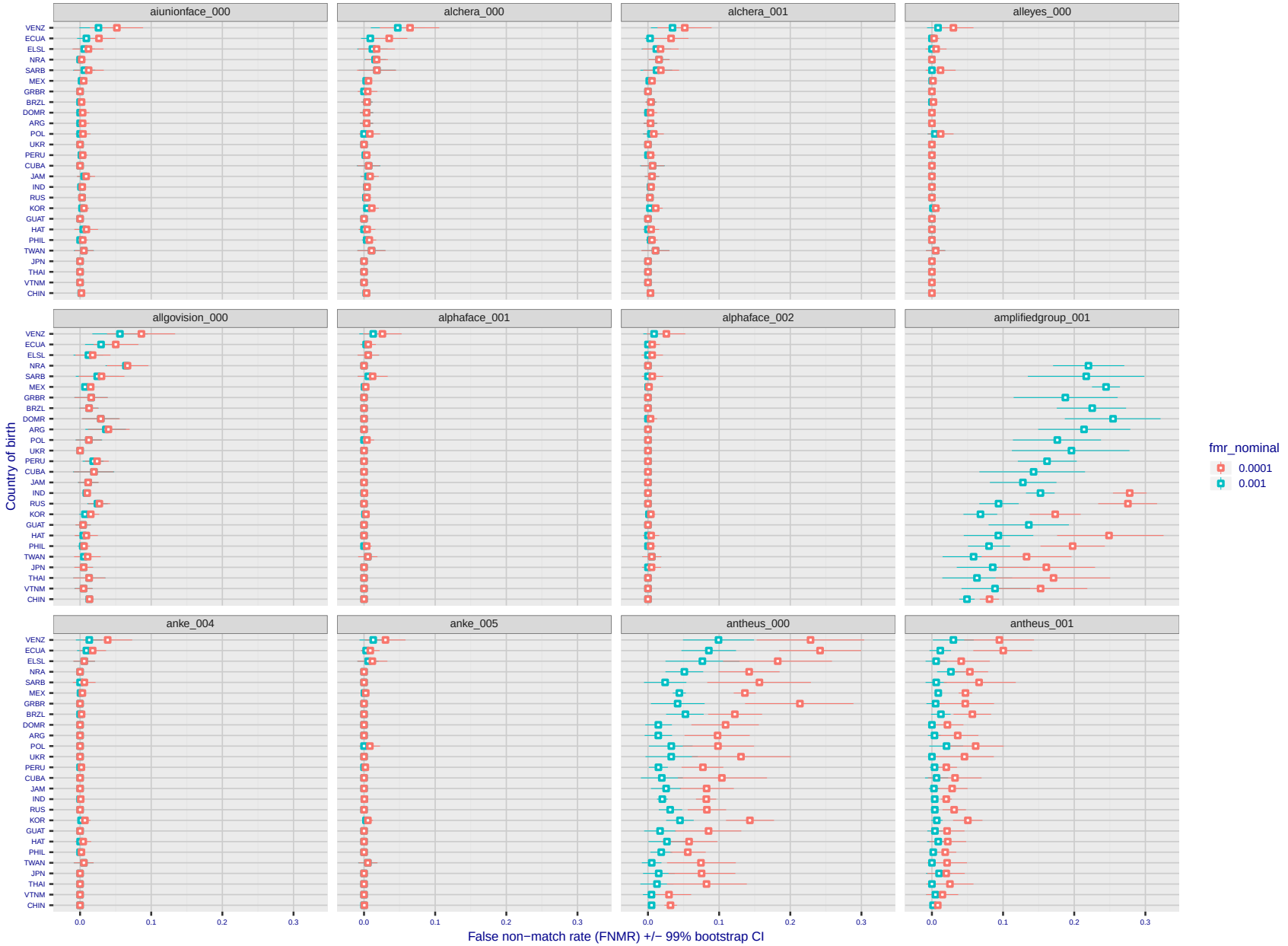

Figure 158: For the visa images, the dots show FNMR by country of birth for two globally set operating thresholds corresponding to FMR = $\{0.001, 0.0001\}$ computed over all on the order of 10^{10} impostor scores. The FMR in each bin will vary also - see subsequent impostor heatmaps in sec. 3.6.1. The figures shows an order of magnitude variation in FNMR across country of birth; these effects are likely due quality variations, then demographics like age and race. The error rates in some cases are zero, and in others the DET is flat so the error rates at the two thresholds are identical. The lines span 1% and 99% of boostrap replicated FNMR estimates.

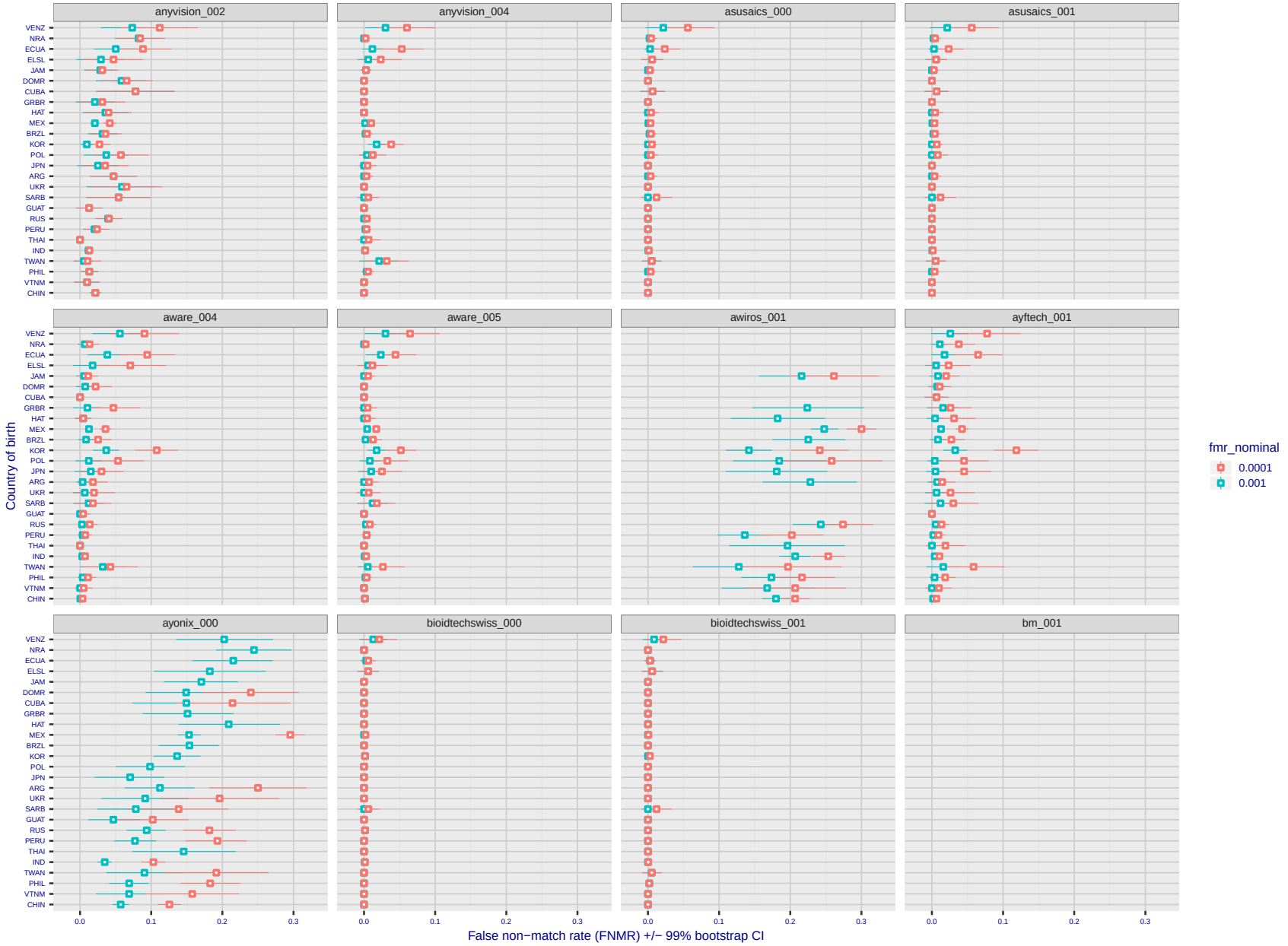

Figure 159: For the visa images, the dots show FNMR by country of birth for two globally set operating thresholds corresponding to FMR = $\{0.001, 0.0001\}$ computed over all on the order of 10^{10} impostor scores. The FMR in each bin will vary also - see subsequent impostor heatmaps in sec. 3.6.1. The figures shows an order of magnitude variation in FNMR across country of birth; these effects are likely due quality variations, then demographics like age and race. The error rates in some cases are zero, and in others the DET is flat so the error rates at the two thresholds are identical. The lines span 1% and 99% of boostrap replicated FNMR estimates.

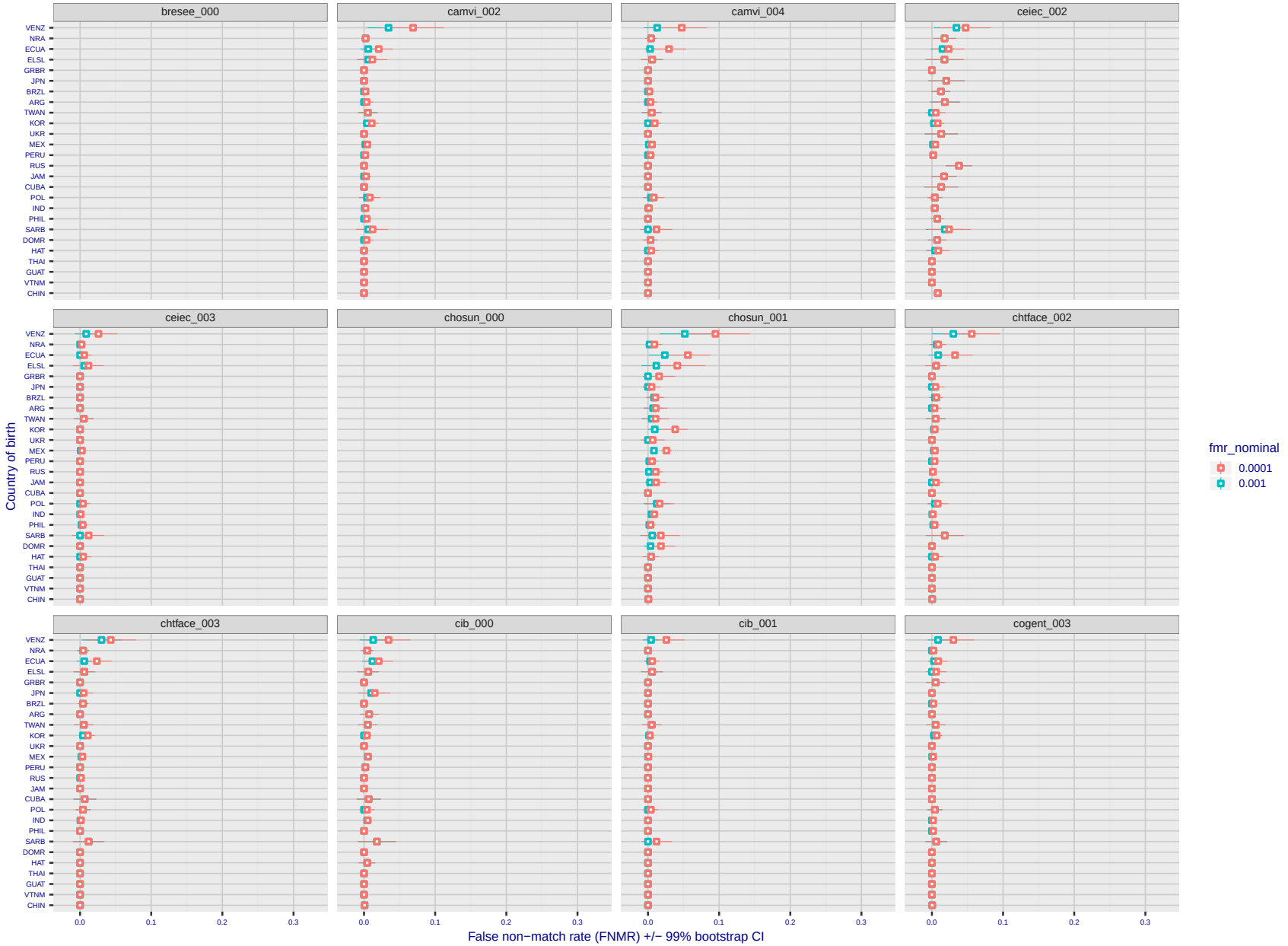

Figure 160: For the visa images, the dots show FNMR by country of birth for two globally set operating thresholds corresponding to FMR = $\{0.001, 0.0001\}$ computed over all on the order of 10^{10} impostor scores. The FMR in each bin will vary also - see subsequent impostor heatmaps in sec. 3.6.1. The figures shows an order of magnitude variation in FNMR across country of birth; these effects are likely due quality variations, then demographics like age and race. The error rates in some cases are zero, and in others the DET is flat so the error rates at the two thresholds are identical. The lines span 1% and 99% of boostrap replicated FNMR estimates.

FNMR(T) "False non-match rate"
FMR(T) "False match rate"

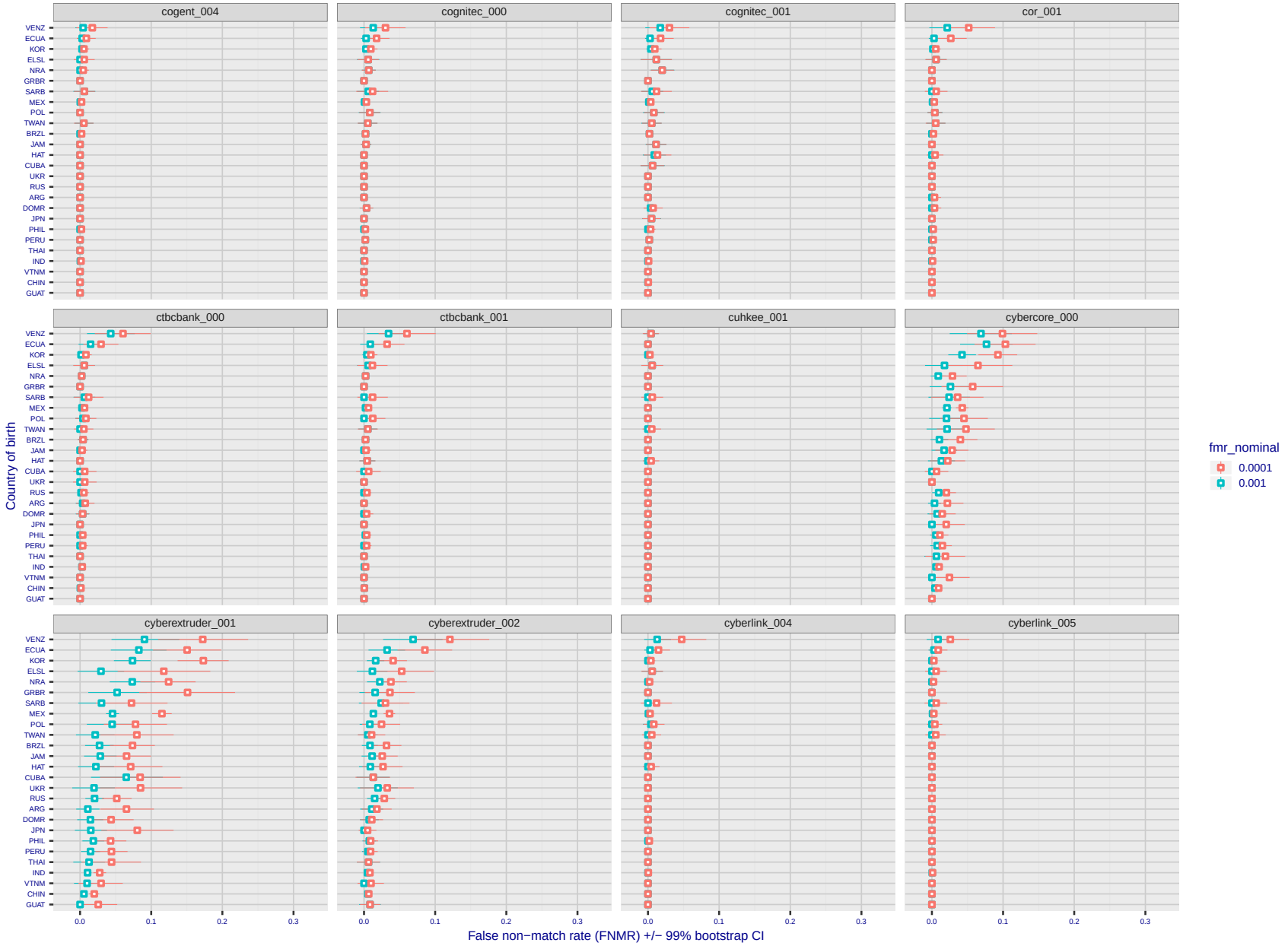

Figure 161: For the visa images, the dots show FNMR by country of birth for two globally set operating thresholds corresponding to FMR = $\{0.001, 0.0001\}$ computed over all on the order of 10^{10} impostor scores. The FMR in each bin will vary also - see subsequent impostor heatmaps in sec. 3.6.1. The figures shows an order of magnitude variation in FNMR across country of birth; these effects are likely due quality variations, then demographics like age and race. The error rates in some cases are zero, and in others the DET is flat so the error rates at the two thresholds are identical. The lines span 1% and 99% of boostrap replicated FNMR estimates.

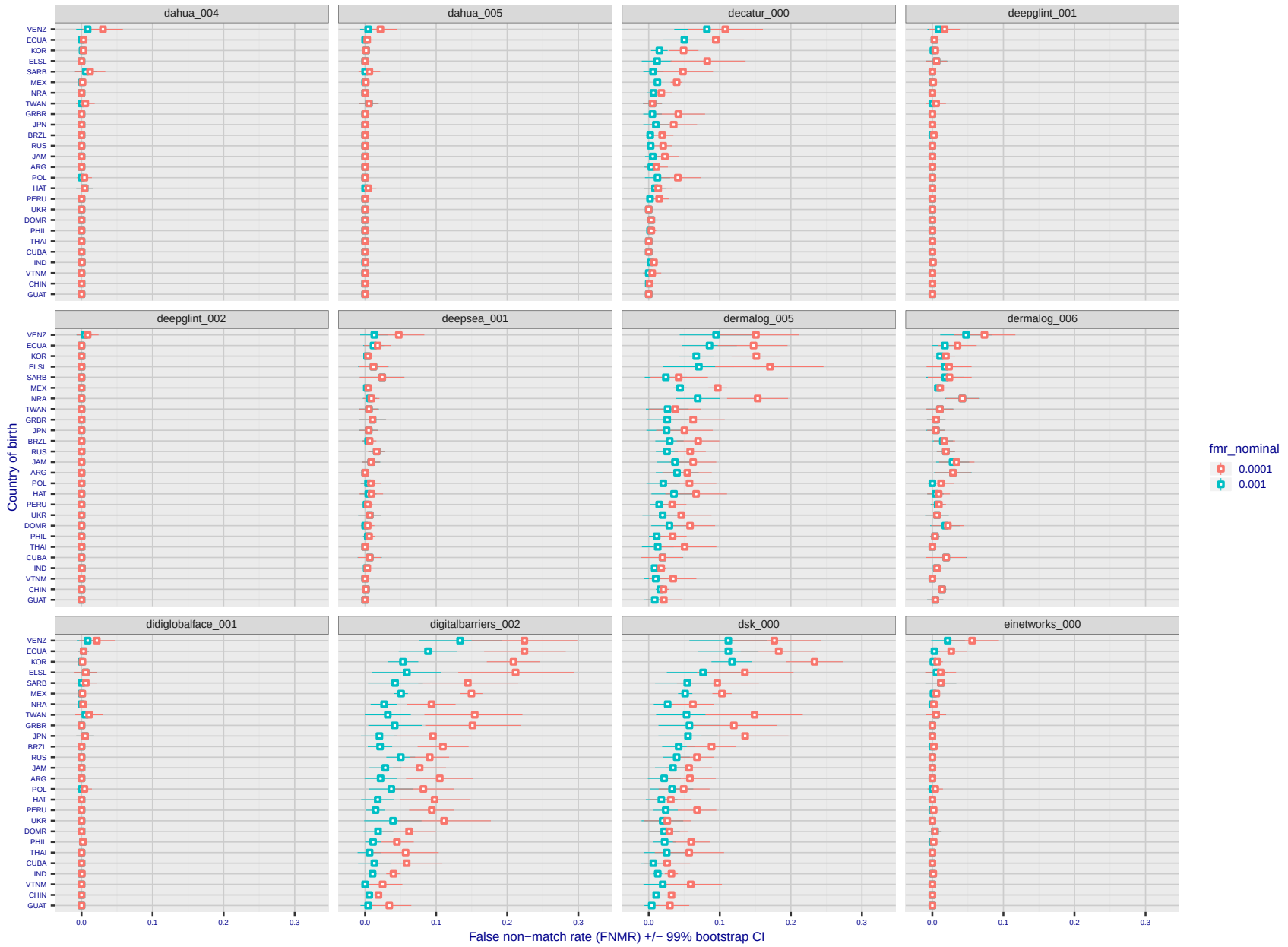

Figure 162: For the visa images, the dots show FNMR by country of birth for two globally set operating thresholds corresponding to FMR = $\{0.001, 0.0001\}$ computed over all on the order of 10^{10} impostor scores. The FMR in each bin will vary also - see subsequent impostor heatmaps in sec. 3.6.1. The figures shows an order of magnitude variation in FNMR across country of birth; these effects are likely due quality variations, then demographics like age and race. The error rates in some cases are zero, and in others the DET is flat so the error rates at the two thresholds are identical. The lines span 1% and 99% of boostrap replicated FNMR estimates.

Figure 163: For the visa images, the dots show FNMR by country of birth for two globally set operating thresholds corresponding to FMR = $\{0.001, 0.0001\}$ computed over all on the order of 10^{10} impostor scores. The FMR in each bin will vary also - see subsequent impostor heatmaps in sec. 3.6.1. The figures shows an order of magnitude variation in FNMR across country of birth; these effects are likely due quality variations, then demographics like age and race. The error rates in some cases are zero, and in others the DET is flat so the error rates at the two thresholds are identical. The lines span 1% and 99% of boostrap replicated FNMR estimates.

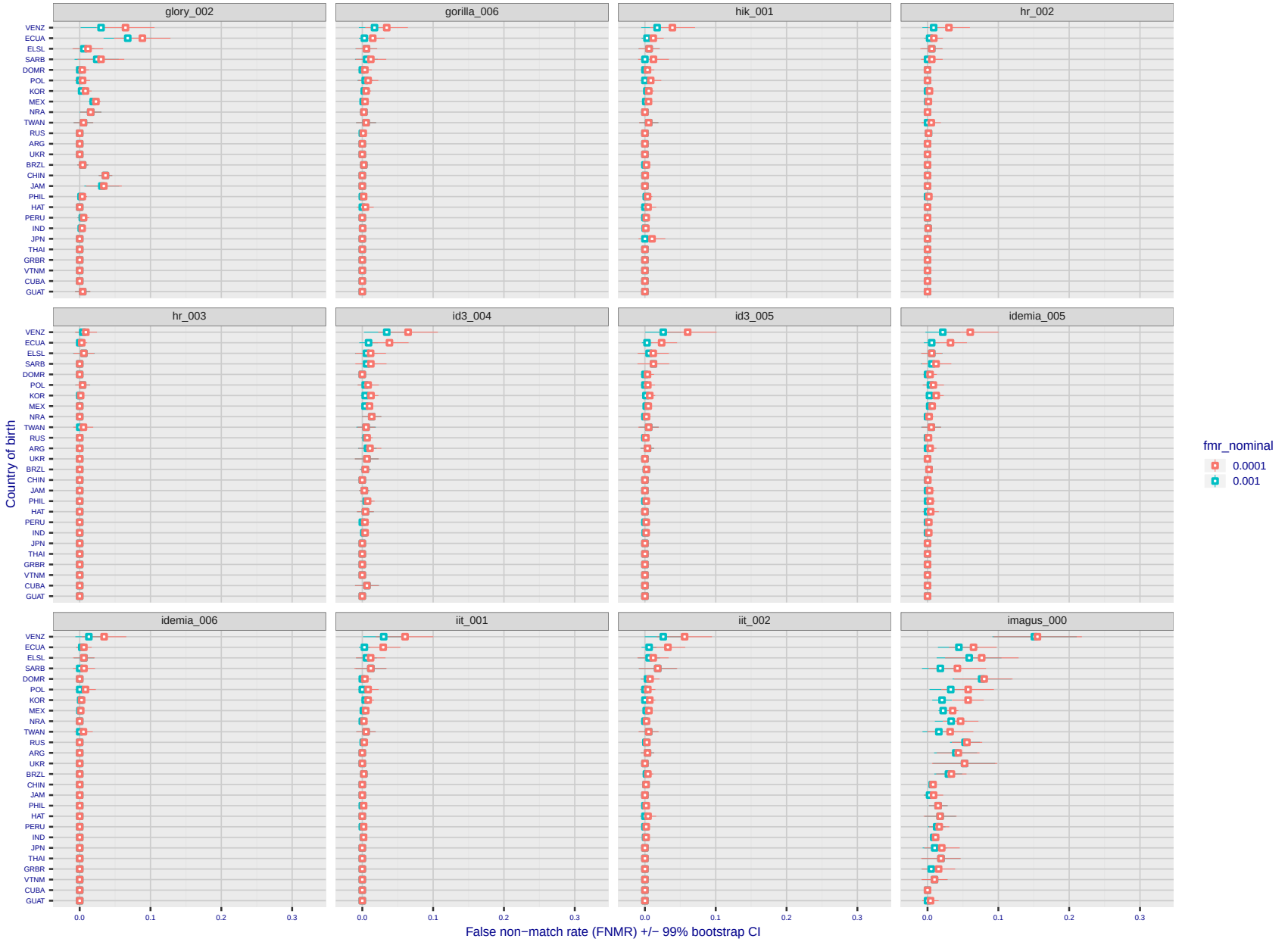

Figure 164: For the visa images, the dots show FNMR by country of birth for two globally set operating thresholds corresponding to FMR = $\{0.001, 0.0001\}$ computed over all on the order of 10^{10} impostor scores. The FMR in each bin will vary also - see subsequent impostor heatmaps in sec. 3.6.1. The figures shows an order of magnitude variation in FNMR across country of birth; these effects are likely due quality variations, then demographics like age and race. The error rates in some cases are zero, and in others the DET is flat so the error rates at the two thresholds are identical. The lines span 1% and 99% of boostrap replicated FNMR estimates.

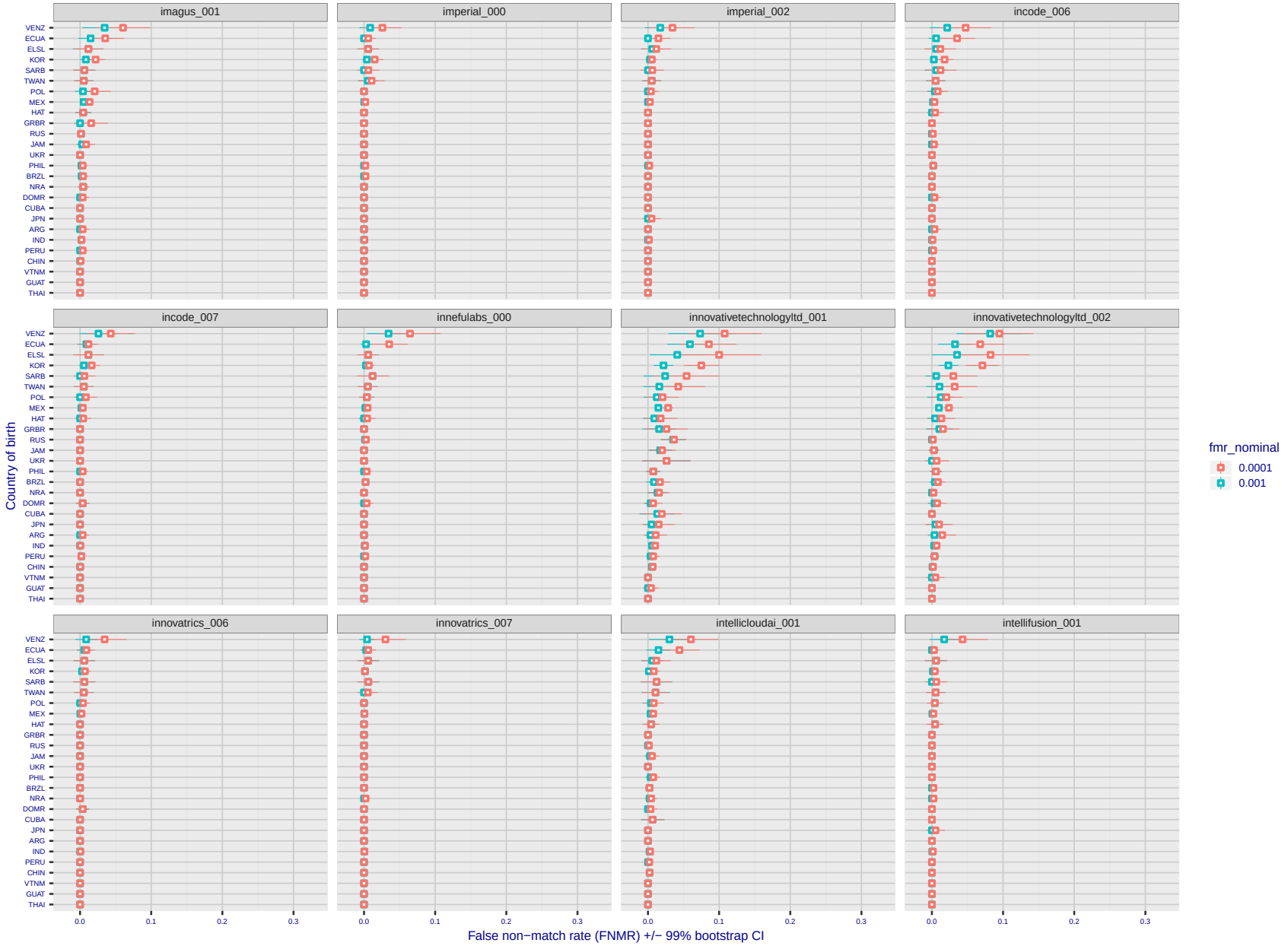

Figure 165: For the visa images, the dots show FNMR by country of birth for two globally set operating thresholds corresponding to FMR = $\{0.001, 0.0001\}$ computed over all on the order of 10^{10} impostor scores. The FMR in each bin will vary also - see subsequent impostor heatmaps in sec. 3.6.1. The figures shows an order of magnitude variation in FNMR across country of birth; these effects are likely due quality variations, then demographics like age and race. The error rates in some cases are zero, and in others the DET is flat so the error rates at the two thresholds are identical. The lines span 1% and 99% of boostrap replicated FNMR estimates.

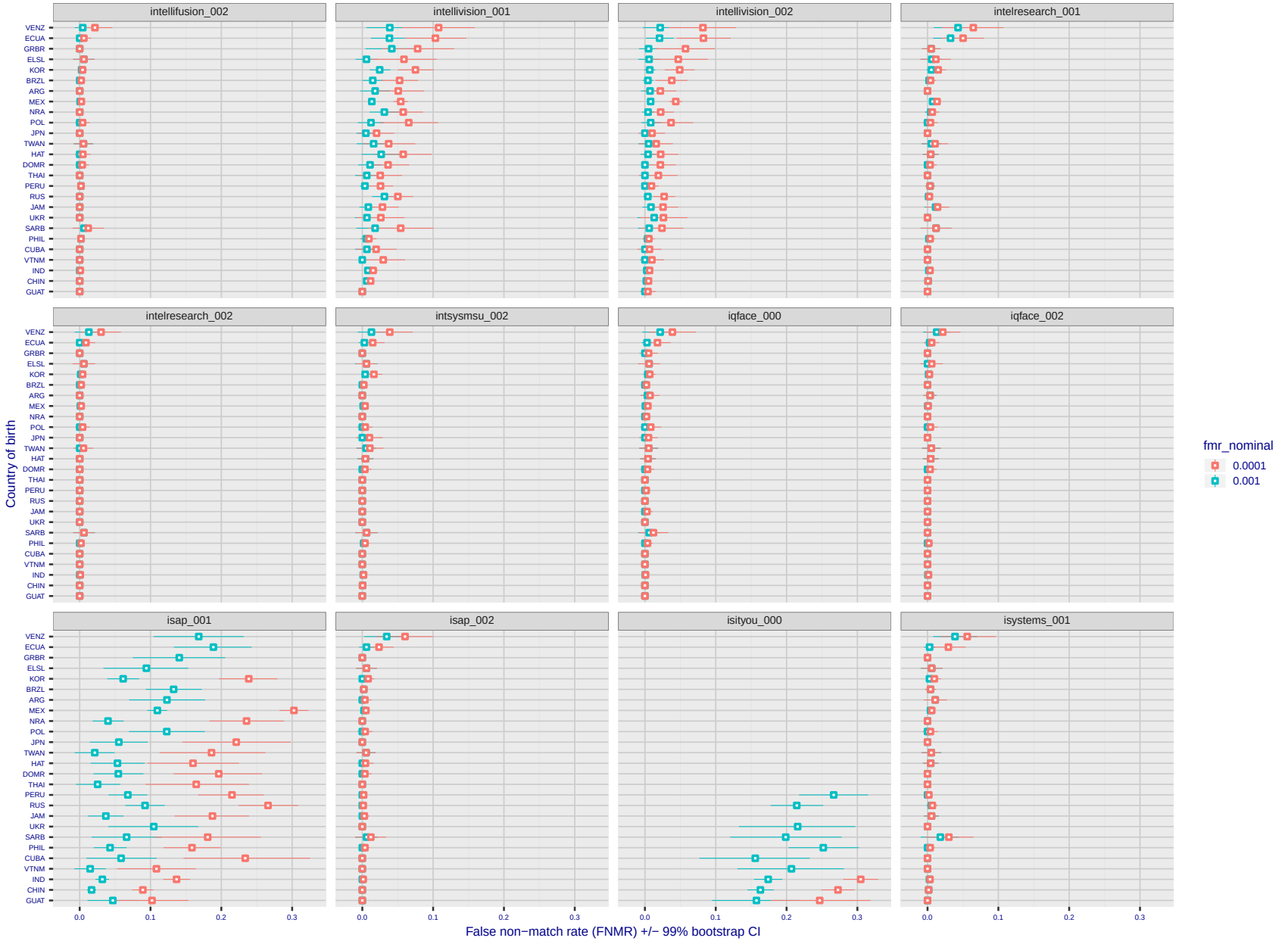

Figure 166: For the visa images, the dots show FNMR by country of birth for two globally set operating thresholds corresponding to FMR = $\{0.001, 0.0001\}$ computed over all on the order of 10^{10} impostor scores. The FMR in each bin will vary also - see subsequent impostor heatmaps in sec. 3.6.1. The figures shows an order of magnitude variation in FNMR across country of birth; these effects are likely due quality variations, then demographics like age and race. The error rates in some cases are zero, and in others the DET is flat so the error rates at the two thresholds are identical. The lines span 1% and 99% of boostrap replicated FNMR estimates.

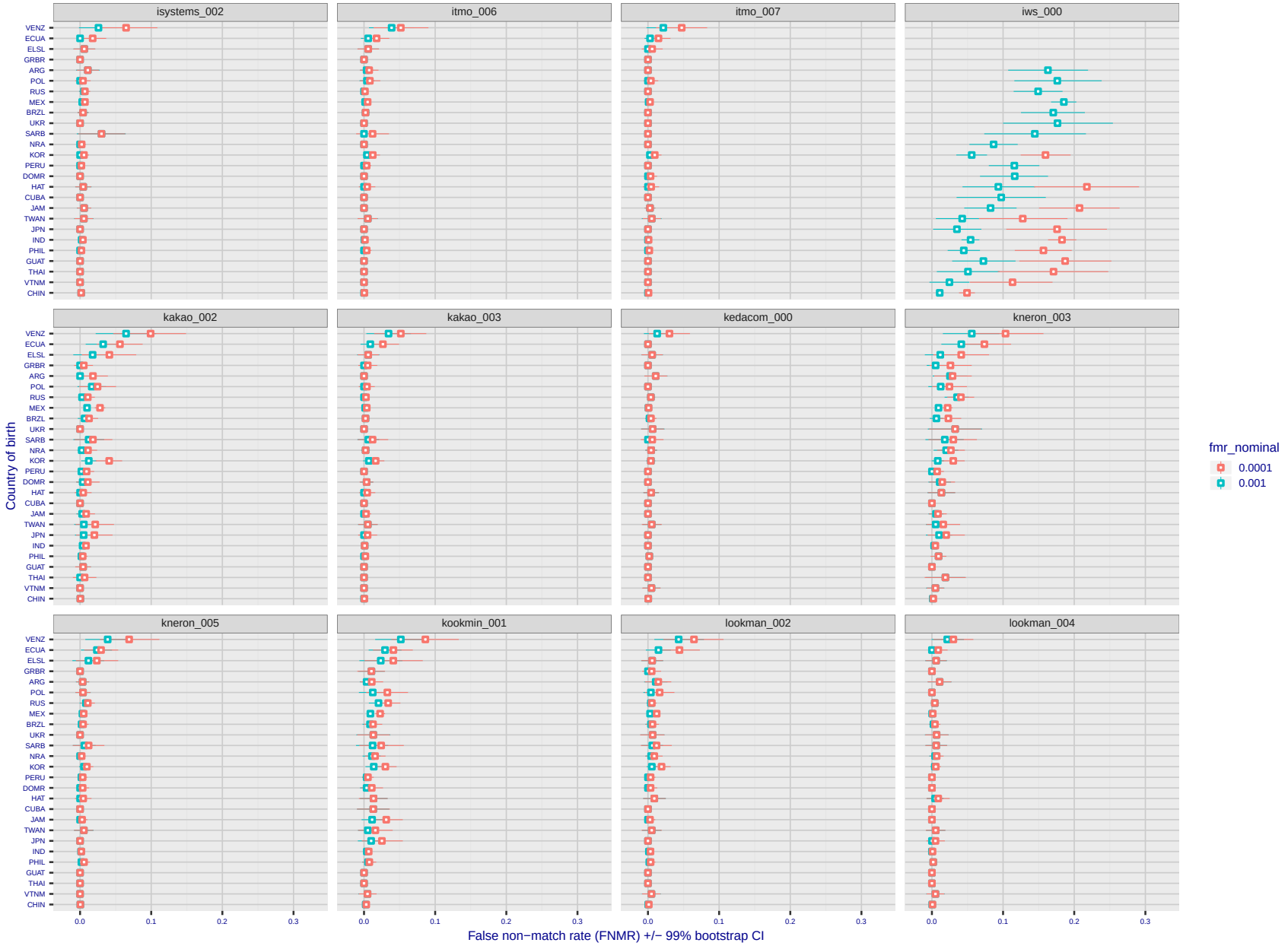

Figure 167: For the visa images, the dots show FNMR by country of birth for two globally set operating thresholds corresponding to FMR = $\{0.001, 0.0001\}$ computed over all on the order of 10^{10} impostor scores. The FMR in each bin will vary also - see subsequent impostor heatmaps in sec. 3.6.1. The figures shows an order of magnitude variation in FNMR across country of birth; these effects are likely due quality variations, then demographics like age and race. The error rates in some cases are zero, and in others the DET is flat so the error rates at the two thresholds are identical. The lines span 1% and 99% of boostrap replicated FNMR estimates.

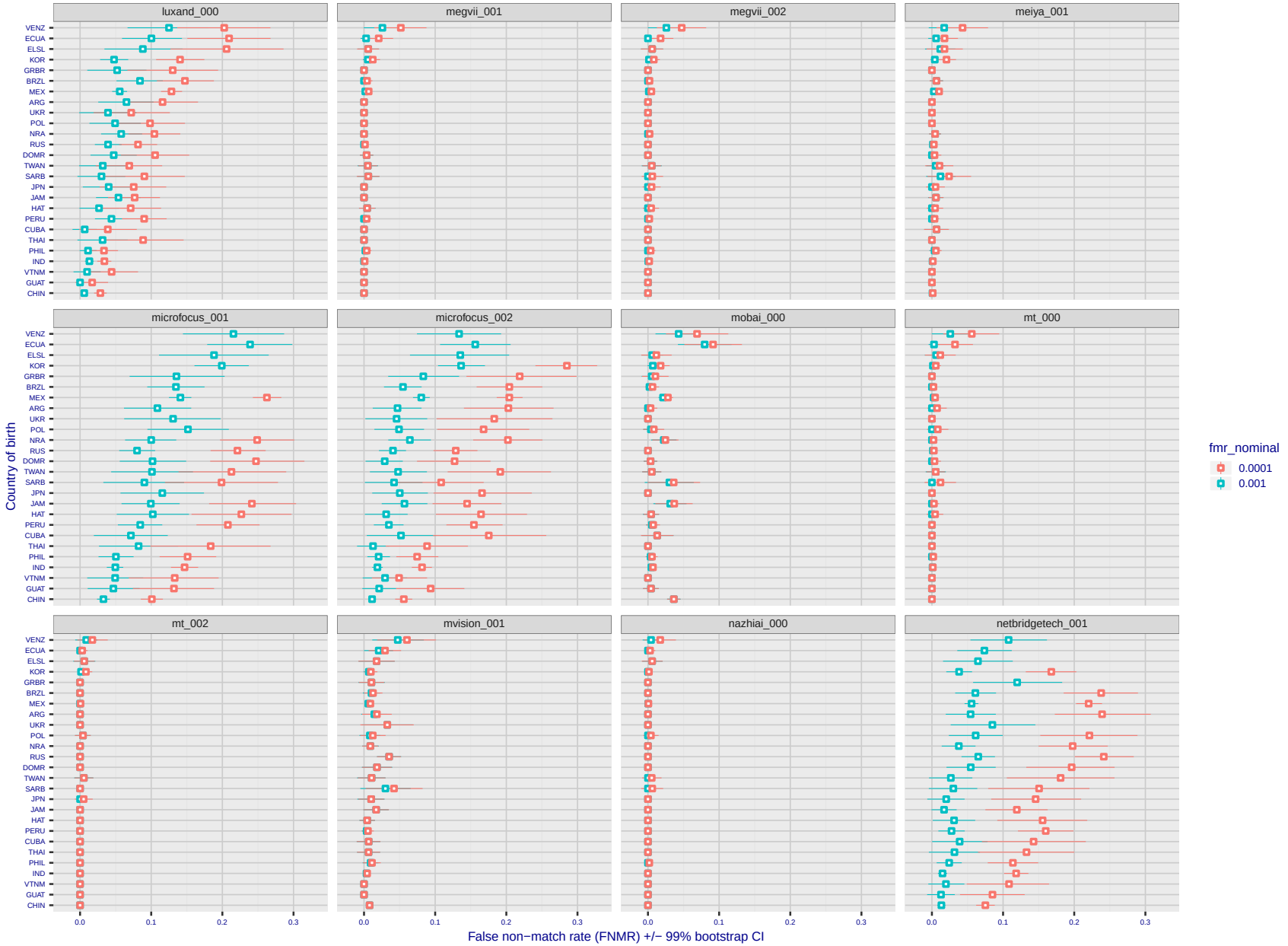

Figure 168: For the visa images, the dots show FNMR by country of birth for two globally set operating thresholds corresponding to FMR = $\{0.001, 0.0001\}$ computed over all on the order of 10^{10} impostor scores. The FMR in each bin will vary also - see subsequent impostor heatmaps in sec. 3.6.1. The figures shows an order of magnitude variation in FNMR across country of birth; these effects are likely due quality variations, then demographics like age and race. The error rates in some cases are zero, and in others the DET is flat so the error rates at the two thresholds are identical. The lines span 1% and 99% of boostrap replicated FNMR estimates.

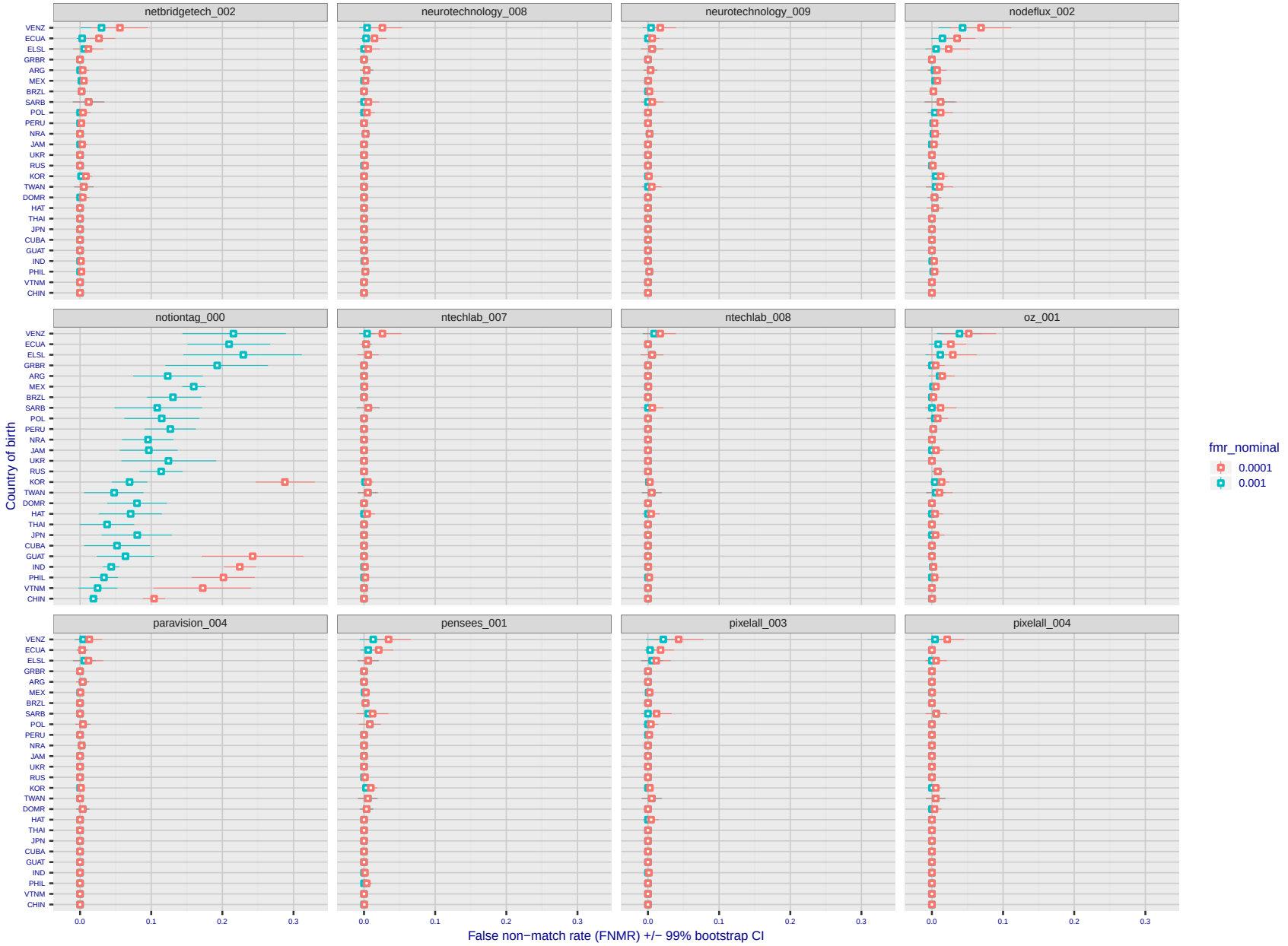

Figure 169: For the visa images, the dots show FNMR by country of birth for two globally set operating thresholds corresponding to FMR = $\{0.001, 0.0001\}$ computed over all on the order of 10^{10} impostor scores. The FMR in each bin will vary also - see subsequent impostor heatmaps in sec. 3.6.1. The figures shows an order of magnitude variation in FNMR across country of birth; these effects are likely due quality variations, then demographics like age and race. The error rates in some cases are zero, and in others the DET is flat so the error rates at the two thresholds are identical. The lines span 1% and 99% of boostrap replicated FNMR estimates.

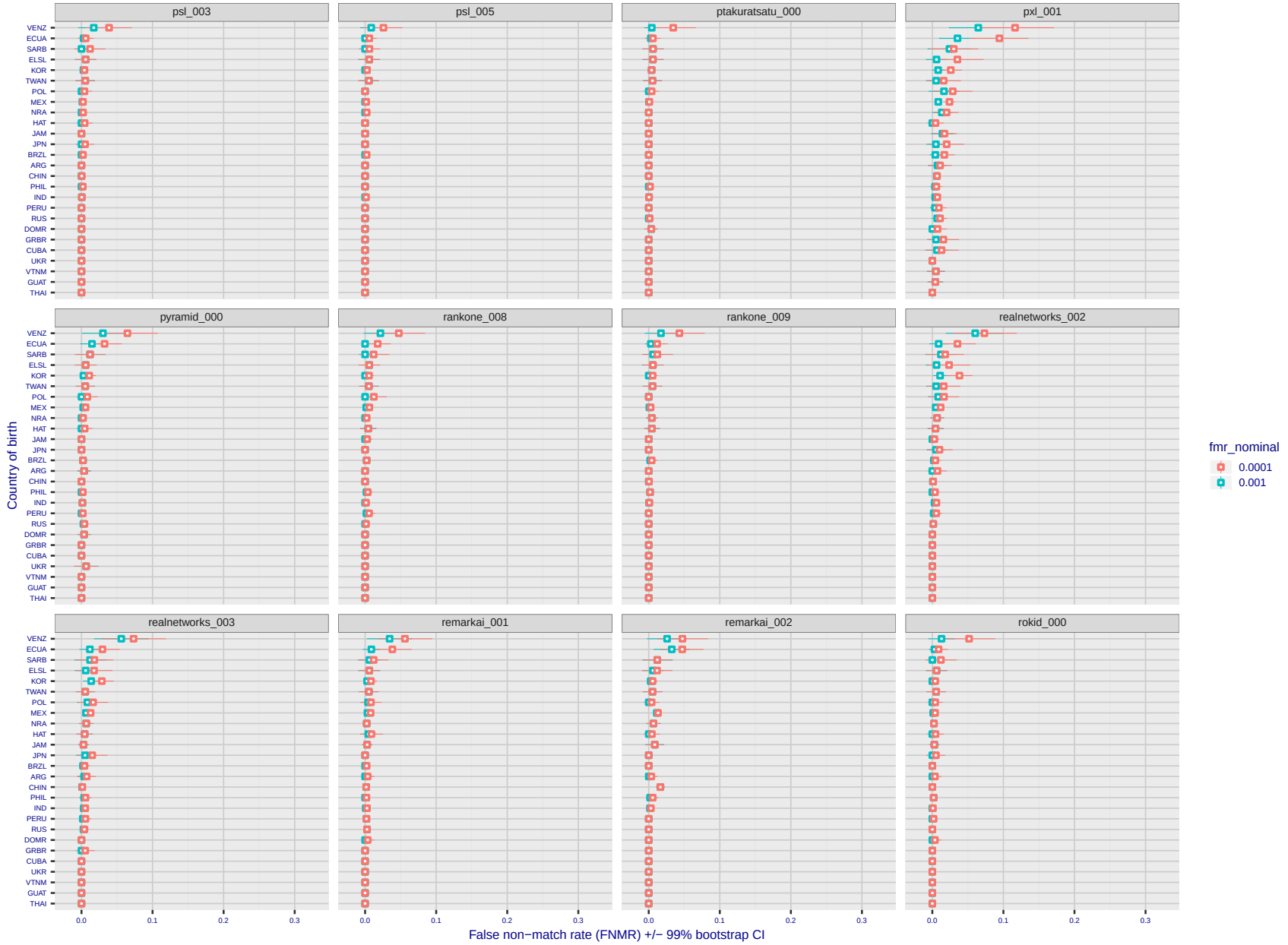

Figure 170: For the visa images, the dots show FNMR by country of birth for two globally set operating thresholds corresponding to FMR = $\{0.001, 0.0001\}$ computed over all on the order of 10^{10} impostor scores. The FMR in each bin will vary also - see subsequent impostor heatmaps in sec. 3.6.1. The figures shows an order of magnitude variation in FNMR across country of birth; these effects are likely due quality variations, then demographics like age and race. The error rates in some cases are zero, and in others the DET is flat so the error rates at the two thresholds are identical. The lines span 1% and 99% of boostrap replicated FNMR estimates.

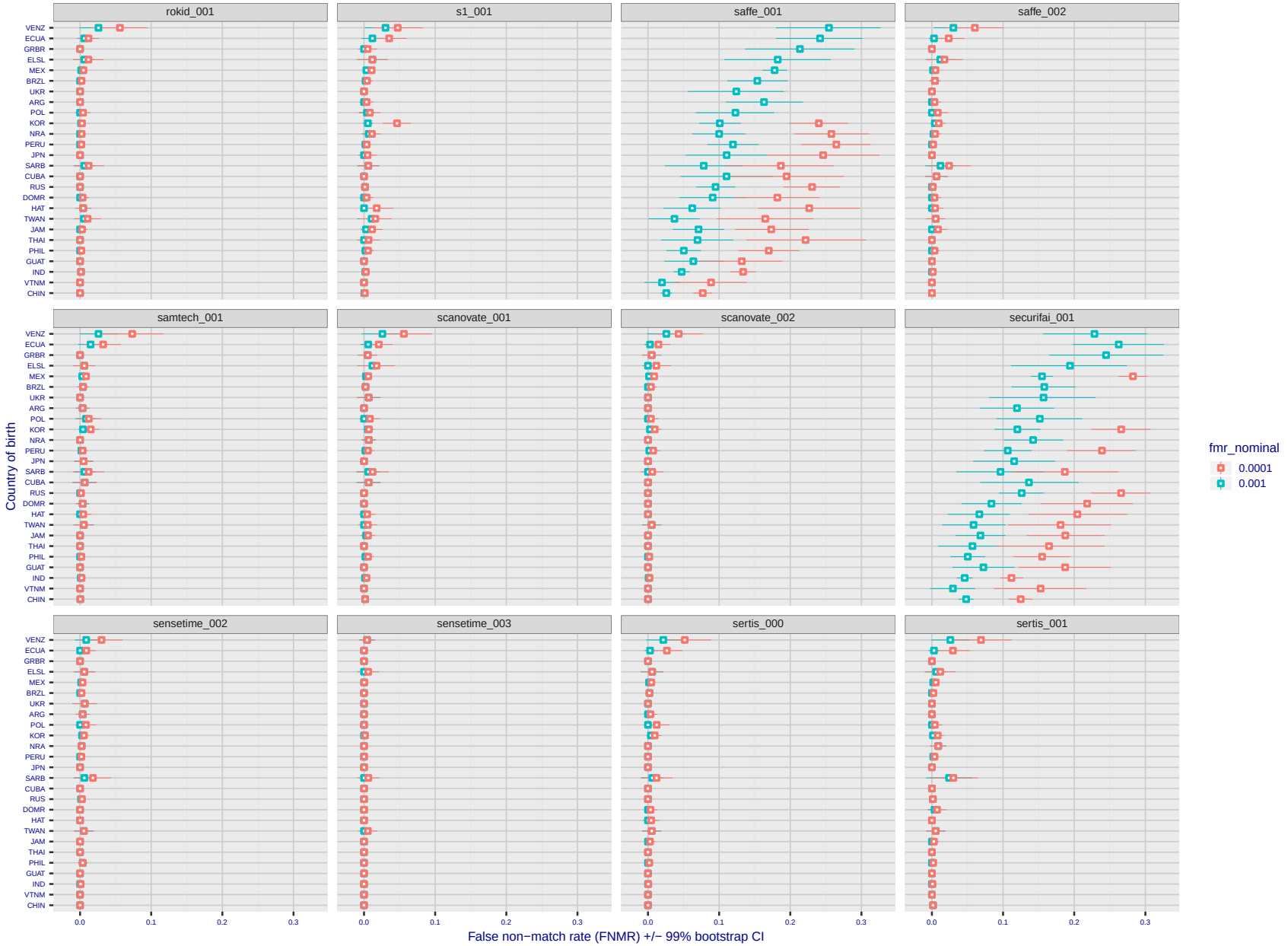

Figure 171: For the visa images, the dots show FNMR by country of birth for two globally set operating thresholds corresponding to FMR = $\{0.001, 0.0001\}$ computed over all on the order of 10^{10} impostor scores. The FMR in each bin will vary also - see subsequent impostor heatmaps in sec. 3.6.1. The figures shows an order of magnitude variation in FNMR across country of birth; these effects are likely due quality variations, then demographics like age and race. The error rates in some cases are zero, and in others the DET is flat so the error rates at the two thresholds are identical. The lines span 1% and 99% of boostrap replicated FNMR estimates.

FNMR(T) "False non-match rate"
FMR(T) "False match rate"

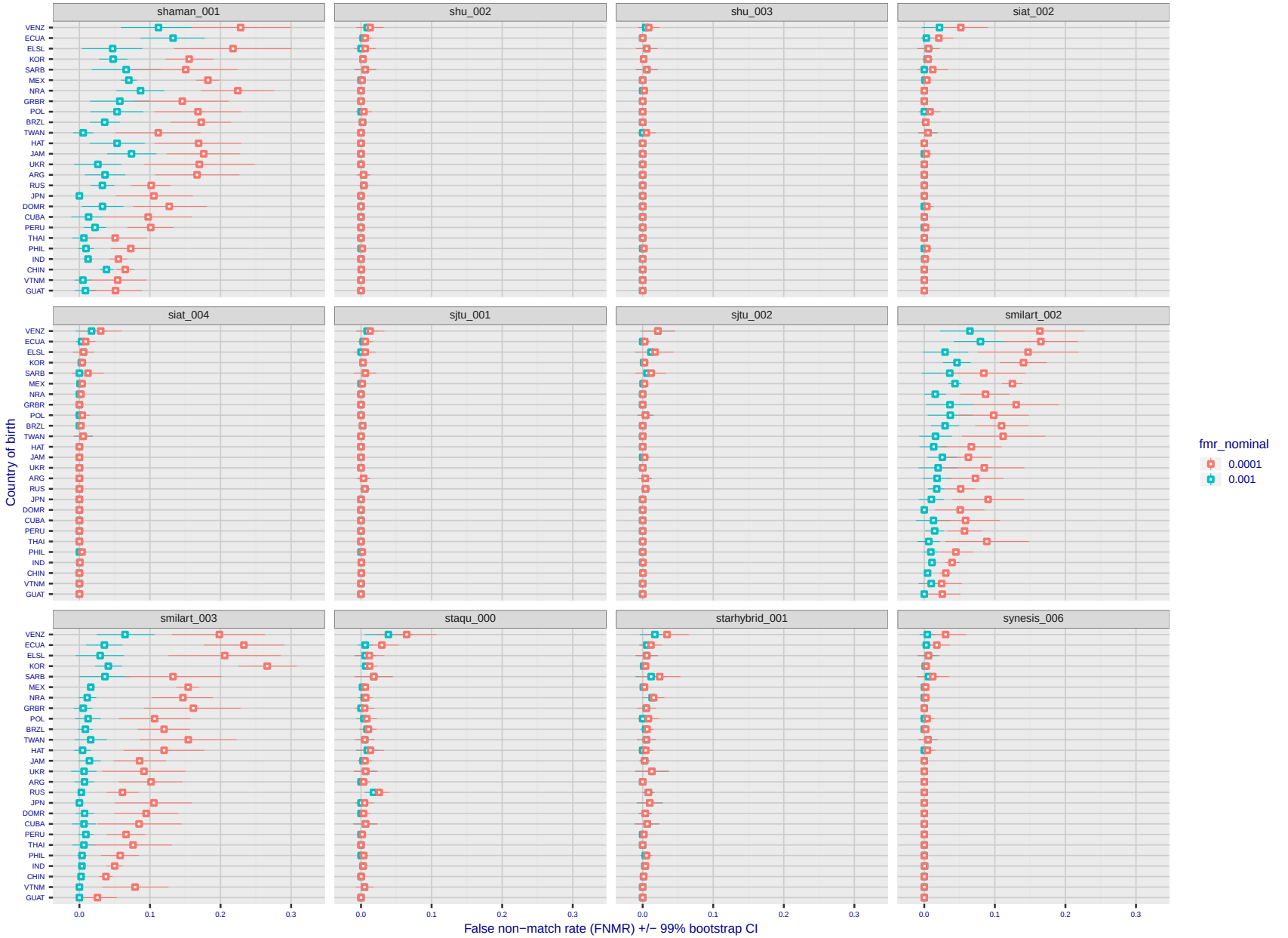

Figure 172: For the visa images, the dots show FNMR by country of birth for two globally set operating thresholds corresponding to FMR = $\{0.001, 0.0001\}$ computed over all on the order of 10^{10} impostor scores. The FMR in each bin will vary also - see subsequent impostor heatmaps in sec. 3.6.1. The figures shows an order of magnitude variation in FNMR across country of birth; these effects are likely due quality variations, then demographics like age and race. The error rates in some cases are zero, and in others the DET is flat so the error rates at the two thresholds are identical. The lines span 1% and 99% of boostrap replicated FNMR estimates.

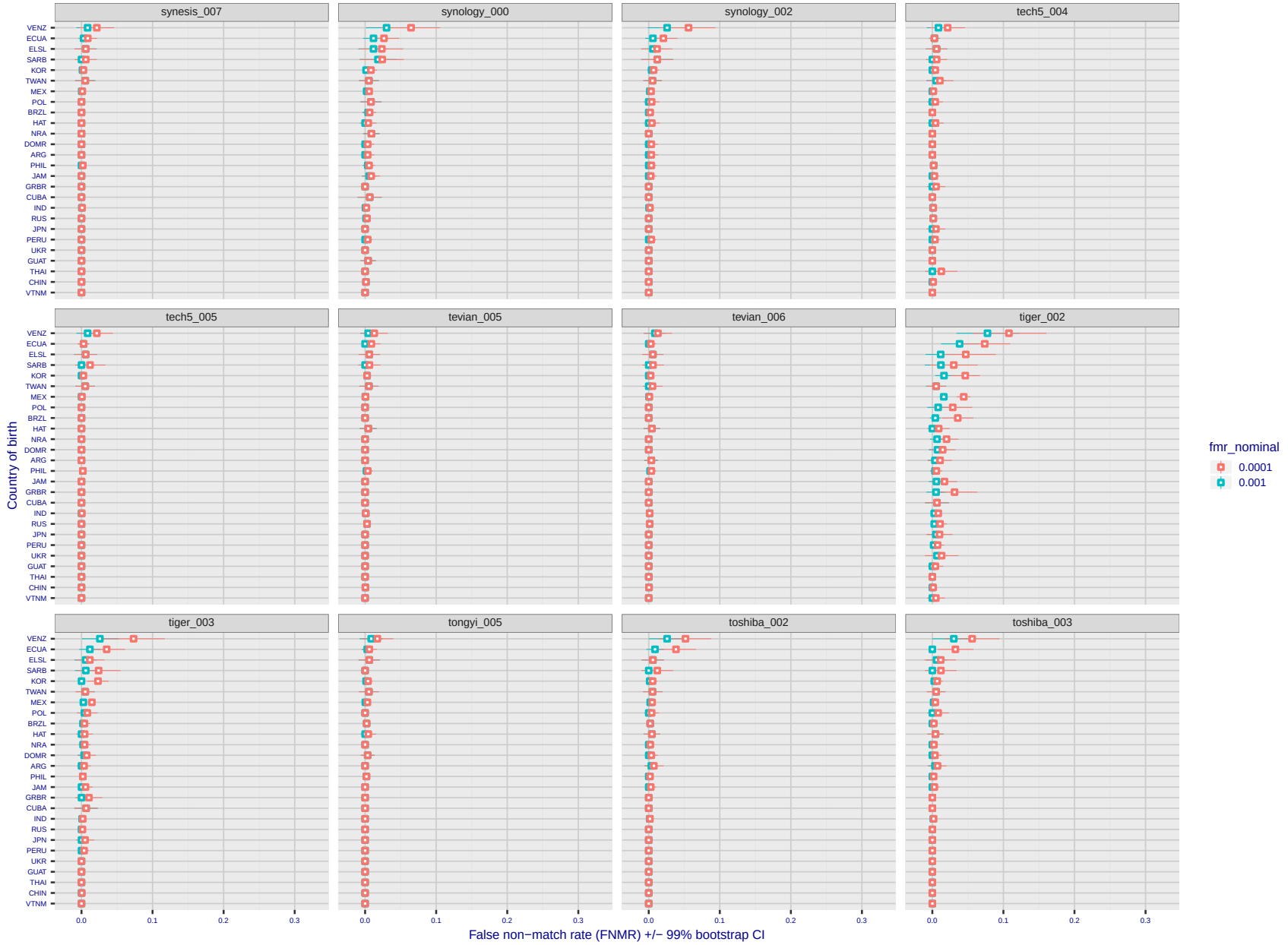

Figure 173: For the visa images, the dots show FNMR by country of birth for two globally set operating thresholds corresponding to FMR = $\{0.001, 0.0001\}$ computed over all on the order of 10^{10} impostor scores. The FMR in each bin will vary also - see subsequent impostor heatmaps in sec. 3.6.1. The figures shows an order of magnitude variation in FNMR across country of birth; these effects are likely due quality variations, then demographics like age and race. The error rates in some cases are zero, and in others the DET is flat so the error rates at the two thresholds are identical. The lines span 1% and 99% of boostrap replicated FNMR estimates.

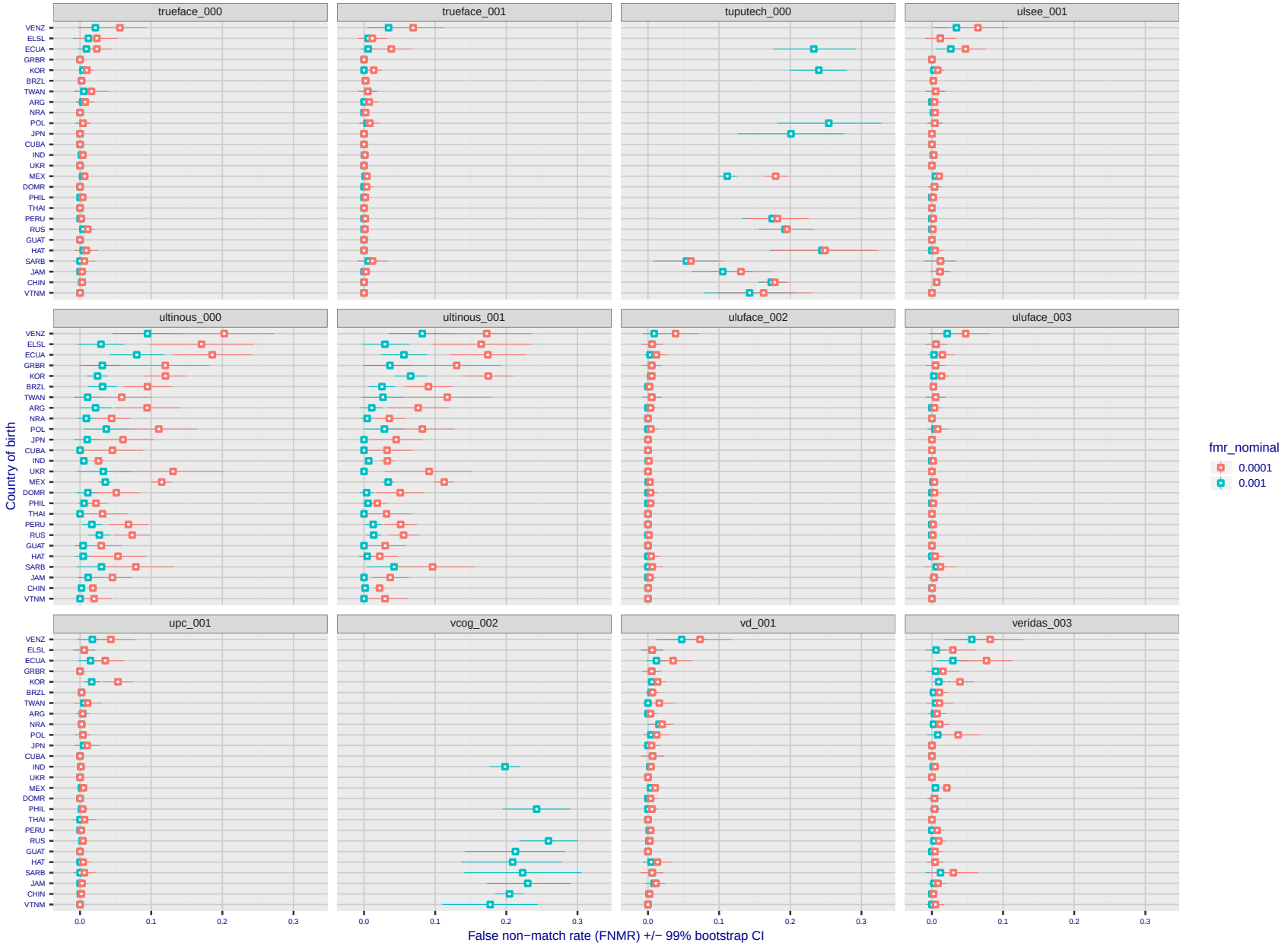

Figure 174: For the visa images, the dots show FNMR by country of birth for two globally set operating thresholds corresponding to FMR = $\{0.001, 0.0001\}$ computed over all on the order of 10^{10} impostor scores. The FMR in each bin will vary also - see subsequent impostor heatmaps in sec. 3.6.1. The figures shows an order of magnitude variation in FNMR across country of birth; these effects are likely due quality variations, then demographics like age and race. The error rates in some cases are zero, and in others the DET is flat so the error rates at the two thresholds are identical. The lines span 1% and 99% of boostrap replicated FNMR estimates.

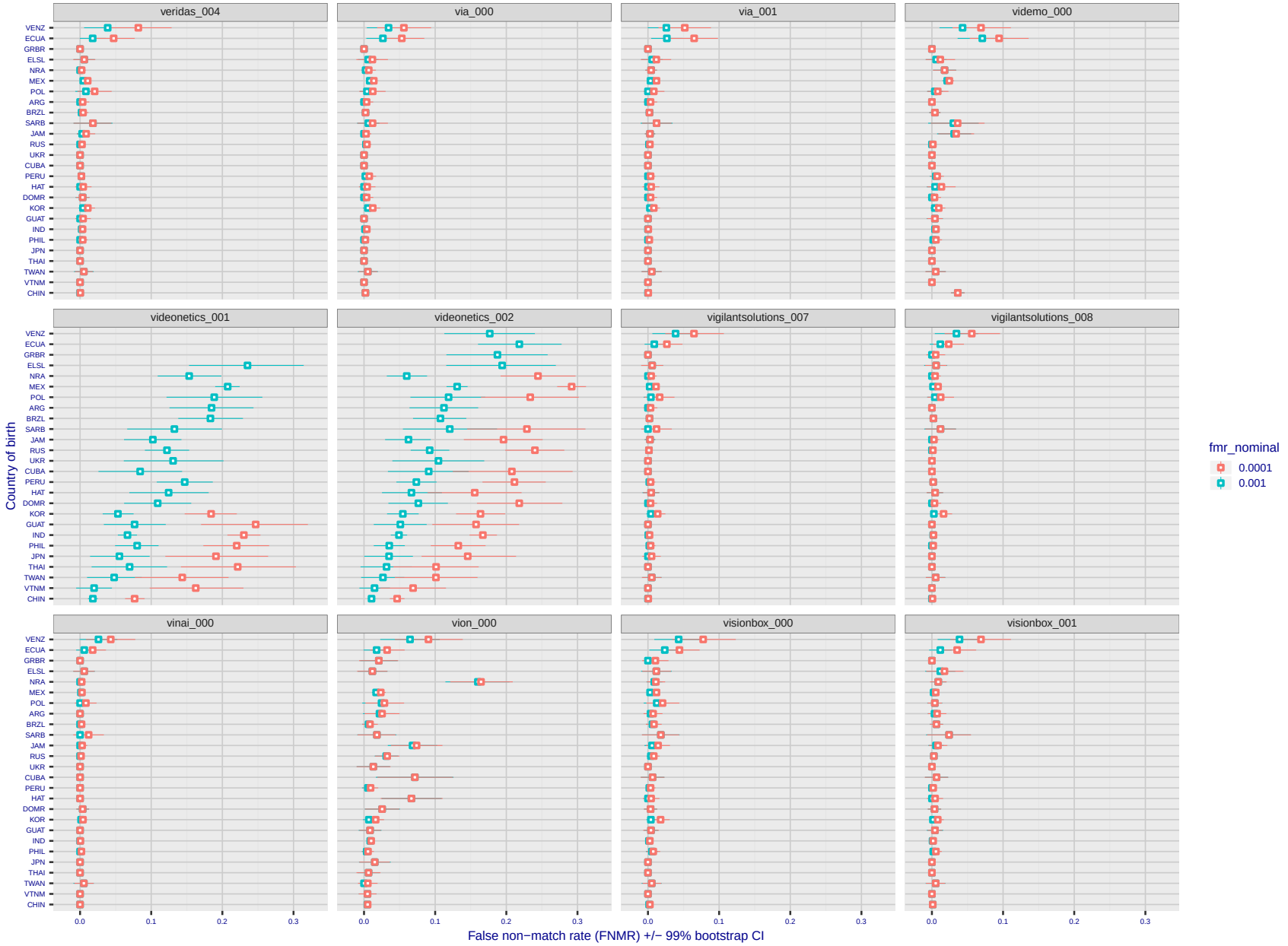

Figure 175: For the visa images, the dots show FNMR by country of birth for two globally set operating thresholds corresponding to FMR = $\{0.001, 0.0001\}$ computed over all on the order of 10^{10} impostor scores. The FMR in each bin will vary also - see subsequent impostor heatmaps in sec. 3.6.1. The figures shows an order of magnitude variation in FNMR across country of birth; these effects are likely due quality variations, then demographics like age and race. The error rates in some cases are zero, and in others the DET is flat so the error rates at the two thresholds are identical. The lines span 1% and 99% of boostrap replicated FNMR estimates.

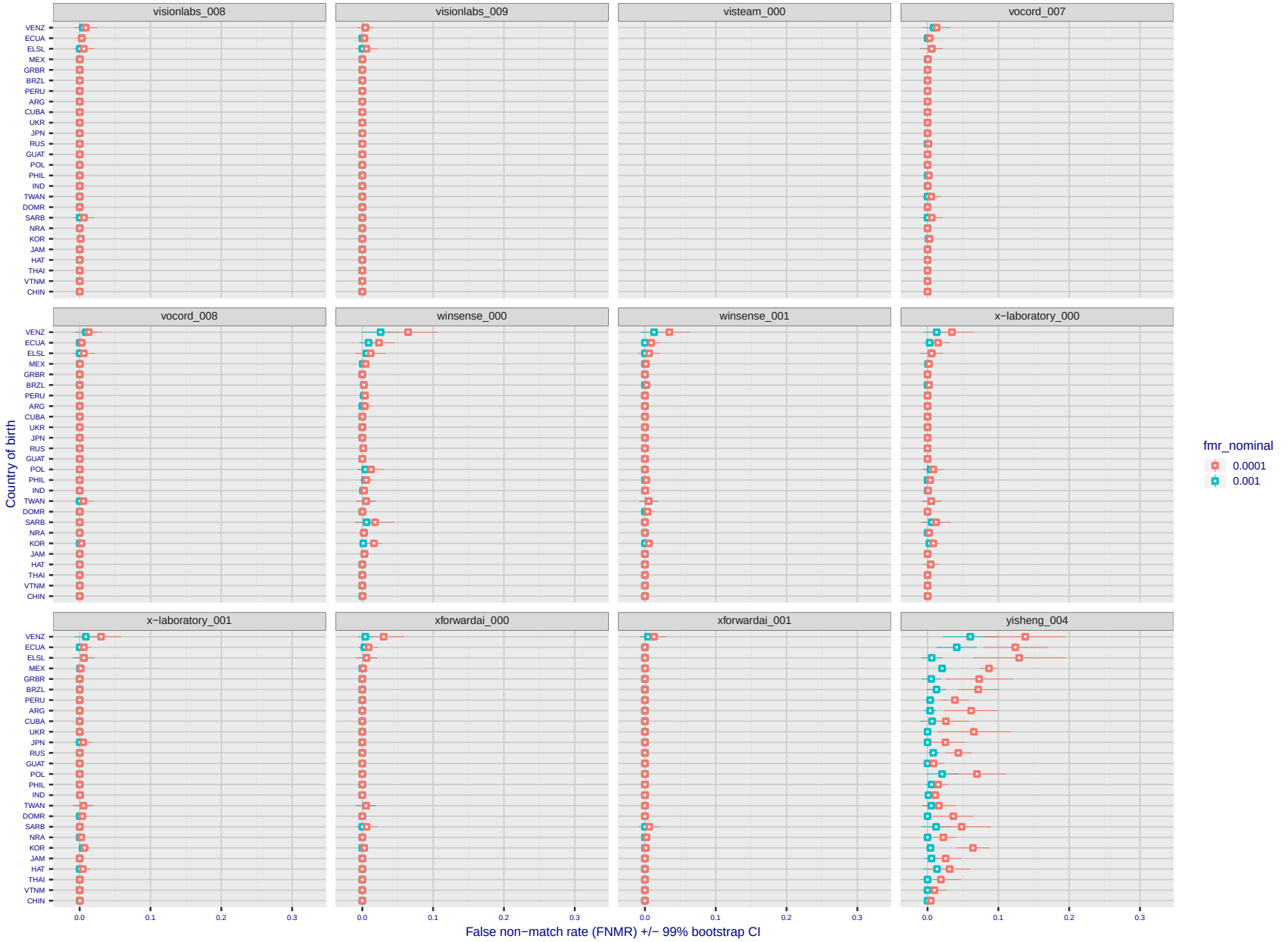

Figure 176: For the visa images, the dots show FNMR by country of birth for two globally set operating thresholds corresponding to FMR = $\{0.001, 0.0001\}$ computed over all on the order of 10^{10} impostor scores. The FMR in each bin will vary also - see subsequent impostor heatmaps in sec. 3.6.1. The figures shows an order of magnitude variation in FNMR across country of birth; these effects are likely due quality variations, then demographics like age and race. The error rates in some cases are zero, and in others the DET is flat so the error rates at the two thresholds are identical. The lines span 1% and 99% of boostrap replicated FNMR estimates.

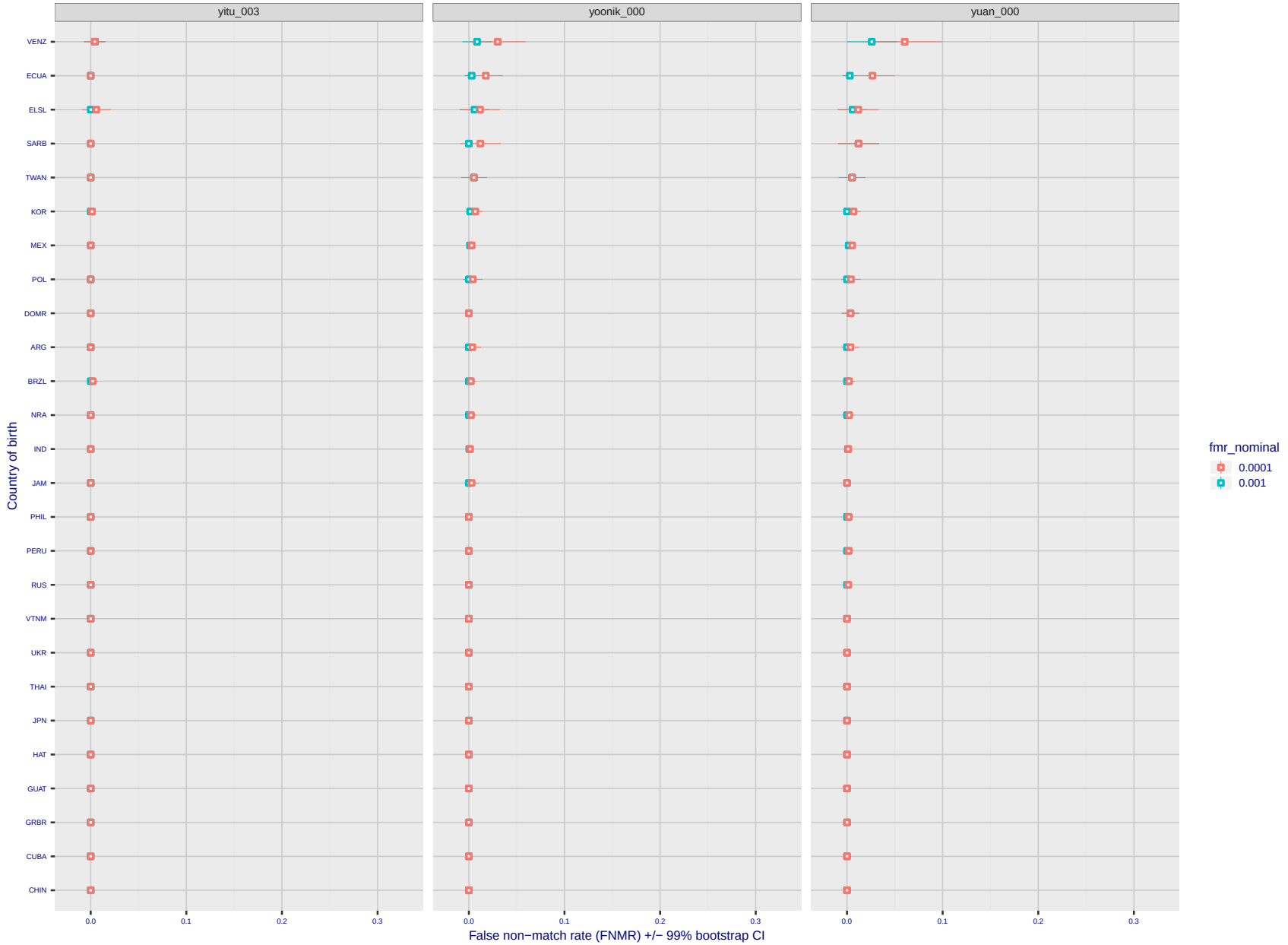

Figure 177: For the visa images, the dots show FNMR by country of birth for two globally set operating thresholds corresponding to FMR = $\{0.001, 0.0001\}$ computed over all on the order of 10^{10} impostor scores. The FMR in each bin will vary also - see subsequent impostor heatmaps in sec. 3.6.1. The figures shows an order of magnitude variation in FNMR across country of birth; these effects are likely due quality variations, then demographics like age and race. The error rates in some cases are zero, and in others the DET is flat so the error rates at the two thresholds are identical. The lines span 1% and 99% of boostrap replicated FNMR estimates.

Caveats: The results may not relate to subject-specific properties. Instead they could reflect image-specific quality differences, which could occur due to collection protocol or software processing variations.

3.5.2 Effect of ageing

Background: Faces change appearance throughout life. This change gradually reduces similarity of a new image to an earlier image. Face recognition algorithms give reduced similarity scores and more frequent false rejections.

Goal: To quantify false non-match rates (FNMR) as a function of elapsed time in an adult population.

Methods: Using the mugshot images, a threshold is set to give FMR = 0.00001 over the entire impostor set. Then FNMR is measured over 1000 bootstrap replications of the genuine scores.

Results: For the visa images, Figure 192 shows how false non-match rates for genuine users, as a function of age group.

FNMR(T) "False non-match rate"
FMR(T) "False match rate"

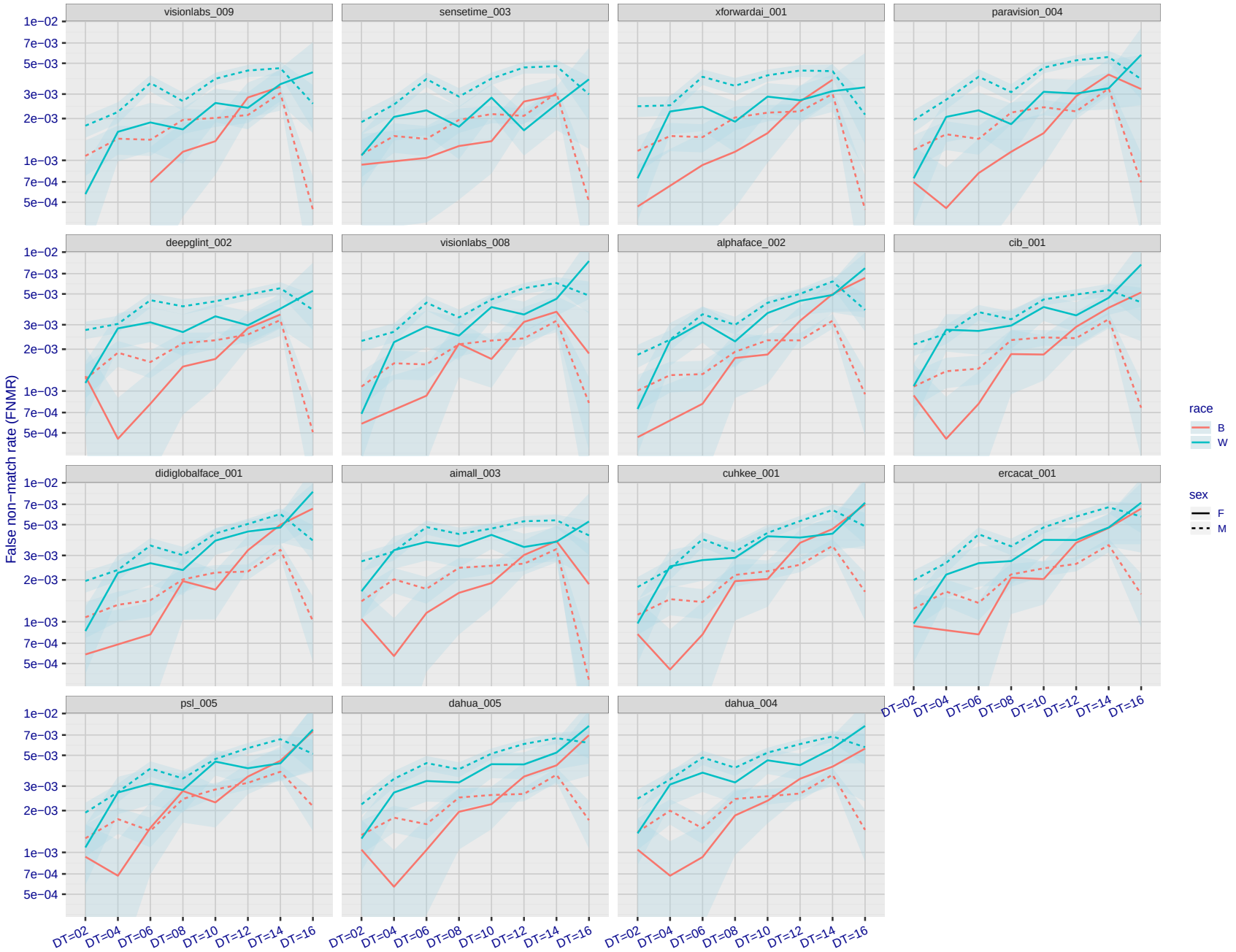

Figure 178: For the mugshot images, FNMR *as a function of elapsed time between initial enrollment and second verification images. The panels appear most accurate first, and vertical scale changes on each page. The four traces correspond to images annotated with codes for black female, black male, white female, white male. The threshold is fixed for each algorithm to give FMR = 0.00001 over all (10^8) impostor comparisons. For short time-lapses, the most accurate algorithms give very few errors (FNMR < 0.001) so that the uncertainty estimates are high.*

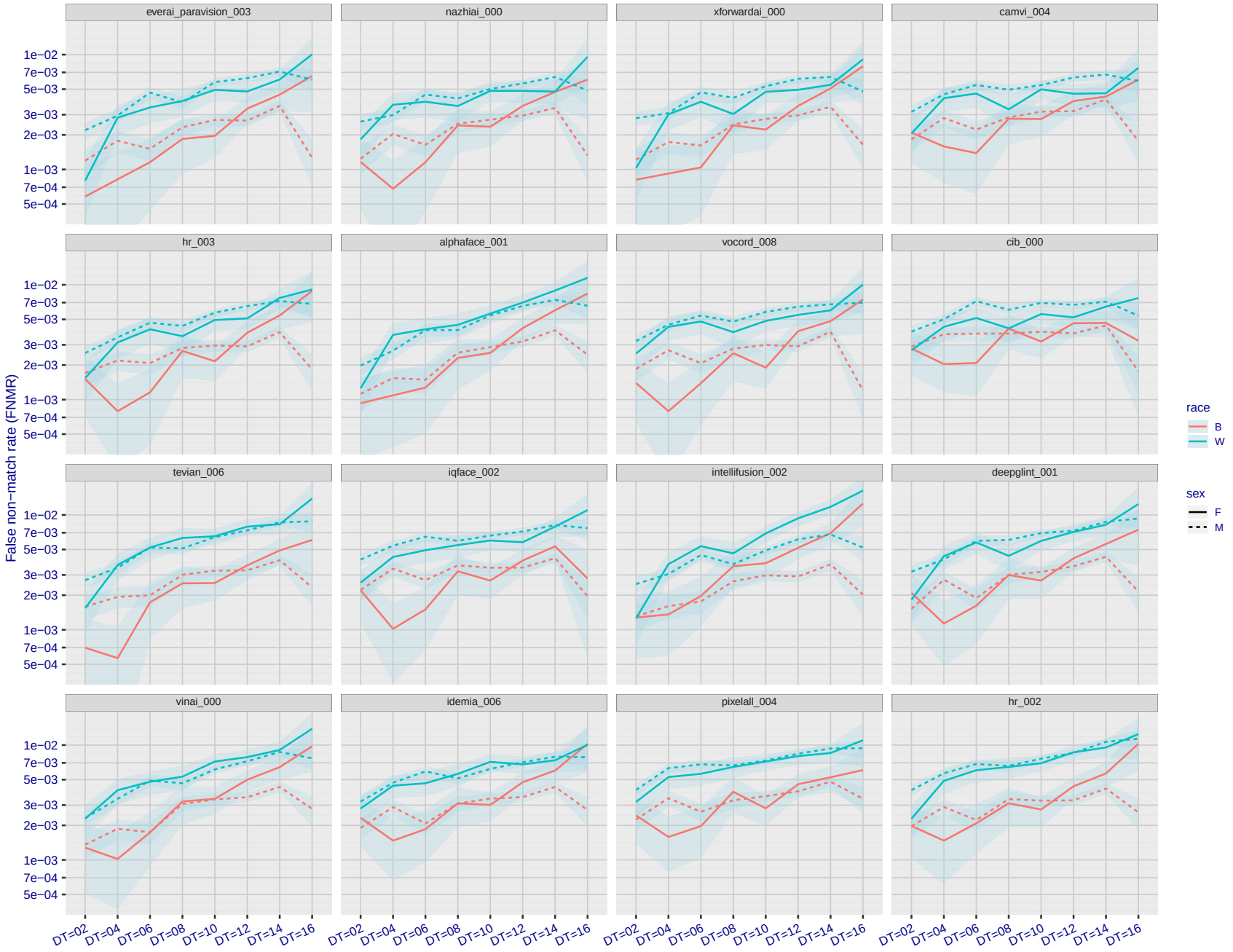

Figure 179: For the mugshot images, FNMR *as a function of elapsed time between initial enrollment and second verification images. The panels appear most accurate first, and vertical scale changes on each page. The four traces correspond to images annotated with codes for black female, black male, white female, white male. The threshold is fixed for each algorithm to give FMR = 0.00001 over all (10^8) impostor comparisons. For short time-lapses, the most accurate algorithms give very few errors (FNMR < 0.001) so that the uncertainty estimates are high.*

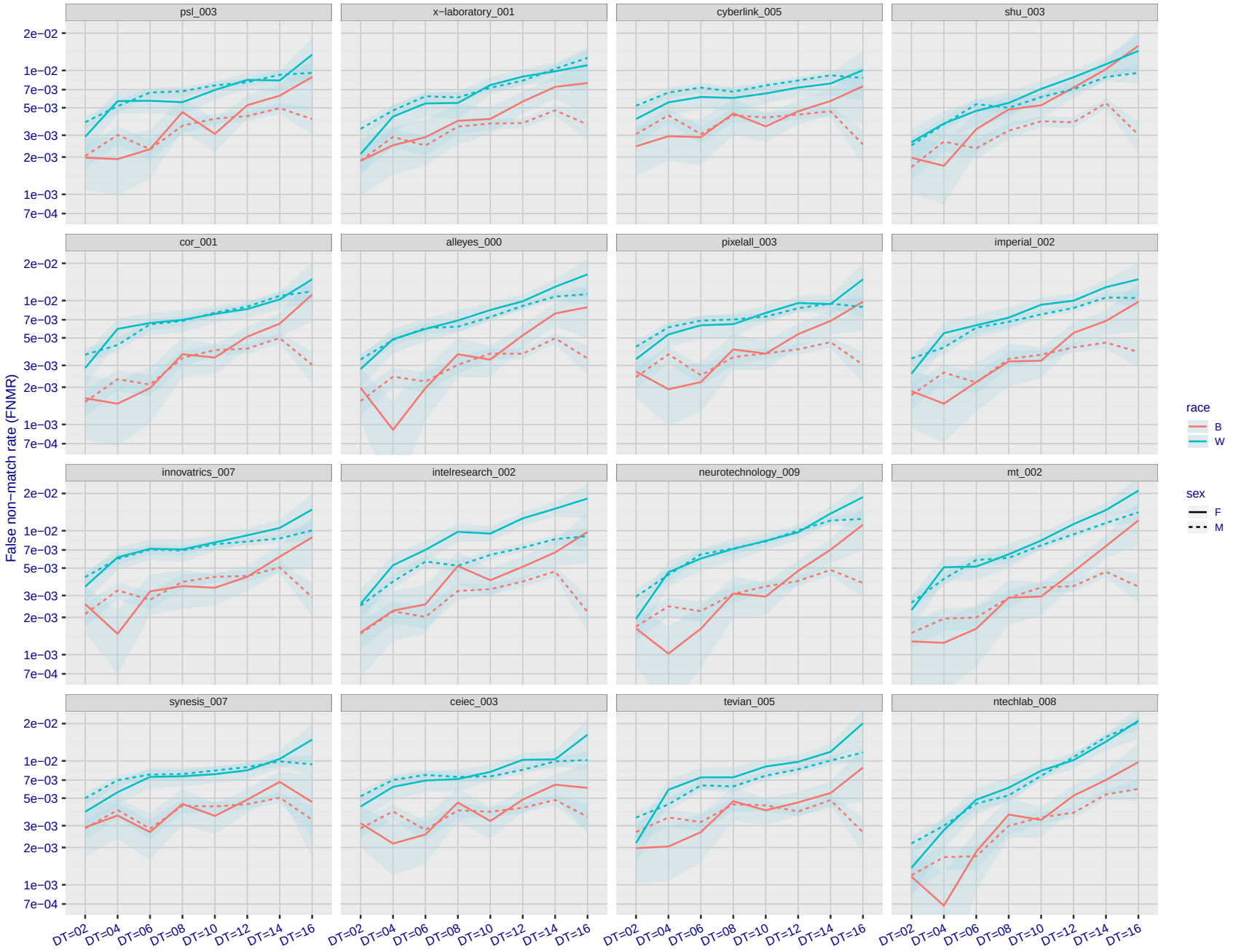

Figure 180: For the mugshot images, FNMR *as a function of elapsed time between initial enrollment and second verification images. The panels appear most accurate first, and vertical scale changes on each page. The four traces correspond to images annotated with codes for black female, black male, white female, white male. The threshold is fixed for each algorithm to give FMR = 0.00001 over all (10^8) impostor comparisons. For short time-lapses, the most accurate algorithms give very few errors (FNMR < 0.001) so that the uncertainty estimates are high.*

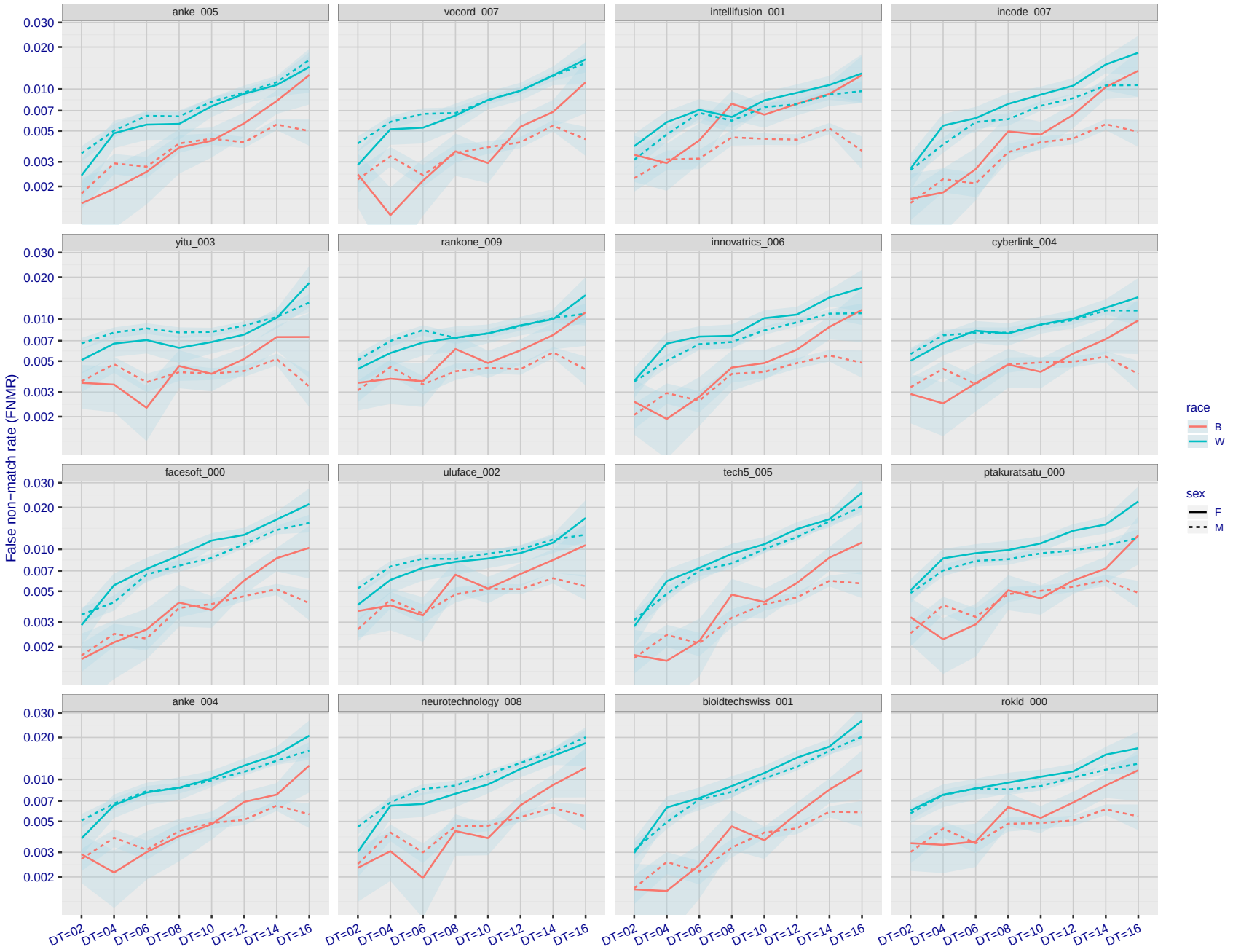

Figure 181: For the mugshot images, FNMR *as a function of elapsed time between initial enrollment and second verification images. The panels appear most accurate first, and vertical scale changes on each page. The four traces correspond to images annotated with codes for black female, black male, white female, white male. The threshold is fixed for each algorithm to give FMR = 0.00001 over all (10^8) impostor comparisons. For short time-lapses, the most accurate algorithms give very few errors (FNMR < 0.001) so that the uncertainty estimates are high.*

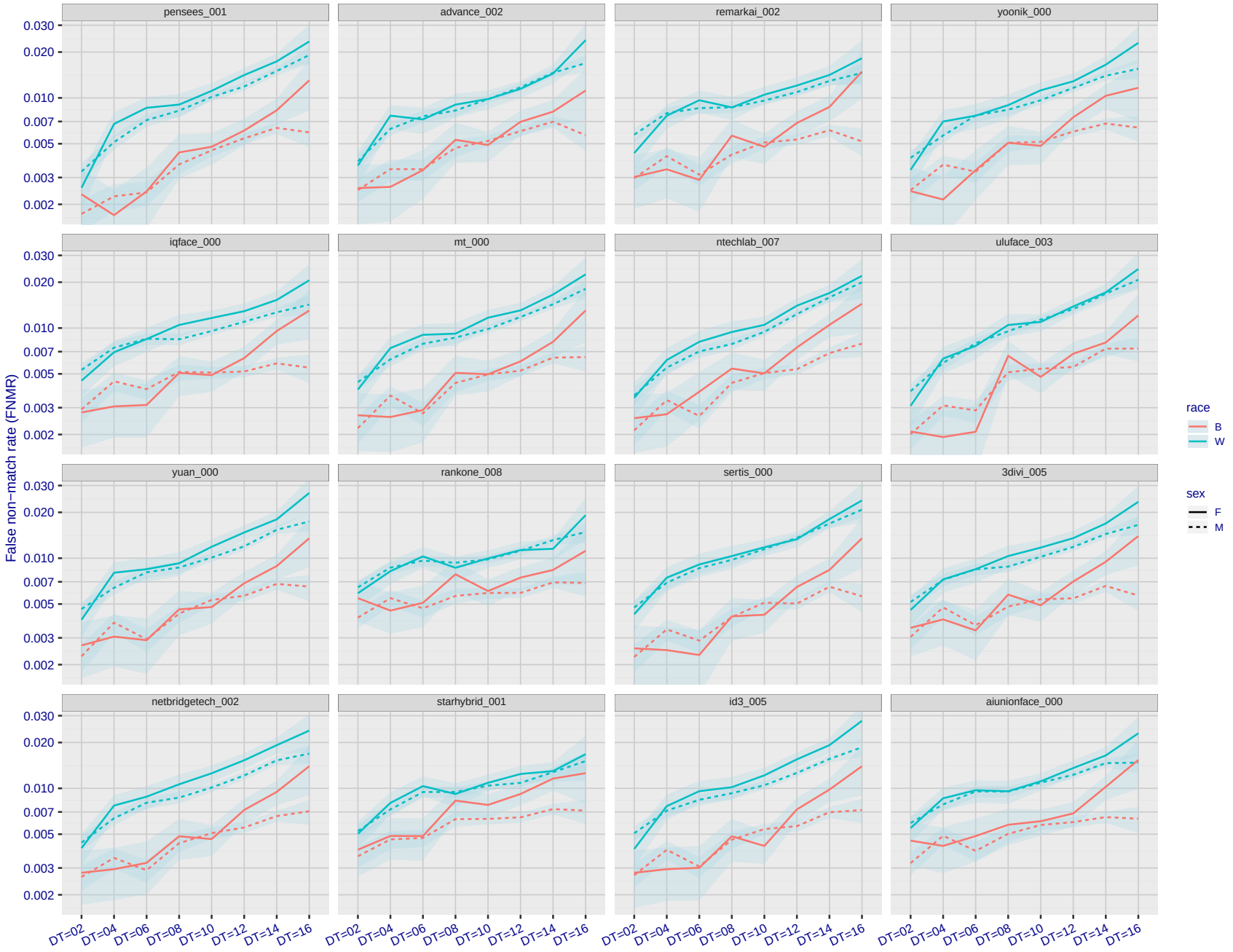

Figure 182: For the mugshot images, FNMR *as a function of elapsed time between initial enrollment and second verification images. The panels appear most accurate first, and vertical scale changes on each page. The four traces correspond to images annotated with codes for black female, black male, white female, white male. The threshold is fixed for each algorithm to give FMR = 0.00001 over all (10^8) impostor comparisons. For short time-lapses, the most accurate algorithms give very few errors (FNMR < 0.001) so that the uncertainty estimates are high.*

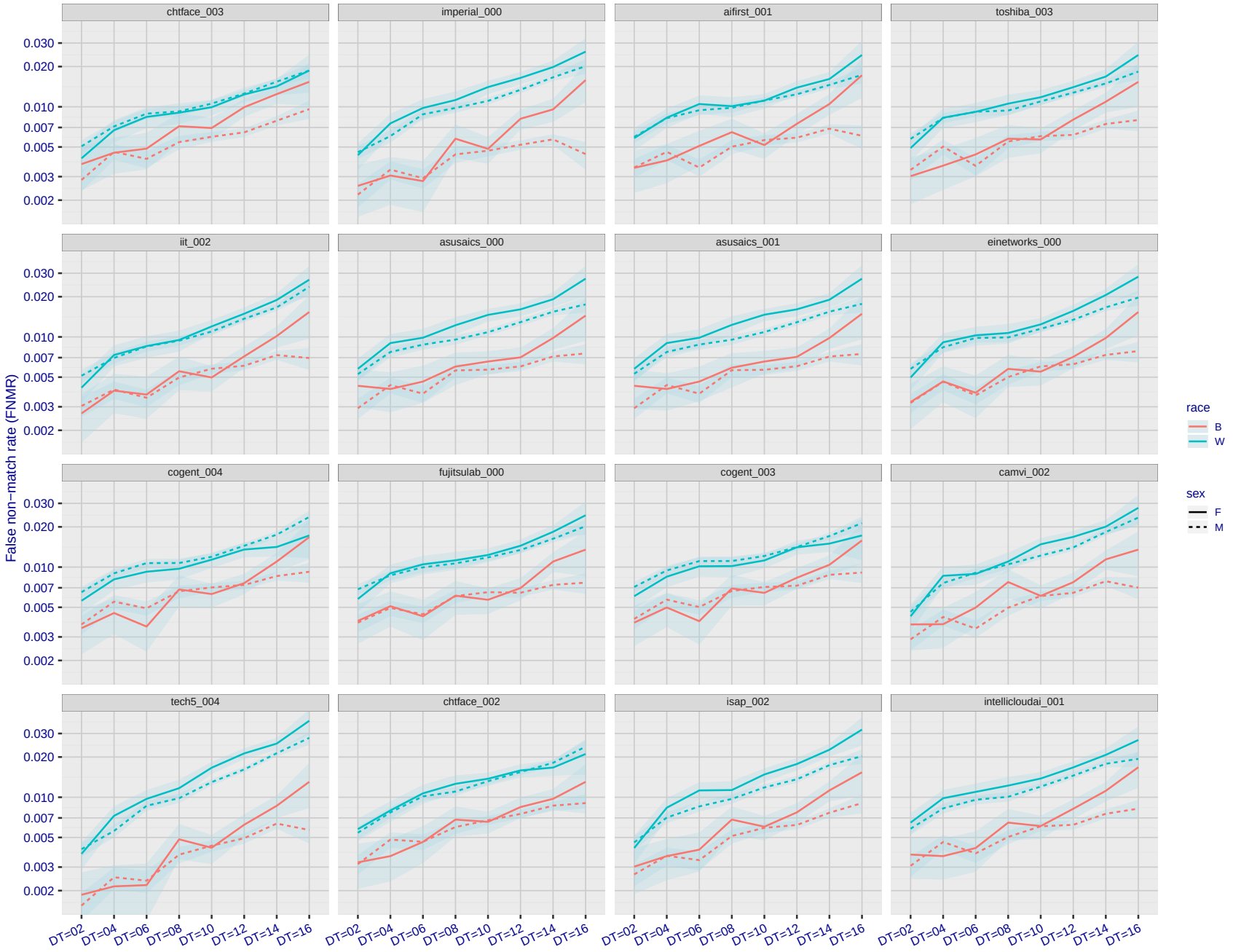

Figure 183: For the mugshot images, FNMR *as a function of elapsed time between initial enrollment and second verification images. The panels appear most accurate first, and vertical scale changes on each page. The four traces correspond to images annotated with codes for black female, black male, white female, white male. The threshold is fixed for each algorithm to give FMR = 0.00001 over all (10^8) impostor comparisons. For short time-lapses, the most accurate algorithms give very few errors (FNMR < 0.001) so that the uncertainty estimates are high.*

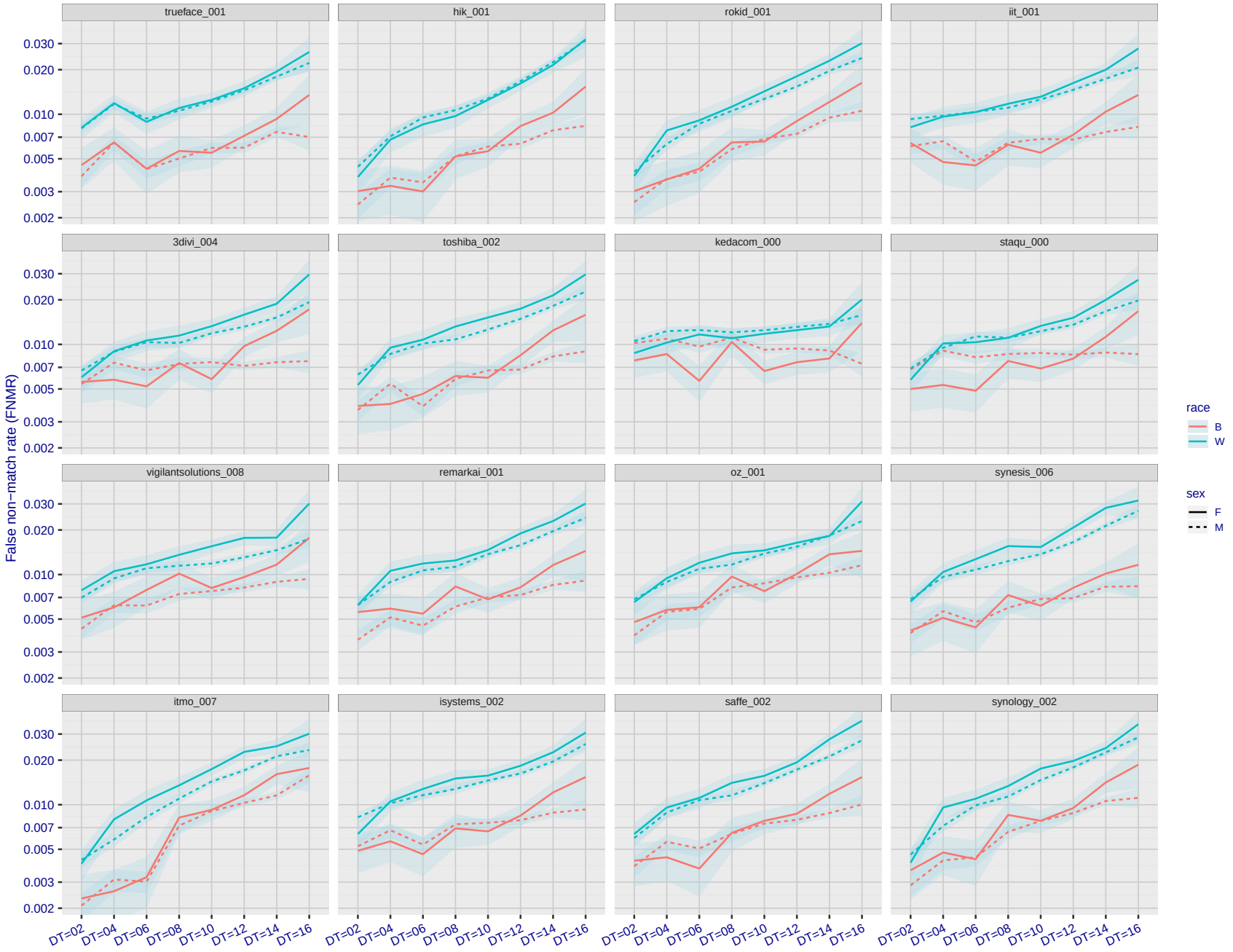

Figure 184: For the mugshot images, FNMR *as a function of elapsed time between initial enrollment and second verification images. The panels appear most accurate first, and vertical scale changes on each page. The four traces correspond to images annotated with codes for black female, black male, white female, white male. The threshold is fixed for each algorithm to give FMR = 0.00001 over all (10^8) impostor comparisons. For short time-lapses, the most accurate algorithms give very few errors (FNMR < 0.001) so that the uncertainty estimates are high.*

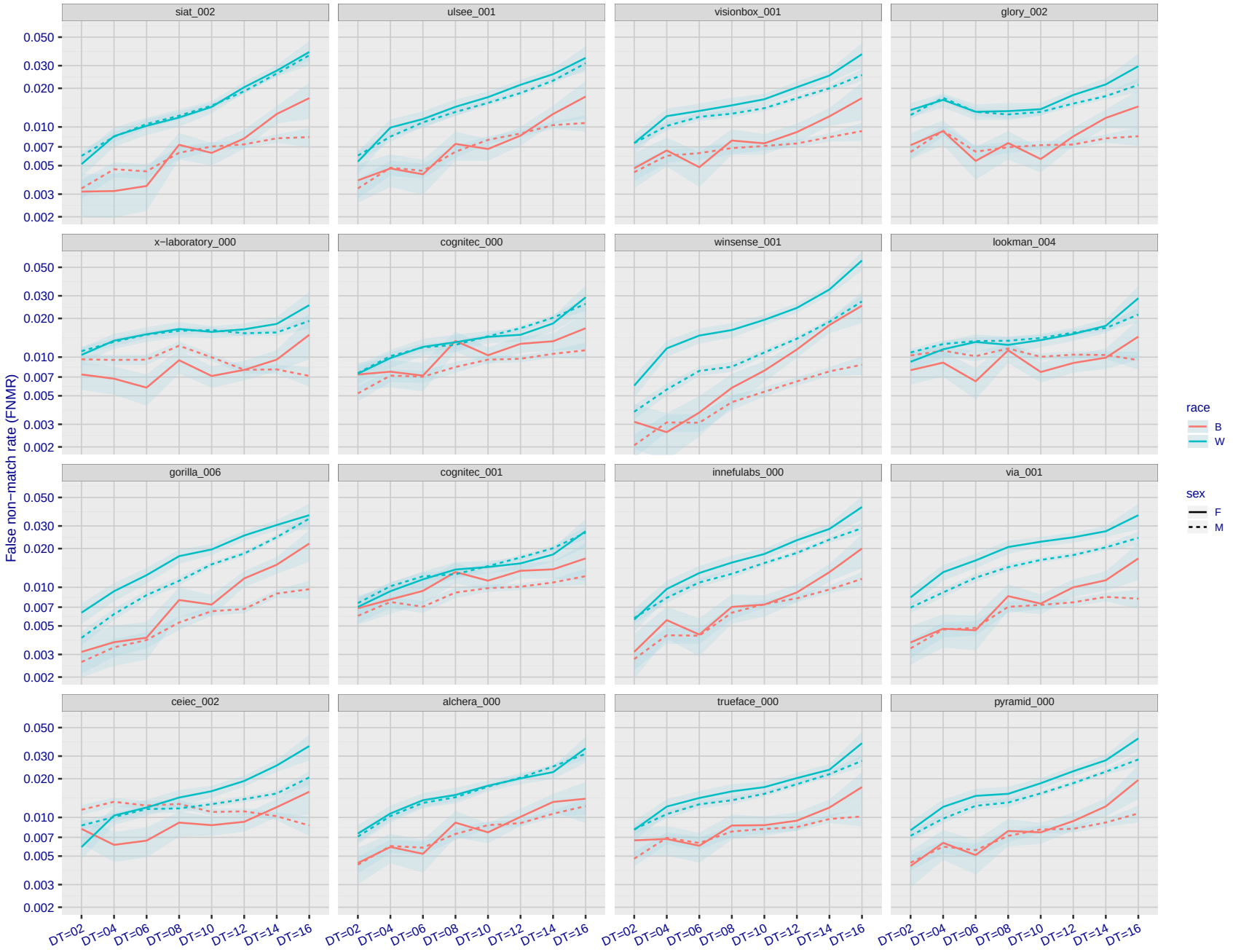

Figure 185: For the mugshot images, FNMR *as a function of elapsed time between initial enrollment and second verification images. The panels appear most accurate first, and vertical scale changes on each page. The four traces correspond to images annotated with codes for black female, black male, white female, white male. The threshold is fixed for each algorithm to give FMR = 0.00001 over all (10^8) impostor comparisons. For short time-lapses, the most accurate algorithms give very few errors (FNMR < 0.001) so that the uncertainty estimates are high.*

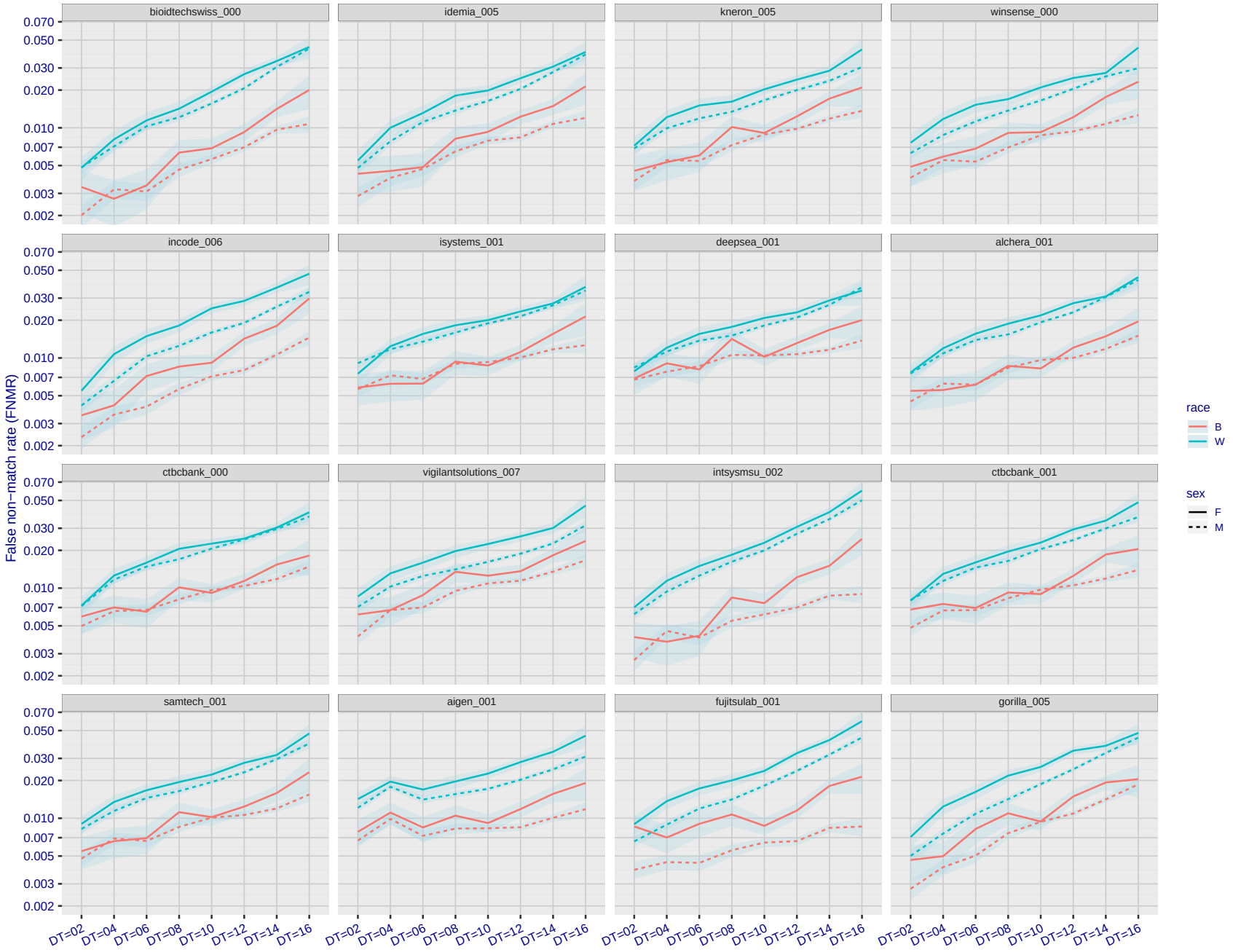

Figure 186: For the mugshot images, FNMR *as a function of elapsed time between initial enrollment and second verification images. The panels appear most accurate first, and vertical scale changes on each page. The four traces correspond to images annotated with codes for black female, black male, white female, white male. The threshold is fixed for each algorithm to give FMR = 0.00001 over all ($\bar{10}^8$) impostor comparisons. For short time-lapses, the most accurate algorithms give very few errors (FNMR < 0.001) so that the uncertainty estimates are high.*

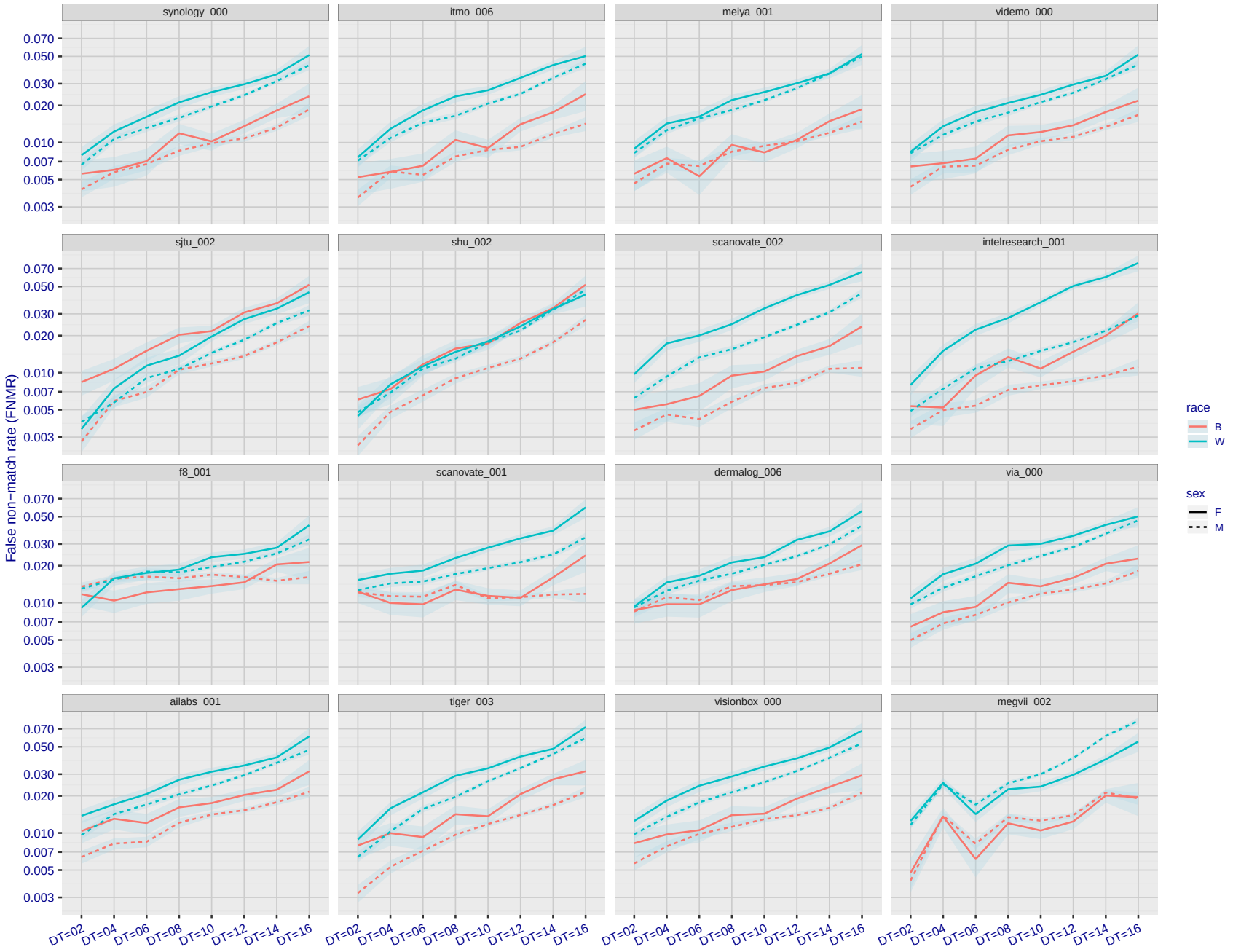

Figure 187: For the mugshot images, FNMR *as a function of elapsed time between initial enrollment and second verification images. The panels appear most accurate first, and vertical scale changes on each page. The four traces correspond to images annotated with codes for black female, black male, white female, white male. The threshold is fixed for each algorithm to give FMR = 0.00001 over all (10^8) impostor comparisons. For short time-lapses, the most accurate algorithms give very few errors (FNMR < 0.001) so that the uncertainty estimates are high.*

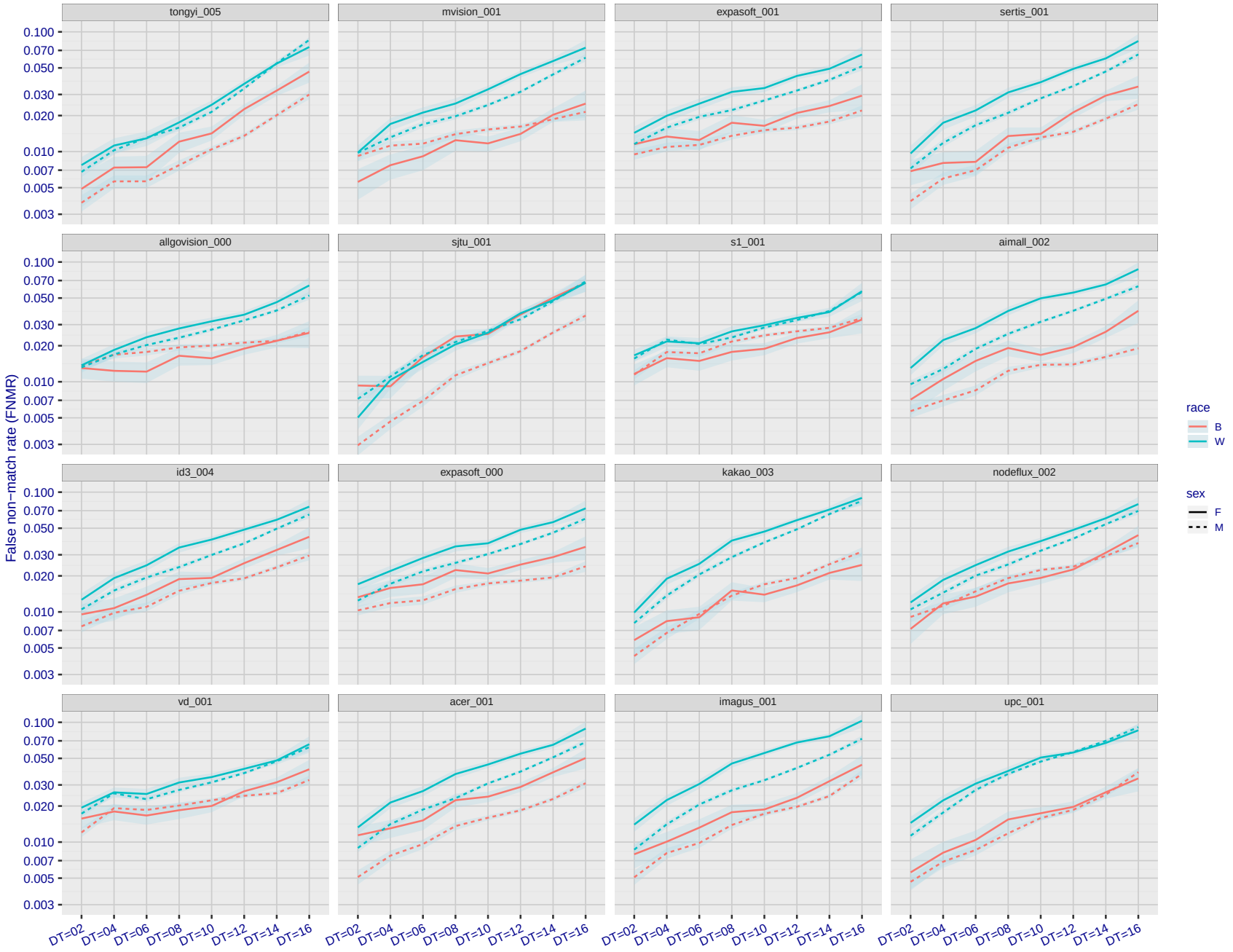

Figure 188: For the mugshot images, FNMR *as a function of elapsed time between initial enrollment and second verification images. The panels appear most accurate first, and vertical scale changes on each page. The four traces correspond to images annotated with codes for black female, black male, white female, white male. The threshold is fixed for each algorithm to give FMR = 0.00001 over all (10^8) impostor comparisons. For short time-lapses, the most accurate algorithms give very few errors (FNMR < 0.001) so that the uncertainty estimates are high.*

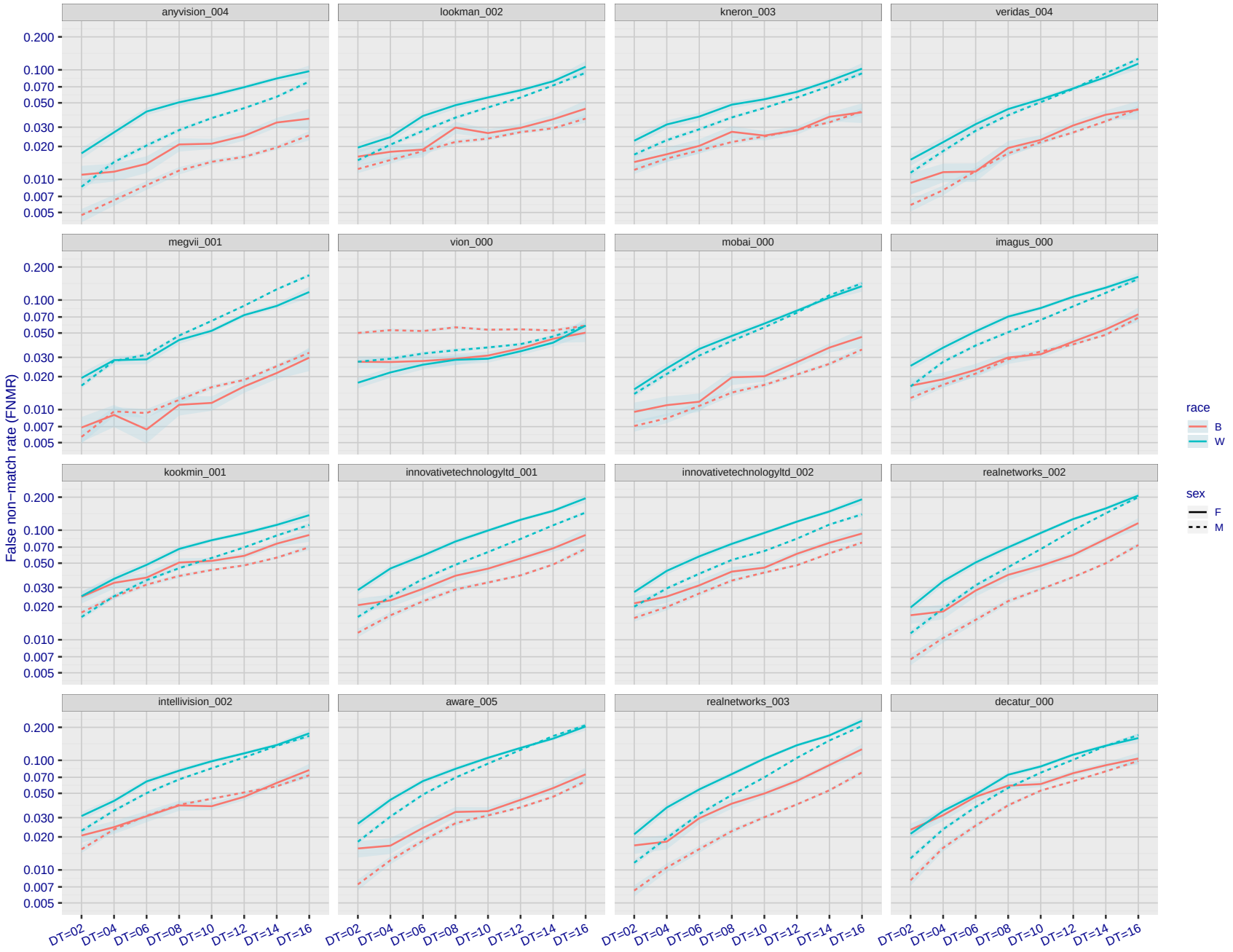

Figure 189: For the mugshot images, FNMR *as a function of elapsed time between initial enrollment and second verification images. The panels appear most accurate first, and vertical scale changes on each page. The four traces correspond to images annotated with codes for black female, black male, white female, white male. The threshold is fixed for each algorithm to give FMR = 0.00001 over all (10^8) impostor comparisons. For short time-lapses, the most accurate algorithms give very few errors (FNMR < 0.001) so that the uncertainty estimates are high.*

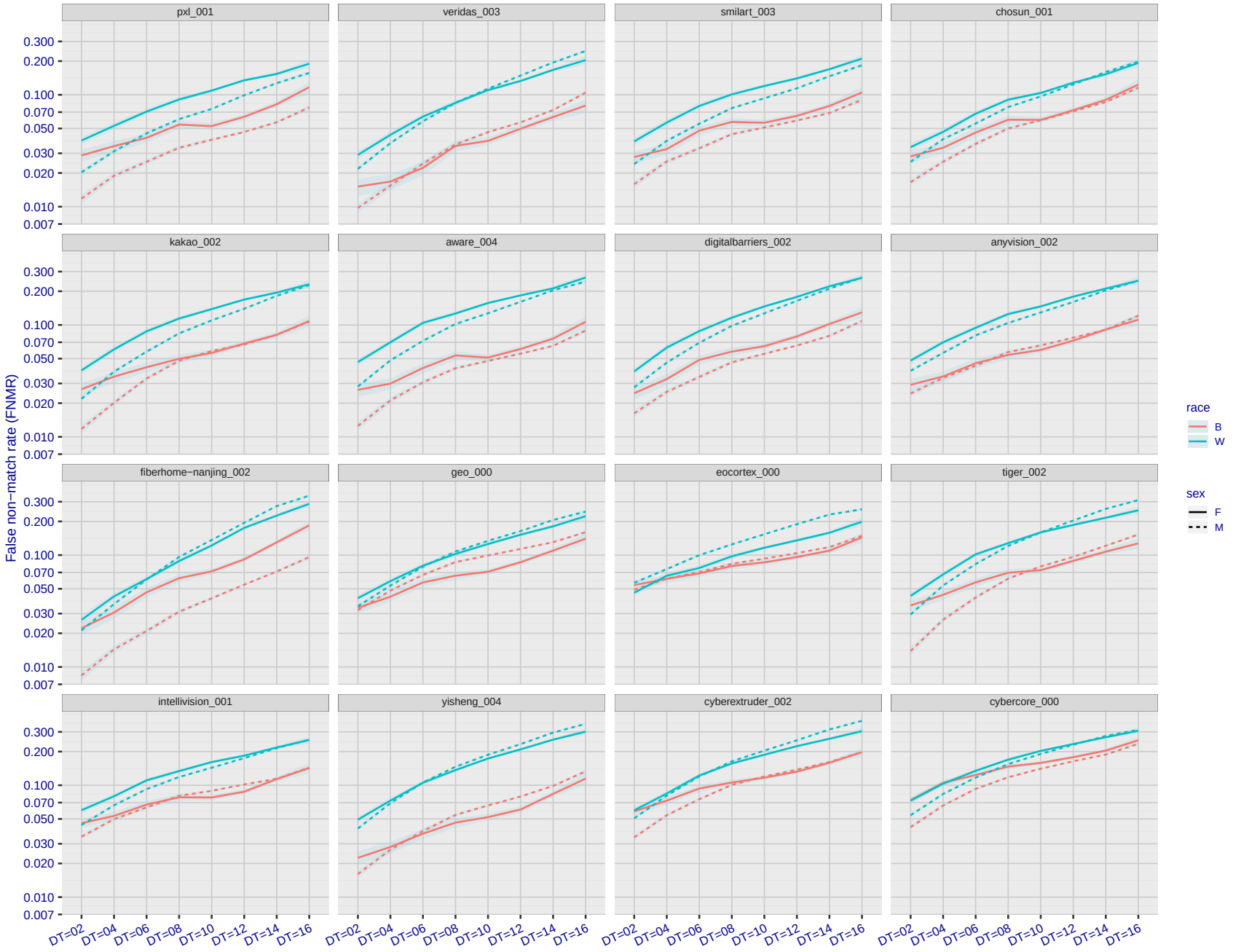

Figure 190: For the mugshot images, FNMR *as a function of elapsed time between initial enrollment and second verification images. The panels appear most accurate first, and vertical scale changes on each page. The four traces correspond to images annotated with codes for black female, black male, white female, white male. The threshold is fixed for each algorithm to give FMR = 0.00001 over all (10^8) impostor comparisons. For short time-lapses, the most accurate algorithms give very few errors (FNMR < 0.001) so that the uncertainty estimates are high.*

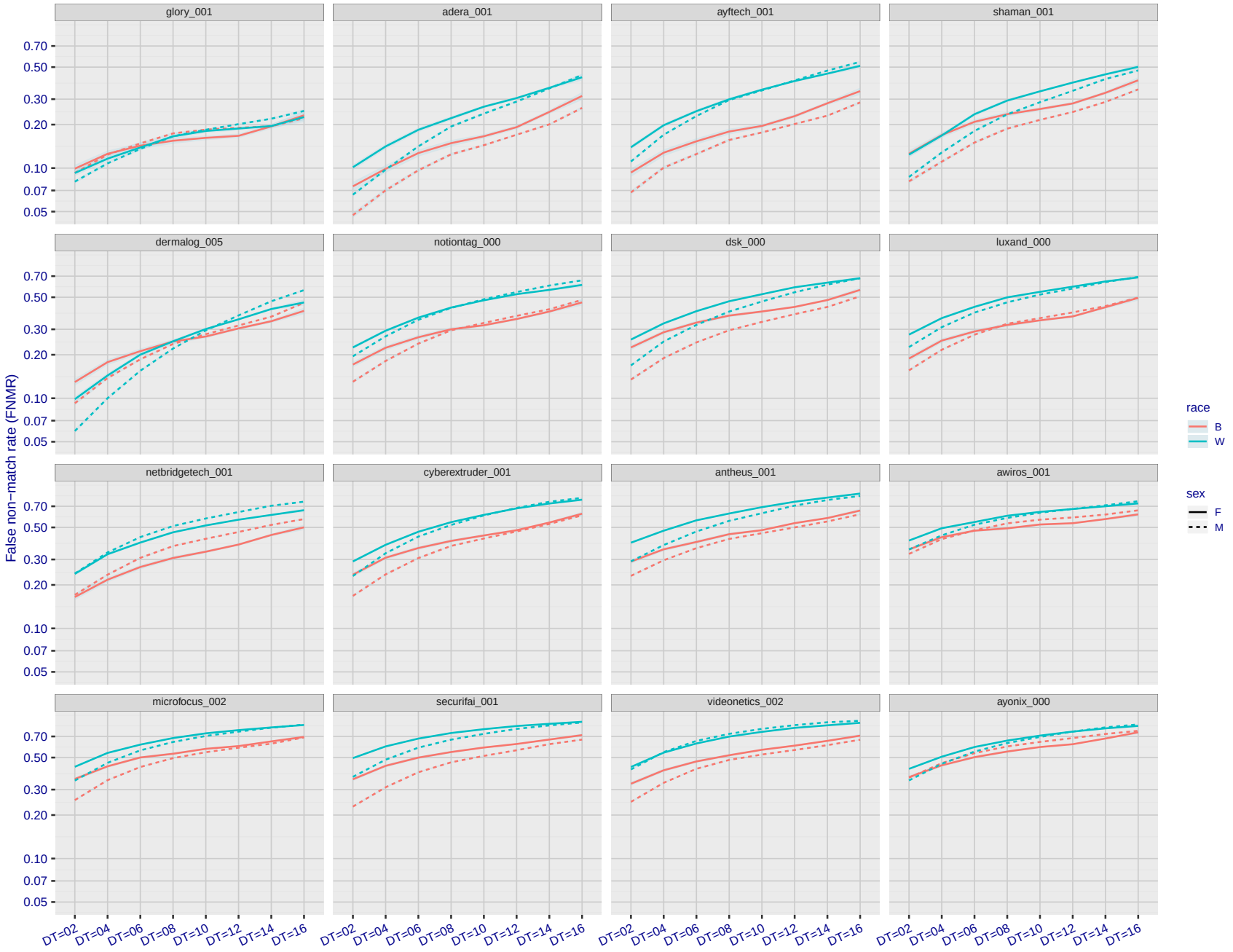

Figure 191: For the mugshot images, FNMR as a function of elapsed time between initial enrollment and second verification images. The panels appear most accurate first, and vertical scale changes on each page. The four traces correspond to images annotated with codes for black female, black male, white female, white male. The threshold is fixed for each algorithm to give FMR = 0.00001 over all (10^8) impostor comparisons. For short time-lapses, the most accurate algorithms give very few errors (FNMR < 0.001) so that the uncertainty estimates are high.

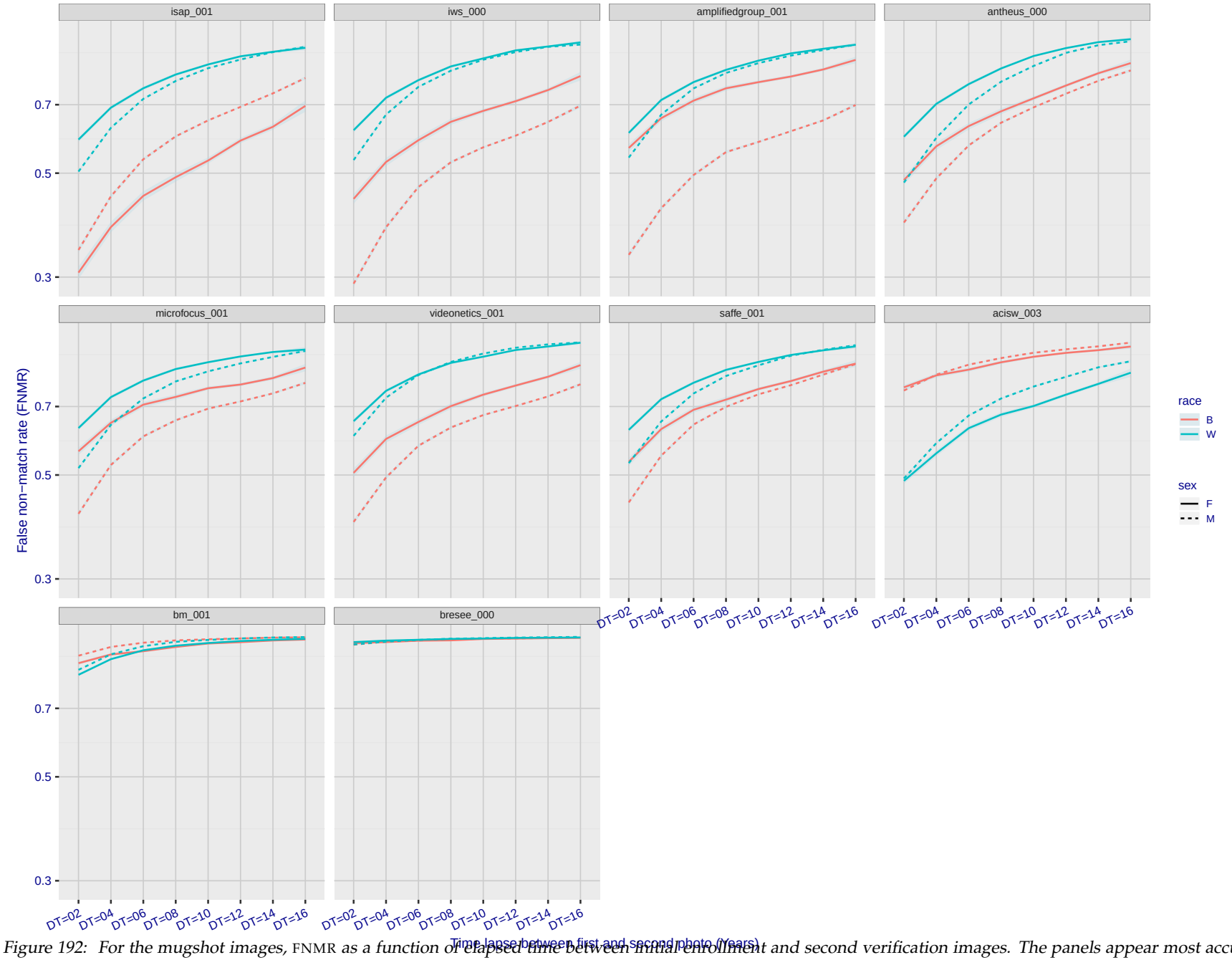

Figure 192: For the mugshot images, FNMR *as a function of elapsed time between initial enrollment and second verification images. The panels appear most accurate first, and vertical scale changes on each page. The four traces correspond to images annotated with codes for black female, black male, white female, white male. The threshold is fixed for each algorithm to give FMR = 0.00001 over all* (10^8) *impostor comparisons. For short time-lapses, the most accurate algorithms give very few errors (FNMR* < 0.001*) so that the uncertainty estimates are high.*

3.5.3 Effect of age on genuine subjects

Background: Faces change appearance throughout life. Face recognition algorithms have previously beeen reported to give better accuracy on older individuals (See NIST IR 8009).

Goal: To quantify false non-match rates (FNMR) as a function of age, without an ageing component.

Methods: Using the visa images, which span fewer than five years, thresholds are determined that give FMR = 0.001 and 0.0001 over the entire impostor set. Then FNMR is measured over 1000 bootstrap replications of the genuine scores.

Results: For the visa images, Figure 213 shows how false non-match rates for genuine users, as a function of age group.

The notable aspects are:

- Younger subjects give considerably higher FNMR. This is likely due to rapid growth and change in facial appearance.
- FNMR trends down throughout life. The last bin, AGE $>$ 72, contains fewer than 140 mated pairs, and may be affected by small sample size.

FNMR(T) "False non-match rate"
FMR(T) "False match rate"

Figure 193: For the visa images, the dots show FNMR by age group for two operating thresholds corresponding to FMR = $\{0.001, 0.0001\}$ computed over all on the order of 10^{10} impostor scores. The FMR in each bin will vary also - see subsequent impostor heatmaps in sec. 3.6.2. Given a pair of face images taken at different times, we assign the comparison to the bin that is the arithmetic average of the subject's ages. This plot shows only the effect of age, not ageing. The number of comparisons in each bin is generally in the thousands, however the first and last bins are computed over 149 and 124 respectively. The error rates in some (adult) cases are zero, and in others the DET is flat so the error rates at the two thresholds are identical. The lines span 1% and 99% of boostrap replicated FNMR estimates.

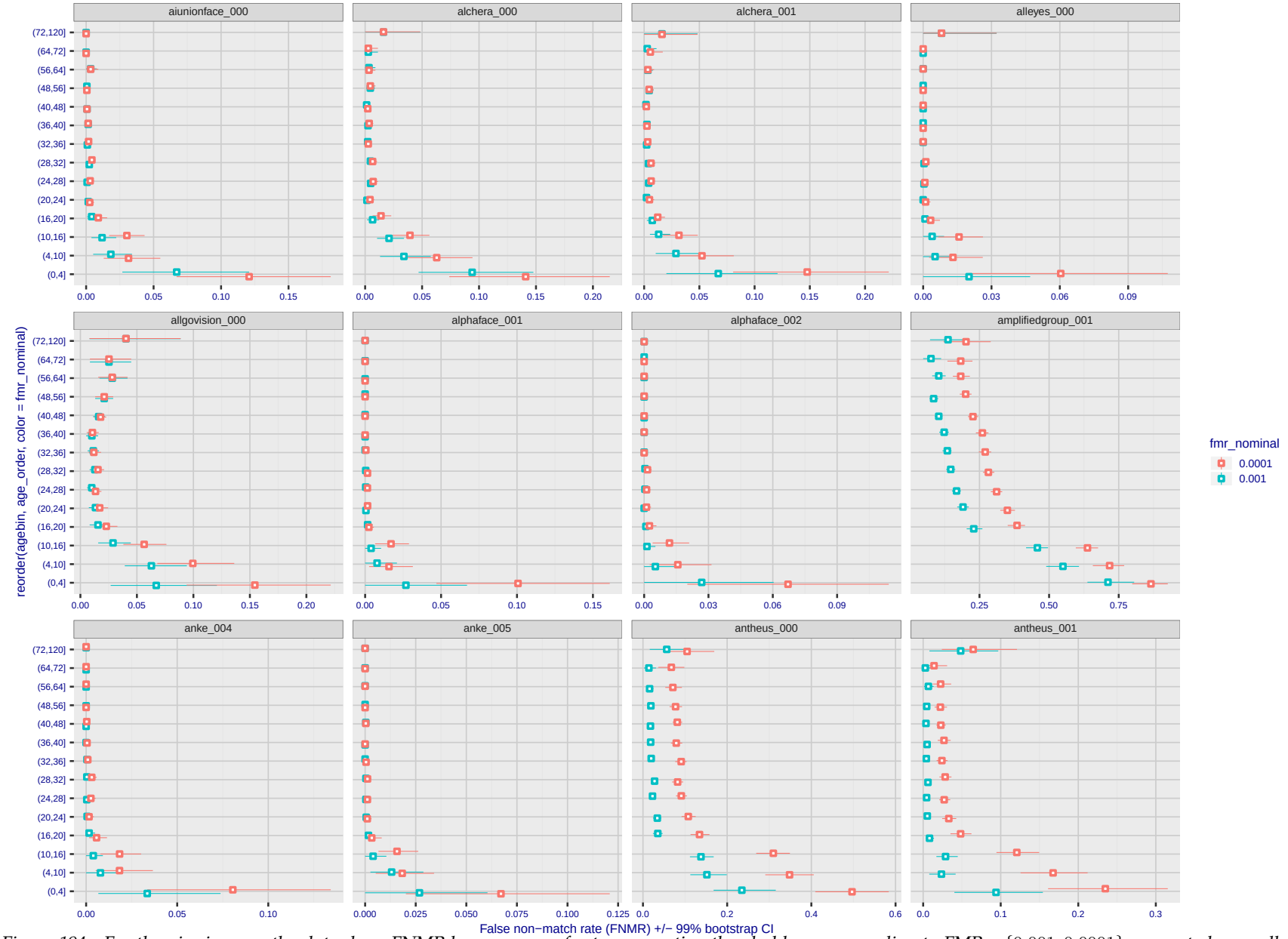

Figure 194: For the visa images, the dots show FNMR by age group for two operating thresholds corresponding to FMR = $\{0.001, 0.0001\}$ computed over all on the order of 10^{10} impostor scores. The FMR in each bin will vary also - see subsequent impostor heatmaps in sec. 3.6.2. Given a pair of face images taken at different times, we assign the comparison to the bin that is the arithmetic average of the subject's ages. This plot shows only the effect of age, not ageing. The number of comparisons in each bin is generally in the thousands, however the first and last bins are computed over 149 and 124 respectively. The error rates in some (adult) cases are zero, and in others the DET is flat so the error rates at the two thresholds are identical. The lines span 1% and 99% of boostrap replicated FNMR estimates.

Figure 195: For the visa images, the dots show FNMR by age group for two operating thresholds corresponding to FMR = $\{0.001, 0.0001\}$ computed over all on the order of 10^{10} impostor scores. The FMR in each bin will vary also - see subsequent impostor heatmaps in sec. 3.6.2. Given a pair of face images taken at different times, we assign the comparison to the bin that is the arithmetic average of the subject's ages. This plot shows only the effect of age, not ageing. The number of comparisons in each bin is generally in the thousands, however the first and last bins are computed over 149 and 124 respectively. The error rates in some (adult) cases are zero, and in others the DET is flat so the error rates at the two thresholds are identical. The lines span 1% and 99% of boostrap replicated FNMR estimates.

Figure 196: For the visa images, the dots show FNMR by age group for two operating thresholds corresponding to FMR = $\{0.001, 0.0001\}$ computed over all on the order of 10^{10} impostor scores. The FMR in each bin will vary also - see subsequent impostor heatmaps in sec. 3.6.2. Given a pair of face images taken at different times, we assign the comparison to the bin that is the arithmetic average of the subject's ages. This plot shows only the effect of age, not ageing. The number of comparisons in each bin is generally in the thousands, however the first and last bins are computed over 149 and 124 respectively. The error rates in some (adult) cases are zero, and in others the DET is flat so the error rates at the two thresholds are identical. The lines span 1% and 99% of boostrap replicated FNMR estimates.

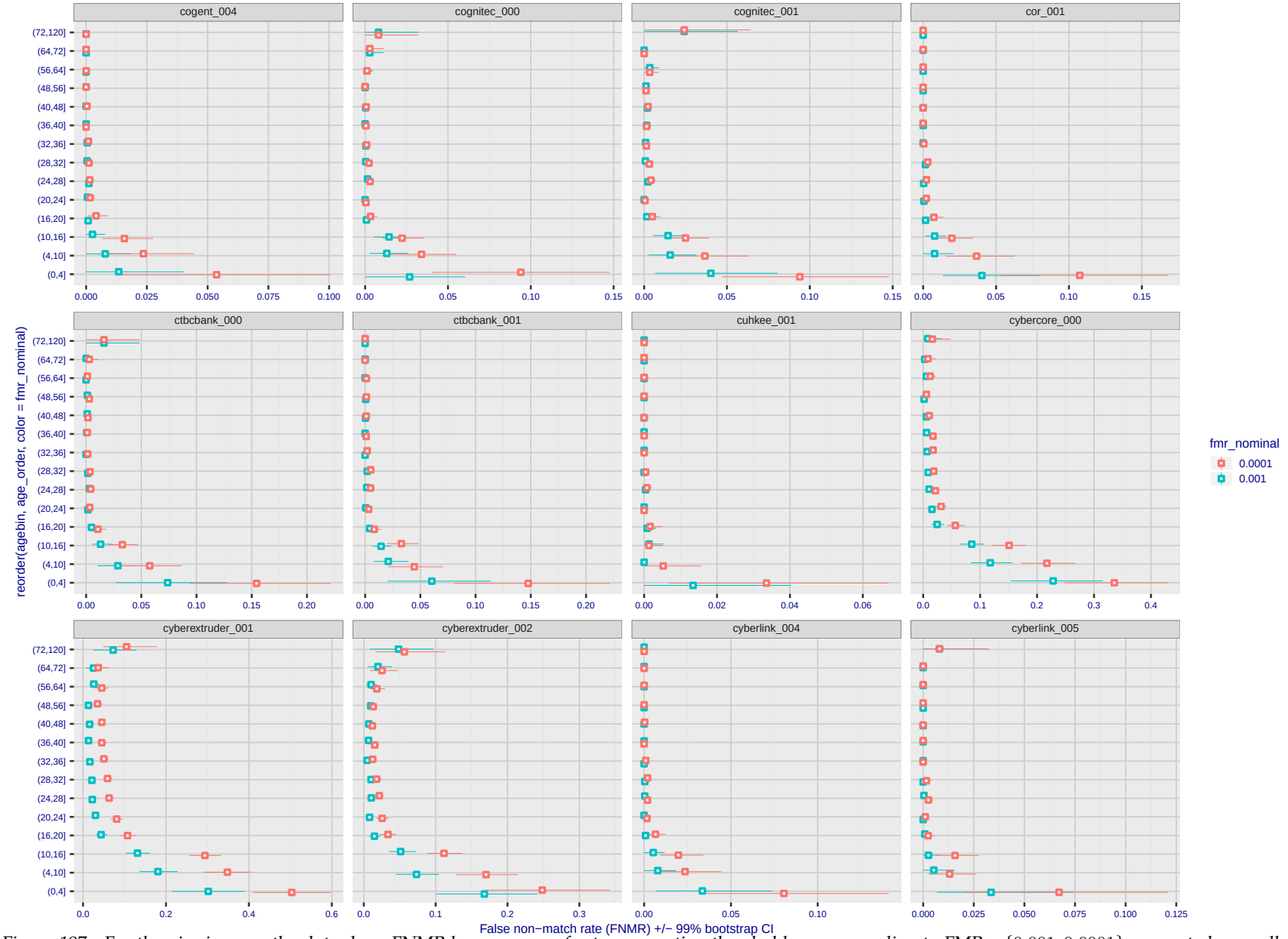

Figure 197: For the visa images, the dots show FNMR by age group for two operating thresholds corresponding to FMR = $\{0.001, 0.0001\}$ computed over all on the order of 10^{10} impostor scores. The FMR in each bin will vary also - see subsequent impostor heatmaps in sec. 3.6.2. Given a pair of face images taken at different times, we assign the comparison to the bin that is the arithmetic average of the subject's ages. This plot shows only the effect of age, not ageing. The number of comparisons in each bin is generally in the thousands, however the first and last bins are computed over 149 and 124 respectively. The error rates in some (adult) cases are zero, and in others the DET is flat so the error rates at the two thresholds are identical. The lines span 1% and 99% of boostrap replicated FNMR estimates.

Figure 198: For the visa images, the dots show FNMR by age group for two operating thresholds corresponding to FMR = $\{0.001, 0.0001\}$ computed over all on the order of 10^{10} impostor scores. The FMR in each bin will vary also - see subsequent impostor heatmaps in sec. 3.6.2. Given a pair of face images taken at different times, we assign the comparison to the bin that is the arithmetic average of the subject's ages. This plot shows only the effect of age, not ageing. The number of comparisons in each bin is generally in the thousands, however the first and last bins are computed over 149 and 124 respectively. The error rates in some (adult) cases are zero, and in others the DET is flat so the error rates at the two thresholds are identical. The lines span 1% and 99% of boostrap replicated FNMR estimates.

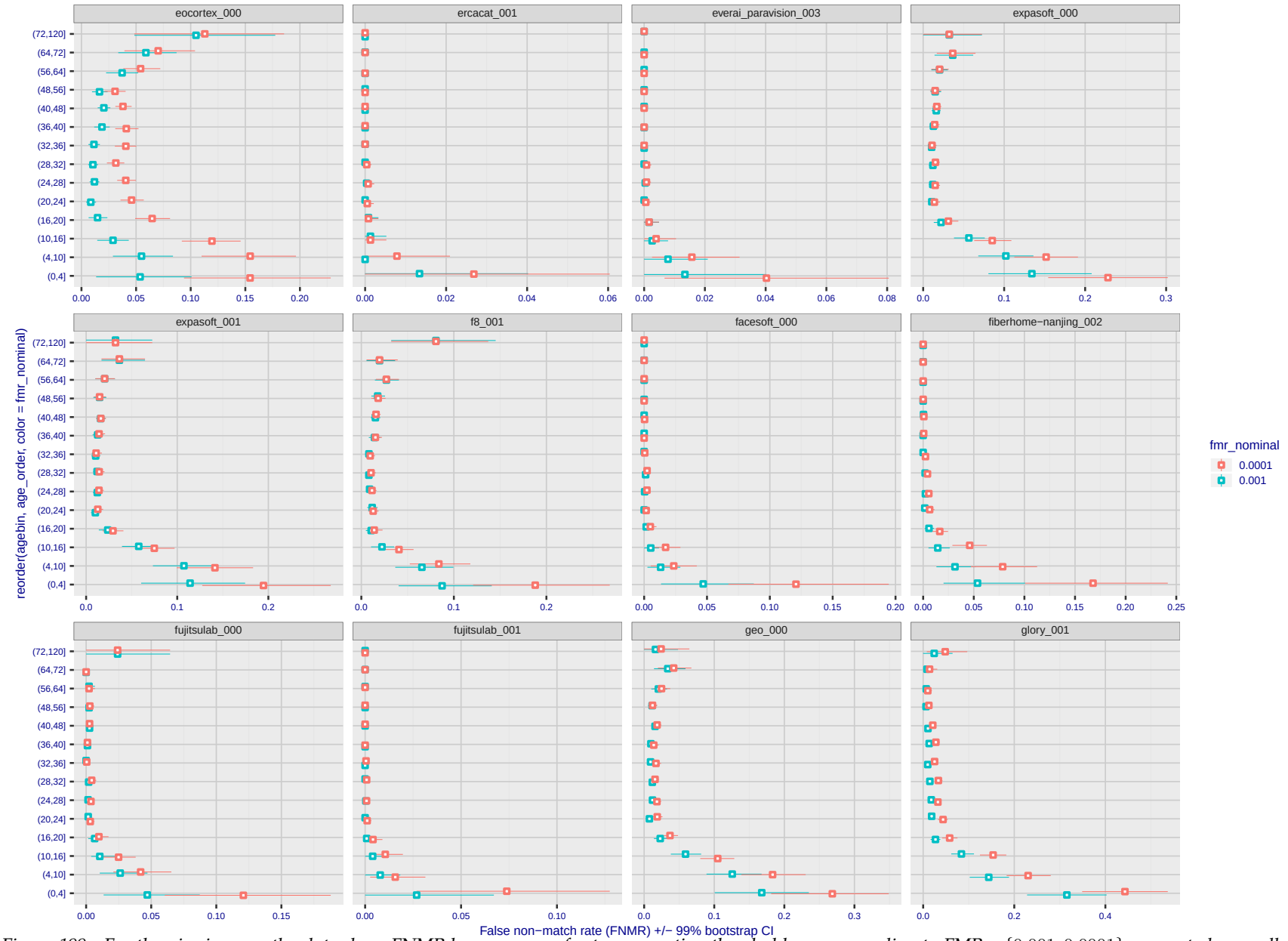

Figure 199: For the visa images, the dots show FNMR by age group for two operating thresholds corresponding to FMR = $\{0.001, 0.0001\}$ computed over all on the order of 10^{10} impostor scores. The FMR in each bin will vary also - see subsequent impostor heatmaps in sec. 3.6.2. Given a pair of face images taken at different times, we assign the comparison to the bin that is the arithmetic average of the subject's ages. This plot shows only the effect of age, not ageing. The number of comparisons in each bin is generally in the thousands, however the first and last bins are computed over 149 and 124 respectively. The error rates in some (adult) cases are zero, and in others the DET is flat so the error rates at the two thresholds are identical. The lines span 1% and 99% of boostrap replicated FNMR estimates.

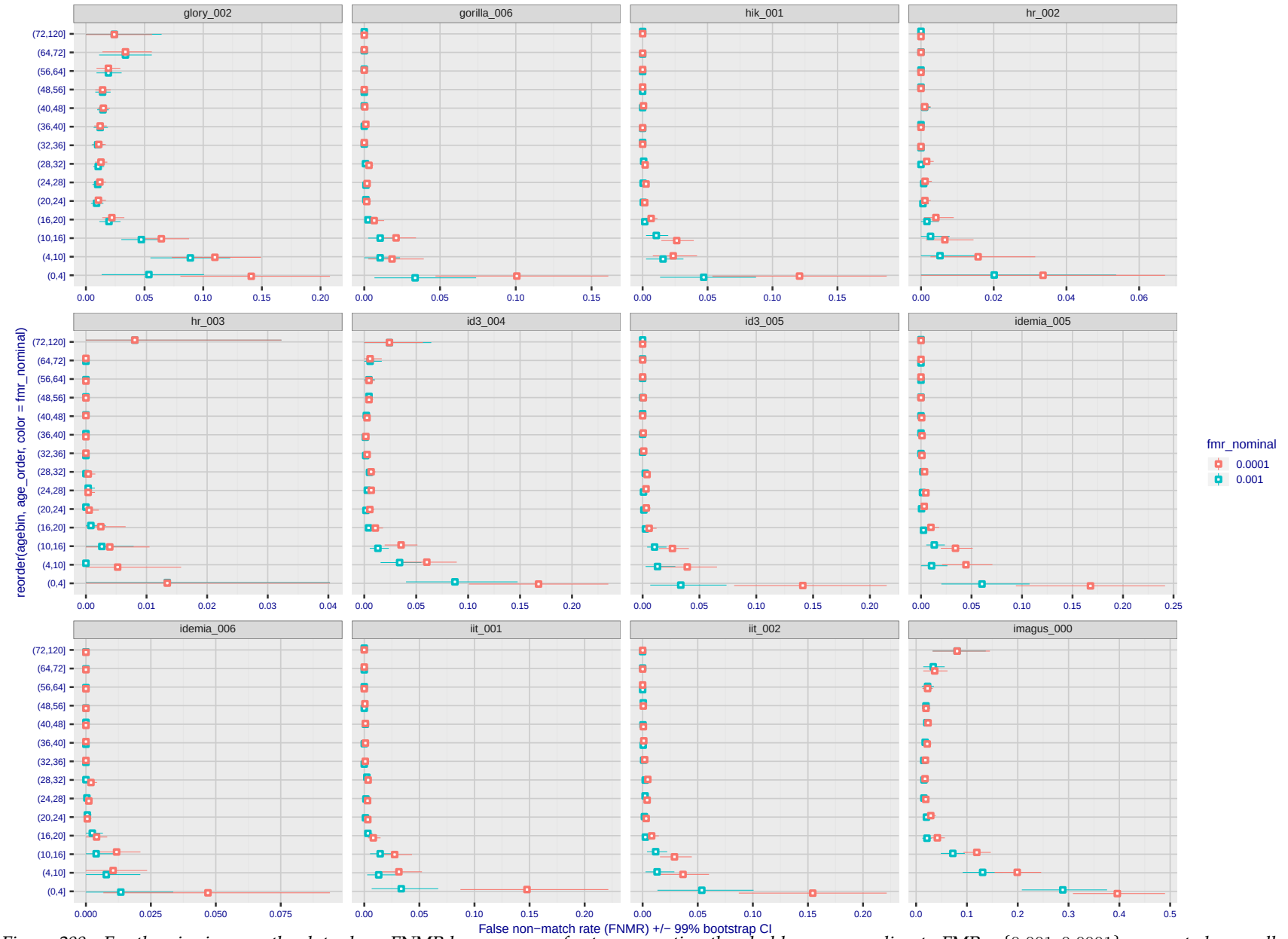

Figure 200: For the visa images, the dots show FNMR by age group for two operating thresholds corresponding to FMR = $\{0.001, 0.0001\}$ computed over all on the order of 10^{10} impostor scores. The FMR in each bin will vary also - see subsequent impostor heatmaps in sec. 3.6.2. Given a pair of face images taken at different times, we assign the comparison to the bin that is the arithmetic average of the subject's ages. This plot shows only the effect of age, not ageing. The number of comparisons in each bin is generally in the thousands, however the first and last bins are computed over 149 and 124 respectively. The error rates in some (adult) cases are zero, and in others the DET is flat so the error rates at the two thresholds are identical. The lines span 1% and 99% of boostrap replicated FNMR estimates.

Figure 201: For the visa images, the dots show FNMR by age group for two operating thresholds corresponding to FMR = $\{0.001, 0.0001\}$ computed over all on the order of 10^{10} impostor scores. The FMR in each bin will vary also - see subsequent impostor heatmaps in sec. 3.6.2. Given a pair of face images taken at different times, we assign the comparison to the bin that is the arithmetic average of the subject's ages. This plot shows only the effect of age, not ageing. The number of comparisons in each bin is generally in the thousands, however the first and last bins are computed over 149 and 124 respectively. The error rates in some (adult) cases are zero, and in others the DET is flat so the error rates at the two thresholds are identical. The lines span 1% and 99% of boostrap replicated FNMR estimates.

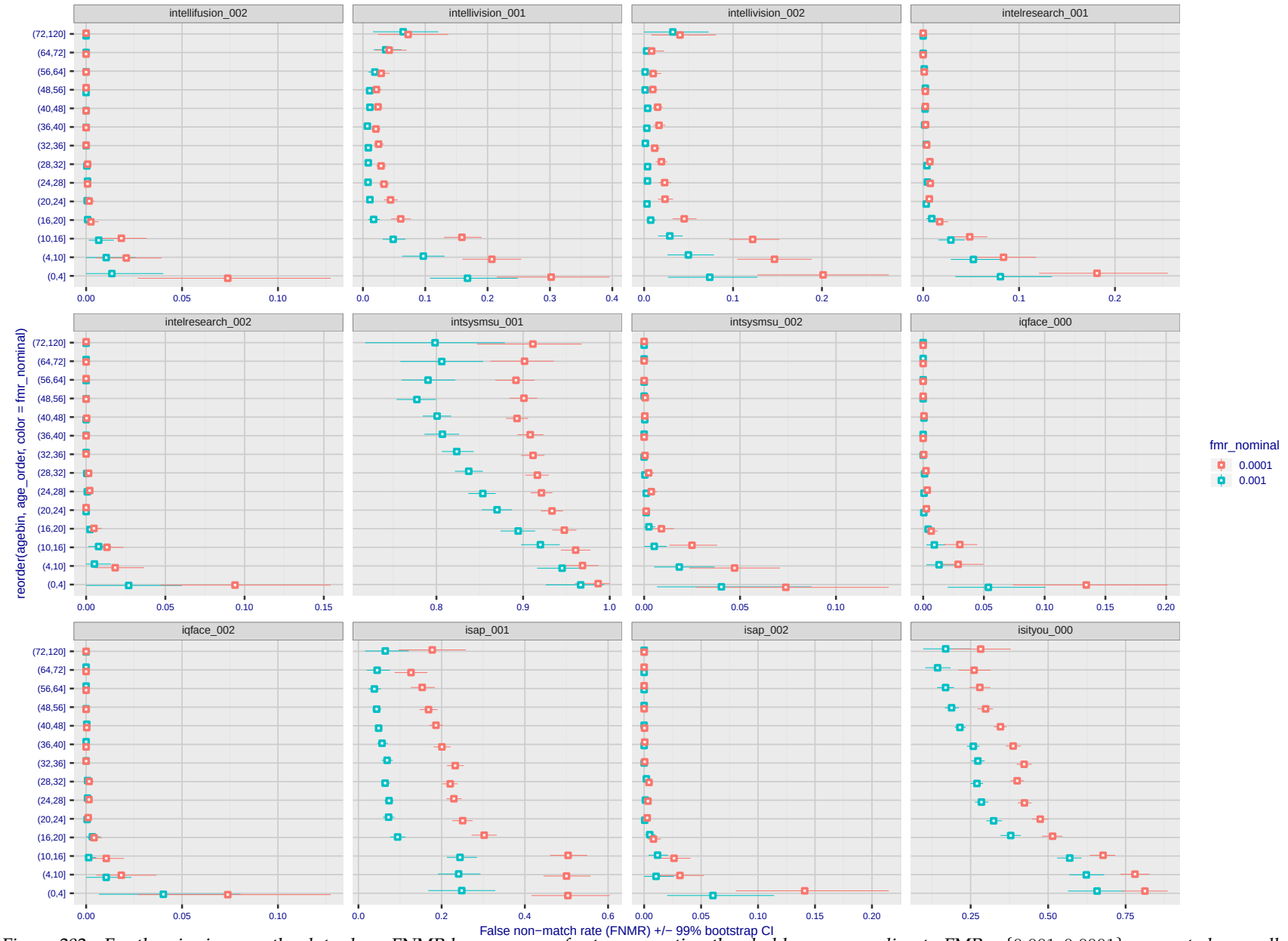

Figure 202: For the visa images, the dots show FNMR by age group for two operating thresholds corresponding to FMR = $\{0.001, 0.0001\}$ computed over all on the order of 10^{10} impostor scores. The FMR in each bin will vary also - see subsequent impostor heatmaps in sec. 3.6.2. Given a pair of face images taken at different times, we assign the comparison to the bin that is the arithmetic average of the subject's ages. This plot shows only the effect of age, not ageing. The number of comparisons in each bin is generally in the thousands, however the first and last bins are computed over 149 and 124 respectively. The error rates in some (adult) cases are zero, and in others the DET is flat so the error rates at the two thresholds are identical. The lines span 1% and 99% of boostrap replicated FNMR estimates.

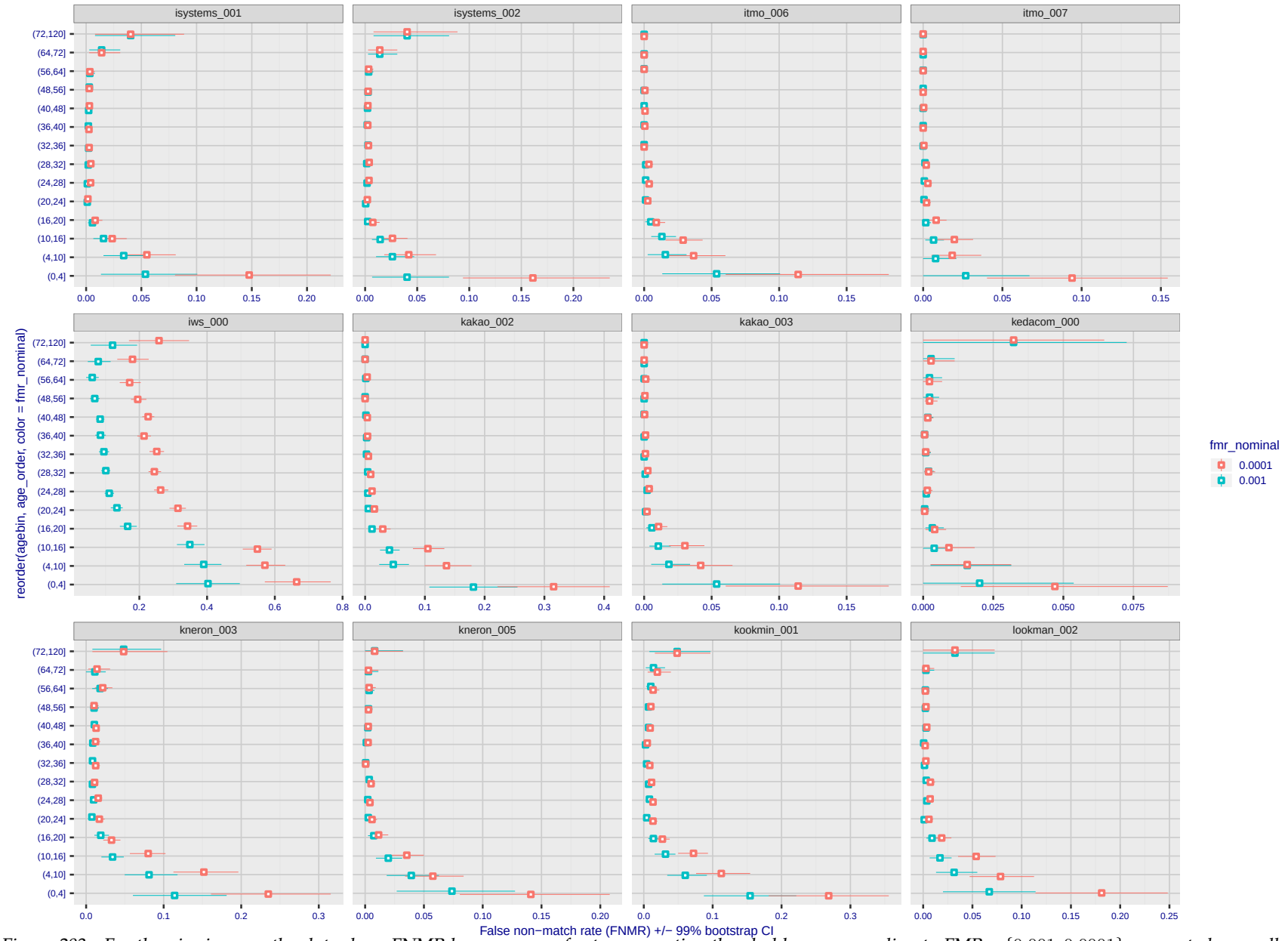

Figure 203: For the visa images, the dots show FNMR by age group for two operating thresholds corresponding to FMR = $\{0.001, 0.0001\}$ computed over all on the order of 10^{10} impostor scores. The FMR in each bin will vary also - see subsequent impostor heatmaps in sec. 3.6.2. Given a pair of face images taken at different times, we assign the comparison to the bin that is the arithmetic average of the subject's ages. This plot shows only the effect of age, not ageing. The number of comparisons in each bin is generally in the thousands, however the first and last bins are computed over 149 and 124 respectively. The error rates in some (adult) cases are zero, and in others the DET is flat so the error rates at the two thresholds are identical. The lines span 1% and 99% of boostrap replicated FNMR estimates.

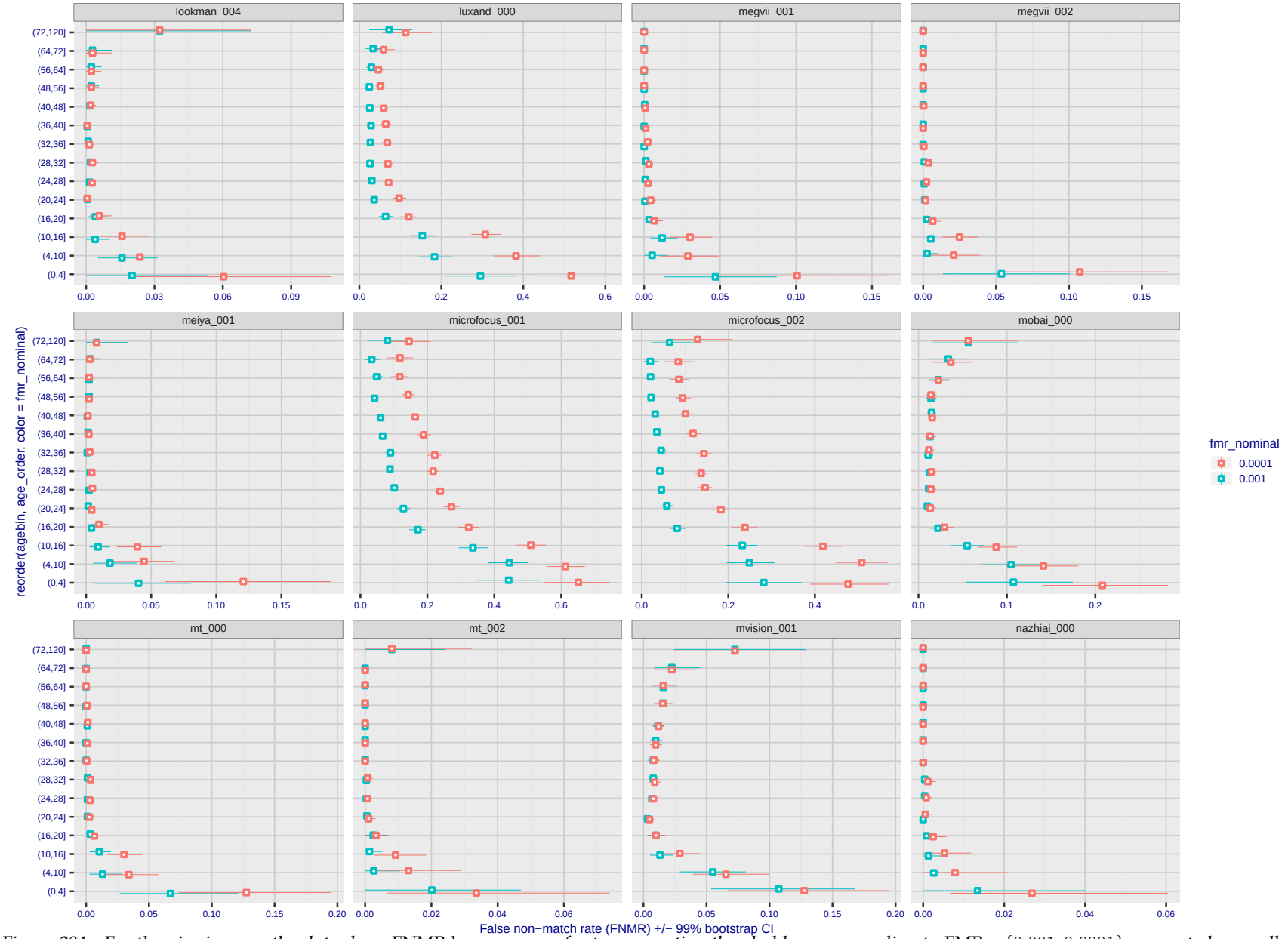

Figure 204: For the visa images, the dots show FNMR by age group for two operating thresholds corresponding to FMR = $\{0.001, 0.0001\}$ computed over all on the order of 10^{10} impostor scores. The FMR in each bin will vary also - see subsequent impostor heatmaps in sec. 3.6.2. Given a pair of face images taken at different times, we assign the comparison to the bin that is the arithmetic average of the subject's ages. This plot shows only the effect of age, not ageing. The number of comparisons in each bin is generally in the thousands, however the first and last bins are computed over 149 and 124 respectively. The error rates in some (adult) cases are zero, and in others the DET is flat so the error rates at the two thresholds are identical. The lines span 1% and 99% of boostrap replicated FNMR estimates.

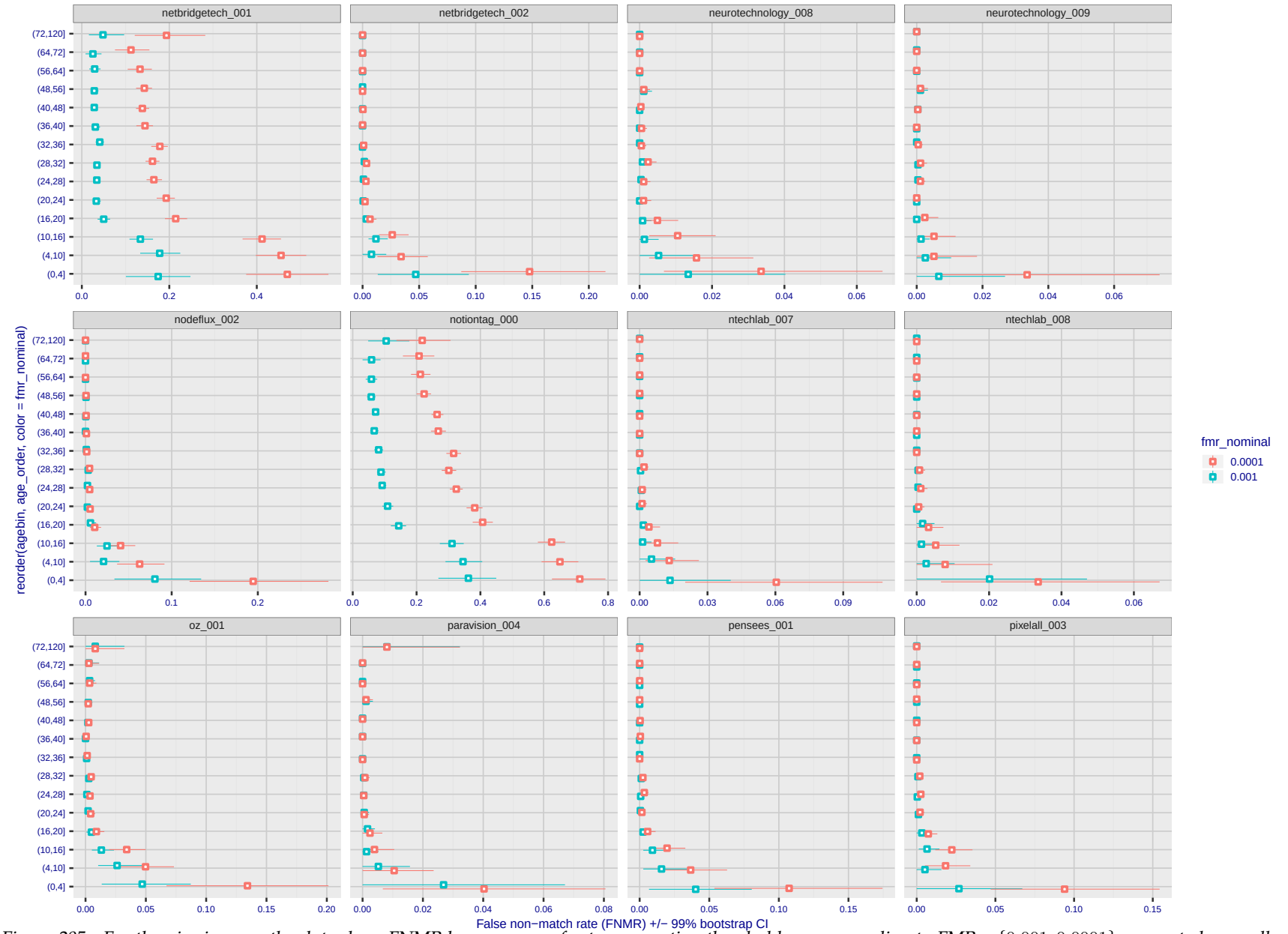

Figure 205: For the visa images, the dots show FNMR by age group for two operating thresholds corresponding to FMR = $\{0.001, 0.0001\}$ computed over all on the order of 10^{10} impostor scores. The FMR in each bin will vary also - see subsequent impostor heatmaps in sec. 3.6.2. Given a pair of face images taken at different times, we assign the comparison to the bin that is the arithmetic average of the subject's ages. This plot shows only the effect of age, not ageing. The number of comparisons in each bin is generally in the thousands, however the first and last bins are computed over 149 and 124 respectively. The error rates in some (adult) cases are zero, and in others the DET is flat so the error rates at the two thresholds are identical. The lines span 1% and 99% of boostrap replicated FNMR estimates.

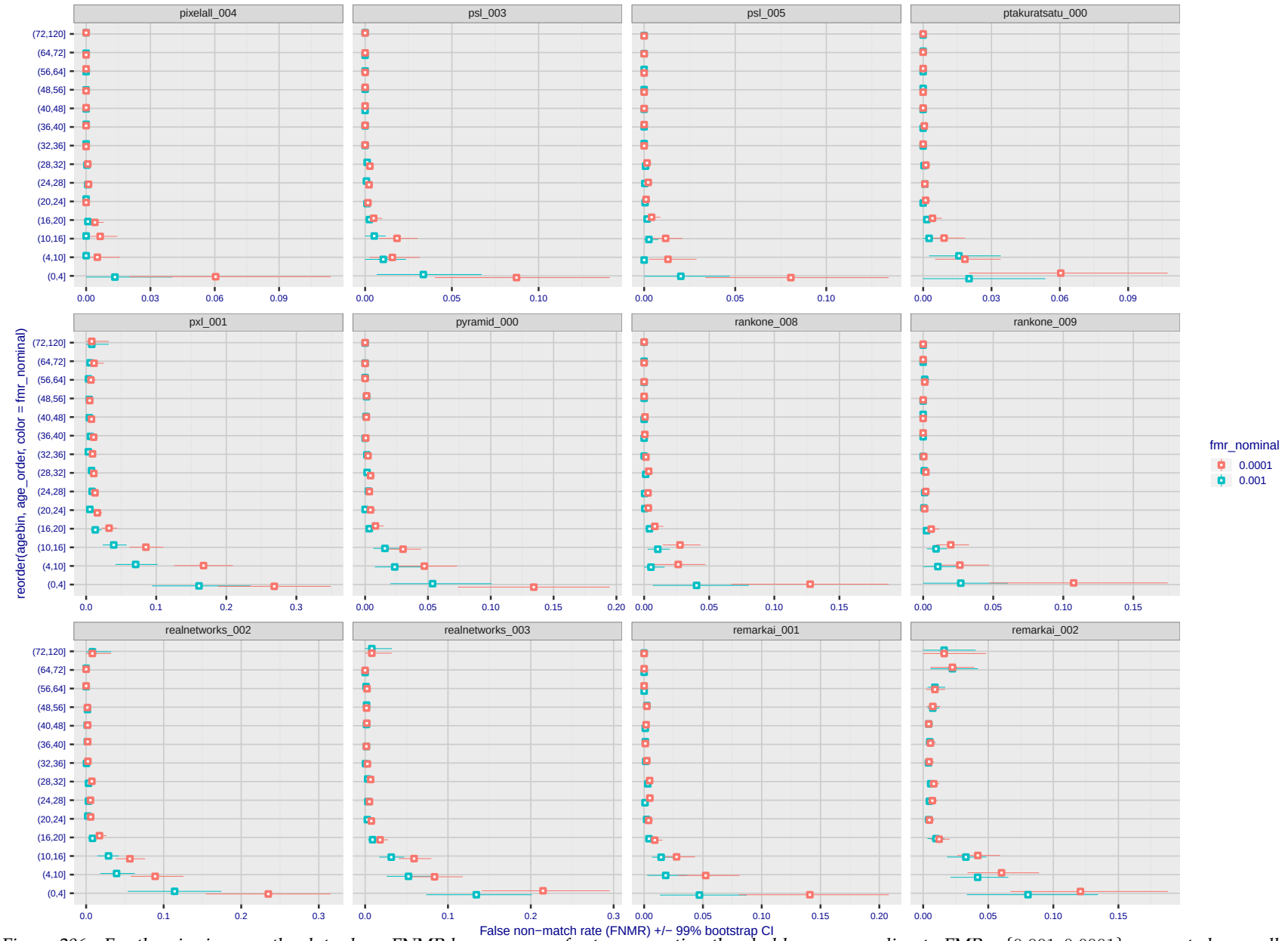

Figure 206: For the visa images, the dots show FNMR by age group for two operating thresholds corresponding to FMR = $\{0.001, 0.0001\}$ computed over all on the order of 10^{10} impostor scores. The FMR in each bin will vary also - see subsequent impostor heatmaps in sec. 3.6.2. Given a pair of face images taken at different times, we assign the comparison to the bin that is the arithmetic average of the subject's ages. This plot shows only the effect of age, not ageing. The number of comparisons in each bin is generally in the thousands, however the first and last bins are computed over 149 and 124 respectively. The error rates in some (adult) cases are zero, and in others the DET is flat so the error rates at the two thresholds are identical. The lines span 1% and 99% of boostrap replicated FNMR estimates.

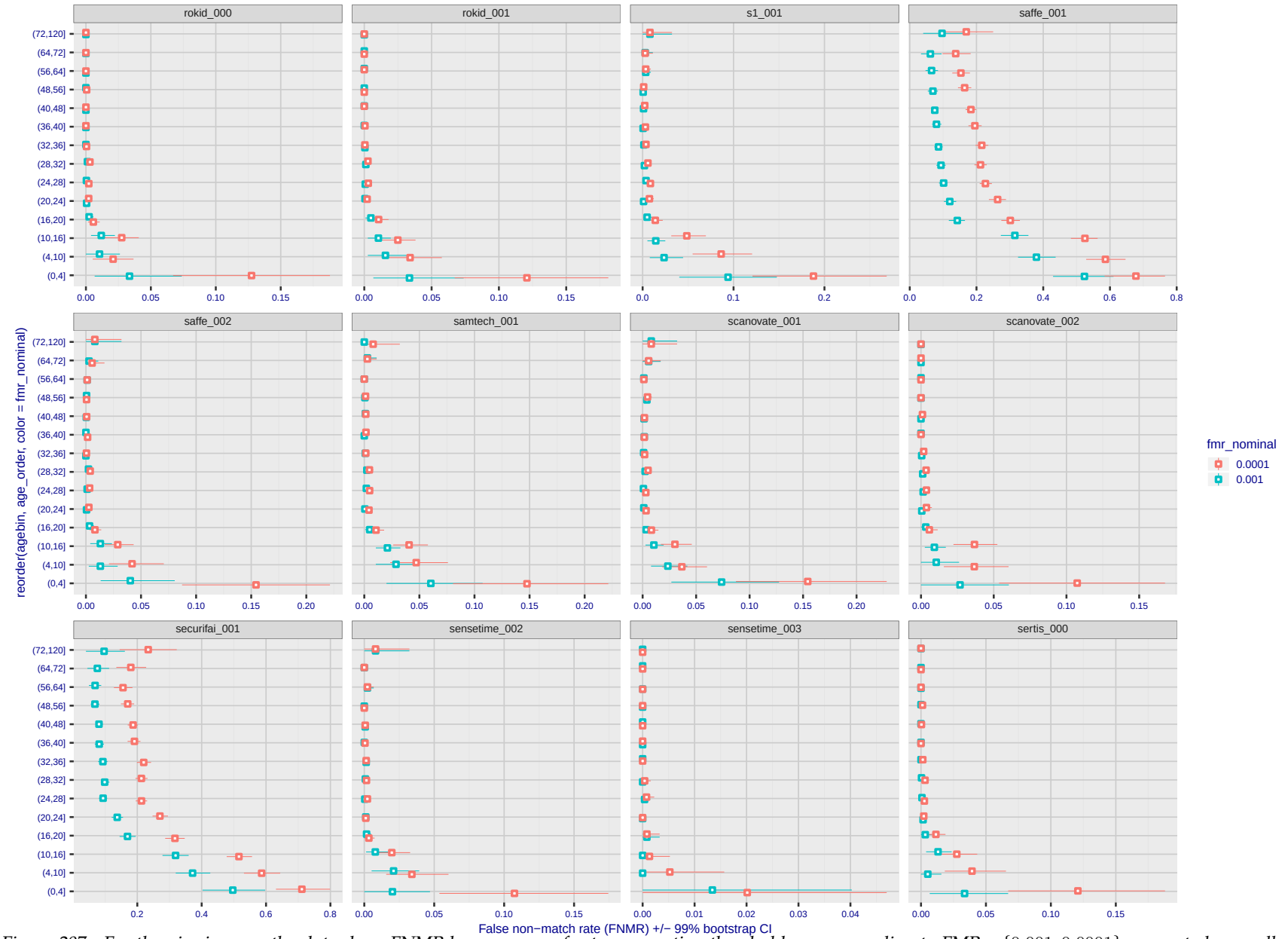

Figure 207: For the visa images, the dots show FNMR by age group for two operating thresholds corresponding to FMR = $\{0.001, 0.0001\}$ computed over all on the order of 10^{10} impostor scores. The FMR in each bin will vary also - see subsequent impostor heatmaps in sec. 3.6.2. Given a pair of face images taken at different times, we assign the comparison to the bin that is the arithmetic average of the subject's ages. This plot shows only the effect of age, not ageing. The number of comparisons in each bin is generally in the thousands, however the first and last bins are computed over 149 and 124 respectively. The error rates in some (adult) cases are zero, and in others the DET is flat so the error rates at the two thresholds are identical. The lines span 1% and 99% of boostrap replicated FNMR estimates.

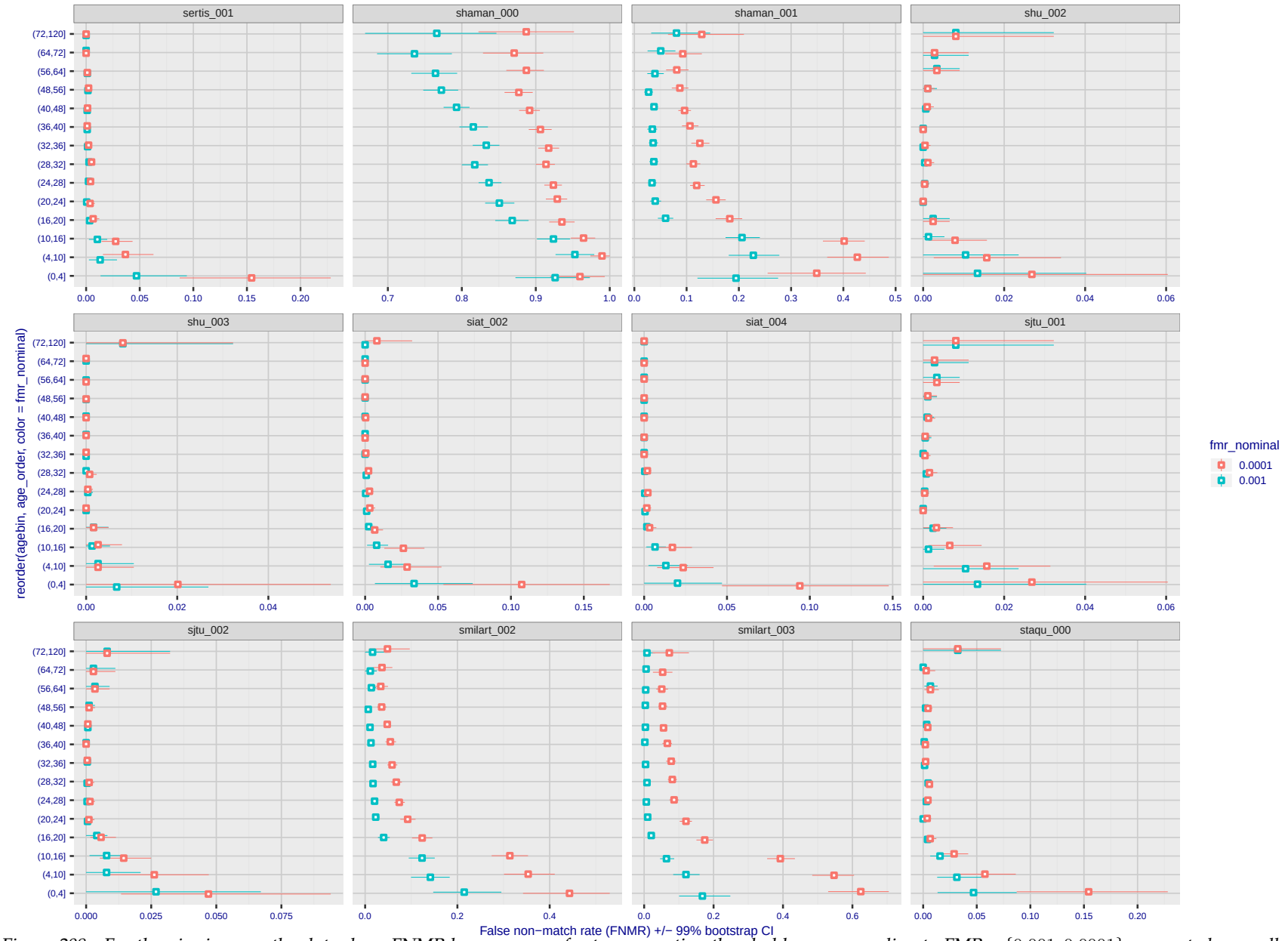

Figure 208: For the visa images, the dots show FNMR by age group for two operating thresholds corresponding to FMR = $\{0.001, 0.0001\}$ computed over all on the order of 10^{10} impostor scores. The FMR in each bin will vary also - see subsequent impostor heatmaps in sec. 3.6.2. Given a pair of face images taken at different times, we assign the comparison to the bin that is the arithmetic average of the subject's ages. This plot shows only the effect of age, not ageing. The number of comparisons in each bin is generally in the thousands, however the first and last bins are computed over 149 and 124 respectively. The error rates in some (adult) cases are zero, and in others the DET is flat so the error rates at the two thresholds are identical. The lines span 1% and 99% of boostrap replicated FNMR estimates.

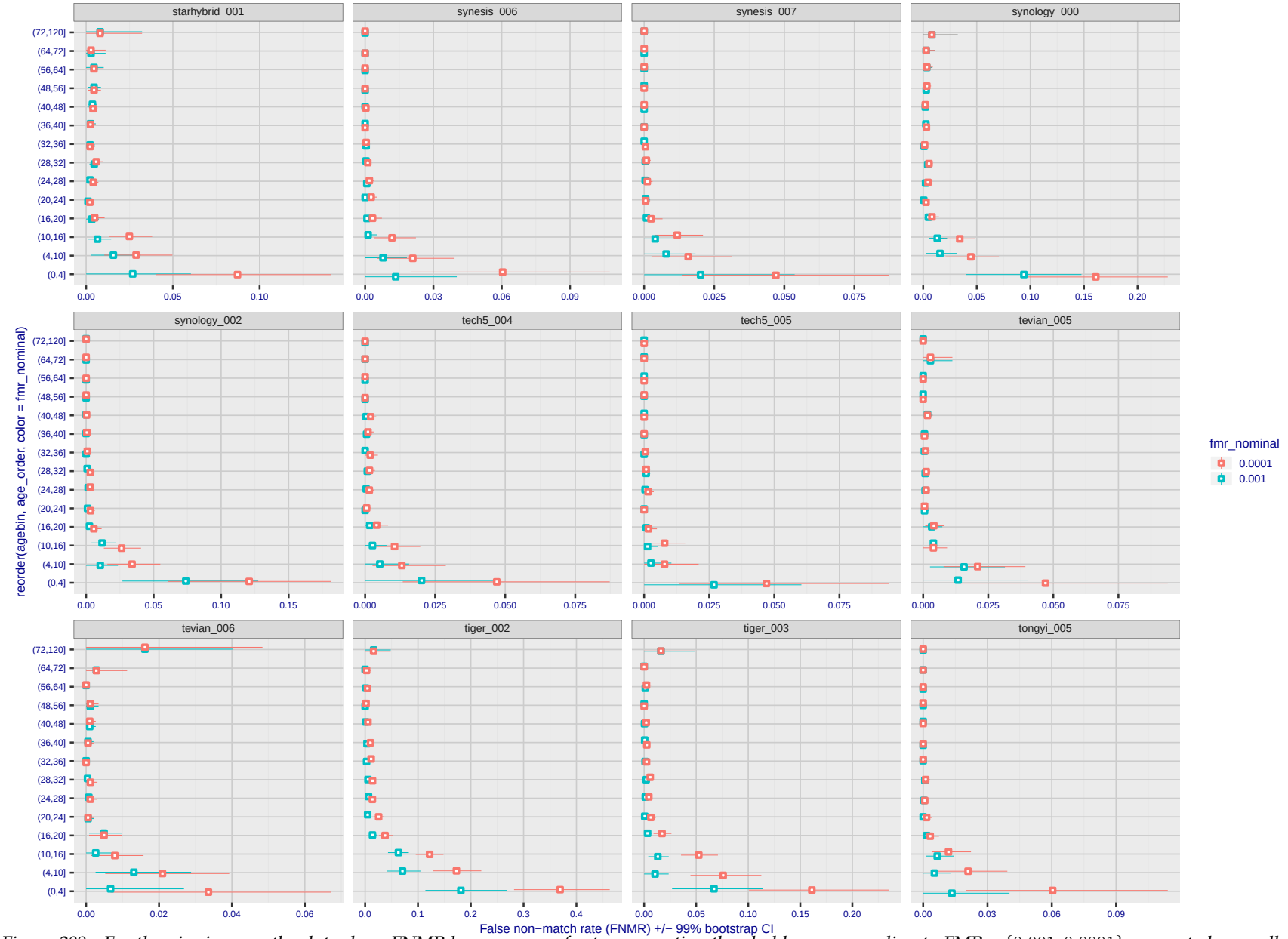

Figure 209: For the visa images, the dots show FNMR by age group for two operating thresholds corresponding to FMR = $\{0.001, 0.0001\}$ computed over all on the order of 10^{10} impostor scores. The FMR in each bin will vary also - see subsequent impostor heatmaps in sec. 3.6.2. Given a pair of face images taken at different times, we assign the comparison to the bin that is the arithmetic average of the subject's ages. This plot shows only the effect of age, not ageing. The number of comparisons in each bin is generally in the thousands, however the first and last bins are computed over 149 and 124 respectively. The error rates in some (adult) cases are zero, and in others the DET is flat so the error rates at the two thresholds are identical. The lines span 1% and 99% of boostrap replicated FNMR estimates.

Figure 210: For the visa images, the dots show FNMR by age group for two operating thresholds corresponding to FMR = $\{0.001, 0.0001\}$ computed over all on the order of 10^{10} impostor scores. The FMR in each bin will vary also - see subsequent impostor heatmaps in sec. 3.6.2. Given a pair of face images taken at different times, we assign the comparison to the bin that is the arithmetic average of the subject's ages. This plot shows only the effect of age, not ageing. The number of comparisons in each bin is generally in the thousands, however the first and last bins are computed over 149 and 124 respectively. The error rates in some (adult) cases are zero, and in others the DET is flat so the error rates at the two thresholds are identical. The lines span 1% and 99% of boostrap replicated FNMR estimates.

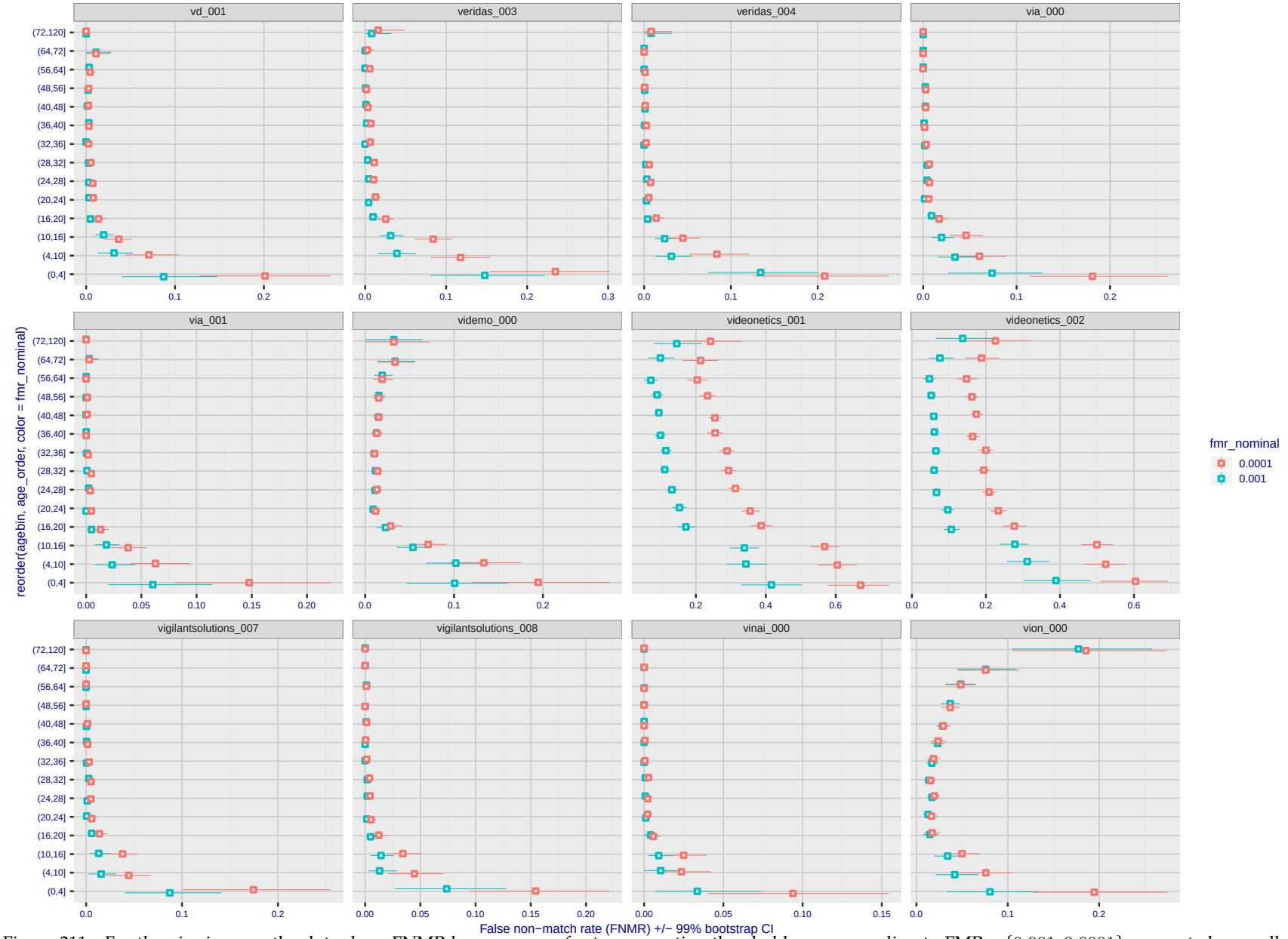

Figure 211: For the visa images, the dots show FNMR by age group for two operating thresholds corresponding to FMR = $\{0.001, 0.0001\}$ computed over all on the order of 10^{10} impostor scores. The FMR in each bin will vary also - see subsequent impostor heatmaps in sec. 3.6.2. Given a pair of face images taken at different times, we assign the comparison to the bin that is the arithmetic average of the subject's ages. This plot shows only the effect of age, not ageing. The number of comparisons in each bin is generally in the thousands, however the first and last bins are computed over 149 and 124 respectively. The error rates in some (adult) cases are zero, and in others the DET is flat so the error rates at the two thresholds are identical. The lines span 1% and 99% of boostrap replicated FNMR estimates.

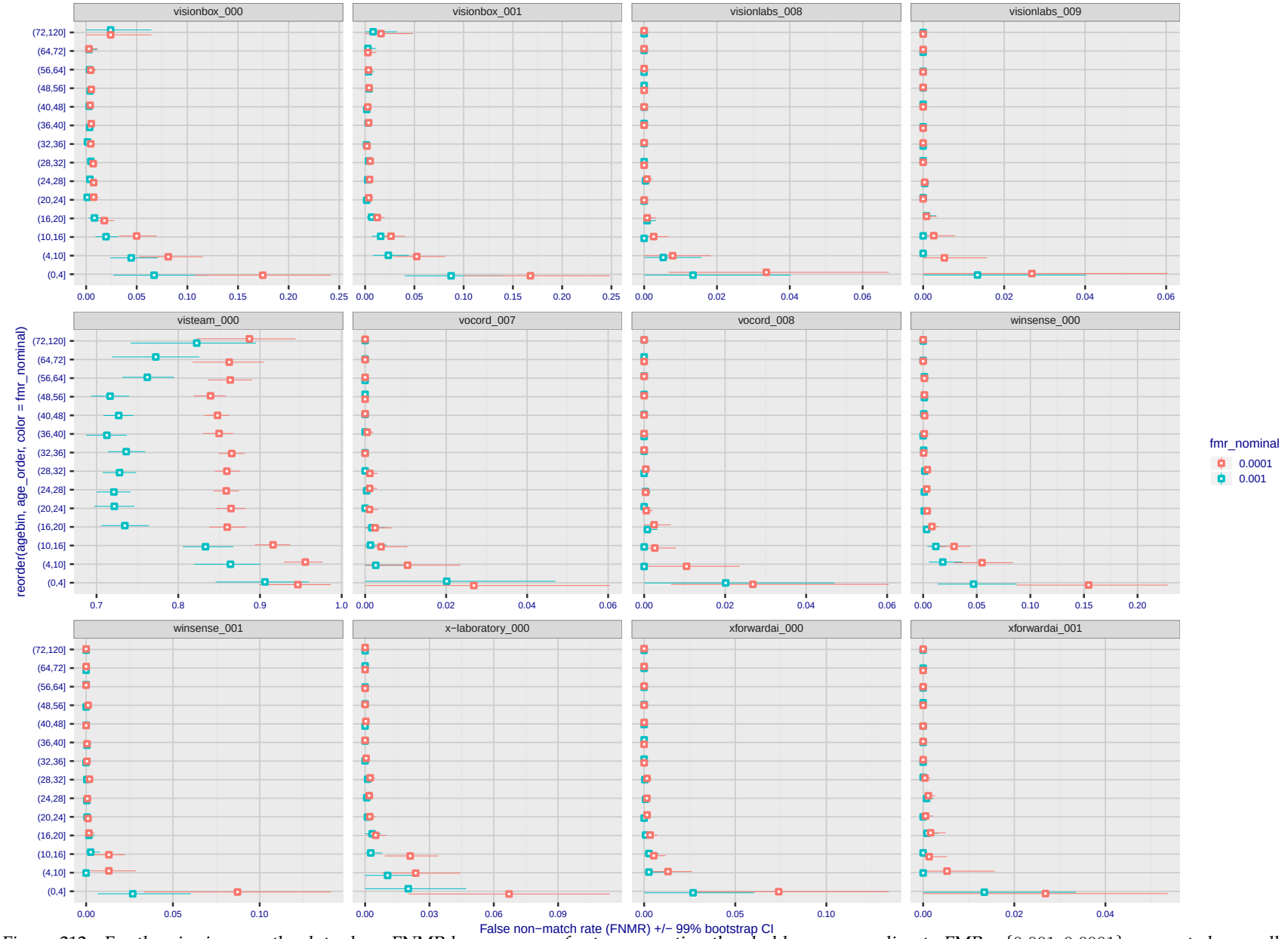

Figure 212: For the visa images, the dots show FNMR by age group for two operating thresholds corresponding to FMR = $\{0.001, 0.0001\}$ computed over all on the order of 10^{10} impostor scores. The FMR in each bin will vary also - see subsequent impostor heatmaps in sec. 3.6.2. Given a pair of face images taken at different times, we assign the comparison to the bin that is the arithmetic average of the subject's ages. This plot shows only the effect of age, not ageing. The number of comparisons in each bin is generally in the thousands, however the first and last bins are computed over 149 and 124 respectively. The error rates in some (adult) cases are zero, and in others the DET is flat so the error rates at the two thresholds are identical. The lines span 1% and 99% of boostrap replicated FNMR estimates.

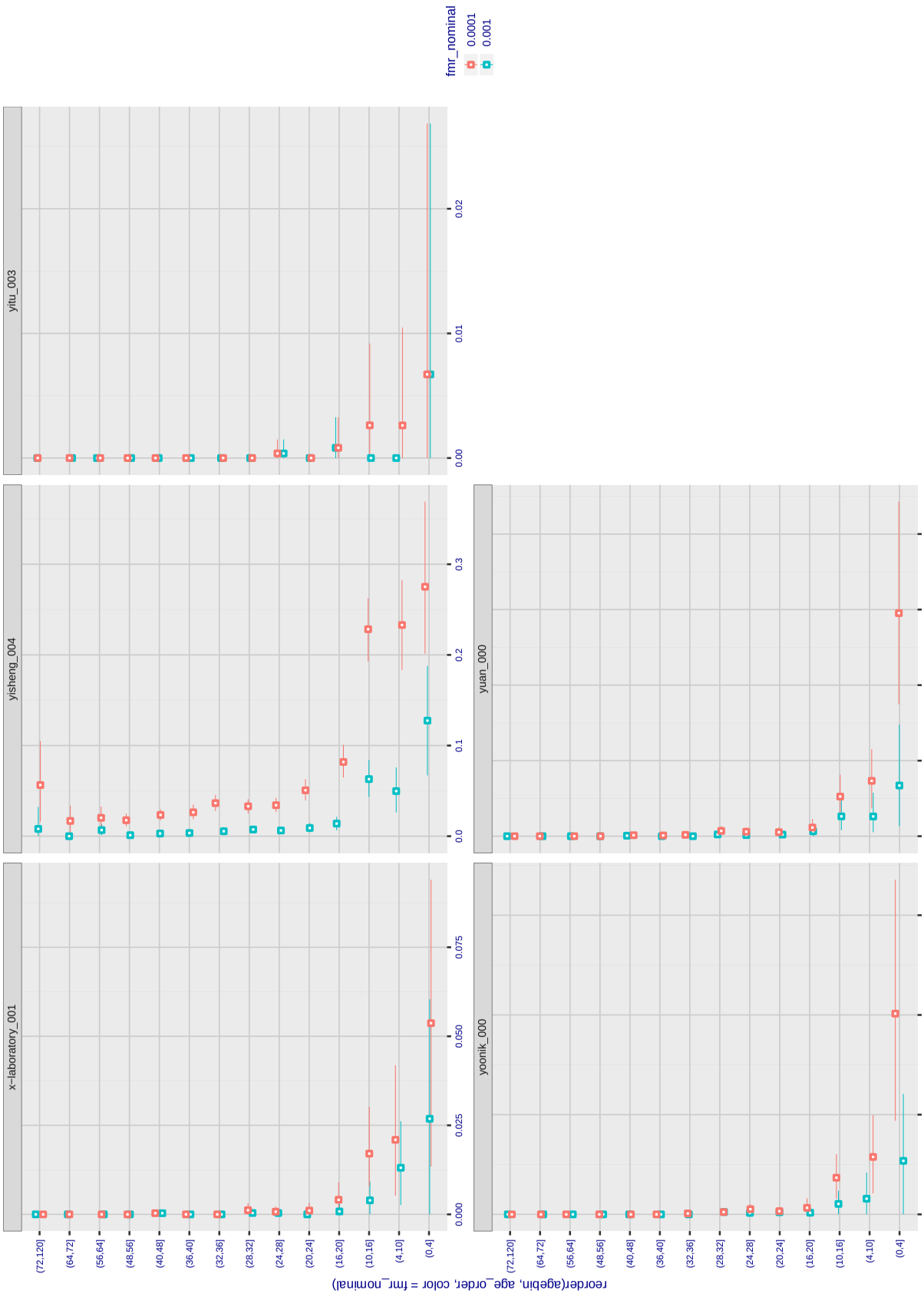

Figure 213: For the visa images, the dots show FNMR by age group for two operating thresholds corresponding to FMR = $\{0.001, 0.0001\}$ computed over all on the order of 10^{10} impostor scores. The FMR in each bin will vary also - see subsequent impostor heatmaps in sec. 3.6.2. Given a pair of face images taken at different times, we assign the comparison to the bin that is the arithmetic average of the subject's ages. This plot shows only the effect of age, not ageing. The number of comparisons in each bin is generally in the thousands, however the first and last bins are computed over 149 and 124 respectively. The error rates in some (adult) cases are zero, and in others the DET is flat so the error rates at the two thresholds are identical. The lines span 1% and 99% of boostrap replicated FNMR estimates.

FNMR(T) "False non-match rate"
FMR(T) "False match rate"

Caveats: None.

3.6 Impostor distribution stability

3.6.1 Effect of birth place on the impostor distribution

Background: Facial appearance varies geographically, both in terms of skin tone, cranio-facial structure and size. This section addresses whether false match rates vary intra- and inter-regionally.

Goals:

- ▷ To show the effect of birth region of the impostor and enrollee on false match rates.
- ▷ To determine whether some algorithms give better impostor distribution stability.

Methods:

- ▷ For the visa images, NIST defined 10 regions: Sub-Saharan Africa, South Asia, Polynesia, North Africa, Middle East, Europe, East Asia, Central and South America, Central Asia, and the Caribbean.
- ▷ For the visa images, NIST mapped each country of birth to a region. There is some arbitrariness to this. For example, Egypt could reasonably be assigned to the Middle East instead of North Africa. An alternative methodology could, for example, assign the Philippines to *both* Polynesia and East Asia.
- ▷ FMR is computed for cases where all face images of impostors born in region r_2 are compared with enrolled face images of persons born in region r_1.

$$\text{FMR}(r_1, r_2, T) = \frac{\sum_{i=1}^{N_{r_1,r_2}} H(s_i - T)}{N_{r_1,r_2}} \tag{5}$$

  where the same threshold, T, is used in all cells, and H is the unit step function. The threshold is set to give FMR(T) = 0.001 over the entire set of visa image impostor comparisons.
- ▷ This analysis is then repeated by country-pair, but only for those country pairs where both have at least 1000 images available. The countries[1] appear in the axes of graphs that follow.
- ▷ The mean number of impostor scores in any cross-region bin is 33 million. The smallest number of impostor scores in any bin is 135000, for Central Asia - North Africa. While these counts are large enough to support reasonable significance, the number of individual faces is much smaller, on the order of $N^{0.5}$.
- ▷ The numbers of impostor scores in any cross-country bin is shown in Figure **??**.

Results: Subsequent figures show heatmaps that use color to represent the base-10 logarithm of the false match rate. Red colors indicate high (bad) false match rates. Dark colors indicate benign false match rates. There are two series of graphs corresponding to aggregated geographical regions, and to countries. The notable observations are:

- ▷ The on-diagonal elements correspond to within-region impostors. FMR is generally above the nominal value of FMR = 0.001. Particularly there is usually higher FMR in, Sub-Saharan Africa, South Asia, and the Caribbean. Europe and Central Asia, on the other hand, usually give FMR closer to the nominal value.
- ▷ The off-diagonal elements correspond to across-region impostors. The highest FMR is produced between the Caribbean and Sub-Saharan Africa.
- ▷ Algorithms vary.

[1] These are Argentina, Australia, Brazil, Chile, China, Costa Rica, Cuba, Czech Republic, Dominican Republic, Ecuador, Egypt, El Salvador, Germany, Ghana, Great Britain, Greece, Guatamala, Haiti, Hong Kong, Honduras, Indonesia, India, Israel, Jamaica, Japan, Kenya, Korea, Lebanon, Mexico, Malaysia, Nepal, Nigeria, Peru, Philippines, Pakistan, Poland, Romania, Russia, South Africa, Saudi Arabia, Thailand, Trinidad, Turkey, Taiwan, Ukraine, Venezuela, and Vietnam.

FNMR(T) "False non-match rate"
FMR(T) "False match rate"

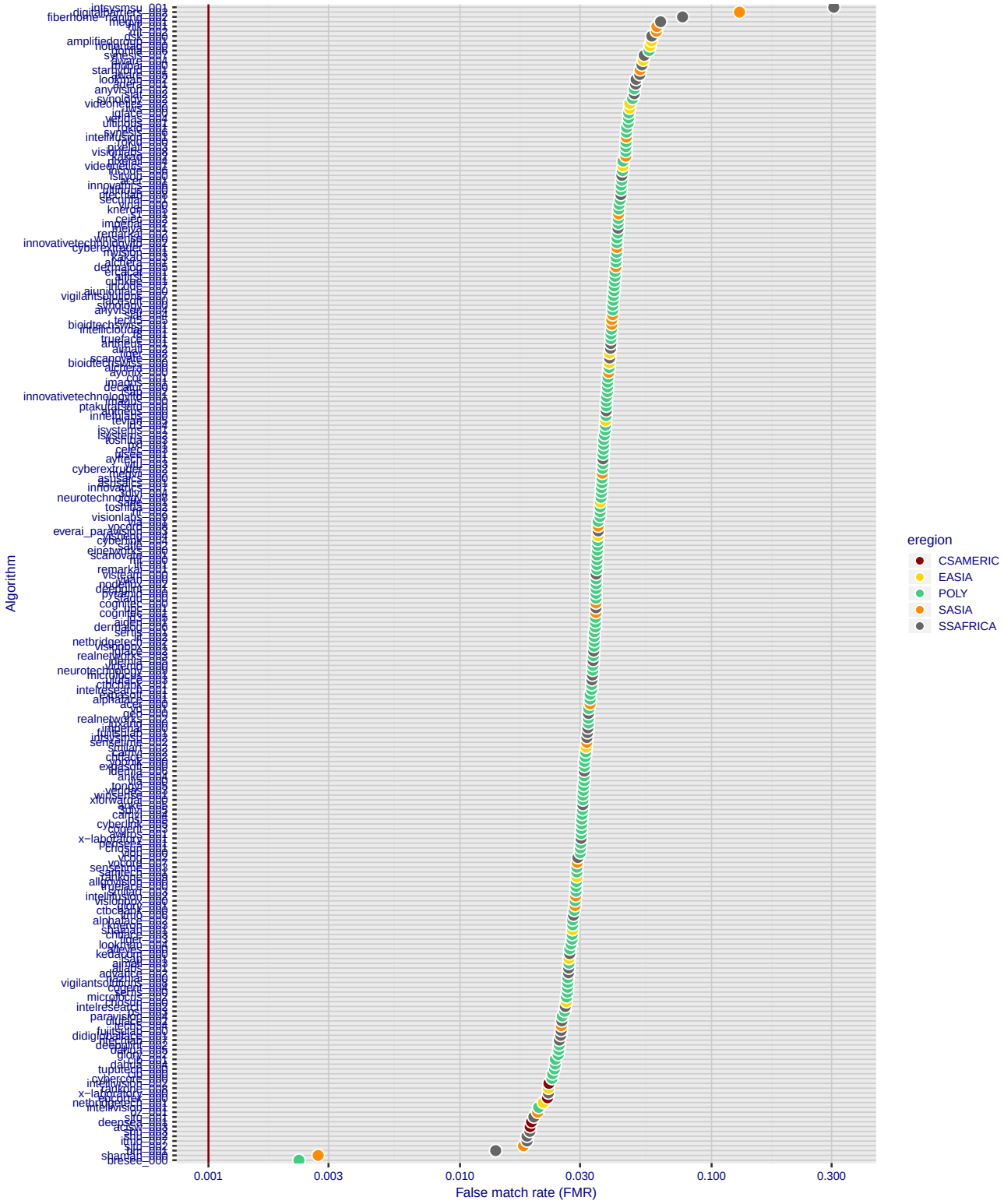

Figure 214: For the visa images, the dots show FMR for impostor comparisons of individuals of the same sex and same age group for the region of the world that gives the worst (highest) FMR when the threshold is set to give FMR = 0.001 (red vertical line) over all on the order of 10^{10} impostor scores i.e. zero-effort. The shift of the dots to right shows massive increases in FMR when impostors have the same sex, age, and region of birth. The color code indicates which region gives the worst case FMR. If the observed variation is due to the prevalence of one kind of images in the training imagery, then algorithms developed on one kind of data might be expected to give higher FMR on other kinds.

FNMR(T) "False non-match rate"
FMR(T) "False match rate"

▷ We computed the same quantities for a global FMR = 0.0001. The effects are similar.

Caveats:

▷ The effects of variable impostor rates on one-to-many identification systems may well differ from what's implied by these one-to-one verification results. Two reasons for this are a) the enrollment galleries are usually imbalanced across countries of birth, age and sex; b) one-to-many identification algorithms often implement techniques aimed at stabilizing the impostor distribution. Further research is necessary.

▷ In principle, the effects seen in this subsection could be due to differences in the image capture process. We consider this unlikely since the effects are maintained across geography - e.g. Caribbean vs. Africa, or Japan vs. China.

FNMR(T) "False non-match rate"
FMR(T) "False match rate"

Figure 215: For visa images, the heatmap shows how the mean of the impostor distribution for the country pair (a,b) is shifted relative to the mean of the global impostor distribution, expressed as a number of standard deviations of the global impostor distribution. This statistic is designed to show shifts in the entire impostor distribution, not just tail effects that manifest as the anomalously high (or low) false match rates that appear in the subsequent figures. The countries are chosen to show that skin tone alone does not explain impostor distribution shifts. The reduced shift in Asian populations with the Yitu and TongYiTrans algorithms, is accompanied by positive shifts in the European populations. This reversal relative to most other algorithms, may derive from use of nationally weighted training sets. The figure is computed from same-sex and same-age impostor pairs.

FNMR(T) "False non-match rate"
FMR(T) "False match rate"

3.6.2 Effect of age on impostors

Background: This section shows the effect of age on the impostor distribution. The ideal behaviour is that the age of the enrollee and the impostor would not affect impostor scores. This would support FMR stability over sub-populations.

Goals:

- ▷ To show the effect of relative ages of the impostor and enrollee on false match rates.
- ▷ To determine whether some algorithms have better impostor distribution stability.

Methods:

- ▷ Define 14 age group bins, spanning 0 to over 100 years old.
- ▷ Compute FMR over all impostor comparisons for which the subjects in the enrollee and impostor images have ages in two bins.
- ▷ Compute FMR over all impostor comparisons for which the subjects are additionally of the same sex, and born in the same geographic region.

Results:

The notable aspects are:

- ▷ Diagonal dominance: Impostors are more likely to be matched against their same age group.
- ▷ Same sex and same region impostors are more successful. On the diagonal, an impostor is more likely to succeed by posing as someone of the same sex. If $\Delta \log_{10}$ FMR $= 0.2$, then same-sex same-region FMR exceeds the all-pairs FMR by factor of $10^{0.2} = 1.6$.
- ▷ Young children impostors give elevated FMR against young children. Older adult impostor give elevated FMR against older adults. These effects are quite large, for example if $\Delta \log_{10}$ FMR $= 1.0$ larger than a 32 year old, then these groups have higher FMR by a factor of $10^1 = 10$. This would imply an FMR above 0.01 for a nominal (global) FMR = 0.001.
- ▷ Algorithms vary.
- ▷ We computed the same quantities for a global FMR = 0.0001. The effects are similar.

Note the calculations in this section include impostors paired across all countries of birth.

Accuracy Terms + Definitions

In biometrics, Type II errors occur when two samples of one person do not match – this is called a **false negative**. Correspondingly, Type I errors occur when samples from two persons do match – this is called a **false positive**. Matches are declared by a biometric system when the native comparison score from the recognition algorithm meets some **threshold**. Comparison scores can be either **similarity scores**, in which case higher values indicate that the samples are more likely to come from the same person, or **dissimilarity scores**, in which case higher values indicate different people. Similarity scores are traditionally computed by **fingerprint** and **face** recognition algorithms, while dissimilarities are used in **iris recognition**. In some cases, the dissimilarity score is a distance; this applies only when **metric** properties are obeyed. In any case, scores can be either **mate** scores, coming from a comparison of one person's samples, or **nonmate** scores, coming from comparison of different persons' samples. The words **genuine** or **authentic** are synonyms for mate, and the word **impostor** is used a synonym for nonmate. The words mate and nonmate are traditionally used in identification applications (such as law enforcement search, or background checks) while genuine and impostor are used in verification applications (such as access control).

A **error tradeoff** characteristic represents the tradeoff between Type II and Type I classification errors. For verification this plots false non-match rate (FNMR) vs. false match rate (FMR) parametrically with T.

The error tradeoff plots are often called **detection error tradeoff (DET)** characteristics or **receiver operating characteristic** (ROC). These serve the same function but differ, for example, in plotting the complement of an error rate (e.g. TMR = 1 – FNMR) and in transforming the axes most commonly using logarithms, to show multiple decades of FMR. More rarely, the function might be the inverse Gaussian function.

More detail and generality is provided in formal biometrics testing standards, see the various parts of ISO/IEC 19795 Biometrics Testing and Reporting. More terms, including and beyond those to do with accuracy, see ISO/IEC 2382-37 Information technology -- Vocabulary -- Part 37: Harmonized biometric vocabulary

FNMR(T) "False non-match rate"
FMR(T) "False match rate"

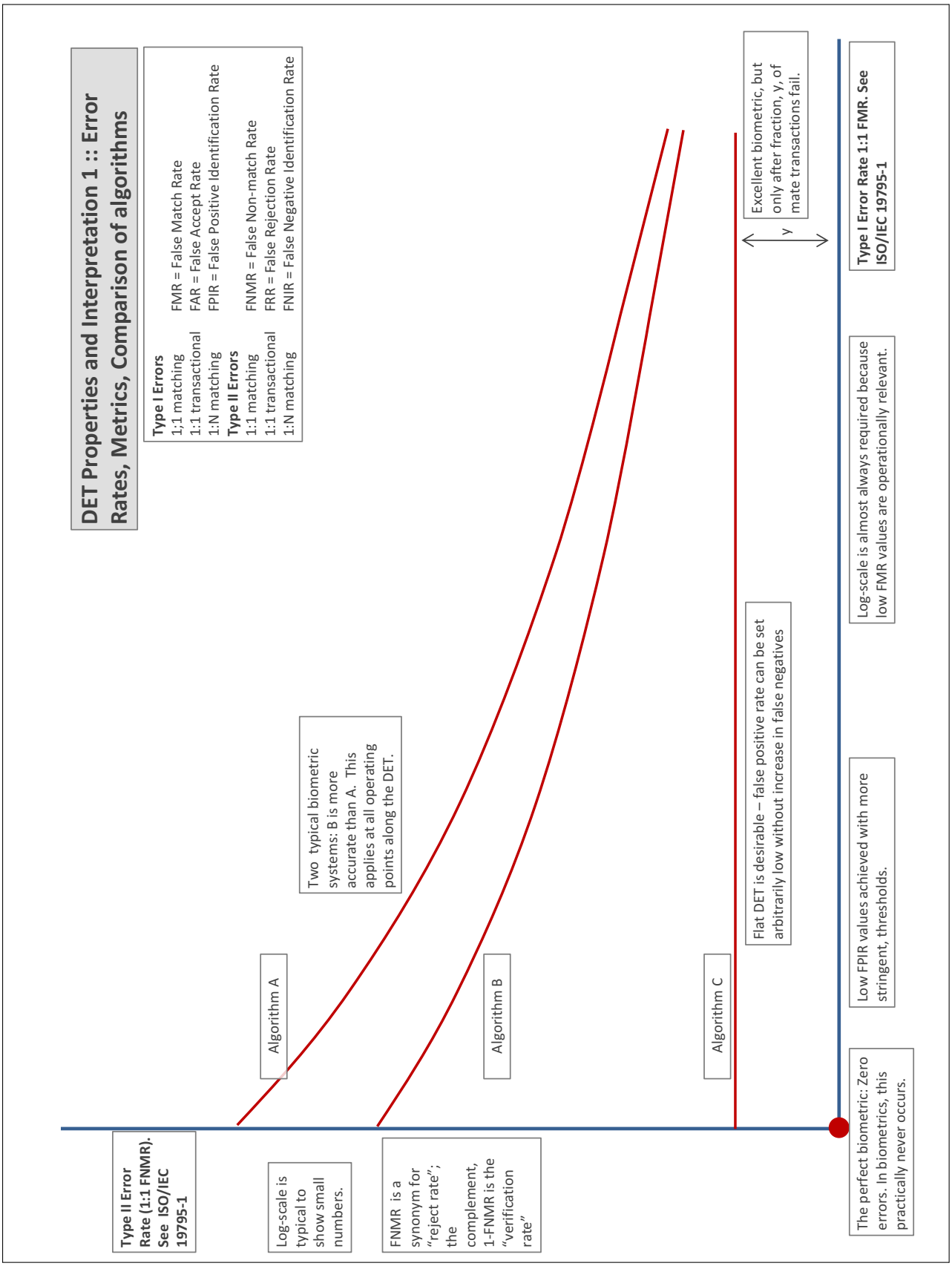

FNMR(T) "False non-match rate"
FMR(T) "False match rate"

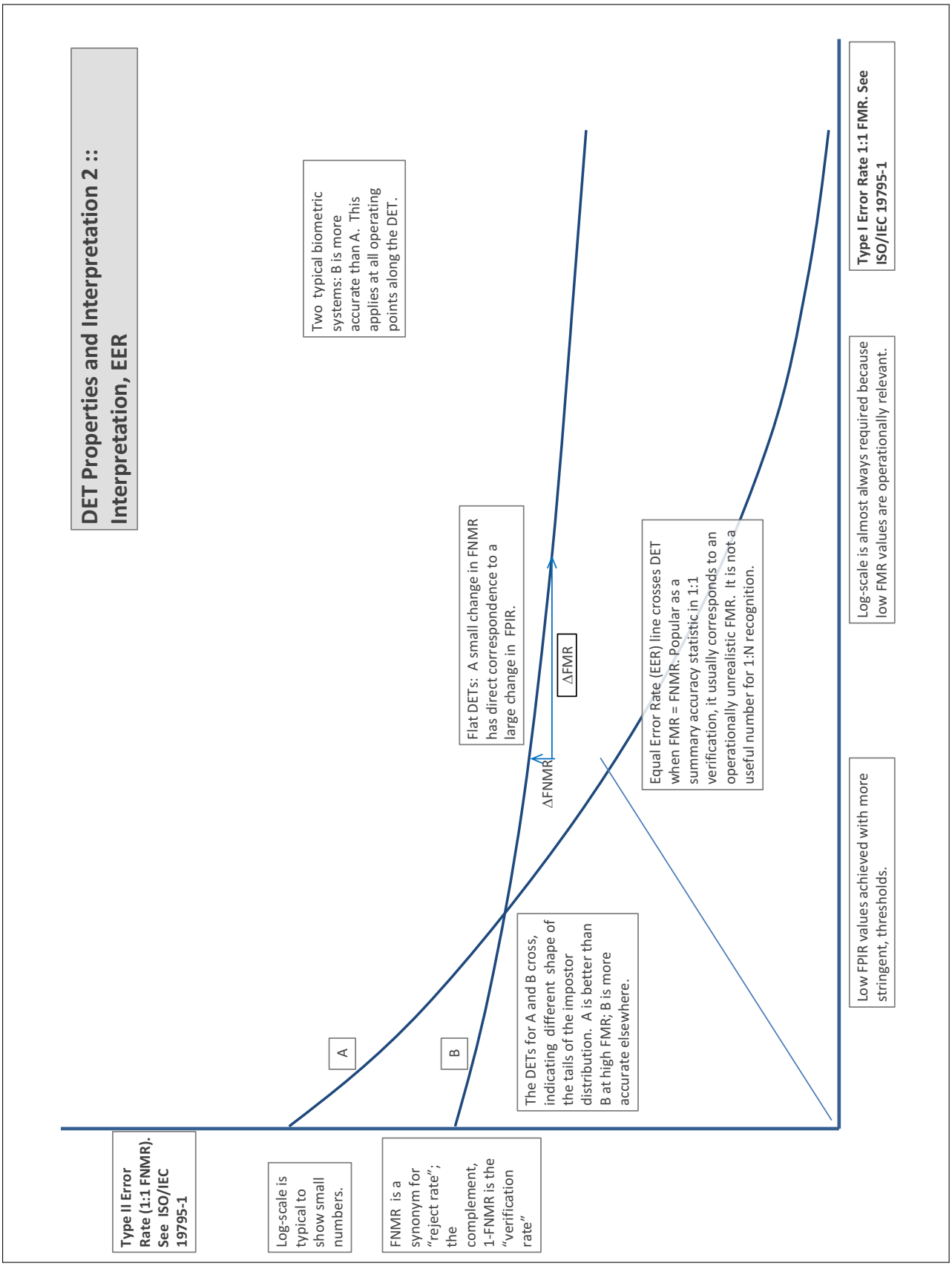

FNMR(T) "False non-match rate"
FMR(T) "False match rate"

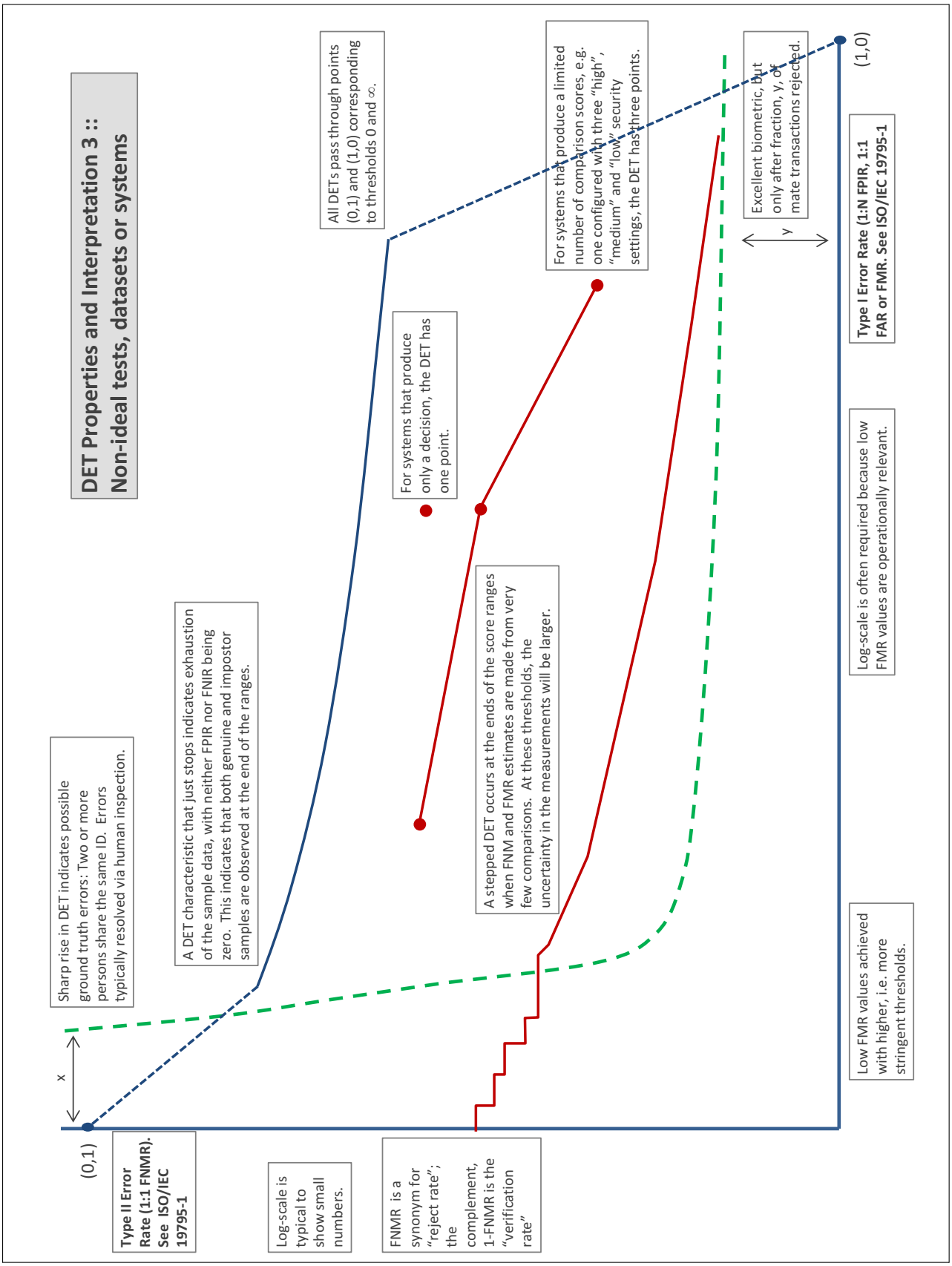

FNMR(T) "False non-match rate"
FMR(T) "False match rate"

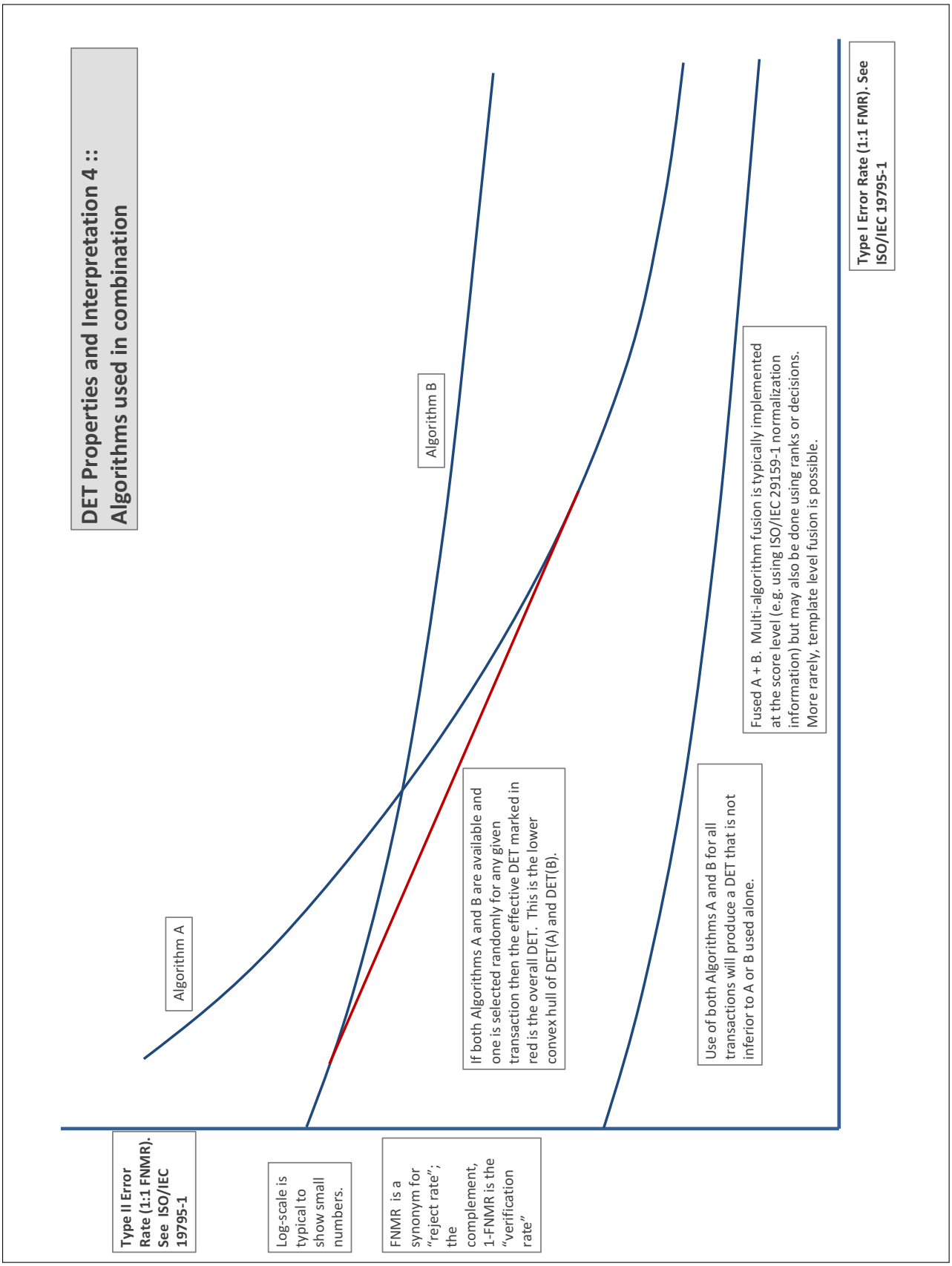

FNMR(T) "False non-match rate"
FMR(T) "False match rate"

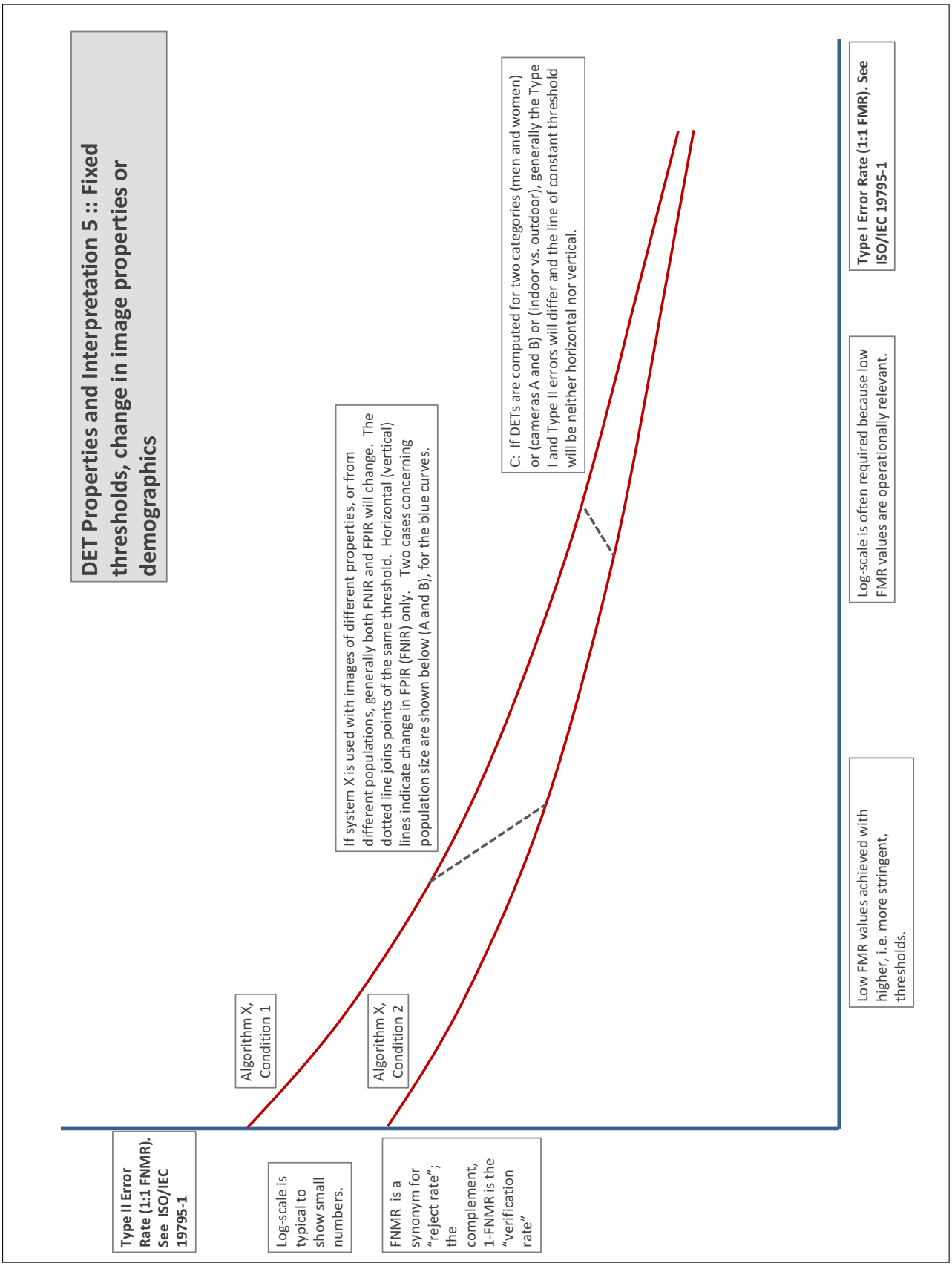

FNMR(T) "False non-match rate"
FMR(T) "False match rate"

References

[1] P. Jonathon Phillips, Amy N. Yates, Ying Hu, Carina A. Hahn, Eilidh Noyes, Kelsey Jackson, Jacqueline G. Cavazos, Géraldine Jeckeln, Rajeev Ranjan, Swami Sankaranarayanan, Jun-Cheng Chen, Carlos D. Castillo, Rama Chellappa, David White, and Alice J. O'Toole. Face recognition accuracy of forensic examiners, superrecognizers, and face recognition algorithms. *Proceedings of the National Academy of Sciences*, 115(24):6171–6176, 2018.